Universitat de València

Programa de Doctorat en Física – 3126

Flavor, Higgses, and CP Violation

Carlos Miró Arenas

IFIC (CSIC – Universitat de València)

Supervised by

Prof. Dr. Francisco José Botella Olcina

Dr. Miguel Rubén Nebot Gómez

Valencia, May 2025

Prof. Dr. Francisco José Botella Olcina, Catedrático de la Universitat de València, y
Dr. Miguel Rubén Nebot Gómez, Profesor Contratado Doctor de la Universitat de València,

CERTIFICAN

Que la presente memoria, *Flavor, Higgses, and CP Violation*, ha sido realizada bajo su dirección en el Instituto de Física Corpuscular, centro mixto de la Universitat de València y del Consejo Superior de Investigaciones Científicas, y en el Departament de Física Teòrica de la Universitat de València, por Carlos Miró Arenas, y constituye su Tesis para optar al título de Doctor en Física.

Y para que así conste, en cumplimiento de la legislación vigente, presentan en el Departament de Física Teòrica de la Universitat de València la referida Tesis Doctoral y firman el presente certificado.

Valencia, mayo de 2025

Francisco José Botella Olcina   Miguel Rubén Nebot Gómez

A mi familia

"When you have eliminated the impossible,
whatever remains, however improbable,
must be the truth."

Sherlock Holmes in *The Sign of the Four*,
by Sir Arthur Conan Doyle

Acknowledgments

En primer lugar, quiero empezar agradeciendo a mis directores, Quico y Miguel, el haber confiado en mí desde un primer momento y haberme dado la oportunidad de adentrarme en el mundo de la investigación. Gracias por todo lo que me habéis enseñado, por hacerme sentir cómodo en todo momento y por darme libertad para explorar nuevos horizontes. Siempre seréis referentes para mí.

Durante esta etapa, he tenido la fortuna de visitar distintas partes del mundo y conocer gente extraordinaria, empezando por Miguel Escudero. Miguel, has sido una persona muy importante en este camino. Siempre te estaré infinitamente agradecido por cuidar de mí en Suiza, por abrirme las puertas del CERN, por darme tantos y tan valiosos consejos, por haberme hecho mejor científico y, sobre todo, por ser un amigo increíble.

De la misma manera, estoy enormemente agradecido a Ben Grinstein. Ben, ojalá algún día pueda llegar a aprender al menos una pequeña parte de todo lo que tú sabes. Eres un ejemplo en todos los sentidos y, sin duda, ha sido un privilegio poder aprender de ti. Por otra parte, quiero dar las gracias a Pablo Quílez. Pablo, gracias por ayudarme siempre que lo necesitaba, por enseñarme tanta Física, y por descubrirme los mejores lugares de San Diego. Hiciste posible que disfrutase cada minuto de la estancia. I am also grateful to Xiaochuan Lu. Xiaochuan, you have been an incredible teacher to me, and I wish I could become as brilliant a scientist as you are. Thank you for helping me every time I needed it. Likewise, I would like to thank Jai for all the great moments we shared together. I feel very lucky to have met you, and I look forward to many more adventures ahead.

I am also grateful to Zoltan Ligeti for welcoming me to Berkeley and giving me the opportunity to experience such an inspiring and unforgettable atmosphere.

Doy gracias también a todos mis compañeros en el Departamento de Física Teórica de la Universitad de Valencia y en el IFIC, los cuales han hecho de este viaje una experiencia inolvidable. A Pablo, por estar ahí siempre que lo he necesitado. Y a Rebeca y Gorka, por haber compartido este camino conmigo desde que empezamos la carrera.

Finalmente, nada hubiera sido posible sin mi familia, a quien está dedicada esta tesis. Gracias a mi madre, a mi padre y a mi hermano por su apoyo incondicional, y por enseñarme con su ejemplo la persona que quiero llegar a ser. A mi sobrino Mateo por hacernos tan felices. A mi abuela por cuidarme tanto durante estos años. Y a mi tía, por todo lo que nos quería.

I acknowledge the valuable comments and suggestions provided by the referees of the various publications that form the basis of this thesis, as well as to the members of the committee for their careful and critical reading of the manuscript. This doctoral thesis is funded by *Conselleria de Educación, Cultura, Universidades y Empleo* from *Generalitat Valenciana* and by *Fondo Social Europeo* under grants ACIF/2021/284, CIBEFP/2022/92, CIBEFP/2023/96, and CIBEFP/2024/37.

List of Publications

This PhD Thesis is based on the following scientific publications:

[1] **Most general EFTs from spurion analysis: Hilbert series and Minimal Lepton Flavor Violation**,
B. Grinstein, X. Lu, C. Miró and P. Quílez,
JHEP **07** (2025) 259, [2412.16285],

[2] **Light states in real multi-Higgs models with spontaneous CP violation**,
C. Miró, M. Nebot and D. Queiroz,
Phys. Rev. D 111 (2025) 11, L111703, [2411.00084],

[3] **How large could the CP violation in neutral B-meson mixing be? Implications for baryogenesis and upcoming searches**,
C. Miró, M. Escudero and M. Nebot,
Phys. Rev. D 110 (2024) 115033, [2410.13936],

[4] **Spontaneous CP violation and $\mu - \tau$ symmetry in two-Higgs-doublet models with flavour conservation**,
J. M. Alves, F. J. Botella, C. Miró and M. Nebot,
Eur. Phys. J. C 83 (2023) 940, [2306.14952],

and proceedings

[5] **How large could CP violation in B meson mixing be? Implications for baryogenesis and future searches**,
C. Miró, M. Escudero and M. Nebot,
PoS DISCRETE2024 (2025) 023.

Other scientific publications and proceedings not included in this manuscript are:

[6] **Accidental symmetries, Hilbert series, and *friends***,
B. Grinstein, X. Lu, C. Miró and P. Quílez,
JHEP **03** (2025) 172, [2412.05359],

[7] **New Physics hints from τ scalar interactions and** $(g-2)_{e,\mu}$,
F. J. Botella, F. Cornet-Gomez, C. Miró and M. Nebot,
J. Phys. G 51 (2024) 025001, [2302.05471],

[8] **Muon and electron $g-2$ anomalies in a flavor conserving 2HDM with an oblique view on the CDF M_W value**,
F. J. Botella, F. Cornet-Gomez, C. Miró and M. Nebot,
Eur. Phys. J. C 82 (2022) 915, [2205.01115],

[9] **Addressing leptonic $g-2$ anomalies in a flavor conserving two-Higgs-doublet model**,
C. Miró,
Frascati Phys. Ser. **72** (2022) 1.

Abbreviations

BAU	Baryon Asymmetry of the Universe
BN	Baryon Number
BSM	Beyond the Standard Model
CKM	Cabibbo-Kobayashi-Maskawa
CL	Confidence Level
CLFV	Charged Lepton Flavor Violation
CP	Charge-Parity
CPT	Charge-Parity-Time reversal
dim	Dimension
dof	Degrees of Freedom
EDM	Electric Dipole Moment
EFT	Effective Field Theory
EW	Electroweak
EWSB	Electroweak Symmetry Breaking
FCNC	Flavor-Changing Neutral Currents
GB	Goldstone Boson
GIM	Glashow-Iliopoulos-Maiani
GUT	Grand Unified Theory
HQE	Heavy Quark Expansion
irrep	Irreducible Representation
OPE	Operator Product Expansion
PDG	Particle Data Group
PMNS	Pontecorvo-Maki-Nakagawa-Sakata
QCD	Quantum Chromodynamics
QED	Quantum Electrodynamics
QFT	Quantum Field Theory
LFUV	Lepton Flavor Universality Violation
LN	Lepton Number

MFV	Minimal Flavor Violation
MHDM	Multi-Higgs-Doublet Model
MLFV	Minimal Lepton Flavor Violation
NFC	Natural Flavor Conservation
NP	New Physics
rep	Representation
RGE	Renormalization Group Evolution
SCPV	Spontaneous Charge-Parity Violation
SFCNC	Scalar Flavor-Changing Neutral Currents
SM	Standard Model
SMEFT	Standard Model Effective Field Theory
SSB	Spontaneous Symmetry Breaking
T	Time reversal
2HDM	Two-Higgs-Doublet Model
UV	Ultraviolet
vev	Vacuum Expectation Value
VIA	Vacuum Insertion Approximation
wbGB	Would-be Goldstone Boson
WB	Weak Basis
WBT	Weak Basis Transformations

Preface

Throughout the history of particle physics, the flavor sector has often anticipated major theoretical breakthroughs. The discovery of the charm quark or the prediction of the third generation of fermions were indeed motivated by the absence of flavor-changing neutral currents, and the evidence of CP-violating meson oscillations, respectively. Flavor transitions are specially sensitive to the quantum footprints that hypothetical particles may leave in rare decays, meson mixings, and subtle CP-violating observables. Therefore, it serves as a powerful probe of new dynamics that may lie far beyond the direct reach of present collider experiments. Today, as experimental facilities like LHCb and Belle II are pushing the boundaries of the high-precision frontier, and as theoretical tools become ever more refined, the flavor sector remains at the forefront to uncover what New Physics lies beyond the Standard Model. Likewise, Flavor sits at the core of some of the most profound open questions in modern physics. *Why Nature abandons minimality and replicates into three generations of fermions? What underlies the hierarchical pattern of fermion masses and mixings?*

On the other hand, the discovery of the Higgs boson in 2012 marked a major milestone in particle physics, and represented a key piece of the experimental confirmation of the Standard Model. Yet, rather than closing this chapter, it opened the door to new fundamental questions—such as the stabilization of the Higgs mass—and raised the intriguing possibility that the scalar sector might be also realized in a non-minimal way. Extensions of the Higgs sector, while often motivated by theories operating at higher energy scales, offer a rich phenomenology, including new sources of CP violation and flavor transitions.

Finally, the violation of the CP symmetry is one of the most intriguing features of fundamental interactions. Within the Standard Model, CP violation arises through a single irremovable phase in the CKM matrix, and although this successfully accounts for all observed phenomena in kaon and B meson physics, it falls dramatically short of explaining the Baryon Asymmetry of the Universe in the context of baryogenesis models. This mismatch suggests that additional sources of CP violation should exist. The search for such sources is not only motivated by cosmological considerations, but also by the rich experimental program exploring CP-violating effects in meson systems, electric dipole moments, and lepton interactions. Understanding the origin and structure of CP violation is thus essential both for uncovering the mechanism behind the primordial matter-antimatter imbalance, as well as guiding the construction of more complete theories of fundamental interactions.

This thesis collects part of my research on the three main topics outlined above: *Flavor, Higgses, and CP Violation*. Although these are often closely interconnected, the contents of this manuscript are organized as follows.

The first part of the thesis serves to introduce the theoretical foundations that underpin our scientific research. This includes a review of the Standard Model framework, analyzing in detail its flavor structure and the emergence of CP violation in the weak interactions. We then turn to the Hilbert series technique with the goal of presenting how it can be applied to particle physics, highlighting it as a powerful tool in symmetry-based analyses. Finally, we discuss the basic features of scalar extensions involving multiple Higgs doublets, with a particular focus on two-Higgs-doublet models. Special attention is given to the appearance of flavor-changing neutral interactions and new sources of CP violation.

The second part of the thesis is dedicated to original scientific research. We start by presenting the most general effective field theories that can be constructed within spurion analyses, taking the Minimal Lepton Flavor Violation paradigm as an illustrative example. On another avenue, the phenomenological implications in the mass spectrum of general multi-Higgs-doublet models where CP is solely broken by the vacuum are presented. The latter condition is also studied in the two-Higgs-doublet model together with the simultaneous requirement of flavor conservation in the lepton sector, focusing on its impact on the structure of the flavor mixing matrix. Finally, we analyze in detail how large CP violation in B meson mixing could be in different scenarios, with special emphasis on its implications for baryogenesis and future experimental searches.

Special effort has been devoted to the appendices, which include detailed calculations and supplementary explanations. These are intended to serve as a useful reference for practitioners interested in the technical aspects underlying our main results, and to provide additional clarity on some of the more involved steps that are only outlined in the main text.

I hope that this thesis, which brings together our findings along with additional open questions that remain to be explored, will serve as a meaningful contribution to the scientific community and a valuable reference for interested readers.

Carlos Miró
Valencia, May 2025

Contents

Theoretical Foundations

1 The Standard Model and the quest for New Physics

The Standard Model (SM) is a Quantum Field Theory (QFT) shaped by the principles of locality, Lorentz-Poincaré invariance, gauge invariance, and renormalizability, that successfully describes the strong, weak, and electromagnetic interactions of all known fundamental particles. These emerge as excitations of quantum fields transforming as representations of the Lorentz group: spin-0 for scalar bosons, spin-1/2 for fermions, and spin-1 for vector bosons. The SM Lagrangian comprises different sectors that can be written as

$$\mathscr{L}_{\text{SM}} = \mathscr{L}_{\text{gauge}} + \mathscr{L}_{\text{scalar}} + \mathscr{L}_{\text{fermion}} + \mathscr{L}_{\text{Y}} + \mathscr{L}_{\text{GF}} + \mathscr{L}_{\text{ghost}}\,. \tag{1.1}$$

The first term in the Lagrangian, $\mathscr{L}_{\text{gauge}}$, describes the pure gauge sector, which is entirely fixed by the requirement of local gauge invariance. The scalar sector of the theory, $\mathscr{L}_{\text{scalar}}$, is then introduced to trigger spontaneous electroweak symmetry breaking, thereby generating masses for the electroweak gauge bosons. Unlike the gauge structure of the theory, its matter content is not dictated by an underlying fundamental principle, but is assumed to consist of quarks and leptons grouped into three generations. Their gauge interactions are described by $\mathscr{L}_{\text{fermion}}$, while their couplings to the scalar fields, encoded in $\mathscr{L}_{\text{Y}}$, give rise to fermion masses after Electroweak Symmetry Breaking (EWSB). This last term is the origin of the flavor structure of the theory, reflecting the replication of fermion families that differ only in their masses. Finally, $\mathscr{L}_{\text{GF}}$ and $\mathscr{L}_{\text{ghost}}$ correspond to the gauge-fixing and ghost terms, respectively. These are required to consistently quantize the theory in a covariant gauge and to properly account for the gauge redundancy in the path integral formalism. While they do not affect physical observables directly, they play a crucial role in ensuring the renormalizability and unitarity of the theory at the quantum level. Altogether, the SM has reigned as an excellent framework for accurately describing the vast majority of particle physics experiments conducted to date.

In this chapter, we provide an overview of the different sectors of the standard theory, with a particular focus on the electroweak interactions, and omitting the technical details related to the gauge-fixing and the ghost fields. Our discussion will place special emphasis on the flavor sector of the theory and the analysis of Charge-Parity (CP) symmetry violation. We should emphasize that this is not intended to be a complete review of the SM, but rather a summary of the theoretical ingredients that will be relevant for the discussions in the following chapters. For a more comprehensive treatment of the topic, we refer to excellent textbooks such as [10–13]. We conclude with a brief discussion of some theoretical and experimental challenges that the SM fails to address, thereby motivating the quest for New Physics (NP) beyond the Standard Model (BSM).

1.1 Gauge sector

The SM is based on the gauge symmetry group

$$G_{\rm SM} = SU(3)_C \times SU(2)_L \times U(1)_Y \,, \tag{1.2}$$

where the $SU(3)_C$ color theory is known as Quantum Chromodynamics (QCD) and controls the strong force, while $SU(2)_L \times U(1)_Y$ corresponds to the unified electroweak (EW) theory [14–16].[1] Any local gauge theory requires the presence of one gauge field for each generator of the group—this means N^2-1 for $SU(N)$ and just one for $U(1)$ factors—in order to preserve the symmetry. Therefore, we have 8 gluon fields G_μ^A ($A=1,\dots,8$) for $SU(3)_C$, 3 gauge fields W_μ^a ($a=1,2,3$) for $SU(2)_L$, and 1 gauge field B_μ for $U(1)_Y$, transforming in the adjoint representation of the corresponding group factor, and invariant under the rest. Their kinetic terms are written as

$$\mathscr{L}_{\rm gauge} = -\frac{1}{4} G_A^{\mu\nu} G_{\mu\nu}^A - \frac{1}{4} W_a^{\mu\nu} W_{\mu\nu}^a - \frac{1}{4} B^{\mu\nu} B_{\mu\nu} \,, \tag{1.3}$$

where we have defined the field strengths tensors[2]

$$G_{\mu\nu}^A = \partial_\mu G_\nu^A - \partial_\nu G_\mu^A - g_s f^{ABC} G_\mu^B G_\nu^C \,, \tag{1.4}$$
$$W_{\mu\nu}^a = \partial_\mu W_\nu^a - \partial_\nu W_\mu^a - g \epsilon^{abc} W_\mu^b W_\nu^c \,, \tag{1.5}$$
$$B_{\mu\nu} = \partial_\mu B_\nu - \partial_\nu B_\mu \,, \tag{1.6}$$

being g_s and g the strong and weak gauge couplings, and f^{ABC} and ϵ^{abc} the structure constants of the $SU(3)_C$ and $SU(2)_L$ non-abelian groups. The latter define the algebra of the Hermitian generators as

$$[t^A, t^B] = i f^{ABC} t^C \,, \qquad [T^a, T^b] = i \epsilon^{abc} T^c \,, \tag{1.7}$$

with ϵ^{abc} fully antisymmetric ($\epsilon^{123} = +1$), and are responsible of the self-interactions among gauge bosons. In their fundamental representation, $t^A = \lambda^A/2$, where λ^A are the Gell-Mann matrices, while $T^a = \sigma^a/2$, with σ^a the Pauli matrices. The generator of the abelian factor $U(1)_Y$ is called weak hypercharge. Throughout this manuscript, we shall discuss very few aspects concerning the strong force, and rather we will essentially focus on the $SU(2)_L \times U(1)_Y$ electroweak theory.

So far, the theory is strictly massless, since the gauge symmetry prevents us from writing down mass terms for the gauge bosons. The short range of the weak interaction suggests, on the contrary, that the force carriers, *i.e.*, the $W^\pm$ and Z bosons, are very heavy. Aiming to generate their masses while preserving gauge invariance, the Higgs mechanism [18, 19] comes into play. The key feature is that the Lagrangian is explicitly gauge-invariant, but the vacuum, that is, the ground state of the theory, is not. This *spontaneous* symmetry breakdown is triggered by an additional scalar $SU(2)_L$ doublet, as we explain in the following section.

[1] Non-abelian gauge theories are often called Yang-Mills theories, and can be understood as a generalization of Quantum Electrodynamics (QED) based on the gauge group $U(1)_{\rm QED} \equiv U(1)_Q$, with Q the electric charge generator.

[2] At this point, we should stress that different sign conventions might be adopted regarding the definitions presented throughout this chapter. We refer the reader to [17] for a comprehensive collection of the different possibilities found in the literature. For concreteness, we choose $\eta = \eta' = \eta_Z = \eta_\theta = \eta_Y = \eta_e = +1$ in the notation of that reference.

1.2 Scalar sector

Before entering into the details of the standard Electroweak Symmetry Breaking, let us briefly introduce the theoretical framework behind the mass generation of gauge boson masses: the Goldstone Theorem and the Higgs Mechanism.

1.2.1 The Goldstone Theorem and the Higgs Mechanism

Goldstone Theorem — In any field theory satisfying locality, Lorentz invariance, and positive-definite norm, if an exact continuous symmetry of the Lagrangian is not a symmetry of the physical vacuum, the theory must contain massless spin-0 particles whose quantum numbers are those of the broken generators of the symmetry.

Let us consider a theory involving a set of n real scalar field components ϕ_i ($i = 1, \dots, n$), transforming as a representation of the symmetry group G in such a way that the scalar potential $\mathscr{V}(\phi_i)$ is invariant under G. At the infinitesimal level, we have

$$\phi_i \quad \xrightarrow{G} \quad \phi'_i = U(\vec{\alpha})_{ij}\phi_j \approx (1 + i\alpha^a R^a)_{ij}\phi_j \equiv \phi_i + \delta\phi_i\,, \qquad \text{with} \qquad \delta\phi_i = i\alpha^a (R^a)_{ij}\phi_j\,, \tag{1.8}$$

with $\vec{\alpha} = (\alpha_1, \dots, \alpha_n)$ a set of real parameters characterizing the elements in the group G, and R^a the generators of the group in the representation of the n real scalar fields. Invariance of the potential implies

$$\delta\mathscr{V}(\phi_i) = 0 \quad \Longleftrightarrow \quad \left(\frac{\partial\mathscr{V}}{\partial\phi_i}\right)\delta\phi_i = 0 \quad \Longleftrightarrow \quad i\alpha^a \left(\frac{\partial\mathscr{V}}{\partial\phi_i}\right)(R^a)_{ij}\phi_j = 0\,. \tag{1.9}$$

This condition should be fulfilled independently of the values of α^a, so that

$$\left(\frac{\partial\mathscr{V}}{\partial\phi_i}\right)(R^a)_{ij}\phi_j = 0\,, \tag{1.10}$$

for all generators R^a. Differentiating with respect to ϕ_k, we find

$$\left(\frac{\partial^2\mathscr{V}}{\partial\phi_k\partial\phi_i}\right)(R^a)_{ij}\phi_j + \left(\frac{\partial\mathscr{V}}{\partial\phi_i}\right)(R^a)_{ij}\delta_{jk} = 0\,. \tag{1.11}$$

We consider now a minimum of the potential to be at $(v_1, \dots, v_n)$, that constitutes the ground state of the theory. The quantum vacuum expectation value (vev) v_i, *i.e.*, the constant field configuration that minimizes the potential can be identified with the classical expectation of the field in the vacuum state $\langle 0|\phi_i|0\rangle \equiv \langle\phi_i\rangle$, meaning that $\langle\phi_i\rangle = v_i$. By definition, the potential is stationary at its minimum, so that

$$\left(\frac{\partial\mathscr{V}}{\partial\phi_i}\right)\Bigg|_{\phi_i = \langle\phi_i\rangle} = 0\,, \tag{1.12}$$

leaving us with

$$\left(\frac{\partial^2\mathscr{V}}{\partial\phi_k\partial\phi_i}\right)\Bigg|_{\phi_i = \langle\phi_i\rangle} (R^a)_{ij}\langle\phi_j\rangle = 0\,. \tag{1.13}$$

The second derivatives of the potential evaluated at its minimum give precisely the (squared) mass matrix of the scalars

$$(M^2)_{ki} = \left(\frac{\partial^2 \mathscr{V}}{\partial \phi_k \partial \phi_i} \right) \Bigg|_{\phi_i = \langle \phi_i \rangle} , \tag{1.14}$$

and thus we have

$$(M^2)_{ki} (R^a)_{ij} \langle \phi_j \rangle = 0 \,. \tag{1.15}$$

There are two possible solutions for the previous equation.

(i) The symmetry is respected by the vacuum, in the sense that

$$\delta \langle \phi_i \rangle = i\alpha^a (R^a)_{ij} \langle \phi_j \rangle = 0 \quad \Longrightarrow \quad (R^a)_{ij} \langle \phi_j \rangle = 0 \,, \tag{1.16}$$

and hence we say that the generator R^a remains *unbroken*. It can be shown that the unbroken generators form a closed commutative subalgebra, and generate a subgroup $H \subset G$ of transformations that do not change the vev at all—the subgroup H is the symmetry group of the vacuum. In this scenario, the symmetry G is *spontaneously* broken to H. The number of unbroken generators is denoted by $\dim H$.

(ii) The symmetry is not respected by the vacuum, *i.e.*,

$$\delta \langle \phi_i \rangle = i\alpha^a (R^a)_{ij} \langle \phi_j \rangle \neq 0 \quad \Longrightarrow \quad (R^a)_{ij} \langle \phi_j \rangle \neq 0 \,, \tag{1.17}$$

and thus we say that the generator R^a is *broken*. The latter generate the coset G/H (the remaining elements of G that are not in H), and take us from one vacuum to another one which is physically equivalent, *i.e.*, has the same energy (same value of the potential), yielding a continuous set of degenerate vacua. The number of broken generators is denoted by $\dim G/H$. The key point to be noticed is that, within this scenario, the mass matrix must contain a zero eigenvalue, one for each broken generator, associated to the eigenvector $R^a \langle \vec{\phi} \rangle$, with $\vec{\phi} = (\phi_1, \ldots, \phi_n)^T$. The corresponding massless scalar particle is known as Nambu-Goldstone boson (GB) [20, 21].

Therefore, there are $\dim G/H = \dim G - \dim H$ massless GBs, one for each broken generator of the continuous symmetry group—more precisely, for each *independent* generator that does not annihilate the vacuum.

Finally, it is important to distinguish between global or gauge (local) continuous symmetries. As we have just checked, a theory where a global continuous symmetry is spontaneously broken possesses massless GBs in their spectrum. Furthermore, Noether's theorem ensures the presence of conserved currents J^a_μ, satisfying $\partial^\mu J^a_\mu = 0$, and their corresponding conserved charges. However, this picture is changed when a continuous symmetry is gauged. In this case, the GBs disappear from the particle spectrum, while the gauge vector bosons associated to the independent broken generators become massive. This is the well-known Higgs Mechanism [18, 19].[3] In the unitary (or physical) gauge, it is said that the degrees of freedom (dof) represented by the *would-be* GBs (wbGBs) are *absorbed* or *eaten* by the gauge bosons in order to gain a mass. In other words, the gauge bosons acquire an additional longitudinal polarization. As a final comment, we should stress that spontaneously broken gauge theories are renormalizable [22], while explicitly broken theories are not.

[3]Likewise, full credit should be given to the contributions on this topic by Anderson, Brout, Englert, Ginzburg, Guralnik, Hagen, Kibble, and Landau, as well as Higgs himself.

1.2.2 Electroweak Symmetry Breaking

Lorentz invariance implies that only scalar fields can acquire a vev, which, in turn, must be constant over space-time by means of the Poincaré symmetry. It is also clear that we need at least three dof in the form of wbGBs to become the longitudinal polarizations of the weak force carriers $W^{\pm}$ and Z bosons. At the same time, the photon must remain massless after spontaneous symmetry breaking (SSB), so that $U(1)_Q$ of electromagnetism is preserved at low energies. With this in mind, as a *minimal* choice, one can consider a complex scalar field Φ, transforming as $\Phi \sim (\mathbf{1}, \mathbf{2}, 1/2)$ under G_{SM}—an $SU(2)_L$ doublet with hypercharge 1/2—, of the form

$$\Phi = \begin{pmatrix} \phi^+ \\ \phi^0 \end{pmatrix} , \tag{1.18}$$

whose vev triggers EWSB:

$$SU(3)_C \times SU(2)_L \times U(1)_Y \ \xrightarrow{\langle\Phi\rangle}\ SU(3)_C \times U(1)_Q \, , \tag{1.19}$$

being $Q = T^3 + Y$ the electric charge generator in QED. The most general Lagrangian involving the scalar doublet Φ is

$$\mathscr{L}_{\text{scalar}} = (D^\mu \Phi)^\dagger (D_\mu \Phi) - \mathscr{V}(\Phi) \, , \tag{1.20}$$

where the scalar potential $\mathscr{V}(\Phi)$ is written as

$$\mathscr{V}(\Phi) = \mu^2 (\Phi^\dagger \Phi) + \lambda (\Phi^\dagger \Phi)^2 \, , \tag{1.21}$$

with $\mu^2, \lambda \in \mathbb{R}$ due to hermiticity, and $\lambda > 0$ to ensure boundedness from below. The covariant derivative is given by

$$D_\mu \Phi = \left(\partial_\mu + i g W^a_\mu \frac{\sigma^a}{2} + i g' B_\mu \frac{1}{2} \right) , \tag{1.22}$$

in order to preserve gauge invariance. The appropriate EWSB in Eq. (1.19) is achieved when the scalar doublet develops a non-trivial vev at

$$\langle \Phi \rangle = \frac{v}{\sqrt{2}} \begin{pmatrix} 0 \\ 1 \end{pmatrix} , \tag{1.23}$$

with $v^2 = -\mu^2/\lambda$, as required by the stationarity condition, and $\mu^2 < 0$ for the vev to be a minimum. Without loss of generality, the vev of the single scalar doublet can be made *real* by means of gauge transformations. Within the SSB framework, all terms in the Lagrangian remain invariant under the gauge group, and it is only the vacuum that breaks the symmetry. One can then expand the scalar field around the selected vacuum as[4]

$$\Phi = \frac{1}{\sqrt{2}} \begin{pmatrix} \sqrt{2}\, G^+ \\ v + h + i G^0 \end{pmatrix} , \tag{1.24}$$

where h is the well-known physical Higgs boson, while G^0 and $G^{\pm}$ represent the unphysical wbGBs that become the longitudinal polarizations of the gauge bosons. In particular, the mass eigenstates are given by

$$W^{\pm}_\mu = \frac{W^1_\mu \mp i W^2_\mu}{\sqrt{2}} \, , \qquad \begin{pmatrix} W^3_\mu \\ B_\mu \end{pmatrix} = \begin{pmatrix} \cos\theta_W & \sin\theta_W \\ -\sin\theta_W & \cos\theta_W \end{pmatrix} \begin{pmatrix} Z_\mu \\ A_\mu \end{pmatrix} , \tag{1.25}$$

[4]The factors $\frac{1}{\sqrt{2}}$ account for the conversion from the canonical normalization of the complex scalar field Φ to that of the real scalar field h.

where $W_\mu^\pm$, Z_μ, and A_μ describe the $W^\pm$, Z, and photon fields, and θ_W is the weak mixing angle

$$\tan\theta_W = \frac{g'}{g}\,. \tag{1.26}$$

The masses of the gauge bosons are fixed by the EW scale v, and the gauge couplings g and g' as

$$M_W = \frac{gv}{2}\,, \qquad M_Z = \frac{v\sqrt{g^2+g'^2}}{2}\,, \qquad M_W = M_Z\cos\theta_W\,. \tag{1.27}$$

Finally, the electromagnetic coupling strength is related to g and g' by

$$e = g\sin\theta_W = g'\cos\theta_W\,, \tag{1.28}$$

being e the electric charge of the proton. It might be instructive to keep track of the number of dof before and after SSB. Before symmetry breaking, the Lagrangian contains three massless $SU(2)_L$ gauge bosons, and one massless $U(1)_Y$ gauge boson, *i.e.*, $4\times 2 = 8$ dof due to the two transverse polarizations of massless spin-1 fields. In addition, we have 4 real scalar fields present in the complex scalar doublet. This gives a total of 12 dof. After symmetry breaking, the three wbGBs become the longitudinal polarizations of the massive $W^\pm$ and Z bosons, while the photon remains massless. Thus, we have $3\times3+2 = 11$ dof in the gauge sector, plus the remaining Higgs particle in the scalar sector. This matches the initial 12 dof. Remarkably, the Higgs boson emerges as a remnant of the spontaneous symmetry breaking mechanism, due to the original scalar doublet containing too many dofs. The Higgs mass is fixed by

$$M_h^2 = 2\lambda v^2\,, \tag{1.29}$$

with an experimental value of $M_h = (125.20 \pm 0.11)$ GeV [23]. The existence of the Higgs boson constitutes a very clear prediction to test the validity of the SM. Its discovery in 2012 by the ATLAS [24] and CMS [25] experiments at CERN confirmed the impressive success of the theory in describing all known experimental data, at least up to energies $\mathcal{O}(v)$.

1.3 Fermion sector

As we have just seen, the gauge principle is extraordinarily predictive when it comes to vector boson interactions. On the other hand, the Higgs Mechanism invokes the presence of a scalar doublet in order to generate the masses of the force carriers in a gauge invariant way. Now, one may ask how fermions couple to gauge bosons. Unfortunately, there is no fundamental principle as a gauge symmetry that automatically determines the fermion sector of the theory. Instead, one includes the matter content by hand, and deduces the corresponding quantum numbers, that is, how the matter fields transform under the gauge group, guided by experiment. For instance, even before the $W^\pm$ and Z bosons were discovered, low-energy experiments suggested that $SU(2)_L$ gauge bosons only coupled to left-handed fermions, *i.e.*, we had a chiral theory that violated parity maximally.

All in all, in the SM spin-1/2 Weyl fermions transform as irreducible representations (irreps) of the gauge group. In particular, left-handed fermions behave as $SU(2)_L$ doublets, while right-handed fermions are $SU(2)_L$ singlets: the weak interactions are chiral, while the strong and electromagnetic interactions are vectorial and invariant under parity. Fermions are classified into quarks and leptons, depending on whether they feel the strong force or not, respectively. In addition, the fermion sector is *non-minimal* in the sense that quarks and leptons appear to be replicated in three generations or families only differing in their masses and mixings, as we will check later. Making manifest their $SU(2)_L$ transformation properties, we can write down

$$Q_L^0 = \left\{ \begin{pmatrix} u_L^0 \\ d_L^0 \end{pmatrix}, \begin{pmatrix} c_L^0 \\ s_L^0 \end{pmatrix}, \begin{pmatrix} t_L^0 \\ b_L^0 \end{pmatrix} \right\}, \qquad d_R^0 = \left\{ d_R^0 , s_R^0 , b_R^0 \right\}, \qquad u_R^0 = \left\{ u_R^0 , c_R^0 , t_R^0 \right\}, \tag{1.30}$$

$$\ell_L^0 = \left\{ \begin{pmatrix} \nu_{eL}^0 \\ e_L^0 \end{pmatrix}, \begin{pmatrix} \nu_{\mu L}^0 \\ \mu_L^0 \end{pmatrix}, \begin{pmatrix} \nu_{\tau L}^0 \\ \tau_L^0 \end{pmatrix} \right\}, \qquad e_R^0 = \left\{ e_R^0 , \mu_R^0 , \tau_R^0 \right\}, \tag{1.31}$$

whose quantum numbers under the Lorentz and gauge groups are summarized in Table 1.1. Each fermion component in the generation space is known as *flavor*: we have u (up), c (charm), t (top), d (down), s (strange), and b (bottom) quarks, as well as e (electron), μ (muon), τ (tau) leptons, and their corresponding neutrinos ν. Flavor indices running over different generations will often be omitted. The superscript "0" indicates that fermions are written in an arbitrary weak basis (WB), also dubbed as interaction or flavor basis, to be distinguished from the mass eigenstate basis, as we will see later. In addition, it is to be noticed that right-handed neutrino singlets are not included within the pure SM framework.

Field	$SO(1,3)$	$SU(3)_C$	$SU(2)_L$	$U(1)_Y$
Q_L^0	$\left(\frac{1}{2},0\right)$	3	2	1/6
u_R^0	$\left(0,\frac{1}{2}\right)$	3	1	2/3
d_R^0	$\left(0,\frac{1}{2}\right)$	3	1	−1/3
ℓ_L^0	$\left(\frac{1}{2},0\right)$	1	2	−1/2
e_R^0	$\left(0,\frac{1}{2}\right)$	1	1	−1

Table 1.1: Fermion quantum numbers under Lorentz and Standard Model gauge groups.

The fermion kinetic terms and their interactions with gauge bosons arise from

$$\mathscr{L}_{\text{fermion}} = i\overline{Q}_L^0\gamma^\mu D_\mu Q_L^0 + i\overline{u}_R^0\gamma^\mu D_\mu u_R^0 + i\overline{d}_R^0\gamma^\mu D_\mu d_R^0 + i\overline{\ell}_L^0\gamma^\mu D_\mu \ell_L^0 + i\overline{e}_R^0\gamma^\mu D_\mu e_R^0 , \tag{1.32}$$

with the covariant derivatives, ensuring gauge invariance, given by

$$D_\mu Q_L^0 = \left[\partial_\mu + ig_s G_\mu^A \frac{\lambda^A}{2} + igW_\mu^a \frac{\sigma^a}{2} + ig' B_\mu \frac{1}{6}\right] Q_L^0 , \tag{1.33}$$

$$D_\mu u_R^0 = \left[\partial_\mu + ig_s G_\mu^A \frac{\lambda^A}{2} + ig' B_\mu \frac{2}{3}\right] u_R^0 , \tag{1.34}$$

$$D_\mu d_R^0 = \left[\partial_\mu + ig_s G_\mu^A \frac{\lambda^A}{2} + ig' B_\mu \left(-\frac{1}{3}\right)\right] d_R^0 , \tag{1.35}$$

$$D_\mu \ell_L^0 = \left[\partial_\mu + igW_\mu^a \frac{\sigma^a}{2} + ig' B_\mu \left(-\frac{1}{2}\right)\right] \ell_L^0 , \tag{1.36}$$

$$D_\mu e_R^0 = \left[\partial_\mu + ig' B_\mu \left(-1\right)\right] e_R^0 . \tag{1.37}$$

Once the fermion quantum numbers are specified, their interactions with gauge bosons are completely determined by the gauge principle in terms of the couplings g_s, g, and g'. For the purposes of upcoming sections, let us specify the form of the interactions between fermions and electroweak gauge bosons in the interaction basis:

$$-\mathscr{L}_W = \frac{g}{\sqrt{2}}\overline{u}_L^0\gamma^\mu d_L^0 W_\mu^+ + \frac{g}{\sqrt{2}}\overline{\nu}_L^0\gamma^\mu e_L^0 W_\mu^+ + \text{H.c.}\,, \tag{1.38}$$

$$-\mathscr{L}_Z = \frac{g}{c_W}\left[\frac{1}{2}\overline{u}_L^0\gamma^\mu u_L^0 - \frac{1}{2}\overline{d}_L^0\gamma^\mu d_L^0 + \frac{1}{2}\overline{\nu}_L^0\gamma^\mu \nu_L^0 - \frac{1}{2}\overline{e}_L^0\gamma^\mu e_L^0 - s_W^2 J_Q^\mu\right] Z_\mu\,, \tag{1.39}$$

$$-\mathscr{L}_A = e J_Q^\mu A_\mu\,, \tag{1.40}$$

where the electromagnetic current J_Q^μ reads

$$J_Q^\mu = \frac{2}{3}\left(\overline{u}_L^0\gamma^\mu u_L^0 + \overline{u}_R^0\gamma^\mu u_R^0\right) - \frac{1}{3}\left(\overline{d}_L^0\gamma^\mu d_L^0 + \overline{d}_R^0\gamma^\mu d_R^0\right) - \left(\overline{e}_L^0\gamma^\mu e_L^0 + \overline{e}_R^0\gamma^\mu e_R^0\right)\,. \tag{1.41}$$

Note that, in this basis, the gauge interactions with fermions are diagonal in flavor space, meaning that they do not mix fermions that belong to different generations.

So far, all quarks and leptons are massless, since the usual Dirac mass term that couples left-handed and right-handed fermions would spoil gauge invariance. Similarly to what happens in the gauge sector, the vev of the scalar doublet Φ can also generate their masses after SSB. To this aim, one is forced to introduce scalar-fermion Yukawa couplings that provide the required chirality-flipping interaction. The fact that u_L^0 and d_L^0 transform collectively in the fundamental representation of $SU(2)_L$ will lead to an interesting flavor phenomenology that we begin to address in the next section.

1.4 Yukawa sector

Aiming for generality, let us promote the subsequent discussion for n_g generations of fermions. This is almost a straightforward step that might prove useful in order to understand some of the key features of the three-generation SM, *e.g.*, the emergence of CP violation.

The most general renormalizable Lagrangian containing the interactions between the fermion fields and the scalar doublet is of the form

$$-\mathscr{L}_Y = \overline{Q}_L^0 Y_u u_R^0 \widetilde{\Phi} + \overline{Q}_L^0 Y_d d_R^0 \Phi + \overline{\ell}_L^0 Y_e e_R^0 \Phi + \text{H.c.}\,, \tag{1.42}$$

where we have defined $\widetilde{\Phi} \equiv \epsilon\Phi^* = i\sigma^2\Phi^*$, transforming as $\widetilde{\Phi} \sim (\mathbf{1}, \mathbf{2}, -1/2)$ under the SM gauge group. The Yukawa coupling matrices are general complex $n_g \times n_g$ matrices, and thus they introduce a large number of free parameters in the model. Nevertheless, as we shall see, not all of them happen to be physical observable quantities, that is, invariant under field redefinitions.[5] On that regard, we must stress that the other pieces of the SM Lagrangian in Eqs. (1.3), (1.20) and (1.32) exhibit a large *global*

[5] In general, field redefinitions should fulfill the following properties: (i) they commute with the Lorentz and gauge groups, (ii) preserve the renormalizability of the theory, and (iii) leave invariant the canonical normalization of the kinetic terms. These conditions constrain the type of transformations one can actually perform, since condition (i) implies that they can only mix fermions with the same quantum numbers, condition (ii) requires them to be linear, and condition (iii) to be unitary. The resulting theory after such a transformation of the fields is completely equivalent to the original one. Physically meaningful observable quantities must therefore be invariant under field redefinitions.

flavor symmetry defined by

$$G_f = U(n_g)_Q \times U(n_g)_u \times U(n_g)_d \times U(n_g)_\ell \times U(n_g)_e \equiv U(n_g)^5 \,, \tag{1.43}$$

where each factor $U(n_g)_f = SU(n_g)_f \times U(1)_f$ $(f = Q, u, d, \ell, e)$ consists of independent unitary transformations in flavor space of the different Weyl fermions in Eqs. (1.30) and (1.31), and are usually known as *weak basis transformations* (WBT). The corresponding transformation properties of the different fields are collected in Table 1.2. This global flavor symmetry is explicitly broken by the Yukawa couplings Y_u, Y_d, and Y_e, and hence one can use the freedom in the previous transformations to remove unphysical parameters—more precisely, one can only use the subgroup of transformations that is actually broken by the Yukawa couplings. Since the analyses of the quark and lepton sectors result to be different due to the absence of right-handed neutrinos, let us treat them separately in what follows.

Field	$SU(n_g)_Q$	$SU(n_g)_u$	$SU(n_g)_d$	$SU(n_g)_\ell$	$SU(n_g)_e$
Q_L^0	$\square$	1	1	1	1
u_R^0	1	$\square$	1	1	1
d_R^0	1	1	$\square$	1	1
ℓ_L^0	1	1	1	$\square$	1
e_R^0	1	1	1	1	$\square$

Table 1.2: Fermion quantum numbers under the non-abelian part of the flavor symmetry group G_f. The boxes denote the Young diagrams of the fundamental representation of the corresponding group factor.

1.4.1 Quark sector

The global flavor symmetry group in the quark sector is broken by the Yukawa couplings Y_u and Y_d as

$$G_q \equiv U(n_g)_Q \times U(n_g)_u \times U(n_g)_d \xrightarrow{Y_u,\,Y_d} H_q \equiv U(1)_{\mathrm{BN}} \,, \tag{1.44}$$

where $H_q \equiv U(1)_{\mathrm{BN}}$ corresponds to the (vectorial) common rephasing of all quark fields, that can be identified as the total baryon number (BN). Taking this into account, one can readily compute the number of real physical parameters, both moduli and phases, that are present in the Yukawa coupling matrices as

$$N_{\mathrm{physical}} = N_{\mathrm{param}} - \dim G_q/H_q = N_{\mathrm{param}} - \big(\dim G_q - \dim H_q\big) \,. \tag{1.45}$$

This counting is summarized in Table 1.3 for the quark sector. This scenario corresponds to the maximal breaking of the flavor symmetry when the Yukawa matrices are completely generic. Indeed, one could expect larger unbroken subgroups if the Yukawa matrices had a symmetric structure or if some of their entries were zero. On the other hand, we should mention that the counting of dof is often carried out after SSB and diagonalization of the quark mass matrices, in the way we shall explain next. In any case, this alternative method might prove useful in other scenarios involving a more complicated diagonalization of the mass matrices [26], *e.g.*, in the lepton sector with right-handed Majorana neutrino fields.

In order to obtain the masses of up-type and down-type quarks, the Yukawa matrices have to be diagonalized. On that regard, any complex matrix can always be diagonalized by means of two different unitary transformations acting on the left and on the right—this is the unitary bidiagonalization pro-

	$N_{\rm param}$	$\dim G_q$	$\dim H_q$	$N_{\rm physical}$
Moduli	$2n_g^2$	$\frac{3n_g(n_g-1)}{2}$	0	$2n_g + \frac{n_g(n_g-1)}{2}$
Phases	$2n_g^2$	$\frac{3n_g(n_g+1)}{2}$	1	$\frac{(n_g-1)(n_g-2)}{2}$
Total	$4n_g^2$	$3n_g^2$	1	n_g^2+1

Table 1.3: Physical parameters in the quark Yukawa sector of the SM.

cedure detailed in App. B. In the quark sector, the unitary rotations provided by G_q are not enough to bidiagonalize simultaneously both Y_u and Y_d without observable consequences in the gauge sector, due to u_L^0 and d_L^0 transforming collectively in the same $SU(2)_L$ doublet representation. Therefore, once spontaneous symmetry breaking takes place and the Higgs field develops a vev, we should rotate the quark fields to the mass basis through unitary transformations of the form

$$u_L^0 = U_{u_L} u_L \,, \qquad u_R^0 = U_{u_R} u_R \,, \qquad d_L^0 = U_{d_L} d_L \,, \qquad d_R^0 = U_{d_R} d_R \,, \tag{1.46}$$

in such a way that the mass matrices, defined by $M_f^0 = \frac{v}{\sqrt{2}} Y_f$, get bidiagonalized:

$$U_{u_L}^\dagger M_u^0 U_{u_R} = M_u = \mathrm{diag}(m_u, m_c, m_t, \dots)\,, \qquad U_{d_L}^\dagger M_d^0 U_{d_R} = M_d = \mathrm{diag}(m_d, m_s, m_b, \dots)\,, \tag{1.47}$$

with m_i the masses of the physical quarks. As commented before, the fact that the transformations in Eq. (1.46) do not correspond to a WBT has observable consequences in other sectors, namely, the charged currents Lagrangian in Eq. (1.38). The mismatch between the unitary transformation of the up-type and down-type left-handed fields leads to

$$-\mathscr{L}_W^{\rm quark} = \frac{g}{\sqrt{2}} \overline{u}_L \gamma^\mu V d_L W_\mu^\dagger + \text{H.c.}\,, \tag{1.48}$$

where $V \equiv U_{u_L}^\dagger U_{d_L}$ is an $n_g \times n_g$ unitary matrix, $VV^\dagger = V^\dagger V = 1_{n_g\times n_g}$. In the SM with $n_g = 3$ generations, this is the well-known Cabibbo-Kobayashi-Maskawa (CKM) matrix [27,28], and its elements are typically labeled as

$$V = \begin{pmatrix} V_{ud} & V_{us} & V_{ub} \\ V_{cd} & V_{cs} & V_{cb} \\ V_{td} & V_{ts} & V_{tb} \end{pmatrix} . \tag{1.49}$$

The CKM matrix controls the pattern of mixings between quarks of different generations in the charged currents interactions, and constitutes the only source of flavor-changing transitions in the SM. Experimentally, the CKM matrix is very close to the identity, meaning that flavor-changing processes are indeed very suppressed by small off-diagonal elements. On the other hand, one can readily check that the neutral current interactions mediated by the Z boson and the photon (as well as gluons) in Eqs. (1.39) and (1.40) remain unchanged under the transformations in Eq. (1.46). Therefore, there are not Flavor-Changing Neutral Currents (FCNC) at tree-level in the SM, and they can only arise at the loop level through W boson exchange—thus involving several powers of the off-diagonal mixing elements. As we can see, the strong suppression of FCNC is a non-trivial phenomenon. In fact, this lead Glashow, Iliopoulos, and Maiani (GIM) to predict the existence of the charm c quark allowing to have two complete generations.[6] Since then, the double suppression due to the unitarity of the quark mixing matrix and the smallness of

[6] By that time only u, d and s quarks were known.

its off-diagonal couplings is known as GIM mechanism [29].

However, not all the parameters contained in this unitary matrix are physical, as we anticipated before. Let us count the number of real dof, this time after SSB. The bidiagonalization of the mass matrices in Eq. (1.47) leaves a residual $[U(1)_{u'} \times U(1)_{d'}]^{n_g}$, where $U(1)_{f'}$ denotes the vectorial component of $U(1)_{f'_L} \times U(1)_{f'_R}$ flavor symmetry.[7] We can use this remaining freedom in order to remove unphysical parameters from V, except for a global common rephasing of all quark fields that leaves V invariant, that is, $U(1)_{\text{BN}}$. Therefore, the number of physical parameters in CKM is:

$$N^{\text{CKM}}_{\text{moduli}} = \frac{n_g(n_g-1)}{2}\,, \qquad N^{\text{CKM}}_{\text{phases}} = \frac{n_g(n_g+1)}{2} - (2n_g - 1) = \frac{(n_g-1)(n_g-2)}{2}\,, \tag{1.50}$$

giving a total of $N^{\text{CKM}}_{\text{total}} = (n_g-1)^2$ real dof. Taking into account that we have $2n_g$ physical quark masses, the results quoted here are in agreement with those presented in Table 1.3. The fact that there are irremovable phases in the CKM matrix for $n_g > 2$ implies that the Lagrangian is not invariant under CP transformations, as we will discuss in Sec. 1.5. Nevertheless, this picture might change if there were mass degeneracies in the up or down sectors. Let us assume, for instance, that there are n_u degenerate up-type quarks and n_d degenerate down-type quarks, with $1 < n_u, n_d \leq n_g$. In that case, the residual freedom to redefine the quark fields is larger, namely, $[U(n_u) \times U(1)^{n_g-n_u}_{u'}] \times [U(n_d) \times U(1)^{n_g-n_d}_{d'}]$, except for a diagonal common rephasing of all quark fields $U(1)_{\text{BN}}$. This freedom can be used to remove additional phases from the CKM matrix, namely:

$$N^{\text{CKM-deg}}_{\text{moduli}} = \frac{n_g(n_g-1)}{2} - \frac{n_u(n_u-1)}{2} - \frac{n_d(n_d-1)}{2}\,, \tag{1.51}$$

$$N^{\text{CKM-deg}}_{\text{phases}} = \frac{(n_g-1)(n_g-2)}{2} - \frac{n_u(n_u-1)}{2} - \frac{n_d(n_d-1)}{2}\,, \tag{1.52}$$

leaving a total of $N^{\text{CKM-deg}}_{\text{total}} = (n-1)^2 - n_u(n_u-1) - n_d(n_d-1)$ real dof.

For concreteness, let us draw the final picture within the SM. For $n_g = 3$ generations, the 3×3 unitary CKM matrix contains 4 real dof that can be well interpreted as 3 Euler angles and 1 complex phase. Remarkably, this irremovable phase is the source of all (weak) CP-violating effects in the SM, as we will explain in Sec. 1.5. Together with the 6 physical quark masses, we are left with a total of 10 dof arising from the quark Yukawa interactions. In the following, we proceed to discuss the fundamental properties of the CKM matrix, as well as some of the relevant parametrizations that can be found in the literature.

Parametrizations of the 3×3 CKM matrix

There are multiple parametrizations of the CKM matrix that accommodate the constraints imposed by 3×3 unitarity, namely, that its rows and columns must be orthonormal vectors. Typically, all of them are chosen in such a way that the elements V_{ud} and V_{us} are real, motivated by neutral kaon physics studies. Here we present the Chau-Keung parametrization [30], adopted by the Particle Data Group (PDG) [23], as well as the famous Wolfenstein parametrization [31]. The latter is specially useful for many purposes since it incorporates our knowledge from experimental data.

[7] We add a prime in f' to distinguish this set of transformations from the $U(1)_f$ factors in the flavor symmetry group of Eq. (1.43).

Chau-Keung parametrization—. The fact that the CKM matrix contains four real dof, three moduli and one phase, suggests its interpretation in terms of three Euler angles θ_{12}, θ_{13}, θ_{23}, and one complex phase δ. The latter has to be introduced in such a way that it cannot be removed by means of a rephasing of the quark fields. Therefore, we can write down three consecutive rotations along the three spatial directions as

$$\begin{aligned} V(\theta_{12},\theta_{13},\theta_{23},\delta) &= \begin{pmatrix} c_{12} & s_{12} & 0 \\ -s_{12} & c_{12} & 0 \\ 0 & 0 & 1 \end{pmatrix} \begin{pmatrix} c_{13} & 0 & s_{13}e^{-i\delta} \\ 0 & 1 & 0 \\ -s_{13}e^{i\delta} & 0 & c_{13} \end{pmatrix} \begin{pmatrix} 1 & 0 & 0 \\ 0 & c_{23} & s_{23} \\ 0 & -s_{23} & c_{23} \end{pmatrix} \\ &= \begin{pmatrix} c_{12}c_{13} & s_{12}c_{13} & s_{13}e^{-i\delta} \\ -s_{12}c_{23} - c_{12}s_{23}s_{13}e^{i\delta} & c_{12}c_{23} - s_{12}s_{23}s_{13}e^{i\delta} & s_{23}c_{13} \\ s_{12}s_{23} - c_{12}c_{23}s_{13}e^{i\delta} & -s_{23}c_{12} - s_{12}c_{23}s_{13}e^{i\delta} & c_{23}c_{13} \end{pmatrix}, \end{aligned} \tag{1.53}$$

where $c_{ij} \equiv \cos\theta_{ij}$ and $s_{ij} \equiv \sin\theta_{ij}$. The angle θ_{12} is also known as the Cabibbo angle for historical reasons. Without loss of generality, one can restrict the rotation angles to the first quadrant, $\theta_{ij} \in [0, \pi/2]$, as long as the complex phase is allowed to be free, $\delta \in [0, 2\pi)$.[8]

Wolfenstein parametrization—. An alternative parametrization of the CKM matrix can be constructed in light of experimental data, in particular: (i) $|V_{us}| \sim \lambda \ll 1$, (ii) $|V_{cb}| \sim |V_{us}|^2$, and (iii) the b quark dominantly decays to c quarks, with $|V_{ub}|/|V_{cb}| \sim \lambda/2$. Taking λ as an expansion parameter and imposing unitarity constraints up to a certain order in λ, one can write down

$$V(\lambda, A, \rho, \eta) = \begin{pmatrix} 1-\frac{\lambda^2}{2} & \lambda & A\lambda^3(\rho - i\eta) \\ -\lambda & 1-\frac{\lambda^2}{2} & A\lambda^2 \\ A\lambda^3(1-\rho-i\eta) & -A\lambda^2 & 1 \end{pmatrix} + \mathcal{O}(\lambda^4)\,. \tag{1.54}$$

Besides $\lambda \approx 0.23$, three additional parameters are introduced: $A \sim 1$ due to the constraint imposed by (ii), and ρ and η which are roughly smaller than $1/2$ as required by (iii). Although we will comment on that later on, it is easy to see that CP-violating effects only enter at $\mathcal{O}(\lambda^3)$. All in all, in the Wolfenstein parametrization the CKM matrix elements are expanded as a power series in λ, and 3×3 unitarity only holds approximately.

Nevertheless, in some phenomenological studies it might be necessary to include higher order terms in the previous expansion to obtain a better level of accuracy. Therefore, it is convenient to derive an exact version of the Wolfenstein parametrization that can be expanded at will. To this aim, one can start from the Chau-Keung parametrization, where unitarity holds exactly, and define the set of parameters $\{\lambda, A, \rho, \eta\}$ in terms of $\{\theta_{12}, \theta_{13}, \theta_{23}, \delta\}$ [32] as

$$s_{12} \equiv \lambda\,, \qquad s_{23} \equiv A\lambda^2\,, \qquad s_{13}e^{-i\delta} \equiv A\lambda^3(\rho - i\eta)\,. \tag{1.55}$$

[8] For instance, let us suppose that one of the angles, say θ_{12}, is in the second quadrant. We can always relate it to an angle θ'_{12} in the first quadrant taking into account that $\cos\theta_{12} = -\cos\theta'_{12}$ and $\sin\theta_{12} = \sin\theta'_{12}$. Then, shifting the value of delta as $\delta = \delta' + \pi$, we change $e^{i\delta} = -e^{i\delta'}$. A final rephasing of u and s quark fields as $V(\theta'_{12}, \theta_{13}, \theta_{23}, \delta') \to \mathrm{diag}(-1,1,1)V(\theta'_{12}, \theta_{13}, \theta_{23}, \delta')\mathrm{diag}(1,-1,1)$ brings V to the form of Eq. (1.53). Hence, we can just drop the primes and assume that all rotation angles lie on the first quadrant.

Fundamental properties of the CKM matrix

Rephasing-invariance—. As we have explained before, after diagonalization of the mass matrices, one still has the freedom to rephase the quark fields as

$$u'_{L_i} = e^{i\alpha_i^u} u_{L_i} \,, \qquad u'_{R_i} = e^{i\alpha_i^u} u_{R_i} \,, \qquad d'_{L_i} = e^{i\alpha_i^d} d_{L_i} \,, \qquad d'_{R_i} = e^{i\alpha_i^d} d_{R_i} \,, \tag{1.56}$$

leaving invariant all terms in the Lagrangian, including the mass terms, except the charged currents. Under these field redefinitions, the CKM matrix changes as

$$V'_{ij} = e^{i(\alpha_j^d - \alpha_i^u)} V_{ij} \,. \tag{1.57}$$

Indeed, we have previously used this rephasing freedom to eliminate $2n_g - 1$ unphysical phases from V (recall that the baryon number transformation of all quark fields leaves V invariant). However, it is clear that physical observables in the CKM mixing must be invariant under such a rephasing. Therefore, one may ask which rephasing-invariant quantities can be built out of the CKM elements. The simplest ones are, of course, the (squared) moduli $|V_{ij}|^2$. The next simplest invariants one can define are quartets of CKM elements of the form

$$Q_{ijkl} \equiv V_{ij} V_{kl} V_{il}^* V_{jk}^* \,, \tag{1.58}$$

with $i \neq k$ and $j \neq l$. Notice that i, k run over the different flavors in the up-type sector, and j, l run in the down-type sector. It is straightforward to check that $Q_{ijkl} = Q_{klij} = Q_{kjil}^* = Q_{ilkj}^*$. In practical terms, the rephasing-invariant quartets are constructed by eliminating $n_g - 2$ out of the n_g rows and columns, and then multiplying one of the diagonals by the complex conjugate of the other one. Therefore, in general we can construct $\binom{n_g}{n_g-2}^2 = \binom{n_g}{2}^2 = \frac{n_g^2(n_g-1)^2}{4}$ quartets from an $n_g \times n_g$ mixing matrix.

Let us consider the SM case with $n_g = 3$ generations. In this particular case, it can be shown that the imaginary parts of all nine quartets are equal up to a sign, due to the orthogonality relations between the rows and columns. Then, it is convenient to define the *Jarlskog invariant* [33] as

$$J \equiv \mathrm{Im}\, Q_{uscb} = \mathrm{Im}\left(V_{us} V_{cb} V_{ub}^* V_{cs}^*\right) \,, \tag{1.59}$$

such that the imaginary parts of the remaining quartets are all equal to J up to a sign. This condition can be written more generally as

$$\mathrm{Im}\, Q_{ijkl} = \mathrm{Im}\left(V_{ij} V_{kl} V_{il}^* V_{kj}^*\right) = J \sum_{m,n} \epsilon_{ikm} \epsilon_{jln} \,, \tag{1.60}$$

for any i, j, k, l. On the other hand, one can compute J within the two parametrizations presented in Eqs. (1.53) and (1.54), yielding

$$\text{Chau-Keung/PDG:} \qquad J = c_{12} s_{12} c_{13}^2 s_{13} c_{23} s_{23} \sin\delta \,, \tag{1.61}$$

$$\text{Wolfenstein:} \qquad J \approx A^2 \lambda^6 \eta \left(1 - \frac{\lambda^2}{2}\right) \,. \tag{1.62}$$

In Sec. 1.5, we show that the Jarlskog invariant is of paramount importance in the study of weak CP violation in the SM. Indeed, $J = 0$ is a necessary and sufficient condition for CP conservation in the SM.

Unitarity—. The CKM mixing matrix is unitary, meaning that its rows and columns can be viewed as orthonormal vectors that satisfy

$$\sum_k |V_{ik}|^2 = \sum_k |V_{ki}|^2 = 1\,, \qquad \forall\, i\,, \tag{1.63}$$

$$\sum_k V_{ik}V_{jk}^* = \sum_k V_{ki}^* V_{kj} = 0\,, \qquad i \neq j\,. \tag{1.64}$$

In the SM case, 3×3 unitarity leads to six orthogonality relations given by

$$\underbrace{V_{ud}V_{cd}^*}_{\mathcal{O}(\lambda)} + \underbrace{V_{us}V_{cs}^*}_{\mathcal{O}(\lambda)} + \underbrace{V_{ub}V_{cb}^*}_{\mathcal{O}(\lambda^5)} = 0\,, \qquad \underbrace{V_{ud}V_{us}^*}_{\mathcal{O}(\lambda)} + \underbrace{V_{cd}V_{cs}^*}_{\mathcal{O}(\lambda)} + \underbrace{V_{td}V_{ts}^*}_{\mathcal{O}(\lambda^5)} = 0\,, \tag{1.65}$$

$$\underbrace{V_{cd}V_{td}^*}_{\mathcal{O}(\lambda^4)} + \underbrace{V_{cs}V_{ts}^*}_{\mathcal{O}(\lambda^2)} + \underbrace{V_{cb}V_{tb}^*}_{\mathcal{O}(\lambda^2)} = 0\,, \qquad \underbrace{V_{us}V_{ub}^*}_{\mathcal{O}(\lambda^4)} + \underbrace{V_{cs}V_{cb}^*}_{\mathcal{O}(\lambda^2)} + \underbrace{V_{ts}V_{tb}^*}_{\mathcal{O}(\lambda^2)} = 0\,, \tag{1.66}$$

$$\underbrace{V_{ud}V_{td}^*}_{\mathcal{O}(\lambda^3)} + \underbrace{V_{us}V_{ts}^*}_{\mathcal{O}(\lambda^3)} + \underbrace{V_{ub}V_{tb}^*}_{\mathcal{O}(\lambda^3)} = 0\,, \qquad \underbrace{V_{ud}V_{ub}^*}_{\mathcal{O}(\lambda^3)} + \underbrace{V_{cd}V_{cb}^*}_{\mathcal{O}(\lambda^3)} + \underbrace{V_{td}V_{tb}^*}_{\mathcal{O}(\lambda^3)} = 0\,. \tag{1.67}$$

They all correspond to three complex numbers that sum up to zero, and thus can be represented as a triangle in the complex plane. As we can see, they have very different shapes: in Eqs. (1.65) and (1.66) one of the sides is much smaller than the other two and thus the triangles are "squashed", while in Eq. (1.67) all sides have similar length. In particular, the triangles on the right-hand side of Eqs. (1.66) and (1.67) play a relevant role in the study of $B_s - \bar{B}_s$ and $B_d - \bar{B}_d$ neutral meson systems, respectively. The last one in Eq. (1.67) is usually called *the unitarity triangle*. Dividing all its sides by $V_{cd}V_{cb}^*$ yields

$$\frac{V_{ud}V_{ub}^*}{V_{cd}V_{cb}^*} + 1 + \frac{V_{td}V_{tb}^*}{V_{cd}V_{cb}^*} = 0\,. \tag{1.68}$$

In order to represent it in the complex plane, one usually defines the coordinates $(\bar{\rho}, \bar{\eta})$ as

$$\bar{\rho} + i\bar{\eta} \equiv -\frac{V_{ud}V_{ub}^*}{V_{cd}V_{cb}^*} = -\frac{\rho + i\eta}{A^2\lambda^4(\rho + i\eta) + \sqrt{\frac{1-A^2\lambda^4}{1-\lambda^2}}}\,, \tag{1.69}$$

where in the last step we have expressed them in terms of the parameters $\{\lambda, A, \rho, \eta\}$ in the exact version of the Wolfenstein parametrization. Then, it is easy to check that $\frac{V_{td}V_{tb}^*}{V_{cd}V_{cb}^*} = -(1 - \bar{\rho} - i\bar{\eta})$. An sketch of the unitarity triangle is illustrated in Fig. 1.1a. Its internal angles are defined as[9]

$$\alpha \equiv \arg\left(-\frac{V_{td}V_{tb}^*}{V_{ud}V_{ub}^*}\right)\,, \qquad \beta \equiv \arg\left(-\frac{V_{cd}V_{cb}^*}{V_{td}V_{tb}^*}\right)\,, \qquad \gamma \equiv \arg\left(-\frac{V_{ud}V_{ub}^*}{V_{cd}V_{cb}^*}\right)\,, \tag{1.70}$$

and satisfy, by construction,

$$\alpha + \beta + \gamma = \arg(-1) = \pi\,. \tag{1.71}$$

We should stress that the previous relation between the angles α, β, and γ is fulfilled by definition, even in the presence of 3×3 unitarity deviations, and thus cannot be interpreted as a test of 3×3 CKM unitarity. In addition, since all the sides of the unitary triangle are of the same order, all internal angles are of $\mathcal{O}(1)$.

[9]The Belle collaboration uses a different notation for the angles of the unitarity triangle, namely, $\phi_1 \equiv \beta$, $\phi_2 \equiv \alpha$, and $\phi_3 \equiv \gamma$.

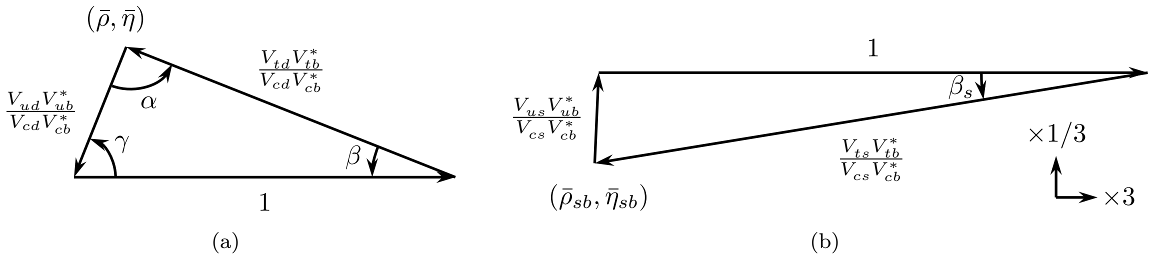

Figure 1.1: Unitarity triangles in the SM: (a) bd sector, (b) bs sector. The x and y directions in the bs unitarity triangle have been rescaled for the purposes of illustration.

Furthermore, it is straightforward to check that the area of the unitarity triangle can be computed as $|\mathrm{Im}\, Q_{udcb}|/2 = |J|/2$, which gives us a geometrical interpretation of the Jarlskog invariant. One can proceed similarly with other triangles, finding that all of them have the same area despite being very different in shape. Indeed, this stems from the fact that the imaginary parts of all quartets are equal to J up to sign.

One may also notice that a rephasing of the quark fields corresponds to a global rotation of the orthogonality relations. In terms of the unitarity triangle, this is equivalent to rotating it as a whole in the complex plane without changing the lengths of its sides or its internal angles, which are rephasing-invariant quantities and thus measurable at experiments. More precisely, the length of the sides encodes the amount of flavor mixing (moduli of CKM elements), while the internal angles are sensitive to CP violation.

In a similar fashion, one can construct the unitarity triangle defined by the right-hand side of Eq. (1.66). Dividing by $V_{cs}V_{cb}^*$, we are left with

$$\frac{V_{us}V_{ub}^*}{V_{cs}V_{cb}^*} + 1 + \frac{V_{ts}V_{tb}^*}{V_{cs}V_{cb}^*} = 0\,. \tag{1.72}$$

In this case, we define the coordinates $(\bar\rho_{sb},\bar\eta_{sb})$ in the complex plane as

$$\bar\rho_{sb} + i\bar\eta_{sb} \equiv -\frac{V_{us}V_{ub}^*}{V_{cs}V_{cb}^*} = -\frac{\lambda^2(\rho+i\eta)}{\sqrt{1-\lambda^2}\sqrt{1-A^2\lambda^4}-A^2\lambda^6(\rho+i\eta)}\,, \tag{1.73}$$

where in the last step we have related them with the parameters $\{\lambda, A, \rho, \eta\}$ in the exact version of the Wolfenstein parametrization. It is easy to check that $\frac{V_{ts}V_{tb}^*}{V_{cs}V_{cb}^*} = -(1-\bar\rho_{sb}-i\bar\eta_{sb})$. This second unitarity triangle is depicted in Fig. 1.1b. Finally, the internal angle β_s is defined as

$$\beta_s \equiv \arg\left(-\frac{V_{ts}V_{tb}^*}{V_{cs}V_{cb}^*}\right)\,. \tag{1.74}$$

Contrary to the previous case, this triangle is almost flat, and the angle β_s is of $\mathcal{O}(\lambda^2)$.

In Fig. 1.2, we illustrate the current status of the CKM unitarity triangle fit, both in the $(\bar\rho,\bar\eta)$ plane and in the $(\bar\rho_{sb},\bar\eta_{sb})$ plane. Overconstraining the elements of the CKM matrix constitutes an important self-consistency check of 3×3 unitarity, which is a neat prediction of the SM. Up to date, excellent agreement with all experimental data on flavor-changing transitions has been found, although some anomalies might still be present.

One final comment is in order. Taking into account the freedom to rephase the quark fields, one can

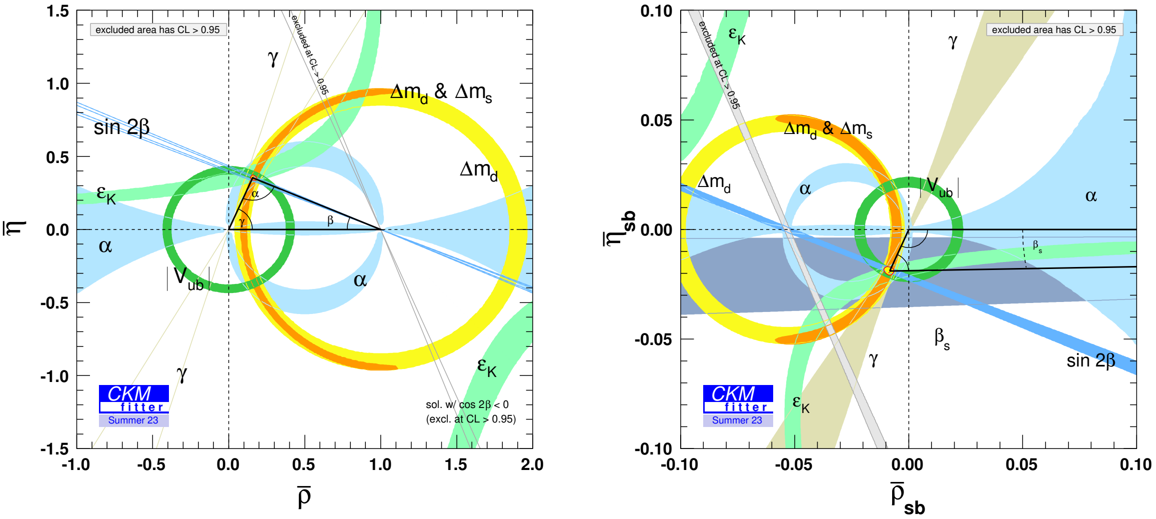

(a) (b)

Figure 1.2: Unitarity triangle fit by the CKMfitter collaboration [34]: (a) bd unitarity triangle in the $(\bar{\rho}, \bar{\eta})$ plane, (b) bs unitarity triangle in the $(\bar{\rho}_{sb}, \bar{\eta}_{sb})$ plane. The colored regions correspond to different experimental constraints, namely: mass differences in B_d and B_s neutral meson systems, $|V_{ub}|$ determination from charmless semileptonic B meson decays, CP violation in neutral kaon mixing ε_K, mixing-induced CP violation $\sin 2\beta$ in the B_d system, mixing-induced CP violation $\sin 2\beta_s$ in the B_s system, and measurements of α and γ from B meson decays.

choose a parametrization of the CKM matrix such that [35]

$$\arg V = \begin{pmatrix} 0 & \beta_K & -\gamma \\ \pi & 0 & 0 \\ -\beta & \pi + \beta_s & 0 \end{pmatrix}, \tag{1.75}$$

where we have introduced $\beta_K \equiv \arg(-V_{us} V_{cd} V^*_{ud} V^*_{cs})$, that is related to ε_K from neutral kaon mixing.

1.4.2 Lepton sector

The global flavor symmetry in the lepton sector of the SM, when right-handed neutrinos are absent, is broken by the Yukawa coupling Y_e as

$$G_\ell \equiv U(n_g)_\ell \times U(n_g)_e \quad \xrightarrow{Y_e} \quad H_\ell \equiv U(1)_e \times U(1)_\mu \times U(1)_\tau \times \dots, \tag{1.76}$$

where the different $U(1)$ factors in H_ℓ correspond to the vectorial component of each family of leptons—*e.g.*, $U(1)_{\mu_L} \times U(1)_{\mu_R}$ for muons—, that can be identified with the individual lepton numbers. The counting of dof is trivial since the unitary rotations in G_ℓ contain enough freedom to bidiagonalize the charged lepton mass matrix after SSB. Therefore, there are only n_g physical parameters corresponding to the charged lepton masses. Since no right-handed neutrinos have been included in the pure SM framework, these remain strictly massless. On the other hand, the gauge interactions are unaffected by the diagonalization of the mass matrices, and thus there is no flavor mixing between leptons of different generations.

Neutrino masses

As we have just seen, neutrinos are massless within the SM. However, neutrino oscillation experiments [36,37] have firmly established that neutrinos do have a mass, providing unequivocal evidence for physics beyond the SM. However, the actual origin of neutrino masses is still one of the most intriguing open fundamental questions in particle physics, as it has to address the fact that they are at least five orders of magnitude smaller than the mass of the electron. Among the plethora of neutrino mass models that have been proposed in the literature, such as the seesaw mechanisms (type I [38–41], type II [42], and type III [43]), radiative neutrino mass models [44], or flavored models [45], we are only introducing those two that are relevant for subsequent chapters. These require the inclusion of right-handed neutrinos to the SM matter content, which will get a mass through their Yukawa couplings or, additionally, by means of a Majorana mass term in the type I seesaw framework. Furthermore, we comment on the possibility to generate neutrino masses from an Effective Field Theory (EFT) perspective through the Weinberg operator [46].

Dirac neutrinos—. Inspired by the quark sector, one can simply add right-handed neutrinos to the SM matter content in order to generate a Dirac mass term after spontaneous symmetry breaking through their Yukawa interactions. To this aim, right-handed neutrinos should transform as $\nu_R^0 \sim (\mathbf{1}, \mathbf{1}, 0)$ under the SM gauge group, *i.e.*, as $SU(2)_L$ singlets with null hypercharge. This means that they do not have gauge interactions, and accordingly they are called *sterile neutrinos*. Within this scenario, the Yukawa couplings in the lepton sector read

$$-\mathscr{L}_Y^{\text{lepton}} = \overline{\ell}_L^0 Y_e e_R^0 \Phi + \overline{\ell}_L^0 Y_\nu \nu_R^0 \widetilde{\Phi} + \text{H.c.} \tag{1.77}$$

The inclusion of right-handed neutrino fields implies that the lepton flavor symmetry group G_ℓ is extended with an additional $U(n_g)_\nu$ factor.[10] Then, the lepton flavor symmetry group is broken as

$$G_\ell \equiv U(n_g)_\ell \times U(n_g)_e \times U(n_g)_\nu \qquad \xrightarrow{Y_e,\, Y_\nu} \qquad H_\ell \equiv U(1)_{\text{LN}} \,, \tag{1.78}$$

where $U(1)_{\text{LN}}$ is the global common rephasing of all lepton fields that can be identified as the total lepton number (LN). The counting of physical dof proceeds analogously to the quark sector, as it was summarized in Table 1.3. On the other hand, after SSB, bidiagonalization of the mass matrices is carried out through the unitary transformations

$$e_L^0 = U_{e_L} e_L \,, \qquad e_R^0 = U_{e_R} e_R \,, \qquad \nu_L^0 = U_{\nu_L} \nu_L \,, \qquad \nu_R^0 = U_{\nu_R} \nu_R \,, \tag{1.79}$$

in such a way that the mass matrices $M_f^0 = \frac{v}{\sqrt{2}} Y_f$ get transformed as

$$U_{e_L}^\dagger M_e^0 U_{e_R} = M_e = \text{diag}(m_e, m_\mu, m_\tau, \dots) \,, \qquad U_{\nu_L}^\dagger M_\nu^0 U_{\nu_R} = M_\nu = \text{diag}(m_{\nu_1}, m_{\nu_2}, m_{\nu_3}, \dots) \,. \tag{1.80}$$

As in the quark sector, the bidiagonalization procedure leads to the appearance of a lepton mixing matrix in the charged currents interactions known as the Pontecorvo-Maki-Nakagawa-Sakata (PMNS) matrix [47,48]:

$$-\mathscr{L}_W^{\text{lepton}} = \frac{g}{\sqrt{2}} \overline{\nu}_L \gamma^\mu U^\dagger e_L W_\mu^\dagger + \text{H.c.} \,, \tag{1.81}$$

[10] We only consider the case where precisely n_g right-handed neutrinos are added, as they can be naturally embedded in the **16**-dimensional spinor representation of $SO(10)$.

with $U \equiv U_{e_L}^{\dagger} U_{\nu_L}$. For $n_g = 3$ generations, its elements are typically labeled as

$$U = \begin{pmatrix} U_{e1} & U_{e2} & U_{e3} \\ U_{\mu 1} & U_{\mu 2} & U_{\mu 3} \\ U_{\tau 1} & U_{\tau 2} & U_{\tau 3} \end{pmatrix}, \tag{1.82}$$

with column indices $j = 1, 2, 3$ denoting the three neutrino mass eigenstates. Within this scenario, the PMNS matrix can be parametrized in terms of three mixing angles θ_{12} (solar angle), θ_{13} (reactor angle), θ_{23} (atmospheric angle), and one complex Dirac phase δ, in a similar fashion to the standard parametrization shown in Eq. (1.53). These, together with two (squared) mass splittings $\Delta m_{21}^2 \equiv m_2^2 - m_1^2$ and $\Delta m_{31}^2 \equiv m_3^2 - m_1^2$, allow to describe the phenomenon of neutrino oscillations [49–51]. While $\Delta m_{21}^2 > 0$ by definition, the sign of Δm_{31}^2 remains unknown and only its absolute value has been determined. This leaves us with two possible orderings for neutrino masses: (i) normal ordering $m_{\nu_1} < m_{\nu_2} < m_{\nu_3}$, or (ii) inverted ordering $m_{\nu_3} < m_{\nu_1} < m_{\nu_2}$, with no strong experimental preference for either. The fact that these two mass splittings have been measured to be different and non-vanishing implies that neutrino masses are all different, with at least two of them being non-zero. On the other hand, we should stress that oscillation data is only sensitive to mass differences, and thus the absolute neutrino mass scale has to be inferred from other experiments. On that regard, recently the DESI collaboration published the most stringent bound on the sum of neutrino masses, given by $\sum m_\nu < 0.072$ eV at 95% CL [52], under the assumption of the standard cosmological model ΛCDM (where CDM stands for Cold Dark Matter, and Λ denotes the cosmological constant) and the three light neutrino paradigm. This bound results from a combination of DESI Baryon Acoustic Oscillations data as well as measurements carried out by the Planck satellite and the ACT telescope. A detailed analysis of this cosmological bound has been addressed in [53]. Alternatively, a bound on the sum of neutrino masses has been set by the KATRIN experiment, namely, $\sum m_\nu < 0.93$ eV at 90% CL [54], based on precision measurements near the endpoint of the tritium β-decay spectrum, and thus independent of the assumed cosmological model.

The fact that generating light neutrino masses at the eV scale requires their Yukawa couplings to be about five orders of magnitude smaller than that of the electron is not a fully satisfactory explanation. A rationale behind the smallness of neutrino masses is in order, as we shall discuss below.

Majorana neutrinos—. The special nature of right-handed neutrinos being singlets under the SM gauge group allows to write down an additional Majorana mass term in Eq. (1.77), namely

$$-\mathscr{L}_{\text{Majorana}} = \frac{1}{2} \overline{(\nu_R^0)^c} M_R \nu_R^0 + \text{H.c.}, \tag{1.83}$$

where M_R is an $n_g \times n_g$ complex symmetric matrix, and $(\nu_R^0)^c \equiv C \overline{\nu}_R^{0\,T}$, with $C = i\gamma^0\gamma^2$ the charge-conjugation matrix. After spontaneous symmetry breaking, the mass terms can be rearranged as

$$-\mathscr{L}_{\text{mass}}^{\text{lepton}} = \overline{e}_L^0 M_e^0 e_R^0 + \frac{1}{2} \begin{pmatrix} \overline{\nu}_L^0 & \overline{(\nu_R^0)^c} \end{pmatrix} \begin{pmatrix} 0 & M_\nu^0 \\ (M_\nu^0)^T & M_R \end{pmatrix} \begin{pmatrix} (\nu_L^0)^c \\ \nu_R \end{pmatrix} + \text{H.c.}, \tag{1.84}$$

where $M_f^0 = \frac{v}{\sqrt{2}} Y_f$, and

$$\mathcal{M} = \begin{pmatrix} 0 & M_\nu^0 \\ (M_\nu^0)^T & M_R \end{pmatrix}, \tag{1.85}$$

is the $2n_g \times 2n_g$ complex symmetric neutrino mass matrix. Block diagonalization of the neutrino mass matrix leads to

$$\mathcal{M}_\nu \approx (M_\nu^0)^T M_R^{-1} M_\nu^0 \sim \frac{v^2 y_\nu^2}{2M}\,. \tag{1.86}$$

We have denoted by M the energy scale of M_R, which in principle could be very large since it is not protected by a symmetry, while v is the EW scale, and y_ν is the order of magnitude of the Yukawa couplings in Y_ν. The relation in Eq. (1.86) summarizes the type I seesaw mechanism: light neutrino masses arise from the hierarchy of scales $v \ll M$. In addition, there are new neutrino states whose masses lie at the heavy scale. For instance, assuming $y_\nu \sim 1$ as in the top quark case, then $M \sim 10^{14}$ GeV would account for light neutrino masses ~ 0.1 eV. Finally, one can check that the neutrino Dirac spinors are indeed Majorana spinors, since they satisfy $\nu = \nu^c$, *i.e.*, neutrinos are its own antiparticle, and thus can be built out of a single two-component Weyl fermion.

It is to be noticed that the Majorana mass term violates lepton number by two units. In particular, the lepton flavor symmetry group is broken as

$$G_\ell \equiv U(n_g)_\ell \times U(n_g)_e \times U(n_g)_\nu \qquad \xrightarrow{Y_e,\,Y_\nu,\,M_R} \qquad H_\ell \equiv \mathbb{Z}_2 = \{1, \mathcal{P}_{\rm LN}\}\,, \tag{1.87}$$

with $\mathcal{P}_{\rm LN} = (-1)^{\rm LN}$ the lepton parity. The counting of real dof present in Y_e, Y_ν, and M_R is summarized in Table 1.4. From the first row, we can read the $3n_g$ masses of charged leptons, light neutrinos, and heavy neutrinos, together with the $n_g(n_g-1)/2$ moduli of the PMNS matrix mixing charged leptons and light neutrinos, and the additional $n_g(n_g-1)/2$ moduli of the complex orthogonal matrix in the Casas-Ibarra parametrization [55]. From the second row, we have the usual $(n_g-1)(n_g-2)/2$ Dirac phases plus (n_g-1) Majorana phases in the PMNS mixing, and $n_g(n_g-1)/2$ phases in the orthogonal complex matrix introduced by Casas-Ibarra.

	$N_{\rm param}$	$\dim G_\ell$	$\dim H_\ell$	$N_{\rm physical}$
Moduli	$2n_g^2 + \frac{n_g(n_g+1)}{2}$	$\frac{3n_g(n_g-1)}{2}$	0	$3n_g + \frac{n_g(n_g-1)}{2} + \frac{n_g(n_g-1)}{2}$
Phases	$2n_g^2 + \frac{n_g(n_g+1)}{2}$	$\frac{3n_g(n_g+1)}{2}$	0	$\frac{(n_g-1)(n_g-2)}{2} + (n_g-1) + \frac{n_g(n_g-1)}{2}$
Total	$4n_g^2 + n_g(n_g+1)$	$3n_g^2$	0	$n_g(2n_g+1)$

Table 1.4: Physical parameters in the lepton Yukawa sector including right-handed neutrinos and a Majorana mass term.

For $n_g = 3$ generations, the PMNS matrix, strictly referring to the mixing of charged leptons and light neutrinos, can be parametrized as

$$U = \begin{pmatrix} c_{12}c_{13} & s_{12}c_{13} & s_{13}e^{-i\delta} \\ -s_{12}c_{23} - c_{12}s_{23}s_{13}e^{i\delta} & c_{12}c_{23} - s_{12}s_{23}s_{13}e^{i\delta} & s_{23}c_{13} \\ s_{12}s_{23} - c_{12}c_{23}s_{13}e^{i\delta} & -s_{23}c_{12} - s_{12}c_{23}s_{13}e^{i\delta} & c_{23}c_{13} \end{pmatrix} \begin{pmatrix} 1 & 0 & 0 \\ 0 & e^{i\phi_1} & 0 \\ 0 & 0 & e^{i\phi_2} \end{pmatrix}, \tag{1.88}$$

where ϕ_1 and ϕ_2 correspond to the two additional Majorana phases arising in the seesaw mechanism. We should recall that neutrino oscillation experiments are not sensitive to Majorana phases.

Besides the dynamical mechanism responsible for generating neutrino masses, the question of whether neutrinos are Dirac or Majorana particles remains one of the most intriguing mysteries in nature. Experiments seeking for neutrinoless double-beta decay ($0\nu\beta\beta$) [56] in which lepton number is violated in two units might shed some light on that respect in the future, apart from giving access to the measurement of Majorana phases. Furthermore, although these experiments do not determine by themselves the neutrino mass generation mechanism, they have the potential to exclude or test some of them.

Weinberg operator—. In the context of the Standard Model Effective Field Theory (SMEFT), one can introduce non-renormalizable operators (with mass dimension larger than four) built out of the SM fields, and endowed with the SM symmetries (Lorentz and gauge) and a power-counting scheme. In particular, each n-dimensional operator is suppressed by $n-4$ powers of a high energy scale Λ, so that they could be interpreted as a perturbation to the low-energy theory, namely, the SM. At the lowest order in the perturbative expansion, the only allowed dim-5 interaction is described by the Weinberg operator [46]:

$$-\mathscr{L}_{\text{Weinberg}} = \frac{1}{2\Lambda}\left[\overline{(\ell_L^0)^c}\widetilde{\Phi}^*\right] C_\nu \left[\widetilde{\Phi}^\dagger \ell_L^0\right] + \text{H.c.}\,, \tag{1.89}$$

where C_ν is an $n_g \times n_g$ complex symmetric matrix. After spontaneous symmetry breaking, this operator generates an effective Majorana mass term for neutrinos, namely,

$$-\mathscr{L}_{\text{Weinberg}} \xrightarrow{\langle\Phi\rangle} \frac{1}{2}\overline{(\nu_L^0)^c}\frac{v^2}{2\Lambda}C_\nu \nu_L^0 + \text{H.c.} = \frac{1}{2}\overline{(\nu_L^0)^c}M_L\nu_L^0 + \text{H.c.}\,, \tag{1.90}$$

with $M_L \equiv \frac{v^2}{2\Lambda}C_\nu$. The well-known seesaw mechanisms (type I, type II and type III) provide three different tree-level realizations of the Weinberg operator. Similarly to the type I seesaw scenario presented above, the Weinberg operator violates lepton number in two units, and the lepton flavor symmetry group is broken as

$$G_\ell \equiv U(n_g)_\ell \times U(n_g)_e \xrightarrow{Y_e,\, C_\nu} H_\ell \equiv \mathbb{Z}_2 = \{1, \mathcal{P}_{\text{LN}}\}\,. \tag{1.91}$$

The counting of physical dof is presented in Table 1.5. Comparing with Table 1.4, one can readily check that the heavy neutrino masses, along with the moduli and phases of the complex orthogonal matrix in the Casas-Ibarra parametrization [55], do not appear explicitly, as they are associated with the ultraviolet (UV) scale and therefore leave no imprint on the low-energy theory.

	N_{param}	$\dim G_\ell$	$\dim H_\ell$	N_{physical}
Moduli	$n_g^2 + \frac{n_g(n_g+1)}{2}$	$\frac{2n_g(n_g-1)}{2}$	0	$2n_g + \frac{n_g(n_g-1)}{2}$
Phases	$n_g^2 + \frac{n_g(n_g+1)}{2}$	$\frac{2n_g(n_g+1)}{2}$	0	$\frac{(n_g-1)(n_g-2)}{2} + (n_g-1)$
Total	$2n_g^2 + n_g(n_g+1)$	$2n_g^2$	0	$n_g(n_g+1)$

Table 1.5: Physical parameters in the lepton Yukawa sector including the dim-5 Weinberg operator.

1.5 Weak CP violation

The CP transformation is physically interpreted as the interchange of particles and antiparticles together with the reflection of all spatial dimensions. At a fundamental level, if a theory is not invariant under CP transformations, it means that the interactions it describes differentiate between particles and antiparticles, as well as between left and right. The weak interactions violate CP, as it was first observed in hadronic kaon decays [57].

Focusing on the electroweak sector of the SM, while parity violation is evident from the different transformation properties of left-handed and right-handed fields, the violation of the CP symmetry emerges in a non-trivial way. We have checked that bidiagonalization of the mass matrices leads to observable consequences in the W boson interactions with quarks, namely, the appearance of a unitary flavor mixing matrix that contains an irremovable phase. The latter is the source of all weak CP-violating effects in the SM, as we proceed to explain.

In general, in order to determine whether CP is conserved or not in a given theory, one first has to define the most general field transformations that can be physically interpreted as charge-parity transformations according to our previous description, including any internal symmetry of the theory. Then, one has to implement those transformations term by term in the Lagrangian. We conclude that there is CP violation if there is not enough freedom in our transformations that allow us to fulfill the restrictions imposed by all terms in the Lagrangian *simultaneously*.

Let us first consider the standard theory after spontaneous symmetry breaking in the mass eigenstate basis. For diagonal mass matrices with non-degenerate eigenvalues, and CKM mixing matrix V emerging in W boson interactions with quarks, one can check that [58]

$$\text{Weak CP conservation} \quad \Longleftrightarrow \quad V_{ij}^{*} = e^{i(\xi+\xi_j-\xi_i)} V_{ij}\,, \tag{1.92}$$

where ξ, ξ_i, and ξ_j are arbitrary phases included in the CP transformation properties of charged bosons, up-type quarks, and down-type quarks, respectively. In general, these CP phases do not provide enough freedom to satisfy the previous condition for all matrix elements in V, and thus CP violation could arise from charged currents interactions in the quark sector. For $n_g = 2$ generations, according to our counting in Table 1.3, there is no physical phase left in the flavor mixing matrix, that is, CKM is real and Eq. (1.92) is trivially satisfied, meaning that CP is conserved. This picture changes when we consider $n_g = 3$ generations. As we have shown before, there is an irremovable physical phase in the flavor mixing matrix. Then, one can check that Eq. (1.92) cannot be fulfilled for all CKM elements, leading to CP violation in the SM with three generations of quarks. This result earned Kobayashi and Maskawa the Nobel Prize *for the discovery of the origin of the broken symmetry which predicts the existence of at least three families of quarks in nature* [28]. On the other hand, it is clear that CP violation can only arise in the quark sector, as there is no analogous mixing matrix in the charged current leptonic interactions—provided that right-handed neutrinos are not included.

Alternatively, one can derive the conditions for CP conservation in the weak eigenstate basis after spontaneous symmetry breaking [59], *i.e.*, the basis where the Lagrangian of the theory is originally written. We should recall that, in this basis, the gauge-fermion interactions are diagonal in flavor space and the mass matrices are complex arbitrary matrices. In this case, the Yukawa sector imposes the following necessary and sufficient conditions for CP conservation:

$$\text{Weak CP conservation} \;\Longleftrightarrow\; \begin{array}{c} K_Q^{\dagger} M_u^0 K_u = (M_u^0)^{*} \\ K_Q^{\dagger} M_d^0 K_d = (M_d^0)^{*} \end{array} \;\Longleftrightarrow\; \begin{array}{c} K_Q^{\dagger} H_u K_Q = H_u^{*} = H_u^{T} \\ K_Q^{\dagger} H_d K_Q = H_d^{*} = H_d^{T} \end{array}\,, \tag{1.93}$$

where $H_u \equiv M_u^0 M_u^{0\dagger}$ and $H_d \equiv M_d^0 M_d^{0\dagger}$ are Hermitian combinations of mass matrices, while K_Q, K_u and K_d are $n_g \times n_g$ unitary rotations in flavor space that mix the left-handed doublets, the right-handed up-type singlets, and the right-handed down-type singlets, respectively. The latter are part of the most general CP transformations of the quark fields. All in all, we learn that CP is conserved in the weak interactions if and only if unitary matrices K_Q, K_u, and K_d exist such that they satisfy Eq. (1.93). Since the matrix K_Q appears in both up-type and down-type quark sectors of Eq. (1.93), as a consequence of W boson interactions connecting u_L^0 and d_L^0, in general the previous conditions cannot be satisfied simultaneously, and thus CP invariance is not guaranteed. This is not the case in the lepton sector, where we only deal with M_e^0: one can always find unitary K_ℓ and K_e such that $K_\ell^\dagger M_e^0 K_e = (M_e^0)^*$, leading to CP conservation.

From Eq. (1.93), it is clear that the presence of complex Yukawa couplings, or equivalently mass matrices, is not the only reason that leads to CP violation, but rather the simultaneous presence of complex Yukawa couplings and left-handed charged currents.

1.5.1 Weak basis invariant conditions for CP conservation

In previous sections, we have argued that physical observables must be invariant under field redefinitions. For the standard gauge theory, these correspond to WBT in Eq. (1.44), namely,

$$Q_L^0 = U_Q Q_L' \,, \qquad u_R^0 = U_u u_R' \,, \qquad d_R^0 = U_d d_R' \,, \tag{1.94}$$

where we have omitted the corresponding transformations in the lepton sector for simplicity. Under WBT, it is easy to see that the mass matrices transform as

$$M_u' = U_Q^\dagger M_u U_u \,, \qquad M_d' = U_Q^\dagger M_d U_d \,, \tag{1.95}$$

and the Hermitian combinations H_u and H_d as

$$H_u' = U_Q^\dagger H_u U_Q \,, \qquad H_d' = U_Q^\dagger H_d U_Q \,. \tag{1.96}$$

Remarkably, WBT contain enough freedom to bidiagonalize one of the mass matrices and make the remaining one Hermitian. Therefore, we can single out two special bases that will prove useful for subsequent calculations:

(i) M_u' real diagonal non-negative, and M_d' Hermitian,

$$\begin{aligned} M_u' &= \mathrm{diag}(m_u, m_c, m_t, \dots) \,, \\ M_d' &= V \mathrm{diag}(m_d, m_s, m_b, \dots) \,, \end{aligned} \qquad \Longrightarrow \qquad \begin{aligned} H_u' &= \mathrm{diag}(m_u^2, m_c^2, m_t^2, \dots) \,, \\ H_d' &= V \mathrm{diag}(m_d^2, m_s^2, m_b^2, \dots) V^\dagger \,, \end{aligned} \tag{1.97}$$

(ii) M_d' real diagonal non-negative, and M_u' Hermitian,

$$\begin{aligned} M_u' &= V^\dagger \mathrm{diag}(m_u, m_c, m_t, \dots) \,, \\ M_d' &= \mathrm{diag}(m_d, m_s, m_b, \dots) \,, \end{aligned} \qquad \Longrightarrow \qquad \begin{aligned} H_u' &= V^\dagger \mathrm{diag}(m_u^2, m_c^2, m_t^2, \dots) V \,, \\ H_d' &= \mathrm{diag}(m_d^2, m_s^2, m_b^2, \dots) \,, \end{aligned} \tag{1.98}$$

where V is the CKM matrix.

By definition, weak basis invariant quantities cannot depend on the transformation matrices U_Q, U_u, and U_d. On that regard, functions of the Hermitian combinations H_u and H_d seem to be good candidates to start with, as their transformation law in Eq. (1.96) only involves the matrix U_Q. In particular, it is enough to take the trace in both sides of Eq. (1.96) to construct our first weak basis invariants, namely, $\mathrm{tr}(H_u') = \mathrm{tr}(H_u)$ and $\mathrm{tr}(H_d') = \mathrm{tr}(H_d)$. More generally, traces of polynomials with arbitrary powers of H_u and H_d are invariant under WBT, hence physically meaningful and measurable. Then, it is convenient to compute such quantities by choosing an appropriate basis, *e.g.*, either of those presented in Eq. (1.97) or in Eq. (1.98). For instance, in this bases, it is straightforward to obtain

$$\mathrm{tr}(H_u^p) = (m_u^2)^p + (m_c^2)^p + (m_t^2)^p + \dots\,, \qquad \mathrm{tr}(H_d^q) = (m_d^2)^q + (m_s^2)^q + (m_b^2)^q + \dots \tag{1.99}$$

In any case, our interest lies in deriving weak basis invariant conditions for CP conservation [59,60]. These are particularly useful for the study of CP violation as they help avoid potential confusion arising from field redefinitions that may introduce spurious phases in the Lagrangian. Likewise, it is more convenient and straightforward to express these conditions in terms of the non-diagonal mass matrices, so that one does not have to care about the specific details concerning their diagonalization. On that regard, one may consider Eq. (1.93) as a benchmark. Under WBT in Eqs. (1.95) and (1.96), it is easy to check that the unitary matrices

$$K'_Q \equiv U_Q K_Q U_Q^T\,, \qquad K'_u \equiv U_u K_u U_u^T\,, \qquad K'_d \equiv U_d K_d U_d^T\,, \tag{1.100}$$

fulfill the conditions in Eq. (1.93) for M'_u, M'_d, H'_u, and H'_d. Since the unitary rotations K_Q, K_u, and K_d are not invariant under a WBT, these must be eliminated from our CP-invariance conditions. To this aim, taking into account the right-hand side of Eq. (1.93), we obtain

$$K_Q^\dagger [H_u, H_d] K_Q = -[H_u, H_d]^T\,, \tag{1.101}$$

and more generally

$$K_Q^\dagger [H_u, H_d]^r K_Q = (-1)^r [H_u, H_d]^{r\,T}\,, \tag{1.102}$$

for r arbitrary powers of the commutator $[H_u, H_d]$. Then, we can take the trace of both sides of Eq. (1.102) to get rid of K_Q, leading to

$$\mathrm{tr}[H_u, H_d]^r = 0\,, \qquad \text{for } r \text{ odd}\,. \tag{1.103}$$

For $r = 1$, Eq. (1.103) does not provide any useful information, as the trace of a commutator is identically zero by itself. Nevertheless, for $r \geq 3$ this yields a necessary condition for CP conservation, which is invariant under WBT and holds for an arbitrary number of generations n_g. In particular, the simplest non-trivial condition can be stated as:

For an arbitrary number of generations,

$$\text{Weak CP conservation} \quad \Longrightarrow \quad \mathrm{tr}[H_u, H_d]^3 = 0\,, \tag{1.104}$$

where

$$\mathrm{tr}[H_u, H_d]^3 = 6i\,\mathrm{Im}\left[\mathrm{tr}\big(H_u^2 H_d^2 H_u H_d\big)\right] = 6i \sum_{i,k=u,c,t,\dots} \; \sum_{j,l=d,s,b,\dots} m_i^4 m_k^2 m_j^4 m_l^2 \,\mathrm{Im}\, Q_{ijkl}\,. \tag{1.105}$$

It is instructive to check the previous condition for two and three generations of quarks. On the one hand, for $n_g = 2$, the only possible quartet that can be constructed, Q_{udcs}, is real due to the orthogonality relations of the 2×2 CKM matrix, and thus Eq. (1.104) is satisfied. Alternatively, one may have realized that, in general, the commutator $[H_1, H_2]^2$, with H_1 and H_2 arbitrary 2×2 Hermitian matrices, is proportional to the identity matrix. Therefore, CP is a good symmetry of the Lagrangian with only two quark generations.

On the other hand, for $n_g = 3$ generations this is not the case anymore. It can be shown that

$\mathrm{tr}[H_u, H_d]^3 = 0$ is indeed a necessary and sufficient condition for CP invariance. Furthermore, by means of the Cayley-Hamilton theorem, $\mathrm{tr}[H_u, H_d]^3 = 3\det[H_u, H_d]$, since $[H_u, H_d]$ is a traceless 3×3 matrix. Therefore:

For $n_g = 3$ generations,

$$\text{Weak CP conservation} \quad \Longleftrightarrow \quad \mathrm{tr}[H_u, H_d]^3 = 0 \quad \Longleftrightarrow \quad \det[H_u, H_d] = 0\,, \tag{1.106}$$

where

$$\mathrm{tr}[H_u, H_d]^3 = 6i\,(m_u^2 - m_c^2)(m_u^2 - m_t^2)(m_c^2 - m_t^2)(m_d^2 - m_s^2)(m_d^2 - m_b^2)(m_s^2 - m_b^2)J\,, \tag{1.107}$$

and $\det[H_u, H_d] = \frac{1}{3}\,\mathrm{tr}[H_u, H_d]^3$.

It is to be noticed that $\mathrm{tr}[H_u, H_d]^3$ have been computed using Eq. (1.60), which accounts for the fact that the imaginary parts of all quartets are equal to the Jarlskog invariant J up to a sign. Since in the SM both up-type and down-type sectors are non-degenerate, there is CP violation if and only if the Jarlskog invariant is different from zero. The requirement imposed in the masses is indeed related to the Jarlskog being non-vanishing because, if there were a degenerate subsector, we could redefine the fields by a unitary rotation in the subspace of the degeneracy, and thus we would have enough freedom to set $J = 0$; in other words, we would be able to remove the remaining physical phase in the CKM, which would be real—see Eq. (1.52).

Two final comments are in order. First, coming back to the geometrical interpretation of the Jarlskog, it is now clear that the area of the unitary triangles is a measure of the amount of CP violation in the SM. Second, one can check that the maximum possible value of the Jarlskog invariant is $1/(6\sqrt{3})$ [61]. This, however, is not the case in the SM, where $J \sim \mathcal{O}(10^{-5})$.

1.5.2 CP violation with massive neutrinos

As we have explained before, the inclusion of right-handed neutrinos in the SM matter content allows to generate a mass term for them, which in turn leads to the appearance of a flavor mixing matrix in the charged current interactions. Contrary to the pure SM framework, CP invariance is not guaranteed in the lepton sector, and thus it is important to identify under which conditions CP is still a good symmetry of the Lagrangian. In the Dirac neutrino scenario, the analysis proceeds analogously to that of the quark sector. This situation changes in the Majorana neutrino scenario due to the presence of the additional term in Eq. (1.83). In that case, one can check that

$$\begin{array}{c}\text{CP conservation}\\ \text{(Majorana neutrinos)}\end{array} \quad \Longleftrightarrow \quad \begin{array}{l} K_\ell^\dagger M_\nu^0 K_\nu = (M_\nu^0)^* \\ K_\ell^\dagger M_e^0 K_e = (M_e^0)^* \\ K_\nu^T M_R K_\nu = M_R^* \end{array}\,, \tag{1.108}$$

where K_ℓ, K_e and K_ν are $n_g \times n_g$ unitary rotations in flavor space that mix the left-handed lepton doublets, the right-handed charged lepton singlets, and the right-handed neutrino singlets, respectively. Therefore, CP is conserved in the lepton interactions if and only if unitary matrices K_ℓ, K_e, and K_ν exist such that they satisfy Eq. (1.108). For the purposes of subsequent chapters, it is sufficient to limit ourselves to this set of conditions, which capture the essential features relevant to our analyses. A more comprehensive study of CP violation in the presence of neutrino masses can be found in [58] and references therein.

1.6 What is beyond? The quest for New Physics

The SM has proven to be a consistent and predictive framework capable of describing all experimental data to date, at least up to energies $\mathcal{O}(v)$. Among its many triumphs, we could mention the prediction of the existence of the $W^{\pm}$ and Z bosons by the gauge symmetry, the charm quark required by the GIM mechanism, or the Higgs boson emerging as a remnant of SSB. Despite its impressive success, several open questions remain for which no compelling explanation exists within the SM. The following is a brief overview of some of the most fascinating challenges we are currently confronted with.

Abundance of free parameters and unification—. Probably, one of the first indications of the SM not being a fully satisfactory theory is the abundance of free parameters it contains. In the most simple scenario, these include: three gauge couplings $\{g_s, g, g'\}$, or equivalently, the two gauge boson masses and the weak mixing angle, $\{M_W, M_Z, \theta_W\}$; two parameters arising from the scalar sector $\{\mu^2, \lambda\}$, which can be traded for the Higgs boson mass and the scalar vev $\{M_h, v\}$; and the numerous parameters arising from the fermion sector, namely, nine fermion masses, three mixing angles, and one complex phase—this gives a total of 18 parameters, not including the hypercharges of the different fields. If we further specify a mass generation mechanism for neutrinos, the number of parameters increases. For Dirac neutrinos, one would have additionally three light neutrino masses, together with three new mixing angles and one complex phase—hence, we are left with a total of 25 parameters. In the type I seesaw framework, six neutrino masses, six mixing angles, and five complex phases add up as parameters of the theory—yielding 35 free parameters in total. Finally, taking into account the theoretical existence of CP violation in the strong interactions, the QCD $\bar{\theta}$ parameter must be included in the previous list.

In addition, it is clear that the presence of three independent gauge couplings, each associated with a different factor in the gauge group G_{SM} in Eq. (1.2), falls short of offering a unified description of the fundamental interactions. Remarkably, a unified framework may naturally account for the observed pattern of charge quantization, namely, why all fundamental particles possess electric charges that are integer multiples of $e/3$, which ultimately guarantees that atoms are electrically neutral.

Flavor puzzle—. Although the SM is extraordinarily accurate in predicting all observed flavor transitions, there is no fundamental principle that justifies the particle structure that emerges in the flavor sector. The Yukawa couplings are introduced as arbitrary complex parameters whose values have to be inferred from experiment, and there is no rationale to explain their hierarchical pattern or, equivalently, of the fermion masses and mixings. In other words, the SM lacks a theory of flavor. In contrast to the gauge interactions, which are fully determined by the gauge principle in terms of three $\mathcal{O}(1)$ coupling constants, the flavor sector introduces the largest amount of free parameters to the theory, which span several orders of magnitude. On the one hand, if we look into the fermion masses, the top quark mass is about five orders of magnitude larger than the mass of the electron. The situation is even worse if we take into account that neutrino masses are extremely small, eleven orders of magnitude (or more) lighter than the top mass. On the other hand, regarding the fermion mixing patterns, the CKM matrix in the quark sector is very close to the identity, with small off-diagonal elements suppressing the mixing between different generations, as illustrated in Fig. 1.3a. The PMNS mixing in the lepton sector is, on the contrary, homogeneous over different generations, as shown in Fig. 1.3b. Finally, despite all terrestrial phenomena could be well explained in terms of (u, d, e^-, ν_e), the fermion sector exhibits a non-minimal structure in Nature: there are three exact replicas or generations which only differ by their masses—and we certainly do not know yet *who ordered that.* All these questions, namely, the hierarchy of fermion masses and mixings as well as the existence of three generations, constitute the SM flavor puzzle.

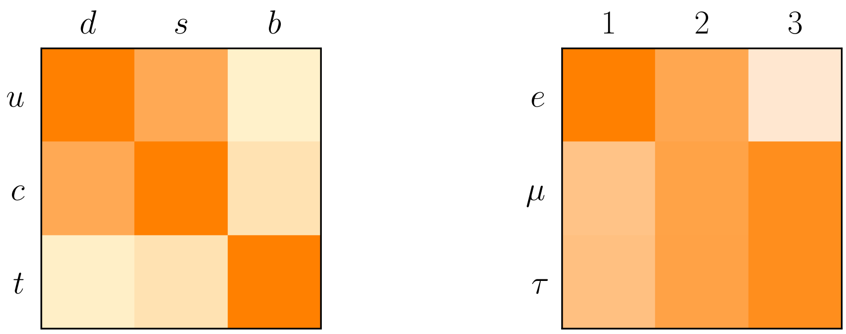

(a) (b)

Figure 1.3: Illustration of the hierarchical patterns of the fermion mixing matrices in the SM: (a) CKM matrix, and (b) PMNS matrix. Darker colors correspond to larger mixing elements.

Neutrino masses—. As we have explained before, neutrino oscillation experiments [36, 37] have established that neutrinos do have a mass, although they are extremely light. The SM framework easily allows to accommodate neutrino masses by including right-handed neutrino fields, in both Dirac and Majorana scenarios. Nevertheless, the concrete mass generation mechanism for neutrinos is still unknown, and other related properties such as their Dirac or Majorana nature remain elusive.

Electroweak or Higgs hierarchy problem—. A Higgs boson mass ($M_h \sim 125$ GeV) close to the EW scale constitutes a self-consistency requirement of the theory—if the Higgs boson had been much heavier, its self-couplings would have been too large in order for a perturbative expansion to be reliable. However, the observed value appears difficult to reconcile with the fact that the tree-level mass is subject to quadratically divergent quantum corrections from higher energy scales. This may be conflict with the *naturalness* paradigm, since *a priori* fine-tuned cancellations would be required to explain the measured value of the Higgs mass.

The fact that stabilizing the Higgs mass may force the scale of NP to lie not far above the EW scale could, in turn, introduce additional tensions with flavor data. In particular, many models proposed to address the Higgs hierarchy problem typically generate FCNC, as well as sizable contributions to electric dipole moments (EDMs) and electroweak precision observables, all of which are tightly constrained by experiment. A straightforward way to evade these bounds is to raise the NP scale, which, however, goes in the opposite direction of what is required for stabilizing the Higgs sector. This tension is commonly referred to as *little hierarchy problem* or *new physics flavor puzzle*, as it might point towards a highly non-trivial or fine-tuned NP flavor structure.

Strong CP problem—. As we know from the weak interactions, CP is not a good symmetry of the Lagrangian. In light of this, the QCD Lagrangian may include a term of the form

$$\mathscr{L}_{\rm QCD} \supset \mathscr{L}_\theta = \theta_{\rm QCD} \frac{g_s}{32\pi^2} G_A^{\mu\nu} \widetilde{G}^A_{\mu\nu} \,, \tag{1.109}$$

where $\widetilde{G}^{A}_{\mu\nu} \equiv \epsilon_{\mu\nu\rho\sigma} G^{A\,\rho\sigma}/2$ is the dual field strength tensor of the gluon, and $\theta_{\rm QCD}$ is a free parameter. One can then construct a single CP-violating phase in the strong sector that is invariant under quark field redefinitions, namely,

$$\bar{\theta} \equiv \theta_{\rm QCD} + \arg\left[\det(M_u M_d)\right] , \tag{1.110}$$

where M_u and M_d are the quark mass matrices. The $\bar{\theta}$ parameter is a physical observable, and stringent bounds have been placed by measurements of the neutron EDM [62], roughly $\bar{\theta} \lesssim 10^{-10}$. The strong CP puzzle stems from the extremely small value of the $\bar{\theta}$ parameter.

Baryon Asymmetry of the Universe—. One of the most fundamental open questions in cosmology and particle physics is why the Universe we observe is almost entirely made of matter structures, with near total absence of antimatter, while the standard cosmological model predicts equal parts of both. This scenario derives from a primordial matter-antimatter imbalance, known as Baryon Asymmetry of the Universe (BAU), given by [63]

$$Y_{\mathcal{B}} \equiv \frac{n_{\mathcal{B}} - n_{\bar{\mathcal{B}}}}{s} = (0.872 \pm 0.004) \times 10^{-10} , \tag{1.111}$$

where $n_{\mathcal{B}}$ ($n_{\bar{\mathcal{B}}}$) is the number of baryon (antibaryons), and s is the entropy density. To generate this primordial asymmetry, many *baryogenesis* models have been proposed in the literature. They all must satisfy the Sakharov conditions [64]: (i) baryon number violation, (ii) C and CP violation, and (iii) departure from thermal equilibrium. However, it is well-known that the amount of CP violation in the SM, either from the weak or strong interactions, is not enough to trigger baryogenesis, and thus new CP-violating sources are needed.

Dark sector—. Measurements of the Cosmic Microwave Background by the Planck satellite [63] indicate that only about 16% of the total matter content of the Universe consists of ordinary baryonic matter, while the remaining 84% must be attributed to a new form of *dark matter* that apparently only manifests through its gravitational interactions. Even more striking is the fact that some form of *dark energy* accounts for almost 70% of the energy density of the Universe and is responsible for its accelerated expansion. The SM lacks any mechanism to explain either of these observations.

Anomalies—. Another source of motivation for physics beyond the SM arises from experimental anomalies, that is, discrepancies between the measured values of certain observables and the corresponding theoretical predictions in the SM. While some of these may ultimately stem from underestimated systematic uncertainties or statistical fluctuations, persistent tensions can point toward NP effects. In the flavor sector, several tensions emerge. At low energies, the Lepton Flavor Universality ratios R_D and R_{D^*}, involving $b \to c\ell\nu$ transitions, show an enhancement of the τ rates over light charged leptons decays of 3.14σ [65] with respect to the SM prediction. Similar deviations have been found in rare decays such as $B^+ \to K^+\nu\nu$, where a significance of 2.7σ above the SM expectation is reported [66]. At high energies, CMS has observed a global excess of 2.8σ in the lepton flavor violating decay $S \to \mu e$ of a neutral scalar with an invariant mass of 146 GeV [67]. On the other hand, the so-called Cabibbo angle anomaly, reflecting deviations from 3×3 unitarity in the first row (and first column) of the CKM matrix, is becoming significant at the 3σ level. These are just a few examples in this regard—for a review, see [68–70]. Although no single measurement provides conclusive evidence for NP, the consistent pattern of deviations across different processes and experiments might draw an interesting picture to be addressed BSM.

The aforementioned points reflect some of the most fundamental open questions in modern physics. To this list, one must add the absence of a consistent quantum theory of gravity, the cosmological constant problem—arguably the worst fine-tuning issue in physics—, or the finely tuned initial conditions at the Big Bang that resulted in the flat, homogeneous, and isotropic Universe we observe.

At this stage, the need for New Physics beyond the Standard Model becomes clear. In the attempt to identify the nature of such NP, one can generally adopt two complementary strategies. The first one is a top-down approach, which consists in proposing a UV complete theory defined at the highest energy scale that can naturally address all (or at least some) of the previous questions. Examples of this include Grand Unified Theories (GUTs) and superstring theories. Another possibility is to follow a bottom-up approach. In this case, the goal is to address specific shortcomings of the SM with particular focus on the phenomenological implications near the EW scale. Typically, within the bottom-up approach the field content is extended beyond minimality, giving rise to new particles that may be understood as remnants of a more fundamental UV theory. In this thesis, we will adopt this second possibility, *e.g.*, in the context of multi-Higgs models, or vector-like quark extensions of the fermion sector. Alternatively, in order to analyze the low-energy behavior of higher mass scales in a model-independent way, one could rely on the EFT framework and, in particular, treat the SM as a low-energy EFT, dubbed SMEFT. We will also explore some of its features in the context of spurion analyses.

2 An introduction to Hilbert Series

Hilbert series constitute a powerful and versatile tool with wide-ranging applications in particle physics. They have proved particularly useful for counting degrees of freedom and enumerating group invariants constructed from a specified set of building blocks, *e.g.*, in the context of flavor physics [71, 72] and neutrino mass models [73, 74], SMEFT [75–81], Higgs EFT [82], the QCD chiral Lagrangian [83], or supersymmetric field theories [84–86], among many others. Furthermore, this technology has been applied to analyze group covariants, that is, non-trivial representations of a symmetry group, in spurion analyses within the Minimal Flavor Violation (MFV) paradigm [1, 87]. Interestingly, Hilbert series have also been employed to gain new insights into the identification of accidental symmetries in EFTs, as illustrated in Ref. [6], where we present a first attempt at developing a systematic approach to this problem.

All in all, and for the purposes of chapter 4, we provide here an introduction to Hilbert series for enumerating group invariants and covariants, with particular emphasis on how to compute them by means of the Molien-Weyl formula, and how to extract information about the underlying algebraic structure of invariants and covariants. Along the way, we highlight some relevant results from the math literature—such as a theorem by Brion [88]—that are pertinent to our discussion. For a more comprehensive review on this topic, we refer the reader to Ref. [87], from which we adopt the notation used throughout this chapter.

2.1 Hilbert series for group invariants and covariants

In QFT, a Lagrangian is constructed from a given set of n building block fields, that we denote as

$$\Phi = \{\Phi_1, \Phi_2, \dots, \Phi_n\}\,, \tag{2.1}$$

where each Φ_i is a Grassmann-even (bosonic) or Grassmann-odd (fermionic) field component with no further internal structure.[1] Typically, the Lagrangian is invariant under some symmetry group G (generally, a product group), under which the building block fields transform as a linear representation (rep) R_Φ of dimension $\dim R_\Phi = n$, namely,

$$\Phi \sim R_\Phi \;\text{ of }\; G: \qquad \Phi \quad \longrightarrow \quad \Phi' \equiv g_{R_\Phi}\Phi\,, \tag{2.2}$$

with g_{R_Φ} the $n \times n$ non-singular matrix representing the element $g \in G$. Only G-invariant polynomials in the field components are then allowed to be part of the Lagrangian of the theory. In general, we will

[1] We will not be concerned with derivative interactions in the Lagrangian; otherwise, field derivatives could be included in the set of building blocks Φ.

collectively denote all polynomials of degree k as

$$\Phi^k \equiv \left\{ \Phi_1^{k_1}\Phi_2^{k_2}\cdots\Phi_n^{k_n}\,, \quad k_i \in \mathbb{N} \;/\; \sum_{i=1}^{n} k_i = k \right\}, \tag{2.3}$$

such that each $\Phi_i^{k_i}$ encodes all possible monomials of Φ_i. In the EFT framework, non-renormalizable interactions are included in the Lagrangian, meaning that the total degree k in Eq. (2.3) could be arbitrarily large. The only restriction comes for fermionic field components, since their anticommuting nature imposes $k_f = 0, 1$. On the contrary, bosonic fields fulfill commutation relations, and thus one can consider arbitrary powers of its components. Since the R_Φ is a linear representation, monomials of degree k and, more generally, polynomials of degree k in the field components only get mixed among themselves, forming a linear representation R_{Φ^k} of G with dimension $\dim R_{\Phi^k} = n^k$.

At this point, one may ask how many invariants can be written at a given power k of the building block fields. This information is encoded in a generating function or partition function known as *Hilbert series*, which is defined as

$$\mathcal{H}_{\text{Inv}}^{G,R_\Phi}(q) \equiv \sum_{k=0}^{\infty} n_{\text{Inv}}(k) q^k\,, \qquad |q| < 1\,, \tag{2.4}$$

where $n_{\text{Inv}}(k)$ gives the number of invariant polynomials at degree k, and q is a grading variable associated to each field component in order to keep track of their powers.[2] As we will check later, this grading variable is required to have modulus $|q| < 1$, so that the Hilbert series converges—often, it can also be summed into an analytical function with a closed form. More generally, one may be interested in the number of covariants that transform as a certain irrep of the group. On that regard, we can extend the definition in Eq. (2.4) to any goal irrep R under consideration:

$$\mathcal{H}_{R}^{G,R_\Phi}(q) \equiv \sum_{k=0}^{\infty} n_R(k) q^k\,, \qquad |q| < 1\,. \tag{2.5}$$

The number $n_R(k)$ gives the multiplicity (number of repetitions) of the irrep R acting on a subspace of Φ^k or, more precisely,

$$R_{\Phi^k} = n_R(k) R \,\oplus\, \text{other irreps of } G\,. \tag{2.6}$$

Then, it is easy to see that the invariant or singlet representation $R = \text{Inv}$ is just a particular case of this more general scenario.

However, as it is common practice in particle physics, our set of building block fields Φ is typically specified as a collection of m irreps ϕ_i, in such a way that R_Φ forms a completely reducible representation of G:

$$\Phi = \{\phi_1, \phi_2, \ldots, \phi_m\}\,, \qquad R_\Phi = \bigoplus_{i=1}^{m} R_{\phi_i}\,, \tag{2.7}$$

with $\dim R_{\phi_i} = n_i$ and $\sum_{i=1}^{m} n_i = n$. It is important to note that each ϕ_i groups together several field components, with the same bosonic or fermionic statistics, that transform collectively under the irrep R_{ϕ_i}. In particular, the representation matrix g_{R_Φ} has a block-diagonal form, meaning that the different subspaces ϕ_i transform independently under $g_{R_{\phi_i}}$ and do not get mixed among themselves. Then, one could opt for a finer grading option, namely, to assign a different grading variable q_i, with $|q_i| < 1$, to each irrep ϕ_i (same grading variable for all of its components). In that case, we can define the multi-graded

[2] Grading variables are always Grassmann-even numbers, regardless of whether they refer to bosonic or fermionic field components.

Hilbert series as

$$\mathcal{H}_R^{G,R_\Phi}(q_1,\ldots,q_m) \equiv \sum_{k_1=0}^{\infty}\cdots\sum_{k_m=0}^{\infty} n_R(k_1,\ldots,k_m) q_1^{k_1}\cdots q_m^{k_m}\,, \qquad |q_i|<1\,, \tag{2.8}$$

and thus $n_R(k_1,\ldots,k_m)$ gives the multiplicity of the goal irrep R acting on the space $\phi_1^{k_1}\cdots\phi_m^{k_m}$, *i.e.*, the space of polynomials of degree $k=\sum_{i=1}^m k_m$ containing k_i components of the irrep ϕ_i. Naturally, we have

$$\lim_{q_i\to q}\mathcal{H}_R^{G,R_\Phi}(q_1,\ldots,q_m) = \mathcal{H}_R^{G,R_\Phi}(q)\,. \tag{2.9}$$

Finally, note that, in the pure fermionic scenario, the Hilbert series is truncated at degree $k_{\max} = \dim R_\Phi$, and thus there is a finite number of invariants and covariants. In such cases, we rather have a finite Hilbert polynomial instead of an infinite series.

2.2 The Molien-Weyl formula

Once we have defined the Hilbert series for group invariants and covariants, we are in good position to introduce how to compute them in a systematic way. Among the various methods to compute Hilbert series, the so-called Molien-Weyl formula [87] will be particularly useful for our purposes. It consists on an integral over the group elements given by

$$\mathcal{H}_R^{G,R_\Phi}(q) = \int \mathrm{d}\mu_G(x)\chi_R^*(x)\left(\prod_{i=1}^{m_b}\frac{1}{\det\Big[1-q\,g_{R_{\phi_i}}(x)\Big]}\right)\left(\prod_{i=1}^{m_f}\det\Big[1+q\,g_{R_{\phi_i}}(x)\Big]\right)\,, \qquad |q|<1\,, \tag{2.10}$$

where q is our grading variable, and x is a set of variables parametrizing the elements in the group G. Note also that $g_{R_{\phi_i}}(x)$ is the representation matrix of each irrep ϕ_i in R_Φ, while 1 stands for the identity matrix in the corresponding representation. Finally, m_b is the number of bosonic irreps and m_f the number of fermionic irreps in the set of building block fields Φ. In general, the integral in Eq. (2.10) should be carried out over all group elements in G. However, for connected Lie groups,[3] this can be restricted to an integral over the Cartan subgroup of G.[4] Then, the integrand in the Molien-Weyl formula is built out of the following three pieces.

(i) **The (modified) Haar measure** $\mathrm{d}\mu_G[g(x)]$. If G is a compact Lie group, this is the unique normalized measure on G which remains invariant under left and right translations performed by any fixed group element $\tilde{g}$. More precisely, when restricted to the Cartan subgroup, we are actually dealing with a modified Haar measure with a non-trivial form. For further details on their derivation, see the appendices in Ref. [79], where the specific form of the Haar measures for the classical Lie groups is also provided.

(ii) **The (Weyl) character** $\chi_R[g(x)]$ **of the goal irrep** R. The character of a group element $g(x)\in G$ is the trace of its corresponding representation matrix, hence it depends on both the group element g and the representation R. When G is a connected Lie group, any element of the group can be related to an element of the Cartan subgroup by conjugation. Since the character function

[3]Connected Lie groups satisfy that any finite group transformation can be obtained as a continuous sequence of infinitesimal transformations generated by the associated Lie algebra.

[4]The Cartan subgroup of a Lie group G is that generated by its Cartan subalgebra, consisting of the maximal number of mutually commuting Hermitian generators of the group.

is invariant under group conjugation, we can restrict ourselves to the characters of the Cartan subgroup, which are known as Weyl characters. An important result in group representation theory is that, for compact continuous groups, the characters of a group element in two unitary irreps are orthonormal upon integration over the Haar measure:[5]

$$\int \mathrm{d}\mu_G[g(x)]\chi^*_{R_1}[g(x)]\chi_{R_2}[g(x)] = \delta_{R_1 R_2}\,, \tag{2.11}$$

where R_1 and R_2 are unitary irreps of G. Importantly, this orthonormality relation holds when we consider instead the modified Haar measure and the Weyl characters over the Cartan subgroup.

(iii) **The graded (Weyl) character of the polynomial ring $\mathbb{r}$ in the building block fields.** As we will develop later, all polynomials in the building block fields, including any degree k, form a ring over the field of complex numbers $\mathbb{C}$, that we denote as $\mathbb{r} = \mathbb{C}[\Phi]$. The factors in parentheses in Eq. (2.10) arise from the evaluation of the sum, for all k, of the character function in the representation R_{Φ^k} graded or multiplied by q^k. Therefore, they encode a graded character over the polynomial ring $\mathbb{r}$ in the building block fields—see [87] for details. It is to be noticed that Eq. (2.10) can be easily extended to the multi-graded case by just assigning a different q_i in the determinant factor associated to each irrep ϕ_i.

In practical terms, the Molien-Weyl integration formula yields a contour integral over a set of r phase variables $z_i(x)$, being r the rank of the group G, *i.e.*, the number of Cartan generators. Then, each phase variable z_i can be integrated over the unit contour $|z_i| = 1$ by means of Cauchy's residue theorem. In this regard, it is important to recall that $|q| < 1$ when identifying the poles within the unit circle. Aiming to automate the different integrations, our `Mathematica` notebook HilbCalc provides general functions for computing each one of the aforementioned factors in the Molien-Weyl formula, and more importantly, it packages them together to calculate the Hilbert series (either single-graded or multi-graded) for group invariants or covariants restricted to the classical Lie groups $SU(n)$, $SO(n)$, $Sp(n = 2r)$, and $U(1)$ factors. Finally, we should note that, if the goal representation R is a completely reducible representation of G, *i.e.*, $R = \bigoplus_i R_i$ with R_i an irrep of G, it is easy to check that

$$\mathcal{H}^{G,R_\Phi}_R(q) = \sum_i \mathcal{H}^{G,R_\Phi}_{R_i}(q)\,. \tag{2.12}$$

All in all, the logic behind the Molien-Weyl formula is to make use of character orthogonality under the Haar measure $\mathrm{d}\mu_G(x)$ to extract the component of our interest irrep R in the graded character of the polynomial ring $\mathbb{r}$ in the building block fields. Although we do not elaborate on the explicit demonstration of the Molien-Weyl integration formula, this allows to obtain a closed form of the analytical function that generates the Hilbert series in Eq. (2.5) when expanding in powers of the grading variable q.

2.3 Algebraic structure of group invariants: polynomial ring

As anticipated before, the set of all polynomials in the building block fields Φ with coefficients in $\mathbb{C}$, denoted as $\mathbb{C}[\Phi]$, forms a polynomial ring $\mathbb{r}$ with the usual operations of addition and multiplication. These operations are closed in $\mathbb{C}[\Phi]$ and satisfy the following properties: (i) $(\mathbb{C}[\Phi], +)$ is an abelian group, (ii) multiplication is associative, and (iii) multiplication is distributive over addition. Furthermore, the

[5] Analogous results apply to discrete/finite groups.

ring is commutative if all building blocks are bosonic. Similarly, it is straightforward to check that the subset of invariant polynomials under the symmetry group G, denoted as $\mathbb{C}[\Phi]^G$, is indeed a subring $\mathbb{r}_{\text{Inv}} \subset \mathbb{r}$, since the previous operations are closed in $\mathbb{C}[\Phi]^G$.

The literature on invariant theory contains many interesting findings. Below, we summarize a selection of those that are particularly relevant to our subsequent analyses. We should point out that the following results only apply for bosonic building blocks. Since this will indeed be our case study in chapter 4, we will not address the fermionic scenario unless explicitly stated otherwise.

First, it is well-known that any G-invariant polynomial in the building block fields can be decomposed in a *unique* way as

$$G\text{-Inv Polynomial} = \sum_{i=0}^{n_S} p_i(P_1, \ldots, P_{n_P}) S_i \,, \tag{2.13}$$

that is, as a linear combination of *secondary invariants* $\{S_i\}_{i=0}^{n_S}$, with $S_0 \equiv 1$, with coefficients that are polynomials in the set of *primary invariants* $\{P_i\}_{i=1}^{n_P}$. This means that, in principle, any power of the primary invariants is needed to construct a G-invariant polynomial, while the secondary invariants only enter linearly. This is called the *Hironaka decomposition* of the G-invariant polynomial. In our previous notation, the number of secondary invariants is $n_S + 1$, and the number of primary invariants is n_P. The latter is also known as the *Krull dimension* and coincides with the number of continuous degrees of freedom in the theory. We should stress that there might be different choices for what we call primary and secondary invariants, but once these are fixed, the Hironaka decomposition of a G-invariant polynomial is indeed unique. Note also that the set of primary invariants forms, in turn, a subring, $\mathbb{r}_{\text{PInv}} \subset \mathbb{r}_{\text{Inv}}$, since addition and multiplication are closed in the subset of primary invariants.

On the other hand, it is also known that for a linear reductive group G—this includes simple[6] compact Lie groups, $U(1)$ abelian factors, finite groups, and their products—there exists a set of primary and secondary invariants from which one can construct the Hironaka decomposition of any G-invariant polynomial. In particular, the Hilbert series has a rational form given by

$$\mathcal{H}_{\text{Inv}}^{G,R_\Phi}(q) = \frac{N_{\text{Inv}}(q)}{D(q)} \qquad \begin{cases} N_{\text{Inv}}(q) = 1 + \displaystyle\sum_{i=1}^{n_S} q^{s_i} \\ D(q) = \displaystyle\prod_{i=1}^{n_P} (1 - q^{p_i}) \end{cases} , \tag{2.14}$$

where p_i and s_i give the order in q of each primary and secondary invariant, respectively. It is then clear that the number of factors in the denominator is n_P, and thus corresponds to the number of dof in the theory. We should emphasize that the Hilbert series in Eq. (2.14) does not identify the primary and secondary invariants explicitly, but rather it encodes how many there are and their corresponding order in q.

Finally, if G is a semisimple[7] Lie group, besides having the form quoted in Eq. (2.14), the numerator of the Hilbert series is palindromic, that is,

$$N_{\text{Inv}}(q) = q^r N_{\text{Inv}}(q^{-1}) \,, \tag{2.15}$$

where r is the highest power in $N_{\text{Inv}}(q)$.

[6] A Lie algebra is said to be simple if it contains no non-trivial invariant subalgebras, which are defined by a subset of generators that is closed under commutation with any element of the algebra.

[7] A Lie algebra is semisimple if it contains no non-trivial abelian invariant subalgebras.

2.4 Algebraic structure of group covariants: module over a ring

Now we turn to the mathematical structure of group covariants transforming under a certain irrep R of G. In contrast to the invariant representation, a general irrep R may have dimension greater than one. As a result, group-covariant polynomials can be viewed as multi-component vectors that transform collectively under R. The set of all rep-R covariant vectors built out of Φ, denoted as $\mathcal{M}_R^{G,R_\Phi}$, forms a module over the ring of invariant polynomials, ${}_{\mathbb{r}_{\text{Inv}}}\mathcal{M}_R^{G,R_\Phi}$, with the usual operations of addition and multiplication. This means: (i) $(\mathcal{M}_R^{G,R_\Phi},+)$ is an abelian group, (ii) multiplication by an element in the ring yields another rep-R covariant vector—this is why the elements in the ring must be invariant polynomials—, (iii) multiplication is distributive over both vector addition and addition of invariants, and associative with respect to multiplication of invariants, (iv) the identity element lies in the ring of invariants. Note that if $\mathbb{r}_{\text{Inv}}$ were a field,[8] then the module would in fact be a genuine vector space. Likewise, one could alternatively define the module over the ring of primary invariants, namely, ${}_{\mathbb{r}_{\text{PInv}}}\mathcal{M}_R^{G,R_\Phi}$.

Following Ref. [87], we proceed to outline the main definitions and properties of a module over a ring.

(i) **(Finite) Generating set**. This is defined as a (finite) set of vectors such that any vector in the module can be written as a linear combination of them with coefficients in the ring. The existence of a finite generating set is not guaranteed in general. A module is said to be finitely generated if there exists a finite generating set.

(ii) **Linear (in)dependence**. A finite set of vectors is linearly independent if there exists no non-trivial linear combination of them with coefficients in the ring that vanishes. Otherwise, the set is linearly dependent.

(iii) **Basis**. Finite generating set of linearly independent vectors. It is important to emphasize that even if a finite generating set exists, it may be linearly dependent. Since the ring of coefficients does not contain an inverse under multiplication, such a set cannot, in general, be reduced to a linearly independent one, and hence to a basis. Not all modules admit a basis; whenever they do, these are called free modules.

(iv) **Rank**. The rank of a module is defined as the maximum number of linearly independent vectors.

Interestingly, Hilbert series encode valuable information about the structure of the module $\mathcal{M}_R^{G,R_\Phi}$ defined over different rings, namely, $\mathbb{r}_{\text{Inv}}$ or $\mathbb{r}_{\text{PInv}}$. In what follows, we summarize how this information can be read out properly from the Hilbert series. As in the case of invariants, we restrict ourselves to bosonic building blocks, since this will be the relevant scenario for the analyses in upcoming chapters.

First of all, we should point out that, when G is a linear reductive group, the modules ${}_{\mathbb{r}_{\text{Inv}}}\mathcal{M}_R^{G,R_\Phi}$ and ${}_{\mathbb{r}_{\text{PInv}}}\mathcal{M}_R^{G,R_\Phi}$ are finetely generated. In particular, the summed Hilbert series for the irrep R is also a rational function [89]:

$$\mathcal{H}_R^{G,R_\Phi}(q) = \frac{N_R(q)}{D(q)}\,, \tag{2.16}$$

where the denominator $D(q)$ is given in Eq. (2.14) and encodes the set of primary invariants. In contrast, $N_R(q)$ is now a polynomial with both positive and negative integer coefficients. When we refer to ${}_{\mathbb{r}_{\text{PInv}}}\mathcal{M}_R^{G,R_\Phi}$, *i.e.*, the module of rep-R covariants over the ring of primary invariants, the positive terms

[8] This would require the existence of an inverse under multiplication for all non-zero elements in the ring of invariants, and commutativity of multiplication.

in the numerator $N_R(q)$ contain the full generating set of the module, and inform us about their number and order. Instead, negative terms represent redundancies in the generating set, that is, linear relations among them. Consequently, the rank of the module ${}_{\mathscr{r}_{\mathrm{PInv}}}\mathcal{M}_R^{G,R_\Phi}$ can be simply computed as

$$\mathrm{rank}\left({}_{\mathscr{r}_{\mathrm{PInv}}}\mathcal{M}_R^{G,R_\Phi}\right) = N_R(q)\big|_{q\to 1} . \tag{2.17}$$

Nevertheless, for the purposes of chapter 4, we will be interested in determining how many independent group covariants built out of a set of bosonic building blocks are present in ${}_{\mathscr{r}_{\mathrm{Inv}}}\mathcal{M}_R^{G,R_\Phi}$, that is, in the module of rep-R covariants over the full ring of invariants. In other words, we want to compute the rank of this module. To this aim, one needs to consider two Hilbert series, namely, $\mathcal{H}_R^{G,R_\Phi}(q)$ and $\mathcal{H}_{\mathrm{Inv}}^{G,R_\Phi}(q)$. In particular, it can be shown—see [87] for details—that their ratio, evaluated at $q = 1$, yields the rank of the module ${}_{\mathscr{r}_{\mathrm{Inv}}}\mathcal{M}_R^{G,R_\Phi}$:

$$\mathrm{rank}\left({}_{\mathscr{r}_{\mathrm{Inv}}}\mathcal{M}_R^{G,R_\Phi}\right) = \left.\frac{\mathcal{H}_R^{G,R_\Phi}(q)}{\mathcal{H}_{\mathrm{Inv}}^{G,R_\Phi}(q)}\right|_{q\to 1} . \tag{2.18}$$

When G is a connected semisimple Lie group, this rank satisfies an upper bound given by

$$\mathrm{rank}\left({}_{\mathscr{r}_{\mathrm{Inv}}}\mathcal{M}_R^{G,R_\Phi}\right) \leq \dim R\,, \tag{2.19}$$

being $\dim R$ the dimension of the goal irrep R. There is *rank saturation* when the equality is fulfilled, meaning that the maximum number of linearly independent rep-R covariants equals the number of its components. Remarkably, the math literature provides a powerful result known as Brion's theorem [88, 89], which establishes the following: let $H \subset G$ be the unbroken subgroup when the building block fields take a *generic* vev $\langle\Phi\rangle$, the rank of the module ${}_{\mathscr{r}_{\mathrm{Inv}}}\mathcal{M}_R^{G,R_\Phi}$ is given by

$$\mathrm{rank}\left({}_{\mathscr{r}_{\mathrm{Inv}}}\mathcal{M}_R^{G,R_\Phi}\right) = \dim R^H\,, \tag{2.20}$$

where R^H denotes the subspace of the goal irrep R that is left invariant by the elements in the subgroup $H \subset G$. In other words, $\dim R^H$ gives the number of invariant irreps in the branching rule of R for $G \to H$. Then, the bound in Eq. (2.19) is evident, since $\dim R^H \leq \dim R$ always holds. When H is the trivial subgroup, it is clear than rank saturation will occur. However, if H is non-trivial, we might reach rank saturation depending on the particular goal irrep R under consideration. We should stress that the concept of *saturation* will be generalized in chapter 4.

To close this section, let us draw one final comment. In the context of spurion analysis, which will be addressed in chapter 4, we are usually interested in evaluating the invariants constructed from a set of building blocks on their specific numerical values or, said differently, on their vacuum expectation values. Then, they reduce to ordinary complex numbers, and the ring of invariants becomes a field. As a result, the notion of a module over a ring translates into that of a conventional vector space over the field of complex numbers. Concepts such as basis and linear independence can then be treated as usual in the language of particle physics. In particular, when there is rank saturation, it is possible to find a basis in the vector space of covariants, and the rank of the module $\mathrm{rank}\left({}_{\mathscr{r}_{\mathrm{Inv}}}\mathcal{M}_R^{G,R_\Phi}\right)$ directly gives us the number of independent components in rep-R covariants.

2.5 Illustrative application to flavor physics

It might be instructive to illustrate some of the properties discussed above by applying the Hilbert series technology to a familiar example: the quark flavor invariants in the SM. This was explored for the first time in Refs. [71, 72], where the analysis was extended to the lepton sector, including neutrino masses through the dim-5 Weinberg operator and within the type I seesaw framework. Here, we revisit some of the results derived in those works. In doing so, we take the opportunity to present an alternative approach to several topics discussed in Secs. 1.4 and 1.5 from chapter 1, such as the counting of physical dof or the question of CP violation.

Let us consider the SM quark sector. As we know, the flavor sector is parametrized in its entirety by two 3×3 Yukawa matrices Y_u and Y_d, together with their hermitian conjugates. Taking into account the flavor symmetry transformations of the quark fields given in Eq. (1.44), the Yukawa couplings get transformed as bifundamental representations in flavor space—see Eq. (1.95). The structure of flavor invariants constructed from the Yukawa matrices, which constitute our bosonic building blocks, is then encoded in the Hilbert series

$$\mathcal{H}_{\text{Inv}}^{\text{SM-quark}}(q) = \frac{1+q^{12}}{(1-q^2)^2(1-q^4)^3(1-q^6)^4(1-q^8)} \,. \tag{2.21}$$

In light of our previous discussion, the number of denominator factors indicates that there are 10 physical dof, corresponding to 6 quark masses, 3 mixing angles, and 1 complex phase.[9] In addition, from the denominator we can also check that there are ten primary invariants, namely, two of order two, three of order four, four of order six, and one of order eight; while the numerator reflects the presence of one secondary invariant of order twelve. Following Ref. [71], we can choose as primary invariants

$$I_{2,0}^P = \mathrm{tr}(H_u)\,, \qquad I_{0,2}^P = \mathrm{tr}(H_d)\,, \tag{2.22}$$
$$I_{4,0}^P = \mathrm{tr}\big(H_u^2\big)\,, \qquad I_{0,4}^P = \mathrm{tr}\big(H_d^2\big)\,, \tag{2.23}$$
$$I_{6,0}^P = \mathrm{tr}\big(H_u^3\big)\,, \qquad I_{0,6}^P = \mathrm{tr}\big(H_d^3\big)\,, \tag{2.24}$$
$$I_{4,2}^P = \mathrm{tr}\big(H_u^2 H_d\big)\,, \qquad I_{2,4}^P = \mathrm{tr}\big(H_u H_d^2\big)\,, \tag{2.25}$$
$$I_{2,2}^P = \mathrm{tr}(H_u H_d)\,, \qquad I_{4,4}^P = \mathrm{tr}\big(H_u^2 H_d^2\big)\,, \tag{2.26}$$

and the single secondary invariant as

$$\begin{aligned} I_{6,6}^S &= \det[H_u, H_d] = \frac{1}{3}\,\mathrm{tr}[H_u, H_d]^3 \\ &= 2i\,(m_u^2 - m_c^2)(m_u^2 - m_t^2)(m_c^2 - m_t^2)(m_d^2 - m_s^2)(m_d^2 - m_b^2)(m_s^2 - m_b^2)J\,, \end{aligned} \tag{2.27}$$

which corresponds to the WB-invariant quantity presented in Eq. (1.107) encoding CP violation. As we can check, all primary invariants are real since they correspond to the traces of hermitian matrices, and thus they are CP-even. In contrast, the secondary invariant is pure imaginary and hence CP-odd. One can check that its square, which is CP-even, can be written as a polynomial in the primary invariants.[10] This is reflected in the Hilbert series by the absence of an $\mathcal{O}(q^{24})$ term in the numerator of Eq. (2.21). Taking into account Eq. (2.13), and for a fixed choice of primary and secondary invariants, any polynomial

[9] The QCD $\bar{\theta}$ parameter does not arise in this context since we are including the anomalous axial $U(1)$ factor in our symmetry transformations.

[10] The relations among invariants are often called *syzygies*.

that is invariant under the quark flavor symmetry group in Eq. (1.44), can be uniquely written as

$$p_0(I^P_{2,0}\,, \,\dots\,, I^P_{4,4}) + p_1(I^P_{2,0}\,, \,\dots\,, I^P_{4,4})I^S_{6,6}\,. \tag{2.28}$$

As we have argued in previous chapters, physical parameters are, by definition, observable quantities, and therefore they must be contained within WB-invariant quantities. In our current language, this means that they are determined by the set of primary and secondary invariants. In particular, from the CP-even primary invariants, one can extract the six quark masses, $\cos\theta_{ij}$ of the three CKM mixing angles, and $\cos\delta$ of the CKM complex phase. Note that, since the mixing angles θ_{ij} are chosen to lie in the first quadrant, they are completely determined at this point. This is not the case for the complex phase δ, because an overall sign is missed. This remaining information is captured by the CP-odd secondary invariant, which allows for the extraction of $\sin\delta$ through the Jarlskog invariant J—see Eq. (1.61). Remarkably, one may have realized that the emergence of CP violation is already determined at the level of the CP-even primary invariants, consistent with the fact that the area of the unitarity triangle is fully fixed by the lengths of its sides. The secondary invariant serves only to resolve a $\mathbb{Z}_2$ ambiguity in the definition of the unitarity triangle.

3 Multi-Higgs-Doublet Models

We have seen before that the scalar sector of the SM is minimal, in the sense that it contains a single scalar $SU(2)_L$ doublet. This naturally raises the question of whether an extension of the scalar sector is possible in the same way as we have multiple generations of fermions. In this regard, one of the most relevant theoretical constraints on the addition of new fundamental scalars comes from the ρ parameter. At tree-level, the SM predicts $\rho = 1$, yielding the relation $M_W = \cos\theta_W M_Z$ among gauge boson masses, which is strongly supported by experimental data [23]. It is well-known that in $SU(3)_C \times SU(2)_L \times U(1)_Y$ gauge theories with additional $SU(2)_L$ doublets with hypercharge $Y = \pm 1/2$ the tree-level value of the ρ parameter is preserved. We will focus on this kind of scenario, namely, scalar extensions consisting of multiple Higgs doublets based on the SM gauge group.

Setting aside the question of (non-)minimality, there are many other theoretical motivations to pursue an enlarged scalar sector. For instance, the origin of neutrino masses in the context of the type II seesaw mechanism is triggered by an $SU(2)_L$ triplet of scalars. Likewise, extensions of the scalar sector allow for new sources of CP violation, either explicitly at the Lagrangian level, or spontaneously through the vacuum structure. This is, of course, relevant to explain the origin of the matter-antimatter asymmetry of the Universe within baryogenesis models. Also related to the question of CP violation, we encounter the strong CP problem, for which a possible solution based on the global $U(1)$ Peccei-Quinn symmetry requires the presence of two Higgs doublets. On another avenue, the minimal supersymmetric extension of the SM contains two scalar doublets in order to give masses to both up-type and down-type quarks, as well as to ensure anomaly cancellation. Interestingly, it is known that some scalar extensions could offer a dark matter candidate, such as the inert model with two Higgs doublets. Finally, we should stress that extended scalar sectors generally lead to a rich phenomenology with many novel features that can be tested at collider experiments, *e.g.*, the appearance of new scalar bosons or FCNC. They could also contribute to alleviate potential tensions arising in low-energy observables, such as leptonic $g-2$ [7,8,90].

Although there is a vast literature in extended scalar sectors, as anticipated before we will exclusively focus on models based on the $SU(3)_C \times SU(2)_L \times U(1)_Y$ gauge group including multiple Higgs doublets and, as a more concrete scenario, in two-Higgs-doublet models (2HDMs). The purpose of this chapter is to introduce the basic and necessary ingredients that will be relevant for our analyses in future chapters. For more detailed and comprehensive reviews on extended Higgs sector, we refer to [58, 91, 92] and references therein.

As a final remark, we should mention that there exist several alternative extensions of the scalar sector, such as composite Higgs models, technicolor, or extra-dimensional frameworks, which we will not consider here. Likewise, we do not focus on GUTs or supersymmetric models, that involve a more elaborate theoretical framework.

3.1 Multiple Higgs doublets

Starting from the SM gauge group, we consider n scalar fields Φ_a, with $n > 1$ and $a = 1, \dots, n$, transforming as $\Phi_a \sim (\mathbf{1}, \mathbf{2}, 1/2)$, that is, as $SU(2)_L$ doublets with hypercharge $1/2$, written as

$$\Phi_a = \begin{pmatrix} \phi_a^+ \\ \phi_a^0 \end{pmatrix} . \tag{3.1}$$

The most general renormalizable scalar Lagrangian reads

$$\mathscr{L}_{\text{scalar}} = (D^\mu \Phi_a)^\dagger (D_\mu \Phi_a) - \mathscr{V}(\Phi_a) , \tag{3.2}$$

with covariant derivative defined in Eq. (1.22),[1] and scalar potential given by

$$\mathscr{V}(\Phi_a) = Y_{ab} \Phi_a^\dagger \Phi_b + Z_{ab,cd} (\Phi_a^\dagger \Phi_b)(\Phi_c^\dagger \Phi_d) , \tag{3.3}$$

where the sum over a, b, c, d is implicit, and parentheses indicate contraction of $SU(2)_L$ indices. One can readily check that $Z_{ab,cd} = Z_{cd,ab}$, and hermiticity of the potential imposes $Y_{ab} = Y_{ba}^*$ and $Z_{ab,cd} = Z_{ba,dc}^*$. Taking this into account, the counting of real dof that are present in the most general scalar potential is summarized in Table 3.1. The quadratic couplings Y_{ab} have dimensions of mass squared, while the quartic couplings $Z_{ab,cd}$ are dimensionless. The latter have to satisfy stability conditions to ensure boundedness from below, as well as perturbative unitarity constraints [93, 94].

	Quadratic	**Quartic**	**Total**
Moduli	$\frac{n(n+1)}{2}$	$\frac{n^2(n^2+3)}{4}$	$\frac{n(n^3+5n+2)}{4}$
Phases	$\frac{n(n-1)}{2}$	$\frac{n^2(n^2-1)}{4}$	$\frac{n(n^3+n-2)}{4}$
Total	n^2	$\frac{n^2(n^2+1)}{2}$	$\frac{n^2(n^2+3)}{2}$

Table 3.1: Real parameters in the multi-Higgs-doublet model scalar potential.

Assuming neutrality of the vacuum in order to have the appropriate EWSB, we have

$$\langle \Phi_a \rangle = \frac{v_a e^{i\theta_a}}{\sqrt{2}} \begin{pmatrix} 0 \\ 1 \end{pmatrix} . \tag{3.4}$$

The parameters $v_a \in \mathbb{R}^+$ and $\theta_a \in [0, 2\pi)$ can be understood as the moduli and phases of complex vevs, respectively. The former are constrained by $\sum_{a=1}^n v_a^2 = v^2$, with $v \simeq 246$ GeV as in the SM, since all scalar doublets are coupled in the same way to electroweak gauge bosons. On the other hand, individual phases have no physical meaning by themselves; in particular, one can always perform a $U(1)_Y$ gauge transformation to set one of them equal to zero, say $\theta_1 = 0$.

The vacuum choice in Eq. (3.4) imposes additional constraints on the parameters of the potential through the stationarity conditions, namely, that the vevs of the scalar fields must be an extremum of the potential:

$$\mathscr{V}(\langle \Phi_1 \rangle, \dots, \langle \Phi_n \rangle) \equiv V(v_1, \dots, v_n, \theta_1, \dots, \theta_n) , \tag{3.5}$$

[1] Non-diagonal kinetic terms can be eliminated by means of a non-unitary rotation at any order of the perturbative expansion.

such that

$$\partial_{v_1} V = \cdots = \partial_{v_n} V = 0\,, \qquad \partial_{\theta_1} V = \cdots = \partial_{\theta_n} V = 0\,, \tag{3.6}$$

where we have introduced the shorthand notation $\partial_x V \equiv \frac{\partial V}{\partial x}$. The lack of physical meaning of individual phases is translated into $\sum_{a=1}^{n} \partial_{\theta_a} V = 0$ by construction, that is, regardless of whether each term is individually zero. Therefore, we are left with $2n-1$ independent minimization conditions. For the purposes of subsequent sections, it is convenient to introduce the $n \times n$ Hermitian matrix $\mathcal{V}$ defined by

$$\mathcal{V}_{ab} \equiv \frac{v_a v_b}{2} e^{i(\theta_a - \theta_b)}\,, \tag{3.7}$$

which is constructed from the vevs of the different Higgs doublets and satisfies $\mathcal{V}_{ab} = \mathcal{V}_{ba}^*$.

Expansion of the fields around the selected vevs can be written as

$$\Phi_a = \frac{e^{i\theta_a}}{\sqrt{2}} \begin{pmatrix} \sqrt{2}\varphi_a^+ \\ v_a + \rho_a + i\eta_a \end{pmatrix}\,, \tag{3.8}$$

where we have factored out the vacuum phase $e^{i\theta_a}$. It is clear that, besides the would-be Goldstone bosons that are absorbed by the $W^\pm$ and Z bosons to gain a mass, there are $n-1$ pairs of charged scalars and $2n-1$ neutral states in a theory with n Higgs doublets. The mass terms contained in $\mathscr{V}$ are of the form

$$-\mathscr{L}_{\text{Mass}} = \vec{C}^\dagger M_\pm^2 \vec{C} + \frac{1}{2} \vec{N}^T M_0^2 \vec{N}\,, \tag{3.9}$$

with $\vec{C}^\dagger = (\varphi_1^+, \ldots, \varphi_n^+)$, $\vec{N}^T = (\rho_1, \ldots, \rho_n, \eta_1, \ldots, \eta_n)$, $M_\pm^2$ the $n \times n$ charged scalar mass matrix, and M_0^2 the $2n \times 2n$ neutral scalar mass matrix. The elements of the mass matrices are computed as

$$(M_\pm^2)_{ij} = \left[\frac{\partial^2 \mathscr{V}}{\partial \varphi_i^+ \partial \varphi_j^-}\right]\,, \tag{3.10}$$

and

$$M_0^2 = \begin{pmatrix} M_\rho^2 & M_{\rho\eta}^2 \\ (M_{\rho\eta}^2)^T & M_\eta^2 \end{pmatrix}\,, \tag{3.11}$$

with

$$M_\rho^2 = \left[\frac{\partial^2 \mathscr{V}}{\partial \rho_i \partial \rho_j}\right]\,, \qquad M_\eta^2 = \left[\frac{\partial^2 \mathscr{V}}{\partial \eta_i \partial \eta_j}\right]\,, \qquad M_{\rho\eta}^2 = \left[\frac{\partial^2 \mathscr{V}}{\partial \rho_i \partial \eta_j}\right]\,. \tag{3.12}$$

The squared brackets indicate that second derivatives are evaluated at $\varphi_a^\pm, \rho_a, \eta_a \to 0$. Given that $M_\rho^2 = (M_\rho^2)^T$ and $M_\eta^2 = (M_\eta^2)^T$, it is clear that M_0^2 is a symmetric matrix, while $M_\pm^2$ is Hermitian.

Finally, it is important to notice that, similarly to what happens with the different flavors in the fermion sector, one is allowed to perform an $n \times n$ unitary rotation of the scalar doublets, which share the same quantum numbers, that leaves the gauge-kinetic terms invariant. In particular, the transformation

$$\Phi_a \quad \longrightarrow \quad \Phi_a' \equiv U_{ab} \Phi_b\,, \tag{3.13}$$

with $UU^\dagger = U^\dagger U = 1_{n\times n}$, yields

$$\mathcal{V}_{ab} \quad \longrightarrow \quad \mathcal{V}_{ab}' \equiv U_{ac} \mathcal{V}_{cd} U_{bd}^*\,, \tag{3.14}$$

while the couplings in the scalar potential transform as

$$Y_{ab} \longrightarrow Y'_{ab} \equiv U_{ac} Y_{cd} U^*_{bd}\,, \qquad Z_{ab,cd} \longrightarrow Z'_{ab,cd} \equiv U_{ap} U_{cr} Z_{pq,rs} U^*_{bq} U^*_{ds}\,. \tag{3.15}$$

The rotation in Eq. (3.13) can be incorporated into the definition of WBT presented before. As a consequence, physically meaningful quantities must be invariant under such transformations in the scalar space.

In the following, we continue our exploration of the basic features of multi-Higgs-doublet models (MHDMs) focusing on their simplest realization: the 2HDM.

3.2 Two-Higgs-Doublet Models

Two-Higgs-doublet models were originally proposed by T. D. Lee [95,96] in 1973 in order to break T (time reversal) and CP spontaneously, thereby placing the breaking of these discrete symmetries on the same footing as the electroweak gauge symmetry breaking. Since then, 2HDMs have been extensively studied in the literature [92], further motivated by the fact that the scalar sector of the minimal supersymmetric SM includes two scalar doublets. In addition, it is well known that 2HDMs exhibit a rich and diverse phenomenology, which we will explore in upcoming chapters.

The most general renormalizable potential constructed from two scalar doublets Φ_1 and Φ_2 reads

$$\begin{aligned}\mathscr{V}(\Phi_1,\Phi_2) = {}& \mu_{11}^2 \Phi_1^\dagger\Phi_1 + \mu_{22}^2 \Phi_2^\dagger\Phi_2 + \left(\mu_{12}^2 \Phi_1^\dagger\Phi_2 + \text{H.c.}\right) \\ & + \lambda_1(\Phi_1^\dagger\Phi_1)^2 + \lambda_2(\Phi_2^\dagger\Phi_2)^2 + 2\lambda_3(\Phi_1^\dagger\Phi_1)(\Phi_2^\dagger\Phi_2) + 2\lambda_4(\Phi_1^\dagger\Phi_2)(\Phi_2^\dagger\Phi_1) \\ & + \lambda_5(\Phi_1^\dagger\Phi_2)^2 + \lambda_6(\Phi_1^\dagger\Phi_1)(\Phi_1^\dagger\Phi_2) + \lambda_7(\Phi_2^\dagger\Phi_2)(\Phi_1^\dagger\Phi_2) + \text{H.c.}\,,\end{aligned} \tag{3.16}$$

where $\{\mu_{11}^2, \mu_{22}^2, \lambda_1, \lambda_2, \lambda_3, \lambda_4\}$ are real, and $\{\mu_{12}^2, \lambda_5, \lambda_6, \lambda_7\}$ are in general complex. This gives a total of fourteen real parameters, ten moduli and four phases, arising from the scalar potential. Nevertheless, not all of them are physical, since an appropriate basis transformation allows one to remove unphysical parameters, leaving only eleven real dof [97, 98]. The parameters in Eq. (3.16) are related to those in Eq. (3.3) as

$$Y_{11} = \mu_{11}^2\,, \qquad Y_{22} = \mu_{22}^2\,, \qquad Y_{12} = \mu_{12}^2\,, \qquad Y_{21} = \mu_{21}^2 = (\mu_{12}^2)^*\,, \tag{3.17}$$

and

$$\begin{aligned}&Z_{1111} = \lambda_1\,, && Z_{2222} = \lambda_2\,, && Z_{1122} = Z_{2211} = \lambda_3\,, && Z_{1221} = Z_{2112} = \lambda_4\,, \\ &Z_{1212} = \lambda_5\,, && Z_{2121} = \lambda_5^*\,, && Z_{1112} = Z_{1211} = \lambda_6/2\,, && Z_{1121} = Z_{2111} = \lambda_6^*/2\,, \\ &Z_{2212} = Z_{1222} = \lambda_7/2\,, && Z_{2221} = Z_{2122} = \lambda_7^*/2\,. && &&\end{aligned} \tag{3.18}$$

In this framework, the scalar spectrum consists of three wbGBs, two physical charged scalars, and three physical neutral states. On that regard, it is clear that the diagonalization of the Hermitian charged scalar mass matrix in Eq. (3.9) is achieved through a unitary transformation, and thus we can use the freedom in Eq. (3.13) to move into the basis where the charged scalars correspond to their mass eigenstates. This basis transformation is of the form

$$\begin{pmatrix} H_1 \\ H_2 \end{pmatrix} = R_\beta \begin{pmatrix} e^{-i\theta_1} & 0 \\ 0 & e^{-i\theta_2} \end{pmatrix} \begin{pmatrix} \Phi_1 \\ \Phi_2 \end{pmatrix}, \qquad \text{with} \qquad R_\beta = \begin{pmatrix} c_\beta & s_\beta \\ -s_\beta & c_\beta \end{pmatrix}, \tag{3.19}$$

being $c_\beta \equiv \cos\beta \equiv v_1/v$, $s_\beta \equiv \sin\beta \equiv v_2/v$, and $t_\beta \equiv \tan\beta = v_2/v_1$, where $\beta \in [0, \pi/2]$ without loss of generality, and $R_\beta R_\beta^T = R_\beta^T R_\beta = 1_{2\times 2}$. Remarkably, in this basis only the doublet H_1 has a vev, namely,

$$\langle H_1 \rangle = \frac{v}{\sqrt{2}} \begin{pmatrix} 0 \\ 1 \end{pmatrix}, \qquad \langle H_2 \rangle = \begin{pmatrix} 0 \\ 0 \end{pmatrix}, \tag{3.20}$$

and the explicit degrees of freedom can be written as

$$H_1 = \frac{1}{\sqrt{2}} \begin{pmatrix} \sqrt{2} G^+ \\ v + H^0 + i G^0 \end{pmatrix}, \qquad H_2 = \frac{1}{\sqrt{2}} \begin{pmatrix} \sqrt{2} H^+ \\ R^0 + i I^0 \end{pmatrix}. \tag{3.21}$$

where

$$\begin{pmatrix} G^+ \\ H^+ \end{pmatrix} = R_\beta \begin{pmatrix} \varphi_1^+ \\ \varphi_2^+ \end{pmatrix}, \qquad \begin{pmatrix} H^0 \\ R^0 \end{pmatrix} = R_\beta \begin{pmatrix} \rho_1 \\ \rho_2 \end{pmatrix}, \qquad \begin{pmatrix} G^0 \\ I^0 \end{pmatrix} = R_\beta \begin{pmatrix} \eta_1 \\ \eta_2 \end{pmatrix}. \tag{3.22}$$

It is straightforward to see that the spontaneous electroweak symmetry breaking is triggered by the vev of the first Higgs doublet, which has the same form as in the SM. Consequently, in this basis, usually called *charged Higgs basis* [99, 100] or *Higgs basis* [60, 101, 102], the fields G^0 and $G^\pm$ can be readily identified as the wbGBs. The scalar potential in the Higgs basis can be written as

$$\begin{aligned} \mathscr{V}(H_1, H_2) = {} & M_{11}^2 H_1^\dagger H_1 + M_{22}^2 H_2^\dagger H_2 + \left(M_{12}^2 H_1^\dagger H_2 + \text{H.c.} \right) \\ & + \Lambda_1 (H_1^\dagger H_1)^2 + \Lambda_2 (H_2^\dagger H_2)^2 + 2\Lambda_3 (H_1^\dagger H_1)(H_2^\dagger H_2) + 2\Lambda_4 (H_1^\dagger H_2)(H_2^\dagger H_1) \\ & + \Lambda_5 (H_1^\dagger H_2)^2 + \Lambda_6 (H_1^\dagger H_1)(H_1^\dagger H_2) + \Lambda_7 (H_2^\dagger H_2)(H_1^\dagger H_2) + \text{H.c.}, \end{aligned} \tag{3.23}$$

with $\{M_{11}^2, M_{22}^2, \Lambda_1, \Lambda_2, \Lambda_3, \Lambda_4\}$ real, and $\{M_{12}^2, \Lambda_5, \Lambda_6, \Lambda_7\}$ complex in general—these can be related to the ones in Eq. (3.16) taking into account Eqs. (3.15) and (3.18). The mass terms for scalars are contained in the quadratic part of the potential, and are of the form

$$\mathscr{V} \supset M_{H^\pm}^2 H^+ H^- + \frac{1}{2} \begin{pmatrix} H^0 & R^0 & I^0 \end{pmatrix} \mathcal{M}_0^2 \begin{pmatrix} H^0 \\ R^0 \\ I^0 \end{pmatrix}, \tag{3.24}$$

where $M_{H^\pm}^2 = M_{22}^2 + v^2 \Lambda_3$ is the mass of physical charged scalars $H^\pm$. In contrast, the neutral states H^0, R^0, and I^0 cannot be identified yet as the mass eigenstates. On that regard, the symmetric neutral scalar mass matrix $\mathcal{M}_0^2$, given by

$$\mathcal{M}_0^2 = \begin{pmatrix} 2v^2 \Lambda_1 & v^2 \text{Re}\,\Lambda_6 & -v^2 \text{Im}\,\Lambda_6 \\ v^2 \text{Re}\,\Lambda_6 & M_{22}^2 + v^2(\Lambda_3 + \Lambda_4 + \text{Re}\,\Lambda_5) & -v^2 \text{Im}\,\Lambda_5 \\ -v^2 \text{Im}\,\Lambda_6 & -v^2 \text{Im}\,\Lambda_5 & M_{22}^2 + v^2(\Lambda_3 + \Lambda_4 - \text{Re}\,\Lambda_5) \end{pmatrix}, \tag{3.25}$$

can be diagonalized through an orthogonal transformation R, with $RR^T = R^T R = 1_{3\times 3}$ and $\det R = 1$, as

$$R^T \mathcal{M}_0^2 R = \text{diag}(M_h^2, M_H^2, M_A^2), \tag{3.26}$$

in such a way that the physical scalars are given by

$$\begin{pmatrix} h \\ H \\ A \end{pmatrix} = R^T \begin{pmatrix} H^0 \\ R^0 \\ I^0 \end{pmatrix} . \tag{3.27}$$

Note that if the parameters in the scalar potential are real, the matrix $\mathcal{M}_0^2$ is block-diagonal, and this feature is, in turn, translated into the diagonalization matrix R. In this case, the physical states $\{h, H\}$ are linear combinations of $\{H^0, R^0\}$, while $A = I^0$. As we shall see in Sec. 3.2.2, this scenario emerges in the absence of CP violation in the scalar sector.

3.2.1 Yukawa sector

We proceed now to discuss the Yukawa sector of the 2HDM, restricting our analysis to the quark sector for the sake of concreteness. The most general Yukawa interactions in the presence of two Higgs doublets can be written as

$$-\mathscr{L}_{\rm Y}^{\rm quark} = \overline{Q_L^0}(Y_1^u\widetilde{\Phi}_1 + Y_2^u\widetilde{\Phi}_2)u_R^0 + \overline{Q_L^0}\left(Y_1^d\Phi_1 + Y_2^d\Phi_2\right) d_R^0 + \text{H.c.}\,, \tag{3.28}$$

where $\widetilde{\Phi}_a \equiv \epsilon\Phi_a^* = i\sigma^2\Phi_a^*$ as usual. In this case, we have two Yukawa matrices Y_a^f $(a = 1, 2)$ in both up-type and down-type sectors $(f = u, d)$, which are $n_g \times n_g$ general complex matrices. Their interpretation is more transparent in the Higgs basis, where we have

$$-\frac{v}{\sqrt{2}}\mathscr{L}_{\rm Y}^{\rm quark} = \overline{Q_L^0}(M_u^0\widetilde{H}_1 + N_u^0\widetilde{H}_2)u_R^0 + \overline{Q_L^0}\left(M_d^0H_1 + N_d^0H_2\right) d_R^0 + \text{H.c.}\,, \tag{3.29}$$

with

$$M_u^0 = \frac{v}{\sqrt{2}}e^{-i\theta_1}\left(c_\beta Y_1^u + e^{-i\theta}s_\beta Y_2^u\right)\,, \qquad M_d^0 = \frac{v}{\sqrt{2}}e^{i\theta_1}\left(c_\beta Y_1^d + e^{i\theta}s_\beta Y_2^d\right)\,, \tag{3.30}$$

$$N_u^0 = \frac{v}{\sqrt{2}}e^{-i\theta_1}\left(-s_\beta Y_1^u + e^{-i\theta}c_\beta Y_2^u\right)\,, \qquad N_d^0 = \frac{v}{\sqrt{2}}e^{i\theta_1}\left(-s_\beta Y_1^d + e^{i\theta}c_\beta Y_2^d\right)\,, \tag{3.31}$$

and $\theta \equiv \theta_2 - \theta_1$. It is then clear that M_f^0 correspond to non-diagonal fermion mass matrices, since they are coupled to the only Higgs doublet that acquires a vev, that is, H_1. Bidiagonalization of the mass matrices proceeds in the same way as presented in Eqs. (1.46) and (1.47)—see App. B for details—, leading to

$$U_{u_L}^\dagger M_u^0 U_{u_R} = M_u = \text{diag}(m_u, m_c, m_t, \dots)\,, \qquad U_{d_L}^\dagger M_d^0 U_{d_R} = M_d = \text{diag}(m_d, m_s, m_b, \dots)\,, \tag{3.32}$$

where U_{f_L} and U_{f_R} are $n_g \times n_g$ unitary matrices, being $V \equiv U_{u_L}^\dagger U_{d_L}$ the CKM unitary matrix. The key difference with respect to the SM lies, of course, in the simultaneous presence of two Yukawa matrices Y_a^f in each fermion sector f. While the unitary transformations U_{f_L} and U_{f_R} allow for the bidiagonalization of the linear combination M_f^0, they do not, in general, diagonalize the individual Yukawa matrices Y_a^f. As a result, the additional combinations encoded in the N_f^0 matrices are not simultaneously diagonalized by the same transformations, leading to the emergence of scalar flavor-changing neutral currents (SFCNC) at tree-level. As we have just mentioned, these are controlled by non-diagonal N_f given by

$$U_{u_L}^\dagger N_u^0 U_{u_R} = N_u\,, \qquad U_{d_L}^\dagger N_d^0 U_{d_R} = N_d\,. \tag{3.33}$$

The appearance of SFCNC is one of the most interesting features of MHDMs and, in particular, of 2HDMs. While offering novel phenomenological possibilities, such couplings are subject to stringent experimental constraints. For instance, the flavor-changing coupling dsH in the down-type sector would induce tree-level contributions to kaon mixing, whereas in the SM this process occurs only at the one-loop level. In light of this, two broad classes of Yukawa sectors in 2HDMs have been extensively studied in the literature, namely: (i) those that entirely forbid the presence of SFCNC, and (ii) those that allow for SFCNC but keep them under control. In the following, we briefly introduce some of the most widely studied realizations within each class.

Natural Flavor Conservation

The Natural Flavor Conservation (NFC) proposal was put forward in 1976 by Glashow and Weinberg [103], and in 1977 by Paschos [104], to ensure the absence of tree-level FCNC in $SU(2)_L \times U(1)_Y$ gauge theories.[2] They established that the necessary and sufficient conditions for this to happen are: (i) all quarks with the same charge and helicity have the same value of the weak isospin T_3, (ii) transform under the same irrep of $SU(2)_L$, and (iii) get their masses either through their couplings to a *single* neutral Higgs field or through an $SU(2)_L$ invariant mass term. Since we already know that weak interactions are chiral, rather than vector-like, an $SU(2)_L$ invariant mass term is dismissed. Therefore, given the SM matter content in Eq. (1.30), with left-handed doublets and right-handed singlets, NFC implies that all right-handed quarks must couple to precisely one Higgs doublet. The latter can only be achieved by introducing additional discrete or continuous symmetries.

Different realizations of NFC based on a $\mathbb{Z}_2$ symmetry are summarized in Table 3.2, where we quote the transformation properties of the right-handed fermions and the scalar doublets, including the lepton sector for completeness. It is worth pointing out that the type II Yukawa interactions arise naturally in both Peccei-Quinn models and supersymmetric frameworks, though as a consequence of a continuous symmetry rather than a discrete one.

	u_R^0	d_R^0	e_R^0	Φ_1	Φ_2
Type I	$+$	$+$	$+$	$-$	$+$
Type II	$+$	$-$	$-$	$-$	$+$
Type X	$+$	$+$	$-$	$-$	$+$
Type Y	$+$	$-$	$+$	$-$	$+$

Table 3.2: Transformation properties of fermions and scalars under $\mathbb{Z}_2$ in 2HDMs with NFC. By convention, right-handed up-type quarks always couple to Φ_2. Notice that the $\mathbb{Z}_2$ symmetry is imposed in the original weak basis of the theory. Type X and type Y scenarios are often called lepton-specific and flipped models, respectively.

As an alternative to the NFC hypothesis, tree-level FCNC can be eliminated by requiring the Yukawa matrices to be proportional to each other, *i.e.*, $Y_1^f \propto Y_2^f$. This leads to the so-called aligned 2HDM [105]. In fact, the four realizations of NFC listed in Table 3.2 can be recovered through specific choices of the three proportionality constants in the aligned 2HDM.

[2]The term *natural* is used in this context to indicate validity for any choice of the parameters of the theory.

Controlling tree-level SFCNC

Rather than imposing the complete absence of SFCNCs, one may consider scenarios in which they are present but, at the same time, they are sufficiently suppressed to remain compatible with current experimental bounds. While raising the scalar mass scale to evade such constraints is certainly a viable option, it may be preferable—especially from the standpoint of discovery prospects—to seek an alternative solution.

Among this class of models, one of the most popular proposals is the Cheng-Sher ansatz [106]. Inspired by the hierarchical pattern of fermion masses, one may take the couplings in $\xi_{ij}\bar{f}_i f_j S$ to be roughly proportional to the geometric mean of the masses of the two fermions normalized to the EW vev, that is, $\xi_{ij} \propto \sqrt{m_i m_j}/v$, with coefficients of order one. In this way, the flavor-changing couplings involving the light generations, which are subject to the most stringent experimental constraints, are naturally suppressed by the smallness of the corresponding fermion masses.

Another interesting possibility to suppress SFCNC is given in Branco-Grimus-Lavoura models [107], where the flavor-changing couplings of scalars to fermions are kept under control by combinations of small off-diagonal CKM elements without introducing additional flavor parameters. Remarkably, these models can be built upon symmetry considerations, so that the flavor-changing couplings are exact radiatively-stable functions of the CKM. They constitute a particular realization of the MFV hypothesis [108, 109], which assumes that all flavor-violating effects at low energies arise from the Yukawa couplings, both in the SM and BSM—the technical aspects of the MFV implementation will be discussed in chapter 4. More recently, Branco-Grimus-Lavoura models have been generalized in [110].

3.2.2 CP violation

As previously mentioned, introducing multiple Higgs doublets allows for new sources of CP violation to emerge from the scalar sector, either explicitly at the Lagrangian level or spontaneously from the vacuum structure. In addition, new CP-violating effects may arise from the clash of the Yukawa and scalar interactions. Before going into details, we should recall that in the SM the scalar sector is CP-conserving, since all parameters in the scalar potential are real due to hermiticity and the vev of the single scalar doublet can be made real by means of gauge transformations. Therefore, in the absence of complex phases in the scalar sector, the Kobayashi–Maskawa phase in the CKM matrix stands as the only source of CP violation in the SM. In the following, we shall see that this picture changes in the presence of two scalar doublets.

Let us start by considering trivial CP transformation properties for fermions and scalars. This means that the unitary rotations K_Q, K_u and K_d in flavor space in Eq. (1.93) are set to the identity in the CP transformations of the fermions fields, while the scalar doublets simply transform as $\Phi_a \longrightarrow \Phi_a^*$. Then, CP invariance of the Lagrangian, together with hermiticity, implies that *all Yukawa couplings and parameters in the scalar potential must be real.* In this way, CP is explicitly conserved at the Lagrangian level. On the other hand, if the vevs of the scalar doublets are assumed to transform identically under CP, it is clear that the vacuum configuration

$$\langle\Phi_1\rangle = \frac{v_1}{\sqrt{2}}\begin{pmatrix}0\\1\end{pmatrix}, \qquad \langle\Phi_2\rangle = \frac{v_2 e^{i\theta}}{\sqrt{2}}\begin{pmatrix}0\\1\end{pmatrix}, \tag{3.34}$$

is not invariant, provided that the relative phase between the vevs of the two Higgs doublets $\theta \neq 0, \pi$.

This leads to *spontaneous CP violation* (SCPV) in the 2HDM. The latter can be present even if the Lagrangian of the theory is explicitly invariant under CP. Nevertheless, in those cases it is important to ensure that the model still generates a complex CKM mixing matrix in agreement with experiment, as was explored, *e.g.*, in Ref. [111].

At this point, we should mention that a $\mathbb{Z}_2$-symmetric scalar sector, such as those arising in any of the NFC implementations collected in Table 3.2, preserves CP invariance. The reason is rather simple: the symmetry eliminates the complex parameters μ_{12}^2, λ_6 and λ_7 from the scalar potential, while the remaining λ_5 can always be made real by an appropriate rephasing of the scalar fields without affecting other parameters. In addition, it can be shown that SCPV cannot occur either once the $\mathbb{Z}_2$ symmetry is imposed. However, CP violation can be restored allowing for soft symmetry-breaking terms in the Lagrangian, that is, operators with mass dimension lower than four which are not invariant under the symmetry. For our case at hand, this would mean $\mathrm{Re}(\mu_{12}^2) \neq 0$. In that way, one could have NFC and, at the same time, incorporate additional sources of CP violation in the scalar sector.

Finally, let us comment on how CP violation manifests in the scalar mixing of Eq. (3.27). It is clear that the neutral scalar H^0, which resides in the SM-like Higgs doublet with a non-vanishing vev, is CP-even, meaning that it remains invariant under CP transformations—in constrast, CP-odd scalars change sign under CP. On the other hand, the fields R^0 and I^0 are, in general, admixtures of CP-even and CP-odd states. If CP is conserved, then we are left with two CP-even states and one CP-odd state that cannot mix. The neutral scalar mass matrix $\mathcal{M}_0^2$ is then block-diagonal and its diagonalization is carried out through a block-diagonal rotation matrix R, yielding two CP-even $\{h, H\}$ and one CP-odd $\{A\}$ neutral mass eigenstates. In particular, it is customary to introduce the parameter α as

$$\begin{pmatrix} h \\ H \end{pmatrix} = R_\alpha^T \begin{pmatrix} \rho_1 \\ \rho_2 \end{pmatrix}, \qquad \text{with} \qquad R_\alpha = \begin{pmatrix} c_\alpha & s_\alpha \\ -s_\alpha & c_\alpha \end{pmatrix}, \tag{3.35}$$

so that the rotation matrix R in Eqs. (3.26) and (3.27) is given by

$$R = \begin{pmatrix} \cos(\alpha+\beta) & \sin(\alpha+\beta) & 0 \\ -\sin(\alpha+\beta) & \cos(\alpha+\beta) & 0 \\ 0 & 0 & 1 \end{pmatrix}. \tag{3.36}$$

This block-diagonal form of the scalar mixing makes CP conservation in the scalar sector manifest.

Weak basis invariant conditions

Similarly to what happens in the SM, the presence of irremovable complex phases in the Lagrangian leads to an explicit violation of the CP symmetry. However, verifying this condition is not always straightforward, as the freedom to perform field redefinitions may introduce or remove spurious phases that do not correspond to genuine CP-violating effects. In light of this, it is desirable to formulate WB-invariant conditions for CP conservation, as was done for the Yukawa sector of the SM in Sec. 1.5. The extension of this method for any gauge theory involving scalars and fermions was addressed in [60]. Here, we reproduce the simplest WB-invariant quantities to determine whether CP is conserved in scalar and scalar-fermion interactions. In general, *all WB-invariants must be real for CP to be conserved.*

When we include the unitary rotation of the scalar doublets in Eq. (3.13) into the definition of WBT, the Yukawa coupling matrices get transformed as

$$Y_i^u \longrightarrow (Y_i^u)' \equiv U_{ij}^* U_Q^\dagger Y_j^u U_u \,, \qquad Y_i^d \longrightarrow (Y_i^d)' \equiv U_{ij} U_Q^\dagger Y_j^d U_d \,, \tag{3.37}$$

where i, j are indices in the scalar space, and U_Q, U_u and U_d are the unitary transformations of fermions in flavor space. One can easily get rid of the matrices U_u and U_d by defining the Hermitian combinations

$$H_{ij}^u \equiv Y_i^u Y_j^{u\dagger} \,, \qquad H_{ij}^d \equiv Y_i^d Y_j^{d\dagger} \,, \tag{3.38}$$

which transform as

$$H_{ij}^u \longrightarrow (H_{ij}^u)' \equiv U_{ik}^* U_{lj} U_Q^\dagger H_{kl}^u U_Q \,, \qquad H_{ij}^d \longrightarrow (H_{ij}^d)' \equiv U_{ik} U_{lj}^* U_Q^\dagger H_{kl}^d U_Q \,. \tag{3.39}$$

On the other hand, under WBT the matrix of scalar vevs $\mathcal{V}_{ij}$, and the parameters of the scalar potential Y_{ab} and $Z_{ij,kl}$, change according to Eqs. (3.14) and (3.15). Then, if we take traces over flavor and scalar indices, the resulting quantities are invariant under the WBT of both fermionic and scalar fields [60].

Scalar sector—. The analysis of CP invariance in the scalar sector requires to construct WB-invariant quantities involving the vevs $\mathcal{V}_{ij}$, and the couplings Y_{ij} and $Z_{ij,kl}$. The most simple invariants that can be complex are defined as [60, 112]

$$J_1 \equiv Y_{ij} Z_{jk,kl} \mathcal{V}_{li} \,, \qquad J_2 \equiv \mathcal{V}_{ij} Y_{jk} Z_{ki,lm} \mathcal{V}_{mn} Y_{nl} \,, \tag{3.40}$$

Therefore, the scalar potential and the vacuum configuration violate CP if either J_1 or J_2 are imaginary. One can readily check this condition for 2HDMs by working in the Higgs basis, where the matrix of vevs takes the simpler form $\mathcal{V}_{11} = v^2/2$, $\mathcal{V}_{22} = \mathcal{V}_{12} = \mathcal{V}_{21} = 0$. We obtain

$$J_1 = -\frac{v^4}{4}\left(2\Lambda_1^2 + 2\Lambda_1\Lambda_4 + \frac{|\Lambda_6|^2}{2} + \frac{\Lambda_6\Lambda_7^*}{2}\right) \quad \Longrightarrow \quad \mathrm{Im}\, J_1 = -\frac{v^4}{8}\mathrm{Im}\,(\Lambda_6\Lambda_7^*) \,, \tag{3.41}$$

$$J_2 = \frac{v^8}{4}\left(\Lambda_1^3 + \frac{\Lambda_1|\Lambda_6|^2}{2} + \frac{\Lambda_5^*\Lambda_6^2}{4}\right) \quad \Longrightarrow \quad \mathrm{Im}\, J_2 = \frac{v^8}{16}\mathrm{Im}\,(\Lambda_5^*\Lambda_6^2) \,, \tag{3.42}$$

where we have used the vacuum stability conditions $M_{11}^2 = -\Lambda_1 v^2$ and $M_{12}^2 = -\Lambda_6 v^2/2$. Therefore, CP-violating effects in the scalar interactions arise from $\mathrm{Im}\,(\Lambda_6\Lambda_7^*)$ and $\mathrm{Im}\,(\Lambda_5^*\Lambda_6^2)$. Interestingly, it can be shown that $\mathrm{Im}\,(\Lambda_5^*\Lambda_6^2)$ is non-vanishing if and only if all neutral scalars have non-degenerate masses and all elements in the first row of the rotation matrix R in Eqs. (3.26) and (3.27) are non-zero [112, 113].

Scalar and Yukawa interactions—. One could also construct WB-invariant conditions to test CP violation in the clash between the scalar and Yukawa sectors. To this aim, the invariants should include traces of the hermitian combinations defined in Eq. (3.38). In particular, one may have, for instance,

$$J_3 \equiv \mathcal{V}_{ij} Y_{jk}\, \mathrm{tr}\big(H_{ki}^d\big) \,, \qquad J_4 \equiv \mathcal{V}_{ij}\, \mathrm{tr}\big(H_{jk}^d\big) Z_{ki,lm} \mathcal{V}_{mn}\, \mathrm{tr}\big(H_{nl}^d\big) \,. \tag{3.43}$$

These can be expressed in terms of fermion and neutral scalar masses, the elements of the rotation matrix R, and the diagonal elements of the Yukawa couplings—see [58] for details. A non-vanishing imaginary part of either J_3 or J_4 would signal CP violation in the clash between the scalar and Yukawa interactions.

Feynman rules

Equivalently, one can verify whether CP is conserved by inspection of the Feynman rules of scalars [58]. In particular, it can be checked that CP violation is present in the scalar mixing if and only if any of the following conditions is fulfilled: (i) all three physical neutral scalars S_i ($S_i = h, H, A$) couple to two Z bosons as $S_i Z_\mu Z^\mu$, (ii) any pair of physical neutral scalars have a derivative interaction with the Z boson of the form $[S_i \partial^\mu S_j - S_j \partial^\mu S_i] Z_\mu$, (iii) any pair of physical neutral scalars exhibits simultaneously both of the previous interactions, and (iv) all three physical neutral scalars couple to charged scalars as $S_i H^+ H^-$. On the other hand, scalar-fermion interactions of the form $S \bar{f}_j (a_{jk} + i b_{jk} \gamma_5) f_k + \mathrm{H.c.}$ (S either neutral or charged) lead to CP violation if $\mathrm{Re}(a_{jk} b_{jk}^*) \neq 0$ [114].

Scientific Research

4 Most general EFTs from spurion analysis: Hilbert Series and Minimal Flavor Violation

The SM provides a successful description of the three generations of quarks and leptons. As we have developed in chapter 1, the flavor structure of quark interactions is fully parametrized by two 3×3 Yukawa matrices Y_u and Y_d or, equivalently, by the six quark masses and the CKM mixing. The model features the GIM mechanism, where an approximate flavor symmetry leads to highly suppressed FCNC. So far, all experimental probes of quark flavor transitions are in agreement with SM predictions, although a few persistent "flavor anomalies" continue to motivate further investigation [70,115]. Likewise, the spontaneous symmetry breaking sector—including both gauge and Higgs interactions—has shown no signs of deviation from the SM picture.

In light of this, a very convenient framework to test the accurate validity of the SM is provided by the SMEFT, where the Lagrangian is extended to include non-renormalizable interactions, *i.e.*, effective operators with mass dimension larger than four involving the SM fields and subject to the SM symmetries. These non-renormalizable interactions, such as four-quark operators at mass dimension 6, generally induce FCNC which would contradict experimental evidences [116].

The MFV [108, 109] hypothesis aims to characterize the class of theories in which FCNC generated by higher-dimensional operators are suppressed by incorporating the GIM mechanism to the SMEFT. In this approach, the Yukawa matrices Y_u and Y_d are treated as *spurions*, that is, as if they were space-time independent fields, with well-defined transformation properties under the quark flavor symmetry group in Eq. (1.44). In particular, given the transformation properties of the quarks with the same quantum numbers, namely,

$$Q_L^0 \longrightarrow U_Q\, Q_L^0\,, \qquad u_R^0 \longrightarrow U_u\, u_R^0\,, \qquad d_R^0 \longrightarrow U_d\, d_R^0\,, \tag{4.1}$$

with $U_Q \in U(3)_Q$, $U_u \in U(3)_u$, $U_d \in U(3)_d$, the quark flavor symmetry, which is explicitly broken by the Yukawa couplings in the SM, can be formally preserved provided that the spurions transform as

$$Y_u \longrightarrow U_Q\, Y_u\, U_u^\dagger\,, \qquad Y_d \longrightarrow U_Q\, Y_d\, U_d^\dagger\,. \tag{4.2}$$

Now, when it comes to higher-dimension operators in the SMEFT, the MFV strategy prescribes that the operator coefficients be constructed as polynomials in the spurions Y_u and Y_d, in such a way that they formally preserve the quark flavor symmetry. Given these constraints, a natural question arises: how many genuinely independent flavor components of the coefficients can be built for a given operator transforming in a specific irrep of the flavor group? In other words, does the MFV principle restrict the operator coefficients to lie along specific directions in flavor space?

To answer the above questions, a systematic investigation on spurion covariants was carried out in Ref. [87]. In particular, the authors extended the Hilbert series technology [71–86] to analyze group covariants, establishing that the number of linearly independent operators under a given irrep of the flavor group G_f, denoted as "Irrep_{G_f}" hereafter, is given by the rank of the module ${}_{\mathbb{F}_{\text{Inv}}}\mathcal{M}_{\text{Irrep}_{G_f}}$. As we have introduced in chapter 2, the latter can be computed by taking the ratio of two Hilbert series:

$$\text{rank}\left({}_{\mathbb{F}_{\text{Inv}}}\mathcal{M}_{\text{Irrep}_{G_f}}\right) = \left.\frac{\mathcal{H}_{\text{Irrep}_{G_f}}(q)}{\mathcal{H}_{\text{Inv}_{G_f}}(q)}\right|_{q\to 1}, \tag{4.3}$$

where "Inv_{G_f}" corresponds to the invariant irrep of the flavor group. In the context of MFV SMEFT, Ref. [87] shows that every direction in the quark flavor space can indeed be fulfilled by the spurion polynomials for any irrep of the quark flavor group, *i.e.*, "(quark) MFV SMEFT = SMEFT". This phenomenon is called "saturation" in Ref. [87]. It is fairly nontrivial, as this is not guaranteed to hold for any combinations of flavor groups and spurions. For example, if one considers a single Yukawa spurion Y_d transforming under the flavor subgroup $U(3)_Q \times U(3)_d$, saturation is not reached. Interestingly, this simplified setup reproduces one of the standard formulations of the MFV principle in the lepton sector: in the minimal SMEFT scenario—assuming massless neutrinos—there is only one available Yukawa coupling, Y_e, which transforms as a bifundamental under $U(3)_\ell \times U(3)_e$.

In this chapter, we extend the concept of saturation discussed in Ref. [87] into a more general result, formulated as a *saturation theorem*—see Eq. (4.10) below—, which applies to a broad class of EFTs constructed from spurion analysis. As we will elaborate in Sec. 4.1, while the EFT constructed using spurions does not necessarily reproduce the full structure of the original EFT, it does saturate a restricted version of it, namely, the one constrained to be invariant under $H_S \subset G_f$, defined as the subgroup that leaves a generic vev of the spurions S unchanged:[1]

$$G_f \xrightarrow{\text{generic } \langle S\rangle} H_S \subset G_f\,. \tag{4.4}$$

In Sec. 4.2, we explore how the MFV principle can be implemented in the lepton sector, dubbed Minimal Lepton Flavor Violation (MLFV). The latter is an interesting framework in its own right [109, 117–119], and its formulation is not a direct extension of the analysis in the quark sector. This is due to the fact that neutrino masses may arise from various mechanisms, each implying a different flavor structure, and hence distinct choices of flavor symmetry groups and spurions. We examine the four MLFV scenarios summarized in Table 4.1, which encompass a range of possible origins for neutrino mass generation. For each case, we employ Eq. (4.3) to determine the number of independent lepton flavor covariant operators at mass dimension 6 in the spurion EFT, and verify the Saturation Theorem introduced in Eq. (4.10). Additionally, for a selected subset of lepton flavor covariants, we provide an explicit choice of linearly independent spurion polynomials, motivated by their phenomenological applications.

We conclude and outline possible future directions in Sec. 4.3. Some of the Hilbert series obtained within the different MLFV realizations are compiled in the publicly available `Mathematica` notebook HilbCalc. This notebook includes general functions for computing Haar measures, Weyl characters, and Hilbert series of invariants and covariants of the classical Lie groups. These tools are readily applicable to a broad range of related calculations. A comprehensive guide to using these functions is provided in App. A.

[1]The subgroup H_S is also referred to as the stabilizer subgroup, little group, or isotropy group, depending on context.

4.1 Spurion analysis for EFTs: the Saturation Theorem

Before presenting the main results of this section, we begin by reviewing the standard procedure for spurion analyses within the EFT framework in Sec. 4.1.1, which also serves to introduce the relevant notation. We then formulate the Saturation Theorem in Sec. 4.1.2.

4.1.1 EFTs from spurion analysis

Consider an EFT defined by a set of dynamical fields $\phi(x)$ and a Lagrangian $\mathscr{L}_{\rm EFT}([\phi])$.[2] As usual, its definition includes a power counting scheme and a set of imposed global and/or gauge symmetries. In addition to these, we can consider a global symmetry G_f that is not imposed in the definition of $\mathscr{L}_{\rm EFT}([\phi])$, *e.g.*, the flavor group in SMEFT. On that regard, in certain situations we may be interested in keeping track of how G_f is broken within $\mathscr{L}_{\rm EFT}([\phi])$, and a standard technique to do so is the spurion analysis.

In this approach, one starts by examining the terms in $\mathscr{L}_{\rm EFT}([\phi])$ that explicitly break G_f at its low orders—typically the leading order, and sometimes also the next-to-leading order. The couplings λ_S associated with these symmetry-breaking operators are then promoted to a set of non-dynamical *spurion fields* S (or simply *spurions*):

$$\lambda_S \quad \longrightarrow \quad S\,. \tag{4.5}$$

We then require S to transform under G_f in such a way that the symmetry is formally restored at the low orders of $\mathscr{L}_{\rm EFT}([\phi])$. In this framework, the G_f-violating couplings λ_S can be interpreted as the vevs of the corresponding spurion fields, namely, $\lambda_S = \langle S\rangle$.

Next, we turn to higher-order interactions in the EFT involving the dynamical fields $\phi(x)$, their derivatives, as well as the spurion fields S, arranged in such a way that the resulting terms are invariant under G_f. These interactions are encoded in the Lagrangian

$$\mathscr{L}_{\rm EFT}([\phi], S)^{G_f}\ , \tag{4.6}$$

where the superscript indicates invariance under G_f. Finally, the *EFT from spurion analysis* is obtained by replacing the spurion fields S by their vevs as

$$\mathscr{L}_{\rm EFT,\,Spurion} \equiv \mathscr{L}_{\rm EFT}([\phi], S)^{G_f}\Big|_{S=\langle S\rangle=\lambda_S}\,. \tag{4.7}$$

In this EFT, G_f invariance is formally preserved, with all breaking effects encoded in the vevs of the spurion fields S. Therefore, this setup gives us control over the breaking of G_f.

Before moving on, we should note that promoting a particular G_f-violating coupling λ_S in the EFT is a common way to introduce a spurion field, but it is not the only possibility. For example, in the case of the QCD chiral Lagrangian, the mass spurion fields (and their transformation properties) are motivated by the UV theory, that is, the QCD Lagrangian, rather than by promoting a coupling in the chiral Lagrangian itself.

[2] The Lagrangian is a polynomial in $\phi(x)$ and their derivatives. Here, we use the shorthand $[\phi] = \{\phi, \partial_\mu\phi, \partial_\mu\partial_\nu\phi, \ldots\}$.

4.1.2 The Saturation Theorem

To what extent is the EFT constructed from spurion analysis in Eq. (4.7) more constrained than the original EFT? To answer this question, let us denote by H_S the subgroup of G_f that remains unbroken under a *generic* vev $\langle S\rangle$ of the spurion fields. Since all sources of G_f breaking in $\mathscr{L}_{\text{EFT, Spurion}}$ originate from the spurion vevs, either generic or special, $\mathscr{L}_{\text{EFT, Spurion}}$ is guaranteed to respect the symmetry imposed by H_S, and thus it is *contained* in $\mathscr{L}_{\text{EFT}}\left([\phi]\right)^{H_S}$:

$$\mathscr{L}_{\text{EFT, Spurion}} \subset \mathscr{L}_{\text{EFT}}\left([\phi]\right)^{H_S} . \tag{4.8}$$

This containing bound "$\subset$" means that the effective operators allowed in $\mathscr{L}_{\text{EFT, Spurion}}$ are a subset of the effective operators allowed in $\mathscr{L}_{\text{EFT}}\left([\phi]\right)^{H_S}$. Said differently, the linear space of Wilson coefficients in $\mathscr{L}_{\text{EFT, Spurion}}$ is a subspace of that in $\mathscr{L}_{\text{EFT}}\left([\phi]\right)^{H_S}$.

The main result of this chapter is formulated as a *saturation theorem*—the bound in Eq. (4.8) is saturated when arbitrary powers of S are included in $\mathscr{L}_{\text{EFT, Spurion}}$ and $\lambda_S = \langle S\rangle$ is a generic vev.

Saturation Theorem — Let H_S be the subgroup of G_f that remains unbroken under a *generic* vev of the spurion fields S:

$$G_f \xrightarrow{\text{generic } \langle S\rangle} H_S \subset G_f . \tag{4.9}$$

Then, the EFT from spurion analysis *saturates* the original EFT with H_S imposed:

$$\mathscr{L}_{\text{EFT, Spurion}} \equiv \mathscr{L}_{\text{EFT}}\left([\phi], S\right)^{G_f}\Big|_{S=\langle S\rangle=\lambda_S} \cong \mathscr{L}_{\text{EFT}}\left([\phi]\right)^{H_S} , \tag{4.10}$$

when all powers of S are included in $\mathscr{L}_{\text{EFT, Spurion}}$ and $\lambda_S = \langle S\rangle$ fulfills a generic vev.

The equivalence symbol "$\cong$" in Eq. (4.10) means that the two EFTs have the same set of allowed effective operators, *i.e.*, $\mathscr{L}_{\text{EFT, Spurion}}$ can reproduce the most general $\mathscr{L}_{\text{EFT}}\left([\phi]\right)^{H_S}$—their Wilson coefficients form the same linear space.

Now let us demonstrate the Saturation Theorem in Eq. (4.10). The EFT from spurion analysis, *i.e.*, $\mathscr{L}_{\text{EFT, Spurion}}$ constructed in Eq. (4.7), consists of a list of effective operators $Q_i[\phi]$ built out of the dynamical fields $\phi(x)$ and their derivatives, which are subject to the usual gauge and space-time symmetry requirements and redundancies. Their corresponding Wilson coefficients $C_i(S)$ are polynomials in the spurion fields S, evaluated at their vevs $\langle S\rangle = \lambda_S$. Each Wilson coefficient transforms under a given irrep of G_f, denoted as "Irrep_{G_f}", such that the number of independent components is given by the rank of the module ${}_{\mathbb{r}_{\text{Inv}}}\mathcal{M}^{G_f, S}_{\text{Irrep}_{G_f}}$, being $\mathbb{r}_{\text{Inv}}$ the ring of the G_f-invariant polynomials in S—see chapter 2 and Ref. [87] for details. According to Brion's theorem [88, 89], this rank satisfies

$$\text{rank}\left({}_{\mathbb{r}_{\text{Inv}}}\mathcal{M}^{G_f, S}_{\text{Irrep}_{G_f}}\right) = \dim\left(\text{Irrep}^{H_S}_{G_f}\right) , \tag{4.11}$$

where $\text{Irrep}^{H_S}_{G_f}$ denotes the subspace of Irrep_{G_f} that is invariant under H_S. Hence $\dim\left(\text{Irrep}^{H_S}_{G_f}\right)$ gives the number of H_S-invariants (*i.e.*, Inv_{H_S}) in the branching rule of Irrep_{G_f}:

$$\text{Irrep}_{G_f} = \dim\left(\text{Irrep}^{H_S}_{G_f}\right) \text{Inv}_{H_S} \oplus \text{non-invariant irreps of } H_S . \tag{4.12}$$

On the other hand, let us check the number of independent operators $Q_i[\phi]$ in the EFT without spurions, but restricted to H_S invariance, *i.e.*, $\mathscr{L}_{\text{EFT}}\left([\phi]\right)^{H_S}$. By construction, we are only retaining the components of the Wilson coefficients accompanying invariant operators under H_S, so the number precisely agrees with the right-hand side of Eq. (4.11). Therefore, the two EFTs, $\mathscr{L}_{\text{EFT, Spurion}}$ and $\mathscr{L}_{\text{EFT}}\left([\phi]\right)^{H_S}$, have the same set of allowed effective operators. This proves the Saturation Theorem in Eq. (4.10).

We should stress two important notes on the previous proof.

(i) Brion's theorem [88,89] in Eq. (4.11) follows from a *generic* vev of the spurion fields $\langle S\rangle$. It is not guaranteed that it also holds for a particular vev structure.

(ii) *All* powers of S should be considered in the construction of $C_i(S)$ in $\mathscr{L}_{\text{EFT, Spurion}}$. With limited powers of the spurions, we might not be able to generate the required Irrep_{G_f} to formally preserve G_f-invariance, and thus $\mathscr{L}_{\text{EFT, Spurion}}$ could be more restrictive.

Before explicitly checking the Saturation Theorem within the MLFV paradigm, let us first illustrate two extreme and simpler scenarios to better see its implications.

- **Extreme scenario 1:** All the spurion fields S are invariants under G_f. In this case, there is no G_f breaking at all and we expect the EFT from spurion analysis to be equivalent with the original EFT restricted to G_f invariance: $\mathscr{L}_{\text{EFT, Spurion}} \cong \mathscr{L}_{\text{EFT}}\left([\phi]\right)^{G_f}$. This scenario is consistent with the Saturation Theorem in Eq. (4.10), because $H_S = G_f$ in this case.
- **Extreme scenario 2:** We have enough spurion fields S transforming non-trivially under G_f such that $H_S = \{\mathbf{e}\}$ (*i.e.*, the identity element only). In this case, the Saturation Theorem in Eq. (4.10) tells us that the EFT from spurion analysis is equivalent to the original EFT: $\mathscr{L}_{\text{EFT, Spurion}} \cong \mathscr{L}_{\text{EFT}}\left([\phi]\right)$. This is in agreement with the reasonable expectation that, with so many spurions, one is able to reconstruct any $C_i(S) \sim \text{Irrep}_{G_f}$ required by $Q_i\left([\phi]\right)$ to preserve G_f-invariance, and thus all operators that appear in the most general EFT $\mathscr{L}_{\text{EFT}}\left([\phi]\right)$ can be retained. This is consistent with the saturation discussed in Ref. [87]—it is a special case of our general Saturation Theorem in Eq. (4.10).

In general, the EFT from spurion analysis, $\mathscr{L}_{\text{EFT, Spurion}}$, will be more restricted compared to the original EFT, $\mathscr{L}_{\text{EFT}}\left([\phi]\right)$, but not as restricted as imposing the full G_f on it:

$$\mathscr{L}_{\text{EFT}}\left([\phi]\right)^{G_f} \quad \subset \quad \mathscr{L}_{\text{EFT, Spurion}} \cong \mathscr{L}_{\text{EFT}}\left([\phi]\right)^{H_S} \quad \subset \quad \mathscr{L}_{\text{EFT}}\left([\phi]\right) . \tag{4.13}$$

In other words, it is in between the two extreme scenarios discussed above, because the unbroken subgroup $H_S \subset G_f$ is generically bigger than the trivial subgroup, and smaller than the full group G_f.

4.2 Minimal Lepton Flavor Violation

In this section, we discuss four possible implementations of the MLFV principle, which are summarized in Table 4.1. We perform a spurion analysis that accounts for how certain couplings break the lepton flavor groups G_{Lf}. We compute Hilbert series to study the group covariants, and use these to check, in each case, the Saturation Theorem in Eq. (4.10). We begin with the SMEFT Cases I and II in Sec. 4.2.1, and then turn to the νSMEFT Cases III and IV in Sec. 4.2.2. The details on the calculation of all Hilbert

Case	ϕ	G_{Lf}	S	H_S
I	SMEFT	$U(3)_\ell \times U(3)_e$	Y_e	$U(1)_e \times U(1)_\mu \times U(1)_\tau$
II			$Y_e,\, C_5$	$\mathbb{Z}_2 = \{1,\, \mathcal{P}_{\rm LN}\}$
III	νSMEFT	$U(3)_\ell \times U(3)_e \times U(3)_\nu$	$Y_e,\, Y_\nu$	$U(1)_{\rm LN}$
IV			$Y_e,\, Y_\nu,\, M_R$	$\mathbb{Z}_2 = \{1,\, \mathcal{P}_{\rm LN}\}$

Table 4.1: MLFV implementations addressed in this section, differing in their content of dynamical fields ϕ and spurion fields S. The SMEFT Cases I and II are discussed in Sec. 4.2.1. The νSMEFT Cases III and IV, where the SMEFT is extended by adding three flavors of right-handed neutrinos ν that transform as gauge singlets, are analyzed in Sec. 4.2.2. The latter include an additional $U(3)_\nu$ factor in the lepton flavor group G_{Lf}. In all cases, the set of spurion fields S implicitly includes the Hermitian conjugates of the listed matrices. Besides the Yukawa couplings Y_e and Y_ν, the coefficient of the dim-5 Weinberg operator, C_5, and the Majorana mass term for right-handed neutrinos, M_R, can be considered. The subgroup of G_{Lf} that is left unbroken by a generic vev of S is indicated as H_S. Among them, the lepton parity is written as $\mathcal{P}_{\rm LN} = (-1)^{\rm LN}$, being LN the total lepton number.

series presented in this section are available in our `Mathematica` notebook HilbCalc, together with other single-graded and additional multi-graded Hilbert series. Some of the single-graded results within Case IV have been omitted from the main text and relegated to App. A.5.

Throughout this section we often use the same symbols for spurion fields, their generic vevs, and their specific values from Lagrangian parameters, for the sake of readability and compactness. In any case, the distinction can be easily inferred from the context.

4.2.1 SMEFT with lepton flavor group $G_{Lf} = U(3)_\ell \times U(3)_e$

We begin analyzing the SMEFT scenarios, in which the dynamical fields $\phi(x)$ are the SM fields:

$$\phi_{\rm SM} \in \Big\{q,\, u,\, d,\, \ell,\, e,\, H,\, G^A_{\mu\nu},\, W^a_{\mu\nu},\, B_{\mu\nu}\Big\} + \Big\{q^c,\, u^c,\, d^c,\, \ell^c,\, e^c,\, H^\dagger,\, \widetilde{G}^A_{\mu\nu},\, \widetilde{W}^a_{\mu\nu},\, \widetilde{B}_{\mu\nu}\Big\}\,, \tag{4.14}$$

where we have adopted the Warsaw basis notation [120] and, in particular, drop the chirality indices L and R for the fermionic fields, namely,

$$q = Q^0_L\,, \qquad u = u^0_R\,, \qquad d = d^0_R\,, \qquad \ell = \ell^0_L\,, \qquad e = e^0_R\,. \tag{4.15}$$

On the other hand, the charge conjugation on Dirac spinors is given by $\psi^c = -i\gamma^2\psi^*$, such that the charge conjugation matrix is $C = i\gamma^0\gamma^2$. Finally, $\widetilde{G}^A_{\mu\nu}$ is the dual field strength tensor in $SU(3)_C$, defined as $\widetilde{G}^A_{\mu\nu} \equiv \epsilon_{\mu\nu\rho\sigma} G^{A\,\rho\sigma}/2$, and analogously for $SU(2)_L$ and $U(1)_Y$ field strengths.

Within this scenario, the lepton flavor group is simply

$$G_{Lf} = U(3)_\ell \times U(3)_e\,, \tag{4.16}$$

under which only ℓ and e, among the dynamical fields, transform:

$$\ell \;\longrightarrow\; U_\ell\, \ell\,, \qquad e \;\longrightarrow\; U_e\, e\,. \tag{4.17}$$

At the leading order of $\mathscr{L}_{\rm SMEFT}$, that is, $\mathscr{L}_{\rm SM}$, the lepton flavor symmetry is broken by the Yukawa matrices Y_e and $Y_e^\dagger$:

$$\mathscr{L}_{\rm SM} \supset -\bar{\ell}\, Y_e\, e\, H + \text{H.c.} \tag{4.18}$$

These Yukawas will be treated as the spurion fields in the Case I listed in Table 4.1. Next, we will move on to the Case II in Table 4.1, where we extend the set of spurion fields S to further include the coupling matrix C_5 (and its hermitian conjugate) of the dim-5 Weinberg operator in SMEFT [46], written as

$$\mathscr{L}_{\rm SMEFT}^{\text{dim-5}} = -\frac{1}{2}\left(\overline{\ell^c}\, \widetilde{H}^*\right) C_5 \left(\widetilde{H}^\dagger \ell\right) + \text{H.c.} = \frac{1}{2}\,\epsilon^{ik}\epsilon^{jl} H_i H_j \left(\ell_k^T\, i\gamma^2\gamma^0\, C_5\, \ell_l\right) + \text{H.c.}\,, \tag{4.19}$$

where $\widetilde{H} \equiv i\sigma^2 H^*$. Here i, j, k, l are $SU(2)_L$ indices, while flavor indices are omitted as in Eq. (4.18). One can readily check that C_5 is a symmetric matrix in flavor space. Taking into account Eq. (4.17), it is straightforward to obtain the transformation law of the spurions Y_e and C_5 under the lepton flavor group $G_{Lf} = U(3)_\ell \times U(3)_e$:

$$Y_e \longrightarrow U_\ell\, Y_e\, U_e^\dagger\,, \qquad Y_e \sim (\mathbf{3}, \bar{\mathbf{3}}) \ \text{ with } \ U(1)_{\ell,\, e} \ \text{ charges } \ (+1, -1)\,, \tag{4.20}$$

$$C_5 \longrightarrow U_\ell^*\, C_5\, U_\ell^\dagger\,, \qquad C_5 \sim (\bar{\mathbf{6}}, \mathbf{1}) \ \text{ with } \ U(1)_{\ell,\, e} \ \text{ charges } \ (-2, 0)\,. \tag{4.21}$$

Notice that only the symmetric component $(\bar{\mathbf{3}} \times \bar{\mathbf{3}})_{\rm sym}$ in the transformation law of C_5 under $SU(3)_\ell$ has been retained since it is a symmetric tensor.

Case I: spurion analysis with $S_{\rm I} = \{Y_e\,, Y_e^\dagger\}$

Due to the smallness of neutrino masses, one may be interested in studying the class of theories that are captured by the MLFV hypothesis in the massless neutrino limit. In these cases, and with the SM matter content, the only spurions responsible for the breaking of G_{Lf} are the charged lepton Yukawas $S_{\rm I} = \{Y_e\,, Y_e^\dagger\}$. This is the Case I listed in Table 4.1. In order to verify the Saturation Theorem in Sec. 4.1, we independently study the operators arising within the EFT Lagrangian from spurion analysis—the left-hand side of Eq. (4.10)—and those arising in the $H_{S_{\rm I}}$-restricted EFT Lagrangian—the right-hand side of Eq. (4.10). For concreteness, we will focus on dim-6 operators in SMEFT and adopt the Warsaw basis [120]. In this basis, the LN-preserving operators are those summarized in Table 4.10, while the LN-violating operators [121] are collected in Table 4.11.

$\mathscr{L}_{{\rm SMEFT},\, S_{\rm I}}$ *from spurion analysis*—. In Tables 4.10 and 4.11, we show the irrep decompositions of the Wilson coefficients under the lepton flavor group $U(3)_\ell \times U(3)_e \times U(3)_\nu$, as required for the operators to satisfy the MLFV criterion. Notice that the transformation properties under $U(3)_\nu$ can be ignored for Cases I and II.

Our aim is to count the different flavor structures that can contribute to the different MLFV SMEFT operators, that is, to obtain how many independent flavor components exist for each Wilson coefficient that transforms under a certain irrep of the lepton flavor group. As developed in [87], a systematic approach to achieve this goal involves calculating the Hilbert series for each of the lepton flavor covariants. Using the unified grading scheme

$$Y_e \sim q\,, \qquad Y_e^\dagger \sim q\,, \tag{4.22}$$

we obtain the following Hilbert series for the LN-preserving covariants in Table 4.10 (computed with our

`Mathematica` notebook HilbCalc):

$$\mathcal{H}_{(\mathbf{1},\mathbf{1})} = \frac{1}{D(q)} = \frac{1}{(1-q^2)\,(1-q^4)\,(1-q^6)}\,, \tag{4.23a}$$

$$\mathcal{H}_{(\mathbf{3},\bar{\mathbf{3}})} = \frac{1}{D(q)}\,q\left(1+q^2+q^4\right), \tag{4.23b}$$

$$\mathcal{H}_{(\mathbf{8},\mathbf{1})} = \frac{1}{D(q)}\,q^2\left(1+q^2\right), \tag{4.23c}$$

$$\mathcal{H}_{(\mathbf{8},\mathbf{8})} = \frac{1}{D(q)}\,q^2\left(1+3q^2+4q^4+2q^6\right), \tag{4.23d}$$

$$\mathcal{H}_{(\mathbf{27},\mathbf{1})} = \frac{1}{D(q)}\,q^4\left(1+q^2+q^4\right), \tag{4.23e}$$

as well as

$$\mathcal{H}_{(\mathbf{1},\mathbf{8})} = \mathcal{H}_{(\mathbf{8},\mathbf{1})}\,, \qquad \mathcal{H}_{(\mathbf{1},\mathbf{27})} = \mathcal{H}_{(\mathbf{27},\mathbf{1})}\,. \tag{4.24}$$

For the LN-violating covariants appearing in Table 4.11, the Hilbert series vanish:

$$\mathcal{H}_{(\bar{\mathbf{3}},\mathbf{1})} = \mathcal{H}_{(\mathbf{1},\bar{\mathbf{3}})} = 0\,. \tag{4.25}$$

As elaborated in Ref. [87], the number of linearly independent operators in a G-irrep is given by the rank of the module ${}_{\mathfrak{r}_{\mathrm{Inv}}}\mathcal{M}_{\mathrm{Irrep}_G}$, which can be computed by taking the ratio of two Hilbert series, as quoted in Eq. (4.3). For our case at hand, one can readily obtain[3]

$$\operatorname{rank}\left({}_{\mathfrak{r}_{\mathrm{Inv}}}\mathcal{M}_{(\mathbf{3},\bar{\mathbf{3}})}\right) = 3\,, \tag{4.26a}$$

$$\operatorname{rank}\left({}_{\mathfrak{r}_{\mathrm{Inv}}}\mathcal{M}_{(\mathbf{8},\mathbf{1})}\right) = \operatorname{rank}\left({}_{\mathfrak{r}_{\mathrm{Inv}}}\mathcal{M}_{(\mathbf{1},\mathbf{8})}\right) = 2\,, \tag{4.26b}$$

$$\operatorname{rank}\left({}_{\mathfrak{r}_{\mathrm{Inv}}}\mathcal{M}_{(\mathbf{8},\mathbf{8})}\right) = 10\,, \tag{4.26c}$$

$$\operatorname{rank}\left({}_{\mathfrak{r}_{\mathrm{Inv}}}\mathcal{M}_{(\mathbf{27},\mathbf{1})}\right) = \operatorname{rank}\left({}_{\mathfrak{r}_{\mathrm{Inv}}}\mathcal{M}_{(\mathbf{1},\mathbf{27})}\right) = 3\,, \tag{4.26d}$$

$$\operatorname{rank}\left({}_{\mathfrak{r}_{\mathrm{Inv}}}\mathcal{M}_{(\bar{\mathbf{3}},\mathbf{1})}\right) = \operatorname{rank}\left({}_{\mathfrak{r}_{\mathrm{Inv}}}\mathcal{M}_{(\mathbf{1},\bar{\mathbf{3}})}\right) = 0\,. \tag{4.26e}$$

Finally, in Tables 4.2 to 4.4, we provide (a choice of) linearly independent covariants for a few modules, namely, ${}_{\mathfrak{r}_{\mathrm{Inv}}}\mathcal{M}_{(\mathbf{3},\bar{\mathbf{3}})}$, ${}_{\mathfrak{r}_{\mathrm{Inv}}}\mathcal{M}_{(\mathbf{8},\mathbf{1})}$, and ${}_{\mathfrak{r}_{\mathrm{Inv}}}\mathcal{M}_{(\mathbf{1},\mathbf{8})}$, where we have introduced the Hermitian combination $h_e \equiv Y_e\,Y_e^\dagger$ for convenience.[4]

q	Y_e
q^3	$h_e Y_e$
q^5	$h_e^2 Y_e$

Table 4.2: Basis of the module ${}_{\mathfrak{r}_{\mathrm{Inv}}}\mathcal{M}_{(\mathbf{3},\bar{\mathbf{3}})}$ in Case I MLFV listed in Table 4.1. This module has rank 3, as shown in Eq. (4.26a).

[3] Taking into account Eq. (2.12), it is clear that the rank of the module ${}_{\mathfrak{r}_{\mathrm{Inv}}}\mathcal{M}_R$, when R is a completely reducible representation of G, can be computed as $\operatorname{rank}({}_{\mathfrak{r}_{\mathrm{Inv}}}\mathcal{M}_R) = \sum_i \operatorname{rank}\left({}_{\mathfrak{r}_{\mathrm{Inv}}}\mathcal{M}_{R_i}\right)$, being R_i the different irreps in the block-diagonal decomposition of R.

[4] It can be shown that these modules are free modules, and the linearly independent covariants presented in each table actually form a basis of the module, that is, a complete set of linearly independent covariants that generate the module.

q^2	$\overline{h_e}$
q^4	$\overline{h_e^2}$

Table 4.3: Basis of the module ${}_{\mathscr{F}_{\text{Inv}}}\mathcal{M}_{(\mathbf{8},\mathbf{1})}$ in Case I MLFV listed in Table 4.1. This module has rank 2, as shown in Eq. (4.26b). An overline denotes the traceless component of a matrix, *i.e.*, $\overline{A} \equiv A - (1/3)\,\mathrm{tr}(A)\, I_3$, with I_3 the 3×3 identity matrix.

q^2	$\overline{Y_e^\dagger Y_e}$
q^4	$\overline{(Y_e^\dagger Y_e\,)^2}$

Table 4.4: Basis of the module ${}_{\mathscr{F}_{\text{Inv}}}\mathcal{M}_{(\mathbf{1},\mathbf{8})}$ in Case I MLFV listed in Table 4.1. This module has rank 2, as shown in Eq. (4.26b). An overline denotes the traceless component of a matrix, *i.e.*, $\overline{A} \equiv A - (1/3)\,\mathrm{tr}(A)\, I_3$, with I_3 the 3×3 identity matrix.

$\mathscr{L}_{\text{SMEFT}}^{U(1)_e\times U(1)_\mu\times U(1)_\tau}$ *with Lepton Flavor Universality Violation*—. In order to check the Saturation Theorem in Eq. (4.10) within this scenario, one has to work out the unbroken subgroup $H_{S_{\text{I}}} \subset G_{Lf}$ by a generic vev of $S_{\text{I}} = \{Y_e\,,\, Y_e^\dagger\}$. We have, for Case I in Table 4.1,

$$G_{Lf} = U(3)_\ell \times U(3)_e \quad \xrightarrow{\langle Y_e\,,\,Y_e^\dagger\rangle} \quad H_{S_{\text{I}}} = U(1)_e \times U(1)_\mu \times U(1)_\tau\,, \tag{4.27}$$

where $U(1)_e \times U(1)_\mu \times U(1)_\tau$ correspond to the three flavor lepton numbers, with $U(1)_\tau$ being the vectorial component of $U(1)_{\tau_L} \times U(1)_{\tau_R}$, and similarly for e and μ. Imposing this symmetry results in a theory with Lepton Flavor Universality Violation (LFUV), in which there are no flavor-changing processes nor any lepton number violation. On the one hand, the LN-violating operators in Table 4.11 are hence immediately ruled out. On the other hand, the LN-preserving operators in Table 4.10 are subject to additional constraints on their lepton flavor structures, as summarized separately in Table 4.12, where we also provide the resulting numbers of allowed operators. It is then straightforward to verify that these numbers match the sum of the ranks of the modules listed in Eq. (4.26), confirming the saturation for Case I MLFV in Table 4.1 at mass dimension 6:

$$\mathscr{L}_{\text{SMEFT},\,S_{\text{I}}}\Big|_{\text{dim-6}} \;\cong\; \mathscr{L}_{\text{SMEFT}}^{U(1)_e\times U(1)_\mu\times U(1)_\tau}\Big|_{\text{dim-6}}\,. \tag{4.28}$$

Importantly, we must stress that the Saturation Theorem is not limited to this explicit verification, but it applies to arbitrary mass dimensions in the SMEFT expansion.

Case II: spurion analysis with $S_{\text{II}} = \{Y_e\,,Y_e^\dagger, C_5, C_5^\dagger\}$

If we stick to the SM matter content, neutrino masses can be generated through the dim-5 Weinberg operator in Eq. (4.19). It is then interesting to study the MLFV SMEFT scenario in which the coefficient of the dim-5 operator is also included into the set of spurions fields, namely, $S_{\text{II}} = \{Y_e\,,Y_e^\dagger, C_5, C_5^\dagger\}$.[5] This is the Case II listed in Table 4.1. We will verify the Saturation Theorem within this scenario following a similar approach to that presented above.

$\mathscr{L}_{\text{SMEFT},\,S_{\text{II}}}$ *from spurion analysis*—. With the new set of spurions $S_{\text{II}} = \{Y_e\,,Y_e^\dagger, C_5, C_5^\dagger\}$, we compute again the Hilbert series for each lepton flavor covariant listed in Tables 4.10 and 4.11. Taking

[5]Note that $C_5^\dagger = C_5^*$, as the matrix of the dim-5 operator in Eq. (4.19) is symmetric.

the unified grading scheme[6]

$$Y_e \sim q\,, \qquad Y_e^\dagger \sim q\,, \qquad C_5 \sim q\,, \qquad C_5^\dagger \sim q\,, \tag{4.29}$$

the Hilbert series of the LN-preserving covariants in Table 4.10 are given by

$$\mathcal{H}_{(\mathbf{1},\mathbf{1})} = \frac{1}{D(q)} \begin{pmatrix} 1+q^6+2q^8+4q^{10}+8q^{12}+7q^{14}+9q^{16}+10q^{18} \\ +9q^{20}+7q^{22}+8q^{24}+4q^{26}+2q^{28}+q^{30}+q^{36} \end{pmatrix}, \tag{4.30a}$$

$$\mathcal{H}_{(\mathbf{3},\bar{\mathbf{3}})} = \frac{1}{D(q)}\, q \begin{pmatrix} 1+2q^2+5q^4+10q^6+21q^8+36q^{10}+55q^{12} \\ +72q^{14}+86q^{16}+90q^{18}+86q^{20}+72q^{22}+55q^{24} \\ +36q^{26}+21q^{28}+10q^{30}+5q^{32}+2q^{34}+q^{36} \end{pmatrix}, \tag{4.30b}$$

$$\mathcal{H}_{(\mathbf{8},\mathbf{1})} = \frac{1}{D(q)}\, q^2 \begin{pmatrix} 2+5q^2+9q^4+19q^6+32q^8+47q^{10}+65q^{12}+77q^{14}+80q^{16} \\ +77q^{18}+65q^{20}+47q^{22}+32q^{24}+19q^{26}+9q^{28}+5q^{30}+2q^{32} \end{pmatrix}, \tag{4.30c}$$

$$\mathcal{H}_{(\mathbf{1},\mathbf{8})} = \frac{1}{D(q)}\, q^2 \begin{pmatrix} 1+2q^2+4q^4+10q^6+21q^8+35q^{10}+53q^{12} \\ +68q^{14}+78q^{16}+83q^{18}+77q^{20}+62q^{22}+46q^{24} \\ +29q^{26}+13q^{28}+6q^{30}+3q^{32}+q^{34}+q^{36}-q^{40} \end{pmatrix}, \tag{4.30d}$$

$$\mathcal{H}_{(\mathbf{8},\mathbf{8})} = \frac{1}{D(q)}\, q^2 \begin{pmatrix} 1+7q^2+26q^4+69q^6+150q^8+273q^{10}+420q^{12} \\ +563q^{14}+664q^{16}+689q^{18}+634q^{20}+515q^{22}+362q^{24} \\ +217q^{26}+108q^{28}+39q^{30}+7q^{32}-2q^{34}-4q^{36}-2q^{38} \end{pmatrix}, \tag{4.30e}$$

$$\mathcal{H}_{(\mathbf{27},\mathbf{1})} = \frac{1}{D(q)}\, q^2 \begin{pmatrix} 1+7q^2+21q^4+52q^6+98q^8+164q^{10} \\ +227q^{12}+281q^{14}+296q^{16}+281q^{18}+227q^{20} \\ +164q^{22}+98q^{24}+52q^{26}+21q^{28}+7q^{30}+q^{32} \end{pmatrix}, \tag{4.30f}$$

$$\mathcal{H}_{(\mathbf{1},\mathbf{27})} = \frac{1}{D(q)}\, q^4 \begin{pmatrix} 1+3q^2+11q^4+29q^6+68q^8+124q^{10}+198q^{12} \\ +263q^{14}+312q^{16}+314q^{18}+281q^{20}+209q^{22}+133q^{24} \\ +62q^{26}+18q^{28}-5q^{30}-9q^{32}-7q^{34}-4q^{36}-2q^{38}-q^{40} \end{pmatrix}, \tag{4.30g}$$

where the denominator factor is

$$\frac{1}{D(q)} = \frac{1}{(1-q^2)^2\,(1-q^4)^3\,(1-q^6)^4\,(1-q^8)^2\,(1-q^{10})}\,. \tag{4.31}$$

For the LN-violating covariants in Table 4.11, the Hilbert series vanish:

$$\mathcal{H}_{(\bar{\mathbf{3}},\mathbf{1})} = \mathcal{H}_{(\mathbf{1},\bar{\mathbf{3}})} = 0\,. \tag{4.32}$$

Again, the number of independent operators is given by the rank of the corresponding module of flavor covariants, which we can compute with the above Hilbert series using Eq. (4.3). In particular, we find that the rank of a flavor irrep in Eq. (4.30) (LN-preserving) equals the dimension of that irrep, while the

[6] Multi-graded Hilbert series can be found in the `Mathematica` notebook HilbCalc.

rank of each irrep in Eq. (4.32) (LN-violating) vanishes:

$$\text{rank}\left({}_{\mathbb{F}_{\text{Inv}}}\mathcal{M}_{\text{Irrep}_G}\right) = \begin{cases} \dim(\text{Irrep}_G) & \text{for } \text{Irrep}_G \text{ in Eq. (4.30)}\,, \\ 0 & \text{for } \text{Irrep}_G \text{ in Eq. (4.32)}\,. \end{cases} \tag{4.33}$$

$\mathscr{L}_{\text{SMEFT}}^{\mathcal{P}_{\text{LN}}}$ with Lepton Parity Conservation—. Under a generic vev of the spurions $S_{\text{II}} = \{Y_e\,, Y_e^\dagger, C_5, C_5^\dagger\}$, the lepton flavor group is broken to the lepton parity as

$$G_{Lf} = U(3)_\ell \times U(3)_e \quad \xrightarrow{\langle Y_e\,, Y_e^\dagger, C_5\,, C_5^\dagger\rangle} \quad H_{S_{\text{II}}} = \mathbb{Z}_2 = \{1, \mathcal{P}_{\text{LN}}\}\,, \tag{4.34}$$

with $\mathcal{P}_{\text{LN}} = (-1)^{\text{LN}}$, since the dim-5 operator breaks the total lepton number by two units. Considering the most general Lagrangian that respects this $\mathbb{Z}_2$ symmetry results in a theory, $\mathscr{L}_{\text{SMEFT}}^{\mathcal{P}_{\text{LN}}}$, with Charged Lepton Flavor Violation (CLFV). The latter yields non-zero decay rates for processes such as $\mu \to e\gamma$. More generally, the theory allows for LN-violating processes in even units of LN.

In terms of the dim-6 operators in SMEFT, the lepton parity does not place further restrictions on the LN-preserving operators in Table 4.10, because it is a subgroup of $U(1)_{\text{LN}}$. Consequently, all flavor combinations are allowed and the number of operators matches the dimension of the representation indicated in Table 4.10. On the other hand, all LN-violating dim-6 operators in Table 4.11 are forbidden by the lepton parity symmetry, as they all violate the total lepton number by one unit [122, 123]. Therefore, it is easy to see that the resulting number of dim-6 operators from imposing lepton parity precisely agree with those from the ranks computed in Eq. (4.33):

$$\mathscr{L}_{\text{SMEFT}, S_{\text{II}}}\Big|_{\text{dim-6}} \cong \mathscr{L}_{\text{SMEFT}}^{\mathcal{P}_{\text{LN}}}\Big|_{\text{dim-6}}\,. \tag{4.35}$$

This verifies the Saturation Theorem in Eq. (4.10) at dim-6 for Case II MLFV in Table 4.1.

4.2.2 νSMEFT with lepton flavor group $G_{Lf} = U(3)_\ell \times U(3)_e \times U(3)_\nu$

Now, we turn to the νSMEFT scenario, where the SMEFT field content is extended with three flavors of right-handed neutrino fields ν that are singlets under the SM gauge group:

$$\phi_{\nu\text{SMEFT}} \in \{\phi_{\text{SM}}\ ,\ \nu\}\,. \tag{4.36}$$

The flavor group in the leptonic sector is now extended to

$$G_{Lf} = U(3)_\ell \times U(3)_e \times U(3)_\nu\,, \tag{4.37}$$

with the following transformation law of the dynamical fields

$$\ell \longrightarrow U_\ell\,\ell\,, \qquad e \longrightarrow U_e\,e\,, \qquad \nu \longrightarrow U_\nu\,\nu\,. \tag{4.38}$$

The G_{Lf}-violating couplings at the renormalizable level of the Lagrangian, $\mathscr{L}_{\nu\text{SM}}$, now include the Yukawa couplings Y_e, Y_ν, and the complex symmetric Majorana mass matrix M_R for the right-handed neutrinos, written here as

$$\mathscr{L}_{\nu\mathrm{SM}} \supset -\frac{1}{2}\,\bar{\nu}\,M_R\,\nu^c - \bar{\ell}\,Y_e\,e\,H - \bar{\ell}\,Y_\nu\,\nu\,\widetilde{H} + \text{H.c.} \tag{4.39}$$

For Case III in Table 4.1, we will only consider the Yukawa matrices Y_e, Y_ν (and their hermitian conjugates) as spurion fields S. In this case, the total lepton number is conserved and the generation of lepton masses is similar to that of the quarks. On the other hand, for Case IV in Table 4.1, we will further include the Majorana mass M_R (and its hermitian conjugate) in the set S. The transformation laws of these spurions under G_{Lf} in Eq. (4.37) read

$$Y_e \longrightarrow U_\ell\,Y_e\,U_e^\dagger\,, \qquad Y_e \sim (\mathbf{3},\bar{\mathbf{3}},\mathbf{1}) \quad \text{with} \quad U(1)_{\ell,\,e,\,\nu} \text{ charges } (+1,-1,0)\,, \tag{4.40}$$

$$Y_\nu \longrightarrow U_\ell\,Y_\nu\,U_\nu^\dagger\,, \qquad Y_\nu \sim (\mathbf{3},\mathbf{1},\bar{\mathbf{3}}) \quad \text{with} \quad U(1)_{\ell,\,e,\,\nu} \text{ charges } (+1,0,-1)\,, \tag{4.41}$$

$$M_R \longrightarrow U_\nu\,M_R\,U_\nu^T\,, \qquad M_R \sim (\mathbf{1},\mathbf{1},\mathbf{6}) \quad \text{with} \quad U(1)_{\ell,\,e,\,\nu} \text{ charges } (0,0,+2)\,. \tag{4.42}$$

Notice that only the $(\mathbf{3}\times\mathbf{3})_{\text{sym}}$ symmetric component in the transformation law of M_R has been retained since it is a symmetric matrix.

Case III: spurion analysis with $S_{\text{III}} = \{Y_e\,, Y_e^\dagger, Y_\nu\,, Y_\nu^\dagger\}$

First, we address Case III in Table 4.1, where the set of spurion fields responsible for the breaking of G_{Lf} is given by $S_{\text{III}} = \{Y_e\,, Y_e^\dagger, Y_\nu\,, Y_\nu^\dagger\}$. Within this framework, it is possible to generate Dirac neutrino masses from the Yukawa coupling Y_ν in Eq. (4.39). This case is in close parallelism with the quark sector of SMEFT, to which all the results presented below apply upon the replacements $Y_e \to Y_d$ and $Y_\nu \to Y_u$.

Since νSMEFT extends the SMEFT field content with three right-handed neutrino fields ν, it has more dim-6 operators on top of those listed in Tables 4.10 and 4.11. The additional LN-preserving operators are collected in Table 4.13, while the LN-violating ones are presented in Table 4.14. As in the previous section, we will verify the Saturation Theorem by comparing the allowed number of dim-6 νSMEFT operators in the EFT from spurion analysis with respect to the H_S-restricted EFT.

$\mathscr{L}_{\nu\text{SMEFT},\,S_{\text{III}}}$ *from spurion analysis*—. Using the unified grading scheme[7]

$$Y_e \sim q\,, \qquad Y_e^\dagger \sim q\,, \qquad Y_\nu \sim q\,, \qquad Y_\nu^\dagger \sim q\,. \tag{4.43}$$

we obtain the following Hilbert series for the LN-preserving covariants that appear in Tables 4.10 and 4.13:

$$\mathcal{H}_{(\mathbf{1},\mathbf{1},\mathbf{1})} = \frac{1}{D(q)}\left(1+q^{12}\right), \tag{4.44a}$$

$$\mathcal{H}_{(\mathbf{3},\bar{\mathbf{3}},\mathbf{1})} = \frac{1}{D(q)}\,q\left(1+2q^2+4q^4+4q^6+4q^8+2q^{10}+q^{12}\right), \tag{4.44b}$$

$$\mathcal{H}_{(\mathbf{1},\bar{\mathbf{3}},\mathbf{3})} = \frac{1}{D(q)}\,q^2\left(1+2q^2+4q^4+4q^6+4q^8+2q^{10}+q^{12}\right), \tag{4.44c}$$

$$\mathcal{H}_{(\bar{\mathbf{3}},\bar{\mathbf{3}},\bar{\mathbf{3}})} = \frac{1}{D(q)}\,q^2\begin{pmatrix}1+4q^2+9q^4+14q^6+15q^8+12q^{10}\\ +5q^{12}-3q^{16}-2q^{18}-q^{20}\end{pmatrix}, \tag{4.44d}$$

[7] Multi-graded Hilbert series are gathered in our `Mathematica` notebook HilbCalc.

$$\mathcal{H}_{(\mathbf{6},\bar{\mathbf{3}},\bar{\mathbf{3}})} = \frac{1}{D(q)}\, q^2 \begin{pmatrix} 1+4q^2+12q^4+22q^6+32q^8+32q^{10}+24q^{12} \\ +8q^{14}-4q^{16}-10q^{18}-8q^{20}-4q^{22}-q^{24} \end{pmatrix}, \tag{4.44e}$$

$$\mathcal{H}_{(\mathbf{8},\mathbf{1},\mathbf{1})} = \frac{1}{D(q)}\, 2q^2 \left(1+2q^2+2q^4+2q^6+q^8\right), \tag{4.44f}$$

$$\mathcal{H}_{(\mathbf{1},\mathbf{8},\mathbf{1})} = \frac{1}{D(q)}\, q^2 \left(1+2q^2+3q^4+4q^6+4q^8+2q^{10}+q^{12}-q^{16}\right), \tag{4.44g}$$

$$\mathcal{H}_{(\mathbf{8},\mathbf{8},\mathbf{1})} = \frac{1}{D(q)}\, q^2 \begin{pmatrix} 1+6q^2+17q^4+30q^6+39q^8+38q^{10}+24q^{12} \\ +6q^{14}-7q^{16}-12q^{18}-9q^{20}-4q^{22}-q^{24} \end{pmatrix}, \tag{4.44h}$$

$$\mathcal{H}_{(\mathbf{1},\mathbf{8},\mathbf{8})} = \frac{1}{D(q)}\, q^4 \begin{pmatrix} 2+8q^2+19q^4+32q^6+40q^8+36q^{10}+21q^{12} \\ +4q^{14}-9q^{16}-12q^{18}-8q^{20}-4q^{22}-q^{24} \end{pmatrix}, \tag{4.44i}$$

$$\mathcal{H}_{(\mathbf{27},\mathbf{1},\mathbf{1})} = \frac{1}{D(q)}\, q^4 \begin{pmatrix} 3+8q^2+17q^4+20q^6+19q^8+8q^{10} \\ -q^{12}-8q^{14}-7q^{16}-4q^{18}-q^{20} \end{pmatrix}, \tag{4.44j}$$

$$\mathcal{H}_{(\mathbf{1},\mathbf{27},\mathbf{1})} = \frac{1}{D(q)}\, q^4 \begin{pmatrix} 1+2q^2+6q^4+10q^6+17q^8+18q^{10}+16q^{12} \\ +6q^{14}-2q^{16}-8q^{18}-7q^{20}-4q^{22}-q^{24} \end{pmatrix}, \tag{4.44k}$$

together with

$$\mathcal{H}_{(\mathbf{3},\mathbf{1},\bar{\mathbf{3}})} = \mathcal{H}_{(\bar{\mathbf{3}},\mathbf{1},\mathbf{3})} = \mathcal{H}_{(\mathbf{3},\bar{\mathbf{3}},\mathbf{1})}\,, \tag{4.45a}$$

$$\mathcal{H}_{(\mathbf{1},\mathbf{1},\mathbf{8})} = \mathcal{H}_{(\mathbf{1},\mathbf{8},\mathbf{1})}\,, \tag{4.45b}$$

$$\mathcal{H}_{(\mathbf{8},\mathbf{1},\mathbf{8})} = \mathcal{H}_{(\mathbf{8},\mathbf{8},\mathbf{1})}\,, \tag{4.45c}$$

$$\mathcal{H}_{(\mathbf{1},\mathbf{1},\mathbf{27})} = \mathcal{H}_{(\mathbf{1},\mathbf{27},\mathbf{1})}\,, \tag{4.45d}$$

where the denominator factor is given by

$$\frac{1}{D(q)} = \frac{1}{(1-q^2)^2\,(1-q^4)^3\,(1-q^6)^4\,(1-q^8)}\,. \tag{4.46}$$

For the LN-violating covariants appearing in Tables 4.11 and 4.14, the Hilbert series vanish:

$$\mathcal{H}_{(\bar{\mathbf{3}},\mathbf{1},\mathbf{1})} = \mathcal{H}_{(\mathbf{1},\bar{\mathbf{3}},\mathbf{1})} = \mathcal{H}_{(\mathbf{1},\mathbf{1},\bar{\mathbf{3}})} = \mathcal{H}_{(\mathbf{1},\mathbf{1},\mathbf{6})} = 0\,. \tag{4.47}$$

As explained before, in order to obtain the number of independent flavor components of each Wilson coefficient, we compute the rank of the corresponding modules by means of Eq. (4.3), and using the Hilbert series quoted above. We find that the rank of a flavor irrep in Eqs. (4.44) and (4.45) (LN-preserving) equals its dimension, while the rank of an irrep in Eq. (4.47) (LN-violating) vanishes:

$$\text{rank}\left({}_{\mathbb{r}_{\text{Inv}}}\mathcal{M}_{\text{Irrep}_G}\right) = \begin{cases} \dim(\text{Irrep}_G) & \text{for Irrep}_G \text{ in Eqs. (4.44) and (4.45)}\,, \\ 0 & \text{for Irrep}_G \text{ in Eq. (4.47)}\,. \end{cases} \tag{4.48}$$

Finally, we provide (a choice of) linearly independent covariants for a few modules, namely, ${}_{\mathbb{r}_{\text{Inv}}}\mathcal{M}_{(\mathbf{3},\bar{\mathbf{3}},\mathbf{1})}$,

${}_{\mathfrak{r}_{\rm Inv}}\mathcal{M}_{(\mathbf{8},\mathbf{1},\mathbf{1})}$, ${}_{\mathfrak{r}_{\rm Inv}}\mathcal{M}_{(\mathbf{3},\mathbf{1},\bar{\mathbf{3}})}$, ${}_{\mathfrak{r}_{\rm Inv}}\mathcal{M}_{(\mathbf{1},\mathbf{3},\bar{\mathbf{3}})}$, and ${}_{\mathfrak{r}_{\rm Inv}}\mathcal{M}_{(\mathbf{1},\mathbf{8},\mathbf{1})}$, collected in Tables 4.5 to 4.9, where we have introduced the Hermitian combination $h_\nu \equiv Y_\nu Y_\nu^\dagger$ for convenience.[8]

q^2		$\overline{h_\nu}$,	$\overline{h_e}$
q^4	$\overline{h_\nu^2}$,	$\overline{h_e^2}$,	$\overline{h_\nu h_e + \text{H.c.}}$
q^6	$\overline{h_\nu^2 h_e + \text{H.c.}}$,		$\overline{h_\nu h_e^2 + \text{H.c.}}$
q^8		$\overline{h_\nu^2 h_e^2 + \text{H.c.}}$	

Table 4.5: A linearly independent set of covariants in the module ${}_{\mathfrak{r}_{\rm Inv}}\mathcal{M}_{(\mathbf{8},\mathbf{1},\mathbf{1})}$ in Case III MLFV listed in Table 4.1. An overline denotes the traceless component of a matrix, *i.e.*, $\overline{A} \equiv A - (1/3)\,\text{tr}(A)\, I_3$, with I_3 the 3×3 identity matrix.

q		Y_ν	
q^3		$h_\nu\, Y_\nu$,	$h_e\, Y_\nu$
q^5	$h_\nu^2\, Y_\nu$,	$h_e^2\, Y_\nu$,	$(h_\nu h_e + \text{H.c.})\, Y_\nu$
q^7	$(h_\nu^2 h_e + \text{H.c.})\, Y_\nu$,		$(h_\nu h_e^2 + \text{H.c.})\, Y_\nu$
q^9		$(h_\nu^2 h_e^2 + \text{H.c.})\, Y_\nu$	

Table 4.6: A linearly independent set of covariants in the module ${}_{\mathfrak{r}_{\rm Inv}}\mathcal{M}_{(\mathbf{3},\mathbf{1},\bar{\mathbf{3}})}$ in Case III MLFV listed in Table 4.1.

q		Y_e	
q^3		$h_\nu\, Y_e$,	$h_e\, Y_e$
q^5	$h_\nu^2\, Y_e$,	$h_e^2\, Y_e$,	$(h_\nu h_e + \text{H.c.})\, Y_e$
q^7	$(h_\nu^2 h_e + \text{H.c.})\, Y_e$,		$(h_\nu h_e^2 + \text{H.c.})\, Y_e$
q^9		$(h_\nu^2 h_e^2 + \text{H.c.})\, Y_e$	

Table 4.7: A linearly independent set of covariants in the module ${}_{\mathfrak{r}_{\rm Inv}}\mathcal{M}_{(\mathbf{3},\bar{\mathbf{3}},\mathbf{1})}$ in Case III MLFV listed in Table 4.1.

$\mathscr{L}_{\nu\text{SMEFT}}^{U(1)_{\rm LN}}$ *with Lepton Number Conservation—.* Similarly to the quark MFV scenario, the lepton flavor group is broken to total lepton number once the Yukawa spurions in $S_{\rm III} = \{Y_e\,, Y_e^\dagger, Y_\nu\,, Y_\nu^\dagger\}$ adopt a generic vev:

$$G_{Lf} = U(3)_\ell \times U(3)_e \times U(3)_\nu \quad \xrightarrow{\langle Y_e\,,\, Y_e^\dagger,\, Y_\nu\,,\, Y_\nu^\dagger \rangle} \quad H_{S_{\rm III}} = U(1)_{\rm LN}\,. \tag{4.49}$$

The most general Lagrangian at mass dimension 6 preserving LN includes all flavor combinations in Tables 4.10 and 4.13, but none of the operators in Tables 4.11 and 4.14. As a consequence, the number of dim-6 operators invariant under $U(1)_{\rm LN}$ exactly matches the ranks computed from the spurion analysis in Eq. (4.48), leading to

$$\mathscr{L}_{\nu\text{SMEFT},\,\text{S}_{\rm III}}\Big|_{\text{dim-6}} \cong \mathscr{L}_{\nu\text{SMEFT}}^{U(1)_{\rm LN}}\Big|_{\text{dim-6}}. \tag{4.50}$$

This verifies the Saturation Theorem in Eq. (4.10) at mass dimension 6 for Case III MLFV in Table 4.1.

[8]Contrary to those in Tables 4.2 to 4.4, the linearly independent covariants here do not form a basis of the module, because the modules are not free and they do not possess a basis.

q^2	$Y_\nu^\dagger Y_e$
q^4	$Y_\nu^\dagger h_\nu Y_e \quad , \quad Y_\nu^\dagger h_e Y_e$
q^6	$Y_\nu^\dagger h_\nu^2 Y_e \quad , \quad Y_\nu^\dagger h_e^2 Y_e \quad , \quad Y_\nu^\dagger (h_\nu h_e + \text{H.c.}) Y_e$
q^8	$Y_\nu^\dagger (h_\nu^2 h_e + \text{H.c.}) Y_e \quad , \quad Y_\nu^\dagger (h_\nu h_e^2 + \text{H.c.}) Y_e$
q^{12}	$Y_\nu^\dagger (h_\nu^2 h_e^2 + \text{H.c.}) Y_e$

Table 4.8: A linearly independent set of covariants in the module ${}_{\mathbb{r}_{\text{Inv}}}\mathcal{M}_{(\mathbf{1},\bar{\mathbf{3}},\mathbf{3})}$ in Case III MLFV listed in Table 4.1.

q^2	$\overline{Y_\nu^\dagger Y_\nu}$
q^4	$\overline{Y_\nu^\dagger h_\nu Y_\nu} \quad , \quad \overline{Y_\nu^\dagger h_e Y_\nu}$
q^6	$\overline{Y_\nu^\dagger h_e^2 Y_\nu} \quad , \quad \overline{Y_\nu^\dagger (h_\nu h_e + \text{H.c.}) Y_\nu}$
q^8	$\overline{Y_\nu^\dagger (h_\nu^2 h_e + \text{H.c.}) Y_\nu} \quad , \quad \overline{Y_\nu^\dagger (h_\nu h_e^2 + \text{H.c.}) Y_\nu}$
q^{12}	$\overline{Y_\nu^\dagger (h_\nu^2 h_e^2 + \text{H.c.}) Y_\nu}$

Table 4.9: A linearly independent set of covariants in the module ${}_{\mathbb{r}_{\text{Inv}}}\mathcal{M}_{(\mathbf{1},\mathbf{1},\mathbf{8})}$ in Case III MLFV listed in Table 4.1. An overline denotes the traceless component of a matrix, *i.e.*, $\overline{A} \equiv A - (1/3)\,\text{tr}(A)\, I_3$, with I_3 the 3×3 identity matrix.

Case IV: spurion analysis with $S_{\text{IV}} = \{Y_e\,, Y_e^\dagger, Y_\nu\,, Y_\nu^\dagger, M_R, M_R^\dagger\}$

Since right-handed neutrinos are singlets under the SM gauge group, we are allowed to write a Majorana mass term for them. Therefore, the most general renormalizable Lagrangian for the lepton sector with three right-handed neutrinos includes all terms in Eq. (4.39). This motivates the study of MFLV with spurions $S_{\text{IV}} = \{Y_e\,, Y_e^\dagger, Y_\nu\,, Y_\nu^\dagger, M_R, M_R^\dagger\}$. Let us verify the Saturation Theorem in Eq. (4.10) by studying the dim-6 operators in Tables 4.10, 4.11, 4.13 and 4.14.

$\mathscr{L}_{\nu\text{SMEFT},\, S_{\text{IV}}}$ *from spurion analysis*—. With a unified grading scheme

$$Y_e \sim q\,, \qquad Y_e^\dagger \sim q\,, \qquad Y_\nu \sim q\,, \qquad Y_\nu^\dagger \sim q\,, \qquad M_R \sim q\,, \qquad M_R^\dagger \sim q\,, \tag{4.51}$$

we have computed the Hilbert series for all the lepton flavor covariants listed in Tables 4.10, 4.11, 4.13 and 4.14. For instance, the Hilbert series for the invariants and the $(\mathbf{1},\mathbf{1},\mathbf{6})$-covariants read

$$\mathcal{H}_{(\mathbf{1},\mathbf{1},\mathbf{1})} = \frac{1}{D(q)} \left(\begin{array}{c} 1 + q^4 + 5q^6 + 9q^8 + 22q^{10} + 61q^{12} + 126q^{14} \\ +273q^{16} + 552q^{18} + 1038q^{20} + 1880q^{22} + 3293q^{24} + 5441q^{26} \\ +8712q^{28} + 13417q^{30} + 19867q^{32} + 28414q^{34} + 39351q^{36} \\ +52604q^{38} + 68220q^{40} + 85783q^{42} + 104588q^{44} + 123852q^{46} \\ +142559q^{48} + 159328q^{50} + 173201q^{52} + 183138q^{54} + 188232q^{56} \\ +188232q^{58} + 183138q^{60} + 173201q^{62} + 159328q^{64} + 142559q^{66} \\ +123852q^{68} + 104588q^{70} + 85783q^{72} + 68220q^{74} + 52604q^{76} \\ +39351q^{78} + 28414q^{80} + 19867q^{82} + 13417q^{84} + 8712q^{86} \\ +5441q^{88} + 3293q^{90} + 1880q^{92} + 1038q^{94} + 552q^{96} + 273q^{98} \\ +126q^{100} + 61q^{102} + 22q^{104} + 9q^{106} + 5q^{108} + q^{110} + q^{114} \end{array} \right), \tag{4.52a}$$

$$\mathcal{H}_{(\mathbf{1},\mathbf{1},\mathbf{6})} = \frac{1}{D(q)}\, q^2 \begin{pmatrix} 1+2q^2+8q^4+24q^6+75q^8+198q^{10}+498q^{12} \\ +1135q^{14}+2434q^{16}+4870q^{18}+9247q^{20}+16622q^{22} \\ +28528q^{24}+46754q^{26}+73518q^{28}+111013q^{30} \\ +161467q^{32}+226415q^{34}+306716q^{36}+401724q^{38} \\ +509439q^{40}+625911q^{42}+745783q^{44}+862182q^{46} \\ +967716q^{48}+1054864q^{50}+1117120q^{52}+1149544q^{54} \\ +1149544q^{56}+1117120q^{58}+1054864q^{60}+967716q^{62} \\ +862182q^{64}+745783q^{66}+625911q^{68}+509439q^{70} \\ +401724q^{72}+306716q^{74}+226415q^{76}+161467q^{78} \\ +111013q^{80}+73518q^{82}+46754q^{84}+28528q^{86} \\ +16622q^{88}+9247q^{90}+4870q^{92}+2434q^{94}+1135q^{96} \\ +498q^{98}+198q^{100}+75q^{102}+24q^{104}+8q^{106}+2q^{108}+q^{110} \end{pmatrix}, \tag{4.52b}$$

where the denominator factor is given by

$$\frac{1}{D(q)} = \frac{1}{(1-q^2)^3(1-q^4)^4(1-q^6)^4(1-q^8)^2(1-q^{10})^2(1-q^{12})^3(1-q^{14})^2(1-q^{16})}\,. \tag{4.53}$$

Since the Hilbert series in this MLFV scenario are lengthy, we relegate the remaining single-graded results to App. A.5.[9] With the Hilbert series given above and the ones collected in App. A.5, once again we can make use of Eq. (4.3) to compute the ranks of the corresponding modules, which give us the number of linearly independent operators in the EFT from spurion analysis. For LN-preserving operators in Tables 4.10 and 4.13, the rank of each flavor irrep equals its dimension:

$$\text{rank}\left({}_{\mathbb{r}_{\text{Inv}}}\mathcal{M}_{\text{Irrep}_G}\right) = \dim(\text{Irrep}_G) \qquad \text{for Irrep}_G \text{ in Tables 4.10 and 4.13}\,. \tag{4.54}$$

For LN-violating operators in Tables 4.11 and 4.14, all ranks vanish except for $(\mathbf{1},\mathbf{1},\mathbf{6})$:

$$\text{rank}\left({}_{\mathbb{r}_{\text{Inv}}}\mathcal{M}_{(\mathbf{1},\mathbf{1},\mathbf{6})}\right) = 6\,, \tag{4.55a}$$

$$\text{rank}\left({}_{\mathbb{r}_{\text{Inv}}}\mathcal{M}_{\text{Irrep}_G}\right) = 0 \qquad \text{for other Irrep}_G \text{ in Tables 4.11 and 4.14}\,. \tag{4.55b}$$

$\mathscr{L}^{\mathcal{P}_{\text{LN}}}_{\nu\text{SMEFT}}$ *with Lepton Parity Conservation*—. Under a generic vev of the set of spurion fields $S_{\text{IV}} = \{Y_e\,, Y_e^\dagger, Y_\nu\,, Y_\nu^\dagger, M_R, M_R^\dagger\}$, the lepton flavor group breaks into the lepton parity as

$$G_{Lf} = U(3)_\ell \times U(3)_e \times U(3)_\nu \xrightarrow{\langle Y_e\,, Y_e^\dagger, Y_\nu\,, Y_\nu^\dagger, M_R, M_R^\dagger \rangle} H_{S_{\text{IV}}} = \mathbb{Z}_2 = \{1, \mathcal{P}_{\text{LN}}\}\,, \tag{4.56}$$

with $\mathcal{P}_{\text{LN}} = (-1)^{\text{LN}}$ as before. Similarly to the case in Eq. (4.34), the Majorana mass term for right-handed neutrinos breaks LN by two units, and thus lepton parity is conserved.

The most general lepton parity-conserving νSMEFT Lagrangian includes all LN-preserving operators in Tables 4.10 and 4.13. Regarding the LN-violating operators in Tables 4.11 and 4.14, most of them are forbidden by the lepton parity $\mathcal{P}_{\text{LN}} = (-1)^{\text{LN}}$ symmetry, except the operator $Q_{\nu\nu\nu\nu}$ in Table 4.14. Comparing with the ranks of the modules obtained in Eqs. (4.54) and (4.55), one can check that

$$\mathscr{L}_{\nu\text{SMEFT},\, S_{\text{IV}}}\Big|_{\text{dim-6}} \cong \mathscr{L}^{\mathcal{P}_{\text{LN}}}_{\nu\text{SMEFT}}\Big|_{\text{dim-6}}\,. \tag{4.57}$$

[9] Hilbert series with a two-variable grading scheme $\{Y_e\,, Y_e^\dagger, Y_\nu\,, Y_\nu^\dagger\} \sim q$ and $\{M_R, M_R^\dagger\} \sim p$ are also available for selected covariants in HilbCalc.

This verifies the Saturation Theorem in Eq. (4.10) at mass dimension 6 for Case IV MLFV in Table 4.1.

4.3 Summary and outlook

In this chapter, we have formulated a saturation theorem—see Eq. (4.10)—that applies to general EFTs constructed from a spurion analysis. When a set of spurion fields S is introduced to gain control over the breaking of a global symmetry G_f in the EFT $\mathscr{L}_{\text{EFT}}([\phi])$, the resulting theory $\mathscr{L}_{\text{EFT, Spurion}}$ *saturates* the original one restricted to be invariant under the subgroup $H_S \subset G_f$ that remains unbroken by a generic vev of the spurions $\langle S \rangle$:

$$\mathscr{L}_{\text{EFT, Spurion}} \equiv \mathscr{L}_{\text{EFT}}([\phi], S)^{G_f}\Big|_{S=\langle S\rangle=\lambda_S} \quad \cong \quad \mathscr{L}_{\text{EFT}}([\phi])^{H_S} \,, \tag{4.58}$$

when *all* powers of S are included in $\mathscr{L}_{\text{EFT, Spurion}}$ and $\lambda_S = \langle S \rangle$ is a *generic* vev. Here the equivalence "$\cong$" means that the two EFTs have the same set of allowed independent effective operators.

We have explored four distinct realizations of the MLFV principle, as outlined in Table 4.1, each corresponding to a different origin of neutrino masses within the SMEFT and νSMEFT frameworks. These scenarios serve as concrete tests to verify the Saturation Theorem at the lowest orders in the EFT expansion. In particular, for each implementation of MLFV, we have analyzed the lepton flavor covariants that contribute at dim-6. The number of linearly independent operators for each covariant has been determined by computing the Hilbert series, and making use of Eq. (4.3). Additionally, for selected flavor covariants, we explicitly provide a choice of linearly independent spurion polynomials that could be useful in phenomenological studies.

The validity of the Saturation Theorem stated in Eq. (4.58) relies on allowing for arbitrary powers of the spurion fields S in the construction of $\mathscr{L}_{\text{EFT, Spurion}}$. However, in many practical applications, one typically restricts the analysis to spurion insertions up to a certain power. Under such conditions, the resulting theory $\mathscr{L}_{\text{EFT, Spurion}}$ may no longer saturate the full set of H_S-invariant operators in $\mathscr{L}_{\text{EFT}}([\phi])^{H_S}$—the theory $\mathscr{L}_{\text{EFT, Spurion}}$ with limited powers of S can be more restricted and hence phenomenologically predictive. A well-motivated example is provided by MLFV scenarios, where the Yukawa couplings Y_e and Y_ν are extremely small, justifying a low-order expansion in these spurions. Moreover, such truncations can occasionally lead to the emergence of accidental symmetries, and one can exploit the method recently developed in [6] to check if any systematic patterns exist for this.

On the other hand, the Saturation Theorem in Eq. (4.58) only holds when the actual couplings $\lambda_S = \langle S \rangle$ fulfill a generic vev. If this condition is not satisfied (for an extreme example, say, experimental measurements suggest that $\lambda_S = 0$), then the residual symmetry may be larger than H_S. In such situations, a larger unbroken subgroup, denoted by H_{Special}, can emerge, even when arbitrary powers of S are included in the EFT construction:

$$H_S \subset H_{\text{Special}} \subset G_f \,. \tag{4.59}$$

It would be worth investigating if saturation still occurs under these circumstances, that is, whether Eq. (4.58) remains valid upon replacing H_S with H_{Special}. We leave a detailed analysis of this possibility for future work.

Here we have implemented the MLFV principle on the maximal lepton flavor groups, *i.e.*, $G_{Lf,\,\mathrm{SMEFT}} = U(3)_\ell \times U(3)_e$ for SMEFT, and $G_{Lf,\,\nu\mathrm{SMEFT}} = U(3)_\ell \times U(3)_e \times U(3)_\nu$ for νSMEFT. An interesting direction is to consider implementing the MLFV principle on a subgroup of these maximal lepton flavor groups. For instance, in νSMEFT, a scenario in which the Majorana neutrino mass term is proportional to the identity would break lepton number but preserve lepton flavor, leading us to consider $G_{Lf} = SU(3)_\ell \times SU(3)_e \times SO(3)_\nu$ instead. This was studied in Ref. [109], and its extension to a local symmetry in [126]. Another possibility is to consider the minimal massive neutrino scenario, where one extends the SM field content with only two generations of right-handed neutrinos, resulting in $G_{Lf} = SU(3)_\ell \times SU(3)_e \times SU(2)_\nu$ or $SU(3)_\ell \times SU(3)_e \times SO(2)_\nu$.

Finally, we have developed a publicly available `Mathematica` code, HilbCalc, that allows to compute general Hilbert series for group invariants and covariants restricted to the classical Lie groups, as explained in detail in App. A. We have applied this code in our MLFV study, but it is intended to be readily accessible for interested readers to use in their own calculations.

$5:\psi^2H^3+\text{H.c.}$		$SU(3)_{\ell,e,\nu}$
Q_{eH}	$(H^\dagger H)(\bar\ell_p e_r H)$	$(\mathbf{3},\bar{\mathbf{3}},\mathbf{1})$
Q_{uH}	$(H^\dagger H)(\bar q_p u_r \widetilde H)$	$(\mathbf{1},\mathbf{1},\mathbf{1})$
Q_{dH}	$(H^\dagger H)(\bar q_p d_r H)$	$(\mathbf{1},\mathbf{1},\mathbf{1})$

$6:\psi^2XH+\text{H.c.}$		$SU(3)_{\ell,e,\nu}$
Q_{eW}	$(\bar\ell_p\sigma^{\mu\nu}e_r)\tau^I HW^I_{\mu\nu}$	$(\mathbf{3},\bar{\mathbf{3}},\mathbf{1})$
Q_{eB}	$(\bar\ell_p\sigma^{\mu\nu}e_r)HB_{\mu\nu}$	$(\mathbf{3},\bar{\mathbf{3}},\mathbf{1})$
Q_{uG}	$(\bar q_p\sigma^{\mu\nu}T^Au_r)\widetilde H\, G^A_{\mu\nu}$	$(\mathbf{1},\mathbf{1},\mathbf{1})$
Q_{uW}	$(\bar q_p\sigma^{\mu\nu}u_r)\tau^I\widetilde H\, W^I_{\mu\nu}$	$(\mathbf{1},\mathbf{1},\mathbf{1})$
Q_{uB}	$(\bar q_p\sigma^{\mu\nu}u_r)\widetilde H\, B_{\mu\nu}$	$(\mathbf{1},\mathbf{1},\mathbf{1})$
Q_{dG}	$(\bar q_p\sigma^{\mu\nu}T^Ad_r)H\, G^A_{\mu\nu}$	$(\mathbf{1},\mathbf{1},\mathbf{1})$
Q_{dW}	$(\bar q_p\sigma^{\mu\nu}d_r)\tau^I H\, W^I_{\mu\nu}$	$(\mathbf{1},\mathbf{1},\mathbf{1})$
Q_{dB}	$(\bar q_p\sigma^{\mu\nu}d_r)H\, B_{\mu\nu}$	$(\mathbf{1},\mathbf{1},\mathbf{1})$

$7:\psi^2H^2D$		$SU(3)_{\ell,e,\nu}$
$Q^{(1)}_{H\ell}$	$(H^\dagger i\overleftrightarrow{D}_\mu H)(\bar\ell_p\gamma^\mu\ell_r)$	$(\mathbf{1}\oplus\mathbf{8},\mathbf{1},\mathbf{1})$
$Q^{(3)}_{H\ell}$	$(H^\dagger i\overleftrightarrow{D}^I_\mu H)(\bar\ell_p\tau^I\gamma^\mu\ell_r)$	$(\mathbf{1}\oplus\mathbf{8},\mathbf{1},\mathbf{1})$
Q_{He}	$(H^\dagger i\overleftrightarrow{D}_\mu H)(\bar e_p\gamma^\mu e_r)$	$(\mathbf{1},\mathbf{1}\oplus\mathbf{8},\mathbf{1})$
$Q^{(1)}_{Hq}$	$(H^\dagger i\overleftrightarrow{D}_\mu H)(\bar q_p\gamma^\mu q_r)$	$(\mathbf{1},\mathbf{1},\mathbf{1})$
$Q^{(3)}_{Hq}$	$(H^\dagger i\overleftrightarrow{D}^I_\mu H)(\bar q_p\tau^I\gamma^\mu q_r)$	$(\mathbf{1},\mathbf{1},\mathbf{1})$
Q_{Hu}	$(H^\dagger i\overleftrightarrow{D}_\mu H)(\bar u_p\gamma^\mu u_r)$	$(\mathbf{1},\mathbf{1},\mathbf{1})$
Q_{Hd}	$(H^\dagger i\overleftrightarrow{D}_\mu H)(\bar d_p\gamma^\mu d_r)$	$(\mathbf{1},\mathbf{1},\mathbf{1})$
Q_{Hud} + h.c.	$i(\widetilde H^\dagger D_\mu H)(\bar u_p\gamma^\mu d_r)$	$(\mathbf{1},\mathbf{1},\mathbf{1})$

$8:(\bar LL)(\bar LL)$		$SU(3)_{\ell,e,\nu}$
$Q_{\ell\ell}$	$(\bar\ell_p\gamma_\mu\ell_r)(\bar\ell_s\gamma^\mu\ell_t)$	$(\mathbf{1}\oplus\mathbf{1}\oplus\mathbf{8}\oplus\mathbf{8}\oplus\mathbf{27},\mathbf{1},\mathbf{1})$
$Q^{(1)}_{qq}$	$(\bar q_p\gamma_\mu q_r)(\bar q_s\gamma^\mu q_t)$	$(\mathbf{1},\mathbf{1},\mathbf{1})$
$Q^{(3)}_{qq}$	$(\bar q_p\gamma_\mu\tau^I q_r)(\bar q_s\gamma^\mu\tau^I q_t)$	$(\mathbf{1},\mathbf{1},\mathbf{1})$
$Q^{(1)}_{\ell q}$	$(\bar\ell_p\gamma_\mu\ell_r)(\bar q_s\gamma^\mu q_t)$	$(\mathbf{1}\oplus\mathbf{8},\mathbf{1},\mathbf{1})$
$Q^{(3)}_{\ell q}$	$(\bar\ell_p\gamma_\mu\tau^I\ell_r)(\bar q_s\gamma^\mu\tau^I q_t)$	$(\mathbf{1}\oplus\mathbf{8},\mathbf{1},\mathbf{1})$

$8:(\bar LL)(\bar RR)$		$SU(3)_{\ell,e,\nu}$
$Q_{\ell e}$	$(\bar\ell_p\gamma_\mu\ell_r)(\bar e_s\gamma^\mu e_t)$	$(\mathbf{1}\oplus\mathbf{8},\mathbf{1}\oplus\mathbf{8},\mathbf{1})$
$Q_{\ell u}$	$(\bar\ell_p\gamma_\mu\ell_r)(\bar u_s\gamma^\mu u_t)$	$(\mathbf{1}\oplus\mathbf{8},\mathbf{1},\mathbf{1})$
$Q_{\ell d}$	$(\bar\ell_p\gamma_\mu\ell_r)(\bar d_s\gamma^\mu d_t)$	$(\mathbf{1}\oplus\mathbf{8},\mathbf{1},\mathbf{1})$
Q_{qe}	$(\bar q_p\gamma_\mu q_r)(\bar e_s\gamma^\mu e_t)$	$(\mathbf{1},\mathbf{1}\oplus\mathbf{8},\mathbf{1})$
$Q^{(1)}_{qu}$	$(\bar q_p\gamma_\mu q_r)(\bar u_s\gamma^\mu u_t)$	$(\mathbf{1},\mathbf{1},\mathbf{1})$
$Q^{(8)}_{qu}$	$(\bar q_p\gamma_\mu T^A q_r)(\bar u_s\gamma^\mu T^A u_t)$	$(\mathbf{1},\mathbf{1},\mathbf{1})$
$Q^{(1)}_{qd}$	$(\bar q_p\gamma_\mu q_r)(\bar d_s\gamma^\mu d_t)$	$(\mathbf{1},\mathbf{1},\mathbf{1})$
$Q^{(8)}_{qd}$	$(\bar q_p\gamma_\mu T^A q_r)(\bar d_s\gamma^\mu T^A d_t)$	$(\mathbf{1},\mathbf{1},\mathbf{1})$

$8:(\bar RR)(\bar RR)$		$SU(3)_{\ell,e,\nu}$
Q_{ee}	$(\bar e_p\gamma_\mu e_r)(\bar e_s\gamma^\mu e_t)$	$(\mathbf{1},\mathbf{1}\oplus\mathbf{8}\oplus\mathbf{27},\mathbf{1})$
Q_{uu}	$(\bar u_p\gamma_\mu u_r)(\bar u_s\gamma^\mu u_t)$	$(\mathbf{1},\mathbf{1},\mathbf{1})$
Q_{dd}	$(\bar d_p\gamma_\mu d_r)(\bar d_s\gamma^\mu d_t)$	$(\mathbf{1},\mathbf{1},\mathbf{1})$
Q_{eu}	$(\bar e_p\gamma_\mu e_r)(\bar u_s\gamma^\mu u_t)$	$(\mathbf{1},\mathbf{1}\oplus\mathbf{8},\mathbf{1})$
Q_{ed}	$(\bar e_p\gamma_\mu e_r)(\bar d_s\gamma^\mu d_t)$	$(\mathbf{1},\mathbf{1}\oplus\mathbf{8},\mathbf{1})$
$Q^{(1)}_{ud}$	$(\bar u_p\gamma_\mu u_r)(\bar d_s\gamma^\mu d_t)$	$(\mathbf{1},\mathbf{1},\mathbf{1})$
$Q^{(8)}_{ud}$	$(\bar u_p\gamma_\mu T^A u_r)(\bar d_s\gamma^\mu T^A d_t)$	$(\mathbf{1},\mathbf{1},\mathbf{1})$

$8:(\bar LR)(\bar LR)+\text{H.c.}$		$SU(3)_{\ell,e,\nu}$
$Q^{(1)}_{quqd}$	$(\bar q^j_p u_r)\epsilon_{jk}(\bar q^k_s d_t)$	$(\mathbf{1},\mathbf{1},\mathbf{1})$
$Q^{(8)}_{quqd}$	$(\bar q^j_p T^A u_r)\epsilon_{jk}(\bar q^k_s T^A d_t)$	$(\mathbf{1},\mathbf{1},\mathbf{1})$
$Q^{(1)}_{\ell equ}$	$(\bar\ell^j_p e_r)\epsilon_{jk}(\bar q^k_s u_t)$	$(\mathbf{3},\bar{\mathbf{3}},\mathbf{1})$
$Q^{(3)}_{\ell equ}$	$(\bar\ell^j_p\sigma_{\mu\nu}e_r)\epsilon_{jk}(\bar q^k_s\sigma^{\mu\nu}u_t)$	$(\mathbf{3},\bar{\mathbf{3}},\mathbf{1})$

$8:(\bar LR)(\bar RL)+\text{H.c.}$		$SU(3)_{\ell,e,\nu}$
$Q_{\ell edq}$	$(\bar\ell^j_p e_r)(\bar d_s q_{tj})$	$(\mathbf{3},\bar{\mathbf{3}},\mathbf{1})$

Table 4.10: Lepton and baryon number preserving fermionic operators in dim-6 SMEFT [120], together with the corresponding spurious transformations of the Wilson coefficients under the non-abelian part of the MLFV group, $SU(3)_{\ell,e,\nu}\equiv SU(3)_\ell\times SU(3)_e\times SU(3)_\nu\subset G_{Lf}$. Transformations under the $U(1)$ factors can be inferred from Eq. (4.38). Operators are organized into eight classes as in Ref. [124], with classes 1-4 collecting bosonic operators not shown here. The subscripts p,r,s,t denote flavor indices. Note that the SMEFT operators, by definition, do not involve right-handed neutrino fields ν, and hence transform trivially under the $SU(3)_\nu$ factor.

	LN- and BN-violating	$SU(3)_{\ell,e,\nu}$	# invariants under lepton parity $\mathcal{P}_{\text{LN}}$
Q_{duq}	$\epsilon_{\alpha\beta\gamma}\epsilon_{jk}\left[(d_p^\alpha)^T C u_r^\beta\right]\left[(q_s^{\gamma j})^T C \ell_t^k\right]$	$(\mathbf{\bar{3}},\mathbf{1},\mathbf{1})$	0
Q_{qqu}	$\epsilon_{\alpha\beta\gamma}\epsilon_{jk}\left[(q_p^{\alpha j})^T C q_r^{\beta k}\right]\left[(u_s^\gamma)^T C e_t\right]$	$(\mathbf{1},\mathbf{\bar{3}},\mathbf{1})$	0
Q_{qqq}	$\epsilon_{\alpha\beta\gamma}\epsilon_{jn}\epsilon_{km}\left[(q_p^{\alpha j})^T C q_r^{\beta k}\right]\left[(q_s^{\gamma m})^T C \ell_t^n\right]$	$(\mathbf{\bar{3}},\mathbf{1},\mathbf{1})$	0
Q_{duu}	$\epsilon_{\alpha\beta\gamma}\left[(d_p^\alpha)^T C u_r^\beta\right]\left[(u_s^\gamma)^T C e_t\right]$	$(\mathbf{1},\mathbf{\bar{3}},\mathbf{1})$	0

Table 4.11: Lepton and baryon number violating fermionic operators in dim-6 SMEFT [120,121], together with the corresponding spurious transformations of the Wilson coefficients under the non-abelian part of the MLFV group, $SU(3)_{\ell,e,\nu} \equiv SU(3)_\ell \times SU(3)_e \times SU(3)_\nu \subset G_{Lf}$. Transformations under the $U(1)$ factors can be inferred from Eq. (4.38). Here $C = i\gamma^0\gamma^2$ is the charge conjugation matrix. The subscripts p, r, s, t denote flavor indices. Note that the SMEFT operators, by definition, do not involve right-handed neutrino fields ν, and hence transform trivially under the $SU(3)_\nu$ factor. All these operators violate the total lepton number $U(1)_{\text{LN}}$, as well as the lepton parity $\mathcal{P}_{\text{LN}} \equiv (-1)^{\text{LN}}$.

	$5 : \psi^2 H^3 + \text{H.c.}$	Restriction	#
Q_{eH}	$(H^\dagger H)(\bar{\ell}_p e_r H)$	$p = r$	3
Q_{uH}	$(H^\dagger H)(\bar{q}_p u_r \widetilde{H})$	–	1
Q_{dH}	$(H^\dagger H)(\bar{q}_p d_r H)$	–	1

	$6 : \psi^2 X H + \text{H.c.}$	Restriction	#
Q_{eW}	$(\bar{\ell}_p \sigma^{\mu\nu} e_r)\tau^I H W^I_{\mu\nu}$	$p = r$	3
Q_{eB}	$(\bar{\ell}_p \sigma^{\mu\nu} e_r) H B_{\mu\nu}$	$p = r$	3
Q_{uG}	$(\bar{q}_p \sigma^{\mu\nu} T^A u_r)\widetilde{H}\, G^A_{\mu\nu}$	–	1
Q_{uW}	$(\bar{q}_p \sigma^{\mu\nu} u_r)\tau^I \widetilde{H}\, W^I_{\mu\nu}$	–	1
Q_{uB}	$(\bar{q}_p \sigma^{\mu\nu} u_r)\widetilde{H}\, B_{\mu\nu}$	–	1
Q_{dG}	$(\bar{q}_p \sigma^{\mu\nu} T^A d_r) H\, G^A_{\mu\nu}$	–	1
Q_{dW}	$(\bar{q}_p \sigma^{\mu\nu} d_r)\tau^I H\, W^I_{\mu\nu}$	–	1
Q_{dB}	$(\bar{q}_p \sigma^{\mu\nu} d_r) H\, B_{\mu\nu}$	–	1

	$7 : \psi^2 H^2 D$	Restriction	#
$Q^{(1)}_{H\ell}$	$(H^\dagger i \overleftrightarrow{D}_\mu H)(\bar{\ell}_p \gamma^\mu \ell_r)$	$p = r$	3
$Q^{(3)}_{H\ell}$	$(H^\dagger i \overleftrightarrow{D}^I_\mu H)(\bar{\ell}_p \tau^I \gamma^\mu \ell_r)$	$p = r$	3
Q_{He}	$(H^\dagger i \overleftrightarrow{D}_\mu H)(\bar{e}_p \gamma^\mu e_r)$	$p = r$	3
$Q^{(1)}_{Hq}$	$(H^\dagger i \overleftrightarrow{D}_\mu H)(\bar{q}_p \gamma^\mu q_r)$	–	1
$Q^{(3)}_{Hq}$	$(H^\dagger i \overleftrightarrow{D}^I_\mu H)(\bar{q}_p \tau^I \gamma^\mu q_r)$	–	1
Q_{Hu}	$(H^\dagger i \overleftrightarrow{D}_\mu H)(\bar{u}_p \gamma^\mu u_r)$	–	1
Q_{Hd}	$(H^\dagger i \overleftrightarrow{D}_\mu H)(\bar{d}_p \gamma^\mu d_r)$	–	1
Q_{Hud} + h.c.	$i(\widetilde{H}^\dagger D_\mu H)(\bar{u}_p \gamma^\mu d_r)$	–	1

	$8 : (\bar{L}L)(\bar{L}L)$	Restriction	#
$Q_{\ell\ell}$	$(\bar{\ell}_p \gamma_\mu \ell_r)(\bar{\ell}_s \gamma^\mu \ell_t)$	$p = r \geq s = t$	6
		$p = t > s = r$	3
$Q^{(1)}_{qq}$	$(\bar{q}_p \gamma_\mu q_r)(\bar{q}_s \gamma^\mu q_t)$	–	1
$Q^{(3)}_{qq}$	$(\bar{q}_p \gamma_\mu \tau^I q_r)(\bar{q}_s \gamma^\mu \tau^I q_t)$	–	1
$Q^{(1)}_{\ell q}$	$(\bar{\ell}_p \gamma_\mu \ell_r)(\bar{q}_s \gamma^\mu q_t)$	$p = r$	3
$Q^{(3)}_{\ell q}$	$(\bar{\ell}_p \gamma_\mu \tau^I \ell_r)(\bar{q}_s \gamma^\mu \tau^I q_t)$	$p = r$	3

	$8 : (\bar{L}L)(\bar{R}R)$	Restriction	#
$Q_{\ell e}$	$(\bar{\ell}_p \gamma_\mu \ell_r)(\bar{e}_s \gamma^\mu e_t)$	$p = r,\ s = t$	9
		$p = t \neq s = r$	6
$Q_{\ell u}$	$(\bar{\ell}_p \gamma_\mu \ell_r)(\bar{u}_s \gamma^\mu u_t)$	$p = r$	3
$Q_{\ell d}$	$(\bar{\ell}_p \gamma_\mu \ell_r)(\bar{d}_s \gamma^\mu d_t)$	$p = r$	3
Q_{qe}	$(\bar{q}_p \gamma_\mu q_r)(\bar{e}_s \gamma^\mu e_t)$	$p = r$	3
$Q^{(1)}_{qu}$	$(\bar{q}_p \gamma_\mu q_r)(\bar{u}_s \gamma^\mu u_t)$	–	1
$Q^{(8)}_{qu}$	$(\bar{q}_p \gamma_\mu T^A q_r)(\bar{u}_s \gamma^\mu T^A u_t)$	–	1
$Q^{(1)}_{qd}$	$(\bar{q}_p \gamma_\mu q_r)(\bar{d}_s \gamma^\mu d_t)$	–	1
$Q^{(8)}_{qd}$	$(\bar{q}_p \gamma_\mu T^A q_r)(\bar{d}_s \gamma^\mu T^A d_t)$	–	1

	$8 : (\bar{R}R)(\bar{R}R)$	Restriction	#
Q_{ee}	$(\bar{e}_p \gamma_\mu e_r)(\bar{e}_s \gamma^\mu e_t)$	$p = r \geq s = t$	6
Q_{uu}	$(\bar{u}_p \gamma_\mu u_r)(\bar{u}_s \gamma^\mu u_t)$	–	1
Q_{dd}	$(\bar{d}_p \gamma_\mu d_r)(\bar{d}_s \gamma^\mu d_t)$	–	1
Q_{eu}	$(\bar{e}_p \gamma_\mu e_r)(\bar{u}_s \gamma^\mu u_t)$	$p = r$	3
Q_{ed}	$(\bar{e}_p \gamma_\mu e_r)(\bar{d}_s \gamma^\mu d_t)$	$p = r$	3
$Q^{(1)}_{ud}$	$(\bar{u}_p \gamma_\mu u_r)(\bar{d}_s \gamma^\mu d_t)$	–	1
$Q^{(8)}_{ud}$	$(\bar{u}_p \gamma_\mu T^A u_r)(\bar{d}_s \gamma^\mu T^A d_t)$	–	1

	$8 : (\bar{L}R)(\bar{L}R) + \text{H.c.}$	Restriction	#
$Q^{(1)}_{quqd}$	$(\bar{q}^j_p u_r)\epsilon_{jk}(\bar{q}^k_s d_t)$	–	1
$Q^{(8)}_{quqd}$	$(\bar{q}^j_p T^A u_r)\epsilon_{jk}(\bar{q}^k_s T^A d_t)$	–	1
$Q^{(1)}_{\ell equ}$	$(\bar{\ell}^j_p e_r)\epsilon_{jk}(\bar{q}^k_s u_t)$	$p = r$	3
$Q^{(3)}_{\ell equ}$	$(\bar{\ell}^j_p \sigma_{\mu\nu} e_r)\epsilon_{jk}(\bar{q}^k_s \sigma^{\mu\nu} u_t)$	$p = r$	3

	$8 : (\bar{L}R)(\bar{R}L) + \text{H.c.}$	Restriction	#
$Q_{\ell edq}$	$(\bar{\ell}^j_p e_r)(\bar{d}_s q_{tj})$	$p = r$	3

Table 4.12: Restrictions from $U(1)_e \times U(1)_\mu \times U(1)_\tau$ invariance on the lepton and baryon number preserving dim-6 SMEFT fermionic operators listed in Table 4.10. These operators generate processes with LFUV, but no CLFV. We indicate the constraints on flavor indices p, r, s, t, as well as the resulting total number of invariants under $U(1)_e \times U(1)_\mu \times U(1)_\tau$. The symbol "–" means that no restrictions are imposed, and thus the resulting number of invariants equals the dimension of the representation.

$5 : \psi^2 H^3 + \text{H.c.}$		$SU(3)_{\ell,e,\nu}$
$Q_{\ell\nu H}$	$(\bar{\ell}_p \nu_r)\tilde{H}(H^\dagger H)$	$(\mathbf{3},\mathbf{1},\bar{\mathbf{3}})$

$6 : \psi^2 X H + \text{H.c.}$		$SU(3)_{\ell,e,\nu}$
$Q_{\nu W}$	$(\bar{\ell}_p \sigma^{\mu\nu}\nu_r)\tau^I \tilde{H} W^I_{\mu\nu}$	$(\mathbf{3},\mathbf{1},\bar{\mathbf{3}})$
$Q_{\nu B}$	$(\bar{\ell}_p \sigma^{\mu\nu}\nu_r)\tilde{H} B_{\mu\nu}$	$(\mathbf{3},\mathbf{1},\bar{\mathbf{3}})$

$7 : \psi^2 H^2 D$		$SU(3)_{\ell,e,\nu}$
$Q_{H\nu}$	$(H^\dagger i\overleftrightarrow{D}_\mu H)(\bar{\nu}_p \gamma^\mu \nu_r)$	$(\mathbf{1},\mathbf{1},\mathbf{1}\oplus\mathbf{8})$
$Q_{H\nu e}$ + h.c.	$i(\widetilde{H}^\dagger D_\mu H)(\bar{\nu}_p \gamma^\mu e_r)$	$(\mathbf{1},\bar{\mathbf{3}},\mathbf{3})$

$8 : (\bar{L}L)(\bar{R}R)$		$SU(3)_{\ell,e,\nu}$
$Q_{\ell\nu}$	$(\bar{\ell}_p \gamma_\mu \ell_r)(\bar{\nu}_s \gamma^\mu \nu_t)$	$(\mathbf{1}\oplus\mathbf{8},\mathbf{1},\mathbf{1}\oplus\mathbf{8})$
$Q_{q\nu}$	$(\bar{q}_p \gamma_\mu q_r)(\bar{\nu}_s \gamma^\mu \nu_t)$	$(\mathbf{1},\mathbf{1},\mathbf{1}\oplus\mathbf{8})$

$8 : (\bar{R}R)(\bar{R}R)$		$SU(3)_{\ell,e,\nu}$
$Q_{\nu\nu}$	$(\bar{\nu}_p \gamma_\mu \nu_r)(\bar{\nu}_s \gamma^\mu \nu_t)$	$(\mathbf{1},\mathbf{1},\mathbf{1}\oplus\mathbf{8}\oplus\mathbf{27})$
$Q_{e\nu}$	$(\bar{e}_p \gamma_\mu e_r)(\bar{\nu}_s \gamma^\mu \nu_t)$	$(\mathbf{1},\mathbf{1}\oplus\mathbf{8},\mathbf{1}\oplus\mathbf{8})$
$Q_{u\nu}$	$(\bar{u}_p \gamma_\mu u_r)(\bar{\nu}_s \gamma^\mu \nu_t)$	$(\mathbf{1},\mathbf{1},\mathbf{1}\oplus\mathbf{8})$
$Q_{d\nu}$	$(\bar{d}_p \gamma_\mu d_r)(\bar{\nu}_s \gamma^\mu \nu_t)$	$(\mathbf{1},\mathbf{1},\mathbf{1}\oplus\mathbf{8})$
$Q_{du\nu e}$ + h.c.	$(\bar{d}_p \gamma_\mu u_r)(\bar{\nu}_s \gamma^\mu e_t)$	$(\mathbf{1},\bar{\mathbf{3}},\mathbf{3})$

$8 : (\bar{L}R)(\bar{L}R) + \text{H.c.}$		$SU(3)_{\ell,e,\nu}$
$Q_{\ell\nu\ell e}$	$(\bar{\ell}^j_p \nu_r)\epsilon_{jk}(\bar{\ell}^k_s e_t)$	$(\bar{\mathbf{3}}\oplus\mathbf{6},\bar{\mathbf{3}},\bar{\mathbf{3}})$
$Q_{\ell\nu qd}$	$(\bar{\ell}^j_p \nu_r)\epsilon_{jk}(\bar{q}^k_s d_t)$	$(\mathbf{3},\mathbf{1},\bar{\mathbf{3}})$
$Q_{\ell dq\nu}$	$(\bar{\ell}^j_p d_r)\epsilon_{jk}(\bar{q}^k_s \nu_t)$	$(\mathbf{3},\mathbf{1},\bar{\mathbf{3}})$

$8 : (\bar{L}R)(\bar{R}L) + \text{H.c.}$		$SU(3)_{\ell,e,\nu}$
$Q_{qu\nu\ell}$	$(\bar{q}_p u_r)(\bar{\nu}_s \ell_t)$	$(\bar{\mathbf{3}},\mathbf{1},\mathbf{3})$

Table 4.13: Lepton and baryon number preserving dim-6 νSMEFT operators involving right-handed neutrino fields ν [125], together with the corresponding spurious transformations of the Wilson coefficients under the non-abelian part of the MLFV group, $SU(3)_{\ell,e,\nu} \equiv SU(3)_\ell \times SU(3)_e \times SU(3)_\nu \subset G_{Lf}$. Transformations under the $U(1)$ factors can be inferred from Eq. (4.38). The subscripts p, r, s, t denote flavor indices.

LN-violating + H.c.		$SU(3)_{\ell,e,\nu}$	# invariants under lepton parity $\mathcal{P}_{\text{LN}}$
$Q_{\nu\nu\nu\nu}$	$(\nu_p C \nu_r)(\nu_s C \nu_t)$	$(\mathbf{1},\mathbf{1},\mathbf{6})$	6

LN- and BN-violating + H.c.		$SU(3)_{\ell,e,\nu}$	# invariants under lepton parity $\mathcal{P}_{\text{LN}}$
$Q_{qqd\nu}$	$\epsilon_{\alpha\beta\gamma}\epsilon_{jk}[(q^{\alpha j}_p)^T C q^{\beta k}_r][(d^\gamma_s)^T C \nu_t]$	$(\mathbf{1},\mathbf{1},\bar{\mathbf{3}})$	0
$Q_{udd\nu}$	$\epsilon_{\alpha\beta\gamma}[(u^\alpha_p)^T C d^\beta_r][(d^\gamma_s)^T C \nu_t]$	$(\mathbf{1},\mathbf{1},\bar{\mathbf{3}})$	0

Table 4.14: Lepton number violating dim-6 νSMEFT operators involving right-handed neutrino fields ν [125], together with the corresponding spurious transformations of the Wilson coefficients under the non-abelian part of the MLFV group, $SU(3)_{\ell,e,\nu} \equiv SU(3)_\ell \times SU(3)_e \times SU(3)_\nu \subset G_{Lf}$. Transformations under the $U(1)$ factors can be inferred from Eq. (4.38). Here $C = i\gamma^0\gamma^2$ is the charge conjugation matrix. The subscripts p, r, s, t denote flavor indices. All these operators violate the total lepton number $U(1)_{\text{LN}}$, among which $Q_{\nu\nu\nu\nu}$ preserves the lepton parity $\mathcal{P}_{\text{LN}} \equiv (-1)^{\text{LN}}$.

5 Light states in multi-Higgs models with spontaneous CP violation

The quest for New Physics phenomena, aiming to solve some of the open problems outlined in chapter 1, usually involves the presence of new particles. Knowing their masses is undoubtedly of paramount importance. In this endeavor, the interplay between theory and experiment, as in many other branches of physics, can be mutually beneficial in obtaining the final answer. We do not need to go back very far in time to find an excellent example, namely, the decades-long history of the Higgs boson that culminated with its glorious discovery in 2012 [24, 25]. Before that moment arrived, there were already indirect experimental hints [127], as well as a variety of theoretical arguments constraining the mass of the scalar boson. Earlier works by Linde [128] and Weinberg [129] set a lower bound on the Higgs mass, order of a few GeV, by requiring vacuum (meta)stability, *i.e.*, the vacuum being a non-trivial (local) minimum of the potential. On the other hand, upper bounds were anticipated by Dicus and Mathur [130], followed by the classical papers of Lee, Quigg, and Thacker [93,94]. In these works, perturbative unitarity bounds on tree-level $2 \to 2$ scattering amplitudes involving the longitudinal polarizations of gauge bosons (or, equivalently, the would-be Goldstone bosons [131]) and scalar bosons were translated into an upper bound on the Higgs quartic coupling and, consequently, to its mass—see Eq. (1.29). As mentioned earlier, the existence of a relatively light Higgs boson in the TeV regime was mandatory for perturbation theory to remain applicable to the weak interaction. Similar conclusions were reached by Veltman [132] when computing radiative corrections from Higgs boson exchange. Later on, Ref. [133] also provided both lower and upper bounds by requiring the vacuum to be an absolute (rather than local) minimum of the perturbatively computed potential, as well as the quartic self-couplings of the Higgs particle to generate a reliable perturbation series, respectively. In the context of GUTs, Ref. [134] set tighter bounds imposing that the breakdown of perturbativity and vacuum instability do not develop up to the unification scale. Alternatively, non-triviality of the renormalized quartic coupling served as well to place upper bounds on the scalar mass [135]. All in all, today we know that the SM-like Higgs boson mass is of around 125 GeV, so that this experimental data might be now used to extract information about the quartic coupling in the scalar potential.

The very same question can be naturally raised in models with more than one Higgs doublet. An important implication of perturbativity requirements on extended scalar sectors featuring spontaneous electroweak symmetry breaking is the existence of a Higgs-like state whose mass cannot be much larger than the EW scale—given by $v \simeq 246$ GeV—, as shown generically in [136, 137]. The case of 2HDMs, first proposed by T. D. Lee [95, 96] with the appealing possibility to have SCPV, has received substantial attention on that regard. Tree-level unitarity bounds on the new scalar masses have been set in the framework of 2HDMs shaped by some symmetry—not of the CP type, but typically a $\mathbb{Z}_2$ discrete symmetry—in [138–142] as well as in more general scenarios in [143,144]. Furthermore, triviality bounds were also addressed in [140]. Other possible scalar sectors such as the singlet extension or minimal supersymmetric realizations were included in [139]. Complementarily, in models with multiple Higgs particles, the scenario with new *heavy* scalars, *i.e.*, scalars with masses much larger than v, was addressed generically in [145], and recently in [146,147] for multi-Higgs-doublet models in connection with symmetries (again, not of the CP type). More precisely, Ref. [146] concluded that, in the absence of small mixing angles and vanishing vevs, all soft symmetry breaking terms must be present in order to have a decoupling regime in the scalar spectrum of MHDMs. Interestingly, Ref. [147] further proved that such a regime is nevertheless accessible in MHDMs satisfying an exact symmetry if and only if the vacuum is also invariant under the symmetry.

Our work is focused in MHDMs with SCPV, that is, described by a CP invariant Lagrangian together with a CP non-invariant vacuum. We will simply refer to them as *real* MHDMs for reasons to become clear later. A possible relationship between the CP properties of the vacuum and the scalar spectrum might not be obvious, and was first suggested in [148]. Concerning real 2HDMs with SCPV, it was realized in [111], and analyzed in detail in [149], that those perturbativity-based bounds on the masses apply to *all* new scalars in the model, one charged and two neutral, in addition to the neutral Higgs-like state—for some phenomenological implications, see [150]. The rationale behind is rather simple. With spontaneous symmetry breaking, there are two types of mass terms in the 2HDM, either dimensionful quadratic couplings or dimensionless quartic couplings multiplied by the square of the vevs. If the quartic couplings are bounded by perturbativity requirements, masses much larger than v can only arise through correspondingly large quadratic couplings. The crucial particularity of the real 2HDM with SCPV is the fact that there are only three quadratic couplings, which is also the number of stationarity conditions imposed on the scalar potential to ensure that the vacuum is an extremum. These stationarity conditions can then be used to trade all three quadratic couplings for quartic couplings multiplied by the square of the vevs. As a consequence, all mass terms are bounded through perturbativity requirements on the quartic couplings. This outcome is indeed peculiar: rather than the generic expectation of having at least one light scalar—the Higgs-like state—, perturbativity requirements bound *the whole scalar spectrum*. This suggests a very interesting question: if instead of a real 2HDM with SCPV, one considers a real MHDM with SCPV, could a similar mechanism be at play? The prospects on that respect are, *a priori*, discouraging: the number of quadratic couplings grows with n^2, while the number of stationarity conditions only scales with n. Does this imply that *all* the masses of the new scalars can be much larger than the EW scale?

The answer to this question, which stands as the main result of this chapter and our contribution to the longstanding research effort in this area, is rather surprising [2]: *for all n, the scalar spectrum necessarily includes one charged and two neutral states (in addition to the neutral Higgs-like particle) that must be light, that is, whose masses cannot be much larger than the EW scale once perturbativity requirements are imposed on the quartic couplings.*

In order to shed some light on this statement, this chapter is organized as follows. In Sec. 5.1, we recall the basic ingredients of the real MHDM with SCPV that are relevant for the subsequent analysis. Then, we carry out a numerical exercise that illustrates our main results in Sec. 5.2, and provide an analytical justification in Sec. 5.3, briefly commenting on the phenomenological prospects. Finally, we summarize our findings in Sec. 5.4.

5.1 Real MHDMs with SCPV

The most general scalar potential involving n Higgs doublets Φ_a $(a = 1, \ldots, n)$, and invariant under the trivial CP transformations of the scalar fields ($\Phi_a \to \Phi_a^*$), can be conveniently written as

$$\mathscr{V}(\Phi_1, \ldots, \Phi_n) = \mathscr{V}_2(\Phi_1, \ldots, \Phi_n) + \mathscr{V}_4(\Phi_1, \ldots, \Phi_n)\,, \tag{5.1}$$

where $\mathscr{V}_2$ represents the quadratic part of the potential given by

$$\mathscr{V}_2(\Phi_1, \ldots, \Phi_n) = \sum_{a=1}^{n} \mu_a^2 \Phi_a^\dagger \Phi_a + \sum_{a=1}^{n-1} \sum_{b=a+1}^{n} \mu_{ab}^2 \mathcal{H}_{ab}\,, \tag{5.2}$$

and $\mathscr{V}_4$ contains quartic interactions of the form

$$\begin{aligned}\mathscr{V}_4(\Phi_1, \ldots, \Phi_n) = &\sum_{a=1}^{n} \lambda_a \left(\Phi_a^\dagger \Phi_a\right)^2 + \sum_{a=1}^{n-1} \sum_{b=a+1}^{n} \lambda_{a,b} \left(\Phi_a^\dagger \Phi_a\right)\left(\Phi_b^\dagger \Phi_b\right) + \sum_{a=1}^{n} \sum_{b=1}^{n-1} \sum_{c=b+1}^{n} \lambda_{a,bc} \left(\Phi_a^\dagger \Phi_a\right) \mathcal{H}_{bc} \\ &+ \sum_{a=1}^{n-1} \sum_{b=a+1}^{n} \sum_{c=1}^{n-1} \sum_{d=c+1}^{n} \Bigg|_{(a,b)\leq(c,d)} \lambda_{ab,cd} \mathcal{H}_{ab} \mathcal{H}_{cd} + \sum_{a=1}^{n-1} \sum_{b=a+1}^{n} \sum_{c=1}^{n-1} \sum_{d=c+1}^{n} \Bigg|_{(a,b)\leq(c,d)} \lambda_{ab,cd}^{\mathcal{A}} \mathcal{A}_{ab} \mathcal{A}_{cd}\,.\end{aligned} \tag{5.3}$$

We have introduced the Hermitian and antihermitian bilinears

$$\mathcal{H}_{ab} = \frac{1}{2}\left(\Phi_a^\dagger \Phi_b + \Phi_b^\dagger \Phi_a\right)\,, \qquad \mathcal{A}_{ab} = \frac{1}{2}\left(\Phi_a^\dagger \Phi_b - \Phi_b^\dagger \Phi_a\right)\,, \tag{5.4}$$

with $a < b$, that transform as $\mathcal{H}_{ab} \to \mathcal{H}_{ab}$ and $\mathcal{A}_{ab} \to -\mathcal{A}_{ab}$ under CP. In particular, the requirement of CP conservation at the Lagrangian level implies that all quadratic couplings $\{\mu_a^2, \mu_{ab}^2\}$ in $\mathscr{V}_2$, as well as all quartic couplings $\{\lambda_a, \lambda_{a,b}, \lambda_{a,bc}, \lambda_{ab,cd}, \lambda_{ab,cd}^{\mathcal{A}}\}$ in $\mathscr{V}_4$ are real—hence *real* MHDMs. The ordering $(a, b) \leq (c, d)$ in the last term of Eq. (5.3) stands for $a < c$ and, in case $a = c$, then $b < d$. It is important to remark that there are n quadratic couplings μ_a^2, and $n(n-1)/2$ couplings μ_{ab}^2, giving a total of $n(n+1)/2$ quadratic couplings.

Following the convention adopted in chapter 3, appropriate EWSB is triggered by

$$\langle \Phi_a \rangle = \frac{v_a e^{i\theta_a}}{\sqrt{2}} \begin{pmatrix} 0 \\ 1 \end{pmatrix}\,, \tag{5.5}$$

so that the expansion of the fields around their corresponding vev reads

$$\Phi_a = \frac{e^{i\theta_a}}{\sqrt{2}} \begin{pmatrix} \sqrt{2}\varphi_a^+ \\ v_a + \rho_a + i\eta_a \end{pmatrix}\,. \tag{5.6}$$

We have $v_a \in \mathbb{R}^+$, $\theta_a \in [0, 2\pi)$, and $\sum_{a=1}^{n} v_a^2 = v^2 \simeq (246\ \text{GeV})^2$. Individual phases have no physical meaning by themselves: all CP violation arising from the vacuum is encoded in the phase differences $\theta_{ab} \equiv \theta_a - \theta_b$. It is also clear that, besides the wbGBs, there are $n-1$ pairs of charged scalars and $2n-1$ neutral states in a theory with n Higgs doublets.

We should recall that the stationarity conditions consist of requiring the vevs of the scalar doublets to be an extremum of the potential:

$$\mathscr{V}(\langle \Phi_1 \rangle, \ldots, \langle \Phi_n \rangle) \equiv V(v_1, \ldots, v_n, \theta_1, \ldots, \theta_n)\,, \tag{5.7}$$

in such a way that

$$\partial_{v_1} V = \cdots = \partial_{v_n} V = 0\,, \qquad \partial_{\theta_1} V = \cdots = \partial_{\theta_n} V = 0\,, \tag{5.8}$$

and where $\sum_{a=1}^{n} \partial_{\theta_a} V = 0$ by construction. Therefore, there are in total $2n-1$ independent stationarity conditions. Taking into account Eqs. (5.2) and (5.3), the derivatives in Eq. (5.8) read

$$\partial_{v_i} V = \mu_i^2 v_i + \frac{1}{2}\sum_{j=i+1}^{n} \mu_{ij}^2 v_j \cos\theta_{ij} + \frac{1}{2}\sum_{j=1}^{i-1} \mu_{ji}^2 v_j \cos\theta_{ji} \quad + \quad [\lambda \text{ terms}]\,, \tag{5.9}$$

$$\partial_{\theta_i} V = -\frac{1}{2}\sum_{j=i+1}^{n} \mu_{ij}^2 v_i v_j \sin\theta_{ij} + \frac{1}{2}\sum_{j=1}^{i-1} \mu_{ji}^2 v_i v_j \sin\theta_{ji} \quad + \quad [\lambda \text{ terms}]\,. \tag{5.10}$$

Notice that in both cases the first and second sums are not present when $i = n$ or $i = 1$, respectively. In order to be concise, we have not displayed the specific dependence on the quartic couplings, simply denoted as [λ terms], since this will not be essential to derive our main results.

On the other hand, the elements of the scalar mass matrices in Eqs. (3.9) to (3.12) are given in this scenario by

$$(M_{\pm}^2)_{ij} = \mu_j^2 \delta_{ji} + \frac{1}{2}\mu_{ij}^2 e^{i\theta_{ij}} \delta_{i<j} + \frac{1}{2}\mu_{ji}^2 e^{-i\theta_{ji}} \delta_{i>j} \quad + \quad [\lambda \text{ terms}]\,, \tag{5.11}$$

$$(M_{\rho}^2)_{ij} = \mu_j^2 \delta_{ji} + \frac{1}{2}\mu_{ij}^2 \cos\theta_{ij} \delta_{i<j} + \frac{1}{2}\mu_{ji}^2 \cos\theta_{ji} \delta_{i>j} \quad + \quad [\lambda \text{ terms}]\,, \tag{5.12}$$

$$(M_{\eta}^2)_{ij} = \mu_j^2 \delta_{ji} + \frac{1}{2}\mu_{ij}^2 \cos\theta_{ij} \delta_{i<j} + \frac{1}{2}\mu_{ji}^2 \cos\theta_{ji} \delta_{i>j} \quad + \quad [\lambda \text{ terms}]\,, \tag{5.13}$$

$$(M_{\rho\eta}^2)_{ij} = \frac{1}{2}\mu_{ij}^2 \sin\theta_{ij} \delta_{i<j} - \frac{1}{2}\mu_{ji}^2 \sin\theta_{ji} \delta_{i>j} \quad + \quad [\lambda \text{ terms}]\,, \tag{5.14}$$

where the $\delta_{i<j}$ ($\delta_{i>j}$) symbol means that the corresponding term only contributes if $i < j$ ($i > j$).

In Table 5.1, we collect the counting of the relevant ingredients for our analysis, namely, the number of quadratic couplings and independent stationarity conditions for a given number of scalar doublets n, particularizing for $n = 2, \ldots, 7$. As already mentioned, for $n = 2$ both numbers match, and the stationarity conditions can be used to trade all quadratic couplings for quartic couplings multiplied by the squared of the vevs. For $n > 2$, one is quickly driven into an overabundance of quadratic couplings with respect to stationarity conditions, showing that for $n = 3$ there is already one free quadratic coupling, for $n = 5$ there are more quadratic couplings than pairs of charged scalars, and for $n = 7$ there are more free quadratic couplings than neutral scalars. One could expect that, beyond $n = 2$, the remaining free quadratic couplings can lead to arbitrarily large *new* scalar masses, *new* meaning neither the wbGBs nor the light Higgs-like state. As we first illustrate numerically and then address analytically, that reasonable expectation is surprisingly misled.

5.2 Numerical analysis

For a given number n of scalar doublets (in particular, we explore the scenarios with $n = 3, 5, 7$), we perform the following numerical exercise.

1. Use the stationarity conditions in Eq. (5.10) to trade all $n-1$ quadratic couplings μ_{1j}^2 ($j = 2, \ldots, n$) in terms of other quadratic μ_{ij}^2 ($i = 2, \ldots, n-1$, and $j = i+1, \ldots, n$) and quartic parameters.

2. Use again the stationarity conditions in Eq. (5.10), together with the ones in Eq. (5.9), to trade

Scalar doublets	n	2	3	4	5	6	7
Quadratic	$\frac{n(n+1)}{2}$	3	6	10	15	21	28
Stationarity	$2n-1$	3	5	7	9	11	13
Free quadratic	$\frac{(n-1)(n-2)}{2}$	0	1	3	6	10	15
Charged scalars	$2(n-1)$	$2{\times}1$	$2{\times}2$	$2{\times}3$	$2{\times}4$	$2{\times}5$	$2{\times}6$
Neutral scalars	$2n-1$	3	5	7	9	11	13

Table 5.1: Number of quadratic couplings, independent stationarity conditions, and physical charged and neutral scalars (*i.e.*, without considering the wbGBs) in a real MHDM with SCPV. The number of free quadratic couplings that are left after imposing the stationarity conditions is also included. All the results are given as a function of the number of scalar doublets n, and particularized for $n = 2, \ldots, 7$. The factors of 2 in orange emphasize that the physical charged scalars can be arranged in pairs with common mass and opposite electric charge.

all n quadratic couplings μ_j^2 $(j = 1, \ldots, n)$ in terms of other quadratic μ_{ij}^2 $(i = 2, \ldots, n-1$, and $j = i+1, \ldots, n)$ and quartic parameters.

3. We are left with $(n-1)(n-2)/2$ free quadratic couplings μ_{ij}^2 $(i = 2, \ldots, n-1$, and $j = i+1, \ldots, n)$. Generate random real values for them in the range $[-k_\mu, k_\mu] \times 10^{10}$ GeV^2, considering separately the cases $k_\mu = 1, 4, 16$.

4. Generate random real values for the quartic couplings in the range $[-k_\lambda, k_\lambda]$, considering separately the cases $k_\lambda = 1, 4, 16$. Notice that we are in a regime where the quadratic couplings can be, in general, much larger than the quartic couplings multiplied by the vevs. The latter, indeed, must satisfy perturbative unitarity bounds.

5. Generate random real values for the moduli of the vevs v_i $(i = 1, \ldots, n)$ in the range $[0, 1]$ GeV, and then rescale them collective to satisfy the constraint $\sum_{i=1}^n v_i^2 = v^2 \simeq (246 \text{ GeV})^2$.

6. Generate random real values for the phases of the vevs θ_i $(i = 1, \ldots, n)$ in the range $[0, 2\pi)$.

7. Compute μ_{1j}^2 $(j = 2, \ldots, n)$ and μ_j^2 $(j = 1, \ldots, n)$ using the previous numerical values, and check if they lie in the range $[-k_\mu, k_\mu] \times 10^{10}$ GeV^2. If this is not the case, go back to the first step and repeat the procedure.

8. Compute the mass matrices $M_\pm^2$ and M_0^2.

9. Compute the eigenvalues of the mass matrices, ordering them according to their absolute values. Notice that we do not require the eigenvalues to be non-negative (which would amount to requiring that the vacuum be a local minimum), nor the quartic couplings to ensure boundedness from below of the potential. As we will comment later, these are not required for the purposes of our analysis.

10. Repeat the whole procedure, $O(10^6)$ times for $n = 3$ and $O(10^3)$ for $n = 7$, and save the largest result for each sorted eigenvalue in the mass matrices $M_\pm^2$ and M_0^2. The number of repetitions is reasonably adapted to the cost of computing time, which grows non-linearly with n.

The results of our numerical analysis, namely, the maximum value of each sorted eigenvalue in the mass matrices normalized to the electroweak vev v, are presented in Fig. 5.1 for charged scalars and in

Fig. 5.2 for neutral scalars. For each case, the left and right panels show the dependence on k_μ and k_λ for a fixed value of k_λ and k_μ, respectively. In turn, each panel is divided in three regions corresponding to 3, 5, and 7HDMs. The key points to stress are the following.

(i) The wbGBs are represented by the points in red. Rather than the analytic zero eigenvalue, they yield values as small as expected considering the finite numerical precision.

(ii) There is one charged light state, represented by the blue points in Fig. 5.1, whose mass cannot exceed the EW scale v, is sensitive to k_λ, and is insensitive to k_μ.

(iii) There are three neutral light states, represented by the blue points in Fig. 5.2. In addition to the expected Higgs-like state, two new neutral states emerge whose masses are close to the EW scale. As before, they are sensitive to k_λ, and insensitive to k_μ.

(iv) The remaining $n-2$ charged and $2n-4$ neutral scalars, represented by the points in brown, are heavy, that is, their masses are much larger than the EW scale. Contrary to the previous cases, they are sensitive to k_μ and insensitive to k_λ.

As a final comment, it is now clear why we could dispense of the additional physical requirements of non-negative eigenvalues and boundedness from below of the potential: the results of our numerical analysis hold in the physically meaningful subspace of the considered parameter space. One could have proceed including the aforementioned physical requirements, but the boundedness from below constraint on the quartic couplings for a generic number of doublets has no analytic answer in the literature, and the required computing time would be unaffordable—we checked that just requiring non-negative eigenvalues already has a very significant impact, with no apparent effect on the results of interest. All in all, the aim of this numerical exploration is to illustrate the unexpected appearance of new light states with masses tied to the EW scale. With this in mind, we now focus on providing an analytical justification for the emergence of these unexpected states.

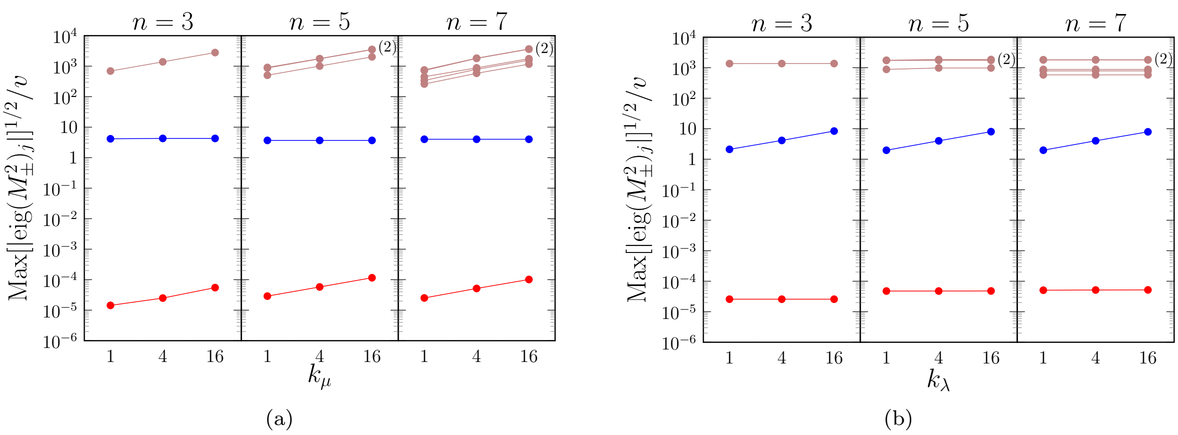

Figure 5.1: Maximum eigenvalues of $M^2_\pm$ normalized to the electroweak scale v for $n = 3, 5, 7$ Higgs doublets: (a) fixed $k_\lambda = 4$, and (b) fixed $k_\mu = 4$. The numbers in parentheses indicate near-degeneracies among different states.

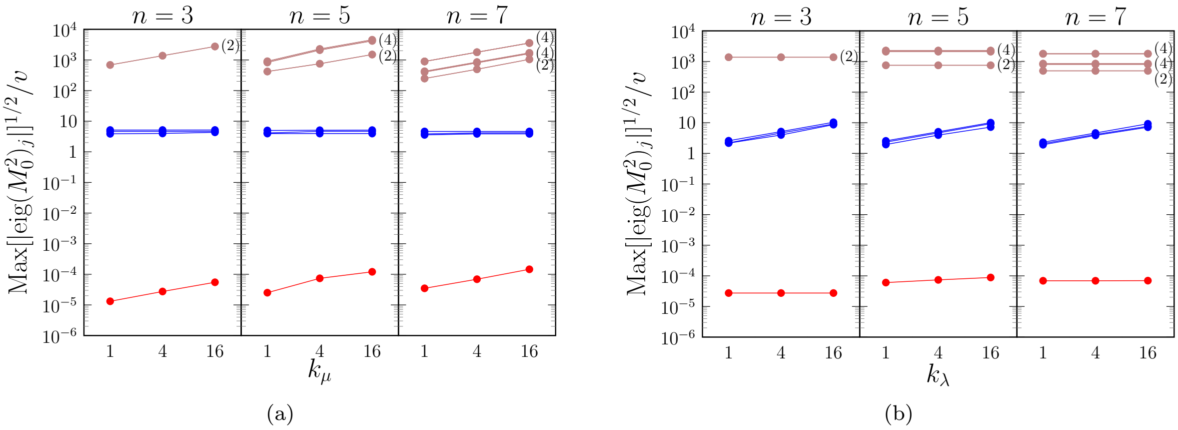

Figure 5.2: Maximum eigenvalues of M_0^2 normalized to the electroweak scale v for $n = 3, 5, 7$ Higgs doublets: (a) fixed $k_\lambda = 4$, and (b) fixed $k_\mu = 4$. The numbers in parentheses indicate near-degeneracies among different states.

5.3 Analytical approach

The obtention of the eigenvalues of the charged and neutral scalar mass matrices for an arbitrary number of Higgs doublets is a task that cannot be carried out analytically. If that was the case, one would simply check that, apart from the massless wbGBs and the Higgs-like scalar, there are one charged and two neutral states that are light, *i.e.*, with masses not exceeding $\mathcal{O}(v)$. Short of that kind of capacity, we might be able to get more insight into the question assisted by the previous numerical exercise. First, pushing the new scalar masses into a decoupling regime requires large quadratic couplings, that is, much larger than v^2. Second, the fact that in our numerical analysis the unexpected light states have eigenvalues apparently insensitive to k_μ suggests that these eigenvalues are independent of the quadratic couplings. Therefore, considering the whole problem, both the stationarity conditions and the mass matrices, without quartic couplings at all would imply that these unexpected states manifest as eigenstates with eigenvalues equal to zero, *i.e.*, null eigenvectors. That is indeed the case, and our way to prove it goes as follows: (i) write down the mass matrices neglecting the quartic couplings, (ii) relate the $n \times n$ charged mass matrix with the $2n \times 2n$ neutral mass matrix in such a way that we can just deal with the charged mass matrix, and (iii) analyze the eigenvectors corresponding to the wbGBs as inspiration to obtaining those associated to the new light states. Afterwards, one can then think about the inclusion of the quartic couplings as a (degenerate) perturbation theory problem, where the contributions to the entries of the mass matrices from the quartic couplings act as the perturbation. Consequently, the null eigenvectors appearing in the reduced problem with only quadratic couplings will not yield scalars with squared masses much larger than the λv^2 perturbation.

In the absence of quartic couplings, the scalar potential in Eqs. (5.1) to (5.3) is simply $\mathscr{V} \to \mathscr{V}_2$. Regarding the stationarity conditions in Eqs. (5.9) and (5.10), and the mass matrix elements in Eqs. (5.11) to (5.14), we just need to take [λ terms] $\to 0$. In this regime, the mass matrices $M^2_\pm$ and M^2_0 read

$$M^2_\pm = \begin{pmatrix} \mu_1^2 & \frac{1}{2}\mu_{12}^2 e^{i\theta_{12}} & \cdots & \\ \frac{1}{2}\mu_{12}^2 e^{-i\theta_{12}} & \mu_2^2 & \cdots & \\ \vdots & \vdots & \ddots & \\ & & & \mu_n^2 \end{pmatrix} , \qquad M_0^2 = \begin{pmatrix} \mathrm{Re}\, M^2_\pm & \mathrm{Im}\, M^2_\pm \\ -\mathrm{Im}\, M^2_\pm & \mathrm{Re}\, M^2_\pm \end{pmatrix} , \tag{5.15}$$

with $\left(\mathrm{Re}\, M^2_\pm\right)^T = \mathrm{Re}\, M^2_\pm$ and $\left(\mathrm{Im}\, M^2_\pm\right)^T = -\mathrm{Im}\, M^2_\pm$. Crucially, $M^2_\pm$ and M^2_0 are related in a simple way. As a consequence, let us analyze what happens in general if there is a null eigenvector in the charged mass matrix, that is, $M^2_\pm\ \vec{c} = \vec{0}_n$, with $\vec{c} \in \mathbb{C}^n$ and $\vec{0}_n$ the n-dimensional null vector. Expanding in real and imaginary parts, one can readily obtain

$$\mathrm{Re}\, M^2_\pm\ \mathrm{Re}\, \vec{c} - \mathrm{Im}\, M^2_\pm\ \mathrm{Im}\, \vec{c} = \vec{0}_n\,, \qquad \mathrm{Re}\, M^2_\pm\ \mathrm{Im}\, \vec{c} + \mathrm{Im}\, M^2_\pm\ \mathrm{Re}\, \vec{c} = \vec{0}_n\,. \tag{5.16}$$

In matrix form, Eq. (5.16) yields

$$M_0^2\ \vec{r}_1 = \vec{0}_{2n}\,, \qquad M_0^2\ \vec{r}_2 = \vec{0}_{2n}\,, \tag{5.17}$$

with

$$\vec{r}_1 = \begin{pmatrix} \mathrm{Re}\, \vec{c} \\ -\mathrm{Im}\, \vec{c} \end{pmatrix} , \qquad \vec{r}_2 = \begin{pmatrix} \mathrm{Im}\, \vec{c} \\ \mathrm{Re}\, \vec{c} \end{pmatrix} , \tag{5.18}$$

and $\vec{r}_1^{\,T} \cdot \vec{r}_2 = 0$. Therefore, once we identify *one* null eigenvector $\vec{c}$ of $M^2_\pm$, we can immediately obtain *two* null eigenvectors $\{\vec{r}_1, \vec{r}_2\}$ of M_0^2.

On this regard, we already know one null eigenvector of $M^2_\pm$, corresponding to the charged wbGB, which is of the form

$$\vec{c}_G^{\,T} = (v_1, \ldots, v_n)\ . \tag{5.19}$$

In particular, it is straightforward to check that

$$M^2_\pm\ \vec{c}_G = \begin{pmatrix} \partial_{v_1} V_2 - i\frac{1}{v_1}\partial_{\theta_1} V_2 \\ \vdots \\ \partial_{v_n} V_2 - i\frac{1}{v_n}\partial_{\theta_n} V_2 \end{pmatrix} . \tag{5.20}$$

Since all entries are expressed as a combination of the derivatives in the stationarity conditions, it is clear that $M^2_\pm\ \vec{c}_G = \vec{0}_n$. The resulting null eigenvectors in M_0^2 are thus

$$\vec{r}_G^{\,T} = \left(\vec{0}_n, v_1, \ldots, v_n\right) , \qquad \vec{r}_h^{\,T} = \left(v_1, \ldots, v_n, \vec{0}_n\right) , \tag{5.21}$$

that satisfy

$$M_0^2\ \vec{r}_G = \vec{0}_{2n}\,, \qquad M_0^2\ \vec{r}_h = \vec{0}_{2n}\,. \tag{5.22}$$

The eigenvector $\vec{r}_G$ corresponds to the neutral wbGB and $\vec{r}_h$ to the Higgs-like scalar. The relevant question to raise is: *is there another null eigenvector of $M^2_\pm$?* If that is the case, it would account precisely for the additional one charged and two neutral states with masses close to the electroweak scale encountered in the numerical exploration. The answer, no wonder, is positive. Out of inspired guessing, consider the complex vector

$$\vec{c}^{\,T} = \left(e^{i2\theta_1} v_1, \ldots, e^{i2\theta_n} v_n\right)\ . \tag{5.23}$$

One can readily obtain

$$M_\pm^2\ \vec{c} = \begin{pmatrix} e^{i2\theta_1}\left(\partial_{v_1}V_2 + i\frac{1}{v_1}\partial_{\theta_1}V_2\right) \\ \vdots \\ e^{i2\theta_n}\left(\partial_{v_n}V_2 + i\frac{1}{v_n}\partial_{\theta_n}V_2\right) \end{pmatrix} . \tag{5.24}$$

As in the previous case, the stationarity conditions make $\vec{c}$ a null eigenvector of $M_\pm^2$. This leads to two null eigenvectors of M_0^2:

$$\begin{aligned} \vec{r}_1^{\,T} &= (v_1\cos 2\theta_1, \ldots, v_n\cos 2\theta_n, -v_1\sin 2\theta_1, \ldots, -v_n\sin 2\theta_n)\ , \\ \vec{r}_2^{\,T} &= (v_1\sin 2\theta_1, \ldots, v_n\sin 2\theta_n, v_1\cos 2\theta_1, \ldots, v_n\cos 2\theta_n)\ , \end{aligned} \tag{5.25}$$

with

$$M_0^2\ \vec{r}_1 = \vec{0}_{2n}\,, \qquad M_0^2\ \vec{r}_2 = \vec{0}_{2n}\,. \tag{5.26}$$

Although $\vec{c}$ and $\vec{c}_G$ are not orthogonal, and correspondingly $\{\vec{r}_1, \vec{r}_2\}$ are not orthogonal to $\{\vec{r}_G, \vec{r}_h\}$, there is no concern on that respect since one can always construct an orthonormal set of eigenvectors by means of the Gram-Schmidt orthonormalization procedure.

So far, we have analyzed the mass matrices in the absence of quartic couplings, obtaining that, besides the expected null eigenvectors of $M_\pm^2$ and M_0^2 associated to the wbGBs and the Higgs-like scalar particle, further null eigenvectors emerge, one of $M_\pm^2$ and two of M_0^2. One can now think about the complete picture, including quartic couplings as a perturbation with respect to the previous analysis—it is indeed degenerate perturbation theory that must be considered. Besides the wbGBs, which remain massless, it is thus clear that out of the additional null eigenvectors of the "no-quartics" mass matrices, $\vec{c}$ in Eq. (5.23), $\vec{r}_1$ and $\vec{r}_2$ in Eq. (5.25), and $\vec{r}_h$ in Eq. (5.22), one charged and three neutral scalars get squared masses of order λv^2. This means they are *light*: after imposing perturbative unitarity constraints on the quartic couplings, their masses cannot be much larger than the electroweak scale, exactly as observed in our illustrative numerical exercise. Of course, more light states might be present when a regime other than $\mu_a^2, \mu_{ab}^2 \gg v^2$ is considered. The novel and relevant point from our study is that with very few assumptions—a real MHDM with SCPV and bounded quartic couplings—, one can establish that, unexpectedly and no matter the number of doublets n, at least three new scalars must be light.

One might reasonably wonder whether the appearance of unexpected null eigenvectors is somehow connected to the spontaneous breaking of a continuous symmetry. First, we should point out that for the vacuum configuration given in Eq. (5.5), the CP-transformed vevs $\langle\Phi_a^*\rangle = \langle\Phi_a\rangle^*$ satisfy

$$\mathscr{V}(\langle\Phi_1\rangle^*, \ldots, \langle\Phi_n\rangle^*) = \mathscr{V}(\langle\Phi_1\rangle, \ldots, \langle\Phi_n\rangle)\,, \tag{5.27}$$

implying that $\langle\Phi_a^*\rangle$ corresponds to a distinct candidate vacuum, obtained by applying a CP transformation to the original one. When the quartic couplings are neglected, the mass terms in $\mathscr{V}_2$ are independent of the vevs. As a result, both the wbGBs associated with the original vacuum and those associated with its CP-transformed counterpart correspond to massless eigenstates at this level. However, since no additional continuous symmetry is spontaneously broken, the latter cannot be regarded as true wbGBs: they acquire masses once the effects of $\mathscr{V}_4$ are taken into account. Their lightness is understood from the fact that, within the approximation that considers $\mathscr{V}_2$ alone, they yield null mass eigenvalues just as the true wbGBs do.[1]

A source of concern is whether radiative corrections could modify the previous picture, potentially inducing large shifts in the masses of the light scalar states. While a thorough analysis of this question lies beyond the scope of the present analysis, some qualitative arguments can still be made. In particular, since the one-loop effective scalar potential is independent of the specific vacuum configuration and preserves CP invariance, it is reasonable to expect that the main conclusions drawn from the tree-level analysis remain unchanged.

Finally, it is clear that the phenomenological implications of our result—*e.g.*, discovery potential at the LHC—deserve attention. This question is also beyond the scope of our analysis here for several reasons. In general, there are three types of interactions involving these new scalars: (i) their interactions with other scalars arising from the quartic couplings in the potential, (ii) their Yukawa interactions with fermions, and (iii) their gauge interactions contained in the covariant derivative. Given the minimality of our starting assumptions, there is still large freedom available to specify both the interactions among the scalars and their couplings to fermions that precludes us from providing any concrete theoretical prediction in that regard. The third type of interaction, involving scalars and gauge bosons, appears *a priori* better suited if observables insensitive to the first two types of interactions were available. However, knowing that scalars with masses close to the electroweak scale (the eigenvalues of the mass matrices) might be present is not sufficient, but a better understanding of the states (the corresponding eigenvectors) is necessary. Even in the regime where, apart from the necessarily light states, all other scalars are much heavier, these eigenvectors—which define the mixings in the scalar sector—depend critically on the quartic couplings. The situation would be even more involved if one is not in that regime and there are more light states, and thus prevents our general approach from guaranteeing discovery prospects. It is worth emphasizing that, within our analysis, there is no requirement for any of the light mass eigenstates to resemble the SM-like Higgs boson—in other words, scalar alignment [151–153] is not enforced. In general, the Higgs-like state can exhibit sizable mixing with the additional light scalars. Experimental constraints, such as the measured signal strengths in processes like $h \to WW^*$, would place strong limits on such mixings, thereby requiring some fine-tuning to ensure the presence of a SM-like Higgs boson in the spectrum.

5.4 Summary

Extended scalar sectors, in particular MHDMs featuring spontaneous electroweak symmetry breaking, necessarily include a Higgs-like state with a mass at the electroweak scale if perturbativity requirements are imposed on the potential. Due to the presence of unconstrained dimensionful quadratic couplings, one naive expectation is that, generically, all new scalars could be made arbitrarily heavy, with masses much larger than the electroweak scale. We have analyzed the case of real MHDM with SCPV and find that, contrary to such expectations and despite the abundance of free quadratic couplings, at least one charged and two additional neutral states have masses that cannot be larger than the electroweak scale, also due to perturbativity requirements on the quartic couplings in the potential. This feature seems to be linked to the existence of an alternative candidate vacuum, with both classes of potential minima related by a CP transformation. To what extent similar conclusions hold for other scalar potentials remains an open question.

[1] The appearance of the $e^{i2\theta_i}$ phases in Eq. (5.23) is merely an artifact of the expansion used in Eq. (5.6), where the vacuum phase $e^{i\theta_a}$ has been explicitly factored out.

We lack a theoretical argument to forbid the presence of additional scalar particles beyond the SM-like Higgs boson, although at the same time the absence of direct experimental evidence, and the severe constraints imposed by flavor data, suggest that their masses may lie well beyond the currently accessible energy scale. Our results in this chapter show that this scenario can be overcome under very few assumptions, and thus we believe this opens up an exciting opportunity for further exploration, both theoretically and experimentally.

6 SCPV and flavor conservation with two Higgs doublets: $\mu - \tau$ symmetric lepton mixing

As we have explored in the previous chapter, MHDMs offer the possibility to break CP invariance from the vacuum configuration, that is, of having SCPV [95,96]. At the same time, they are generally affected by the presence of SFCNC at tree-level, which are severely constrained by experiment [116], hence requiring a mechanism to guarantee their absence or, at least, keep them under control. The combination of these two features could constitute an appealing motivation both from a theoretical and a phenomenological point of view. However, in [154] Branco gave a strong argument for this not to be possible: for any number of Higgs doublets and fermion generations, if CP is solely broken by the vacuum and SFCNC are absent by means of the simultaneous bidiagonalization of all Yukawa couplings, the CKM mixing matrix does not violate CP. The particular case of 2HDMs with NFC *à la* Glashow-Weinberg [103] was presented. Later on, Refs. [155] and [156] found a way, and provided a counter-example, to evade Branco's argument. However, they ended up with a very specific structure for the CKM matrix: two rows or two columns should have the same moduli. While the latter implementation is not phenomenologically viable in the quark sector, we address the feasibility of this idea in the lepton sector of a 2HDM, where the PMNS mixing matrix, as a consequence of the simultaneous requirement of SCPV and flavor conservation presents a $\mu - \tau$ symmetric [157] structure compatible with experiment. On that regard, one should specify a mass generation mechanism for neutrinos, and therefore distinguish between their Dirac or Majorana nature.

The structure of this chapter is the following. In Sec. 6.1, we recall some basic features of 2HDMs that are relevant for our subsequent analysis. Then, in Sec. 6.2, we revisit the CP-conserving mixing argument given by Branco in [154], and confront it to the counter-example presented in Refs. [155] and [156]. A more general approach to the question is addressed in detail in Sec. 6.3. We present our minimal model with Dirac neutrinos, together with a straightforward extension to a type I seesaw scenario, and discuss some relevant phenomenological consequences in Sec. 6.4. Finally, we summarize our findings in Sec. 6.5. We devote to App. D the analysis of the stability under renormalization group evolution (RGE) of the Yukawa matrices, including extensions of the minimal model presented here.

6.1 Flavor Conservation in 2HDMs

As anticipated in Sec. 3.2.1, the Yukawa interactions of quarks with two Higgs doublets in an arbitrary weak basis read

$$-\mathscr{L}_{\mathrm{Y}}^{\mathrm{quark}} = \overline{Q_L^0}(Y_1^u\widetilde{\Phi}_1 + Y_2^u\widetilde{\Phi}_2)u_R^0 + \overline{Q_L^0}\left(Y_1^d\Phi_1 + Y_2^d\Phi_2\right)d_R^0 + \mathrm{H.c.} \tag{6.1}$$

Rotation into the Higgs basis [60, 101, 102] by means of the transformation in Eq. (3.19) leads to

$$-\frac{v}{\sqrt{2}}\mathscr{L}_{\mathrm{Y}}^{\text{quark}} = \overline{Q_L^0}(M_u^0\widetilde{H}_1 + N_u^0\widetilde{H}_2)u_R^0 + \overline{Q_L^0}\left(M_d^0 H_1 + N_d^0 H_2\right)d_R^0 + \text{H.c.}\,, \tag{6.2}$$

where the non-diagonal mass matrices are given by

$$M_u^0 = \frac{v}{\sqrt{2}}e^{-i\theta_1}\left(c_\beta Y_1^u + e^{-i\theta}s_\beta Y_2^u\right)\,, \qquad M_d^0 = \frac{v}{\sqrt{2}}e^{i\theta_1}\left(c_\beta Y_1^d + e^{i\theta}s_\beta Y_2^d\right)\,, \tag{6.3}$$

and the additional scalar-fermion couplings are

$$N_u^0 = \frac{v}{\sqrt{2}}e^{-i\theta_1}\left(-s_\beta Y_1^u + e^{-i\theta}c_\beta Y_2^u\right)\,, \qquad N_d^0 = \frac{v}{\sqrt{2}}e^{i\theta_1}\left(-s_\beta Y_1^d + e^{i\theta}c_\beta Y_2^d\right)\,. \tag{6.4}$$

with $\theta \equiv \theta_2 - \theta_1$, and θ_i the complex phase of the vev of each doublet. The usual bidiagonalization procedure—see App. B—allows us to bring M_f^0 ($f = u, d$) into a diagonal form. In particular, the Hermitian combinations $M_f^0 M_f^{0\dagger}$ and $M_f^{0\dagger}M_f^0$ get diagonalized as

$$U_{f_L}^\dagger M_f^0 M_f^{0\dagger} U_{f_L} = \operatorname{diag}(m_{f_1}^2, m_{f_2}^2, m_{f_3}^2)\,, \qquad U_{f_R}^\dagger M_f^{0\dagger} M_f^0 U_{f_R} = \operatorname{diag}(m_{f_1}^2, m_{f_2}^2, m_{f_3}^2)\,, \tag{6.5}$$

with U_{f_L} and U_{f_R} the unitary 3×3 transformations of the quark fields, $f_L^0 = U_{f_L} f_L$ and $f_R^0 = U_{f_R} f_R$, to their mass basis.[1] Consequently, the individual mass matrices transform as

$$U_{f_L}^\dagger M_f^0 U_{f_R} = M_f = \operatorname{diag}(m_{f_1}, m_{f_2}, m_{f_3})\,, \tag{6.6}$$

where m_{f_i} are the real and positive fermion masses. However, the additional Yukawa couplings in Eq. (6.4) are not, in general, bidiagonalized by the same transformations, and thus they encode dangerous SFCNC that are severely constrained by experiment. Then, flavor conservation would require

$$\text{Flavor Conservation} \quad \Longleftrightarrow \quad U_{f_L}^\dagger N_f^0 U_{f_R} = N_f = \operatorname{diag}(n_{f_1}, n_{f_2}, n_{f_3})\,, \tag{6.7}$$

with general complex n_{f_i}.

On the other hand, it is important to recall that invariance of the Lagrangian under standard CP transformations [58] forces all Yukawa couplings and parameters in the scalar potential to be real. Therefore, CP violation solely arises from the vacuum configuration provided that $\theta \neq 0, \pi$, *i.e.*, there is SCPV.

6.2 Evading a CP-conserving fermion mixing

We begin by requiring that CP violation arises exclusively from the vacuum phase $\theta \neq 0, \pi$, and that all Yukawa couplings Y_a^f are real.

Our second requirement is flavor conservation, that is, the absence of SFCNC at tree-level. On that regard, the argument presented by Branco [154] works as follows. As previously mentioned, flavor conservation stems from the simultaneous bidiagonalization of M_f^0 and N_f^0 or, equivalently, both Y_1^f and Y_2^f. Since the Yukawa matrices Y_a^f are real, the bidiagonalization procedure is carried out by real

[1] For concreteness, we stick here to three generations of fermions.

orthogonal matrices, such that

$$O_{f_L}^T Y_a^f O_{f_R} = \mathrm{diag}\left(y_{a1}^f, y_{a2}^f, y_{a3}^f\right)\,, \quad y_{ai}^f \in \mathbb{R}^+ \qquad \Longrightarrow \qquad O_{f_L}^T M_f^0 O_{f_R}\,,\; O_{f_L}^T N_f^0 O_{f_R}\ \text{diagonal}\,. \tag{6.8}$$

This leads to a CKM mixing of the form $V = R_u^\dagger O_{u_L}^T O_{d_L} R_d$, with R_f diagonal rephasings: the CKM matrix is essentially real, thus CP-conserving.

Although compelling, the previous argument can be surpassed. As shown in [155, 156], even if the matrices Y_a^f are real, they can have complex conjugate eigenvalues and, consequently, they might not necessarily be diagonalized with real orthogonal matrices. An illustrative example of this kind of scenario was presented in [155], in the context of a 2HDM with four quark generations, where

$$Y_a^u = O^T \begin{pmatrix} y_{a1}^u & 0 & 0 & 0 \\ 0 & y_{a2}^u & 0 & 0 \\ 0 & 0 & c_a & s_a \\ 0 & 0 & -s_a & c_a \end{pmatrix}\,, \qquad Y_a^d = \mathrm{diag}\left(y_{a1}^d, y_{a2}^d, y_{a3}^d, y_{a4}^d\right)\,, \tag{6.9}$$

being O a real orthogonal matrix, and $Y_a^f = Y_a^{f*}$, as required by CP invariance. The crucial ingredient are the 2×2 blocks in Y_a^u, namely,

$$B_a^u = \begin{pmatrix} c_a & s_a \\ -s_a & c_a \end{pmatrix}\,. \tag{6.10}$$

There are several points that should be noticed in this regard.

(i) The combinations $B_a^u B_a^{uT}$ and $B_a^{uT} B_a^u$ (no sum over a) have two *degenerate* real eigenvalues $c_a^2 + s_a^2$. In particular, they satisfy $B_a^u B_a^{uT} = B_a^{uT} B_a^u = (c_a^2 + s_a^2)\, 1_{2\times 2}$, where $1_{2\times 2}$ is the 2×2 identity matrix.

(ii) The individual matrices B_a^u have two complex conjugate eigenvalues $c_a \pm i s_a$, corresponding to *complex conjugate* eigenvectors, and are *unitarily* diagonalized as[2]

$$U_0^\dagger B_a^u U_0 = \begin{pmatrix} c_a + i s_a & 0 \\ 0 & c_a - i s_a \end{pmatrix}\,, \qquad \text{with} \qquad U_0 = \frac{1}{\sqrt{2}}\begin{pmatrix} 1 & 1 \\ i & -i \end{pmatrix}\,. \tag{6.11}$$

(iii) The unitary matrix U_0 does not depend on the specific eigenvalues, and thus diagonalizes *simultaneously* both B_a^u blocks ($a = 1, 2$).

Turning to Y_1^u and Y_2^u, this implies that they are *simultaneously* and *unitarily* diagonalized:

$$\hat{U}_{uL}^\dagger Y_a^u \hat{U}_{uR} = \mathrm{diag}\left(y_{a1}^u, y_{a2}^u, c_a + i s_a, c_a - i s_a\right)\,, \tag{6.12}$$

with

$$\hat{U}_{uL} = O^T \mathcal{U}\,, \qquad \hat{U}_{uR} = \mathcal{U}\,, \qquad \mathcal{U} = \begin{pmatrix} 1_{2\times 2} & 0 \\ 0 & U_0 \end{pmatrix}\,. \tag{6.13}$$

The diagonalization of the mass matrices involves additional diagonal rephasings in order to have real mass terms. The resulting CKM mixing matrix, up to these diagonal rephasings, is given by

$$\hat{V} \equiv \hat{U}_{uL}^\dagger \hat{U}_{dL} = \mathcal{U}^\dagger O\,, \tag{6.14}$$

[2] There is still freedom in U_0, since a diagonal rephasing $U_0 \to U_0 \times \mathrm{diag}(e^{i\alpha}, e^{i\beta})$ does not change Eq. (6.11).

which satisfies $\hat{V}_{4i}=\hat{V}_{3i}^{*}=\frac{1}{\sqrt{2}}\left(O_{3i}+iO_{4i}\right)$, and thus the rephasing invariant relation

$$|\hat{V}_{3i}|=|\hat{V}_{4i}|\,,\quad \forall\, i\,. \tag{6.15}$$

Although the CKM mixing is actually CP-violating, the particular structure reflected by Eq. (6.15) is not phenomenologically viable. The implementation of this idea with three generations of quarks would not be either: experimentally, two CKM elements in the same column cannot have the same modulus. Likewise, we should emphasize that the Yukawa couplings in Eq. (6.9) are not enforced by a symmetry, and thus the model is in principle not stable under RGE.

From the phenomenological point of view, this possibility remains open if one considers instead the PMNS lepton mixing matrix. Before addressing this scenario in Sec. 6.4, we devote next section to present a more general approach that might allow us to gain more insight into the question.

6.3 General approach

Aiming to evade the "CP-conserving mixing argument" provided in [154], one has to identify the conditions under which the bidiagonalization—see App. B for details—of the Yukawa coupling matrices fails. In a fermion sector f, with CP invariance assumed to hold at the Lagrangian level, this implies that the matrices $Y_a^f Y_a^{f\,T}$ and $Y_a^{f\,T} Y_a^f$ have real *degenerate* eigenvalues. In turn, this allows for a simultaneous unitary diagonalization of the Yukawa matrices that involves complex conjugate eigenvectors and leads to a CP-violating mixing matrix.

We develop this question in detail and provide a more transparent understanding of the conclusions reached in [156], clarifying in the process how the simultaneous unitary diagonalization of the Yukawa matrices arises. For concreteness, we circumscribe our discussion to three generations of fermions. Furthermore, since the key ingredient is the degeneracy of the eigenvalues of $Y_a^f Y_a^{f\,T}$ and $Y_a^{f\,T} Y_a^f$, we discuss separately the case of two degenerate eigenvalues, and the case of all three eigenvalues degenerate. Finally, we analyze the resulting structure of the fermion mixing matrix.

Two degenerate eigenvalues

Let us first consider that $Y_a^f Y_a^{f\,T}$ and $Y_a^{f\,T} Y_a^f$ have eigenvalues $\{(y_{a1}^f)^2,(y_{a2}^f)^2,(y_{a2}^f)^2\}$, with $(y_{ai}^f)^2\in\mathbb{R}$, $(y_{ai}^f)^2\geq 0$, and $(y_{a1}^f)^2\neq(y_{a2}^f)^2$. The previous symmetric combinations are diagonalized as

$$O_{f_L}^T Y_a^f Y_a^{f\,T} O_{f_L}=O_{f_R}^T Y_a^{f\,T} Y_a^f O_{f_R}=D_a^f=\mathrm{diag}\left((y_{a1}^f)^2,(y_{a2}^f)^2,(y_{a2}^f)^2\right)\,, \tag{6.16}$$

where O_{f_L} and O_{f_R} are real orthogonal matrices.[3] Then, we can write down

$$D_a^f=O_{f_L}^T Y_a^f Y_a^{f\,T} O_{f_L}=\left(O_{f_L}^T Y_a^f O_{f_R}\right)\left(O_{f_L}^T Y_a^f O_{f_R}\right)^T=\Delta_a^f\Delta_a^{f\,T}\quad\longrightarrow\quad D_a^f\Delta_a^f=\Delta_a^f\Delta_a^{f\,T}\Delta_a^f\,, \tag{6.17}$$

$$D_a^f=O_{f_R}^T Y_a^{f\,T} Y_a^f O_{f_R}=\left(O_{f_L}^T Y_a^f O_{f_R}\right)^T\left(O_{f_L}^T Y_a^f O_{f_R}\right)=\Delta_a^{f\,T}\Delta_a^f\quad\longrightarrow\quad \Delta_a^f D_a^f=\Delta_a^f\Delta_a^{f\,T}\Delta_a^f\,, \tag{6.18}$$

[3] This does not fix $O_{f_{L/R}}$ completely, since Eq. (6.16) is invariant under

$$O_{f_{L/R}}\longrightarrow O_{f_{L/R}}\begin{pmatrix}1 & 0_{1\times 2}\\ 0_{2\times 1} & O_2\end{pmatrix}\,,\qquad \text{with}\qquad O_2\in O(2,\mathbb{R})\,.$$

where we have defined $\Delta_a^f \equiv O_{f_L}^T Y_a^f O_{f_R}$. Combining the right-hand side of Eqs. (6.17) and (6.18), it is clear that

$$D_a^f \Delta_a^f - \Delta_a^f D_a^f = 0 \quad \longrightarrow \quad \left[\left(D_a^f\right)_{ii} - \left(D_a^f\right)_{jj} \right] \left(\Delta_a^f\right)_{ij} = 0 \,. \tag{6.19}$$

Assuming that $(y_{ai}^f)^2 \neq 0$, and taking into account the degeneracy between two of the eigenvalues in D_a^f, Eq. (6.19) yields the following structure for Δ_a^f:

$$\Delta_a^f = \begin{pmatrix} b_a^f & 0_{1\times 2} \\ 0_{2\times 1} & B_a^f \end{pmatrix} . \tag{6.20}$$

being B_a^f a 2×2 block. The left-hand side of Eqs. (6.17) and (6.18) fixes

$$(b_a^f)^2 = (y_{a1}^f)^2 \,, \qquad B_a^f B_a^{f\,T} = B_a^{f\,T} B_a^f = (y_{a2}^f)^2 \; 1_{2\times 2} \,, \tag{6.21}$$

meaning that $(y_{a2}^f)^{-1} B_a^f \in O(2,\mathbb{R})$. Choosing $b_a^f = y_{a1}^f$, we are left with Yukawa couplings Y_a^f of the form

$$Y_a^f = y_{a2}^f \, O_{f_L} \begin{pmatrix} y_{a1}^f / y_{a2}^f & 0_{1\times 2} \\ 0_{2\times 1} & O_2 \end{pmatrix} O_{f_R}^T \,, \tag{6.22}$$

where $y_{ai}^f \in \mathbb{R}$, $y_{ai}^f \neq 0$, and O_2 is a 2×2 real orthogonal matrix. This is the most general Y_a^f compatible with $Y_a^f Y_a^{f\,T}$ and $Y_a^{f\,T} Y_a^f$ having two degenerate eigenvalues. The appearance of an orthogonal submatrix is most important. There are two possible choices for O_2 depending on the value of its determinant. On the one hand, if $O_2 \in SO(2,\mathbb{R})$, that is, $\det O_2 = +1$, then it can be parametrized as

$$O_2 \in SO(2,\mathbb{R}) \qquad \Longleftrightarrow \qquad O_2 = \begin{pmatrix} \cos\alpha & \sin\alpha \\ -\sin\alpha & \cos\alpha \end{pmatrix} , \quad \alpha \in [0, 2\pi) \,. \tag{6.23}$$

This matrix has complex conjugate eigenvalues $e^{\pm i\alpha}$ corresponding to complex conjugate eigenvectors $\vec{v}_\pm = \frac{1}{\sqrt{2}} \left(\begin{smallmatrix} 1 \\ \pm i \end{smallmatrix} \right)$, with $\vec{v}_- = (\vec{v}_+)^*$. Since they are orthonormal, the following unitary diagonalization exists

$$U_0^\dagger \begin{pmatrix} \cos\alpha & \sin\alpha \\ -\sin\alpha & \cos\alpha \end{pmatrix} U_0 = \mathrm{diag}\left(e^{i\alpha}, e^{-i\alpha}\right) , \qquad \text{with} \qquad U_0 = \frac{1}{\sqrt{2}} \begin{pmatrix} 1 & 1 \\ i & -i \end{pmatrix} . \tag{6.24}$$

Remarkably, the matrix U_0 does not depend on the specific value of α: all $SO(2,\mathbb{R})$ matrices are simultaneously diagonalizable. Therefore, the structure in Eq. (6.22) contains all the ingredients of the counter-example presented in [155]. It is sufficient to realize that the 2×2 block in Eq. (6.10) can be written as

$$B_a^u = \sqrt{c_a^2 + s_a^2} \begin{pmatrix} \frac{c_a}{\sqrt{c_a^2+s_a^2}} & \frac{s_a}{\sqrt{c_a^2+s_a^2}} \\ \frac{-s_a}{\sqrt{c_a^2+s_a^2}} & \frac{c_a}{\sqrt{c_a^2+s_a^2}} \end{pmatrix} , \qquad \text{with} \qquad \left(c_a^2 + s_a^2\right)^{-1/2} B_a^u \in SO(2,\mathbb{R}) \,. \tag{6.25}$$

On the other hand, orthogonal matrices $O_2 \notin SO(2,\mathbb{R})$, that is, with $\det O_2 = -1$, are parametrized as

$$O_2 \notin SO(2,\mathbb{R}) \qquad \Longleftrightarrow \qquad O_2 = \begin{pmatrix} \cos\alpha & \sin\alpha \\ \sin\alpha & -\cos\alpha \end{pmatrix} , \quad \alpha \in [0, 2\pi) \,. \tag{6.26}$$

They have real eigenvalues ± 1 and, although the degeneracy in $Y_a^f Y_a^{f\,T}$ and $Y_a^{f\,T} Y_a^f$ is still present, there is no simultaneous unitary diagonalization such as Eq. (6.24).

Three degenerate eigenvalues

Once we have stressed the important role of orthogonal matrices, the case of $Y_a^f Y_a^{f\,T}$ and $Y_a^{f\,T} Y_a^f$ with all three degenerate eigenvalues, namely $\{(y_{a1}^f)^2, (y_{a1}^f)^2, (y_{a1}^f)^2\}$, becomes almost straightforward. One simply has

$$Y_a^f Y_a^{f\,T} = Y_a^{f\,T} Y_a^f = (y_{a1}^f)^2 \; 1_{3\times 3} \,, \tag{6.27}$$

meaning that $(y_{a1}^f)^{-1}\, Y_a^f \in O(3,\mathbb{R})$, with $y_{a1}^f \in \mathbb{R}$ and $y_{a1}^f \neq 0$. All $O(3,\mathbb{R})$ matrices have two complex conjugate eigenvalues with corresponding complex conjugate eigenvectors, and a real unit eigenvalue corresponding to a real eigenvector (a short reminder regarding the diagonalization of $O(3,\mathbb{R})$ matrices is provided in App. C). We emphasize two important points: (i) since the eigenvectors are orthonormal, a unitary diagonalization of Y_a^f exists, and (ii) the eigenvectors do not depend on the specific eigenvalues, and thus there are different $O(3,\mathbb{R})$ matrices that can be unitarily diagonalized simultaneously. Therefore, it is possible to construct counter-examples to the "CP-conserving mixing argument" extending the case analyzed in [155] in a transparent manner via $Y_a^f = y_{a1}^f O_a^f$, with $y_{a1}^f \in \mathbb{R}$, $O_a^f \in O(3,\mathbb{R})$, and all O_a^f simultaneously diagonalizable unitarily.

In [155, 156] there is no mention to the intimate connection between degeneracies, the role of orthogonal matrices, the presence of complex conjugate eigenvalues corresponding to complex conjugate eigenvectors, and a simultaneous unitary diagonalization. Our previous discussion makes it clear without invalidating, of course, the results in these references.

Fermion mixing

Concerning the resulting fermion mixing matrices, the common feature that should be noticed in the previous two cases, either $Y_a^f Y_a^{f\,T}$ having two or three degenerate eigenvalues, is the following. The columns of the unitary matrix $\mathcal{U}$ that simultaneously diagonalizes all Y_a^f (that is, for all a), seen as vectors, are $\{\vec{r}, \vec{v}_+, \vec{v}_-\}$, which constitutes an orthonormal set and, crucially, $\vec{v}_- = (\vec{v}_+)^*$, while $\vec{r}$ is real. Taking this into account, we end up with three different possible structures for the fermion mixing, up to diagonal rephasings, depending on the choice of the couplings Y_a^f in each fermion sector f.

(i) Fermion mixing given by $\hat{V} = \mathcal{U}^\dagger O_3$, being O_3 a 3×3 real orthogonal matrix with column vectors denoted by $\vec{o}_i$. We obtain

$$\hat{V}_{3i} = \vec{v}_+ \cdot \vec{o}_i = (\vec{v}_- \cdot \vec{o}_i)^* = \hat{V}_{2i}^* \qquad \Longrightarrow \qquad |\hat{V}_{3i}| = |\hat{V}_{2i}| \,, \tag{6.28}$$

that is, the moduli of the second and third rows are equal, which is of course a rephasing-invariant relation. Furthermore, this mixing matrix is CP-violating, as one can readily check by computing $J \neq 0$.

(ii) Fermion mixing given by $\hat{V} = O_3 \mathcal{U}$. In this case,

$$\hat{V}_{i3} = \vec{o}_i \cdot \vec{v}_- = (\vec{o}_i \cdot \vec{v}_+)^* = \hat{V}_{i2}^* \qquad \Longrightarrow \qquad |\hat{V}_{i3}| = |\hat{V}_{i2}| \,, \tag{6.29}$$

such that there is equality of moduli in the second and third columns of the mixing matrix. The latter is, again, CP-violating since $J \neq 0$.

(iii) Fermion mixing given by $\hat{V} = \mathcal{U}^\dagger \mathcal{U}'$, with $\mathcal{U}'$ an analogous unitary matrix with column vectors

$\{\vec{r}\,', \vec{v}_+', \vec{v}_-'\}$. The resulting $\hat{V}$ satisfies

$$\hat{V} = \begin{pmatrix} \vec{r}\cdot\vec{r}\,' & \vec{r}\cdot\vec{v}_+' & \vec{r}\cdot\vec{v}_-' \\ \vec{v}_+\cdot\vec{r}\,' & \vec{v}_+\cdot\vec{v}_+' & \vec{v}_+\cdot\vec{v}_-' \\ \vec{v}_-\cdot\vec{r}\,' & \vec{v}_-\cdot\vec{v}_+' & \vec{v}_-\cdot\vec{v}_-' \end{pmatrix} \qquad \Longrightarrow \qquad \begin{cases} \hat{V}_{12} = \hat{V}_{13}^*\,, & \hat{V}_{21} = \hat{V}_{31}^*\,, \\ \hat{V}_{22} = \hat{V}_{33}^*\,, & \hat{V}_{23} = \hat{V}_{32}^*\,. \end{cases} \tag{6.30}$$

This particular structure is not phenomenologically viable neither for CKM nor for PMNS. Besides the equality of moduli, the resulting mixing is CP-conserving [156], as $J = 0$.

Notice that starting with a different ordering of the columns of $\mathcal{U}$, the equality of moduli of the elements of $\hat{V}$ would apply to the correspondingly permuted rows for case (i) or columns for case (ii). It is thus clear how, in general, the basic ingredient underlying the particular example of Sec. 6.2 can yield a mixing matrix with the same kind of specific property: equality of moduli in pairs of rows/columns. As mentioned before, this property is ruled out in the quark sector, but not in the lepton sector, to which we now turn our attention.

6.4 Lepton models

As we have just shown, in MHDMs the simultaneous requirement of neutral flavor conservation and spontaneous CP breaking leads to an irreducibly complex unitary mixing matrix for which two rows or two columns must have equal moduli. The latter structure is not feasible in the quark sector. Consequently, one would need to relax one of the previous assumptions, namely, allow for SFCNC while keeping them under control, in order to have SCPV and a complex CKM compatible with experiment, as done in [111]. Nevertheless, the idea can still work in the lepton sector. Lepton mixing inevitably requires to specify a mechanism to generate neutrino masses. On that regard, we present a simple implementation with Dirac neutrinos in Sec. 6.4.1, and extend it to the case of Majorana neutrinos in Sec. 6.4.2. Some relevant phenomenological consequences concerning both neutrino and charged lepton interactions are discussed in Sec. 6.4.3.

6.4.1 Dirac neutrinos

Let us introduce three right-handed neutrino fields ν_R^0 which are singlets under the SM gauge group. The Yukawa interactions of leptons with two Higgs doublets in an arbitrary weak basis read

$$-\mathscr{L}_{\mathrm{Y}}^{\mathrm{lepton}} = \overline{\ell_L^0}(Y_1^\nu\widetilde{\Phi}_1 + Y_2^\nu\widetilde{\Phi}_2)\nu_R^0 + \overline{\ell_L^0}\left(Y_1^\ell\Phi_1 + Y_2^\ell\Phi_2\right)e_R^0 + \mathrm{H.c.}\,, \tag{6.31}$$

where the Yukawa matrices are of the form

$$Y_a^\nu = \mathrm{diag}\,(y_{a1}^\nu, y_{a2}^\nu, y_{a3}^\nu)\;, \qquad Y_a^\ell = O_{\ell_L}\; y_{a2}^\ell \begin{pmatrix} y_{a1}^\ell/y_{a2}^\ell & 0 & 0 \\ 0 & \cos\varphi_a & \sin\varphi_a \\ 0 & -\sin\varphi_a & \cos\varphi_a \end{pmatrix} O_{\ell_R}^T\,, \tag{6.32}$$

with $y_{ai}^f \in \mathbb{R}$, $\varphi_a \in [0, 2\pi)$, and $O_{\ell_{L/R}}$ real orthogonal 3×3 matrices. It is then clear that $\mathscr{L}_{\mathrm{Y}}^{\mathrm{lepton}}$ is CP-invariant. Rotating the scalar doublets into the Higgs basis [60, 101, 102], the Yukawa interactions are written as

$$-\frac{v}{\sqrt{2}}\mathscr{L}_{\mathrm{Y}}^{\mathrm{lepton}} = \overline{\ell_L^0}(M_\nu^0\widetilde{H}_1 + N_\nu^0\widetilde{H}_2)\nu_R^0 + \overline{\ell_L^0}\left(M_\ell^0 H_1 + N_\ell^0 H_2\right)e_R^0 + \mathrm{H.c.}\,, \tag{6.33}$$

with mass matrices

$$M_\nu^0 = \frac{v}{\sqrt{2}}e^{-i\theta_1}\left(c_\beta Y_1^\nu + s_\beta e^{-i\theta}Y_2^\nu\right)\,, \qquad M_\ell^0 = \frac{v}{\sqrt{2}}e^{i\theta_1}\left(c_\beta Y_1^\ell + s_\beta e^{i\theta}Y_2^\ell\right)\,, \tag{6.34}$$

and additional Yukawa couplings

$$N_\nu^0 = \frac{v}{\sqrt{2}}e^{-i\theta_1}\left(-s_\beta Y_1^\nu + c_\beta e^{-i\theta}Y_2^\nu\right)\,, \qquad N_\ell^0 = \frac{v}{\sqrt{2}}e^{i\theta_1}\left(-s_\beta Y_1^\ell + c_\beta e^{i\theta}Y_2^\ell\right)\,. \tag{6.35}$$

On the one hand, the neutrino mass matrix M_ν^0 and the couplings N_ν^0 are already diagonal, and only a diagonal rephasing of the right-handed fields is required in order to have real neutrino masses. On the other hand, the diagonalization of the charged lepton mass matrix M_ℓ^0 is carried out as

$$\begin{aligned} U_{\ell_L}^\dagger M_\ell^0 U_{\ell_R} &= M_\ell = \mathrm{diag}\left(m_e, m_\mu, m_\tau\right) = \\ &= \frac{v}{\sqrt{2}}\begin{pmatrix} |c_\beta y_{11}^\ell + s_\beta y_{21}^\ell e^{i\theta}| & 0 & 0 \\ 0 & |c_\beta y_{12}^\ell e^{i\varphi_1} + s_\beta y_{22}^\ell e^{i\theta}e^{i\varphi_2}| & 0 \\ 0 & 0 & |c_\beta y_{12}^\ell e^{-i\varphi_1} + s_\beta y_{22}^\ell e^{i\theta}e^{-i\varphi_2}| \end{pmatrix}\,, \end{aligned} \tag{6.36}$$

where

$$U_{\ell_L} = O_{\ell_L}\mathcal{U}\,, \qquad U_{\ell_R} = O_{\ell_R}\mathcal{U}R_{\ell_R}\,, \qquad \mathcal{U} = \begin{pmatrix} 1 & 0 & 0 \\ 0 & \frac{1}{\sqrt{2}} & \frac{1}{\sqrt{2}} \\ 0 & \frac{i}{\sqrt{2}} & \frac{-i}{\sqrt{2}} \end{pmatrix}\,, \tag{6.37}$$

with diagonal rephasing R_{ℓ_R} to ensure real diagonal elements given by[4]

$$R_{\ell_R} = e^{-i\theta_1}\mathrm{diag}\left(e^{-i\gamma_1}, e^{-i\gamma_2}, e^{-i\gamma_3}\right) \qquad \begin{cases} \gamma_1 = \arg\left(c_\beta y_{11}^\ell + s_\beta y_{21}^\ell e^{i\theta}\right)\,, \\ \gamma_2 = \arg\left(c_\beta y_{12}^\ell e^{i\varphi_1} + s_\beta y_{22}^\ell e^{i\theta}e^{i\varphi_2}\right)\,, \\ \gamma_3 = \arg\left(c_\beta y_{12}^\ell e^{-i\varphi_1} + s_\beta y_{22}^\ell e^{i\theta}e^{-i\varphi_2}\right)\,. \end{cases} \tag{6.38}$$

Similarly, $N_\ell = U_{\ell_L}^\dagger N_\ell^0 U_{\ell_R}$. It is important to notice that the couplings N_ℓ are diagonal as well—there is flavor conservation—, but not necessarily real, and this has potential implications for CP violation to be addressed later. All in all, the resulting PMNS mixing matrix (up to rephasings) is

$$\hat{U} \equiv U_{\ell_L}^\dagger U_{\nu_L} = \mathcal{U}^\dagger O_{\ell_L}^T\,, \tag{6.39}$$

leading to the rephasing-invariant property

$$|\hat{U}_{2i}| = |\hat{U}_{3i}|\,, \qquad \forall\, i\,. \tag{6.40}$$

Therefore, the PMNS matrix exhibits a "$\mu-\tau$ symmetry" [157]. An immediate consequence is that, in the standard PDG parametrization [23,30], the atmospheric angle $\theta_{23} = \pi/4$ and the Dirac CP-violating

[4] The diagonalization in Eq. (6.36) allows for an additional common rephasing of the lepton fields, namely, $U_{\ell_L} \to U_{\ell_L}R_\ell$ and $U_{\ell_R} \to U_{\ell_R}R_\ell$, with $R_\ell = \mathrm{diag}\left(e^{i\delta_1}, e^{i\delta_2}, e^{i\delta_3}\right)$.

phase is $\delta = 3\pi/2$. At the same time, there is enough parametric freedom in O_{ℓ_L} to fix the values of the remaining parameters in agreement with experiment [49–51]. The following comments are in order.

(i) CP violation in the PMNS matrix is independent on the specific value of θ, as long as $\theta \neq 0, \pi$: the Dirac CP phase is fixed to $\delta = 3\pi/2$, in agreement with current global fits on neutrino oscillation data.

(ii) Checking CP violation at the level of WB-invariants is crucial in this context. Translating Eq. (1.106) to the lepton sector, it is straightforward to see that CP violation in the PMNS matrix requires any pair of charged leptons or neutrinos to be non-degenerate. In particular, from Eq. (6.36), we derive

$$m_\mu \neq m_\tau \qquad \Longleftrightarrow \qquad c_\beta s_\beta y^\ell_{12} y^\ell_{22} \sin(\varphi_2 - \varphi_1) \sin\theta \neq 0 \,. \tag{6.41}$$

It is then clear that we must have two non-vanishing vevs, that is, $c_\beta s_\beta \neq 0$, with a relative complex phase $\theta \neq 0, \pi$. Furthermore, we need both 2×2 orthogonal blocks to be present in Y^ℓ_1 and Y^ℓ_2, *i.e.*, $y^\ell_{12} y^\ell_{22} \neq 0$, and they must not be proportional, $\sin(\varphi_2 - \varphi_1) \neq 0$.

(iii) The choice of Yukawa coupling matrices in Eq. (6.32) is the only viable implementation in order to generate a CP-violating PMNS mixing matrix with the requirements of SCPV and flavor conservation. Relations like Eq. (6.40) for other rows, or columns if one exchanges the roles $Y^\nu_a \leftrightarrows Y^\ell_a$, are not compatible with our current knowledge of the PMNS matrix [49–51]. On the other hand, if we had considered couplings like Y^ℓ_a in Eq. (6.32) for both neutrino and charged lepton sectors, equality of moduli would not extend to the whole row/column, but it would not be phenomenologically acceptable either, and the resulting PMNS would be CP-conserving, contrary to the intended goal.

(iv) The diagonalization of the neutrino mass matrix has played no role in the obtention of the $\mu - \tau$ symmetric PMNS (we have indeed chosen diagonal Y^ν_a couplings to start with).

(v) The resulting $\mu - \tau$ symmetry in the PMNS mixing matrix does not derive from a fundamental symmetry of the model. As discussed in App. D, this means that the minimal implementation of the basic idea—combining SCPV, flavor conservation, and a CP-violating mixing—, is not stable under one-loop RGE. Nevertheless, one-loop stability can be obtained within non-minimal implementations.

Therefore, we have achieved our main goal: the Yukawa couplings in Eq. (6.32) together with SCPV shape a model without SFCNC at tree-level, and where the PMNS matrix is not only CP-violating, but also $\mu - \tau$ symmetric and compatible with experiment. In App. D, we discuss the stability of this scenario under RGE.

6.4.2 Majorana neutrinos — type I seesaw

Considering that the diagonalization of the neutrino mass matrix plays only a secondary role in our previous Dirac neutrino model, it is natural and simple to extend this scenario with the inclusion of Majorana mass terms for the right-handed neutrinos. These provide a rationale for the smallness of neutrino masses at the cost of violating lepton number in two units. Aiming for simplicity, we introduce diagonal Majorana mass terms as

$$-\mathscr{L}_{\text{Majorana}} = \frac{1}{2}\left[\overline{(\nu^0_R)^c}\, M_R\, \nu^0_R + \overline{\nu^0_R}\, M_R\, (\nu^0_R)^c\right] \,, \tag{6.42}$$

where $(\nu_R^0)^c \equiv C\overline{\nu_R^0}^T$, and $M_R = \mathrm{diag}\,(M_{R1}, M_{R2}, M_{R3})$, with $M_{Ri} \in \mathbb{R}$. Given that M_R is real, CP conservation at the Lagrangian level is preserved—see Eq. (1.108). The mass term for neutrinos thus reads

$$-\mathscr{L}^\nu_{\text{mass}} = \frac{1}{2}\begin{pmatrix}\overline{(\nu_L^0)^c} & \overline{\nu_R^0}\end{pmatrix}\mathcal{M}^*\begin{pmatrix}\nu_L^0 \\ (\nu_R^0)^c\end{pmatrix} + \text{H.c.}\,, \tag{6.43}$$

being

$$\mathcal{M} = \begin{pmatrix} 0 & M_\nu^0 \\ (M_\nu^0)^T & M_R\end{pmatrix}\,. \tag{6.44}$$

For the sake of clarity, let us introduce

$$\mu_i \equiv (M_\nu^0)^*_{ii} = \frac{v}{\sqrt{2}}e^{i\theta_1}\left(c_\beta y^\nu_{1i} + s_\beta y^\nu_{2i}e^{i\theta}\right)\,. \tag{6.45}$$

With M_ν^0 and M_R diagonal, the diagonalization of $\mathcal{M}$ can be carried out as

$$\mathcal{U}^T\mathcal{M}^*\,\mathcal{U} = \begin{pmatrix} m_{\text{light}} & 0_{3\times3} \\ 0_{3\times3} & m_{\text{heavy}}\end{pmatrix}\,, \tag{6.46}$$

where

$$\mathcal{U} = \begin{pmatrix} C & S \\ -S^* & C\end{pmatrix}\begin{pmatrix} R_\nu & 0_{3\times3} \\ 0_{3\times3} & 1_{3\times3}\end{pmatrix} \qquad \begin{cases} C = \mathrm{diag}\,(\cos\alpha_1, \cos\alpha_2, \cos\alpha_3)\,, \\ S = \mathrm{diag}\left(e^{i\beta_1}\sin\alpha_1, e^{i\beta_2}\sin\alpha_2, e^{i\beta_3}\sin\alpha_3\right)\,, \\ R_\nu = i\;\mathrm{diag}\left(e^{i\beta_1}, e^{i\beta_2}, e^{i\beta_3}\right)\,, \end{cases} \tag{6.47}$$

and

$$\tan 2\alpha_i = 2\frac{|\mu_i|}{M_{R_i}}\,, \qquad \beta_i = -\arg\,(\mu_i)\,. \tag{6.48}$$

The resulting m_{light} and m_{heavy} are 3×3 real diagonal matrices given by

$$(m_{\text{light}})_{ij} = \delta_{ij}|\mu_i|\tan\alpha_i \simeq \delta_{ij}\frac{|\mu_i|^2}{M_{Ri}}\,, \qquad (m_{\text{heavy}})_{ij} = \delta_{ij}M_{Ri}\frac{\tan 2\alpha_i}{2\tan\alpha_i} \simeq \delta_{ij}M_{Ri}\,. \tag{6.49}$$

Assuming $|\mu_i|$ to have the same mass scale of charged leptons and quarks, such that $|\mu_i| \ll M_{Ri}$, we are left with three heavy neutrino states as well as three light neutrinos whose masses are suppressed by a factor $|\mu_i|/M_{Ri}$, as in the usual type I seesaw mechanism for neutrino mass generation—see Eq. (1.86). The corresponding transformation of the neutrino fields reads

$$\nu_L^0 = \begin{pmatrix} CR_\nu & S\end{pmatrix}\begin{pmatrix}\nu_L^{\text{light}} \\ \nu_L^{\text{heavy}}\end{pmatrix}\,, \qquad \nu_R^0 = \begin{pmatrix} -SR_\nu^* & C\end{pmatrix}\begin{pmatrix}(\nu_L^{\text{light}})^c \\ (\nu_L^{\text{heavy}})^c\end{pmatrix}\,, \tag{6.50}$$

Therefore, it is easy to see that light neutrinos are mostly ν_L^0, while heavy neutrinos are mostly ν_R^0. In addition, one can check that the Dirac spinors $\nu^{\text{light}} = \nu_L^{\text{light}} + (\nu_L^{\text{light}})^c$ and $\nu^{\text{heavy}} = \nu_L^{\text{heavy}} + (\nu_L^{\text{heavy}})^c$ are indeed Majorana spinors since $\nu^{\text{light}} = (\nu^{\text{light}})^c$ and $\nu^{\text{heavy}} = (\nu^{\text{heavy}})^c$. Finally, the 3×6 lepton mixing matrix, up to diagonal rephasings of the charged lepton fields,[5] is

$$\hat{U}_{3\times6} = U^\dagger_{\ell_L}\begin{pmatrix} CR_\nu & S\end{pmatrix}\,, \tag{6.51}$$

[5]The presence of Majorana mass terms do not allow for a common rephasing of left-handed and right-handed neutrino fields.

with U_{ℓ_L} in Eq. (6.37). The PMNS mixing, as it is usually defined, refers solely to the light neutrino sector, namely, the 3×3 matrix given by

$$\hat{U} = U_{\ell_L}^{\dagger} C R_{\nu} \,. \tag{6.52}$$

Deviations of 3×3 unitarity in the light sector are thus controlled by small $\sin \alpha_i$ factors, and Majorana phases can be read from R_ν. As in the previous scenario with Dirac neutrinos, the resulting PMNS mixing is CP-violating, and exhibits $\mu - \tau$ symmetry—in fact, this property holds at the level of $\hat{U}_{3\times 6}$ in Eq. (6.51). Regarding neutral flavor conservation, this is maintained in the charged lepton sector, but SFCNC arise in the neutrino sector. The latter, together with other phenomenological implications, are discussed in next section.

6.4.3 Phenomenological implications

Finally, we address some relevant phenomenological implications of the previous scenarios. We discuss separately neutrino and charged lepton interactions.

Neutrino sector

In the Dirac neutrino case, both N_ν^0 and N_ν are diagonal, and there are no SFCNC. Furthermore, if M_ν^0 does not involve large cancellations, one reasonably has $(N_\nu)_{ii} \sim m_{\nu_i}$, and thus the additional flavor-conserving Yukawa interactions of neutrinos appear to be safely negligible with a $\frac{m_{\nu_i}}{v} \sim 10^{-13}$ suppression factor.

Concerning the Majorana neutrinos of the seesaw scenario, it is important to recall that each of the components in ν_L^0 and ν_R^0 is an admixture of one light and one heavy state, as quoted in Eq. (6.50), being ν_L^0 mostly light and ν_R^0 mostly heavy. Since M_ν^0 and N_ν^0 are diagonal, couplings between different pairs are absent. Consequently, the Yukawa interactions in the light-light and heavy-heavy sectors are flavor-conserving and, in particular, they are suppressed by small factors $\sin \alpha_i$. There are, nevertheless, SFCNC involving one light and one heavy neutrino (one non-vanishing coupling for each independent pair): since our concern lies with effects not at the large scale M_{R_i}, we do not discuss them further.

As a final comment on the neutrino sector, while the original motivation—obtaining a CP-violating PMNS mixing matrix when one requires that (i) the only source of CP violation is the vacuum state, and that (ii) there are no SFCNC—fully applies in the Dirac neutrino case, this motivation is weakened in the second scenario with Majorana neutrinos, since neutrino masses arise differently (they involve a different diagonalization). However, it is remarkable that the most relevant features of the Dirac neutrino case in Sec. 6.4.1, that is, a $\mu - \tau$ symmetric PMNS and no SFCNC for charged leptons, are preserved in the simple seesaw Majorana scenario of Sec. 6.4.2.

Charged lepton sector

The most relevant sources of potential phenomenological concern are the flavor-conserving couplings of the charged leptons in N_ℓ. These are given by

$$\begin{aligned}
n_e \equiv (N_\ell)_{ee} &= \frac{v^2}{2m_e}\left\{c_\beta s_\beta\left[(y^\ell_{21})^2-(y^\ell_{11})^2\right]+y^\ell_{11}y^\ell_{21}\left(c^2_\beta-s^2_\beta\right)\cos\theta+iy^\ell_{11}y^\ell_{21}\sin\theta\right\}\,,\\
n_\mu \equiv (N_\ell)_{\mu\mu} &= \frac{v^2}{2m_\mu}\left\{c_\beta s_\beta\left[(y^\ell_{22})^2-(y^\ell_{12})^2\right]+y^\ell_{12}y^\ell_{22}(c^2_\beta-s^2_\beta)\cos(\theta+\varphi)+iy^\ell_{12}y^\ell_{22}\sin(\theta+\varphi)\right\}\,,\\
n_\tau \equiv (N_\ell)_{\tau\tau} &= \frac{v^2}{2m_\tau}\left\{c_\beta s_\beta\left[(y^\ell_{22})^2-(y^\ell_{12})^2\right]+y^\ell_{12}y^\ell_{22}(c^2_\beta-s^2_\beta)\cos(\theta-\varphi)+iy^\ell_{12}y^\ell_{22}\sin(\theta-\varphi)\right\}\,,
\end{aligned} \tag{6.53}$$

with $\varphi\equiv\varphi_2-\varphi_1$, and where we have taken into account that, from Eq. (6.36),

$$\begin{aligned}
\frac{2m_e^2}{v^2} &= c^2_\beta(y^\ell_{11})^2+s^2_\beta(y^\ell_{21})^2+2c_\beta s_\beta y^\ell_{11}y^\ell_{21}\cos\theta\,,\\
\frac{2m_\mu^2}{v^2} &= c^2_\beta(y^\ell_{12})^2+s^2_\beta(y^\ell_{22})^2+2c_\beta s_\beta y^\ell_{12}y^\ell_{22}\cos(\theta+\varphi)\,,\\
\frac{2m_\tau^2}{v^2} &= c^2_\beta(y^\ell_{12})^2+s^2_\beta(y^\ell_{22})^2+2c_\beta s_\beta y^\ell_{12}y^\ell_{22}\cos(\theta-\varphi)\,.
\end{aligned} \tag{6.54}$$

The interactions of the charged leptons with the physical neutral scalars are of the form

$$\mathscr{L}_{S\ell\ell} = -S_j\,\bar{\ell}\left(a^\ell_j+ib^\ell_j\gamma_5\right)\ell\,, \tag{6.55}$$

with $\ell=e,\mu,\tau$, and $j=1,2,3$ corresponding to $\{S_1,S_2,S_3\}=\{h,H,A\}$. The previous couplings read

$$a^\ell_j = R_{1j}\,\frac{m_\ell}{v}+R_{2j}\,\frac{\mathrm{Re}(n_\ell)}{v}-R_{3j}\,\frac{\mathrm{Im}(n_\ell)}{v}\,, \tag{6.56}$$

$$b^\ell_j = R_{2j}\,\frac{\mathrm{Im}(n_\ell)}{v}+R_{3j}\,\frac{\mathrm{Re}(n_\ell)}{v}\,, \tag{6.57}$$

where R_{jk} is the scalar mixing in Eqs. (3.26) and (3.27).

The observables that can be affected by the presence of the previous couplings and deserve some attention are listed below.

- Signal strengths of the 125 GeV scalar boson in $\ell^+\ell^-$ decays.
- Scalar resonances in $pp\to S\to\ell^+\ell^-$, with invariant mass of the lepton pair $q^2\sim M_S^2$. One may also consider the production of charged scalars $H^\pm$ and their leptonic decays $H^+\to\ell^+\nu$ and $H^-\to\ell^-\bar{\nu}$, but they are controlled by the same couplings and the sensitivity is poorer.
- Precision observables sensitive to loops involving new scalars, such as the $g-2$ of the electron and the muon, the electron EDM, and $\mu\to e\gamma$ transitions. In App. E, we provide a detailed calculation of scalar loop contributions to lepton dipole moments.

One could address them through a full numerical exploration of the parameter space of the model (which in principle has enough parametric freedom to satisfy those constraints), but that is beyond the scope of the present study—establishing that the model can be viable—, and would require, in addition, to specify the quark sector. In any case, our analysis in Refs. [7, 8], may provide a satisfactory answer. There, we considered a general flavor conserving 2HDM to address potential deviations from SM expectations in both $g-2$ of the electron and the muon. The complete numerical analysis includes the Higgs signal strengths and bounds on resonant production of new scalars as relevant constraints. In particular, they are satisfied despite the fact that the N_ℓ couplings required to obtain sizable contributions to $(g-2)_{e,\mu}$ are much larger than the corresponding charged lepton masses—in addition, the scalar sector must be close to the scalar alignment limit. Since here we do not necessarily require such values of the couplings, no problem is to be expected from these observables. However, this might not be the case with the electron EDM, d_e, as CP conservation is assumed in [7, 8], and the most recent experimental bound is $|d_e| < 4.1\times 10^{-30}\ e\cdot\mathrm{cm} = 2.1\times 10^{-16}\ e\cdot\mathrm{GeV}^{-1}$ at 90% CL [158]. Hence, let us briefly analyze the neutral scalar contributions to this precision observable in some detail. These arise from one-loop and two-loop (Barr-Zee) diagrams depicted in Fig. 6.1.

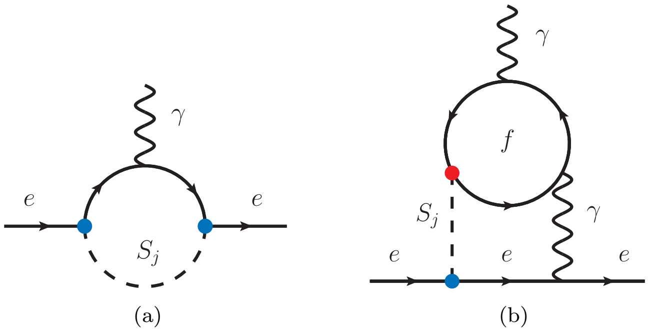

Figure 6.1: Neutral scalar loop contributions to the electron EDM: (a) one-loop, and (b) two-loop Barr-Zee. The blue vertices represent the couplings of the electron to neutral scalars as given in Eqs. (6.55) and (6.56). We distinguish in red the coupling of either a quark or a lepton to a neutral scalar in the closed fermion loop of the Barr-Zee diagram.

On the one hand, with the couplings in Eq. (6.55), one-loop neutral scalar contributions to the electron EDM in Fig. 6.1a—check App. E.1 for the full calculation—are given by

$$|\delta d_e^{(1)}| \simeq \frac{e m_e}{8\pi^2}\left|\sum_j \frac{a_j^e b_j^e}{M_{S_j}^2}\left[\frac{3}{2}+\ln\left(\frac{m_e^2}{M_{S_j}^2}\right)\right]\right| . \tag{6.58}$$

As a simple numerical exercise, one can consider the contribution of a single neutral scalar with mass $M_{S_j} = 500$ GeV and couplings $a_{S_j}^e = b_{S_j}^e = 10(m_e/v)$. With these values, one obtains $|\delta d_e^{(1),\,S_j}| \simeq 2.9\times 10^{-19}\ e\cdot\mathrm{GeV}^{-1}$. It is thus clear that, even for a scalar S_j not too heavy that presents enhanced scalar and pseudoscalar couplings $a_{S_j}^e$ and $b_{S_j}^e$ with respect to the SM-like coupling m_e/v, the corresponding contribution is not expected to be in conflict with the experimental bound on d_e.

On the other hand, for a given scalar S_j and fermion f, two-loop Barr-Zee diagrams in Fig. 6.1b generate a contribution to the electron EDM of the form

$$|\delta d_e^{(2),\,(S_j,\,f)}| = \frac{e\alpha}{8\pi^3}\frac{N_C^f Q_f^2}{m_f}\left| a_j^e b_j^f\ f\left(\frac{m_f^2}{M_{S_j}^2}\right) + b_j^e a_j^f\ g\left(\frac{m_f^2}{M_{S_j}^2}\right)\right| , \tag{6.59}$$

where N_C^f and Q_f are the number of colors and the electric charge of fermion f, and the functions $f(z)$ and $g(z)$ are given in App. E.3. Notice that one of the "small" electron Yukawa couplings is replaced by the scalar or pseudoscalar couplings of the fermion f, which are analogous to the ones quoted in

Eq. (6.55).[6] With the previous values $M_{S_j} = 500$ GeV, $a_j^e = b_j^e = 10(m_e/v)$, and an internal top quark $f = t$ with couplings $a_j^t = b_j^t = m_t/v$, we obtain $|\delta d_e^{(2),\,(S_j,\,t)}| \simeq 3\times 10^{-13}\ e\cdot\mathrm{GeV}^{-1}$, which is incompatible with the experimental bound. From this rough estimate, it is clear that the electron EDM is indeed a relevant constraint, and these illustrative values (considered simultaneously) are too naive or generic: although not automatically granted, compatibility with experiment can be regained by a combination of heavier scalars, smaller Yukawa couplings of the electron,[7] smaller Yukawa couplings of the top quark (presumably the dominant fermion contribution unless the bottom quark couplings are much more enhanced), and even cancellations between the different scalar contributions. As an example, let us consider the joint contribution of all three scalars with masses $M_{S_1} = M_{S_2} = M_{S_3} = 2$ TeV, with couplings to the electron and the top quark given by $n_e = (e^{i\pi/4}/20)m_e$ and $n_t = (e^{i\pi/4}/20)m_t$, respectively, and non-vanishing scalar mixings $R_{11} = 1$ (corresponding to the scalar alignment limit), $R_{22} = R_{33} = \cos\theta_{23}$ and $R_{23} = -R_{32} = \sin\theta_{23}$, with $\theta_{23} = 0.2$. With these illustrative values, we obtain $|\delta d_e^{(2),\,(S_1,\,t)} + \delta d_e^{(2),\,(S_2,\,t)} + \delta d_e^{(2),\,(S_3,\,t)}| \simeq 1.5\times 10^{-16}\ e\cdot\mathrm{GeV}^{-1}$, in agreement with experiment. All in all, one can readily see that the model remains viable, but the electron EDM plays an important role in shaping the available parameter space.

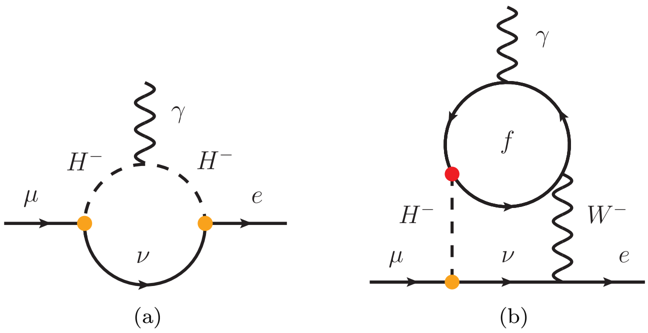

Figure 6.2: Scalar loop contributions to $\mu\to e\gamma$: (a) one-loop, and (b) two-loop Barr-Zee. The orange vertices represent the couplings of the leptons to charged scalars. We distinguish in red the coupling of either a quark or a lepton to the charged scalar in the closed fermion loop of the Barr-Zee diagram.

One might also worry about potentially dangerous contributions to $\mu\to e\gamma$ transitions such as those in Fig. 6.2. For Dirac neutrinos, the smallness of neutrino masses and couplings $(N_\nu)_{ii} \sim m_{\nu_i}$ safely suppress $\mu\to e\gamma$ transitions. For Majorana neutrinos in the type I seesaw scenario presented in Sec. 6.4.2, one might worry about the contributions coming from internal heavy neutrinos, which are mostly ν_R^0. One expects again suppressed contributions from the large heavy neutrino masses in the one-loop diagrams and, less transparently—see [159]—, from the heavy neutrino in the initial-to-final fermion line together with the heavy W in the internal vector boson line. Nevertheless, although plausible, this does not guarantee automatic agreement with experimental constraints on $\mu\to e\gamma$ transitions, and similarly to the case of the electron EDM, they can play a relevant role in constraining the parameter space in more thorough phenomenological studies.

[6] The only relevant change for fermions with opposite sign weak isospin, *i.e.*, neutrinos and up-type quarks, is that the scalar mixing $R_{3j}\to -R_{3j}$.

[7] Smaller Yukawa couplings are in fact to be expected since the couplings in Eq. (6.55) involve the interplay between the real and imaginary parts of n_e and the scalar mixings R_{jk}.

6.5 Summary

In the context of 2HDM, we have analyzed how the simultaneous requirement of (i) SCPV and (ii) the absence of SFCNC can lead to a fermion mixing matrix that violates CP, evading the argument given in [154]. To this aim, the real Yukawa couplings must exhibit a very particular structure, as shown in [155], satisfying two important conditions: (i) the symmetric combinations $Y_a^f Y_a^{f\,T}$ and $Y_a^{f\,T} Y_a^f$ have real *degenerate* eigenvalues, and (ii) the corresponding Yukawa coupling Y_a^f presents complex conjugate eigenvalues corresponding to *complex conjugate* eigenvectors, which are *orthonormal* and *do not depend on the specific eigenvalues*. The latter allows for a *simultaneous unitary* diagonalization of all Y_a^f ($a = 1, 2$), and thus guarantees the absence of SFCNC. At the same time, the fact that the eigenvectors are complex conjugate of one another forces the fermion mixing matrix to have two rows/columns of equal moduli. Our analysis provides a general approach to the model presented in [155, 156], and emphasizes the important role of orthogonal matrices together with their intimate connection with degeneracies, complex eigenvalues, and a simultaneous unitary diagonalization of the Yukawa couplings. Although the previous framework is not viable in the quark sector, we extend this idea to the lepton sector, considering both Dirac and Majorana neutrinos (in a type I seesaw scenario). The resulting PMNS mixing matrix, as a consequence of the simultaneous requirement of SCPV and the absence of SFCNC, is $\mu - \tau$ symmetric and compatible with current experimental data. Finally, we have discussed some additional phenomenological implications, and argued that observables such as the electron EDM and $\mu \to e\gamma$ transitions would play a fundamental role in constraining the parameter space of the model.

7 CP violation in B meson mixing: baryogenesis and upcoming searches

As developed in chapter 1, the phenomenon of CP violation in the SM is a consequence of the existence of three generations of fermions, predicted by Kobayashi and Maskawa [28], and beautifully confirmed by an array of measurements in the quark sector [23, 116]. However, CP violation has not yet been observed in all quark flavor transitions. In this chapter, we will focus on the yet-to-be-measured CP violation in neutral B meson mixing.

Neutral B mesons are eigenstates of the strong and electromagnetic interactions with quark flavor content $B_q = \bar{b}q$ and $\bar{B}_q = b\bar{q}$, being $q = d, s$. Like kaons and D mesons, they are not mass eigenstates once the weak interaction comes into play, but they form an ultradegenerate oscillating system $B_q \leftrightarrow \bar{B}_q$, with $\Delta M_{B_d}/M_{B_d} \simeq 10^{-13}$ and $\Delta M_{B_s}/M_{B_s} \simeq 10^{-12}$. In addition, we know that the actual mass eigenstates are not eigenstates of CP, and that this symmetry is violated in meson-antimeson oscillations at the level of 10^{-3} in both kaon and D meson systems. On the other hand, the SM predicts that the amount of CP violation in B meson mixing is $\mathcal{O}(10^{-4}\text{–}10^{-5})$ [160]:

$$A_{\mathrm{SL}}^{d,\mathrm{SM}} \simeq -5 \times 10^{-4} \qquad [\text{SM prediction}]\,, \tag{7.1}$$

$$A_{\mathrm{SL}}^{s,\mathrm{SM}} \simeq +2 \times 10^{-5} \qquad [\text{SM prediction}]\,. \tag{7.2}$$

Here, as it is common practice, A_{SL}^{q} quantifies CP violation in neutral B meson mixing, with SL standing for "semileptonic", which are the typical modes where these observables are searched for.

From the more theoretical point of view, the analysis of CP violation in neutral B meson oscillations is appealing for two reasons.

(i) This is a highly suppressed phenomenon in the SM, meaning that, if it was measured, it would constitute a clear signal of NP.

(ii) Since this type of CP violation arises in mixing, its effects are imprinted into *any* B meson decay, and in particular into novel BSM decays of B mesons. In this context, the B-mesogenesis mechanism [161–163]—see also [164–170]—combined precisely these two features, namely, CP violation in mixing and the existence of a new decay mode of B mesons into a baryon and a dark sector antibaryon, aiming to generate both the observed matter-antimatter asymmetry as well as the dark matter abundance in the early Universe. Notably, within this mechanism, *the baryon asymmetry of the Universe is directly proportional to the amount of CP violation in neutral B meson mixing,* requiring in particular [163]:[1]

$$A_{\rm SL}^q > +10^{-4} \qquad \text{[required for baryogenesis]}\,. \tag{7.3}$$

Hence, the magnitude of CP violation in neutral B meson mixing could be a sensitive probe for many NP scenarios that modify neutral meson mixing, and also be at the origin of the asymmetry between matter and antimatter in the Universe. Unfortunately, it turns out that the CP asymmetry in the SM falls short by about an order of magnitude—compare Eqs. (7.1) and (7.2) with Eq. (7.3)—to generate the observed baryon asymmetry quoted in Eq. (1.111), thus requiring the presence of new CP-violating sources in B meson oscillations.

The modification of B meson mixing and its CP-violating effects has been broadly addressed in the literature in the context of NP models—see [172–181] for global analyses, and [182–198] for specific models. Nevertheless, the extent to which these models can alter the amount of CP violation in B mixing has not been recently analyzed. The latest detailed studies date from over a decade, when the D0 collaboration reported an anomalously large CP asymmetry involving both B_d and B_s decays [199–201]. After new measurements by LHCb, Belle and BaBar, it has become clear that global averages are compatible with the absence of CP violation in neutral B meson mixing [65]:

$$A_{\rm SL}^{d,\rm Exp} = (-21 \pm 17) \times 10^{-4} \qquad \text{[world average 2025]}\,, \tag{7.4}$$
$$A_{\rm SL}^{s,\rm Exp} = (\;\;-6 \pm 28) \times 10^{-4} \qquad \text{[world average 2025]}\,. \tag{7.5}$$

In this context, we believe there are three more reasons to explore this subject again.

(i) The LHC has provided many new measurements of CP-violating observables in the B meson sector, which have implications for this type of models.

(ii) The CP asymmetries encoding the amount of CP violation in mixing will be measured with higher precision at LHCb as well as in Belle II in the upcoming years.

(iii) NP models that can alter these CP asymmetries face many novel bounds from the LHC as a result of the plethora of stringent searches for new phenomena, which in general require $\Lambda_{\rm NP} > 1$ TeV, being $\Lambda_{\rm NP}$ the NP energy scale.

All in all, our main goal in this chapter is to understand how large CP violation in neutral B meson mixing can be. As previously mentioned, this is important in order to highlight what the relevance of future measurements of this quantity at collider experiments is, its implications for BSM models (that is, what sort of NP could be at play if a non-standard value is measured), and finally to understand which conditions are needed BSM to generate a large enough CP asymmetry allowing for successful B-mesogenesis.

To this aim, we consider three different scenarios. (i) Models where the main modification to B meson mixing arises from contributions to the *mass mixing* M_{12}^q. These are the most standard modifications, as M_{12}^q mediates virtual transitions, and thus heavy particles inaccessible to the LHC could contribute to it. (ii) NP models with additional vector-like quarks inducing deviations from 3×3 CKM unitarity. The motivation for this type of extensions follows from the original purpose of introducing three quarks

[1] Recently, it has been pointed out that radiative decays and inverse decays of resonant vector mesons $B_q^* \leftrightarrow B_q + \gamma$ will act as to suppress the generation of the baryon asymmetry within B-mesogenesis, and probably one would need a semileptonic asymmetry larger than in Eq. (7.3) [171].

in the SM to allow for CP violation. In our case, we want to understand how they change the relevant CP asymmetries. (iii) NP models that contribute to the *decay width mixing* Γ_{12}^q. In principle, these scenarios necessarily involve rather light states, and as we will check, they are highly constrained by LHC searches and measurements of the meson mass differences.

Overall, our main conclusions are that upcoming measurements of CP violation in B mixing will not be able to test the most generic NP models, and that the B-mesogenesis mechanism is to some extent theoretically depreciated due to the difficulty to obtain large enough CP asymmetries BSM. A visual description of these results is displayed in Fig. 7.8.

This chapter is structured as follows. In Sec. 7.1, we present an overview of neutral B meson systems as well as the current status of the relevant mixing observables. In Sec. 7.2, we perform a global analysis of NP models which affect the mass mixing. Then, in Sec. 7.3, we focus on the impact that deviations of 3×3 CKM unitarity induced by the presence of vector-like quarks have on the CP asymmetries. Sec. 7.5 is devoted to BSM scenarios that can also modify the decay mixing. In Sec. 7.6 we discuss our results and compare them with the minimal requirements needed for successful B-mesogenesis as well as upcoming sensitivities from LHCb and Belle II. Finally, we draw our conclusions in Sec. 7.7. We refer the practitioners to App. F. There we discuss in depth the effective 2×2 Hamiltonian for $B_q-\bar{B}_q$ meson systems and review the SM calculation of the mixing parameters in App. F.1. We also include a fully detailed computation of the novel contributions arising in vector-like quark models in App. F.2.

7.1 Neutral $B_q-\bar{B}_q$ meson mixing

In this section, we revisit the fundamental concepts related to the phenomenon of neutral B meson oscillations. Furthermore, we compare the SM prediction with the latest experimental results on the mixing observables that are of interest for the subsequent analyses.

7.1.1 General framework and experimental status

The mesons $B_q = \bar{b}q$ and $\bar{B}_q = b\bar{q}$, with $q = d, s$, are eigenstates of the strong and electromagnetic interactions with opposite flavor content. Once the weak interaction is considered, they both mix and decay to other states. In the Weisskopf-Wigner approximation [202, 203], the time evolution of a superposition of neutral B mesons,

$$|\psi(t)\rangle = a(t)|B_q\rangle + b(t)|\bar{B}_q\rangle\,, \tag{7.6}$$

with t measured in the rest frame of the $B_q-\bar{B}_q$ system, is controlled by the Hamiltonian

$$\mathcal{H}^q = M^q - i\frac{\Gamma^q}{2} = \begin{pmatrix} M_{11}^q - i\Gamma_{11}^q/2 & M_{12}^q - i\Gamma_{12}^q/2 \\ M_{21}^q - i\Gamma_{21}^q/2 & M_{22}^q - i\Gamma_{22}^q/2 \end{pmatrix}\,, \tag{7.7}$$

that is,

$$\mathcal{H}^q|\psi(t)\rangle = i\frac{d}{dt}|\psi(t)\rangle\,, \qquad |\psi(t)\rangle = \exp(-i\mathcal{H}^q t)|\psi(0)\rangle\,, \tag{7.8}$$

with $M^q = M^{q\dagger}$ and $\Gamma^q = \Gamma^{q\dagger}$. The Hamiltonian is not diagonal in the $\{|B_q\rangle, |\bar{B}_q\rangle\}$ basis, meaning that neutral B mesons will *oscillate*, *i.e.*, have a time-dependent varying flavor content in terms of B_q and $\bar{B}_q$. Furthermore, CPT invariance, which is assumed hereafter, leads to $M_{11}^q = M_{22}^q$ and $\Gamma_{11}^q = \Gamma_{22}^q$.

The off-diagonal elements are precisely the ones responsible for the $B_q \leftrightarrow \bar{B}_q$ transitions in two possible ways: (i) through intermediate virtual (off-shell) states encoded in the *mass mixing* M_{12}^q, or (ii) through intermediate real (on-shell) states related to the *decay width mixing* Γ_{12}^q. For further details on the physical meaning of these quantities and their relation to the underlying fundamental interactions, see App. F. The mass and decay width differences between the heavy (H) and light (L) eigenstates of the Hamiltonian can be expressed,[2] up to $\mathcal{O}(|\Gamma_{12}^q/M_{12}^q|^2)$, as

$$\Delta M_q \equiv M_H^q - M_L^q \simeq 2|M_{12}^q|\,, \tag{7.9}$$

$$\Delta\Gamma_q \equiv \Gamma_L^q - \Gamma_H^q \simeq 2|\Gamma_{12}^q|\cos\phi_{12}^q\,, \tag{7.10}$$

where

$$\phi_{12}^q \equiv \arg\left(-\frac{M_{12}^q}{\Gamma_{12}^q}\right)\,. \tag{7.11}$$

This relative phase is directly related to the phenomenon of CP violation in B meson mixing, which will translate into a deviation of Γ_{12}^q/M_{12}^q from being a real quantity. In particular, ϕ_{12}^q emerges in the computation of CP asymmetries involving flavor-specific decays characterized by a final state f such that $B_q \nrightarrow \bar{f}$ and $\bar{B}_q \nrightarrow f$ (*i.e.*, B_q cannot decay into $\bar{f}$ and $\bar{B}_q$ cannot decay into f), and $\langle f|\mathcal{T}|B_q\rangle = \langle \bar{f}|\mathcal{T}|\bar{B}_q\rangle$, where $\mathcal{T}$ is the transition matrix describing the underlying fundamental interactions that control these processes. In particular, one can consider the semileptonic decay modes $B_q \to X\ell^+\nu_\ell$ and $\bar{B}_q \to X\ell^-\bar{\nu}_\ell$, where the charge of the final state lepton projects the flavor content of the B meson at the time of decay (the $\Delta F = \Delta Q$ rule of charged current weak interactions).[3] In those cases, the semileptonic asymmetries are defined as

$$A_{\rm SL}^q \equiv \frac{\Gamma(\bar{B}_q(t)\to f) - \Gamma(B_q(t)\to \bar{f})}{\Gamma(\bar{B}_q(t)\to f) + \Gamma(B_q(t)\to \bar{f})}\,. \tag{7.12}$$

Notice that, in the previous equation, we have explicitly included the time dependence of the meson states to make clear that, although they are produced as a B_q ($\bar{B}_q$) meson at the initial time, they may oscillate into a $\bar{B}_q$ (B_q) and then decay to $\bar{f}$ (f). Therefore, the semileptonic asymmetries are actually measuring the difference between the probability of $\bar{B}_q$ mixing into B_q, and B_q mixing into $\bar{B}_q$, that is, CP violation *in mixing*. Furthermore, it is interesting to remark that a positive value of $A_{\rm SL}^q$ indicates that it is more likely that a $\bar{B}_q$ oscillates into a B_q than the other way around, which is precisely the scenario where the B-mesogenesis mechanism can generate the observed BAU. Taking into account the time evolution of B mesons, it is straightforward to check that, up to $\mathcal{O}(|\Gamma_{12}^q/M_{12}^q|^2)$,

$$A_{\rm SL}^q = {\rm Im}\left(\frac{\Gamma_{12}^q}{M_{12}^q}\right) = \left|\frac{\Gamma_{12}^q}{M_{12}^q}\right|\sin\phi_{12}^q\,, \tag{7.13}$$

so that a signal of CP violation in mixing, *i.e.*, $A_{\rm SL}^q \neq 0$, is due to a non-vanishing imaginary part of the ratio Γ_{12}^q/M_{12}^q. For completeness, we point out that, up to $\mathcal{O}(|\Gamma_{12}^q/M_{12}^q|^2)$, one also has

$$\frac{\Delta\Gamma_q}{\Delta M_q} = -{\rm Re}\left(\frac{\Gamma_{12}^q}{M_{12}^q}\right) = \left|\frac{\Gamma_{12}^q}{M_{12}^q}\right|\cos\phi_{12}^q\,. \tag{7.14}$$

All in all, we have related the three relevant observables for the study of $B_q-\bar{B}_q$ meson mixing with the parameters $|M_{12}^q|$, $|\Gamma_{12}^q|$ and ϕ_{12}^q. The most recent experimental measurements of these quantities

[2] The eigenvalues of $\mathcal{H}^q$ are $\mu_H^q = M_H^q - i(\Gamma_H^q/2)$ and $\mu_L^q = M_L^q - i(\Gamma_L^q/2)$, with $M_H^q, M_L^q, \Gamma_H^q, \Gamma_L^q \in \mathbb{R}$, and $M_H^q > M_L^q$ by definition. Notice the flipped $H \leftrightarrows L$ convention in $\Delta\Gamma_q$ with respect to ΔM_q, commonly used in the literature and in agreement with the PDG notation [23].

[3] The $\bar{b}$ quark of the B_q meson decays into a positive charged lepton by emitting a W^+ boson.

are [65]:

$$\Delta M_d^{\rm Exp} = 0.5069(19)\ {\rm ps}^{-1}\,, \qquad \Delta M_s^{\rm Exp} = 17.766(6)\ {\rm ps}^{-1}\,, \tag{7.15}$$

$$\frac{\Delta\Gamma_d^{\rm Exp}}{\Gamma_d^{\rm Exp}} = 0.001(10)\,, \qquad \Delta\Gamma_s^{\rm Exp} = 0.0781(35)\ {\rm ps}^{-1}\,, \tag{7.16}$$

$$A_{\rm SL}^{d,{\rm Exp}} = (-21 \pm 17) \times 10^{-4}\,, \qquad A_{\rm SL}^{s,{\rm Exp}} = (-6 \pm 28) \times 10^{-4}\,, \tag{7.17}$$

with a correlation coefficient for the semileptonic asymmetries of $\rho(A_{\rm SL}^{d,{\rm Exp}}, A_{\rm SL}^{s,{\rm Exp}}) = -0.054$. Notice that the latter are still compatible with zero. The projected 1σ sensitivities $\delta A_{\rm SL}^q$ for the semileptonic asymmetries from LHCb and Belle II, according to [163, 204–206], are the following:

$$\delta A_{\rm SL}^s = 10 \times 10^{-4} \qquad [{\rm LHCb}\,(23\,{\rm fb}^{-1}) - 2025]\,, \tag{7.18}$$

$$\delta A_{\rm SL}^s = 3 \times 10^{-4} \qquad [{\rm LHCb}\,(300\,{\rm fb}^{-1}) - 2040]\,, \tag{7.19}$$

$$\delta A_{\rm SL}^d = 8 \times 10^{-4} \qquad [{\rm LHCb}\,(23\,{\rm fb}^{-1}) - 2025]\,, \tag{7.20}$$

$$\delta A_{\rm SL}^d = 2 \times 10^{-4} \qquad [{\rm LHCb}\,(300\,{\rm fb}^{-1}) - 2040]\,, \tag{7.21}$$

$$\delta A_{\rm SL}^d = 5 \times 10^{-4} \qquad [{\rm Belle\ II}\,(50\,{\rm ab}^{-1}) - 2035]\,, \tag{7.22}$$

where the year is set based on the expected date at which such luminosity will be collected. We should point out that, despite the impressive sensitivity of a few parts in 10^{-4} that will be reached at the end of the HL-LHC era, this is still far from saturating the current theoretical uncertainties within the SM, as we will check later. Looking forward ahead, it is expected that FCC-ee [207] will be able to measure these asymmetries with high precision. Although no dedicated final sensitivity studies are available yet, it has been suggested [208] that FCC-ee could achieve a sensitivity at the level of a few parts in 10^{-5} for $A_{\rm SL}^s$, and hence capable of testing the SM prediction.

7.1.2 The Standard Model prediction for the mixing observables

In the SM, the transitions $\bar{B}_q \leftrightarrow B_q$ occur at a fundamental level via box diagrams with W boson exchange, as depicted in Fig. 7.1—see App. F.1 for details.

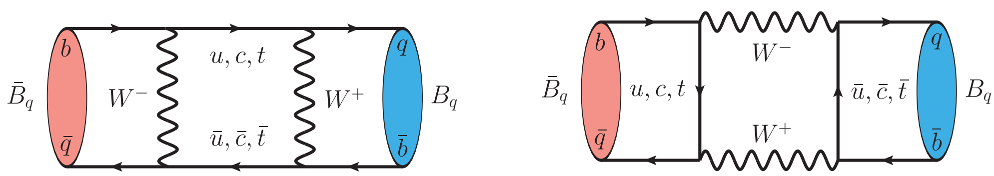

Figure 7.1: SM box diagrams mediating $B_q - \bar{B}_q$ mixing.

On the one hand, $M_{12}^{q,{\rm SM}}$ arises from the dispersive part of these diagrams and is dominated by the virtual top quark contribution [58, 209]:

$$M_{12}^{q,{\rm SM}} = \frac{G_F^2 M_W^2}{12\pi^2} (\lambda_{bq}^t)^2 S_0(x_t) M_{B_q} f_{B_q}^2 B_{B_q} \hat{\eta}_B\,, \tag{7.23}$$

with G_F the Fermi constant, and M_W the mass of the W boson. We will be using the shorthand $\lambda_{bq}^{\alpha} \equiv V_{\alpha b} V_{\alpha q}^*$ for the corresponding combination of CKM elements and $x_\alpha \equiv m_\alpha^2/M_W^2$. The Inami-Lim function $S_0(x)$ [210] is given by

$$S_0(x) = \frac{x}{(1-x)^2}\left[1 - \frac{11x}{4} + \frac{x^2}{4} - \frac{3x^2\ln x}{2(1-x)}\right], \tag{7.24}$$

and is evaluated at $x_t = \bar{m}_t^2(\bar{m}_t)/M_W^2$, where $\bar{m}_t(\bar{m}_t)$ is the top quark mass in the $\overline{\text{MS}}$ scheme [211], yielding $S_0(x_t) \simeq 2.29$. The parameter M_{B_q} is the common mass of the B_q and $\bar{B}_q$ mesons under the strong and electromagnetic interactions. Non-perturbative QCD and hadronization effects are encoded in the product $f_{B_q}^2 B_{B_q}(\bar{m}_b)$, where f_{B_q} is the B_q meson decay constant and $B_{B_q}(\bar{m}_b)$ the bag parameter evaluated at the $\bar{m}_b$ scale. These two parameters have to be determined using non-perturbative methods such as lattice QCD [212, 213] or QCD sum rules [214–216]. In this sense, we should point out that, for the purpose of our analysis, we find more transparent to follow the lattice results from [212] in order to take a particular value of the previous product in both B_d and B_s systems together with their correlation. We note that the semileptonic asymmetries are not particularly sensitive to these parameters and, as such, choosing any other set would not impact significantly our results and final conclusions. We also refer to [217] for an updated discussion on the various calculations of B_q meson parameters from the lattice and future prospects. Finally, the factor $\hat{\eta}_B$ [218] includes two-loop perturbative QCD corrections and is chosen to be renormalization scale and scheme independent. It accounts for the running from the $\bar{m}_t$ scale to the $\bar{m}_b$ scale.[4] In App. F.1.1, we provide further details on the calculation of $M_{12}^{q,\text{SM}}$.

The mixing phenomenon in B_q meson systems is triggered dominantly by the mass difference between the heavy and light eigenstates, that is, ΔM_q. The oscillations are considerably faster for B_s mesons (around 35 times faster) than for B_d mesons. This is due to the hierarchy $|V_{ts}| \gg |V_{td}|$ between the CKM elements appearing in the result for $M_{12}^{q,\text{SM}}$. The most recent SM prediction for the meson mass differences reads [160]:

$$\Delta M_d^{\text{SM}} = 0.535 \pm 0.021\ \text{ps}^{-1}, \qquad \Delta M_s^{\text{SM}} = 18.23 \pm 0.63\ \text{ps}^{-1}. \tag{7.25}$$

The connection with the rephasing-invariant angles β and β_s of the unitarity triangles corresponding to the B_d and B_s systems—see Fig. 1.1—is most important. Their definition, as introduced in chapter 1, is given by

$$\beta \equiv \arg\left(-\frac{V_{cd}V_{cb}^*}{V_{td}V_{tb}^*}\right), \qquad \beta_s \equiv \arg\left(-\frac{V_{ts}V_{tb}^*}{V_{cs}V_{cb}^*}\right). \tag{7.26}$$

These control the time-dependent CP asymmetries, $S_{J/\Psi K_S} \simeq -\eta_{J/\Psi K_S}\sin 2\beta$ and $S_{J/\Psi\Phi} \simeq \eta_{J/\Psi\Phi}\sin 2\beta_s$ (η_f is the CP eigenvalue of the final state f), in the gold-plated modes[5] $B_d \to J/\Psi K_S$ and $B_s \to J/\Psi\Phi$ due to the interference between the decays with and without mixing. As we can see, the latter have a clear theoretical interpretation in terms of the angles of the unitarity triangles, although this remains true when only tree-level contributions to the decays are considered (and CP violation in kaon mixing is neglected in $B_d \to J/\Psi K_S$). On that regard, gluon penguin exchange diagrams can also arise in the SM giving a contribution of order 1° [222–231], which is at the level of the current experimental precision [65, 232, 233], hence will be determinant if one considers the expected experimental sensitivity at LHCb [204] and Belle II [205]. Therefore, the so-called "penguin pollution" must be taken into account in order not to misidentify potential NP effects. In this sense, we conveniently write the SM prediction

[4] An alternative choice for the product of the two-loop perturbative QCD correction factor times the bag parameter can be found in the literature, namely, $\hat{\eta}_B B_{B_q} = \eta_B \hat{B}_{B_q}$. On the left hand side, all renormalization scale and scheme dependence enters on the bag parameter B_{B_q}, while, on the right hand side, it is translated into η_B. The second possibility is used, for instance, by the Flavor Lattice Averaging Group (FLAG) [219].

[5] The gold-plated modes [220, 221] correspond to decays into CP eigenstates common to B_q and $\bar{B}_q$ that occur at tree-level. In those cases, hadronic effects cancel in the ratio of the decay amplitudes of $B_q \to f$ and $\bar{B}_q \to f$.

for the phases controlling the time-dependent CP asymmetries as:

$$\phi_d^{\rm SM} = 2\beta + \phi_d^{\rm SM,peng}\,, \tag{7.27}$$
$$\phi_s^{\rm SM} = -2\beta_s + \phi_s^{\rm SM,peng}\,. \tag{7.28}$$

The first angle on the right-hand side of Eqs. (7.27) and (7.28) arises from the argument of $M_{12}^{q,\rm SM}$ normalized to the relative phase between the tree-level decays $B_d \to J/\Psi K_S$ or $B_s \to J/\Psi\Phi$ and their corresponding CP-conjugate processes $\bar{B}_d \to J/\Psi K_S$ or $\bar{B}_s \to J/\Psi\Phi$. In particular, we have

$$2\beta = \arg(M_{12}^{d,\rm SM}) - 2\arg(V_{cb}V_{cd}^*)\,, \tag{7.29}$$
$$-2\beta_s = \arg(M_{12}^{s,\rm SM}) - 2\arg(V_{cb}V_{cs}^*)\,. \tag{7.30}$$

The parametrization of the CKM matrix can be chosen in such a way that the second term on the right-hand side vanishes—see, *e.g.*, Eq. (1.75).

On the other hand, the theoretical determination of $\Gamma_{12}^{q,\rm SM}$ is much more challenging. It arises from the absorptive part of box diagrams in Fig. 7.1 with real intermediate up and charm quarks. The way to proceed with the computation consists of performing a first Operator Product Expansion (OPE) where all degrees of freedom heavier than the b quark are integrated out (similarly to the $M_{12}^{q,\rm SM}$ case). Then, a second OPE in inverse powers of the heavy b quark mass, the so-called Heavy Quark Expansion (HQE) [234], is carried out. Consequently, this procedure yields $\Gamma_{12}^{q,\rm SM}$ as a power series in $1/m_b$,[6] being m_b the mass of the b quark, where each term is the product of a perturbative Wilson coefficient and a non-perturbative matrix element between the B_q and $\bar{B}_q$ meson states. In turn, the Wilson coefficients may receive QCD corrections at higher orders in the strong coupling α_s. On that respect, contributions at $\mathcal{O}(\alpha_s)$ [235–238] and $\mathcal{O}(\alpha_s^2)$ [239–243] have been computed for the $1/m_b^3$ power, while only leading order terms in QCD are known for $1/m_b^4$ [244] and $1/m_b^5$ [245] powers. Regarding non-perturbative calculations, the hadronic scale fixed by the matrix elements, Λ, is naively expected to be of the order of $\Lambda_{\rm QCD}$, but its specific value must be extracted individually for each term. As previously commented, non-perturbative matrix elements of dim-6 operators are computed in the framework of lattice QCD [212, 213] or QCD sum rules [214–216]. More recently, a novel determination of matrix elements of dim-7 operators was achieved in [246]. In App. F.1.2, details on the computation of $\Gamma_{12}^{q,\rm SM}$ at the lowest order in the HQE and QCD corrections can be found. The latest update of the SM prediction for the decay width differences of B mesons is given by [160]

$$\Delta\Gamma_d^{\rm SM} = (2.7 \pm 0.4)\times 10^{-3}\ {\rm ps}^{-1}\,, \qquad \Delta\Gamma_s^{\rm SM} = (9.1 \pm 1.5)\times 10^{-2}\ {\rm ps}^{-1}\,. \tag{7.31}$$

In any case, we are mostly interested in the ratio $\Gamma_{12}^{q,\rm SM}/M_{12}^{q,\rm SM}$, which can be expressed as

$$\frac{\Gamma_{12}^{q,\rm SM}}{M_{12}^{q,\rm SM}} = -\frac{(\lambda_{bq}^c)^2\Gamma_{12}^{q,cc} + 2\lambda_{bq}^c\lambda_{bq}^u\Gamma_{12}^{q,uc} + (\lambda_{bq}^u)^2\Gamma_{12}^{q,uu}}{(\lambda_{bq}^t)^2\tilde{M}_{12}^{q,\rm SM}}\,, \tag{7.32}$$

where $\tilde{M}_{12}^{q,\rm SM}$ contains the CKM-independent part of $M_{12}^{q,\rm SM}$, and $\Gamma_{12}^{q,\rm SM}$ has been decomposed into different CKM structures coming from uu, uc and cc quark contributions. The latter have very similar

[6] In the case of Γ_{12}^q, the HQE starts at order $1/m_b^3$.

size, that is, $\Gamma_{12}^{q,cc} \simeq \Gamma_{12}^{q,uc} \simeq \Gamma_{12}^{q,uu}$ [247]. Defining the coefficients

$$c_q = -\frac{\Gamma_{12}^{q,cc}}{\tilde{M}_{12}^{q,\mathrm{SM}}}\,, \qquad a_q = 2\frac{\Gamma_{12}^{q,uc} - \Gamma_{12}^{q,cc}}{\tilde{M}_{12}^{q,\mathrm{SM}}}\,, \qquad b_q = \frac{2\Gamma_{12}^{q,uc} - \Gamma_{12}^{q,cc} - \Gamma_{12}^{q,uu}}{\tilde{M}_{12}^{q,\mathrm{SM}}}\,, \tag{7.33}$$

and applying 3×3 CKM unitarity in the form $\lambda_{bq}^u + \lambda_{bq}^c + \lambda_{bq}^t = 0$, one obtains

$$\frac{\Gamma_{12}^{q,\mathrm{SM}}}{M_{12}^{q,\mathrm{SM}}} = c_q + \left(\frac{\lambda_{bq}^u}{\lambda_{bq}^t}\right) a_q + \left(\frac{\lambda_{bq}^u}{\lambda_{bq}^t}\right)^2 b_q\,. \tag{7.34}$$

The numerical values of the coefficients c_q, a_q and b_q extracted from [179] are

$$c_d = (-49.5 \pm 8.5) \times 10^{-4}\,, \qquad c_s = (-48.0 \pm 8.3) \times 10^{-4}\,, \tag{7.35}$$
$$a_d = (11.7 \pm 1.3) \times 10^{-4}\,, \qquad a_s = (12.3 \pm 1.4) \times 10^{-4}\,, \tag{7.36}$$
$$b_d = (0.24 \pm 0.06) \times 10^{-4}\,, \qquad b_s = (0.79 \pm 0.12) \times 10^{-4}\,, \tag{7.37}$$

for the B_d and B_s systems, in accordance with the fact that $\Gamma_{12}^{q,cc} \simeq \Gamma_{12}^{q,uc} \simeq \Gamma_{12}^{q,uu}$. At this point, it is justified to neglect terms of $\mathcal{O}(|\Gamma_{12}^q/M_{12}^q|^2)$ in the expressions for the relevant mixing observables, since $|\Gamma_{12}^q/M_{12}^q| \sim 5\times 10^{-3}$ in the SM.[7] There is a strong hierarchy in the numerical values, namely, $|c_q| > a_q \gg b_q$, due to the GIM suppression affecting a_q and b_q, which vanish in the limit $m_c \to m_u$. Furthermore, the terms proportional to a_q and b_q in Eq. (7.34) are CKM-suppressed, with

$$\frac{\lambda_{bq}^u}{\lambda_{bq}^t} = \begin{cases} 1.7\times 10^{-2} - 4.2\times 10^{-1}\, i\,, & q = d\,, \\ -8.8\times 10^{-3} + 1.8\times 10^{-2}\, i\,, & q = s\,, \end{cases} \tag{7.38}$$

$$\left(\frac{\lambda_{bq}^u}{\lambda_{bq}^t}\right)^2 = \begin{cases} -1.8\times 10^{-1} - 1.5\times 10^{-2}\, i\,, & q = d\,, \\ -2.5\times 10^{-4} - 3.2\times 10^{-4}\, i\,, & q = s\,. \end{cases} \tag{7.39}$$

It is then clear that the real part of the previous ratio is dominated by the real c_q contribution, while for the imaginary part only the term proportional to a_q contributes significantly. In particular, given that a_d and a_s are of the same order, the hierarchy in the values of the semileptonic asymmetries in each system is determined by the fact that the imaginary part of $\lambda_{bq}^u/\lambda_{bq}^t$ is around 20 times larger in the B_d sector than in the B_s sector, having both opposite sign. The latest update from [160] on the SM prediction for the semileptonic asymmetries reads

$$A_{\mathrm{SL}}^{d,\mathrm{SM}} = (-5.1 \pm 0.5) \times 10^{-4}\,, \tag{7.40}$$
$$A_{\mathrm{SL}}^{s,\mathrm{SM}} = (0.22 \pm 0.02) \times 10^{-4}\,. \tag{7.41}$$

All in all, the semileptonic asymmetries in the SM are small, with room for variation at the 10% level, and fully compatible with the current experimental results. Comparing Eq. (7.17) with Eqs. (7.40) and (7.41), one can readily check that the experimental uncertainty is about 3 times larger than the corresponding SM central value in the B_d system, and 130 times larger in the B_s system. This means that there is *a priori* ample room to accommodate NP effects affecting the semileptonic asymmetries, thus providing new sources of CP violation in B meson mixing.

In summary, there are two ingredients that suppress the imaginary part of the ratio $\Gamma_{12}^{q,\mathrm{SM}}/M_{12}^{q,\mathrm{SM}}$

[7] More precisely, corrections to the mixing observables are of $\mathcal{O}((1/8)|\Gamma_{12}^q/M_{12}^q|^2 \sin^2\phi_{12}^q)$, that is, $\mathcal{O}(10^{-8})$ for B_d and $\mathcal{O}(10^{-11})$ for B_s in the SM, thus completely negligible given the current experimental precision.

and, in particular, that align the phases of $\Gamma_{12}^{q,{\rm SM}}$ and $M_{12}^{q,{\rm SM}}$: (i) the dominant top contribution in $M_{12}^{q,{\rm SM}}$, and (ii) 3×3 CKM unitarity and GIM cancellation. Aiming to analyze how this suppression can be evaded BSM, we explore different frameworks in the following. In Sec. 7.2, we adopt a model-independent approach to scenarios where only M^q_{12} is modified. In Sec. 7.3, the inclusion of vector-like quark singlets is considered. Finally, modifications of Γ^q_{12} are addressed in Sec. 7.5.

7.2 $A^q_{\rm SL}$ with heavy New Physics affecting M^q_{12}

First of all, we consider the possibility of *heavy* NP affecting $B_q-\bar{B}_q$ oscillations. The effects of short-distance contributions can be addressed in the EFT framework through higher dimension operators built out of SM light fields (below the m_b scale). On the one hand, in the context of perturbation theory in the weak interactions, M^q_{12} corresponds to $\Delta B=2$ transitions through intermediate virtual states. These arise at the one-loop level in the SM and they are CKM-suppressed, so that M^q_{12} could be a sensitive probe to elucidate heavy NP effects which might compete with the corresponding SM contribution. On the other hand, Γ^q_{12} corresponds to two $\Delta B=1$ transitions through an intermediate real state that is common to both B_q and $\bar{B}_q$ mesons. $\Delta B=1$ transitions arise at tree-level in the SM, so that if NP entered also at tree-level, its effects would be in any case suppressed with respect to the SM by powers of $(M_W/\Lambda_{\rm NP})^2$, being $\Lambda_{\rm NP}$ the NP scale. Therefore, it seems reasonable to neglect heavy NP contributions in Γ^q_{12} at first instance and circumscribe its effects to M^q_{12}.

In this context, we consider a general model-independent modification of M^q_{12}, such that it could be the benchmark to analyze a great variety of models including, *e.g.*, leptoquarks [186, 187, 189], a heavy Z' [189, 196, 197], 2HDMs [183, 188, 190, 191], axion-like particles [192, 198], supersymmetric models [167, 193], dark sector particles [194], or $SU(2)_L$ triplets of heavy gauge bosons [195], among other extensions. We should point out that although previous analyses addressing the impact of NP in B meson mixing have been performed in the literature in a similar fashion—see, *e.g.*, [173–181, 185]—, we rather focus our attention on the question of how large $A^q_{\rm SL}$ can be. On that regard, modifications of these quantities triggered the attention from the theoretical particle physics community some time ago due to the anomalous value of the like-sign dimuon asymmetry reported by the D0 Collaboration [199–201]. Now, we are also encouraged by the fact that the potential size of the semileptonic asymmetries might play a relevant role in generating the observed matter-antimatter asymmetry in the Universe [161]. Finally, it might be convenient to revisit these analyses in light of the most recent experimental data, such as the latest results presented by LHCb concerning the phases that control CP violation in the interference between mixing and decay of B mesons [232, 233].

Following previous studies [176, 179], we can write down

$$M^q_{12}=M_{12}^{q,{\rm SM}}\Delta_q=M_{12}^{q,{\rm SM}}|\Delta_q|e^{i\phi^\Delta_q}\,, \tag{7.42}$$
$$\Gamma^q_{12}=\Gamma_{12}^{q,{\rm SM}}\,, \tag{7.43}$$
$$\phi^q_{12}=\phi_{12}^{q,{\rm SM}}+\phi^\Delta_q\,, \tag{7.44}$$

being $|\Delta_q|$ and ϕ^Δ_q the modulus and the phase of the complex number Δ_q that parametrizes the modification of M^q_{12} with respect to the SM.[8] It is clear that the absence of NP translates into $(|\Delta_q|,\phi^\Delta_q)=(1,0)$. In EFT framework, Δ_q can be understood as a modification of the Wilson coefficient accompanying the

[8]Other authors [178,180,181] opt to parametrize the deviation of the pure NP contribution with respect to the SM, that is, the ratio $M_{12}^{q,{\rm NP}}/M_{12}^{q,{\rm SM}}$. It is straightforward to relate both parametrizations as $M^q_{12}/M_{12}^{q,{\rm SM}}=1+M_{12}^{q,{\rm NP}}/M_{12}^{q,{\rm SM}}$.

dim-6 operator that contributes to $M_{12}^{q,\mathrm{SM}}$. In this way, the mixing observables are modified according to

$$\Delta M_q = 2|M_{12}^{q,\mathrm{SM}}||\Delta_q| = \Delta M_q^{\mathrm{SM}}|\Delta_q|\,, \tag{7.45}$$

$$\Delta\Gamma_q = 2|\Gamma_{12}^{q,\mathrm{SM}}|\cos(\phi_{12}^{q,\mathrm{SM}} + \phi_q^\Delta) = \Delta\Gamma_q^{\mathrm{SM}}\cos\phi_q^\Delta - \Delta M_q^{\mathrm{SM}} A_{\mathrm{SL}}^{q,\mathrm{SM}}\sin\phi_q^\Delta\,, \tag{7.46}$$

$$A_{\mathrm{SL}}^q = \frac{1}{|\Delta_q|}\left|\frac{\Gamma_{12}^{q,\mathrm{SM}}}{M_{12}^{q,\mathrm{SM}}}\right|\sin(\phi_{12}^{q,\mathrm{SM}} + \phi_q^\Delta) = \frac{1}{|\Delta_q|}\left[A_{\mathrm{SL}}^{q,\mathrm{SM}}\cos\phi_q^\Delta + \left(\frac{\Delta\Gamma_q^{\mathrm{SM}}}{\Delta M_q^{\mathrm{SM}}}\right)\sin\phi_q^\Delta\right]. \tag{7.47}$$

The phase controlling the time-dependent CP asymmetries gets modified as

$$\phi_q = \phi_q^{\mathrm{SM}} + \phi_q^\Delta\,, \tag{7.48}$$

where ϕ_q^{SM} is given in Eqs. (7.27) and (7.28). In Eq. (7.48), we are assuming that NP does not enter in tree-level decays nor through penguin topologies, while Eq. (7.47) highlights the strong correlation between A_{SL}^q and ϕ_q^Δ.

Aiming to understand how large the semileptonic asymmetries can be within this scenario, we perform a global fit to constrain all independent parameters: $\{|\Delta_d|, |\Delta_s|, \phi_d^\Delta, \phi_s^\Delta, f_{B_d}^2 B_{B_d}, f_{B_s}^2 B_{B_s}, \theta_{12}, \theta_{13}, \theta_{23}, \delta\}$, being θ_{ij} and δ the three rotation angles and the complex phase of the 3×3 unitary CKM matrix. Without loss of generality, one can restrict the angles to lie in the first quadrant provided that the phase is allowed to be free. In particular, we adopt the Chau-Keung parameterization [30] used by the PDG [23]. The set of relevant constraints includes the following.

- B meson mass differences ΔM_d and ΔM_s. The combination of all available measurements is summarized in [65], and given in Eq. (7.15). These are extraordinary well measured observables, with uncertainties well below 1%.

- CP-violating phases arising in the interference between mixing and decay of B mesons. These can be measured in different decay channels governed by the quark level transition $b \to c\bar{c}s$. On the one hand, $\sin\phi_d$ is obtained from the analysis of final states such as $J/\Psi K_{S/L}$, $\Psi(2S)K_S$, or $\chi_{c1}K_S$. On the other hand, ϕ_s is extracted using final states like $J/\Psi\Phi$, $\Psi(2S)\Phi$, or $D_s^+D_s^-$. LHCb has recently published the most precise single measurements of $\sin\phi_d$ [232] and ϕ_s [233] using the decays $B_d \to \Psi(\to \ell^+\ell^-)K_S(\to \pi^+\pi^-)$ and $B_s \to J/\Psi(\to \mu^+\mu^-)K^+K^-$, respectively. A detailed breakdown of the different determinations of the CP-violating phases can be found in Refs. [65] and [23]. Here, we use the average including the latest results from LHCb, namely,[9]

$$\sin\phi_d^{\mathrm{Exp}} = 0.709 \pm 0.011\,, \tag{7.49}$$

$$\phi_s^{\mathrm{Exp}} = -0.052 \pm 0.013\,. \tag{7.50}$$

  As previously commented, one should care about the contributions coming from penguin diagrams when implementing this constraint. The penguin pollution in the SM is estimated to be of order 1° (~ 0.017 rad), while NP penguins are much less constrained. In this sense, we add in quadrature the potential size of penguin topologies and the experimental uncertainty in the measurement of the previous mixing-induced CP phases, and treat the result as a total uncertainty for this constraint. Our limited knowledge on the penguin effects, and even more on the NP penguin contributions

[9]For online updates of these quantities, we refer to the HFLAV webpage, and the PDG Live results.

(that depend on the specific model), should be appropriately covered in this way. One may also worry about the channel dependence of the penguin pollution,[10] since we are actually taking an experimental average over different decay modes where the mixing-induced CP phases have been measured. An analysis of different decay channels besides the gold-plated ones has been carried out, *e.g.*, in [223, 225], where the penguin effects are expected to be of order 1° as well. Hence, these further effects are also accommodated within our approach.

- Lattice QCD results for the products $f_{B_d}^2 B_{B_d}$ and $f_{B_s}^2 B_{B_s}$, together with their correlation, are taken from [212]:

$$f_{B_d}^2 B_{B_d}(\bar{m}_b) = 0.0342(29)(7)\,\mathrm{GeV}^2\,, \tag{7.51}$$
$$f_{B_s}^2 B_{B_s}(\bar{m}_b) = 0.0498(30)(10)\,\mathrm{GeV}^2\,, \tag{7.52}$$
$$\rho(f_{B_d}^2 B_{B_d}, f_{B_s}^2 B_{B_s}) = 0.968\,, \tag{7.53}$$

where the first number in parentheses is the "total error" accounting for all statistical and systematic uncertainties in the lattice simulation, and the second number in parentheses corresponds to the "charm sea error". We add these two contributions in quadrature.

- CKM entries $|V_{ud}|$, $|V_{us}|$, $|V_{ub}|$, $|V_{cb}|$ and the angle $\gamma \equiv \arg(-V_{ud}V_{cb}V_{ub}^*V_{cd}^*)$. As we will highlight later in next section, in the context of vector-like quark extensions it is crucial to further include the $|V_{tb}|$ constraint, and thus we quote its value in the list below. The experimental values reported by the PDG [23] are:

$$|V_{ud}| = 0.97367 \pm 0.00032\,, \tag{7.54}$$
$$|V_{us}| = 0.22431 \pm 0.00085\,, \tag{7.55}$$
$$|V_{ub}| = (3.82 \pm 0.20) \times 10^{-3}\,, \tag{7.56}$$
$$|V_{cb}| = (41.1 \pm 1.2) \times 10^{-3}\,, \tag{7.57}$$
$$|V_{tb}| = 1.010 \pm 0.027\,, \tag{7.58}$$
$$\gamma = (65.7 \pm 3.0)^\circ\,. \tag{7.59}$$

One may worry about the longstanding discrepancy between the inclusive and exclusive determinations of $|V_{cb}|$ and $|V_{ub}|$, which reach the level of $\sim 3\sigma$ and $\lesssim 2\sigma$, respectively. More precisely, they are given by $|V_{cb}|_{\rm incl} = (42.2\pm0.5)\times10^{-3}$, $|V_{cb}|_{\rm excl} = (39.8\pm0.6)\times10^{-3}$, $|V_{ub}|_{\rm incl} = (4.13\pm0.26)\times10^{-3}$, and $|V_{ub}|_{\rm excl} = (3.67 \pm 0.15) \times 10^{-3}$, with inclusive measurements being generally larger than the exclusive ones. As we will check later, the use of the average values in Eqs. (7.56) and (7.57) or the incl./excl. measurements of these quantities would not change our conclusions, and thus in the following we stick to the combined results recommended by the PDG.

- B meson decay width differences $\Delta\Gamma_d$ and $\Delta\Gamma_s$ [65], as given in Eq. (7.16).

- Semileptonic asymmetries $A_{\rm SL}^d$ and $A_{\rm SL}^s$ [65] in Eq. (7.17). They are measured in flavor-specific decay modes such as $B_q \to D_q^{(*)-}\mu^+\nu X$.

[10]In particular, the penguin pollution encodes non-perturbative hadronic effects involving the initial and final states of the transition amplitude. Other factors such as the polarization of the final state particles might also have an impact on this estimation, as it happens for instance in the gold-plated mode $B_s \to J/\Psi\Phi$. A more extensive explanation can be found in [179].

- Parameters c_q, a_q, and b_q in Eqs. (7.35) to (7.37) entering the ratio Γ_{12}^q/M_{12}^q. It is worth mentioning that their uncertainties are "theoretical". We explore two extreme options: (i) allowing them to vary freely within the range given by the central values plus/minus the uncertainties, and (ii) fixing them to their central values. The results obtained with one or the other option differ at a negligible level. A more realistic approach would allow them to vary in a correlated manner, but since the extreme options make essentially no difference, that more realistic approach cannot neither.

Other input parameters used in the analysis are given in Table 7.1.

Parameter	**Value**	**Units**	**Reference**
G_F	$1.1663788(6) \times 10^{-5}$	GeV^{-2}	[23]
$\hat{\eta}_B$	0.84	1	[218]
M_W	80.377(12)	GeV	[23]
$\bar{m}_t(\bar{m}_t)$	161.98(75)	GeV	[248]
M_{B_d}	5.27963(20)	GeV	[23]
M_{B_s}	5.36691(11)	GeV	[23]

Table 7.1: Input parameters.

The previous constraints are implemented in terms of Gaussian likelihoods or equivalent χ^2 terms (except for the parameters c_q, a_q, and b_q, as mentioned before). The global χ^2 is sampled via Markov chain Monte Carlo techniques in order to represent the relevant regions for the different parameters and observables.

Our results are summarized in Fig. 7.2, where we present the allowed regions in the $A_{\rm SL}^s$–$A_{\rm SL}^d$ plane. In particular, at 68% CL, we have

$$A_{\rm SL}^d|_{\rm w/\,peng} = (-9.1 \pm 3.6) \times 10^{-4}\,, \tag{7.60}$$
$$A_{\rm SL}^s|_{\rm w/\,peng} = (-0.04 \pm 1.21) \times 10^{-4}\,, \tag{7.61}$$
$$\rho(A_{\rm SL}^d, A_{\rm SL}^s)|_{\rm w/\,peng} = -0.113\,, \tag{7.62}$$

including the penguin pollution, and

$$A_{\rm SL}^d|_{\rm w/o\,peng} = (-9.4 \pm 3.2) \times 10^{-4}\,, \tag{7.63}$$
$$A_{\rm SL}^s|_{\rm w/o\,peng} = (-0.01 \pm 0.83) \times 10^{-4}\,, \tag{7.64}$$
$$\rho(A_{\rm SL}^d, A_{\rm SL}^s)|_{\rm w/o\,peng} = -0.110\,, \tag{7.65}$$

if penguins effects are ignored. Both results are fully compatible with the SM prediction at 95% CL, and compatible with zero within 1σ in the B_s system and less than 3σ in the B_d system. We can check that the potential size of the semileptonic asymmetries, as allowed by current data, is $\mathcal{O}(10^{-3})$ for $A_{\rm SL}^d$ and $\mathcal{O}(10^{-4})$ for $A_{\rm SL}^s$, which are still below the projected sensitivity at LHCb with 23 fb^{-1},

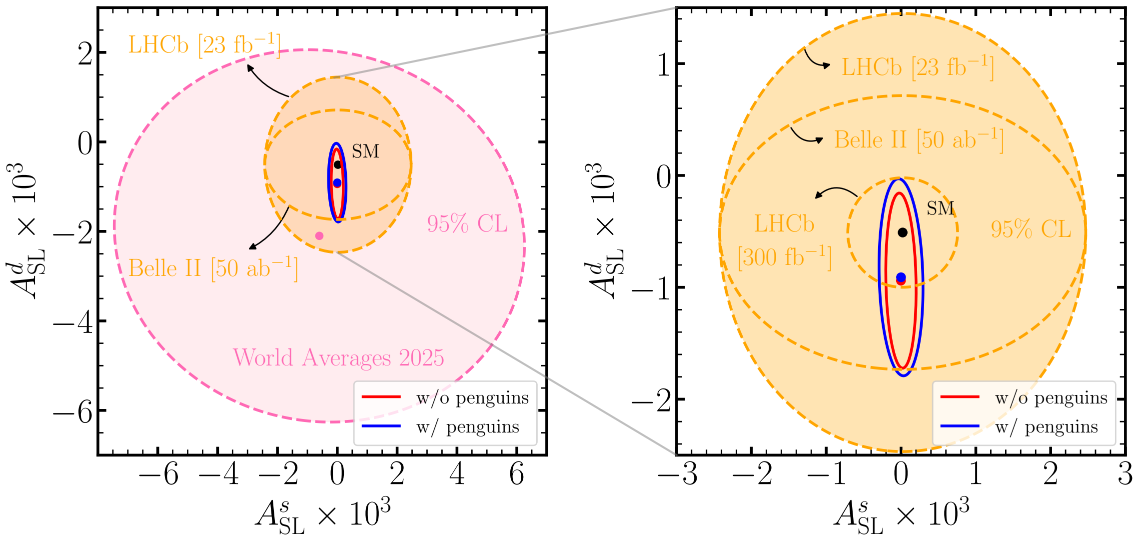

Figure 7.2: Allowed regions for $A_{\rm SL}^d$ and $A_{\rm SL}^s$ with heavy NP solely affecting M_{12}^q. All contours are shown at 95% CL (2D-$\Delta\chi^2 = 5.99$), together with the corresponding best fit point. In the left panel, the pink ellipse represents the current experimental world averages for the semileptonic asymmetries measurements as of 2025, while the ellipses in orange project the future expected sensitivity at LHCb with 23 fb^{-1}, and Belle II with 50 ab^{-1} of collected data. The blue and red contours show the results of our analysis within the scenario presented in Sec. 7.2, corresponding to the case where SM gluon penguin contributions have been included or neglected, respectively. The point in black is the SM prediction, whose uncertainties are not visible in these axes. In the right panel, we provide the detail of our results along with the projected sensitivities at LHCb (23 fb^{-1}) and Belle II (50 ab^{-1}), and, in addition, at LHCb with 300 fb^{-1} of collected data.

and Belle II with 50 ab^{-1} of collected data. Only LHCb at 300 fb^{-1} is expected to effectively constrain the allowed range for $A_{\rm SL}^d$, as it is shown in Fig. 7.2. The vanishing correlation coefficient between the semileptonic asymmetries in our analyses traces back to the absence of correlation in the measurements of the mixing-induced CP phases that constrain the parameters ϕ_q^Δ in B_d and B_s meson systems.

For completeness, we provide in the following the values of the parameters $|\Delta_q|$ and ϕ_q^Δ that modify the modulus and the phase of $M_{12}^{q,\rm SM}$ in this scenario:

$$|\Delta_d|_{\rm w/\,peng} = 0.98^{+0.10}_{-0.07}\,, \qquad \phi_d^\Delta|_{\rm w/\,peng} = -0.071^{+0.058}_{-0.057}\,, \tag{7.66}$$
$$|\Delta_s|_{\rm w/\,peng} = 1.00^{+0.06}_{-0.04}\,, \qquad \phi_s^\Delta|_{\rm w/\,peng} = -0.004^{+0.025}_{-0.027}\,, \tag{7.67}$$

and

$$|\Delta_d|_{\rm w/o\,peng} = 0.90^{+0.13}_{-0.07}\,, \qquad \phi_d^\Delta|_{\rm w/o\,peng} = -0.055^{+0.048}_{-0.059}\,, \tag{7.68}$$
$$|\Delta_s|_{\rm w/o\,peng} = 0.92^{+0.10}_{-0.05}\,, \qquad \phi_s^\Delta|_{\rm w/o\,peng} = -0.006^{+0.018}_{-0.019}\,. \tag{7.69}$$

On the one hand, the parameters $|\Delta_q|$ are close to their SM value with uncertainties of $\mathcal{O}(10\%)$, as one could have expected from the agreement between the measurements and the SM prediction of the meson mass differences ΔM_q. Therefore, they do not contribute substantially to enhance the values of the semileptonic asymmetries with respect to the SM. On the other hand, despite the small values of ϕ_s^Δ, they can enhance $A_{\rm SL}^s$ at the 10^{-4} level. In the case of $A_{\rm SL}^d$, the phases ϕ_d^Δ could be large enough to saturate the experimental lower bound expected from Belle II (50 ab^{-1}).

The previous results have been obtained considering the average experimental values of $|V_{cb}|$ and $|V_{ub}|$ provided by the PDG. On that regard, aiming to maximize the values of the semileptonic asymmetries, we could have used instead the exclusive determination of $|V_{cb}|$ together with the inclusive determination of $|V_{ub}|$, as this choice would allow for larger values of the angles β and β_s in the corresponding unitarity triangles, and thus for the asymmetries—see Eq. (7.47). Ignoring the fact that using the exclusive measurements in one case and the inclusive ones in the other might be in some sense inconsistent, we have checked that this would imply a shift in the central values of the asymmetries, in particular to larger negative values of A^d_{SL} and larger positive values of A^s_{SL}, without altering the ranges of variation driven by the corresponding uncertainties. Although this means that a small region of the parameters could actually be tested by upcoming measurements at Belle II (50 ab^{-1}), our conclusions in terms of compatibility with the B-mesogenesis mechanism do not change, as we will check later.

7.3 A^q_{SL} with non-unitary CKM mixing

We consider in this section models where the SM quark content is extended through the inclusion of "vector-like" quarks.[11] These "exotic fermions" naturally arise in a number of theoretically top-down motivated scenarios such as GUTs [249, 250], extra-dimensional models [251], or composite Higgs models [252]. From a bottom-up perspective, models with vector-like quarks provide an interestingly rich phenomenology [253–261]. We will focus on the simplest cases within that large class of models, that is, models with either one up-type or one down-type quark singlet (to be referred in the following as UVLQ and DVLQ, respectively), since they already introduce the modifications of interest. Two important features are present in these models.

(i) The CKM matrix is not anymore 3×3 unitary, but part of larger unitary matrix. In the UVLQ case, CKM is 4×3, while in DVLQ models, CKM is 3×4. Notably, in both cases CKM mixing is embedded in a 4×4 unitary matrix. Just for illustration, although we do not consider such a scenario, adding simultaneously one up-type and one down-type vector-like quark singlets, CKM would be 4×4 and would be embedded in a larger 5×5 unitary matrix.

(ii) In UVLQ scenario, there are tree-level Z-FCNC in the up quark sector, but not in the down quark sector. On the contrary, in the DVLQ case, there are tree-level Z-FCNC in the down quark sector, but not in the up quark sector. For illustration again, with both one up-type and one down-type vector-like quark singlets, tree-level Z-FCNC are present in both the up and down quark sectors.

Focusing on B_d and B_s neutral meson mixings, there are novel contributions to the mixing parameters.

(i) Contributions to M^q_{12}. In UVLQ models, they correspond to additional SM-like box diagrams, as those in Fig. 7.1, including the new up-type quark T in the loop. These contributions depend on the mass m_T and the combinations $V_{Tb}V^*_{Tq}$ of the enlarged CKM matrix. More precisely, we obtain

$$\frac{M_{12}^{q,\text{UVLQ}}}{M_{12}^{q,\text{SM-like}}} = 1 + \frac{\lambda^T_{bq}}{\lambda^t_{bq}} \frac{C_1^{\text{UVLQ}}(x_t, x_T)}{S_0(x_t)} + \left(\frac{\lambda^T_{bq}}{\lambda^t_{bq}}\right)^2 \frac{C_2^{\text{UVLQ}}(x_T)}{S_0(x_t)}\,, \tag{7.70}$$

[11] "Vector-like" meaning that new left-handed and right-handed fields are added together, with the same $SU(2)_L$ assignment, and thus they are *harmless* from the point of view of anomaly cancellations.

where

$$C_1^{\rm UVLQ}(x_t,x_T)=2S_0(x_t,x_T)\,,\qquad C_2^{\rm UVLQ}(x_T)=S_0(x_T)\,, \tag{7.71}$$

On the other hand, in the DVLQ case, the new contributions involve tree-level flavor-changing neutral vertices, as illustrated in Fig. 7.3, that depend on the 3×3 unitarity violations $(D_L)_{qb}=V_{ub}V_{uq}^*+V_{cb}V_{cq}^*+V_{tb}V_{tq}^*\neq0$, but not on the mass of the new down-type quark. In particular, we find

$$\frac{M_{12}^{q,\rm DVLQ}}{M_{12}^{q,\rm SM\text{-}like}}=1+\frac{(D_L)_{qb}}{\lambda_{bq}^t}\frac{C_1^{\rm DVLQ}(x_t)}{S_0(x_t)}+\left(\frac{(D_L)_{qb}}{\lambda_{bq}^t}\right)^2\frac{C_2^{\rm DVLQ}}{S_0(x_t)}\,, \tag{7.72}$$

where

$$C_1^{\rm DVLQ}(x_t)=-4Y(x_t),\quad C_2^{\rm DVLQ}=\frac{2\sqrt{2}\pi^2}{G_FM_W^2}\,, \tag{7.73}$$

and the Inami-Lim function given by

$$Y(x)=\frac{x}{4(x-1)}\left[x-4+\frac{3x\ln x}{x-1}\right]\,. \tag{7.74}$$

The factor $M_{12}^{q,\rm SM\text{-}like}$ denotes the SM-like contribution quoted in Eq. (7.23), although one could expect different values for the CKM elements since 3×3 unitarity does not hold within these scenarios. A detailed breakdown of the calculation of the different contributions is provided in Apps. F.2.1 and F.2.2.

(ii) Contributions to Γ_{12}^q. There are no new contributions in the UVLQ scenario, contrary to the DVLQ case, where new contributions involving one or two Z flavor-changing vertices are present. These new contributions in the DVLQ case are nevertheless negligible, as we will discuss later.

All in all, the inclusion of vector-like quarks provides two ingredients—a non 3×3 unitary CKM matrix together with new contributions to M_{12}^q—that have the potential to induce a significant misalignment of Γ_{12}^q/M_{12}^q with respect to the SM.

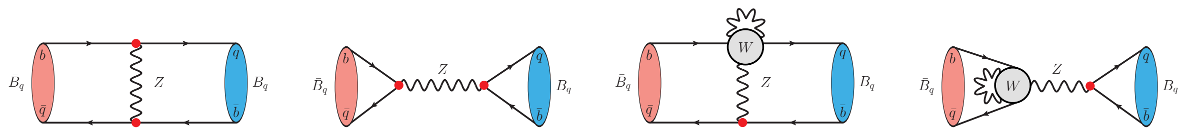

Figure 7.3: Tree-level and one-loop diagrams contributing to $B_q-\bar{B}_q$ mixing in DVLQ models. The red vertex corresponds to the flavor-changing coupling $Z\bar{d}_id_j$ generated in this type of models. The blob in gray represents all possible flavor-changing one-loop topologies arising from the exchange of one or two W bosons, including those where the Z couples directly to one of the external lines. In this case, the other topologies where the red vertex and the gray blob exchange positions are not shown, but appropriately included in the calculations—see App. F.2.2 for details.

The analyses within this scenario are conducted in the same way as those of Sec. 7.2 with the following changes. Since the CKM matrix is not 3×3 unitary but part of a larger 4×4 unitary matrix in both UVLQ and DVLQ analyses, rather than the 4 parameters required in Sec. 7.2 to describe CKM mixing, 5 additional parameters are needed, namely, 3 new mixing angles $\{\theta_{14},\theta_{24},\theta_{34}\}$, and 2 new phases $\{\delta_{14},\delta_{24}\}$ in a PDG-like parametrization. In this way, the extended CKM matrix (4×3 in the UVLQ case, and 3×4 in the DVLQ case), together with the Z tree-level flavor-changing couplings are properly covered.

It is to be mentioned that, in the DVLQ scenario, we ignore the mass of the new down-type quark since it does not enter the quantities of interest, that is, Γ_{12}^q and M_{12}^q. In the UVLQ case, the mass of the new up-type quark m_T is, on the contrary, very relevant. The results shown in Fig. 7.4 correspond to $m_T = 1.6$ TeV. This value is chosen to avoid direct lower bounds [262, 263].[12] We have also checked that for values of $m_T \in [1.6, 5]$ TeV, the range of potential enhancement of the asymmetries $A^q_{\rm SL}$ is unchanged. Concerning the penguin pollution discussed in Sec. 7.2, we only consider in this section analyses that include it, without further mention.

There is an important aspect of our analyses that deserves clarification. For both UVLQ and DVLQ scenarios, we consider the same set of constraints discussed in Sec. 7.2, and used in the model-independent analyses presented there. In principle, this set could be extended to include other relevant constraints (*e.g.*, B_q rare decays, electroweak precision data and oblique parameters, kaon mixing observables, rare kaon decays, *etc.*, to name a few), if we were to perform detailed phenomenological analyses of these scenarios. We stick to the constraints of Sec. 7.2 since that is not our goal. As a consequence, the results obtained in this section, in particular the ranges in $A^d_{\rm SL}$ and $A^s_{\rm SL}$, come with a qualification. It is not guaranteed that the full range of variation of $A^d_{\rm SL}$ and $A^s_{\rm SL}$ would be allowed if additional constraints were to be included. What is guaranteed, however, is that values of $A^d_{\rm SL}$ and $A^s_{\rm SL}$ outside the allowed regions emerging from the analyses cannot be accommodated in any case in these scenarios. Since the regions that we have obtained are already very limited, further constraining them would not change our conclusions in terms of their testability in upcoming measurements at LHCb and Belle II, and their compatibility with the B-mesogenesis mechanism, as we will check later.

Furthermore, we have explored the size of the 3×3 unitarity deviations that our analyses allow for, finding, in the DVLQ case $|(D_L)_{db}| < 5 \times 10^{-4}$ and $|(D_L)_{sb}| < 2 \times 10^{-3}$, while in the UVLQ case $|\lambda^T_{bd}| < 10^{-3}$ and $|\lambda^T_{bs}| < 5 \times 10^{-3}$. Since part of these ranges can indeed be in conflict with other constraints not included, we have also analyzed the minimal sizes of these 3×3 unitarity deviations required to produce the full range of variation of $A^d_{\rm SL}$ and $A^s_{\rm SL}$. We find $|(D_L)_{db}| \sim 2 \times 10^{-4}$ and $|(D_L)_{sb}| \sim 5 \times 10^{-4}$ in the DVLQ case, and $|\lambda^T_{bd}| \sim 4 \times 10^{-4}$ and $|\lambda^T_{bs}| \sim 8 \times 10^{-4}$ in UVLQ models. These values appear to be sufficiently safe from the point of view of other B_d and B_s related constraints [261] not considered here. As a bonus, it is also clear from the values of these 3×3 unitarity deviations that the new contributions to Γ^q_{12} in the DVLQ scenario mentioned before are much suppressed with respect to the usual ones: $|(D_L)_{db}| \ll |\lambda^u_{bd}|, |\lambda^c_{bd}| \sim \mathcal{O}(\lambda^3)$ and $|(D_L)_{sb}| \le |\lambda^u_{bs}| \sim \mathcal{O}(\lambda^4) \ll |\lambda^c_{bs}| \sim \mathcal{O}(\lambda^2)$, with $\lambda \simeq 0.23$ in the Wolfenstein parametrization of CKM.

As a last comment concerning the constraints, the one on $|V_{tb}|$ deserves some attention. When CKM is assumed to be 3×3 unitary—as in Sec. 7.2—, the constraints on $|V_{cb}|$ and $|V_{ub}|$ already force $|V_{tb}| = 1 - \mathcal{O}(\lambda^4)$ with an uncertainty of $\mathcal{O}(\lambda^6)$, while the uncertainty in the experimental determination of $|V_{tb}|$ is (numerically) in the $\mathcal{O}(\lambda^2)$ to $\mathcal{O}(\lambda^3)$ ballpark. This means that the role of this constraint when 3×3 unitarity is assumed is irrelevant. However, that is not the case anymore when CKM is not 3×3 but part of a larger unitary matrix, since unitarity bounds the moduli of the elements of that extended matrix beyond the third row and column.

The main result of this section is shown in Fig. 7.4. As in Fig. 7.2 in Sec. 7.2, the allowed region for the semileptonic asymmetries in the $A^d_{\rm SL}$–$A^s_{\rm SL}$ plane is shown, together with the experimental projected sensitivities. For comparison, the allowed region obtained in the analysis of Sec. 7.2, the NP 3×3 case, is also displayed. One can observe that the enhancements of $A^d_{\rm SL}$ and $A^s_{\rm SL}$ in these simple scenarios are similar to the ones achieved in Sec. 7.2, with values of $A^d_{\rm SL}$ at the 10^{-3} level, values of $A^s_{\rm SL}$ at the 10^{-4}

[12] We should point out, however, that such direct bounds typically assume patterns of decays, including dominance of decays into the third quark generation, that do not necessarily hold, and thus they are not absolute and could be evaded. In any case, we play safe setting $m_T = 1.6$ TeV.

level, and a small correlation. More precisely, we obtain

$$A^d_{\rm SL} = (-8.0 \pm 2.9) \times 10^{-4}\,, \tag{7.75}$$
$$A^s_{\rm SL} = (-0.08 \pm 0.97) \times 10^{-4}\,, \tag{7.76}$$
$$\rho(A^d_{\rm SL}, A^s_{\rm SL}) = -0.094\,, \tag{7.77}$$

in UVLQ models, and

$$A^d_{\rm SL} = (-10.3 \pm 2.9) \times 10^{-4}\,, \tag{7.78}$$
$$A^s_{\rm SL} = (-0.47 \pm 0.96) \times 10^{-4}\,, \tag{7.79}$$
$$\rho(A^d_{\rm SL}, A^s_{\rm SL}) = -0.101\,, \tag{7.80}$$

in DVLQ extensions. At a finer level of detail, one may notice that these regions, although similar, are both slightly smaller than in the NP 3×3 case, covering practically the same region in $A^s_{\rm SL}$ but a smaller one in $A^d_{\rm SL}$. In addition, there is a small shift of around $\sim 2\times10^{-4}$ in the central value of $A^d_{\rm SL}$ in the UVLQ case with respect to the DVLQ scenario.

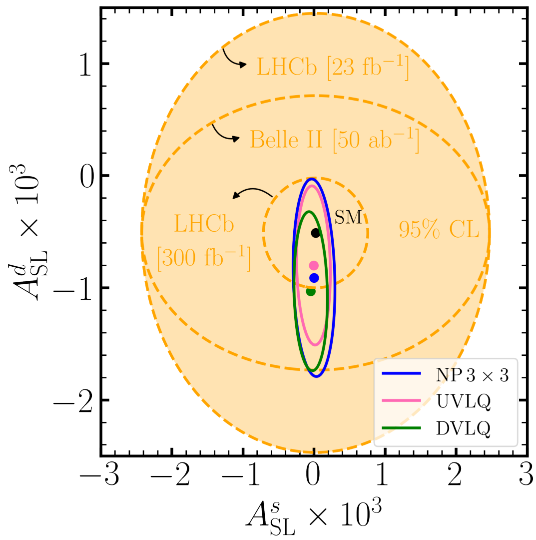

Figure 7.4: Allowed regions for $A^d_{\rm SL}$ and $A^s_{\rm SL}$ within vector-like quark singlet extensions. All contours are shown at 95% CL (2D-$\Delta\chi^2 = 5.99$), together with the corresponding best fit point. The pink and green contours correspond to UVLQ and DVLQ models, respectively. In blue, we further include the result of our previous analysis with heavy NP affecting M^q_{12} for comparison. All results are obtained including the penguin pollution as discussed in Sec. 7.2.

7.4 Enhancements of $A^q_{\rm SL}$ in detail

Once we have analyzed the enhancements of $A^d_{\rm SL}$ and $A^s_{\rm SL}$ that can be obtained with heavy NP solely affecting M^q_{12}, as well as in vector-like quark extensions triggering deviations of CKM unitarity, it is interesting to understand how these enhancements are actually achieved. While the physically meaningful, rephasing-invariant observables are the semileptonic asymmetries themselves, our goal is to determine whether their potential enhancement originates from modifications to M_{12}^q, Γ_{12}^q, or both. At first glance, such an analysis might appear somewhat meaningless, as the moduli of these quantities are rephasing-invariant, but not their arguments. However, the following discussion should be understood as an exploration of how much variation is permitted within the parametric freedom available in each scenario. Although this exercise is, strictly speaking, carried out within a fixed phase convention, it may still offer useful insights into the mechanisms driving the main results. Our strategy is the following.

We first perform a SM analysis using the same set of constraints applied in the previous studies. From this, we extract the best fit values of the CKM parameters, the lattice inputs $f_{B_d}^2 B_{B_d}$ and $f_{B_s}^2 B_{B_s}$, as well as the parameters c_q, a_q, b_q, that enter the expression for Γ_{12}^q.[13] Using these inputs, we compute reference SM values of the mixing amplitudes, denoted as $\Gamma_{12}^{q,\mathrm{SM}_0}$ and M_{12}^{q,SM_0}. Then, we consider the ratios $\Gamma_{12}^q/\Gamma_{12}^{q,\mathrm{SM}_0}$ and $M_{12}^q/M_{12}^{q,\mathrm{SM}_0}$, with Γ_{12}^q and M_{12}^q in the corresponding BSM scenario, so that we can read out the room for variation that each scenario allows with respect to a SM reference value. For completeness, the same analysis is also done for the "SM itself". The relevant results are depicted in Fig. 7.5, where we have only included the results of DVLQ models in the context of vector-like quark scenarios since the results for the UVLQ case do not differ significantly.

Before going into details, let us first recall some basic implications of 3×3 CKM unitarity. In the bd sector, the unitarity triangle is defined by the relation $\lambda_{bd}^t + \lambda_{bd}^c + \lambda_{bd}^u = 0$, with all three sides of similar size $\mathcal{O}(\lambda^3)$, as shown in Fig. 1.1a. On the other hand, the unitarity triangle in the bs sector is determined by $\lambda_{bs}^t + \lambda_{bs}^c + \lambda_{bs}^u = 0$, where $\lambda_{bs}^t \sim \mathcal{O}(\lambda^2)$, $\lambda_{bs}^c \sim \mathcal{O}(\lambda^2)$ and $\lambda_{bs}^u \sim \mathcal{O}(\lambda^4)$, that is, the triangle is squashed, as one can check in Fig. 1.1b. In terms of the room for variation allowed by tree-level dominated data (moduli of the first two rows in the CKM and the angle γ), the bd triangle allows for larger absolute deformations (in particular the $\mathcal{O}(1)$ relative phase between λ_{bd}^t and λ_{bd}^c, that is, β) than the bs triangle can allow for (in particular the $\mathcal{O}(\lambda^2)$ relative phase between λ_{bs}^t and λ_{bs}^c, that is, β_s).

We have

$$\frac{\Gamma_{12}^q}{\Gamma_{12}^{q,\mathrm{SM}_0}} = -\frac{\Gamma_{12}^{q,uc}(\lambda_{bq}^c + \lambda_{bq}^u)^2 + (\Gamma_{12}^{q,cc} - \Gamma_{12}^{q,uc})(\lambda_{bq}^c)^2 + (\Gamma_{12}^{q,uu} - \Gamma_{12}^{q,uc})(\lambda_{bq}^u)^2}{\Gamma_{12}^{q,\mathrm{SM}_0}}\,, \tag{7.81}$$

with $\Gamma_{12}^{q,cc} \simeq \Gamma_{12}^{q,uc} \simeq \Gamma_{12}^{q,uu}$, as mentioned in Sec. 7.1, in such a way that the first term gives the leading contribution in both B_d and B_s systems. When 3×3 CKM unitarity holds, this can be readily identified as $\Gamma_{12}^{q,uc}(\lambda_{bq}^t)^2$. The point is that its phase, within the parametric freedom allowed by the CKM, has $\mathcal{O}(1)$ room for variation in the B_d system while only $\mathcal{O}(\lambda^2)$ room for variation in the B_s system. At the level of the semileptonic asymmetries, this variation is matched by a dominant contribution to M_{12}^q that is proportional to $(\lambda_{bq}^t)^2$, leading to the expected SM regions shown in Fig. 7.5.

B_d system

The results for the B_d system are presented in Figs. 7.5a and 7.5b. The span of the SM region, essentially due to the uncertainties in the experimental constraints, is below the ± 0.1 level in both $\arg(\Gamma_{12}^d/\Gamma_{12}^{d,\mathrm{SM}_0})$ and $\arg(M_{12}^d/M_{12}^{d,\mathrm{SM}_0})$. Most importantly, that region is aligned with the diagonal $\arg(\Gamma_{12}^d/\Gamma_{12}^{d,\mathrm{SM}_0}) = \arg(M_{12}^d/M_{12}^{d,\mathrm{SM}_0})$, further illustrating the reduced range of variation of A_{SL}^d within the SM. Beyond the SM, it is interesting to notice that the allowed regions in the NP 3×3 case displayed in Fig. 7.5a,

[13] Regarding the parameters c_q, a_q, and b_q, since the SM fit is insensitive to them—in the considered ranges, their profile likelihoods are simply flat—, there is no reason for consider their best fit values, and hence we choose to take the central values in Eqs. (7.35) to (7.37). In any case, the following results would be essentially unchanged if we had used best fit values instead.

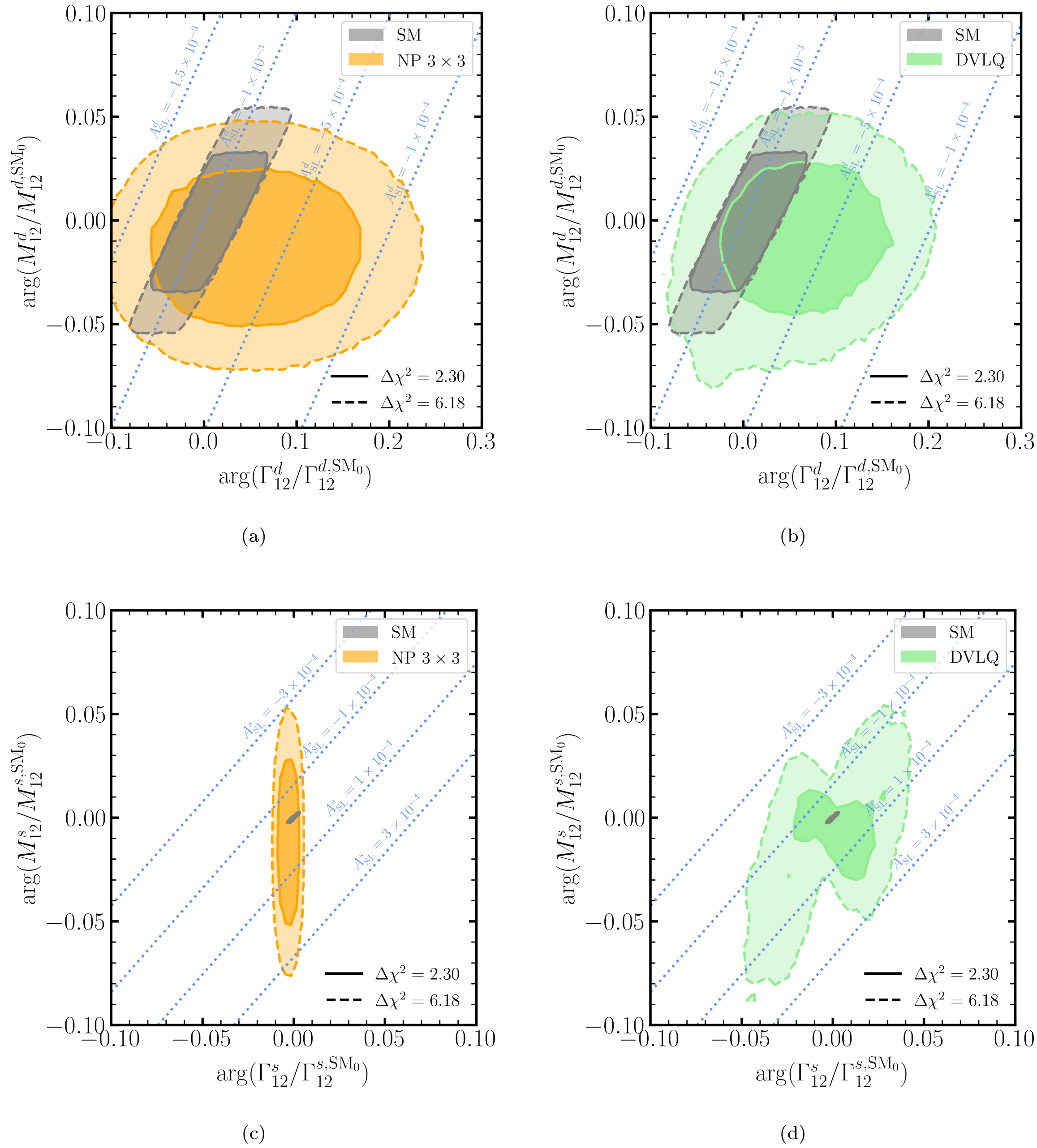

Figure 7.5: Allowed regions in the $\arg(M_{12}^q/M_{12}^{q,\rm SM_0})$ vs. $\arg(\Gamma_{12}^q/\Gamma_{12}^{q,\rm SM_0})$ plane regarding the analyses of Secs. 7.2 and 7.3: (a) B_d system, NP 3×3 scenario, (b) B_d system, DVLQ scenario, (c) B_s system, NP 3×3 scenario, (d) B_s system, DVLQ scenario. The SM region, as discussed in the text, is depicted in gray. Dashed isocontours of the semileptonic asymmetries are included for reference: they are represented assuming $|M_{12}^q/M_{12}^{q,\rm SM_0}| = |\Gamma_{12}^q/\Gamma_{12}^{q,\rm SM_0}| = 1$. Note the change of scale in the horizontal axis from the upper panels to the lower ones.

and in the DVLQ case in Fig. 7.5b, are rather similar: $\arg(M_{12}^d/M_{12}^{d,\text{SM}_0})$ essentially spans the same range as in the SM, while $\arg(\Gamma_{12}^d/\Gamma_{12}^{d,\text{SM}_0})$ covers a much wider range. This is somehow unexpected. Fig. 7.5a suggests that, in the NP 3×3 case, the freedom introduced by the new parameter ϕ_d^Δ in M_{12}^d does not enlarge the room for variation of $\arg(M_{12}^d)$ itself, but instead it allows for a sizable variation of $\arg(\Gamma_{12}^d)$, triggering the enhancement of A_{SL}^d. The reason is that $\arg(\Gamma_{12}^d/\Gamma_{12}^{d,\text{SM}_0})$ varies as much as tree-level CKM data allows for, while the freedom in ϕ_d^Δ is used to put "in place" $\arg(M_{12}^d)$ in order to satisfy the $B_d \to J/\Psi K_S$ CP asymmetry constraint, which is quite restrictive. On the other hand, observing Fig. 7.5b, it seems that a similar argument applies for the enhancement of A_{SL}^d in the DVLQ (and UVLQ) scenario, with the role of ϕ_d^Δ played by the new contributions to M_{12}^d.

B_s system

Turning to the B_s system, the SM allowed region displayed in Figs. 7.5c and 7.5d looks tiny, in line with the expectations discussed before. Beyond the SM, the situation differs significantly from that of the B_d system, and is not similar in the NP 3×3 case and the VLQ models.

On the one hand, within the NP 3×3 scenario, although there is some room for variation in $\arg(\Gamma_{12}^s/\Gamma_{12}^{s,\text{SM}_0})$ at the 10^{-2} level, the key feature is the larger freedom in $\arg(M_{12}^s/M_{12}^{s,\text{SM}_0})$. In contrast to the B_d system, the constraint from the CP asymmetry in $B_s \to J/\Psi\Phi$ is much weaker, allowing the phase ϕ_s^Δ to induce variations in $\arg(M_{12}^s/M_{12}^{s,\text{SM}_0})$ at the ± 0.05 level.

In the DVLQ scenario presented in Fig. 7.5d, apart from the effect on $\arg(M_{12}^s/M_{12}^{s,\text{SM}_0})$, we also observe sizable deviations in $\arg(\Gamma_{12}^s/\Gamma_{12}^{s,\text{SM}_0})$ of comparable magnitude. However, the allowed region does not exhibit a simple elliptical shape, suggesting a more intricate behavior: deviations from 3×3 CKM unitarity not only introduce new contributions to M_{12}^s, but also misalign Γ_{12}^s with respect to the SM. What becomes clear is that deviations in M_{12}^s, in Γ_{12}^s, or both, are possible and can contribute to an enhancement of A_{SL}^s.

As a final comment, regarding the moduli $|M_{12}^q/M_{12}^{q,\text{SM}_0}|$ and $|\Gamma_{12}^q/\Gamma_{12}^{q,\text{SM}_0}|$, we obtain

$$\begin{aligned}
|M_{12}^d/M_{12}^{d,\text{SM}_0}| &= 1.00 \pm 0.01\,,\\
|\Gamma_{12}^d/\Gamma_{12}^{d,\text{SM}_0}| &= 1.00 \pm 0.15\,,\\
|M_{12}^s/M_{12}^{s,\text{SM}_0}| &= 1.000 \pm 0.001\,,\\
|\Gamma_{12}^s/\Gamma_{12}^{s,\text{SM}_0}| &= 1.00 \pm 0.08\,.
\end{aligned} \tag{7.82}$$

For $|M_{12}^q/M_{12}^{q,\text{SM}_0}|$, the results align with expectations based on the measured values of ΔM_q. In contrast, $|\Gamma_{12}^q/\Gamma_{12}^{q,\text{SM}_0}|$ exhibits a larger degree of variation $\mathcal{O}(10\%)$. Nevertheless, such variation alone can only induce a corresponding $\mathcal{O}(10\%)$ change in A_{SL}^d and A_{SL}^s with respect to their SM predictions. This underscores that the potential for sizable enhancements of the semileptonic asymmetries lies primarily in the arguments of M_{12}^q and Γ_{12}^q, rather than in their moduli.

7.5 A_{SL}^q with modifications to Γ_{12}^q

Finally, we explore scenarios which could also generate new contributions to Γ_{12}^q, focusing on its impact on A_{SL}^q. This idea was explored before in a range of models after the anomalously large asymmetries reported by D0 more than a decade ago—see [199–201] for the measurements, and [172, 182–185] for several phenomenological studies.

In general, we should remark that any time we write a diagram that mediates neutral B meson mixing, we always get a contribution to M^q_{12} (*off-shell*) and, in principle, also to Γ^q_{12} (*on-shell*), although the latter is not always guaranteed. That is, one cannot modify Γ^q_{12} without affecting M^q_{12}. We also know that the new contributions to M^q_{12} are strongly constrained by the measurements of the meson mass differences, and thus small deviations with respect to its SM value are expected. This, in turn, has an impact on the potential size of the new contributions to Γ^q_{12}. Furthermore, the existence of LHC bounds on colorful mediators generically impose $\Lambda_{\rm NP} \gtrsim 1$ TeV. Therefore, *a priori* this is not the most favorable scenario for our ultimate purpose of enhancing the values of the semileptonic asymmetries, since the ratio Γ^q_{12}/M^q_{12} typically scales as $\Gamma^q_{12}/M^q_{12} \sim m_b^2/m^2_{\rm virtual}$, which would require rather light NP. Although this is a very general argument that might be surpassed in more tuned BSM scenarios, it anticipates that the present task is, at least, very challenging from the point of view of model building.

To address this question we opt for two avenues. First, we review existing studies in the literature that explore various possible common final states for the B_q and $\bar{B}_q$ mesons, thus with the potential to modify Γ^q_{12}. Second, we explicitly calculate how large the semileptonic asymmetries can be within the minimal realization of the B-mesogenesis paradigm, which contains a color-triplet scalar mediating $B_q - \bar{B}_q$ mixing and, in particular, modifying Γ^q_{12}.

7.5.1 Possible decay channels contributing to Γ^q_{12}

It has been known for a while that there are not many possible channels that can accommodate substantial modifications to Γ^q_{12}. The viable options as of 2010 were [172]: (i) $b \to u_i \bar{u}_j q$ decays ($u_i = u, c$), (ii) $b \to \tau\bar{\tau}s$ decays, and (iii) decays including invisible particles in the final state. Overall, they were viable because for case (i) substantial BSM effects could hide within large hadronic uncertainties, and modes (ii) and (iii) involve particles that are hard to detect so that large branching fractions could still be allowed. The current status for each case is different, and here we provide a summary and reinterpretation of recent works for options (i) and (ii). In next section, we will provide specific examples for cases (i) and (iii) within the B-mesogenesis framework.

Modifying Γ^q_{12} with $b \to u_i \bar{u}_j q$ decays at the EFT level

Recent global analyses of effective operators that can modify $b \to u_i \bar{u}_j q$ decays include [247, 264–267]. In full generality, 20 combinations of $\Delta B = 1$ operators $(\bar{u}_i \Gamma b)(\bar{u}_j \Gamma q)$ can be constructed with the quarks in different color and Lorentz structures encoded in Γ. Out of those, most of them cannot lead to significant contributions to Γ^q_{12} because, rather generically, they also substantially contribute radiatively to rare processes in the SM, such as $b \to q\gamma$ and $b \to q\ell\ell$ decays—see, *e.g.*, [264] for their relationship, and [268–270] for recent global analyses of these modes. On the one hand, among the different operators investigated in [264–266], color-rearranged structures of the form $Q_1^{d,cc} = (\bar{c}_\beta \gamma^\mu P_L b_\alpha)(\bar{d}_\alpha \gamma_\mu P_L c_\beta)$, being α, β color indices, can generate an effect that saturates the current experimental limit on $A^d_{\rm SL}$, namely, $|A^d_{\rm SL}| \lesssim 2 \times 10^{-3}$. On the other hand, Γ^s_{12} is strongly dominated by $b \to c\bar{c}s$ decays, but in this scenario operators of the type $Q_1^{s,cc}$ are severely constrained by $b \to s\gamma$, while color-singlet operators of the type $Q_2^{s,cc} = (\bar{c}_\alpha \gamma^\mu P_L b_\alpha)(\bar{s}_\beta \gamma_\mu P_L c_\beta)$ can also reach values of $|A^s_{\rm SL}| \lesssim 2 \times 10^{-3}$.

Modifying Γ_{12}^q with $b \to \tau\bar{\tau}s$ decays at the EFT level

The recent global analysis in [271] addressed the current status of all possible effective operators that can significantly contribute to Γ_{12}^s through $b \to \tau\bar{\tau}s$ decays—see also [175]. Although in [271] the authors restricted themselves to real Wilson coefficients, their results can be extended to show that in the presence of complex Wilson coefficients one could have $|A_{\rm SL}^s| \lesssim 10^{-3}$, again a rather large number.[14]

Modifying Γ_{12}^q within UV complete models

The previous studies worked in terms of effective $\Delta B = 1$ operators involving light states (below the m_b scale), whose Wilson coefficients are appropriately constrained by all relevant observables, including, in particular, the meson mass differences ΔM_q that are generated through $\Delta B = 2$ transitions. As discussed in the introduction of this section, it is crucial to check that contributions to ΔM_q controlled by heavier states do not spoil the agreement between the experimental measurement and the SM. To understand this observation, it is illustrative to think, for instance, in the SM case: as $\Delta M_q^{\rm SM}$ is top-dominated, in an effective theory such as those proposed in the previous studies this contribution would be missed. Therefore, we include in this section a review of some UV completions capable of generating the aforementioned $\Delta B = 1$ operators in order to check the actual enhancement of $A_{\rm SL}^q$ one is able to achieve.

Recent examples of UV models featuring $\Delta B = 1$ operators include Ref. [273] for type (i) operators, and Ref. [274] for operators of the type (ii). Taking the parameter space in [273] at face value, the authors report that $A_{\rm SL}^s$ could be as large as $A_{\rm SL}^s = -4 \times 10^{-5}$, and hence only a factor of two larger than the SM prediction in Eq. (7.41), and roughly 50 times smaller than what appears to be allowed when considering only $\Delta B = 1$ operators. Regarding type (ii) operators, the UV complete model that realizes potentially large $b \to \tau\bar{\tau}s$ transitions in [274] would allow for contributions $A_{\rm SL}^s \lesssim 10^{-5}$, again a rather small number and comparable to the effects one can find by solely modifying the phase of M_{12}^q.

Therefore, although this does not constitute an exhaustive list of UV completions, it generically highlights that, indeed, in UV theories that could potentially induce modifications to Γ_{12}^q it is not easy to find large values of the CP asymmetries. The reasons are rather simple: (i) the contribution of Γ_{12}^q appears from tree-level decays and mediators of these interactions are generically constrained to have $M \gtrsim 1$ TeV from LHC searches, leading to very suppressed contributions to Γ_{12}^q, and (ii) new contributions to M_{12}^q must survive the stringent constraints placed by the meson mass differences.

To complete this section, in what follows, we consider the minimal scenario capable of triggering B-mesogenesis in order to check whether it can lead to substantially large CP asymmetries. This is motivated because it can contribute both to $\Delta B = 2$ transitions as well as to $\Delta B = 1$ operators of the type (i) $b \to u_i \bar{u}_j q$, and those of the type (iii) involving a new invisible particle.

7.5.2 Minimal B-mesogenesis contributions to Γ_{12}^q

Before going into the details of our analyses, let us provide a brief overview of how the B-mesogenesis mechanism [161, 163] operates. We start with a massive scalar particle that decays, out of thermal equilibrium, into $b\bar{b}$ pairs, late enough so that the Universe is cool enough for b quarks to hadronize.

[14] Notice that the case of $b \to \tau\bar{\tau}d$ is significantly more constrained than that of $b \to \tau\bar{\tau}s$ because ${\rm Br}(B_d \to \tau\bar{\tau}) < 2.3 \times 10^{-3}$ while ${\rm Br}(B_s \to \tau\bar{\tau}) < 6.8 \times 10^{-3}$ at 90% CL [272]. Thus, there appears to be more room for $b \to \tau\bar{\tau}s$ transitions as compared to $b \to \tau\bar{\tau}d$ ones, although a dedicated study is not currently available in the literature.

Then, as we already know, neutral B mesons exhibit CP-violating oscillations. Finally, in order to violate baryon number, the authors proposed a new decay mode of B mesons into a dark sector antibaryon ψ, a visible baryon, and any number of light mesons. The key point is that dark matter is charged under baryon number, so that the total baryon number of the Universe is conserved, and the last Sakharov condition is relaxed into an apparent violation of baryon number in the visible sector. Therefore, if $\bar{B}_q$ mesons are more likely to oscillate into B_q mesons, which implies a *positive* semileptonic asymmetry, we will get an excess of baryons in the visible sector that is exactly compensated by an excess of antibaryons in the dark sector. As previously mentioned, within this framework, the primordial baryon asymmetry is related to collider observables, namely, the branching ratio of the new B meson decay mode, as well as the semileptonic asymmetries. More precisely, in order to have successful baryogenesis we need: (i) at least one of the asymmetries to be positive, and (ii) given the existing upper bounds on the new branching ratio, they have to be larger than 10^{-4}, *i.e.*, roughly an order of magnitude larger than the SM prediction.

The minimal realization of this mechanism [161, 163] involves a scalar boson Y, transforming as $Y \sim (\mathbf{3}, \mathbf{1}, -1/3)$ under the SM gauge group and triggering the novel decay mode of B mesons, as well as a Dirac dark sector antibaryon ψ.[15] The most general renormalizable interaction Lagrangian reads

$$-\mathscr{L}_{-1/3} = \sum_{i,j=1}^{3} y_{u_i d_j} Y^* \bar{u}_{iR} d^c_{jR} + \sum_{k=1}^{3} y_{\psi d_k} Y d^c_{kR} \bar{\psi} + \text{H.c.}\,, \tag{7.83}$$

where $y_{u_i d_j}$ and $y_{\psi d_k}$ represent (complex) coupling constants, and $f^c = C\bar{f}^T$, as usual.[16] It is to be stressed that, while Y features a coupling to two quarks, once we impose baryon number conservation through $B(\psi) = -1$ and $B(Y) = -2/3$, proton decay is evaded by kinematics if $m_\psi > m_p - m_e$.

As already mentioned, the above interactions would generate new contributions to both Γ_{12}^q and M_{12}^q. On that regard, we can conveniently write

$$A_{\rm SL}^q = \text{Im}\left(\frac{\Gamma_{12}^{q,\rm SM} + \Gamma_{12}^{q,\rm NP}}{M_{12}^{q,\rm SM} + M_{12}^{q,\rm NP}}\right) \simeq \text{Im}\left(\frac{\Gamma_{12}^{q,\rm SM}}{M_{12}^{q,\rm SM} + M_{12}^{q,\rm NP}}\right) + \text{Im}\left(\frac{\Gamma_{12}^{q,\rm NP}}{M_{12}^{q,\rm SM}}\right)\,, \tag{7.84}$$

where in the last step we have neglected the contribution $M_{12}^{q,\rm NP}$ in the second term as it can be at most 10% of the SM. One should notice that the first term is precisely the one that we have explored in a model-independent way in Sec. 7.2. We can further split the purely NP contributions as

$$\Gamma_{12}^{q,\rm NP} = \Gamma_{12}^{q,\rm NP}(\psi) + \Gamma_{12}^{q,\rm NP}(\not\psi)\,, \qquad M_{12}^{q,\rm NP} = M_{12}^{q,\rm NP}(\psi) + M_{12}^{q,\rm NP}(\not\psi)\,, \tag{7.85}$$

depending on whether they involve the ψ mediation or not. In the following, we will focus on quantifying the contributions to the semileptonic asymmetries generated by $\Gamma_{12}^{q,\rm NP}$.

Modifying Γ_{12}^q with semi-invisible $b \to \psi\bar{\psi}q$ decays

The ψ fermion and Y boson mediate the transition amplitudes shown in Fig. 7.6. They contribute to M_{12}^q, but also to Γ_{12}^q via $b \to \psi\bar{\psi}q$ decays provided that $m_\psi < m_b/2 + m_q$. In this kinematical regime,

[15] Not to be confused with the J/Ψ hadronic resonance.

[16] We should point out that there exists an alternative version of the model where the scalar boson Y has hypercharge 2/3. Nevertheless, we expect even smaller contributions to Γ_{12}^q in that scenario—see [163] for a phenomenological study.

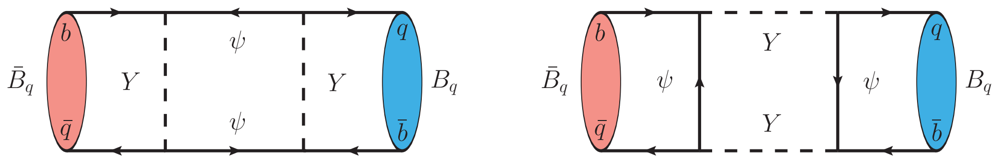

Figure 7.6: Box diagrams triggering $B_q-\bar{B}_q$ mixing from ψ–Y mediation.

and considering $m_q = 0$, direct computation leads to

$$\Gamma_{12}^{q,\rm NP}(\psi) = -\frac{f_{B_q}^2 M_{B_q}}{256\pi}\frac{(y_{\psi q}y_{\psi b}^*)^2 m_b^2}{M_Y^4}\left(1-\frac{2}{3}\frac{m_\psi^2}{m_b^2}\right)\sqrt{1-4\frac{m_\psi^2}{m_b^2}}\,, \tag{7.86}$$

and

$$M_{12}^{q,\rm NP}(\psi) = \frac{f_{B_q}^2 M_{B_q}}{384\pi^2}\frac{(y_{\psi q}y_{\psi b}^*)^2}{M_Y^2}G(x_{\psi Y})\,, \tag{7.87}$$

with $x_{\psi Y} = m_\psi^2/M_Y^2$, and

$$G(x) = \frac{1+x}{(1-x)^2} + \frac{2x\ln x}{(1-x)^3}\,. \tag{7.88}$$

For the relevant range of parameters, $G \sim 1$. Furthermore, it is to be mentioned that we are working in the vacuum insertion approximation (VIA), *i.e.*, $B_{B_q} = 1$.

From our previous analyses, we know that any NP contribution to M_{12}^q is bounded to be at most $\sim 10\%$ of the SM one, as we can check from Eqs. (7.66) and (7.67). Taking into account the result quoted in Eq. (7.87), one can derive the following upper bounds on the products of $y_{\psi d_k}$ couplings:

$$|y_{\psi d}y_{\psi b}^*| \lesssim 0.01 \times \frac{M_Y}{500\ \text{GeV}}\,, \qquad |y_{\psi s}y_{\psi b}^*| \lesssim 0.05 \times \frac{M_Y}{500\ \text{GeV}}\,, \tag{7.89}$$

which have been normalized considering that $M_Y > 500$ GeV is the most conservative limit from direct LHC searches on pair-produced Y resonances [275–278].[17] In light of these constraints, the NP contribution from the last term in Eq. (7.84), involving ψ exchange and considering the most favorable scenario where $\arg\left(\Gamma_{12}^{q,\rm NP}/M_{12}^{q,\rm SM}\right) = \pm\pi/2$, is bounded to be

$$|A_{\rm SL}^{q,\rm NP}(\psi)| \lesssim 4\times 10^{-5}\left(\frac{500\ \text{GeV}}{M_Y}\right)^2\,. \tag{7.90}$$

These contributions to the semileptonic asymmetries are smaller than the ones coming from $M_{12}^{q,\rm NP}$ in Eq. (7.84), as one can check from Eqs. (7.60) and (7.61).

Modifying Γ_{12}^q with $b \to u_i\bar{u}_j q$ decays

The scalar boson Y can also mediate a transition amplitude introducing the quark-quark coupling in Eq. (7.83) through the box diagrams depicted in Fig. 7.7. Working in the VIA by setting $B_{B_q} = 1$, these

[17] More restrictive LHC bounds on M_Y may apply from single resonant production and decays into jets plus missing energy. We refer to [163] for a detailed assessment of these bounds.

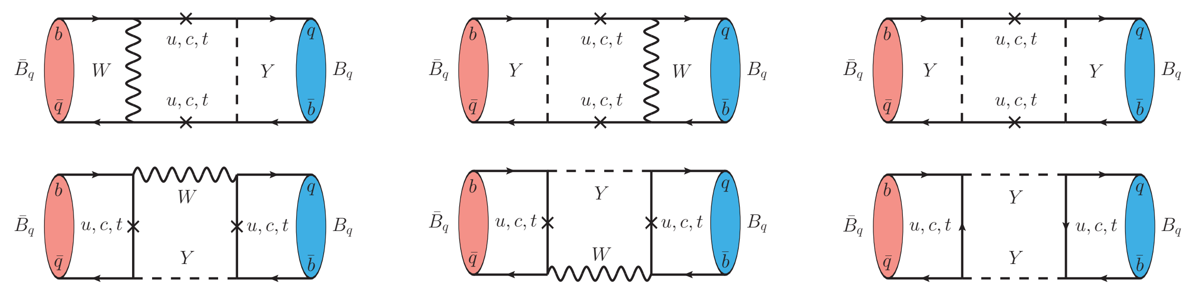

Figure 7.7: Box diagrams triggering $B_q - \bar{B}_q$ mixing from u_i–Y/W mediation.

generate

$$\Gamma_{12}^{q,\rm NP}(\not{y}) = \frac{f_{B_q}^2 M_{B_q}}{384\pi^2} \sum_{i,j=u,c} \frac{\pi\sqrt{\lambda(m_b^2, m_i^2, m_j^2)}}{m_b^2}$$
$$\times \left[(y_{iq} y_{jb}^* V_{ib} V_{jq}^*) \frac{m_i m_j}{M_W^2 M_Y^2} 8g^2 - (y_{iq} y_{jb}^* y_{jq} y_{ib}^*) \frac{m_b^2}{12 M_Y^4} (8H_1^{ij} + 5H_2^{ij}) \right], \tag{7.91}$$

and

$$M_{12}^{q,\rm NP}(\not{y}) = -\frac{f_{B_q}^2 M_{B_q}}{384\pi^2} \sum_{i,j=u,c,t} \left[(y_{iq} y_{jb}^* V_{ib} V_{jq}^*) \frac{m_i m_j}{M_W^2 M_Y^2} g^2 J_1^{ij} - (y_{iq} y_{jb}^* y_{jq} y_{ib}^*) \frac{1}{M_Y^2} J_2^{ij} \right],$$

where $\lambda(x, y, z) = x^2 + y^2 + z^2 - 2xy - 2xz - 2xy$ is the Källen function, and

$$H_1^{ij} = \frac{\lambda(m_b^2, m_i^2, m_j^2)}{m_b^4}, \tag{7.92}$$

$$H_2^{ij} = \frac{2\left[m_b^4 + m_b^2(m_i^2 + m_j^2) + 4m_i^2 m_j^2 - 2(m_i^4 + m_j^4)\right]}{m_b^4}, \tag{7.93}$$

$$J_1^{ij} = \frac{x_{iW}(x_{iW} - 4)\ln x_{iY}}{(x_{iW} - 1)(x_{iY} - 1)(x_{iW} - x_{jW})} + \frac{x_{jW}(x_{jW} - 4)\ln x_{jY}}{(x_{jW} - 1)(x_{jY} - 1)(x_{jW} - x_{iW})}$$
$$- \frac{3\ln x_{WY}}{(x_{iW} - 1)(x_{jW} - 1)(x_{WY} - 1)}, \tag{7.94}$$

$$J_2^{ij} = \frac{1}{(x_{iY} - 1)(x_{jY} - 1)} + \frac{x_{iY}^2 \ln x_{iY}}{(x_{iY} - x_{jY})(x_{iY} - 1)^2} + \frac{x_{jY}^2 \ln x_{jY}}{(x_{jY} - x_{iY})(x_{jY} - 1)^2}, \tag{7.95}$$

with the usual definition $x_{\alpha\beta} = m_\alpha^2/m_\beta^2$. On the one hand, the functions H_1^{ij} and H_2^{ij} are of $\mathcal{O}(1)$:

$$H_1^{uu} \simeq 1, \qquad H_1^{cc} \simeq -0.6, \qquad H_1^{uc} = H_1^{cu} \simeq -0.8, \tag{7.96}$$

$$H_2^{uu} \simeq 2, \qquad H_2^{cc} \simeq 2.41, \qquad H_2^{uc} = H_2^{cu} \simeq 2.16. \tag{7.97}$$

On the other hand, the functions J_1^{ij} and J_2^{ij} are numerically of $\mathcal{O}(1-10)$. A rough approximation for the latter reads

$$J_1^{ii} \simeq \begin{cases} -6\ln\left(\frac{m_i}{M_Y}\right), & i \neq t \\ -2\ln\left(\frac{m_t}{M_Y}\right), & i = t \end{cases}, \qquad J_1^{ij}(i \neq j) \simeq \frac{2}{3}\ln\left(\frac{m_i}{M_Y}\right)\ln\left(\frac{m_j}{M_Y}\right), \qquad J_2^{ij} \simeq -1. \tag{7.98}$$

Our results coincide with those computed in [163, 279] within the same framework.

From Eq. (7.91), one can check that Γ_{12}^q will be dominated by the $b \to c\bar{c}q$ channel. In contrast, if one reasonably assumes that $y_{iq} \lesssim \mathcal{O}(10^{-1})$, then M_{12}^q will be top-dominated. Consequently, the ratio Γ_{12}^q/M_{12}^q will be highly suppressed, as will the semileptonic asymmetries. In order to maximize the size of $A_{\rm SL}^q$, let us consider a more favorable (and tuned) scenario where only the $b \to c\bar{c}q$ channel contributes both to M_{12}^q and Γ_{12}^q. In that case, the dominant contribution to $M_{12}^{q,\rm NP}$ arises from the second term in Eq. (7.92). Requiring again that $|M_{12}^{q,\rm NP}|$ does not exceed more than 10% of the SM one—see Eqs. (7.66) and (7.67)—, we find

$$|y_{cd}y_{cb}^*| \lesssim 0.01 \times \frac{M_Y}{500\ \text{GeV}}\,, \qquad |y_{cs}y_{cb}^*| \lesssim 0.05 \times \frac{M_Y}{500\ \text{GeV}}\,. \tag{7.99}$$

Similarly to what has been done before, noting that at least $M_Y > 500$ GeV from LHC searches, and taking $\arg\left(\Gamma_{12}^{q,\rm NP}/M_{12}^{q,\rm SM}\right) = \pm\pi/2$ to maximize the imaginary part of the ratio, we obtain

$$|A_{\rm SL}^{q,\rm NP}(\not{y})| \lesssim 10^{-4}\,. \tag{7.100}$$

This means that even in the best case scenario where only the $c\bar{c}$ channel dominates both Γ_{12}^q and M_{12}^q, the new contributions to $A_{\rm SL}^q$ generated by the $\Gamma_{12}^{q,\rm NP}$ are small. This results from the strong bounds placed by the ΔM_q constraint on the new contributions to M_{12}^q—see Eq. (7.99)—, and from LHC constraints on the mass of the new color-triplet scalar mediator—at least, $M_Y > 500$ GeV. For completeness, we have checked that using $b \to u\bar{c}q$, $b \to c\bar{u}q$, and $b \to u\bar{u}q$ decays leads to even smaller asymmetries than the ones quoted in Eq. (7.100).

Therefore, we conclude that, in the absence of fine-tuning, the maximum values of the semileptonic asymmetries within the minimal realization of the B-mesogenesis mechanism are mainly dominated by the $\sim 1^\circ$ phase that the color-triplet scalar boson could induce to M_{12}^q, and not by the novel contributions to Γ_{12}^q. This means that the same limits we found in Sec. 7.2 for generic heavy NP scenarios that only modify the phase and magnitude of M_{12}^q still apply, *i.e.*, the semileptonic asymmetries cannot be larger than those in Eqs. (7.60) and (7.61). An exception to this conclusion may arise in the following case: there are large contributions to Γ_{12}^q from a given channel, say $b \to c\bar{c}q$, but the contributions from this channel to M_{12}^q are compensated by those from a different channel with opposite sign, say from the top. Then, ΔM_q would still be in agreement with the SM prediction. While this is in principle possible, it is finely tuned as it requires very specific phases and hierarchies of coupling constants. The lesson we learn is thus clear: it is in general very difficult to generate large semileptonic asymmetries BSM, meaning that, if a non-standard value of these observables were measured, it would point to a very specific pattern of NP.

In this context, let us finally comment on two additional options that have been invoked in the literature to enlarge the CP asymmetries with light new particles. Ref. [184] considered a new hidden pseudoscalar that mixes with B_q and $\bar{B}_q$. In order for the CP asymmetries to be enlarged this new state should have a mass $M \simeq M_{B_q}$ and very specific decay modes. Alternatively, Ref. [280] considered the contributions from a very light Z' with $M_{Z'} \lesssim M_{B_q}$. Significant enhancements of the CP asymmetries can be obtained by considering only bq couplings, but the necessary presence of other types of interactions are likely to strongly constrain this possibility—see [281].

7.6 Implications for B-mesogenesis and future searches

Having performed global analyses to explore the magnitude of the semileptonic CP asymmetries in neutral B meson mixing within (i) heavy NP scenarios modifying the mass mixing in Sec. 7.2, (ii) scenarios featuring vector-like quarks that lead to a non-unitary CKM in Sec. 7.3, and (iii) scenarios modifying decay width mixing Γ_{12}^q in Sec. 7.5, we are now in good position to compare our findings with the expected experimental sensitivity for these quantities from LHCb and Belle II in Eqs. (7.18) to (7.22), and with their minimum required value for a successful B-mesogenesis.

As anticipated before, in the B-mesogenesis framework [161–163] the amount of CP violation in neutral B meson mixing is directly proportional to the BAU. In particular, a minimal requirement is that [163][18]

$$A_{\rm SL}^q > +10^{-4}\,. \tag{7.101}$$

Importantly, at least one of the asymmetries must be positive because we live in a Universe dominated by matter. The prediction for the baryon asymmetry does depend upon the sign and magnitude of both $A_{\rm SL}^d$ and $A_{\rm SL}^s$ (as each meson system oscillates at a different rate and they are produced in different numbers in the early Universe), but also upon the branching ratio of the new decay mode of a B meson into a dark sector antibaryon, a visible baryon, and any number of light mesons, that is, ${\rm Br}(B \to \text{baryon}+\psi+\text{mesons})$. These two parameters are strongly correlated, with the latter constrained by direct searches at B factories [282–284] and from a recast of old searches at LEP [163]—see also [285–288] for refined theoretical predictions. While these bounds depend upon the ψ mass, a rather global conservative constraint is ${\rm Br} \lesssim 1\%$ for $m_\psi \sim 1$ GeV. For heavier ψ masses and depending on the particular flavor combination that dominates in Eq. (7.83), the bound can actually be more restrictive, namely, ${\rm Br} < (0.01-1)\%$. The smaller this branching ratio, the larger the CP asymmetries must be in magnitude to account for the observed BAU.

We depict the parameter space studied in [163] in Fig. 7.8. Here we illustrate the $A_{\rm SL}^d$–$A_{\rm SL}^s$ plane (in logarithmic scale), highlighting in red the region of the parameter space where B-mesogenesis generates the observed baryon asymmetry according to [163]. In addition, we show in orange the current experimental world averages, the projected sensitivities from LHCb and Belle II, and most importantly the allowed regions we have obtained for the scenario where M_{12}^q is modified by heavy NP. We exclusively include this case because, as we have checked in the previous sections, scenarios with a non-unitary CKM or UV complete models that could modify Γ_{12}^q cannot lead to larger CP asymmetries. In light of this, Fig. 7.8 allows us to state two of our key results.

(i) *New measurements of the semileptonic asymmetries at LHCb and Belle II are not expected to test the most generic NP scenarios.* All models that we have considered feature smaller asymmetries than their future sensitivity. This covers any BSM scenario that modifies mass mixing M_{12}^q, scenarios including vector-like quarks with a non-unitary CKM, and non-tuned UV complete models which can also contribute to decay width mixing Γ_{12}^q. The only scenarios that could generate large asymmetries are those that introduce substantial modifications to Γ_{12}^q while also requiring finely tuned contributions to M_{12}^q to evade the stringent constraints from ΔM_q.

(ii) *The small CP asymmetries that can be obtained BSM place the B-mesogenesis mechanism in theoretical tension.* As shown in red, the mechanism requires positive and rather large CP asymmetries

[18] See also footnote 1.

in order to explain the matter-antimatter asymmetry of the Universe. However, only the region with $A^s_{\rm SL} \simeq (1-5)\times 10^{-4}$ and $A^d_{\rm SL} \simeq A^{d,\rm SM}_{\rm SL}$ can be theoretically achieved from a generic contribution to M^q_{12}. In the rest of the parameter space, and in the absence of tuning, there is no BSM scenario explored in our study which can lead to the required CP asymmetries to trigger baryogenesis. We note that, while Br $< 1\%$ is a rather conservative constraint on the new decay mode $B \to$ baryon $+\,\psi\,+$ mesons, in many regions of the parameter space this bound is stronger, and thus the tension is even larger.

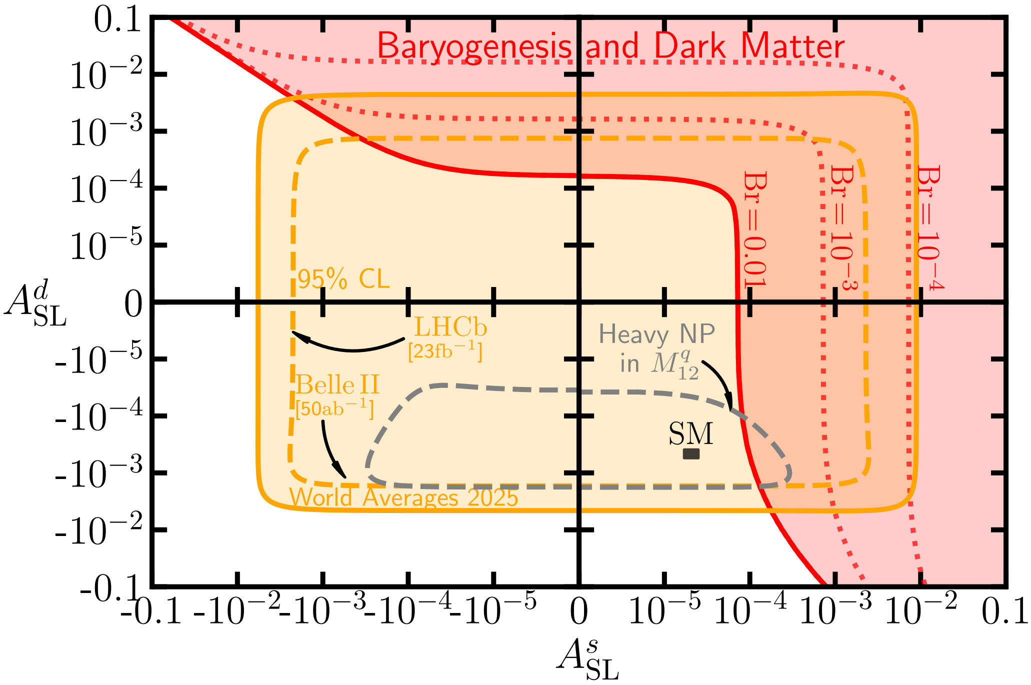

Figure 7.8: Semileptonic asymmetries for the B_d and B_s systems in logarithmic scale. In orange we show the experimentally allowed regions at 95% CL (2D-$\Delta\chi^2 = 5.99$) as of 2025—Eq. (7.17)—, and in dashed orange the expected sensitivity from LHCb—Eqs. (7.18) and (7.20)—and Belle II—Eq. (7.22)—assuming that their measurements are centered at the SM prediction—Eqs. (7.40) and (7.41). In red we highlight the region of the parameter space identified in [163] in which the baryon asymmetry can be explained through the B-mesogenesis mechanism [161–163]. The dashed red lines correspond to isocontours of Br($B \to$ baryon $+\,\psi\,+$ mesons). Only the region of parameter space with Br < 0.01 is shown since larger branching ratios are conservatively excluded: depending upon other parameters, the constraints can reach up to Br $< 10^{-4}$. The dashed gray line is one of the main results of our study and highlights the values of the semileptonic asymmetries that heavy NP models contributing to M^q_{12} can generate according to Eqs. (7.60) and (7.61). We see that the overlap between the red and the gray dashed regions is small, which implies that the B-mesogenesis mechanism is in tension, as it would require that B mesons posses an inclusive $\mathcal{O}(1\%)$ branching ratio into a baryon, any number of light mesons, and missing energy. As discussed in Sec. 7.5, we finally note that semileptonic asymmetries larger than those contained in the gray contour might be obtained in tuned scenarios where Γ^q_{12} is modified.

7.7 Summary

In this chapter, we have addressed in detail how large CP violation in neutral B meson mixing could be beyond the SM. This is motivated by the intimate link with baryogenesis in the B-mesogenesis framework, for which the SM prediction falls short by roughly an order magnitude, as well as the important constraints that the B factories and the LHC have placed over the B_d and B_s mixing parameters.

To this aim, we have first considered in Sec. 7.2 a very general scenario where heavy NP solely affects the mass mixing M_{12}^q. In particular, we have followed a model-independent approach allowing the modulus and phase of M_{12}^d and M_{12}^s to vary. Our global analysis of these quantities and the CKM mixing matrix including all relevant flavor data, specially the constraints from the meson mass differences and mixing-induced CP-violating phases, produce 68% CL results for the semileptonic asymmetries given by

$$A_{\rm SL}^d|_{\rm w/\,peng} = (-9.1 \pm 3.6) \times 10^{-4}\,, \tag{7.102}$$

$$A_{\rm SL}^s|_{\rm w/\,peng} = (-0.04 \pm 1.21) \times 10^{-4}\,, \tag{7.103}$$

$$\rho(A_{\rm SL}^d, A_{\rm SL}^s)|_{\rm w/\,peng} = -0.113\,. \tag{7.104}$$

Effectively, these results are driven in part by the $\sim 1^\circ$ precision measurements of mixing-induced CP violation constraining the phase of M_{12}^d and M_{12}^s, and partly from the allowed freedom in the CKM parameters.

In Sec. 7.3, we have studied the scenario in which the inclusion of one up-type or one down-type vector-like quark singlet leads to a non-unitary CKM matrix. This is motivated because one of the ingredients that suppresses CP violation in B meson mixing in the SM is precisely the unitarity of the CKM matrix. Our results from an enlarged global CKM fit show that these scenarios can produce similar CP asymmetries to the ones in Eq. (7.102), but not larger in magnitude. The main reasons why the CP asymmetries are not substantially larger stem from the fact that the allowed deviations of 3×3 CKM unitarity are small, and up-type vector-like quarks are constrained to be rather heavy by direct searches, thus unable to generate large effects on the relation between Γ_{12}^q and M_{12}^q.

Finally, in Sec. 7.5 we have explored scenarios that can also alter the decay width mixing Γ_{12}^q. While at first sight it appears that, in an EFT built out of $\Delta B = 1$ operators that contribute to Γ_{12}^q, the CP asymmetries could be large, the actual results in UV complete models show that the resulting contribution to the CP asymmetries from Γ_{12}^q ends up being significantly smaller than those in Eq. (7.102). Likewise, we have presented the first full calculation of the CP asymmetries within the minimal realization of B-mesogenesis in Sec. 7.5.2. The overall difficulty in obtaining large contributions to $A_{\rm SL}^q$ from Γ_{12}^q in a UV complete model is due to several reasons. First, one cannot ignore the new contributions to M_{12}^q, whose modulus should be within $\sim 10\%$ of the SM value and its phase within 1°, as required by the meson mass differences and the mixing-induced CP violation constraints, respectively. These have, in turn, an impact on the potential size of Γ_{12}^q. Second, the LHC sets very strong constraints on the mass of the NP mediators, $M_{\rm heavy}$, hence further suppressing the effects on Γ_{12}^q. Third, the ratio Γ_{12}^q/M_{12}^q typically scales as $\Gamma_{12}^q/M_{12}^q \sim m_b^2/M_{\rm heavy}^2$, which clearly limits the enhancements one can achieve for the semileptonic asymmetries.

Finally, in Sec. 7.6 we have put our results in context by comparing these findings with the expected sensitivity at LHCb and Belle II regarding CP violation in B meson mixing. Our main results are summarized in Fig. 7.8, highlighting that: (i) we do not expect upcoming measurements of the CP asymmetries to test any of the NP models we have considered in this study (unless significant tunings are present), and (ii) the B-mesogenesis mechanism is in theoretical tension. The latter stems from the rather large and positive CP asymmetries needed for the mechanism to be successful, which are difficult to feature BSM. The only region of parameter space that could be covered is the one with $A_{\rm SL}^s \simeq (1-5)\times 10^{-4}$ and $A_{\rm SL}^d \simeq A_{\rm SL}^{d,{\rm SM}}$. Remarkably, in this region of the parameter space B mesons should have a rather large branching ratio $(0.2-1\%)$ into a visible baryon, missing energy, and any number of light mesons. While this represents a strong requirement, it makes the mechanism even more predictive, and we note that its minimal realization could actually incorporate the two necessary ingredients for baryogenesis: the required amount of CP violation in mixing (from the triplet scalar contributions to M_{12}^s), as well as the required branching ratio for the new decay mode.

Overall, we find that it appears challenging to significantly enlarge CP violation in the mixing of neutral B mesons beyond the SM. This has implications both for the interpretation of future LHCb and Belle II measurements of the semileptonic asymmetries as well as for the B-mesogenesis mechanism, as mentioned before. Despite the rich ongoing flavor physics program at LHC and Belle II, we expect our results not to be significantly altered in the next 5–10 years. The reason is that the ranges of the CP asymmetries found in Eq. (7.102) are primarily driven by the measurements of the phase of M_{12}^q from time-dependent CP asymmetries. The latter, ϕ_d and ϕ_s, have been measured with $\sim 1^\circ$ precision, which is precisely the expected size of the SM penguin pollution, and thus contain irreducible uncertainties at first sight.

The quest for New Physics beyond the Standard Model continues, but our study highlights that it is likely not to be found for the most generic models through upcoming measurements of CP violation in B meson mixing. Very high precision measurements of these asymmetries at a future Tera-Z factory such as FCC-ee [207, 208] or finely tuned contributions to B meson mixing may change this picture.

Concluding Remarks

Conclusions

Throughout the history of particle physics, the flavor sector has often played a relevant role in anticipating the existence of new dynamics beyond the current understanding of the time. Major examples include he prediction of the charm quark, as required by the GIM mechanism for the suppression of FCNC, or the postulation of a third quark generation to account for CP violation within the Kobayashi-Maskawa paradigm. On the other hand, the discovery of the Higgs boson, while being the last piece of confirmation of the SM, it underscored the need for a deeper understanding of the scalar sector.

This thesis presents our research on the flavor and the scalar sectors beyond the SM, with special emphasis on the related phenomenon of CP violation. Following a bottom-up approach, we are mostly interested in investigating the phenomenological implications of different NP scenarios.

We begin by formulating a Saturation Theorem for EFTs constructed from spurion analysis. When a set of spurion fields S is introduced to organize the breaking of a global symmetry G_f in an EFT $\mathscr{L}_{\text{EFT}}([\phi])$, the resulting EFT $\mathscr{L}_{\text{EFT, Spurion}}$ *saturates* (or reproduces) the original one restricted to be invariant under $H_S \subset G_f$, being H_S the unbroken subgroup under a generic vev of the spurions $\langle S\rangle$. More precisely, we have

$$\mathscr{L}_{\text{EFT, Spurion}} \equiv \mathscr{L}_{\text{EFT}}([\phi], S)^{G_f}\Big|_{S=\langle S\rangle=\lambda_S} \quad \cong \quad \mathscr{L}_{\text{EFT}}([\phi])^{H_S} \,, \tag{7.105}$$

where "$\cong$" means that the two EFTs have the same set of allowed independent effective operators. Importantly, *all* powers of S should be included in $\mathscr{L}_{\text{EFT, Spurion}}$ and $\lambda_S = \langle S\rangle$ must fulfill a *generic* vev. Regarding the latter, it would be interesting to explore in a future work if our Saturation Theorem is still valid when the vev of the spurion fields presents a specific structure rather than being completely generic, as in that case the unbroken subgroup will be presumably larger.

As a relevant case study in flavor physics, we have considered four implementations of the MFV hypothesis in the lepton sector, summarized in Table 7.2, which stem from different neutrino mass generation mechanisms. In particular, we have explicitly checked the Saturation Theorem at mass dimension 6 in the EFT expansion, although it holds for higher dimension operators. In this task, we have developed a publicly available `Mathematica` notebook, HilbCalc, for the computation of single-graded and multi-graded Hilbert series restricted to the classical Lie groups.

Turning to model building, we have investigated extensions of the scalar sector, based on the SM gauge group, that include several Higgs doublets. First, we examine the intriguing relation between the scalar mass spectrum and the CP properties of the vacuum in real MHDMs, that is, when CP invariance is imposed in the scalar potential but it is spontaneously broken by the vacuum. Naively, one would expect that, for a sufficiently large number of scalar doublets, the overabundance of dimensionful quadratic couplings in the scalar potential would lead to a regime with arbitrary heavy scalars, *i.e.*, with masses that could be much larger than the EW scale. Rather unexpectedly, we find that, once perturbativity requirements are imposed on the quartic couplings of the potential, there must be at least one charged scalar and two neutral scalars—besides the wbGBs and the Higgs-like state—, whose masses are close to the EW scale. This feature seems to be related to the existence of an alternative candidate vacuum that is obtained from the original one by means of a CP transformation. The question of whether this conclusion extends to other scalar potentials remains to be answered. Likewise, it would be interesting to address in detail the discovery prospects of these new light states within a more complete framework where the Yukawa and gauge interactions are also specified.

We continue exploring the appealing possibility of having SCPV in two-Higgs-doublet models where neutral flavor conservation is also imposed, that is, where FCNC are completely absent at tree-level. A major obstacle to the viability of this model is that the orthogonal bidiagonalization of the real Yukawa couplings—as imposed by CP invariance at the Lagrangian level—leads to a real CKM matrix [154]. However, the latter can be evaded when the Yukawa matrices exhibit a particular structure—see Eq. (6.32)—, that fulfills two important conditions [155, 156]: (i) the symmetric combinations $Y_a^f Y_a^{f\,T}$ and $Y_a^{f\,T} Y_a^f$ have real *degenerate* eigenvalues, and (ii) the corresponding Yukawa matrix Y_a^f have complex conjugate eigenvalues corresponding to *complex conjugate* eigenvectors, which are *orthonormal* and *independent of the specific eigenvalues*. This allows for a *simultaneous unitary* diagonalization of all Y_a^f $(a = 1, 2)$, which guarantees the absence of SFCNC. Importantly, the fact that the eigenvectors are complex conjugate of one another leads to a fermion mixing matrix where two rows or two columns have equal moduli. While it is clear that this particular structure is ruled out in the quark sector, it remains an interesting open possibility in the lepton sector: the PMNS mixing matrix is CP-violating and $\mu - \tau$ symmetric. At this point, additional experimental constraints such as the electron EDM and the rare decay $\mu \to e\gamma$ are expected to play a key role in constraining the parameter space of the model.

On another avenue, we have analyzed to which extent CP is violated in neutral B meson mixing within different BSM scenarios. One of the main motivations for this study is its direct connection to the baryon asymmetry of the Universe within the B-mesogenesis framework. In particular, we have considered: (i) the effects of heavy NP in the mass mixing M_{12}^q following a model-independent approach, (ii) the implications of 3×3 CKM unitarity deviations in vector-like quark singlet extensions of the fermion sector, and (iii) the role of new contributions to the decay width mixing Γ_{12}^q.

Within the first scenario, based on a general modification of M_{12}^q, we obtain enhancements of the semileptonic asymmetries at the 10^{-3} level for the B_d system, and 10^{-4} for the B_s system:

$$A_{\rm SL}^d = (-9.1 \pm 3.6) \times 10^{-4}\,, \qquad A_{\rm SL}^s = (-0.04 \pm 1.21) \times 10^{-4}\,, \tag{7.106}$$

mainly driven by the $\mathcal{O}(1^\circ)$ phases controlling CP violation in the interference between mixing and decay. Similar results are obtained in extensions of the fermion sector including one up-type or one down-type vector-like quark singlet, which induce deviations of 3×3 CKM unitarity. Finally, we find that NP models where Γ_{12}^q is also modified lead to much smaller enhancements of the semileptonic asymmetries in realistic UV completions, *e.g.*, the minimal realization of the B-mesogenesis mechanism.

These results have been compared with the expected sensitivity at LHCb and Belle II in the measurements of CP violation in B meson mixing. From Fig. 7.8, it is clear that: (i) we do not expect upcoming measurements of the CP asymmetries to probe new regions of the parameter space (unless substantial fine-tunings are involved), and (ii) the B-mesogenesis mechanism is placed in tension. The latter stems from the overall difficulty to generate sufficiently large values of the semileptonic asymmetries BSM.

The only viable region of the parameter space appears to be $A_{\rm SL}^s \simeq (1-5)\times 10^{-4}$ and $A_{\rm SL}^d \simeq A_{\rm SL}^{d,\rm SM}$. Importantly, in this region B mesons should have a rather large branching ratio $(0.2-1\%)$ into a visible baryon, missing energy, and any number of light mesons. Therefore, our analysis highlights that NP is not likely to be found for the most generic models through upcoming measurements of CP violation in B meson mixing, although this picture may change in future high precision measurements of these asymmetries at a Tera-Z factory such as FCC-ee. Conversely, if a non-standard signal were detected in these observables, it would certainly point toward a highly non-trivial NP structure.

Finally, it is important to highlight that the flavor and scalar sectors, as well as the phenomenon of CP violation, sit at the core of numerous fundamental questions that remain to be answered. Although this thesis has focused on a limited set of well-motivated NP scenarios in this context, many other interesting possibilities exist that deserve thorough investigation. Looking ahead, the high-precision era we are entering at experiments such as LHCb, Belle II, and future facilities will be crucial for uncovering potential deviations from the SM. At the same time, theoretical research will be essential to guide and interpret experimental progress. This thesis represents our specific contribution to a field with many challenges ahead, but with great potential for unexpected discoveries in the not-so-distant future.

Resumen de la tesis

Sabor, Higgses y Violación de CP

El campo de la física de sabor constituye una ventana única para la exploración de Nueva Física (NP) más allá del Modelo Estándar (SM). Su alta sensibilidad a correcciones virtuales de estados más pesados, directamente fuera del alcance de los colisionadores actuales, impone algunas de las restricciones más fuertes sobre los diferentes modelos de NP. Esto último, enmarcado dentro de la era de alta precisión en la que nos adentramos con experimentos dedicados como LHCb o Belle II, hace que el análisis de desintegraciones raras, oscilaciones de mesones neutros, y otros observables sensibles a la violación de la simetría Carga-Paridad (CP) cobren una gran relevancia y se conviertan en una herramienta especialmente poderosa tanto para el descubrimiento indirecto de NP como para la puesta a prueba de la estructura de sabor del SM.

Por otra parte, el descubrimiento del bosón de Higgs en el año 2012 relanzó el estudio detallado del sector escalar, el cual se ha convertido en una tarea central en la física de altas energías hasta la fecha. Si bien el SM contiene un único doblete de Higgs, responsable de la generación de masas de los bosones de gauge y las partículas materiales a través de la rotura espontánea de la simetría electrodébil, existen fuertes motivaciones teóricas para considerar sectores escalares extendidos. Es bien sabido que éstos pueden ofrecer una fenomenología variada no muy alejada de la escala electrodébil, incluyendo, entre otros efectos, la existencia de nuevos escalares neutros y cargados. Al mismo tiempo, resulta esencial confrontar dichos modelos con los datos que proporciona la física de sabor, por ejemplo, aquéllos relacionados con la presencia de corrientes neutras con cambio de sabor.

Finalmente, conviene recordar que la violación de la simetría CP constituye un ingrediente clave para entender por qué la gran mayoría de estructuras que componen nuestro Universo están hechas de materia en lugar de antimateria. Esta observación deriva de una ligera asimetría entre la cantidad de materia y antimateria en el Universo primitivo, conocida como asimetría bariónica primordial. Para entender su origen dinámicamente, se proponen los conocidos como modelos de bariogénesis. Todos ellos deben satisfacer las condiciones establecidas por Sakharov, a saber: (i) violación del número bariónico, (ii) violación de C y CP, y (iii) ausencia de equilibrio térmico. En el marco del SM, la única fuente de violación de CP es la fase compleja presente en la matriz de Cabibbo-Kobayashi-Maskawa (CKM) responsable de los procesos con cambio de sabor, la cual resulta insuficiente para explicar la bariogénesis. Por lo tanto, nuevas fuentes de violación de CP más allá del SM son necesarias. Éstas pueden surgir de forma explícita (a nivel del Lagrangiano) o espontánea (a través de la configuración del vacío de la teoría). En este sentido, diferentes extensiones del sector de Higgs permiten esta última posibilidad, estableciendo un vínculo directo entre la dinámica escalar y el origen fundamental de la violación de CP.

Con todo, el análisis y entendimiento del sector de sabor, el sector escalar y la violación de CP más allá del SM, y concretamente la conexión que se establece entre ellos, es una labor fundamental para el campo de la física de partículas. La presente tesis se centra en el estudio de estos tres temas, *Sabor, Higgses y Violación de CP*, poniendo especial énfasis en algunas de sus implicaciones fenomenológicas.

Objetivos

Tal y como acabamos de mencionar, esta tesis se centra en explorar el sector de sabor y el sector escalar, así como posibles fuentes de violación de la simetría CP, en el marco de diferentes modelos de NP más allá del SM. Nuestro trabajo se estructura en torno a cuatro artículos de investigación cuyos objetivos principales pasamos a detallar.

En el capítulo 4, analizamos las Teorías Efectivas de Campos (EFTs) más generales que pueden construirse en el contexto de un análisis con espuriones. En particular, en este terreno se encuentran los modelos que implementan la hipótesis de Violación Mínima de Sabor (MFV), la cual consiste en asumir que la única fuente de ruptura de la simetría de sabor a bajas energías, tanto en el SM como en modelos de NP, son los acoplamientos de Yukawa. Utilizando la tecnología de las series de Hilbert, establecemos un criterio claro para determinar cuál es la teoría efectiva más general en este escenario.

A continuación, nos centramos en el estudio de modelos concretos de NP: extensiones del sector escalar con múltiples dobletes de Higgs basadas en el grupo de gauge del SM. En primer lugar, en el capítulo 5, analizamos la interesante conexión entre el espectro de masas de los modelos que preservan la invariancia CP a nivel del Lagrangiano en el sector escalar y las propiedades de CP del vacío.

Más adelante, el capítulo 6 vuelve a centrarse en la violación espontánea de CP, aunque esta vez en el contexto de los modelos con sólo dos dobletes de Higgs donde se impone la conservación del sabor. Concretamente, examinamos las implicaciones fenomenológicas del requirimento simultáneo de: (i) la rotura espontánea de la simetría CP, (ii) la ausencia de corrientes neutras escalares que cambien el sabor, y (iii) la generación de una mezcla fermiónica que viole CP, en concordancia con los datos experimentales.

Finalmente, en el capítulo 7 tratamos de cuantificar cuán grande puede ser la violación de CP en la mezcla de mesones B dentro de diferentes escenarios de NP más allá del SM. Dicho análisis está motivado por la relación directa que se establece con la asimetría bariónica primordial en el mecanismo de B-mesogénesis. Entre los escenarios de NP considerados, se incluyen las extensiones del sector fermiónico con quarks vectoriales que se transforman como singletes bajo el grupo de gauge del SM. Estos últimos plantean la interesante posibilidad de introducir desviaciones con respecto a la unitariedad 3×3 en la matriz CKM. Asimismo, en este capítulo buscamos establecer si las futuras búsquedas de violación de CP en la mezcla de mesones B, tanto en LHCb como en Belle II, serán capaces de probar nuevas regiones del espacio de parámetros.

Antes de profundizar en los detalles de nuestra investigación, los tres primeros capítulos de esta tesis contienen una introducción teórica autocontenida a los diferentes marcos de trabajo que se utilizan en los capítulos subsiguientes. En primer lugar, el capítulo 1 repasa los fundamentos básicos del SM, con especial atención en su estructura de sabor y el origen de la violación de CP en el paradigma de CKM. En el capítulo 2, presentamos los aspectos técnicos de las series de Hilbert, junto con un conjunto seleccionado de resultados matemáticos que serán relevantes para nuestros análisis, como por ejemplo la fórmula de Molien-Weyl y el teorema de Brion. Las características principales de los modelos con múltiples dobletes de Higgs y, en particular, los modelos con dos dobletes de Higgs, se recogen en el capítulo 3.

Esfuerzo especial se ha dedicado a la preparación de un conjunto de apéndices que incluyen cálculos detallados y explicaciones complementarias omitidas en el texto principal. En concreto, el apéndice A contiene una guía de usuario de nuestro cuaderno de `Mathematica` HilbCalc, el cual permite el cálculo automatizado de series de Hilbert restringidas a los grupos de Lie clásicos. Los apéndices B, C y D recogen los detalles del proceso de bidiagonalización unitaria, la diagonalización de matrices ortogonales $O(3,\mathbb{R})$ y la evolución bajo el grupo de renormalización de las matrices de Yukawa, respectivamente, los cuales resultan relevantes para el capítulo 6. Finalmente, los apéndices E y F contienen cálculos detallados de las contribuciones de escalares a un bucle a los momentos dipolares leptónicos, así como de las diferentes contribuciones a la mezcla de mesones B en los modelos considerados en el capítulo 7.

Metodología

Esta tesis se basa en el uso de un conjunto de herramientas teóricas y computacionales orientadas al análisis de diferentes escenarios de NP más allá del SM. En este sentido, combinamos un enfoque basado en modelos concretos de NP con estrategias más generales que no requiren de la especificación del modelo en cuestión.

Por un lado, el formalismo de las teorías efectivas de campos permite capturar los efectos de una amplia gama de modelos completos en el ultravioleta (UV) a escalas de energía más bajas y sin necesidad de concretar sus características particulares. En este contexto, destacamos la teoría efectiva del SM (SMEFT), en la que se incluyen operadores de dimensión mayor que cuatro construidos a partir de los campos del SM y respetando sus simetrías gauge. Dicho marco teórico, es utilizado en los análisis con espuriones que implementan la hipótesis de MFV. Este tipo de análisis resulta, a su vez, útil para controlar los efectos de ruptura de una cierta simetría global en el Lagrangiano.

Por otra parte, hacemos uso extensivo de la teoría de representación de grupos, así como de la tecnología de las series de Hilbert. También se emplean resultados matemáticos de interés, como la fórmula de Molien-Weyl y el teorema de Brion. Cabe destacar que, como parte de esta tesis, hemos desarrollado un código en `Mathematica` de acceso público, HilbCalc, para el cálculo automatizado de series de Hilbert restringidas a los grupos de Lie clásicos $SU(n)$, $SO(n)$, $Sp(n)$ y factores $U(1)$.

Complementando el enfoque general ofrecido por las EFTs, exploramos modelos específicos de NP incluyendo, por ejemplo, los modelos con múltiples dobletes de Higgs y las extensiones del sector fermiónico con quarks vectoriales de tipo singlete. Este enfoque dependiente del modelo nos permite investigar en detalle la fenomenología asociada—existencia de nuevos bosones escalares, corrientes neutras con cambio de sabor, o violación espontánea de CP—en un marco completamente definido.

Dada la naturaleza teórica de este proyecto de tesis, se hace uso de las técnicas usuales de Teoría Cuántica de Campos, como son la teoría de perturbaciones y el cálculo de amplitudes a nivel árbol y a un bucle. Nuestros cálculos analíticos se apoyan en herramientas computacionales como `Mathematica`, que permiten llevar a cabo las evaluaciones numéricas pertinentes.

Finalmente, con el fin de evaluar la viabilidad de los modelos de NP propuestos, realizamos análisis estadísticos de naturaleza frecuentista. En particular, las restricciones experimentales relevantes se implementan mediante procedimientos estándar de minimización de la función χ^2. Para la exploración de espacios de parámetros multidimensionales se recurre a los métodos de Monte Carlo basados en cadenas de Markov. Todas estas técnicas nos permiten identificar las regiones del espacio de parámetros del modelo que resultan compatibles con las medidas existentes, así como prever la sensibilidad de futuras búsquedas experimentales.

Resultados

La búsqueda de Nueva Física más allá del Modelo Estándar

El SM ha demostrado ser un marco teórico tremendamente exitoso a la hora de describir todos los resultados experimentales en física de partículas obtenidos hasta la fecha, al menos a la escala de energía electrodébil. No obstante, es bien sabido que éste no proporciona una respuesta satisfactoria, o directamente no es capaz de abordar, varias cuestiones fundamentales en diferentes frentes. Entre los problemas más relevantes que permanecen sin resolver pueden destacarse los siguientes.

En primer lugar, la gran cantidad de parámetros libres presentes en el SM pone de manifiesto que éste se encuentra lejos de ser una teoría definitiva de las interacciones entre partículas elementales. En su versión mínima, es decir, ignorando las masas de los neutrinos, hay un total de 19 parámetros libres. Si, además, especificamos un mecanismo para la generación de masa de los neutrinos, este número puede ascender hasta 26 en el caso de neutrinos de Dirac, o incluso hasta 36 dentro del modelo de balancín de tipo I. Relacionado con el número de parámetros libres, se encuentra el hecho de que el grupo de simetría gauge $SU(3)_C \times SU(2)_L \times U(1)_Y$ es más bien complejo y, en particular, introduce tres acoplamientos independientes correspondientes a cada uno de los factores del grupo. De nuevo, esta descripción queda lejos de ser un marco unificado de las interacciones fundamentales.

Dentro del conjunto de parámetros libres, se puede comprobar que la inmensa mayoría proviene del sector de sabor. De hecho, en rigor, el SM no está provisto de una teoría del sabor, sino que los acoplamientos de Yukawa se introducen como números complejos arbitrarios que deben determinarse experimentalmente. Sorprendentemente, dichos acoplamientos abarcan varios órdenes de magnitud, lo cual resulta poco natural—por ejemplo, existe una diferencia de cinco órdenes de magnitud entre el acoplamiento de Yukawa del quark top y el del electrón. Además, las masas y mezclas de los fermiones responden a un patrón jerarquizado cuyo origen se desconoce: éste es el conocido como *problema del sabor*. Del mismo modo, no existe una explicación para la existencia de tres (y sólo tres) generaciones de fermiones o, dicho de otro modo, no entendemos por qué la Naturaleza se manifiesta de una forma no mínima en este sector.

Como se ha mencionado anteriormente, es importante incorporar un mecanismo de generación de masas para los neutrinos, tal y como indican de manera inequívoca los experimentos de oscilaciones. Al mismo tiempo, dicho mecanismo debe tener en cuenta que las masas de los neutrinos son extremadamente pequeñas en comparación con el leptón cargado más ligero, es decir, el electrón.

Por otro lado, el sector escalar también plantea cuestiones teóricas profundas como la estabilización de la masa del bosón de Higgs. Las correcciones cuánticas de orden superior por parte de escalas de energía más altas introducen una contribución a la masa del Higgs que diverge cuadráticamente. Dado que el bosón escalar observado en el LHC tiene una masa $M_h \sim 125$ GeV, *a priori* debería existir una importante cancelación de las contribuciones de orden superior, lo cual se considera antinatural. Éste es el denominado *problema de jerarquía electrodébil o del Higgs*. La existencia de NP no muy alejada de la escala electrodébil podría aliviar este problema, aunque, al mismo tiempo, las restricciones experimentales provenientes de la física del sabor descartarían esta posibilidad. Esta contraposición genera un *pequeño problema de jerarquía*.

Otro problema teórico que suscita gran interés es el llamado *problema de CP fuerte*. La evidencia experimental en las interacciones débiles nos muestra que CP no es una buena simetría de la Naturaleza. Por tanto, no hay nada que impida incluir un parámetro que viole CP, $\bar{\theta}$, en el Lagrangiano de las interacciones fuertes. Sin embargo, a pesar de su legítima existencia teórica, las medidas del momento dipolar eléctrico del neutrón restringen este parámetro a valores extremadamente pequeños, a saber, $\bar{\theta} \lesssim 10^{-10}$.

Tal y como anticipábamos anteriormente, la violación de la simetría CP está relacionada con una de las preguntas más fundamentales en física de partículas y cosmología: ¿cuál es el origen de la asimetría materia-antimateria en el Universo? La cantidad de violación de CP proporcionada por el SM, incluyendo tanto la interacción débil como la fuerte, no es suficiente. Es decir, son necesarias nuevas fuentes de violación de CP más allá del SM.

Otro problema en el ámbito cosmológico es el entendimiento del sector oscuro. Por un lado, existe evidencia sólida de la existencia de una nueva forma de *materia oscura* que, aparentemente, sólo se manifiesta a través de su interacción gravitatoria, pero representa el 26% del contenido energético del Universo—muy por encima de la contribución de la materia bariónica ordinaria. Por otro lado, casi un 70% de la densidad de energía corresponde a cierto tipo de *energía oscura* responsable de la expansión acelerada del Universo. El SM no ofrece siquiera un candidato a materia oscura.

En definitiva, existen numerosos frentes abiertos que el SM no puede abordar, lo cual hace evidente la necesidad de NP. En este contexto, nos centramos en analizar las implicaciones fenomenológicas que se desprenden del sector de sabor y el sector escalar en diferentes modelos de NP, prestando especial atención al fenómeno de violación de CP. Para ello, hacemos uso de distintos marcos de trabajo y herramientas teóricas que pasamos a describir.

El método de las series de Hilbert

Las series de Hilbert constituyen una poderosa herramienta con un amplio rango de aplicaciones en física de partículas. En nuestro caso, utilizamos este método en el contexto de un análisis con espuriones en EFTs y, más concretamente, dentro del paradigma de MFV.

Dado un conjunto de campos fundamentales Φ que transforman bajo una cierta representación R_Φ del grupo de simetría G, es posible contabilizar el número de invariantes que pueden construirse a una determinada potencia de los campos mediante una función de partición conocida como serie de Hilbert. Ésta viene dada por la expresión

$$\mathcal{H}_{\text{Inv}}^{G,R_\Phi}(q) \equiv \sum_{k=0}^{\infty} n_{\text{Inv}}(k) q^k \,, \qquad |q| < 1 \,, \tag{7.107}$$

donde $n_{\text{Inv}}(k)$ es el número de polinomios invariantes de grado k que pueden construirse a partir de los campos, y q es una variable de graduación asociada a cada uno de ellos, la cual permite hacer seguimiento de sus potencias. Es importante destacar que la variable de graduación debe satisfacer la condición $|q| < 1$ con tal de que la serie de Hilbert converja.

Asimismo, este método puede extenderse fácilmente para otros covariantes del grupo de simetría, es decir, para representaciones irreducibles (irreps) de G distintas a la trivial. De forma similar, se tiene que

$$\mathcal{H}_R^{G,R_\Phi}(q) \equiv \sum_{k=0}^{\infty} n_R(k) q^k \,, \qquad |q| < 1 \,, \tag{7.108}$$

lo cual constituye una generalización de la ecuación (7.107)—de hecho, la serie de Hilbert para invariantes corresponde al caso particular $R = \mathrm{Inv}$.

Entre las distintas posibilidades existentes en la literatura, la fórmula de Molien-Weyl nos permite calcular la serie de Hilbert en términos de una integral de contorno que puede resolverse aplicando el teorema de Cauchy. Una vez resuelta, basta con expandir en potencias de q para obtener los diferentes términos de la serie de Hilbert. En caso de tener un conjunto de campos exclusivamente bosónicos, la fórmula de Molien-Weyl se escribe como

$$\mathcal{H}_R^{G,R_\Phi}(q) = \int \mathrm{d}\mu_G(x) \chi_R^*(x) \frac{1}{\det[1 - q\, g_{R_\Phi}(x)]} \,, \qquad |q| < 1 \,. \tag{7.109}$$

Los distintos elementos que aparecen bajo el signo integral son: la variable de graduación q, la medida de Haar $\mathrm{d}\mu_G(x)$ del grupo G, el carácter $\chi_R(x)$ de la representación objetivo R, la matriz de la representación g_{R_Φ}, y un conjunto de variables x que parametrizan los elementos del grupo.

Modelos con múltiples dobletes de Higgs

Algunos de los problemas para los cuales el SM no ofrece una respuesta satisfactoria pueden abordarse a través de diferentes extensiones del sector escalar, como ocurre con la estabilización del sector de Higgs en modelos supersimétricos, el origen de la masa de los neutrinos en el mecanismo de balancín de tipo II, o el problema de CP fuerte a través de la solución de Peccei-Quinn. Además, dichas extensiones suelen ofrecer una fenomenología variada relacionada con la dinámica en el sector de sabor, en muchos casos contribuyendo a reducir posibles tensiones entre el SM y los datos experimentales. En nuestro caso, nos centramos en modelos que incluyen múltiples dobletes de Higgs, y realizaciones particulares con únicamente dos dobletes, como extensiones del sector escalar basadas en el grupo gauge del SM.

El potencial escalar más general en presencia de n dobletes de Higgs puede escribirse como

$$\mathscr{V}(\Phi_1, \dots, \Phi_n) = Y_{ab} \Phi_a^\dagger \Phi_b + Z_{ab,cd} (\Phi_a^\dagger \Phi_b)(\Phi_c^\dagger \Phi_d) \,, \tag{7.110}$$

donde Y_{ab} son acoplamientos cuadráticos con dimensión de energía al cuadrado, y $Z_{ab,cd}$ son acoplamientos cuárticos adimensionales. Es fácil comprobar que $Z_{ab,cd} = Z_{cd,ab}$, mientras que la hermiticidad del potencial implica que $Y_{ab} = Y_{ba}^*$ y $Z_{ab,cd} = Z_{ba,dc}^*$. Teniendo esto en cuenta, el recuento de parámetros reales presentes en los acoplamientos del potencial escalar se presenta en la tabla 3.1 para un número arbitrario de dobletes de Higgs.

El mínimo del potencial viene dado por el valor esperado en el vacío (vev) de los dobletes escalares. Suponiendo que el vacío conserva la carga eléctrica y desencadena correctamente la ruptura de la simetría electrodébil, se tiene que

$$\langle \Phi_a \rangle = \frac{v_a e^{i\theta_a}}{\sqrt{2}} \begin{pmatrix} 0 \\ 1 \end{pmatrix} \,, \tag{7.111}$$

donde $v_a \in \mathbb{R}^+$ y $\theta_a \in [0, 2\pi)$, con la condición $\sum_{a=1}^n v_a^2 = v^2 \approx (246 \text{ GeV})^2$. La estabilidad del vacío requiere que éste sea un extremo del potencial, es decir,

$$\mathscr{V}\left(\langle\Phi_1\rangle,\ldots,\langle\Phi_n\rangle\right)\equiv V(v_1,\ldots,v_n,\theta_1,\ldots,\theta_n)\,, \tag{7.112}$$

tal que

$$\partial_{v_1}V=\cdots=\partial_{v_n}V=0\,,\qquad \partial_{\theta_1}V=\cdots=\partial_{\theta_n}V=0\,. \tag{7.113}$$

Es importante señalar que las fases individuales θ_a no tienen significado físico por sí mismas, lo cual se pone de manifiesto a través de la condición $\sum_{a=1}^{n}\partial_{\theta_a}V=0$, con independencia de que cada término se anule por separado. Por tanto, existen $2n-1$ condiciones de minimización independientes. De forma general, éstas permiten expresar un subconjunto de acoplamientos cuadráticos en términos de los cuárticos, lo cual permite establecer cotas superiores sobre las masas de los nuevos escalares.

En lo que se refiere a la violación de CP originada en el sector escalar, la invariancia bajo las transformaciones estándar de CP de los campos impone que todos los acoplamientos en el potencial sean reales. No obstante, esto no asegura completamente la invariancia CP, ya que esta simetría puede romperse espontáneamente a través de la configuración del vacío. En concreto, la violación espontánea de CP se debe a la presencia de fases relativas entre los vevs de los diferentes dobletes escalares.

Pasamos ahora a introducir las interacciones de Yukawa entre los dobletes escalares y los fermiones. Para mayor claridad y concreción, desarrollamos este punto en el contexto de los modelos con sólo dos dobletes de Higgs y centrándonos en el sector de quarks. Así pues, los acoplamientos de Yukawa vienen dados por

$$-\mathscr{L}_{\rm Y}^{\rm quark}=\overline{Q_L^0}(Y_1^u\widetilde{\Phi}_1+Y_2^u\widetilde{\Phi}_2)u_R^0+\overline{Q_L^0}\left(Y_1^d\Phi_1+Y_2^d\Phi_2\right)d_R^0+\text{H.c.}\,, \tag{7.114}$$

donde $\widetilde{\Phi}_a\equiv\epsilon\Phi_a^*=i\sigma^2\Phi_a^*$. Como podemos observar, en este caso contamos con dos matrices de Yukawa Y_a^f $(a=1,2)$ en cada sector $(f=u,d)$, a diferencia de lo que ocurre en el SM. Su interpretación es más transparente en la denominada base de Higgs, definida por

$$\begin{pmatrix}H_1\\H_2\end{pmatrix}=R_\beta\begin{pmatrix}e^{-i\theta_1}&0\\0&e^{-i\theta_2}\end{pmatrix}\begin{pmatrix}\Phi_1\\\Phi_2\end{pmatrix}\,,\qquad\text{con}\qquad R_\beta=\begin{pmatrix}c_\beta&s_\beta\\-s_\beta&c_\beta\end{pmatrix}\,, \tag{7.115}$$

donde $c_\beta\equiv\cos\beta\equiv v_1/v$, $s_\beta\equiv\sin\beta\equiv v_2/v$, $t_\beta\equiv\tan\beta=v_2/v_1$, y con $\beta\in[0,\pi/2]$ sin pérdida de generalidad. En esta base, tan solo el doblete escalar H_1 adquiere un vev, v, por lo que éste presenta la misma forma que el doblete escalar del SM. Las interacciones de Yukawa toman la forma

$$-\frac{v}{\sqrt{2}}\mathscr{L}_{\rm Y}^{\rm quark}=\overline{Q_L^0}(M_u^0\widetilde{H}_1+N_u^0\widetilde{H}_2)u_R^0+\overline{Q_L^0}\left(M_d^0H_1+N_d^0H_2\right)d_R^0+\text{H.c.}\,, \tag{7.116}$$

con

$$M_u^0=\frac{v}{\sqrt{2}}e^{-i\theta_1}\left(c_\beta Y_1^u+e^{-i\theta}s_\beta Y_2^u\right)\,,\qquad M_d^0=\frac{v}{\sqrt{2}}e^{i\theta_1}\left(c_\beta Y_1^d+e^{i\theta}s_\beta Y_2^d\right)\,, \tag{7.117}$$

$$N_u^0=\frac{v}{\sqrt{2}}e^{-i\theta_1}\left(-s_\beta Y_1^u+e^{-i\theta}c_\beta Y_2^u\right)\,,\qquad N_d^0=\frac{v}{\sqrt{2}}e^{i\theta_1}\left(-s_\beta Y_1^d+e^{i\theta}c_\beta Y_2^d\right)\,, \tag{7.118}$$

y $\theta\equiv\theta_2-\theta_1$. Así pues, queda claro que las matrices M_f^0 corresponden a las matrices de masa fermiónicas no diagonales, al estar acopladas al único doblete escalar que adquiere un vev. Éstas pueden diagonalizarse mediante el procedimiento habitual de bidiagonalización unitaria. Ahora bien, las mismas transformaciones unitarias no diagonalizan, en general, los términos adicionales N_f^0, permitiendo la aparición de corrientes neutras escalares con cambio de sabor a nivel árbol. Dadas las fuertes restricciones experimentales sobre este tipo de interacciones, se hace necesario evitar su aparición o, al menos, mantenerlas bajo control. Entre la primera clase de modelos, encontramos aquéllos que implementan la Conservación Natural del Sabor (NFC) *à la* Glashow-Weinberg-Paschos, donde se incluyen los modelos con dos dobletes de Higgs con una simetría $\mathbb{Z}_2$ presentados en la tabla 3.2, entre otros. Por otro lado, encontramos una segunda clase de modelos en los que sí se permite la aparición de corrientes neutras con cambio de sabor siempre y cuando su intensidad se mantenga bajo control, como es el caso de la propuesta de Cheng-Sher, o los modelos de Branco-Grimus-Lavoura en el marco de MFV.

Por último, conviene señalar que la invariancia de las interacciones de Yukawa bajo las transformaciones estándar de CP, implica que los acoplamientos de Yukawa son reales. En esos casos, es importante asegurar, no obstante, que la matriz de mezcla fermiónica viole CP, tal y como establecen los datos experimentales.

EFTs más generales en un análisis con espuriones: el Teorema de Saturación

En el capítulo 4, derivamos un teorema de saturación que permite determinar cuál es la EFT más general que puede construirse a partir de un conjunto de espuriones S.

De forma general, una EFT viene definida por un conjunto de campos dinámicos $\phi(x)$ y sus derivadas, un conjunto de simetrías globales y/o gauge, y una expansión en serie de potencias que involucra una escala de energía superior Λ. El Lagrangiano de la EFT, $\mathscr{L}_{\text{EFT}}\left([\phi]\right)$, contiene entonces todos los operadores que puedan construirse a partir de los campos y respeten las simetrías impuestas, de tal forma que los operadores de dimensión mayor que cuatro queden suprimidos por el correspondiente número de potencias de Λ.

Por otra parte, en un análisis con espuriones, se empieza identificando los operadores de menor dimensión que violen una cierta simetría global G_f no impuesta originalmente en $\mathscr{L}_{\text{EFT}}\left([\phi]\right)$. A continuación, los acoplamientos λ_S de dichos operadores pasan a tratarse como campos espuriónicos (no dinámicos) S con las propiedades adecuadas de transformación bajo G_f que permitan restaurar la simetría a los órdenes más bajos de la EFT. En este sentido, los acoplamientos que originalmente rompían la simetría G_f pueden interpretarse como los vevs de los campos espuriónicos, es decir, $\lambda_S = \langle S \rangle$. A partir de aquí, los operadores de mayor dimensión se construyen teniendo en cuenta los campos dinámicos $\phi(x)$, con coeficientes construidos a partir los campos espuriónicos S para garantizar la invariancia bajo G_f. Finalmente, la EFT resultante del análisis con espuriones se define evaluando los campos espuriónicos en sus correspondientes vevs:

$$\mathscr{L}_{\text{EFT, Spurion}} \equiv \mathscr{L}_{\text{EFT}}\left([\phi], S\right)^{G_f}\Big|_{S=\langle S\rangle=\lambda_S} . \tag{7.119}$$

Nuestro Teorema de Saturación establece que la EFT con espuriones *satura* (o reproduce) la EFT original restringida a ser invariante bajo $H_S \subset G_f$, siendo H_S el subgrupo de transformaciones que dejan invariante un vev genérico de los espuriones $\lambda_S = \langle S \rangle$:

$$\mathscr{L}_{\text{EFT, Spurion}} \equiv \mathscr{L}_{\text{EFT}}\left([\phi], S\right)^{G_f}\Big|_{S=\langle S\rangle=\lambda_S} \quad \cong \quad \mathscr{L}_{\text{EFT}}\left([\phi]\right)^{H_S} , \tag{7.120}$$

donde se admiten todas las potencias de S en $\mathscr{L}_{\text{EFT, Spurion}}$. Conviene señalar que la equivalencia "$\cong$" significa que ambas EFTs contienen el mismo conjunto de operadores efectivos independientes.

Una vez formulado el Teorema de Saturación, hemos comprobado su validez en las cuatro imple-

Caso	ϕ	G_{Lf}	S	H_S
I	SMEFT	$U(3)_\ell \times U(3)_e$	Y_e	$U(1)_e \times U(1)_\mu \times U(1)_\tau$
II			$Y_e,\, C_5$	$\mathbb{Z}_2 = \{1,\, \mathcal{P}_{\rm LN}\}$
III	νSMEFT	$U(3)_\ell \times U(3)_e \times U(3)_\nu$	$Y_e,\, Y_\nu$	$U(1)_{\rm LN}$
IV			$Y_e,\, Y_\nu,\, M_R$	$\mathbb{Z}_2 = \{1,\, \mathcal{P}_{\rm LN}\}$

Table 7.2: Implementaciones de MLFV analizadas en el capítulo 4.

mentaciones del principio de Violación Mínima de Sabor Leptónico (MLFV), recogidas en la tabla 7.2, al orden más bajo de la expansión EFT (dimensión 6). Cada uno de los casos considerados da cuenta de un mecanismo de generación de masa diferente para los neutrinos en la SMEFT y la νSMEFT (donde se incluyen neutrinos dextrógiros). En particular, encontramos que

$$\text{Caso I:} \qquad \mathscr{L}_{\text{SMEFT},\, S_{\rm I}}\Big|_{\text{dim-6}} \cong \mathscr{L}_{\text{SMEFT}}^{U(1)_e \times U(1)_\mu \times U(1)_\tau}\Big|_{\text{dim-6}}, \tag{7.121}$$

$$\text{Caso II:} \qquad \mathscr{L}_{\text{SMEFT},\, S_{\rm II}}\Big|_{\text{dim-6}} \cong \mathscr{L}_{\text{SMEFT}}^{\mathcal{P}_{\rm LN}}\Big|_{\text{dim-6}}, \tag{7.122}$$

$$\text{Caso III:} \qquad \mathscr{L}_{\nu\text{SMEFT},\, \text{S}_{\rm III}}\Big|_{\text{dim-6}} \cong \mathscr{L}_{\nu\text{SMEFT}}^{U(1)_{\rm LN}}\Big|_{\text{dim-6}}, \tag{7.123}$$

$$\text{Caso IV:} \qquad \mathscr{L}_{\nu\text{SMEFT},\, S_{\rm IV}}\Big|_{\text{dim-6}} \cong \mathscr{L}_{\nu\text{SMEFT}}^{\mathcal{P}_{\rm LN}}\Big|_{\text{dim-6}}, \tag{7.124}$$

para operadores de dimensión 6. En cualquier caso, el Teorema de Saturación se cumple para todos los órdenes de la expansión en la EFT.

Estados ligeros en modelos con múltiples dobletes de Higgs y violación espontánea de CP

En el capítulo 5, trabajamos en el marco de los modelos con múltiples dobletes de Higgs. En concreto, asumimos que CP es una simetría exacta del Lagrangiano en el sector escalar, la cual es rota espontáneamente por la configuración del vacío. Aunque la conexión entre las propiedades de CP del vacío y el espectro de masas de los escalares no es evidente en un primer momento, nuestro análisis refleja un resultado inesperado: para cualquier número de dobletes de Higgs, y una vez se imponen las restricciones de perturbatividad en los acoplamientos cuárticos del potencial, debe existir al menos un escalar cargado y dos escalares neutros—más allá del bosón de Higgs de 125 GeV y los que serían los bosones de Goldstone—cuyas masas están próximas a la escala electrodébil. Veámoslo con algo más de detalle.

Tras la ruptura espontánea de la simetría electrodébil, el potencial escalar genera dos tipos de contribuciones a los términos de masa de los escalares: las que provienen de los acoplamientos cuadráticos con dimensiones de masa (al cuadrado), y aquéllas que involucran los acoplamientos cuárticos multiplicados por los vevs (al cuadrado) de los escalares. Dado que los acoplamientos cuárticos están restringidos por condiciones de perturbatividad, valores de las masas muy por encima de la escala electrodébil sólo pueden originarse a partir de términos cuadráticos grandes. Sin embargo, las condiciones de estabilidad del vacío en la ecuación (7.113) permiten expresar algunos de los acoplamientos cuadráticos en términos de los cuárticos, estableciendo así una cota superior sobre las masas de los escalares. Así pues, uno podría pensar que esta última restricción podría eludirse en modelos que contengan muchos dobletes de Higgs: mientras que el número de términos cuadráticos independientes crece cuadráticamente con el número de dobletes n, el número de condiciones de estacionariedad del vacío únicamente crece linealmente—véase la tabla 5.1. Por tanto, podríamos esperar que, para n suficientemente grande, todos los escalares pudieran ser arbitrariamente pesados.

Los resultados de nuestro análisis numérico, presentados en las figuras 5.1 y 5.2, muestran que esta expectativa razonable no se cumple en modelos con múltiples dobletes de Higgs donde se impone la invariancia CP en el potencial escalar—acoplamientos reales—, pero el vacío rompe espontáneamente esta simetría. Por un lado, los puntos azules en las figuras 5.1 y 5.2 indican, respectivamente, la presencia de un estado cargado ligero y dos escalares neutros—además del bosón de Higgs observado—cuyas masas no están muy alejadas de la escala electrodébil. Por otro lado, los que serían los bosones de Goldstone sin masa corresponden a los puntos en rojo, mientras que los restantes $n-2$ escalares cargados y $2n-4$ escalares neutros vienen dados por las líneas marrones, pudiendo tener masas mucho mayores que la escala electrodébil.

Con tal de obtener un enfoque analítico de este resultado, hemos examinado un escenario simplificado en el que los acoplamientos cuadráticos se consideran mucho mayores que la escala electrodébil, por lo que podemos despreciar los acoplamientos cuárticos. En este contexto, encontramos que los estados escalares ligeros que emergen en el anterior análisis numérico se manifiestan, efectivamente, como autoestados con autovalores nulos.

Este resultado inesperado parece estar relacionado con la existencia de un vacío físicamente equivalente al original, ambos relacionados mediante una transformación de CP. No obstante, en qué medida estas conclusiones pueden extrapolarse a otros potenciales escalares es una cuestión a explorar en el futuro.

Violación espontánea de CP y conservación del sabor con dos dobletes de Higgs: matriz PMNS con simetría $\mu-\tau$

En el capítulo 6, dentro del marco de los modelos con dos dobletes de Higgs, hemos analizado las implicaciones fenomenológicas que surgen del requerimiento simultáneo de: (i) un origen espontáneo de la violación de CP, (ii) la ausencia de corrientes neutras escalares con cambio de sabor, y (iii) la generación de una matriz de mezcla fermiónica (en las corrientes cargadas) que viole CP y sea compatible con los datos experimentales.

En nuestro estudio, hemos comprobado que estas tres condiciones se cumplen simultáneamente cuando los acomplamientos de Yukawa satisfacen: (i) las combinaciones simétricas $Y_a^f Y_a^{f\,T}$ y $Y_a^{f\,T} Y_a^f$, ya sea en el sector "up" o en el sector "down", tienen autovalores reales y degenerados, y (ii) la matriz Y_a^f tiene autovalores complejo conjugados asociados a autovectores complejo conjugados entre sí, los cuales son ortonormales e independientes de los valores específicos de sus autovalores. Esto garantiza la diagonalización unitaria simultánea de todas las Y_a^f $(a=1,2)$, eliminando así las corrientes neutras con cambio de sabor a nivel árbol. Además, el hecho de que los autovalores sean el uno complejo conjugado del otro conduce a una matriz de mezcla con dos filas o columnas de módulos idénticos. En este sentido, si bien esta configuración resulta fenomenológicamente inviable en el sector de quarks, puede implementarse exitosamente en el sector leptónico tanto para neutrinos de Dirac como neutrinos de Majorana en el modelo de balancín de tipo I. Como resultado, la matriz de Pontecorvo-Maki-Nakagawa-Sakata (PMNS) posee la simetría $\mu-\tau$ (su segunda y tercera filas tienen el mismo módulo) y es compatible con las medidas experimentales actuales. En cualquier caso, conviene señalar que observables como el momento dipolar eléctrico del electrón o la desintegración $\mu \to e\gamma$ juegan un papel importante a la hora de establecer el espacio de parámetros permitidos del modelo.

La violación de CP en la mezcla de mesones B podría ser insuficiente para la bariogénesis

En el capítulo 7, hemos investigado cuán grande puede ser la violación de CP en la mezcla de mesones neutros B_d y B_s más allá del SM. En concreto, la cantidad de violación de CP queda reflejada a través de las asimetrías semileptónicas de CP. Dado que se trata de un fenómeno altamente suprimido en el SM—tiene lugar a un bucle—, éste constituye una prueba sensible para la detección de NP. Asimismo, la violación de CP en la mezcla de mesones B se puede relacionar directamente con la asimetría bariónica primordial a través del mecanismo de B-mesogénesis.

Con tal de responder a esta cuestión, adoptamos en primer lugar un enfoque independiente del modelo en el que la NP pesada modifica exclusivamente la mezcla de masas M_{12}^q $(q = d, s)$ en el sistema de mesones B_q. Del análisis global que incluye todas las restricciones experimentales relevantes se desprenden los siguientes resultados:

$$A_{\rm SL}^d = (-9.1 \pm 3.6) \times 10^{-4}\,, \qquad A_{\rm SL}^s = (-0.04 \pm 1.21) \times 10^{-4}\,, \tag{7.125}$$

determinados principalmente por las medidas precisas de la fase de violación de CP en la interferencia entre mezcla y desintegración, $\mathcal{O}(1^\circ)$, que restringen la fase de M_{12}^q.

En segundo lugar, consideramos escenarios que incluyen quarks vectoriales de tipo singlete, los cuales inducen desviaciones respecto a la unitariedad 3×3 de la matriz CKM. Dichos modelos resultan de interés ya que uno de los ingredientes que conduce a pequeñas asimetrías de CP en el SM es, precisamente, la unitariedad de CKM. En cualquier caso, encontramos resultados muy similares al escenario general anterior.

En tercer lugar, examinamos varios escenarios que permiten incluir modificaciones en la mezcla de desintegración Γ_{12}^q. Aunque en principio dichas contribuciones podrían llegar a ser grandes, permitiendo obtener grandes valores de las asimetrías de CP, esto no ocurre cuando se consideran modelos UV completos debido a las fuertes restricciones impuestas por las medidas de las diferencias de masas de los mesones, las cotas inferiores altas sobre la masa de los mediadores provenientes del LHC, y la relación $\Gamma_{12}^q/M_{12}^q \sim m_b^2/M_{\rm pesada}^2$.

A la luz de los resultados obtenidos, concluimos que la dificultad general para generar valores grandes de las asimetrías semileptónicas más allá del SM pone en tensión el mecanismo de B-mesogénesis. En particular, sólo una pequeña región donde $A_{\rm SL}^s \simeq (1-5)\times 10^{-4}$ y $A_{\rm SL}^d \simeq A_{\rm SL}^{d,\rm SM}$ es todavía viable.

Finalmente, analizamos las perspectivas de las próximas medidas de las asimetrías de CP en LHCb (23 fb^{-1}) y Belle II (50 ab^{-1}), concluyendo que ninguno de los escenarios de NP considerados—en ausencia de ajustes finos de los parámetros del modelo—podrá ser probado en un futuro próximo.

Conclusiones

La investigación desarrollada en el marco de esta tesis recoge resultados originales relacionados con el sector de sabor y el sector escalar más allá del SM, con especial atención en la violación de la simetría CP, tanto desde el punto de vista teórico como fenomenológico. Nuestro trabajo analiza una variedad de escenarios de NP más allá del SM que incluyen el paradigma de MFV, extensiones del sector escalar con múltiples dobletes de Higgs, la ruptura espontánea de CP a partir del vacío, y nuevas fuentes de violación de CP en la mezcla de mesones B, entre otros.

Con este objetivo, hemos combinado tanto métodos analíticos como numéricos que resultan esenciales para llevar a cabo los cálculos de interés y delimitar el espacio de parámetros permitidos de los modelos considerados. Más allá de los resultados específicos antes presentados, esta tesis proporciona herramientas que esperamos sean útiles para la comunidad científica, como nuestro código de acceso público HilbCalc.

Finalmente, es importante señalar que los sectores de sabor y escalar son el origen de numerosas preguntas que todavía hoy buscan una respuesta a nivel fundamental. Aunque esta tesis se ha centrado en un conjunto limitado de escenarios de NP bien motivados, existen muchas otras posibilidades interesantes que merecen una investigación profunda y detallada. De cara al futuro, la era de alta precisión en la que nos adentramos con experimentos como LHCb, Belle II y futuras instalaciones, será crucial para descubrir posibles desviaciones respecto al SM. Al mismo tiempo, la investigación teórica será indispensable para guiar e interpretar los avances experimentales. Esta tesis representa nuestra contribución particular a un campo que plantea un futuro desafiante, pero que todavía alberga un gran potencial para descubrimientos inesperados en un futuro no demasiado lejano.

Appendices

A Computing Hilbert Series with HilbCalc

In this appendix, we provide an introductory guide on how to use our `Mathematica` notebook HilbCalc to calculate a general Hilbert series (either single-graded or multi-graded) for group invariants and covariants restricted to the classical Lie groups $SU(n)$, $SO(n)$, $Sp(n=2r)$, and $U(1)$ abelian factors.

Suppose that we have a set of spurion fields Φ, which form a representation of a symmetry group G, and we are interested in its polynomials. In particular, given each irrep of G, denoted "Irrep_G" below, we would like to know how many of them can be made by Φ polynomials. This is encoded in the Hilbert series $\mathcal{H}^{G,\,\Phi}_{\mathrm{Irrep}_G}$. It has several inputs to take:

- The group G, which is a product group in general.
- The G-irrep of interest, *i.e.*, the goal Irrep_G.
- The spurions Φ, which we will refer to as "building block fields". They are assigned grading variables to keep track of their powers in the polynomials. Each G-irrep component of Φ can be assigned a distinct grading variable.

The key formula underlying the calculation of a Hilbert series for group invariants and covariants is the Molien-Weyl formula [87]:

$$\mathcal{H}^{G,\,\Phi}_{\mathrm{Irrep}_G}(q) = \int \mathrm{d}\mu_G(x)\, \chi^*_{\mathrm{Irrep}_G}(x)\, \chi_{\mathbb{r}_\Phi}(q,x)\,, \qquad \text{with} \qquad |q| < 1\,. \tag{A.1}$$

The integrand consists of three factors:

(i) **The Haar measure** $\mathrm{d}\mu_G(x)$.

(ii) **The Weyl character** $\chi^*_{\mathrm{Irrep}_G}(x)$ **of the goal** Irrep_G.

(iii) **The graded Weyl character** $\chi_{\mathbb{r}_\Phi}(q,x)$ **of the polynomial ring** $\mathbb{r}_\Phi$ **in the building block fields**.

As explained in chapter 2, the Molien-Weyl formula makes use of character orthogonality under the Haar measure $\mathrm{d}\mu_G(x)$ to extract the component of our interest Irrep_G in the graded character $\chi_{\mathbb{r}_\Phi}(q,x)$ of the polynomial ring $\mathbb{r}_\Phi$ in the building block fields.

Our `Mathematica` notebook HilbCalc provides general functions for calculating each of the above three factors, packaging them together to calculate the Hilbert series for a general set of group invariants or covariants that is asked by the user. In what follows, we navigate through it to explain how to use it for computing each of these three factors: Haar measures in App. A.1, Weyl characters in App. A.2, graded characters of polynomial rings in App. A.3, and finally their combination in the Molien-Weyl formula in App. A.4. In App. A.5, we include the remaining Hilbert series for our MLFV Case IV in Sec. 4.2.2, that have been computed using HilbCalc.

We highlight that a more comprehensive list of demonstration examples are provided in the notebook. It also collects a more complete list of the Hilbert series for the four cases of MLFV implementations discussed in Sec. 4.2.

A.1 Haar measure calculations

A Haar measure $\mathrm{d}\mu_G(x)$ is parametrized by r phase variables, $x = \{x_1, \cdots, x_r\}$, where r is the rank of the group G. In the Molien-Weyl formula in Eq. (A.1), each phase variable x_i is integrated over the contour of the unit circle. To compute a Haar measure with `HilbCalc`, one simply uses the function `HaarGroup` as

```
In[1]:= HaarGroup[gp,chvars]
```

As indicated above, two input arguments are required:

- `gp` is a `Symbol` that specifies the group G among `U1`, `SUn`, `SOn`, or `Spn`, where `n` is an integer. For instance, one can type `SU3`, `SO7`, `Sp10`, and so on.
- `chvars` is a `List` that contains the r variables parametrizing the Haar measure, *e.g.*, $\{x_1, x_2\}$ for a group with rank $r = 2$.

Let us compute a simple example—the Haar measure of $SU(3)$:

$$\text{In[2]:= HaarGroup[SU3,}\{x_1,x_2\}]$$

$$\text{Out[2]=} \quad \frac{\left(1-\frac{1}{x_1 x_2^2}\right)\left(1-\frac{1}{x_1^2 x_2}\right)\left(1-\frac{x_1}{x_2}\right)\left(1-\frac{x_2}{x_1}\right)\left(1-x_1^2 x_2\right)\left(1-x_1 x_2^2\right)}{6 x_1 x_2}$$

In case the integrand in the Molien-Weyl formula is symmetric under the Weyl group, the Haar measures can be further simplified or *reduced*. To get the reduced version of the Haar measures, one can use the function `HaarReducedGroup` instead as

$$\text{In[3]:= HaarReducedGroup[SU3,}\{x_1,x_2\}]$$

$$\text{Out[3]=} \quad \frac{\left(1-\frac{x_1}{x_2}\right)\left(1-x_1^2 x_2\right)\left(1-x_1 x_2^2\right)}{x_1 x_2}$$

To deal with a product group $G = G_1 \times G_2 \times \cdots \times G_k$, one uses the following two extended functions

```
In[4]:= HaarProductGroup[gplist,chvarsGps]
```

```
In[5]:= HaarReducedProductGroup[gplist,chvarsGps]
```

with input arguments given by

- `gplist` is a `List` of `gp`, *e.g.*, `{SU3,U1}`.
- `chvarsGps` is a `List` of `chvars`, such as `{{x1,x2},{x}}`.

Taking $SU(3) \times U(1)$ as an example, one can readily check that

```
In[6]:= HaarReducedProductGroup[{SU3,U1},{{x1,x2},{x}}]
```

$$\text{Out[6]=} \quad \frac{\left(1-\frac{x_1}{x_2}\right)\left(1-x_1^2 x_2\right)\left(1-x_1 x_2^2\right)}{x\ x_1 x_2}$$

A.2 Weyl character calculations

The Weyl character $\chi_{\mathrm{Irrep}_G}(x)$ depends on the irrep specified. In `HilbCalc`, we use the highest weight vectors to label irreps of a Lie algebra. We provide auxiliary functions to automatically translate between a highest weight vector and the Dynkin labels of an irrep, as the latter are also frequently used for referring to an irrep. Furthermore, we also provide a function for computing the dimension of irreps. For user convenience, we include a function that generates a table summarizing the Dynkin labels, dimensions, and highest weight vectors for the irreps of a given group, up to a specified maximum Dynkin label. These auxiliary functions are

```
In[7]:= DynkinLabelsFromIrrephwt[gp, irrephwt]
```

```
In[8]:= IrrephwtFromDynkinLabels[gp, dynkinlabels]
```

```
In[9]:= DimIrrephwt[gp, irrephwt]
```

```
In[10]:= IrrepTableGroup[gp, maxdynkinlabel]
```

In all cases, the first input argument `gp` specifies the group of interest, as explained in App. A.1. In addition, a second argument is required, as we explain below.

- `irrephwt` is a `List` of r components, being r the rank of the group. Taking $SU(3)$ for example, we have `{1,0}` for the fundamental irrep, `{1,1}` for the antifundamental, and `{2,1}` for the adjoint.[1]
- `dynkinlabels` is a `List` of r non-negative `Integers`.
- `maxdynkinlabel` is a non-negative `Integer` that that sets the maximum value for each component of the Dynkin labels of the irreps included in the table.

As an illustrative example, one can check the conversion from highest weight vector to Dynkin labels, and viceversa, for the adjoint irrep of $SU(3)$:

```
In[11]:= DynkinLabelsFromIrrephwt[SU3,{2,1}]
```

[1] For $SU(n = r + 1)$ groups, we embed the weight lattice in the $(r + 1)$-dimensional space, such that the components of the weight vectors are all integers. The $(r + 1)$-th component of a highest weight vector is zero, and we can view it as a vector with r components, as in the $SU(3)$ examples given above. With this convention, for a given $SU(n = r + 1)$ irrep, there is a convenient map between its highest weight vector and its Young diagram—the k-th component of `irrephwt` gives the number of boxes in the k-th row of the Young diagram.

```
Out[11]= {1,1}

In[12]:= IrrephwtFromDynkinLabels[SU3,{1,1}]

Out[12]= {2,1}
```

One can also generate a table of the $SU(3)$ irreps with Dynkin labels smaller than 2:

```
In[13]:= IrrepTableGroup[SU3,2]
```

Out[13]=

Summary of SU3 irreps

Dynkin Label	Dimension	Highest weight vector
$\{0,0\}$	1	$\{0,0\}$
$\{0,1\}$	3	$\{1,1\}$
$\{0,2\}$	6	$\{2,2\}$
$\{1,0\}$	3	$\{1,0\}$
$\{1,1\}$	8	$\{2,1\}$
$\{1,2\}$	15	$\{3,2\}$
$\{2,0\}$	6	$\{2,0\}$
$\{2,1\}$	15	$\{3,1\}$
$\{2,2\}$	27	$\{4,2\}$

With the irrep convention established, one can compute a Weyl character with the function

```
In[14]:= WeylChGroup[gp, chvars, irrephwt]
```

for a single group, and

```
In[15]:= WeylChProductGroup[gplist, chvarsGps, irrephwtGps]
```

for product groups, where `irrephwtGps` is a `List` of `irrephwt`, such as `{{1,0},{+1}}`. Coming back to our previous $SU(3)\times U(1)$ example, the Weyl character for the fundamental irrep with charge $+1$ reads

```
In[16]:= WeylChProductGroup[{SU3,U1},{{x1,x2},{x}}, {{1,0},{+1}}]
```

Out[16]= $x\, x_1 + \frac{x}{x_1 x_2} + x\, x_2$

A.3 Graded character of the polynomial ring in the building block fields

The remaining piece of the integrand in the Molien-Weyl formula, namely, $\chi_{\mathbf{r}_\Phi}(q,x)$, is the graded character of the polynomial ring in a set of building block fields `BBFlist`. It is a `List` of `BBF`, and each `BBF` is a `List` with the following three components.

- `BBF[[1]]` is a `Symbol` referring to the grading variable of the building block field, *e.g.*, ϕ or `q`.

- BBF[[2]] is an Integer that takes values 0 or 1 for Grassmann-even and Grassmann-odd fields, respectively.
- BBF[[3]] has the format of the irrephwtGps presented before, which is a List of highest weight vectors irrephwt.

Then, the graded character of a polynomial ring in a given set of building block fields can be readily computed for a single group or a product group by using

```
In[17]:= GradedRingChGroup[gp, chvars, BBFlist]
```

```
In[18]:= GradedRingChProductGroup[gplist, chvarsGps, BBFlist]
```

Let us consider our recurrent example $SU(3) \times U(1)$ from bosonic fundamental ϕ with charge +1 and antifundamental ϕ_d with charge -1. The graded character of the polynomial ring is given by

```
In[19]:= φBBF = {φ, 0, {{1,0}, {+1}}};
         φdBBF = {φd, 0, {{1,1}, {-1}}};
         GradedRingChProductGroup[{SU3,U1},{{x1,x2},{x}},{φBBF,φdBBF}]
```

Out[19]=
$$\frac{1}{\left(1-\mathrm{x}\mathrm{x}_1\phi\right)\left(1-\frac{\mathrm{x}\phi}{\mathrm{x}_1\mathrm{x}_2}\right)\left(1-\mathrm{x}\mathrm{x}_2\phi\right)\left(1-\frac{\phi_\mathrm{d}}{\mathrm{x}\mathrm{x}_1}\right)\left(1-\frac{\phi_\mathrm{d}}{\mathrm{x}\mathrm{x}_2}\right)\left(1-\frac{\mathrm{x}_1\mathrm{x}_2\phi_\mathrm{d}}{\mathrm{x}}\right)}$$

A.4 Hilbert series evaluations

Finally, we present the main functions of HilbCalc. These are

```
In[20]:= HilbertSeriesBBFGRCh[gplist, chvarsGps, irrephwtGps, BBFgrch]
```

```
In[21]:= HilbertSeriesBBFlist[gplist, chvarsGps, irrephwtGps, BBFlist]
```

The sole difference between these two functions is in their last input argument. The former requires to take the graded character of the polynomial ring BBFgrch computed separately as an input; the latter directly takes the list of building block fields BBFlist as an input. One should notice that the input argument irrephwtGps here refers to the goal irrep for which we are computing the Hilbert—it is not about the irreps of the building block fields.

It is instructive to present a simple example computation to clearly illustrate the different calls of our main functions—the multi-graded Hilbert series for $SU(3)$ invariants made out of bosonic fundamental ϕ and antifundamental ϕ_d. We have

```
In[22]:= gplist = {SU3}
         chvarsGps = {{x1,x2}}
         irrephwtGps = {{0,0}}
         φBBF = {φ, 0, {{1,0}}}
         φdBBF = {φd, 0, {{1,1}}}
         BBFlist = {φBBF, φdBBF}
         BBFGRCh = GradedRingChProductGroup[gplistchvarsGpsBBFlist]
```

where the last line uses the function explained in App. A.3 to compute the graded character BBFgrch of the polynomial ring in ϕ and $\phi_\mathtt{d}$. After evaluating the above entries, we can call the two main functions:

```
In[23]:= HilbertSeriesBBFGRCh[gplist,chvarsGps,irrephwtGps,BBFGRCh]
```

```
In[23]:= HilbertSeriesBBFlist[gplist,chvarsGps,irrephwtGps,BBFlist]
```

They both yield

$$\text{Out[23]=}\quad -\frac{1}{-1+\phi\phi_\mathtt{d}}$$

Although the second main function is clearly more direct, the first one might be useful when we are given a fixed set of building block fields and want to compute the Hilbert series for different goal irreps, as encountered in the case of calculating the MLFV Hilbert series.

A.5 More Hilbert series for spurions $S_{\mathrm{IV}} = \{Y_e\,, Y_e^\dagger, Y_\nu\,, Y_\nu^\dagger, M_R, M_R^\dagger\}$

Some single-graded Hilbert series for the MLFV Case IV in Table 4.1 have already been presented in Sec. 4.2.2. Those that correspond to the remaining relevant covariants read:

$$\mathcal{H}_{(\mathbf{3},\bar{\mathbf{3}},\mathbf{1})} = \frac{1}{D(q)}\, q \begin{pmatrix} 1+2q^2+6q^4+17q^6+49q^8 \\ +134q^{10}+350q^{12}+840q^{14}+1884q^{16}+3945q^{18} \\ +7804q^{20}+14617q^{22}+26075q^{24}+44374q^{26}+72312q^{28} \\ +113032q^{30}+169916q^{32}+246022q^{34}+343750q^{36}+464054q^{38} \\ +606096q^{40}+766599q^{42}+939899q^{44}+1117832q^{46}+1290454q^{48} \\ +1446692q^{50}+1575652q^{52}+1667681q^{54}+1715623q^{56}+1715623q^{58} \\ +1667681q^{60}+1575652q^{62}+1446692q^{64}+1290454q^{66}+1117832q^{68} \\ +939899q^{70}+766599q^{72}+606096q^{74}+464054q^{76}+343750q^{78} \\ +246022q^{80}+169916q^{82}+113032q^{84}+72312q^{86}+44374q^{88} \\ +26075q^{90}+14617q^{92}+7804q^{94}+3945q^{96}+1884q^{98} \\ +840q^{100}+350q^{102}+134q^{104}+49q^{106}+17q^{108} \\ +6q^{110}+2q^{112}+q^{114} \end{pmatrix}, \tag{A.2a}$$

$$\mathcal{H}_{(\mathbf{3},\mathbf{1},\bar{\mathbf{3}})} = \frac{1}{D(q)}\, q \begin{pmatrix} 1+3q^2+10q^4+29q^6+85q^8 \\ +227q^{10}+565q^{12}+1301q^{14}+2808q^{16}+5694q^{18} \\ +10927q^{20}+19911q^{22}+34597q^{24}+57471q^{26}+91526q^{28} \\ +140038q^{30}+206279q^{32}+293018q^{34}+401993q^{36}+533306q^{38} \\ +684938q^{40}+852425q^{42}+1028814q^{44}+1204999q^{46}+1370374q^{48} \\ +1513873q^{50}+1625094q^{52}+1695561q^{54}+1719690q^{56}+1695561q^{58} \\ +1625094q^{60}+1513873q^{62}+1370374q^{64}+1204999q^{66}+1028814q^{68} \\ +852425q^{70}+684938q^{72}+533306q^{74}+401993q^{76}+293018q^{78} \\ +206279q^{80}+140038q^{82}+91526q^{84}+57471q^{86}+34597q^{88} \\ +19911q^{90}+10927q^{92}+5694q^{94}+2808q^{96}+1301q^{98} \\ +565q^{100}+227q^{102}+85q^{104}+29q^{106}+10q^{108} \\ +3q^{110}+q^{112} \end{pmatrix}, \tag{A.2b}$$

$$\mathcal{H}_{(\mathbf{1},\bar{\mathbf{3}},\mathbf{3})} = \frac{1}{D(q)}\, q^2 \left(\begin{array}{c} 1 + 3q^2 + 10q^4 + 29q^6 + 85q^8 \\ +227q^{10} + 565q^{12} + 1301q^{14} + 2808q^{16} + 5694q^{18} \\ +10927q^{20} + 19911q^{22} + 34597q^{24} + 57471q^{26} + 91526q^{28} \\ +140038q^{30} + 206279q^{32} + 293018q^{34} + 401993q^{36} + 533306q^{38} \\ +684938q^{40} + 852425q^{42} + 1028814q^{44} + 1204999q^{46} + 1370374q^{48} \\ +1513873q^{50} + 1625094q^{52} + 1695561q^{54} + 1719690q^{56} + 1695561q^{58} \\ +1625094q^{60} + 1513873q^{62} + 1370374q^{64} + 1204999q^{66} + 1028814q^{68} \\ +852425q^{70} + 684938q^{72} + 533306q^{74} + 401993q^{76} + 293018q^{78} \\ +206279q^{80} + 140038q^{82} + 91526q^{84} + 57471q^{86} + 34597q^{88} \\ +19911q^{90} + 10927q^{92} + 5694q^{94} + 2808q^{96} + 1301q^{98} \\ +565q^{100} + 227q^{102} + 85q^{104} + 29q^{106} + 10q^{108} \\ +3q^{110} + q^{112} \end{array} \right), \tag{A.2c}$$

$$\mathcal{H}_{(\bar{\mathbf{3}},\bar{\mathbf{3}},\bar{\mathbf{3}})} = \frac{1}{D(q)}\, q^2 \left(\begin{array}{c} 1 + 5q^2 + 18q^4 + 60q^6 + 187q^8 \\ +534q^{10} + 1391q^{12} + 3326q^{14} + 7385q^{16} + 15337q^{18} \\ +30005q^{20} + 55565q^{22} + 97839q^{24} + 164360q^{26} + 264230q^{28} \\ +407535q^{30} + 604396q^{32} + 863519q^{34} + 1190500q^{36} + 1585985q^{38} \\ +2044114q^{40} + 2551484q^{42} + 3087009q^{44} + 3622873q^{46} + 4126606q^{48} \\ +4564184q^{50} + 4903632q^{52} + 5118801q^{54} + 5192510q^{56} + 5118801q^{58} \\ +4903632q^{60} + 4564184q^{62} + 4126606q^{64} + 3622873q^{66} + 3087009q^{68} \\ +2551484q^{70} + 2044114q^{72} + 1585985q^{74} + 1190500q^{76} + 863519q^{78} \\ +604396q^{80} + 407535q^{82} + 264230q^{84} + 164360q^{86} + 97839q^{88} \\ +55565q^{90} + 30005q^{92} + 15337q^{94} + 7385q^{96} + 3326q^{98} \\ +1391q^{100} + 534q^{102} + 187q^{104} + 60q^{106} + 18q^{108} \\ +5q^{110} + q^{112} \end{array} \right), \tag{A.2d}$$

$$\mathcal{H}_{(\mathbf{6},\bar{\mathbf{3}},\bar{\mathbf{3}})} = \frac{1}{D(q)}\, q^2 \left(\begin{array}{c} 1 + 5q^2 + 22q^4 + 79q^6 + 263q^8 \\ +789q^{10} + 2153q^{12} + 5362q^{14} + 12317q^{16} + 26332q^{18} \\ +52792q^{20} + 99846q^{22} + 179004q^{24} + 305426q^{26} + 497663q^{28} \\ +776610q^{30} + 1163530q^{32} + 1677151q^{34} + 2330050q^{36} + 3124799q^{38} \\ +4050510q^{40} + 5080558q^{42} + 6172107q^{44} + 7267977q^{46} + 8300935q^{48} \\ +9200124q^{50} + 9898773q^{52} + 10342078q^{54} + 10494032q^{56} + 10342078q^{58} \\ +9898773q^{60} + 9200124q^{62} + 8300935q^{64} + 7267977q^{66} + 6172107q^{68} \\ +5080558q^{70} + 4050510q^{72} + 3124799q^{74} + 2330050q^{76} + 1677151q^{78} \\ +1163530q^{80} + 776610q^{82} + 497663q^{84} + 305426q^{86} + 179004q^{88} \\ +99846q^{90} + 52792q^{92} + 26332q^{94} + 12317q^{96} + 5362q^{98} \\ +2153q^{100} + 789q^{102} + 263q^{104} + 79q^{106} + 22q^{108} \\ +5q^{110} + q^{112} \end{array} \right), \tag{A.2e}$$

$$\mathcal{H}_{(\mathbf{8},\mathbf{1},\mathbf{1})} = \frac{1}{D(q)}\, q^2 \begin{pmatrix} 2 + 5q^2 + 12q^4 + 40q^6 + 112q^8 \\ +289q^{10} + 714q^{12} + 1611q^{14} + 3393q^{16} + 6766q^{18} \\ +12737q^{20} + 22782q^{22} + 38933q^{24} + 63600q^{26} + 99615q^{28} \\ +150049q^{30} + 217608q^{32} + 304399q^{34} + 411450q^{36} + 537876q^{38} \\ +680816q^{40} + 835311q^{42} + 993980q^{44} + 1147895q^{46} + 1287364q^{48} \\ +1402451q^{50} + 1484543q^{52} + 1527391q^{54} + 1527391q^{56} + 1484543q^{58} \\ +1402451q^{60} + 1287364q^{62} + 1147895q^{64} + 993980q^{66} + 835311q^{68} \\ +680816q^{70} + 537876q^{72} + 411450q^{74} + 304399q^{76} + 217608q^{78} \\ +150049q^{80} + 99615q^{82} + 63600q^{84} + 38933q^{86} + 22782q^{88} \\ +12737q^{90} + 6766q^{92} + 3393q^{94} + 1611q^{96} + 714q^{98} \\ +289q^{100} + 112q^{102} + 40q^{104} + 12q^{106} + 5q^{108} \\ +2q^{110} \end{pmatrix}, \tag{A.2f}$$

$$\mathcal{H}_{(\mathbf{1},\mathbf{8},\mathbf{1})} = \frac{1}{D(q)}\, q^2 \begin{pmatrix} 1 + 2q^2 + 5q^4 + 17q^6 + 48q^8 \\ +129q^{10} + 341q^{12} + 818q^{14} + 1823q^{16} + 3819q^{18} \\ +7531q^{20} + 14065q^{22} + 25037q^{24} + 42494q^{26} + 69019q^{28} \\ +107591q^{30} + 161204q^{32} + 232605q^{34} + 323883q^{36} + 435640q^{38} \\ +566745q^{40} + 713995q^{42} + 871679q^{44} + 1032049q^{46} + 1185866q^{48} \\ +1322840q^{50} + 1433093q^{52} + 1508353q^{54} + 1542422q^{56} + 1532485q^{58} \\ +1479449q^{60} + 1387420q^{62} + 1263554q^{64} + 1117253q^{66} + 958504q^{68} \\ +797340q^{70} + 642747q^{72} + 501508q^{74} + 378271q^{76} + 275530q^{78} \\ +193418q^{80} + 130565q^{82} + 84618q^{84} + 52445q^{86} + 30957q^{88} \\ +17363q^{90} + 9176q^{92} + 4511q^{94} + 2065q^{96} + 846q^{98} \\ +288q^{100} + 77q^{102} + 8q^{104} - 12q^{106} - 5q^{108} \\ -3q^{110} - 3q^{112} - q^{118} \end{pmatrix}, \tag{A.2g}$$

$$\mathcal{H}_{(\mathbf{1},\mathbf{1},\mathbf{8})} = \frac{1}{D(q)}\, q^2 \begin{pmatrix} 2 + 6q^2 + 17q^4 + 55q^6 + 147q^8 \\ +362q^{10} + 855q^{12} + 1866q^{14} + 3828q^{16} + 7470q^{18} \\ +13812q^{20} + 24335q^{22} + 41056q^{24} + 66350q^{26} + 102994q^{28} \\ +153978q^{30} + 221909q^{32} + 308789q^{34} + 415557q^{36} + 541264q^{38} \\ +683030q^{40} + 835922q^{42} + 992658q^{44} + 1144473q^{46} + 1281880q^{48} \\ +1395164q^{50} + 1475916q^{52} + 1518049q^{54} + 1518049q^{56} + 1475916q^{58} \\ +1395164q^{60} + 1281880q^{62} + 1144473q^{64} + 992658q^{66} + 835922q^{68} \\ +683030q^{70} + 541264q^{72} + 415557q^{74} + 308789q^{76} + 221909q^{78} \\ +153978q^{80} + 102994q^{82} + 66350q^{84} + 41056q^{86} + 24335q^{88} \\ +13812q^{90} + 7470q^{92} + 3828q^{94} + 1866q^{96} + 855q^{98} \\ +362q^{100} + 147q^{102} + 55q^{104} + 17q^{106} + 6q^{108} + 2q^{110} \end{pmatrix}, \tag{A.2h}$$

$$\mathcal{H}_{(\mathbf{8},\mathbf{8},\mathbf{1})} = \frac{1}{D(q)}\,q^2 \begin{pmatrix} 1+6q^2+21q^4+66q^6+211q^8 \\ +642q^{10}+1794q^{12}+4605q^{14}+10879q^{16}+23850q^{18} \\ +48978q^{20}+94762q^{22}+173526q^{24}+302042q^{26}+501409q^{28} \\ +796121q^{30}+1212242q^{32}+1774100q^{34}+2500075q^{36}+3398116q^{38} \\ +4461005q^{40}+5662924q^{42}+6958390q^{44}+8283152q^{46}+9558406q^{48} \\ +10698365q^{50}+11619006q^{52}+12247840q^{54}+12533352q^{56}+12451260q^{58} \\ +12007813q^{60}+11239510q^{62}+10207802q^{64}+8991266q^{66}+7676604q^{68} \\ +6348371q^{70}+5080394q^{72}+3930093q^{74}+2934908q^{76}+2112248q^{78} \\ +1462265q^{80}+971443q^{82}+617446q^{84}+374142q^{86}+215164q^{88} \\ +116692q^{90}+59222q^{92}+27807q^{94}+11827q^{96}+4402q^{98} \\ +1324q^{100}+223q^{102}-60q^{104}-73q^{106}-44q^{108}-19q^{110} \\ -6q^{112}-4q^{114}-2q^{116} \end{pmatrix}, \tag{A.2i}$$

$$\mathcal{H}_{(\mathbf{8},\mathbf{1},\mathbf{8})} = \frac{1}{D(q)}\,q^2 \begin{pmatrix} 1+11q^2+53q^4+192q^6+618q^8 \\ +1765q^{10}+4531q^{12}+10692q^{14}+23397q^{16}+47841q^{18} \\ +92146q^{20}+168024q^{22}+291252q^{24}+481825q^{26}+763013q^{28} \\ +1159515q^{30}+1694813q^{32}+2387110q^{34}+3244911q^{36}+4263103q^{38} \\ +5419291q^{40}+6672187q^{42}+7962912q^{44}+9218234q^{46}+10356836q^{48} \\ +11298070q^{50}+11970601q^{52}+12321008q^{54}+12321008q^{56}+11970601q^{58} \\ +11298070q^{60}+10356836q^{62}+9218234q^{64}+7962912q^{66}+6672187q^{68} \\ +5419291q^{70}+4263103q^{72}+3244911q^{74}+2387110q^{76}+1694813q^{78} \\ +1159515q^{80}+763013q^{82}+481825q^{84}+291252q^{86}+168024q^{88} \\ +92146q^{90}+47841q^{92}+23397q^{94}+10692q^{96}+4531q^{98} \\ +1765q^{100}+618q^{102}+192q^{104}+53q^{106}+11q^{108}+q^{110} \end{pmatrix}, \tag{A.2j}$$

$$\mathcal{H}_{(\mathbf{1},\mathbf{8},\mathbf{8})} = \frac{1}{D(q)}\,q^4 \begin{pmatrix} 3+17q^2+68q^4+241q^6+748q^8 \\ +2072q^{10}+5239q^{12}+12196q^{14}+26370q^{16}+53445q^{18} \\ +102130q^{20}+184889q^{22}+318496q^{24}+523840q^{26}+824951q^{28} \\ +1247143q^{30}+1813728q^{32}+2541921q^{34}+3438559q^{36}+4495578q^{38} \\ +5686764q^{40}+6966845q^{42}+8272540q^{44}+9526785q^{46}+10646058q^{48} \\ +11548761q^{50}+12164637q^{52}+12443893q^{54}+12363141q^{56}+11928468q^{58} \\ +11175185q^{60}+10162800q^{62}+8967543q^{64}+7673690q^{66}+6363636q^{68} \\ +5109663q^{70}+3968445q^{72}+2977438q^{74}+2154635q^{76}+1501165q^{78} \\ +1004704q^{80}+644098q^{82}+394197q^{84}+229314q^{86}+126009q^{88} \\ +64902q^{90}+30976q^{92}+13413q^{94}+5088q^{96}+1558q^{98} \\ +261q^{100}-90q^{102}-115q^{104}-77q^{106}-38q^{108} \\ -14q^{110}-6q^{112}-2q^{114} \end{pmatrix}, \tag{A.2k}$$

$$\mathcal{H}_{(\mathbf{27},\mathbf{1},\mathbf{1})} = \frac{1}{D(q)}\, q^4 \left(\begin{array}{c} 3 + 11q^2 + 43q^4 + 144q^6 + 450q^8 \\ +1247q^{10} + 3160q^{12} + 7309q^{14} + 15717q^{16} + 31534q^{18} \\ +59603q^{20} + 106489q^{22} + 180873q^{24} + 292898q^{26} + 453886q^{28} \\ +674573q^{30} + 963970q^{32} + 1326706q^{34} + 1761692q^{36} + 2259769q^{38} \\ +2803593q^{40} + 3367158q^{42} + 3918081q^{44} + 4419761q^{46} + 4835781q^{48} \\ +5133621q^{50} + 5289064q^{52} + 5289064q^{54} + 5133621q^{56} + 4835781q^{58} \\ +4419761q^{60} + 3918081q^{62} + 3367158q^{64} + 2803593q^{66} + 2259769q^{68} \\ +1761692q^{70} + 1326706q^{72} + 963970q^{74} + 674573q^{76} + 453886q^{78} \\ +292898q^{80} + 180873q^{82} + 106489q^{84} + 59603q^{86} + 31534q^{88} \\ +15717q^{90} + 7309q^{92} + 3160q^{94} + 1247q^{96} + 450q^{98} \\ +144q^{100} + 43q^{102} + 11q^{104} + 3q^{106} \end{array} \right), \tag{A.2l}$$

$$\mathcal{H}_{(\mathbf{1},\mathbf{27},\mathbf{1})} = \frac{1}{D(q)}\, q^4 \left(\begin{array}{c} 1 + 2q^2 + 8q^4 + 26q^6 + 86q^8 \\ +261q^{10} + 751q^{12} + 1953q^{14} + 4694q^{16} + 10414q^{18} \\ +21637q^{20} + 42206q^{22} + 77874q^{24} + 136246q^{26} + 227110q^{28} \\ +361556q^{30} + 551490q^{32} + 807563q^{34} + 1137804q^{36} + 1544738q^{38} \\ +2024038q^{40} + 2562314q^{42} + 3137396q^{44} + 3718391q^{46} + 4268636q^{48} \\ +4748621q^{50} + 5120979q^{52} + 5354610q^{54} + 5429035q^{56} + 5337006q^{58} \\ +5085679q^{60} + 4695810q^{62} + 4198772q^{64} + 3632883q^{66} + 3038298q^{68} \\ +2453038q^{70} + 1908536q^{72} + 1427889q^{74} + 1024161q^{76} + 701624q^{78} \\ +456541q^{80} + 280052q^{82} + 159908q^{84} + 83269q^{86} + 37831q^{88} \\ +13366q^{90} + 1777q^{92} - 2554q^{94} - 3363q^{96} - 2760q^{98} - 1858q^{100} \\ -1084q^{102} - 562q^{104} - 258q^{106} - 106q^{108} - 40q^{110} \\ -15q^{112} - 5q^{114} - 2q^{116} - q^{118} \end{array} \right), \tag{A.2m}$$

$$\mathcal{H}_{(\mathbf{1},\mathbf{1},\mathbf{27})} = \frac{1}{D(q)}\, q^2 \left(\begin{array}{c} 1 + 7q^2 + 26q^4 + 95q^6 + 290q^8 \\ +809q^{10} + 2029q^{12} + 4728q^{14} + 10214q^{16} + 20735q^{18} \\ +39649q^{20} + 71948q^{22} + 124208q^{24} + 204900q^{26} + 323684q^{28} \\ +491100q^{30} + 716847q^{32} + 1008738q^{34} + 1370233q^{36} + 1799319q^{38} \\ +2286404q^{40} + 2814348q^{42} + 3358130q^{44} + 3887064q^{46} + 4366822q^{48} \\ +4763465q^{50} + 5046825q^{52} + 5194518q^{54} + 5194518q^{56} + 5046825q^{58} \\ +4763465q^{60} + 4366822q^{62} + 3887064q^{64} + 3358130q^{66} + 2814348q^{68} \\ +2286404q^{70} + 1799319q^{72} + 1370233q^{74} + 1008738q^{76} + 716847q^{78} \\ +491100q^{80} + 323684q^{82} + 204900q^{84} + 124208q^{86} + 71948q^{88} \\ +39649q^{90} + 20735q^{92} + 10214q^{94} + 4728q^{96} + 2029q^{98} \\ +809q^{100} + 290q^{102} + 95q^{104} + 26q^{106} + 7q^{108} + q^{110} \end{array} \right), \tag{A.2n}$$

where the denominator factor is given by

$$\frac{1}{D(q)} = \frac{1}{(1-q^2)^3\,(1-q^4)^4\,(1-q^6)^4\,(1-q^8)^2\,(1-q^{10})^2\,(1-q^{12})^3\,(1-q^{14})^2\,(1-q^{16})}\,. \tag{A.3}$$

B | Unitary bidiagonalization

Any arbitrary complex matrix can be diagonalized by means of two different unitary transformations, acting on the left and on the right, with real and positive eigenvalues. This procedure is known as unitary bidiagonalization.

Let M be an arbitrary complex matrix. The Hermitian combinations $MM^\dagger$ and $M^\dagger M$ are diagonalized through unitary transformations U_L and U_R, respectively. Their eigenvalues are real (due to hermiticity) and non-negative, since

$$\left.\begin{aligned} &\vec{u}^\dagger MM^\dagger \vec{u} = \lambda_{\vec{u}}\ \vec{u}^\dagger \cdot \vec{u} = \lambda_{\vec{u}} \left\|\vec{u}\right\|^2 = \lambda_{\vec{u}} \\ &\vec{u}^\dagger MM^\dagger \vec{u} = \left\|M^\dagger \vec{u}\right\|^2 \geq 0 \end{aligned}\right\} \quad \lambda_{\vec{u}} \geq 0\,, \tag{B.1}$$

$$\left.\begin{aligned} &\vec{v}^\dagger M^\dagger M \vec{v} = \lambda_{\vec{v}}\ \vec{v}^\dagger \cdot \vec{v} = \lambda_{\vec{v}} \left\|\vec{v}\right\|^2 = \lambda_{\vec{v}} \\ &\vec{v}^\dagger M^\dagger M \vec{v} = \left\|M \vec{v}\right\|^2 \geq 0 \end{aligned}\right\} \quad \lambda_{\vec{v}} \geq 0\,, \tag{B.2}$$

where $\vec{u}$ and $\vec{v}$ are (normalized) eigenvectors of $MM^\dagger$ and $M^\dagger M$ with eigenvalues $\lambda_{\vec{u}}$ and $\lambda_{\vec{v}}$, respectively. As both $MM^\dagger$ and $M^\dagger M$ share the same characteristic polynomial, they have common real and non-negative eigenvalues, which we can simply denote as m_i^2. Therefore, we can write

$$U_L^\dagger MM^\dagger U_L = U_R^\dagger M^\dagger M U_R = D = \mathrm{diag}\left(m_1^2, m_2^2, \dots\right)\,, \quad m_i^2 \in \mathbb{R}\,,\ m_i^2 \geq 0\,. \tag{B.3}$$

From the previous line, we obtain

$$D = U_L^\dagger MM^\dagger U_L = \left(U_L^\dagger M U_R\right)\left(U_L^\dagger M U_R\right)^\dagger = \hat{M}_D \hat{M}_D^\dagger \quad \longrightarrow \quad D\hat{M}_D = \hat{M}_D \hat{M}_D^\dagger \hat{M}_D\,, \tag{B.4}$$

$$D = U_R^\dagger M^\dagger M U_R = \left(U_L^\dagger M U_R\right)^\dagger \left(U_L^\dagger M U_R\right) = \hat{M}_D^\dagger \hat{M}_D \quad \longrightarrow \quad \hat{M}_D D = \hat{M}_D \hat{M}_D^\dagger \hat{M}_D\,, \tag{B.5}$$

where we have defined $\hat{M}_D \equiv U_L^\dagger M U_R$, yielding

$$D\hat{M}_D - \hat{M}_D D = 0 \quad \longrightarrow \quad \left(D_{ii} - D_{jj}\right)\left(\hat{M}_D\right)_{ij} = 0\,. \tag{B.6}$$

Assuming that the elements of D are all different and non-vanishing, Eq. (B.6) implies that $\left(\hat{M}_D\right)_{ij} = 0$ for $i \neq j$, that is, $\hat{M}_D$ is also a diagonal matrix with $\left(\hat{M}_D\right)_{ii} = m_i\, e^{i\varphi_i}$, being $m_i \in \mathbb{R}^+$. Taking into account the definition of $\hat{M}_D$, we are left with

$$U_L^\dagger M U_R = C M_D = M_D C\,, \tag{B.7}$$

where $M_D \equiv \mathrm{diag}\left(m_1, m_2, \dots\right)$ and $C \equiv \mathrm{diag}\left(e^{i\varphi_1}, e^{i\varphi_2}, \dots\right)$. An additional diagonal rephasing is required in order to remove the phases in C.

Similarly, it is straightforward to apply this procedure to an arbitrary real matrix M. In this case, the symmetric combinations MM^T and M^TM are diagonalized through orthogonal transformations O_L and O_R, respectively, as

$$O_L^T M M^T O_L = O_R^T M^T M O_R = D = \mathrm{diag}\left(m_1^2, m_2^2, \dots\right) , \quad m_i^2 \in \mathbb{R} ,\ m_i^2 \geq 0 , \tag{B.8}$$

thus leading to

$$O_L^T M O_R = M_D = \mathrm{diag}\left(m_1, m_2, \dots\right) , \quad m_i \in \mathbb{R}^+ . \tag{B.9}$$

Notice that no additional diagonal rephasing is left in the real scenario.

Let us finally stress that two important assumptions have been made in the previous argument, namely, that the combinations $MM^\dagger$ (MM^T) and $M^\dagger M$ (M^TM) have (i) non-degenerate, and (ii) non-vanishing eigenvalues.

C | Orthogonal matrices $O(3,\mathbb{R})$

Matrices $O \in SO(3,\mathbb{R})$ can be parametrized as $O = e^{\alpha A}$, with $\alpha \in [0, 2\pi)$ and A a normalized real antisymmetric matrix of the form

$$A = \begin{pmatrix} 0 & \hat{n}_3 & -\hat{n}_2 \\ -\hat{n}_3 & 0 & \hat{n}_1 \\ \hat{n}_2 & -\hat{n}_1 & 0 \end{pmatrix}, \qquad \hat{n}_j \in \mathbb{R}\,, \qquad \hat{n}_1^2 + \hat{n}_2^2 + \hat{n}_3^2 = 1\,. \tag{C.1}$$

It is easy to check that the eigenvalues of A and their corresponding normalized eigenvectors are

$$\lambda_0 = 0\,, \qquad \vec{v}_0^{\,T} = (\hat{n}_1, \hat{n}_2, \hat{n}_3) = (\sin\vartheta\cos\varphi, \sin\vartheta\sin\varphi, \cos\vartheta)\,, \tag{C.2}$$

$$\lambda_+ = i\,, \qquad \vec{v}_+^{\,T} = \frac{1}{\sqrt{2}}(-\cos\vartheta\cos\varphi + i\sin\varphi, -\cos\vartheta\sin\varphi - i\cos\varphi, \sin\vartheta)\,, \tag{C.3}$$

$$\lambda_- = -i\,, \qquad \vec{v}_- = (\vec{v}_+)^*\,, \tag{C.4}$$

where, for convenience, we have parametrized the real unit vector $(\hat{n}_1, \hat{n}_2, \hat{n}_3)$ using spherical coordinates. Since the eigenvectors $\{\vec{v}_0, \vec{v}_+, \vec{v}_-\}$ are orthonormal,[1] A is diagonalized with a unitary transformation U as

$$U^\dagger A U = \mathrm{diag}(0, i, -i)\,, \qquad \text{with} \qquad U = \begin{pmatrix} \uparrow & \uparrow & \uparrow \\ \vec{v}_0 & \vec{v}_+ & \vec{v}_- \\ \downarrow & \downarrow & \downarrow \end{pmatrix}. \tag{C.5}$$

Then, the eigenvalues of $O = e^{\alpha A}$ are $\{1, e^{i\alpha}, e^{-i\alpha}\}$, with corresponding eigenvectors $\{\vec{v}_0, \vec{v}_+, \vec{v}_-\}$ given above. Its unitary diagonalization reads

$$U^\dagger O U = \mathrm{diag}(1, e^{i\alpha}, e^{-i\alpha})\,. \tag{C.6}$$

Geometrically, O represents a rotation of angle α in $\mathbb{R}^3$ along the direction $(\hat{n}_1, \hat{n}_2, \hat{n}_3)$—in terms of A, one has the compact expression $O = 1 + A\sin\alpha + A^2(1-\cos\alpha)$.

From the previous construction, it is clear that the eigenvectors of O do not depend on α, meaning that $O_1 = \exp(\alpha_1 A)$ and $O_2 = \exp(\alpha_2 A)$, with $\alpha_1 \neq \alpha_2$ and the same A in Eq. (C.1), can be simultaneously diagonalized by the same unitary transformation.

Finally, note also that, if $O' \in O(3,\mathbb{R})$ with $\det O' = -1$, *i.e.*, $O' \notin SO(3,\mathbb{R})$, the previous discussion applies straightforwardly taking into account that $-O' \in SO(3,\mathbb{R})$.

[1] This is guaranteed since $\vec{v}_j$ ($j = 0, \pm$) are eigenvectors of the real symmetric (semipositive definite) matrix $A^T A$.

D Renormalization Group Evolution

The particular structure of the Yukawa matrices of the model presented in chapter 6, and consequently, the $\mu-\tau$ symmetric character of the PMNS mixing, does not derive from an imposed symmetry in the Lagrangian. Hence, it is important to analyze how this picture is changed under one-loop renormalization group evolution, with particular focus on: (i) the potential appearance of SFCNC at one-loop, (ii) the possibility to avoid SFCNC, while maintaining the essential ingredients of the model, if we depart from its minimal implementation with only two Higgs doublets.

The one-loop renormalization group equations of the lepton Yukawa couplings are

$$\begin{aligned}\mathcal{D}Y_a^\ell &= c_\ell Y_a^\ell + \sum_{j=1}^{n}\left[3\,\mathrm{tr}\left(Y_a^\ell Y_j^{\ell\dagger}+Y_a^{\nu\dagger}Y_j^\nu\right)+\mathrm{tr}\left(Y_a^\ell Y_j^{\ell\dagger}+Y_a^{\nu\dagger}Y_j^\nu\right)\right]Y_j^\ell \\ &+\sum_{j=1}^{n}\left[-2Y_j^\nu Y_a^{\nu\dagger}Y_j^\ell + Y_a^\ell Y_j^{\ell\dagger}Y_j^\ell+\frac{1}{2}Y_j^\nu Y_j^{\nu\dagger}Y_a^\ell+\frac{1}{2}Y_j^\ell Y_j^{\ell\dagger}Y_a^\ell\right],\end{aligned} \tag{D.1}$$

$$\begin{aligned}\mathcal{D}Y_a^\nu &= c_\nu Y_a^\nu + \sum_{j=1}^{n}\left[3\,\mathrm{tr}\left(Y_a^\nu Y_j^{\ell\dagger}+Y_a^{\nu\dagger}Y_j^\nu\right)+\mathrm{tr}\left(Y_a^\ell Y_j^{\ell\dagger}+Y_a^{\nu\dagger}Y_j^\nu\right)\right]Y_j^\nu \\ &+\sum_{j=1}^{n}\left[-2Y_j^\ell Y_a^{\ell\dagger}Y_j^\nu + Y_a^\nu Y_j^{\nu\dagger}Y_j^\nu+\frac{1}{2}Y_j^\ell Y_j^{\ell\dagger}Y_a^\nu+\frac{1}{2}Y_j^\nu Y_j^{\nu\dagger}Y_a^\nu\right],\end{aligned} \tag{D.2}$$

where c_ℓ and c_ν are linear combinations of the squared of the gauge couplings $\{g_s, g, g'\}$, the number of Higgs doublets is n, and $\mathcal{D}\equiv 16\pi^2\frac{\mathrm{d}}{\mathrm{d}\ln\mu}$, with μ the energy scale.

From Eqs. (D.1) and (D.2), it is clear that SFCNC arise through one-loop RGE: if flavor conservation is imposed at some scale μ_{FC}, one would expect SFCNC at a scale μ proportional to $\ln(\mu/\mu_{\mathrm{FC}})$, which might be sufficient to keep them under control. One can readily check that, indeed, the terms that introduce deviations from flavor conservation involve the products of three Yukawa matrices in the second line of Eqs. (D.1) and (D.2). However, the terms $Y_a^\ell Y_j^{\ell\dagger}Y_j^\ell$ and $Y_j^\ell Y_j^{\ell\dagger}Y_a^\ell$ have the same structure as Y_a^ℓ in Eq. (6.32), and thus are simultaneously diagonalized unitarily, while the terms $Y_a^\nu Y_j^{\nu\dagger}Y_j^\nu$ and $Y_j^\nu Y_j^{\nu\dagger}Y_a^\nu$ are diagonal like Y_a^ν. Therefore, these pieces do not generate SFCNC at one-loop. On the contrary, from the point of view of flavor conservation, the potential source of concern are the terms $Y_j^\nu Y_a^{\nu\dagger}Y_j^\ell$ and $Y_j^\nu Y_j^{\nu\dagger}Y_a^\ell$ in Eq. (D.1), as well as $Y_j^\ell Y_a^{\ell\dagger}Y_j^\nu$ and $Y_j^\ell Y_j^{\ell\dagger}Y_a^\nu$ in Eq. (D.2). On the one hand, one can get rid of the terms $Y_j^\nu Y_a^{\nu\dagger}Y_j^\ell$ and $Y_j^\ell Y_a^{\ell\dagger}Y_j^\nu$ if no Higgs doublet couples simultaneously to e_R^0 and ν_R^0. On the other hand, the latter condition does not eliminate the terms $Y_j^\nu Y_j^{\nu\dagger}Y_a^\ell$ and $Y_j^\ell Y_j^{\ell\dagger}Y_a^\nu$. In fact, since the combinations $Y_j^\nu Y_j^{\nu\dagger}$ and $Y_j^\ell Y_j^{\ell\dagger}$ are guaranteed to be non-vanishing, one would need them to be proportional to the identity matrix in order to avoid the appearance of SFCNC.

Let us consider an example scenario with five Higgs doublets and Dirac neutrinos where SFCNC do not arise through RGE, the only source of CP violation is the vacuum, and the PMNS matrix is

CP-violating. In this model, the real Yukawa couplings read

$$\ell \text{ sector:} \quad Y_1^\ell = \lambda_1 O_{\ell 1}\,, \quad Y_2^\ell = \lambda_2 O_{\ell 2}\,, \quad Y_j^\ell = 0 \;\; (j = 3,4,5)\,, \tag{D.3}$$

$$\nu \text{ sector:} \quad Y_j^\nu = 0 \;\; (j = 1,2)\,, \quad Y_3^\nu = O_\nu^T \mathrm{diag}(y,0,0)\,, \quad Y_4^\nu = O_\nu^T \mathrm{diag}(0,y,0)\,, \quad Y_5^\nu = O_\nu^T \mathrm{diag}(0,0,y)\,, \tag{D.4}$$

where $O_{\ell 1}, O_{\ell 2}, O_\nu \in O(3,\mathbb{R})$, and $O_{\ell 1}, O_{\ell 2}$ have the same set of eigenvectors, but different eigenvalues. The vevs of the scalar doublets Φ_a $(a = 3,4,5)$ need to be chosen in such a way that $m_{\nu_1} = yv_3/\sqrt{2}$, $m_{\nu_2} = yv_4/\sqrt{2}$, and $m_{\nu_3} = yv_5/\sqrt{2}$ (hence, the hierarchy between the vevs of the Higgs doublets is responsible of the ordering of light neutrino masses). In this way, we obtain

$$\sum_{j=1}^{5} Y_j^\nu Y_a^{\nu\dagger} Y_j^\ell = 0\,, \qquad \sum_{j=1}^{5} Y_j^\ell Y_a^{\ell\dagger} Y_j^\nu = 0\,, \tag{D.5}$$

$$\sum_{j=1}^{5} Y_j^\nu Y_j^{\nu\dagger} = \sum_{j=1}^{5} Y_j^{\nu\dagger} Y_j^\nu = y^2 1_{3\times 3}\,, \tag{D.6}$$

$$\sum_{j=1}^{5} Y_j^\ell Y_j^{\ell\dagger} = \sum_{j=1}^{5} Y_j^{\ell\dagger} Y_j^\ell = (\lambda_1^2 + \lambda_2^2) 1_{3\times 3}\,, \tag{D.7}$$

so that both Y_a^ℓ and $\mathcal{D}Y_a^\ell$, as well as Y_a^ν and $\mathcal{D}Y_a^\nu$, are simultaneously diagonalizable: SFCNC do not arise through one-loop RGE.

E Scalar loop contributions to $(g-2)_\ell$ and ℓEDM

In this appendix, we provide detailed steps on the computation of one-loop diagrams mediated by neutral and charged scalars that contribute to the $g-2$ and EDM of lepton ℓ. For completeness, the results arising from the relevant two-loop Barr-Zee diagrams are also presented without further derivation. We consider a flavor-conserving scenario where the scalar-fermion couplings are diagonal in flavor space, that is, they do not mix fermions of different generations. The interaction Lagrangian for leptons reads

$$\mathscr{L}_\ell = -S\bar{\ell}\left(a_S^\ell + i b_S^\ell \gamma_5\right)\ell - C^-\bar{\ell}\left(a_C^\ell + i b_C^\ell\gamma_5\right)\nu - C^+\bar{\nu}\left(a_C^{\ell *} + i b_C^{\ell *}\gamma_5\right)\ell\,, \quad \text{with} \quad a_S^\ell\,, b_S^\ell \in \mathbb{R}\,. \tag{E.1}$$

The magnetic and electric dipole moments of lepton ℓ are two of the quantities characterizing its interaction with an external electromagnetic field. This is described through the diagram

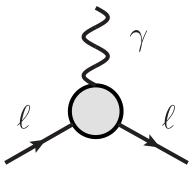

$$= \quad \left(-i\eta_e e Q_\ell\right)\, \bar{u}(p+q)\Gamma^\mu(q)u(p)\,, \tag{E.2}$$

where the vertex function $\Gamma^\mu(q)$ can be written in terms of Lorentz-invariant form factors [289] as

$$\Gamma^\mu(q) = \gamma^\mu F_E(q^2) + i\frac{\sigma^{\mu\nu}q_\nu}{2m_\ell}F_M(q^2) + \frac{\sigma^{\mu\nu}q_\nu}{2m_\ell}\gamma_5 F_D(q^2) + \frac{q^2\gamma^\mu - q^\mu \not{q}}{m_\ell^2}\gamma_5 F_A(q^2)\,, \tag{E.3}$$

encoding all higher-order corrections to the process $\ell^-(p)\,\gamma(q) \to \ell^-(p+q)$. The momentum of the incoming photon line is q, and the external lepton states satisfy the on-shell conditions $p^2 = (p+q)^2 = m_\ell^2$, with m_ℓ the physical (pole) mass. The amplitude in Eq. (E.2), hereafter denoted $i\mathcal{M}^\mu$, should be further contracted with the corresponding polarization vector of the incoming photon $\epsilon_\mu(q)$ to obtain the full amplitude of the process. The prefactor contains the physical electric charge e (with $\alpha = e^2/(4\pi)$ from QED), $Q_\ell = -1$ for the lepton particle, and $\eta_e = \pm 1$ depending on the sign convention used for the $U(1)_{\text{QED}}$ covariant derivative [17].

Regarding the vertex function, the first term in Eq. (E.3) contributes to the renormalization of the electric charge, fixed by the condition $F_E(0) = 1$, while $F_A(0)$ is the unphysical anapole moment that can be absorbed into four-fermion operators. The form factors $F_M(0)$ and $F_D(0)$ evaluated at $q^2 = 0$ define the anomalous magnetic moment a_ℓ and the electric dipole moment d_ℓ of the lepton:

$$a_\ell \equiv \frac{(g-2)_\ell}{2} = F_M(0)\,, \qquad d_\ell = -eQ_\ell\frac{F_D(0)}{2m_\ell}\,. \tag{E.4}$$

In the following, we explicitly compute the one-loop contributions generated by the neutral and charged scalar interactions in Eq. (E.1) to the anomalous magnetic moment of the lepton $\{\delta a_\ell^{(1),\,S}, \delta a_\ell^{(1),\,C}\}$, as well as its electric dipole moment $\{\delta d_\ell^{(1),\,S}, \delta d_\ell^{(1),\,C}\}$. These arise from the diagrams in Figs. E.1a and E.1b. For the sake of clarity, our choice for the momentum flow is specified in Figs. E.2a and E.2b. In addition, the relevant two-loop Barr-Zee diagram is shown in Fig. E.1c. Notice that, in the latter, the loop connected to the external photon line involves any charged fermion f, not necessarily a lepton, which are coupled to neutral scalars with analogous interactions to the ones quoted in Eq. (E.1).

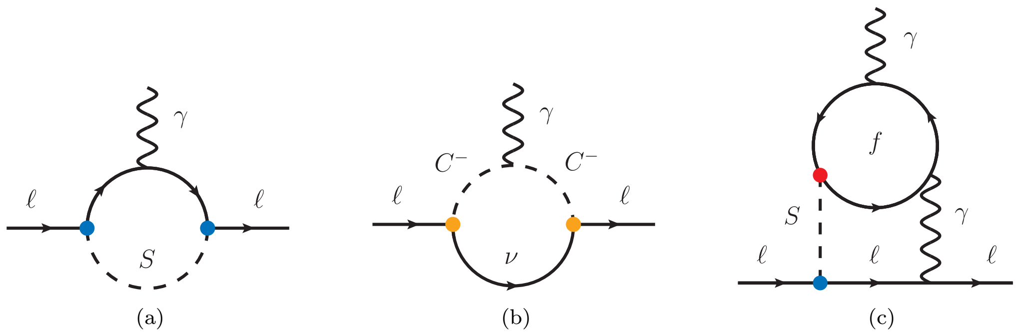

Figure E.1: Scalar loop contributions to $(g-2)_\ell$ and ℓEDM: (a) one-loop diagram mediated by a neutral scalar, (b) one-loop diagram mediated by charged scalars, and (c) two-loop diagram of Barr-Zee type. The blue and orange vertices represent the couplings of the lepton to neutral and charged scalars, respectively, as given in Eq. (E.1). We distinguish in red the coupling of either a quark or a lepton to a neutral scalar in the closed fermion loop of the Barr-Zee diagram.

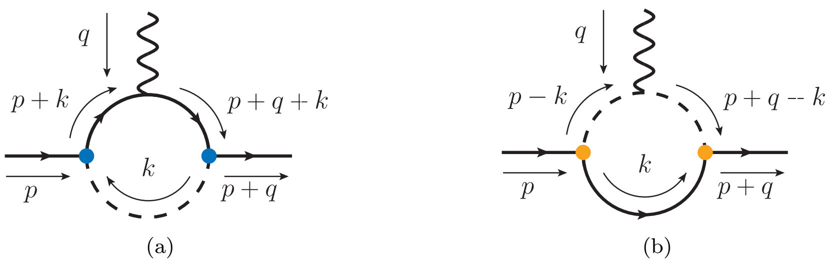

Figure E.2: Momentum flow assignments in scalar one-loop contributions to $(g-2)_\ell$ and ℓEDM: (a) diagram mediated by a neutral scalar, and (b) diagram mediated by charged scalars.

E.1 One-loop neutral scalar contributions

The amplitude associated to diagram in Fig. E.2a reads

$$
\begin{aligned}
i\mathcal{M}_S^\mu = &\int \frac{\mathrm{d}^d k}{(2\pi)^d}\Bigg[\bar{u}(p+q)(-i)\left(a_S^\ell + i b_S^\ell \gamma_5\right)\frac{i(\not{p}+\not{q}+\not{k}+m_\ell)}{(p+q+k)^2-m_\ell^2}\left(-i\eta_e e Q_\ell \gamma^\mu\right)\\
&\times \frac{i(\not{p}+\not{k}+m_\ell)}{(p+k)^2-m_\ell^2}(-i)\left(a_S^\ell + i b_S^\ell \gamma_5\right)u(p)\Bigg]\frac{i}{k^2-M_S^2}\\
= &\ \eta_e e Q_\ell\ \bar{u}(p+q)\left\{\int \frac{\mathrm{d}^d k}{(2\pi)^d}\frac{(a_S^\ell + i b_S^\ell\gamma_5)(\not{p}+\not{q}+\not{k}+m_\ell)\gamma^\mu(\not{p}+\not{k}+m_\ell)(a_S^\ell + i b_S^\ell\gamma_5)}{(k^2-M_S^2)\left[(p+k)^2-m_\ell^2\right]\left[(p+q+k)^2-m_\ell^2\right]}\right\}u(p)\\
= &\ \eta_e e Q_\ell\ \bar{u}(p+q)\left\{\int \frac{\mathrm{d}^d k}{(2\pi)^d}\frac{N_S^\mu}{D_S}\right\}u(p)\,,
\end{aligned}
\tag{E.5}
$$

where we have defined

$$
N_S^\mu = (a_S^\ell + i b_S^\ell\gamma_5)(\not{p}+\not{q}+\not{k}+m_\ell)\gamma^\mu(\not{p}+\not{k}+m_\ell)(a_S^\ell + i b_S^\ell\gamma_5)\,, \tag{E.6}
$$

$$
D_S = (k^2-M_S^2)\left[(p+k)^2-m_\ell^2\right]\left[(p+q+k)^2-m_\ell^2\right]\,. \tag{E.7}
$$

The spinorial structure of the numerator in Eq. (E.6) can be reduced using the equations of motion for spinors

$$
\bar{u}(p+q)(\not{p}+\not{q}) = m_\ell \bar{u}(p+q)\,, \qquad \not{p}u(p) = m_\ell u(p)\,, \tag{E.8}
$$

together with the Dirac algebra relations

$$
\{\gamma^\mu,\gamma^\nu\} = 2\eta^{\mu\nu} = 2\,\mathrm{diag}(1,-1,-1,-1)\,, \qquad \{\gamma^\mu,\gamma_5\} = 0\,, \qquad (\gamma_5)^2 = 1\,. \tag{E.9}
$$

Acting on the left with $\bar{u}(p+q)$ and on the right with $u(p)$, we obtain

$$
\bar{u}(p+q)(a_S^\ell + i b_S^\ell\gamma_5)(\not{p}+\not{q}+\not{k}+m_\ell) = \bar{u}(p+q)\left[2m_\ell a_S^\ell + (a_S^\ell + i b_S^\ell\gamma_5)\not{k}\right]\,, \tag{E.10}
$$

$$
(\not{p}+\not{k}+m_\ell)(a_S^\ell + i b_S^\ell\gamma_5)u(p) = \left[2m_\ell a_S^\ell + \not{k}(a_S^\ell + i b_S^\ell\gamma_5)\right]u(p)\,, \tag{E.11}
$$

yielding

$$
\begin{aligned}
\bar{u}(p+q)N_S^\mu u(p) &= \bar{u}\left[2m_\ell a_S^\ell + (a_S^\ell + i b_S^\ell\gamma_5)\not{k}\right]\gamma^\mu\left[2m_\ell a_S^\ell + \not{k}(a_S^\ell + i b_S^\ell\gamma_5)\right]u\\
&= \bar{u}\left[(2m_\ell a_S^\ell)^2\gamma^\mu + (a_S^\ell + i b_S^\ell\gamma_5)\not{k}\gamma^\mu\not{k}(a_S^\ell + i b_S^\ell\gamma_5) + 4m_\ell a_S^\ell k^\mu(a_S^\ell + i b_S^\ell\gamma_5)\right]u\\
&= \bar{u}\left\{\left[(2m_\ell a_S^\ell)^2 - k^2\left((a_S^\ell)^2+(b_S^\ell)^2\right)\right]\gamma^\mu + 2\left[(a_S^\ell)^2+(b_S^\ell)^2\right]\not{k}k^\mu + 4m_\ell a_S^\ell k^\mu(a_S^\ell + i b_S^\ell\gamma_5)\right\}u\,,
\end{aligned}
\tag{E.12}
$$

where we have used $\{\gamma^\mu,\not{k}\} = 2k^\mu$ and $\not{k}^2 = k^2$. The first term in brackets, proportional to γ^μ, contributes to the renormalization of the electric charge. As our concern relies exclusively on the contributions to the lepton dipole moments, we will assiduously ignore this type of structure in the next steps. Thus, we simply have

$$
\bar{u}(p+q)N_S^\mu u(p) = \bar{u}(p+q)\left(\alpha_S^\ell \not{k}k^\mu + \beta_S^\ell k^\mu\right)u(p)\,, \tag{E.13}
$$

with

$$
\alpha_S^\ell = 2\left[(a_S^\ell)^2+(b_S^\ell)^2\right]\,, \qquad \beta_S^\ell = 4m_\ell a_S^\ell(a_S^\ell + i b_S^\ell\gamma_5)\,. \tag{E.14}
$$

On the other hand, it is convenient to express the denominator in Eq. (E.7) making use of the Feynman parametrization [10], *i.e.*,

$$\frac{1}{A_1 A_2 A_3} = \int_0^1 \mathrm{d}x_1 \mathrm{d}x_2 \mathrm{d}x_3 \delta(x_1 + x_2 + x_3 - 1) \frac{2}{(x_1 A_1 + x_2 A_2 + x_3 A_3)^3} . \tag{E.15}$$

In our case, defining

$$A_1 = k^2 - M_S^2 , \qquad A_2 = (p+k)^2 - m_\ell^2 , \qquad A_3 = (p+q+k)^2 - m_\ell^2 , \tag{E.16}$$

we are left with

$$\begin{aligned} x_1 A_1 + x_2 A_2 + x_3 A_3 &= x_1 k^2 + x_2 (p+k)^2 + x_3 (p+q+k)^2 - x_1 M_S^2 - (x_2 + x_3) m_\ell^2 \\ &= (x_1 + x_2 + x_3) k^2 + 2k \cdot [x_2 p + x_3 (p+q)] - x_1 M_S^2 , \end{aligned} \tag{E.17}$$

where we have taken into account the on-shell conditions $p^2 = (p+q)^2 = m_\ell^2$. The integration over one of the Feynman parameters, say x_1, can be done straightforwardly due to the presence of the Dirac delta function, leading to

$$\frac{1}{D_S} = \int_0^1 \mathrm{d}x_2 \int_0^{1-x_2} \mathrm{d}x_3 \frac{2}{\{k^2 + 2k \cdot [x_2 p + x_3 (p+q)] - (1 - x_2 - x_3) M_S^2\}^3} . \tag{E.18}$$

Therefore, the loop integral in Eq. (E.5) is translated into

$$I^\mu = \int \frac{\mathrm{d}^d k}{(2\pi)^d} \int_0^1 \mathrm{d}x_2 \int_0^{1-x_2} \mathrm{d}x_3 \frac{2 \left(\alpha_S^\ell \not{k} k^\mu + \beta_S^\ell k^\mu\right)}{\{k^2 + 2k \cdot [x_2 p + x_3 (p+q)] - (1 - x_2 - x_3) M_S^2\}^3} . \tag{E.19}$$

At this point, we apply the variable change

$$l = k + x_2 p + x_3 (p+q) , \tag{E.20}$$

such that

$$\begin{aligned} l^2 &= k^2 + 2k \cdot [x_2 p + x_3 (p+q)] + [x_2 p + x_3 (p+q)]^2 \\ &= k^2 + 2k \cdot [x_2 p + x_3 (p+q)] + x_2^2 m_\ell^2 + x_3^2 m_\ell^2 + 2 x_2 x_3 (m_\ell^2 + p \cdot q) \\ &= k^2 + 2k \cdot [x_2 p + x_3 (p+q)] + (x_2 + x_3)^2 m_\ell^2 - x_2 x_3 q^2 , \end{aligned} \tag{E.21}$$

where in the second-to-last step we have used that $q^2 = -2(p \cdot q)$. In this way, the denominator in Eq. (E.19) only depends quadratically in the loop momentum l. Thus, if we define

$$\Delta^2 = (x_2 + x_3)^2 m_\ell^2 + (1 - x_2 - x_3) M_S^2 - x_2 x_3 q^2 , \tag{E.22}$$

after variable change the loop integral will read

$$I^\mu = \int \frac{\mathrm{d}^d l}{(2\pi)^d} \int_0^1 \mathrm{d}x_2 \int_0^{1-x_2} \mathrm{d}x_3 \frac{2 N_S^\mu}{(l^2 - \Delta^2)^3} , \tag{E.23}$$

with

$$N_S^\mu = \alpha_S^\ell \left[\not{l} - x_2 \not{p} - x_3 (\not{p} + \not{q})\right] [l - x_2 p - x_3 (p+q)]^\mu + \beta_S^\ell [l - x_2 p - x_3 (p+q)]^\mu . \tag{E.24}$$

It is easy to see that the terms containing odd powers of l in the numerator N_S^μ vanish under integration. Furthermore, the structure $\not{l} l^\mu$ gives rise to a contribution proportional to γ^μ by Lorentz covariance, and thus it is involved in the renormalization of the electric charge. Finally, using the Dirac equations for spinors in Eq. (E.8), we can trade

$$\bar{u}(p+q)\left[x_2\not{p} + x_3(\not{p}+\not{q})\right] u(p) = m_\ell(x_2+x_3)\bar{u}(p+q)u(p)\,, \tag{E.25}$$

yielding

$$I^\mu = \int \frac{\mathrm{d}^d l}{(2\pi)^d} \int_0^1 \mathrm{d}x_2 \int_0^{1-x_2} \mathrm{d}x_3 \frac{2\left[\alpha_S^\ell m_\ell(x_2+x_3) - \beta_S^\ell\right]\left[x_2 p + x_3(p+q)\right]^\mu}{\left(l^2-\Delta^2\right)^3}\,. \tag{E.26}$$

The integration over loop momentum in $d=4$ dimensions is convergent, and is given by [10]

$$\int \frac{\mathrm{d}^4 l}{(2\pi)^4} \frac{1}{\left(l^2-\Delta^2\right)^3} = -\frac{i}{(4\pi)^2}\frac{1}{2\Delta^2}\,, \tag{E.27}$$

such that

$$I^\mu = -\frac{i}{(4\pi)^2}\int_0^1 \mathrm{d}x_2 \int_0^{1-x_2} \mathrm{d}x_3 \frac{\left[\alpha_S^\ell m_\ell(x_2+x_3) - \beta_S^\ell\right]\left[x_2 p + x_3(p+q)\right]^\mu}{(x_2+x_3)^2 m_\ell^2 + (1-x_2-x_3)M_S^2 - x_2 x_3 q^2}\,. \tag{E.28}$$

One may notice that the denominator in Eq. (E.28) together with the first factor in the numerator are symmetric under the exchange $x_2 \leftrightarrow x_3$. Let us collectively call this piece $S(x_2,x_3)$, which obviously satisfies that $S(x_2,x_3) = S(x_3,x_2)$. We can conveniently write

$$\begin{aligned}
&\int_0^1 \mathrm{d}x_2 \int_0^{1-x_2} \mathrm{d}x_3 S(x_2,x_3)\left[x_2 p + x_3(p+q)\right]^\mu \\
&= \int_0^1 \mathrm{d}x_2 \int_0^{1-x_2} \mathrm{d}x_3 S(x_2,x_3)\frac{\left[x_2 p + x_3(p+q)\right]^\mu}{2} + \int_0^1 \mathrm{d}x_3 \int_0^{1-x_3} \mathrm{d}x_2 S(x_3,x_2)\frac{\left[x_3 p + x_2(p+q)\right]^\mu}{2}\,.
\end{aligned} \tag{E.29}$$

where we have exchanged $x_2 \leftrightarrow x_3$ in the second term. Then, taking into account that $S(x_2,x_3) = S(x_3,x_2)$ and that the integration domain satisfies

$$\int_0^1 \mathrm{d}x_3 \int_0^{1-x_3} \mathrm{d}x_2 = \int_0^1 \mathrm{d}x_2 \int_0^{1-x_2} \mathrm{d}x_3\,, \tag{E.30}$$

the integral reduces to

$$I^\mu = -\frac{i}{(4\pi)^2}\frac{(2p+q)^\mu}{2}\int_0^1 \mathrm{d}x_2 \int_0^{1-x_2} \mathrm{d}x_3 \frac{\alpha_S^\ell m_\ell(x_2+x_3)^2 - \beta_S^\ell(x_2+x_3)}{(x_2+x_3)^2 m_\ell^2 + (1-x_2-x_3)M_S^2 - x_2 x_3 q^2}\,. \tag{E.31}$$

Our next step consists of applying the change of variables defined by

$$y = x_2 + x_3\,, \qquad z = x_2 - x_3\,, \qquad \mathrm{d}x_2\mathrm{d}x_3 = \frac{1}{2}\mathrm{d}y\mathrm{d}z\,, \qquad \text{with} \qquad y\in[0,1]\,,\ z\in[-y,+y]\,. \tag{E.32}$$

This leads to

$$I^\mu = -\frac{i}{(4\pi)^2}\frac{(2p+q)^\mu}{4}\int_0^1 \mathrm{d}y \int_{-y}^{+y} \mathrm{d}z \frac{\alpha_S^\ell m_\ell y^2 - \beta_S^\ell y}{m_\ell^2 y^2 + (1-y)M_S^2 + (z^2-y^2)q^2/4}\,. \tag{E.33}$$

As the dipole moments are measured at energies $q^2 \ll m_\ell^2$, we set now $q^2 = 0$. Then, the integration over z can be easily done, and we are left with

$$I^\mu = -\frac{i}{(4\pi)^2}\frac{(2p+q)^\mu}{2m_\ell^2}\left[\alpha_S^\ell m_\ell I_3(x) - \beta_S^\ell I_2(x)\right] , \tag{E.34}$$

where we have defined

$$I_2(x) = \int_0^1 \mathrm{d}y \frac{y^2}{y^2+(1-y)/x} , \qquad I_3(x) = \int_0^1 \mathrm{d}y \frac{y^3}{y^2+(1-y)/x} , \tag{E.35}$$

with $x = m_\ell^2/M_S^2$. The details on the computation of these integrals will be addressed later. Meanwhile, let us simply quote the result of their evaluation:

$$\begin{aligned} I_2(x) &= 1 + \frac{1-2x}{2x\sqrt{1-4x}}\ln\left(\frac{1+\sqrt{1-4x}}{1-\sqrt{1-4x}}\right) + \frac{1}{2x}\ln x \\ &= x\left(-\frac{3}{2} - \ln x\right) + x^2\left(-\frac{16}{3} - 4\ln x\right) + \mathcal{O}(x^3) , \end{aligned} \tag{E.36}$$

$$\begin{aligned} I_3(x) &= \frac{1}{2} + \frac{1}{x} + \frac{1-3x}{2x^2\sqrt{1-4x}}\ln\left(\frac{1+\sqrt{1-4x}}{1-\sqrt{1-4x}}\right) + \frac{1-x}{2x^2}\ln x \\ &= x\left(-\frac{11}{6} - \ln x\right) + x^2\left(-\frac{89}{12} - 5\ln x\right) + \mathcal{O}(x^3) . \end{aligned} \tag{E.37}$$

After integration, the amplitude $i\mathcal{M}_S^\mu$ reads

$$\begin{aligned} i\mathcal{M}_S^\mu &= \eta_e e Q_\ell \frac{-i}{(4\pi)^2}\frac{(2p+q)^\mu}{2m_\ell^2}\bar{u}(p+q)\left[\alpha_S^\ell m_\ell I_3(x) - \beta_S^\ell I_2(x)\right] u(p) \\ &= -i\eta_e e Q_\ell \frac{(2p+q)^\mu}{2m_\ell^2}\frac{1}{8\pi^2}\bar{u}(p+q)\left\{(a_S^\ell)^2\left[I_3(x) - 2I_2(x)\right] + (b_S^\ell)^2 I_3(x) - i2a_S^\ell b_S^\ell I_2(x)\gamma_5\right\} u(p) , \end{aligned} \tag{E.38}$$

where in the last step we have taken into account our definitions of α_S^ℓ and β_S^ℓ in Eq. (E.14), and arranged separately the scalar and pseudoscalar currents as each of them will generate a separate contribution to a_ℓ and d_ℓ, respectively. The latter can be made clear by means of the Gordon identities:

$$(2p+q)^\mu \bar{u}_{f_1}(p+q)u_{f_2}(p) = (m_{f_1}+m_{f_2})\bar{u}_{f_1}(p+q)\gamma^\mu u_{f_2}(p) - \bar{u}_{f_1}(p+q)i\sigma^{\mu\nu}q_\nu u_{f_2}(p) , \tag{E.39}$$

$$(2p+q)^\mu \bar{u}_{f_1}(p+q)\gamma_5 u_{f_2}(p) = (m_{f_1}-m_{f_2})\bar{u}_{f_1}(p+q)\gamma^\mu\gamma_5 u_{f_2}(p) - \bar{u}_{f_1}(p+q)i\sigma^{\mu\nu}q_\nu\gamma_5 u_{f_2}(p) , \tag{E.40}$$

for two different fermions f_1 and f_2. In our case, $f_1 = f_2$, and thus we obtain

$$\begin{aligned} i\mathcal{M}_S^\mu =& -i\eta_e e Q_\ell\left[\bar{u}(p+q)i\frac{\sigma^{\mu\nu}q_\nu}{2m_\ell}u(p)\right]\frac{1}{8\pi^2}\left\{(a_S^\ell)^2\left[2I_2(x) - I_3(x)\right] - (b_S^\ell)^2 I_3(x)\right\} \\ & -i\eta_e e Q_\ell\left[\bar{u}(p+q)\sigma^{\mu\nu}q_\nu\gamma_5 u(p)\right]\left\{-\frac{1}{8\pi^2}\frac{a_S^\ell b_S^\ell}{m_\ell}I_2(x)\right\} . \end{aligned} \tag{E.41}$$

Comparing with Eqs. (E.2) and (E.3), it is straightforward to identify

$$F_M(0) = \frac{1}{8\pi^2}\left\{(a_S^\ell)^2\left[2I_2(x) - I_3(x)\right] - (b_S^\ell)^2 I_3(x)\right\} , \qquad \frac{F_D(0)}{2m_\ell} = -\frac{1}{8\pi^2}\frac{a_S^\ell b_S^\ell}{m_\ell}I_2(x) . \tag{E.42}$$

Therefore, the one-loop contributions of a neutral scalar S to the lepton dipole moments defined in Eq. (E.4) are given by

$$\delta a_\ell^{(1),\,S} = \frac{1}{8\pi^2}\left\{(a_S^\ell)^2\left[2I_2\left(\frac{m_\ell^2}{M_S^2}\right) - I_3\left(\frac{m_\ell^2}{M_S^2}\right)\right] - (b_S^\ell)^2 I_3\left(\frac{m_\ell^2}{M_S^2}\right)\right\}\,, \tag{E.43}$$

$$\delta d_\ell^{(1),\,S} = \frac{eQ_\ell}{8\pi^2}\frac{a_S^\ell b_S^\ell}{m_\ell} I_2\left(\frac{m_\ell^2}{M_S^2}\right)\,. \tag{E.44}$$

In what follows, we provide the details on the computation of the integrals $I_2(x)$ and $I_3(x)$ in Eq. (E.35).

Computing $I_2(x)$ and $I_3(x)$

The integral $I_2(x)$ can be readily solved by decomposing the integrand in simple fractions, that is,

$$\frac{y^2}{y^2 + (1-y)/x} = 1 + \frac{a_+}{y - y_+} + \frac{a_-}{y - y_-}\,, \tag{E.45}$$

where

$$a_\pm = \pm\frac{y_\pm^2}{y - y_\pm}\,, \qquad y_\pm = \frac{1 \pm \sqrt{1-4x}}{2x}\,, \tag{E.46}$$

being $y_\pm$ the roots of the denominator in the integrand. In this form, it is straightforward to evaluate the integral over y as

$$I_2(x) = 1 + \frac{1}{y_+ - y_-}\left[y_+^2 \ln\left(\frac{y_+ - 1}{y_+}\right) - y_-^2 \ln\left(\frac{y_- - 1}{y_+}\right)\right]\,, \tag{E.47}$$

such that, substituting the values of $y_\pm$, we obtain

$$I_2(x) = 1 + \frac{1-2x}{2x\sqrt{1-4x}}\ln\left(\frac{1+\sqrt{1-4x}}{1-\sqrt{1-4x}}\right) + \frac{1}{2x}\ln x\,. \tag{E.48}$$

In order to solve the integral $I_3(x)$, we can make use of the previous decomposition by noticing that

$$\frac{y^3}{y^2 + (1-y)/x} = y + \frac{a_+ y}{y - y_+} + \frac{a_- y}{y - y_-} = y + a_+ + a_- + \frac{a_+ y_+}{y - y_+} + \frac{a_- y_-}{y - y_-}\,. \tag{E.49}$$

Again, the evaluation of the integral can be done straightforwardly:

$$I_3(x) = \frac{1}{2} + y_+ + y_- + \frac{1}{y_+ - y_-}\left[y_+^3 \ln\left(\frac{y_+ - 1}{y_+}\right) - y_-^3 \ln\left(\frac{y_- - 1}{y_+}\right)\right]\,, \tag{E.50}$$

leading to

$$I_3(x) = \frac{1}{2} + \frac{1}{x} + \frac{1-3x}{2x^2\sqrt{1-4x}}\ln\left(\frac{1+\sqrt{1-4x}}{1-\sqrt{1-4x}}\right) + \frac{1-x}{2x^2}\ln x\,. \tag{E.51}$$

E.2 One-loop charged scalar contributions

From Fig. E.2b, one can write down the amplitude

$$
\begin{aligned}
i\mathcal{M}_C^\mu = & \int \frac{\mathrm{d}^d k}{(2\pi)^d}\left[\bar{u}(p+q)(-i)(a_C^\ell + i b_C^\ell\gamma_5)\frac{i(\not{k}+m_\nu)}{k^2-m_\nu^2}(-i)(a_C^{\ell *} + i b_C^{\ell *}\gamma_5)u(p)\right] \\
& \times(-i)\eta_e e Q_\ell (2p+q-2k)^\mu \frac{i}{(p+q-k)^2-M_C^2}\frac{i}{(p-k)^2-M_C^2} \\
= & \, \eta_e e Q_\ell\, \bar{u}(p+q)\left\{\int\frac{\mathrm{d}^d k}{(2\pi)^d}\frac{(2p+q-2k)^\mu(a_C^\ell + i b_C^\ell\gamma_5)(\not{k}+m_\nu)(a_C^{\ell *} + i b_C^{\ell *}\gamma_5)}{(k^2-m_\nu^2)[(p+q-k)^2-M_C^2][(p-k)^2-M_C^2]}\right\}u(p) \\
= & \, \eta_e e Q_\ell\, \bar{u}(p+q)\left\{\int\frac{\mathrm{d}^d k}{(2\pi)^d}\frac{N_C^\mu}{D_C}\right\}u(p)\,,
\end{aligned}
\tag{E.52}
$$

where we have defined

$$N_C^\mu \equiv (2p+q-2k)^\mu(a_C^\ell + i b_C^\ell\gamma_5)(\not{k}+m_\nu)(a_C^{\ell *} + i b_C^{\ell *}\gamma_5)\,, \tag{E.53}$$

$$D_C \equiv (k^2-m_\nu^2)[(p+q-k)^2-M_C^2][(p-k)^2-M_C^2]\,. \tag{E.54}$$

Using Eqs. (E.8) and (E.9), the numerator N_C^μ can be reduced as

$$N_C^\mu = A^\mu + B^{\mu\nu}k_\nu + C_\nu k^\mu k^\nu\,, \tag{E.55}$$

with

$$A^\mu \equiv (2p+q)^\mu m_\nu\left[|a_C^\ell|^2 - |b_C^\ell|^2 + i2\mathrm{Re}(a_C^\ell b_C^{\ell *})\gamma_5\right]\,, \tag{E.56}$$

$$B^{\mu\nu} \equiv (2p+q)^\mu\gamma^\nu\left[|a_C^\ell|^2 + |b_C^\ell|^2 - 2\mathrm{Im}(a_C^\ell b_C^{\ell *})\gamma_5\right] - 2g^{\mu\nu}m_\nu\left[|a_C^\ell|^2 - |b_C^\ell|^2 + i2\mathrm{Re}(a_C^\ell b_C^{\ell *})\gamma_5\right]\,, \tag{E.57}$$

$$C_\nu \equiv -2\gamma_\nu\left[|a_C^\ell|^2 + |b_C^\ell|^2 - 2\mathrm{Im}(a_C^\ell b_C^{\ell *})\gamma_5\right]\,, \tag{E.58}$$

in such a way that we have singled out the dependence on the loop momentum k for later convenience.

On the other hand, we introduce the Feynman parametrization in Eq. (E.15), with

$$A_1 = k^2 - m_\nu^2\,, \qquad A_2 = (p+q-k)^2 - M_C^2\,, \qquad A_3 = (p-k)^2 - M_C^2\,, \tag{E.59}$$

to express the denominator D_C as

$$\frac{1}{D_C} = \int_0^1 \mathrm{d}x_2 \int_0^{1-x_2}\mathrm{d}x_3 \frac{2}{\{k^2 - 2k\cdot[x_2(p+q)+x_3 p] - (x_2+x_3)(M_C^2-m_\ell^2) - (1-x_2-x_3)m_\nu^2\}^3}\,, \tag{E.60}$$

where we have taken into account the on-shell conditions $p^2 = (p+q)^2 = m_\ell^2$, and already integrated out the variable x_1.

Therefore, our loop integral in Eq. (E.52) reads

$$I^\mu = \int\frac{\mathrm{d}^d k}{(2\pi)^d}\int_0^1 \mathrm{d}x_2\int_0^{1-x_2}\mathrm{d}x_3 \frac{2\,(A^\mu + B^{\mu\nu}k_\nu + C_\nu k^\mu k^\nu)}{\{k^2 - 2k\cdot[x_2(p+q)+x_3 p] - (x_2+x_3)(M_C^2-m_\ell^2) - (1-x_2-x_3)m_\nu^2\}^3}\,. \tag{E.61}$$

At this point, we apply the change of variable

$$l = k - x_2(p+q) - x_3 p\,, \tag{E.62}$$

such that

$$l^2 = k^2 - 2k \cdot [x_2(p+q) + x_3 p] + (x_2+x_3)^2 m_\ell^2 - x_2 x_3 q^2\,, \tag{E.63}$$

with $q^2 = -2(p\cdot q)$ after applying the on-shell conditions of the external charged lepton state. This leaves us with

$$I^\mu = \int \frac{\mathrm{d}^d l}{(2\pi)^d} \int_0^1 \mathrm{d}x_2 \int_0^{1-x_2} \mathrm{d}x_3 \frac{2N_C^\mu}{(l^2-\Delta^2)^3}\,, \tag{E.64}$$

defining, as usual,

$$\Delta^2 \equiv (x_2+x_3)^2 m_\ell^2 + (x_2+x_3)(M_C^2 - m_\ell^2) + (1-x_2-x_3)m_\nu^2 - x_2x_3q^2\,, \tag{E.65}$$

and

$$N_C^\mu = A^\mu + B^{\mu\nu}[l + x_2(p+q) + x_3p]_\nu + C_\nu[l + x_2(p+q) + x_3p]^\mu [l + x_2(p+q) + x_3p]^\nu\,. \tag{E.66}$$

It is clear that the terms proportional to an odd number of powers of l vanish under integration over loop momentum. On the other hand, by Lorentz covariance, the structure $l^\mu l^\nu$ in the integrand yields a contribution proportional to the metric tensor $g^{\mu\nu}$, which in turn leads to $C^\mu \propto \gamma^\mu, \gamma^\mu\gamma_5$. These structures do not contribute to the form factors related to the lepton dipole moments, and thus we will simply drop them from the computation—we will assiduously do so in other steps of the calculation. All in all, we are left with

$$I^\mu = \int \frac{\mathrm{d}^d l}{(2\pi)^d} \int_0^1 \mathrm{d}x_2 \int_0^{1-x_2} \mathrm{d}x_3 \frac{2\left\{A^\mu + B^{\mu\nu}[x_2(p+q)+x_3p]_\nu + C_\nu[x_2(p+q)+x_3p]^\mu[x_2(p+q)+x_3p]^\nu\right\}}{(l^2-\Delta^2)^3}\,. \tag{E.67}$$

Now we can use the external spinors in order to express the last two contributions in the numerator as

$$\begin{aligned}&\bar{u}(p+q)B^{\mu\nu}[x_2(p+q)+x_3p]_\nu u(p) = \\ &\quad = \bar{u}(p+q)\begin{pmatrix} (2p+q)^\mu(x_2+x_3)m_\ell\left(|a_C^\ell|^2+|b_C^\ell|^2\right) \\ -2(2p+q)^\mu(x_2-x_3)m_\ell \mathrm{Im}(a_C^\ell b_C^{\ell*})\gamma_5 \\ -2[x_2(p+q)+x_3p]^\mu m_\nu\left(|a_C^\ell|^2-|b_C^\ell|^2+i2\mathrm{Re}(a_C^\ell b_C^{\ell*})\gamma_5\right)\end{pmatrix}u(p)\,,\end{aligned} \tag{E.68}$$

and

$$\begin{aligned}&\bar{u}(p+q)C_\nu[x_2(p+q)+x_3p]^\mu[x_2(p+q)+x_3p]^\nu u(p) = \\ &\quad = \bar{u}(p+q)\begin{pmatrix} -2[x_2(p+q)+x_3p]^\mu(x_2+x_3)m_\ell\left(|a_C^\ell|^2+|b_C^\ell|^2\right) \\ +4[x_2(p+q)+x_3p]^\mu(x_2-x_3)m_\ell\mathrm{Im}(a_C^\ell b_C^{\ell*})\gamma_5\end{pmatrix}u(p)\,.\end{aligned} \tag{E.69}$$

Summing up all terms we obtain

$$\begin{aligned}N_C^\mu = {}&(2p+q)^\mu\begin{pmatrix} m_\nu\left(|a_C^\ell|^2-|b_C^\ell|^2+i2\mathrm{Re}(a_C^\ell b_C^{\ell*})\gamma_5\right) + (x_2+x_3)m_\ell\left(|a_C^\ell|^2+|b_C^\ell|^2\right) \\ -2(x_2-x_3)m_\ell\mathrm{Im}(a_C^\ell b_C^{\ell*})\gamma_5\end{pmatrix} \\ &+[x_2(p+q)+x_3p]^\mu\begin{pmatrix} -2m_\nu\left(|a_C^\ell|^2-|b_C^\ell|^2+i2\mathrm{Re}(a_C^\ell b_C^{\ell*})\gamma_5\right) - 2(x_2+x_3)m_\ell\left(|a_C^\ell|^2+|b_C^\ell|^2\right) \\ +4(x_2-x_3)m_\ell\mathrm{Im}(a_C^\ell b_C^{\ell*})\gamma_5\end{pmatrix}\,,\end{aligned} \tag{E.70}$$

On the other hand, the integration over loop momentum l is convergent in $d=4$ dimensions. Then, using the result in Eq. (E.27), we obtain

$$I^\mu = -\frac{i}{(4\pi)^2}\int_0^1 \mathrm{d}x_2 \int_0^{1-x_2} \mathrm{d}x_3 \frac{N_C^\mu}{(x_2+x_3)^2 m_\ell^2 + (x_2+x_3)(M_C^2 - m_\nu^2) + (1-x_2-x_3)m_\nu^2 - x_2 x_3 q^2}\,. \tag{E.71}$$

Similarly to what has been done in Eqs. (E.29) and (E.30) for the computation of the neutral scalar contribution, it is convenient to symmetrize the integrand in the remaining Feynman parameters (x_2, x_3). After this process is carried out, the numerator in the loop integral takes the form

$$\begin{aligned} N_C^\mu = {} & (2p+q)^\mu (1-x_2-x_3)\left\{ m_\nu \left(|a_C^\ell|^2 - |b_C^\ell|^2 + i2\mathrm{Re}(a_C^\ell b_C^{\ell *})\gamma_5\right) + (x_2+x_3) m_\ell \left(|a_C^\ell|^2 + |b_C^\ell|^2\right)\right\} \\ & + 2q^\mu (x_2 - x_3)^2 m_\ell \mathrm{Im}(a_C^\ell b_C^{\ell *})\gamma_5\,. \end{aligned} \tag{E.72}$$

The second line in the numerator, containing the Lorentz structure $q^\mu\gamma_5$, contributes to other form factors different from the ones related to the dipole moments, and thus we can drop this term. If we further perform the change of variables proposed in Eq. (E.32), we can write down

$$I^\mu = -\frac{i}{(4\pi)^2}\frac{(2p+q)^\mu}{2}\int_0^1 \mathrm{d}y \int_{-y}^{+y} \mathrm{d}z \frac{(1-y)\left\{ m_\nu \left(|a_C^\ell|^2 - |b_C^\ell|^2 + i2\mathrm{Re}(a_C^\ell b_C^{\ell *})\gamma_5\right) + y m_\ell \left(|a_C^\ell|^2 + |b_C^\ell|^2\right)\right\}}{y^2 m_\ell^2 + y(M_C^2 - m_\ell^2) + (1-y)m_\nu^2 + (z^2 - y^2)q^2/4}\,. \tag{E.73}$$

Once we set $q^2 = 0$, the integral over z can be done straightforwardly. Then, we can write down

$$I^\mu = -\frac{i}{(4\pi)^2}\frac{(2p+q)^\mu}{2m_\ell^2}\begin{pmatrix} 2m_\ell \left(|a_C^\ell|^2 + |b_C^\ell|^2\right) J_2(x,x_\nu) + 2m_\nu \left(|a_C^\ell|^2 - |b_C^\ell|^2\right) J_1(x,x_\nu) \\ +4m_\nu \mathrm{Re}(a_C^\ell b_C^{\ell *}) i\gamma_5 J_1(x,x_\nu)\end{pmatrix}, \tag{E.74}$$

where $x \equiv m_\ell^2/M_C^2$, $x_\nu \equiv m_\nu^2/m_\ell^2$, and

$$J_1(x,x_\nu) = \int_0^1 \mathrm{d}y \frac{y^2(1-y)}{y^2 + y\frac{1-x}{x} + (1-y)x_\nu}\,, \qquad J_2(x,x_\nu) = \int_0^1 \mathrm{d}y \frac{y(1-y)}{y^2 + y\frac{1-x}{x} + (1-y)x_\nu}\,. \tag{E.75}$$

It is easy to check that the first line in parentheses in Eq. (E.74) gives a contribution to the magnetic dipole moment of lepton ℓ, while the second line in parentheses generates a contribution to its electric dipole moment. This is more transparent when we make use of the Gordon identities in Eq. (E.39). The total amplitude can then be written as

$$i\mathcal{M}_C^\mu = -i\eta_e e Q_\ell \left[\bar{u}(p+q) i\frac{\sigma^{\mu\nu}q_\nu}{2m_\ell}u(p)\right]\left\{-\frac{1}{8\pi^2}\begin{pmatrix} \left(|a_C^\ell|^2 + |b_C^\ell|^2\right) J_2(x,x_\nu) \\ +x_\nu \left(|a_C^\ell|^2 - |b_C^\ell|^2\right) J_1(x,x_\nu)\end{pmatrix}\right\} \tag{E.76}$$

$$-i\eta_e e Q_\ell \left[\bar{u}(p+q)\sigma^{\mu\nu}q_\nu\gamma_5 u(p)\right]\left\{\frac{1}{8\pi^2}\frac{x_\nu}{m_\ell}\mathrm{Re}(a_C^\ell b_C^{\ell *}) J_1(x,x_\nu)\right\}\,. \tag{E.77}$$

Comparing with Eqs. (E.2) and (E.3), one can readily identify

$$F_M(0) = -\frac{1}{8\pi^2}\left[\left(|a_C^\ell|^2 + |b_C^\ell|^2\right) J_2(x,x_\nu) + x_\nu\left(|a_C^\ell|^2 - |b_C^\ell|^2\right) J_1(x,x_\nu)\right]\,, \tag{E.78}$$

$$\frac{F_D(0)}{2m_\ell} = \frac{1}{8\pi^2}\frac{x_\nu}{m_\ell}\mathrm{Re}(a_C^\ell b_C^{\ell *}) J_1(x,x_\nu)\,, \tag{E.79}$$

Therefore, the one-loop contribution of charged scalars $C^\pm$ to the lepton dipole moments in Eq. (E.4) is given by

$$\delta a_\ell^{(1),C} = -\frac{1}{8\pi^2}\left[\left(|a_C^\ell|^2 + |b_C^\ell|^2\right) J_2(x,x_\nu) + x_\nu\left(|a_C^\ell|^2 - |b_C^\ell|^2\right) J_1(x,x_\nu)\right]\,, \tag{E.80}$$

$$\delta d_\ell^{(1),\,C} = -\frac{eQ_\ell}{8\pi^2}\frac{x_\nu}{m_\ell}\mathrm{Re}(a_C^\ell b_C^{\ell *})J_1(x,x_\nu)\,. \tag{E.81}$$

In the limit of massless neutrinos, *i.e.*, $x_\nu \to 0$, the contribution to the electric dipole moment vanishes, but there remains a contribution to the magnetic dipole moment. Within this scenario, the only relevant integral is $J_2(x,0)$, namely,

$$J_2(x,0) = \int_0^1 \mathrm{d}y \frac{y(1-y)}{y+\frac{1-x}{x}}\,. \tag{E.82}$$

This can be easily solved by noticing that the integrand can be expressed as

$$\frac{y(1-y)}{y+a} = 1 + a - y - \frac{a(1+a)}{y+a}\,, \qquad \text{with} \qquad a \equiv \frac{1-x}{x}\,. \tag{E.83}$$

Then, it is straightforward to obtain

$$\begin{aligned} H(x) \equiv J_2(x,0) &= -\frac{1}{2} + \frac{1}{x} + \frac{1-x}{x^2}\ln(1-x) \\ &= \frac{x}{6} + \frac{x^2}{12} + \mathcal{O}(x^3)\,, \end{aligned} \tag{E.84}$$

leaving us with

$$\delta a_\ell^{(1),\,C} = -\frac{1}{8\pi^2}\left(|a_C^\ell|^2 + |b_C^\ell|^2\right)H(x)\,. \tag{E.85}$$

E.3 Two-loop Barr-Zee contributions

The relevant two-loop contributions for our analysis arise from Barr-Zee diagrams of the class depicted in Fig. E.1c. As previously commented, the closed fermion loop includes all possible charged states f, not necessarily leptons, whose interaction with a neutral scalar S is given by

$$\mathscr{L}_{Sff} = -S\bar{f}\left(a_S^f + ib_S^f\gamma_5\right)f\,, \qquad \text{with} \qquad a_S^f\,,\, b_S^f \in \mathbb{R}\,, \tag{E.86}$$

analogous to the lepton sector quoted in Eq. (E.1). The corresponding two-loop contribution to the dipole moments of lepton ℓ reads [159, 290]

$$\delta a_\ell^{(2),\,S} = -\sum_f \frac{\alpha}{4\pi^3}\frac{m_\ell^2}{m_f^2}N_C^f Q_f^2\left[a_S^f a_S^\ell f\left(\frac{m_f^2}{M_S^2}\right) - b_S^f b_S^\ell g\left(\frac{m_f^2}{M_S^2}\right)\right]\,, \tag{E.87}$$

$$\delta d_\ell^{(2),\,S} = \sum_f \frac{e\alpha}{8\pi^3}\frac{N_C^f Q_f^2}{m_f}\left[a_S^\ell b_S^f f\left(\frac{m_f^2}{M_S^2}\right) + b_S^\ell a_S^f g\left(\frac{m_f^2}{M_S^2}\right)\right]\,, \tag{E.88}$$

where N_C^f is the number of colors of fermion f, and

$$f(z) = \frac{z}{2}\int_0^1 \mathrm{d}x \frac{1-2x(1-x)}{x(1-x)-z}\ln\left[\frac{x(1-x)}{z}\right]\,, \tag{E.89}$$

$$g(z) = \frac{z}{2}\int_0^1 \mathrm{d}x \frac{1}{x(1-x)-z}\ln\left[\frac{x(1-x)}{z}\right]\,. \tag{E.90}$$

For a complete review of two-loop diagrams (both Barr-Zee and non-Barr-Zee) contributing to the anomalous magnetic moment in the context of 2HDMs, see [291]. Electric dipole moments in 2HDMs are reviewed in [290].

F Neutral $B_q - \bar{B}_q$ meson mixing calculations

This appendix is devoted to a detailed derivation of the theoretical results presented in chapter 7 regarding neutral $B_q - \bar{B}_q$ meson mixing. First, we address the computation of the relevant mixing matrix elements in the SM in App. F.1, and then present the novel contributions arising in models that include vector-like quarks in App. F.2.

F.1 Standard Model calculation

The theoretical determination of the mass mixing $M_{12}^{q,\mathrm{SM}}$ and the decay width mixing $\Gamma_{12}^{q,\mathrm{SM}}$ controlling neutral $B_q - \bar{B}_q$ mesons oscillations is broadly addressed in the literature. However, different choices regarding the definition of the relevant matrix elements and normalization factors are usually encountered. In light of this, we believe it might be useful for the reader to settle down which convention we have adopted and compare with other references in order to avoid potential confusion on that regard. Furthermore, we take the opportunity to provide additional details on the technical aspects and the physical meaning of the different approximations used in the calculations, which are performed in a general R_ξ-gauge.

As introduced in chapter 7, M_{12}^q and Γ_{12}^q are the off-diagonal elements of the 2×2 Hamiltonian in Eq. (7.7), which acts on the Hilbert space of the $\{|B_q\rangle, |\bar{B}_q\rangle\}$ mesons and controls their time evolution. The effects of the underlying fundamental physics can be encoded into the matrix elements of the Hamiltonian $\mathcal{H}^q$ using the framework of perturbation theory, in particular:

$$M_{12}^q = \langle B_q|\mathcal{H}_W|\bar{B}_q\rangle + \sum_n \mathrm{P}\frac{\langle B_q|\mathcal{H}_W|n\rangle\langle n|\mathcal{H}_W|\bar{B}_q\rangle}{M_{B_q} - E_n} + \dots\,, \tag{F.1}$$

$$\Gamma_{12}^q = 2\pi \sum_n \delta(M_{B_q} - E_n)\langle B_q|\mathcal{H}_W|n\rangle\langle n|\mathcal{H}_W|\bar{B}_q\rangle + \dots\,, \tag{F.2}$$

where the summation over the n states does not include the B_q and $\bar{B}_q$ mesons themselves, and P stands for "principal part". In the SM, it is clear that $\mathcal{H}_W$ denotes the standard weak interactions, which play the role of the perturbation in the previous expansion and are responsible for the flavor-changing transitions we are interested in. Likewise, it is important to remark that Eqs. (F.1) and (F.2) are obtained using a non-covariant normalization of the states, that is, $\langle\vec{p}|\vec{p}\,'\rangle = (2\pi)^3\delta^{(3)}(\vec{p}-\vec{p}\,')$, and they are usually written in this way in the literature [58, 292]. In this work, we are adopting a covariant (relativistic) normalization—see, *e.g.*, [11] for a review—, $\langle\vec{p}|\vec{p}\,'\rangle = 2E_{\vec{p}}\,(2\pi)^3\delta^{(3)}(\vec{p}-\vec{p}\,') \equiv \Delta_{\vec{p}\vec{p}\,'}$; therefore, at some point one has to correct the previous equations with a factor $(2M_{B_q})^{-1}$, since we are considering the mesons to be in their rest frame.

F.1.1 Mass mixing $M_{12}^{q,\mathrm{SM}}$

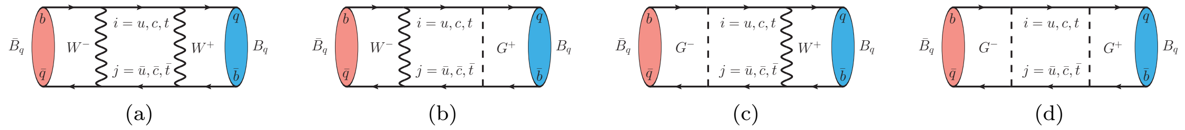

Figure F.1: Set I of box diagrams triggering neutral B_q $(q = d, s)$ meson mixing through the exchange of $W^\pm$ gauge bosons and $G^\pm$ Goldstone bosons: (a) W^-W^+ contribution, (b) W^-G^+ contribution, (c) G^-W^+ contribution, and (d) G^-G^+ contribution.

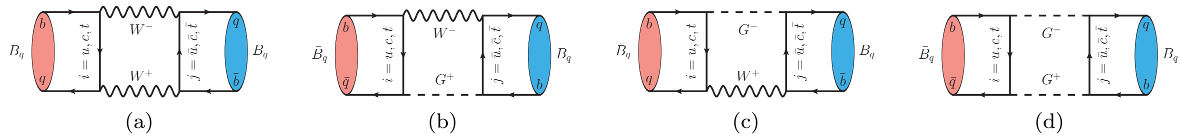

Figure F.2: Set II of box diagrams triggering neutral B_q $(q = d, s)$ meson mixing through the exchange of $W^\pm$ gauge bosons and $G^\pm$ Goldstone bosons: (a) W^-W^+ contribution, (b) W^-G^+ contribution, (c) G^-W^+ contribution, and (d) G^-G^+ contribution.

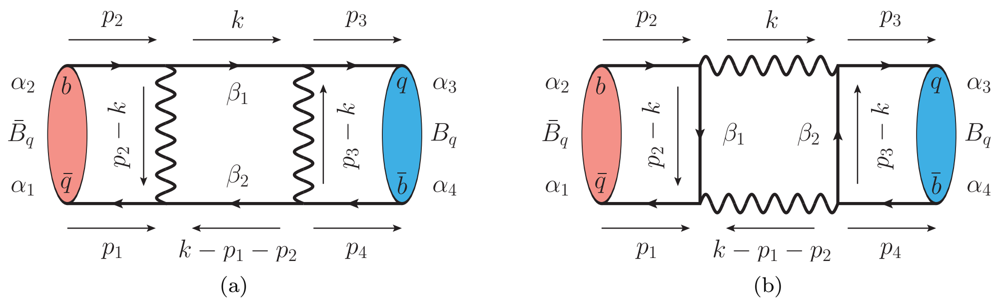

Figure F.3: Momentum flow assignments in box diagrams triggering neutral B_q $(q = d, s)$ meson mixing: (a) set I, and (b) set II. The indices α_i $(i = 1, \ldots, 4)$ and β_i $(i = 1, 2)$ are the color indices of the quark fields.

Let us first analyze the contributions to $M_{12}^{q,\mathrm{SM}}$. It is clear that the first order term of the perturbative expansion in Eq. (F.1) represents a $\Delta B = 2$ transition, namely, $\bar{B}_q \to B_q$. The leading contribution mediating this process arises at fourth order in the weak coupling, $\mathcal{O}(g^4)$, through the two sets of box diagrams depicted in Figs. F.1 and F.2. The latter involve the exchange of virtual (off-shell) up-type quarks and W bosons. In addition, since we choose to work in an R_ξ-gauge, one must include the contributions from the corresponding charged Goldstone bosons. This first order term in the perturbative expansion of $M_{12}^{q,\mathrm{SM}}$ is usually referred to as *short distance* contribution because $\Delta t \sim (\Delta E)^{-1} = (M - m_b)^{-1} \ll \Lambda_{\mathrm{QCD}}^{-1}$ (being $M = M_W, m_t$), *i.e.*, the time scale of the interaction is much smaller than the characteristic scale of strong interactions. All in all, it is important to remark that $M_{12}^{q,\mathrm{SM}}$ is sensitive to heavy virtual particles running in the loop, and thus to potential heavy NP effects.

On the other hand, the second order term in Eq. (F.1) corresponds to two $\Delta B = 1$ transitions involving low-mass (on-shell) intermediate states that are common to both B_q and $\bar{B}_q$ mesons, and thus they represent *long distance* contributions. These are further suppressed by $M_{B_q} \sim m_b$ and will be neglected in the computation of $M_{12}^{q,\mathrm{SM}}$.

Once the one-loop integrals are performed, one can insert the resulting local $\mathcal{H}^{\Delta B=2}_{\text{dis,eff}}$ into the perturbative expansion and compute $M_{12}^{q,\text{SM}}$. The details of the strong interactions that bind the quarks together into the meson states will be appropriately encoded in the relevant matrix elements of the effective dim-6 local operator involving the quark fields. Note that the subscript "dis" in the effective Hamiltonian states for *dispersive*, as $M_{12}^{q,\text{SM}}$ arises from the real part of the box diagrams.

As previously mentioned, there are two sets of contributing diagrams, depending on whether the external quarks legs are connected from the initial-to-final state as in Fig. F.1, or among themselves in the initial or final states as in Fig. F.2. Our choice for the momentum flow is illustrated in Fig. F.3, where we have also included the color indices indices of the quarks fields. A simplifying assumption can be carried out when computing the dispersive part of the box diagrams, namely, taking the limit of massless external particles and zero external momenta. The latter approximation is justified because the relevant contribution to the one-loop integral lies around the interval centered at $k^2 \sim M^2$ (being M the largest scale in the box, *i.e.*, m_t or M_W for the SM case), which is a much larger energy scale than the one associated to the external states ($p_1^2 = p_3^2 = m_q^2$ and $p_2^2 = p_4^2 = m_b^2$). With all these ingredients, and focusing on the set I of diagrams represented in Fig. F.1, the SM amplitude can be written as

$$
\begin{aligned}
i\mathcal{M}_{\text{I}} = \sum_{\beta_1,\beta_2} & \delta_{\alpha_1\beta_2}\delta_{\alpha_2\beta_1}\delta_{\alpha_3\beta_1}\delta_{\alpha_4\beta_2}\left(i\frac{g}{\sqrt{2}}\right)^4 \\
\times \sum_{i,j=u,c,t} & \lambda^i_{bq}\lambda^j_{bq}\int\frac{\mathrm{d}^d k}{(2\pi)^d}\Bigg\{(-\eta)^4\frac{[\bar{u}_q(0)\gamma^\rho P_L i(\not{k}+m_i)\gamma^\nu P_L u_b(0)]\,[\bar{v}_q(0)\gamma^\mu P_L i(\not{k}+m_j)\gamma^\sigma P_L v_b(0)]}{D_i(k)D_j(k)} \\
& \times i\left[-\frac{g_{\mu\nu}}{D_W(k)}+\frac{k_\mu k_\nu}{M_W^2}\left(\frac{1}{D_W(k)}-\frac{1}{D_g(k)}\right)\right] \\
& \times i\left[-\frac{g_{\rho\sigma}}{D_W(k)}+\frac{k_\rho k_\sigma}{M_W^2}\left(\frac{1}{D_W(k)}-\frac{1}{D_g(k)}\right)\right] \\
& +(-\eta)^2\frac{[\bar{u}_q(0)P_R i(\not{k}+m_i)\gamma^\nu P_L u_b(0)]\,[\bar{v}_q(0)\gamma^\mu P_L i(\not{k}+m_j)P_L v_b(0)]}{D_i(k)D_j(k)} \\
& \times\frac{m_i m_j}{M_W^2}\times i\left[-\frac{g_{\mu\nu}}{D_W(k)}+\frac{k_\mu k_\nu}{M_W^2}\left(\frac{1}{D_W(k)}-\frac{1}{D_g(k)}\right)\right]\times\frac{i}{D_g(k)} \\
& +(-\eta)^2\frac{[\bar{u}_q(0)\gamma^\rho P_L i(\not{k}+m_i)P_L u_b(0)]\,[\bar{v}_q(0)P_R i(\not{k}+m_j)\gamma^\sigma P_L v_b(0)]}{D_i(k)D_j(k)} \\
& \times\frac{m_i m_j}{M_W^2}\times i\left[-\frac{g_{\rho\sigma}}{D_W(k)}+\frac{k_\rho k_\sigma}{M_W^2}\left(\frac{1}{D_W(k)}-\frac{1}{D_g(k)}\right)\right]\times\frac{i}{D_g(k)} \\
& +\frac{[\bar{u}_q(0)P_R i(\not{k}+m_i)P_L u_b(0)]\,[\bar{v}_q(0)P_R i(\not{k}+m_j)P_L v_b(0)]}{D_i(k)D_j(k)} \\
& \times\frac{m_i^2 m_j^2}{M_W^4}\times\frac{i}{D_g(k)}\times\frac{i}{D_g(k)}\Bigg\}\,,
\end{aligned}
\tag{F.3}
$$

with $\lambda^i_{bq} = V_{ib}V^*_{iq}$, and

$$
D_i(k) = k^2 - m_i^2\,, \qquad D_W(k) = k^2 - M_W^2\,, \qquad D_g(k) = k^2 - \xi_W M_W^2\,, \tag{F.4}
$$

in the corresponding propagators, being ξ_W a gauge-fixing parameter. On the other hand, the parameter η arising from the W couplings to fermions can be $\eta = \pm 1$ depending on the sign convention used in the definition of the $SU(2)_L$ covariant derivative [17], although it is easy to see that this does not play a critical role in the calculation. Taking into account some fundamental properties of the chiral projectors in the Dirac algebra, namely,

$$P_{L/R} = \frac{1 \mp \gamma_5}{2}\,, \qquad P_L P_R = P_R P_L = 0\,, \qquad (P_{L/R})^2 = P_{L/R}\,, \qquad \gamma^\mu P_{L/R} = P_{R/L}\gamma^\mu\,, \tag{F.5}$$

we can simplify the previous expression as

$$\begin{aligned} i\mathcal{M}_{\rm I} = \delta_{\alpha_1\alpha_4}\delta_{\alpha_2\alpha_3}\frac{g^4}{4} &\sum_{i,j=u,c,t} \lambda^i_{bq}\lambda^j_{bq} \int \frac{\mathrm{d}^d k}{(2\pi)^d}\frac{1}{D_i(k)D_j(k)} \\ \times \Bigg\{ & [\bar{u}_q(0)\gamma^\rho \not{k}\gamma^\nu P_L u_b(0)]\,[\bar{v}_q(0)\gamma^\mu \not{k}\gamma^\sigma P_L v_b(0)] \\ & \times \left[-\frac{g_{\mu\nu}}{D_W(k)} + \frac{k_\mu k_\nu}{M_W^2}\left(\frac{1}{D_W(k)} - \frac{1}{D_g(k)}\right)\right]\left[-\frac{g_{\rho\sigma}}{D_W(k)} + \frac{k_\rho k_\sigma}{M_W^2}\left(\frac{1}{D_W(k)} - \frac{1}{D_g(k)}\right)\right] \\ & + \frac{2m_i^2 m_j^2}{M_W^2}\,[\bar{u}_q(0)\gamma^\nu P_L u_b(0)]\,[\bar{v}_q(0)\gamma^\mu P_L v_b(0)]\left[-\frac{g_{\mu\nu}}{D_W(k)} + \frac{k_\mu k_\nu}{M_W^2}\left(\frac{1}{D_W(k)} - \frac{1}{D_g(k)}\right)\right]\frac{1}{D_g(k)} \\ & + \frac{m_i^2 m_j^2}{M_W^4}\,[\bar{u}_q(0)\not{k}P_L u_b(0)]\,[\bar{v}_q(0)\not{k}P_L v_b(0)]\,\frac{1}{D_g^2(k)}\Bigg\}\,. \end{aligned} \tag{F.6}$$

Notice that both diagrams with $W^\pm G^\mp$ exchange give rise to the very same contribution to the amplitude. We can perform the contractions in the first two terms in the curly brackets, using that $\not{k}^2 = k^2$, and then separate the gauge-independent and gauge-dependent terms. This yields

$$\begin{aligned} i\mathcal{M}_{\rm I} = \delta_{\alpha_1\alpha_4}\delta_{\alpha_2\alpha_3}\frac{g^4}{4} &\sum_{i,j=u,c,t} \lambda^i_{bq}\lambda^j_{bq} \int \frac{\mathrm{d}^d k}{(2\pi)^d}\frac{1}{D_i(k)D_j(k)} \\ \times \Bigg\{ & \frac{1}{D_W^2(k)}\left(\frac{k^4}{M_W^4}[\not{k}P_L]\,[\not{k}P_L] - \frac{2k^4}{M_W^2}[\gamma^\mu P_L]\,[\gamma_\mu P_L] + [\gamma^\nu\not{k}\gamma^\mu P_L]\,[\gamma_\mu\not{k}\gamma_\nu P_L]\right) \\ & + \frac{k^4 - m_i^2 m_j^2}{M_W^4}\left(\frac{1}{D_g^2(k)} - \frac{2}{D_W(k)D_g(k)}\right)[\not{k}P_L]\,[\not{k}P_L] + \frac{k^4 - m_i^2 m_j^2}{M_W^2}\frac{2}{D_W(k)D_g(k)}[\gamma^\mu P_L]\,[\gamma_\mu P_L]\Bigg\}\,, \end{aligned} \tag{F.7}$$

where we have introduced the shorthand $[\ldots][\ldots] = [\bar{u}_q(0)\ldots u_b(0)]\,[\bar{v}_q(0)\ldots v_b(0)]$. The second line in the curly brackets contains all gauge dependence. The latter, nevertheless, vanishes due to 3×3 CKM unitarity, which manifests through

$$\sum_{i=u,c,t}\lambda^i_{bq} = \lambda^u_{bq} + \lambda^c_{bq} + \lambda^t_{bq} = 0\,, \qquad (q = d, s)\,, \tag{F.8}$$

that is, the orthogonality relation between columns. Therefore, using that

$$k^4 - m_i^2 m_j^2 = -D_i(k)D_j(k) + k^2\,[D_i(k) + D_j(k)]\,, \tag{F.9}$$

we are left with

$$\begin{aligned} i\mathcal{M}_{\rm I} = \delta_{\alpha_1\alpha_4}\delta_{\alpha_2\alpha_3}\frac{g^4}{4M_W^2} &\sum_{i,j=u,c,t} \lambda^i_{bq}\lambda^j_{bq} \int \frac{\mathrm{d}^d k}{(2\pi)^d}\frac{1}{D_i(k)D_j(k)D_W^2(k)} \\ \times & \left(\frac{m_i^2 m_j^2}{M_W^2}[\not{k}P_L]\,[\not{k}P_L] - 2m_i^2 m_j^2\,[\gamma^\mu P_L]\,[\gamma_\mu P_L] + M_W^2\,[\gamma^\nu\not{k}\gamma^\mu P_L]\,[\gamma_\mu\not{k}\gamma_\nu P_L]\right)\,. \end{aligned} \tag{F.10}$$

At this point, one has to perform the corresponding one-loop integrals,[1] which are convergent in $d = 4$ dimensions. To this aim, it is convenient to reexpress the denominator introducing Feynman parameters. In particular, we have

$$\begin{aligned}\frac{1}{D_i(k)D_j(k)D_W^2(k)} &= \int_0^1 \mathrm{d}x_1\mathrm{d}x_2\mathrm{d}x_3\delta(x_1+x_2+x_3-1)\frac{6x_3}{[x_1D_i(k)+x_2D_j(k)+x_3D_W(k)]^4} \\ &= \int_0^1 \mathrm{d}x_1\mathrm{d}x_2\mathrm{d}x_3\delta(x_1+x_2+x_3-1)\frac{6x_3}{\left[(x_1+x_2+x_3)k^2-x_1m_i^2-x_2m_j^2-x_3M_W^2\right]^4} \\ &= \int_0^1 \mathrm{d}x_2\int_0^{1-x_2}\mathrm{d}x_3\frac{6x_3}{\left[k^2-m_i^2+(m_i^2-m_j^2)x_2+(m_i^2-M_W^2)x_3\right]^4}\,. \end{aligned} \tag{F.11}$$

We can change variables as $x = 1 - x_2$ and $y = x_3$, such that

$$\begin{aligned}\frac{1}{D_i(k)D_j(k)D_W^2(k)} &= \int_0^1 \mathrm{d}x\int_0^x \mathrm{d}y\frac{6y}{\left[k^2-m_j^2-(m_i^2-m_j^2)x-(M_W^2-m_j^2)y\right]^4} \\ &= \int_0^1 \mathrm{d}x\int_0^x \mathrm{d}y\frac{6y}{(k^2-\Delta^2)^4}\,, \end{aligned} \tag{F.12}$$

with

$$\Delta^2 = m_j^2+(m_i^2-m_j^2)x+(M_W^2-m_j^2)y\,. \tag{F.13}$$

There are thus two types of one-loop integrals in Eq. (F.10) attending to their Lorentz structure. They are given by [10]

$$\int\frac{\mathrm{d}^4k}{(2\pi)^4}\frac{1}{(k^2-\Delta^2)^4} = \frac{i}{(4\pi)^2}\frac{1}{6\Delta^4}\,, \tag{F.14}$$

$$\int\frac{\mathrm{d}^4k}{(2\pi)^4}\frac{k^\alpha k^\beta}{(k^2-\Delta^2)^4} = \frac{g^{\alpha\beta}}{4}\int\frac{\mathrm{d}^4k}{(2\pi)^4}\frac{k^2}{(k^2-\Delta^2)^4} = -\frac{i}{(4\pi)^2}\frac{g^{\alpha\beta}}{12\Delta^2}\,. \tag{F.15}$$

Then, the amplitude in Eq. (F.10) now reads

$$\begin{aligned} i\mathcal{M}_\mathrm{I} = {}& \delta_{\alpha_1\alpha_4}\delta_{\alpha_2\alpha_3}\frac{-ig^4}{64\pi^2M_W^2}\sum_{i,j=u,c,t}\lambda^i_{bq}\lambda^j_{bq}\int_0^1\mathrm{d}x\int_0^y\mathrm{d}y \\ &\times\left(\frac{m_i^2m_j^2}{2M_W^2\Delta^2}\left[\gamma^\mu P_L\right]\left[\gamma_\mu P_L\right]+\frac{2m_i^2m_j^2}{\Delta^4}\left[\gamma^\mu P_L\right]\left[\gamma_\mu P_L\right]+\frac{M_W^2}{2\Delta^2}\left[\gamma^\nu\gamma^\alpha\gamma^\mu P_L\right]\left[\gamma_\mu\gamma_\alpha\gamma_\nu P_L\right]\right)y\,. \end{aligned} \tag{F.16}$$

The Dirac structure in the last term in parenthesis can be further reduced to

$$\left[\gamma^\nu\gamma^\alpha\gamma^\mu P_L\right]\otimes\left[\gamma_\mu\gamma_\alpha\gamma_\nu P_L\right] = 4\left[\gamma^\mu P_L\right]\otimes\left[\gamma_\mu P_L\right]\,, \tag{F.17}$$

by means of the identities

$$\gamma^\mu\gamma^\nu\gamma^\alpha = g^{\mu\nu}\gamma^\alpha - g^{\mu\alpha}\gamma^\nu + g^{\nu\alpha}\gamma^\mu + i\epsilon^{\mu\nu\alpha\beta}\gamma_\beta\gamma_5\,, \qquad \epsilon^{\mu\nu\alpha\beta}\epsilon_{\mu\nu\alpha\rho} = -6\delta^\beta_\rho\,, \qquad \gamma_5P_{L/R} = \mp P_{L/R}\,. \tag{F.18}$$

[1]One-loop integrals can be computed using `Package X` [293]. Unfortunately, new versions of this software are not available anymore.

This leads to

$$
\begin{aligned}
i\mathcal{M}_{\mathrm{I}} = \delta_{\alpha_1\alpha_4}\delta_{\alpha_2\alpha_3}\frac{-ig^4}{64\pi^2 M_W^2}\,[\bar{u}_q(0)\gamma^\mu P_L u_b(0)]\,[\bar{v}_q(0)\gamma_\mu P_L v_b(0)] \\
\times \sum_{i,j=u,c,t}\lambda^i_{bq}\lambda^j_{bq}\int_0^1 \mathrm{d}x\int_0^y \mathrm{d}y\left(\frac{m_i^2 m_j^2}{2M_W^2\Delta^2}+\frac{2m_i^2 m_j^2}{\Delta^4}+\frac{2M_W^2}{\Delta^2}\right)y\,,
\end{aligned}
\tag{F.19}
$$

with Δ^2 given in Eq. (F.13). It is common practice in the literature to introduce the Fermi coupling constant in the prefactor using that $G_F/\sqrt{2} = g^2/(8M_W^2)$. Once the integration over the Feynman parameters is performed, we obtain

$$
i\mathcal{M}_{\mathrm{I}} = \delta_{\alpha_1\alpha_4}\delta_{\alpha_2\alpha_3}\frac{iG_F^2 M_W^2}{2\pi^2}\,[\bar{u}_q(0)\gamma^\mu P_L u_b(0)]\,[\bar{v}_q(0)\gamma_\mu P_L v_b(0)]\sum_{i,j=u,c,t}\lambda^i_{bq}\lambda^j_{bq}F(x_i,x_j)\,,
\tag{F.20}
$$

with $x_i = m_i^2/M_W^2$, and

$$
F(x_i,x_j) = \frac{1}{(1-x_i)(1-x_j)}\left(\frac{7x_ix_j}{4}-1\right)+\frac{\left(1-2x_j+\frac{x_ix_j}{4}\right)x_i^2\ln x_i}{(x_j-x_i)(1-x_i)^2}+\frac{\left(1-2x_i+\frac{x_ix_j}{4}\right)x_j^2\ln x_j}{(x_i-x_j)(1-x_j)^2}\,.
\tag{F.21}
$$

As one could have expected, the function $F(x_i,x_j)$ is symmetric in its arguments, *i.e.*, $F(x_i,x_j) = F(x_j,x_i)$. The 3×3 unitarity of the CKM matrix allows us to eliminate λ^u_{bq} from the last sum in Eq. (F.20) as

$$
\begin{aligned}
\sum_{i,j=u,c,t}\lambda^i_{bq}\lambda^j_{bq}F(x_i,x_j) &= -\sum_{i,j=c,t}\lambda^i_{bq}\lambda^j_{bq}\left[F(x_u,x_i)+F(x_u,x_j)-F(x_u,x_u)-F(x_i,x_j)\right] \\
&= -\left(\lambda^c_{bq}\right)^2\left[2F(x_u,x_c)-F(x_u,x_u)-F(x_c,x_c)\right] \\
&\quad -\left(\lambda^t_{bq}\right)^2\left[2F(x_u,x_t)-F(x_u,x_u)-F(x_t,x_t)\right] \\
&\quad -2\lambda^c_{bq}\lambda^t_{bq}\left[F(x_u,x_c)+F(x_u,x_t)-F(x_u,x_u)-F(x_c,x_t)\right]\,.
\end{aligned}
\tag{F.22}
$$

Taking the limit $x_u \to 0$, one can define

$$
S_0(x_i,x_j) \equiv \lim_{x_u\to 0}\left[F(x_u,x_i)+F(x_u,x_j)-F(x_u,x_u)-F(x_i,x_j)\right]\,,
\tag{F.23}
$$

$$
S_0(x_i) \equiv \lim_{x_u\to 0}\left[2F(x_u,x_i)-F(x_u,x_u)-F(x_i,x_i)\right]\,,
\tag{F.24}
$$

such that $S_0(x_i) = \lim_{x_j\to x_i} S_0(x_i,x_j)$. In this limit, the final amplitude corresponding to the set I of diagrams in Fig. F.1 is given by

$$
\begin{aligned}
i\mathcal{M}_{\mathrm{I}} = -\frac{iG_F^2 M_W^2}{2\pi^2}\left[(\lambda^t_{bq})^2 S_0(x_t)+(\lambda^c_{bq})^2 S_0(x_c)+2\lambda^c_{bq}\lambda^t_{bq}S_0(x_c,x_t)\right] \\
\times\,\delta_{\alpha_1\alpha_4}\delta_{\alpha_2\alpha_3}\,[\bar{u}_q(0)\gamma^\mu P_L u_b(0)]\,[\bar{v}_q(0)\gamma_\mu P_L v_b(0)]\,,
\end{aligned}
\tag{F.25}
$$

where the explicit form of the well-known Inami-Lim functions in Eqs. (F.23) and (F.24) reads

$$
S_0(x_i,x_j) = x_ix_j\left[-\frac{3}{4(1-x_i)(1-x_j)}+\frac{(1-2x_i+x_i^2/4)\ln x_i}{(x_i-x_j)(1-x_i)^2}+\frac{(1-2x_j+x_j^2/4)\ln x_j}{(x_j-x_i)(1-x_j)^2}\right],
\tag{F.26}
$$

$$
S_0(x_i) = \frac{x_i}{(1-x_i)^2}\left[1-\frac{11x_i}{4}+\frac{x_i^2}{4}-\frac{3x_i^2\ln x_i}{2(1-x_i)}\right]\,.
\tag{F.27}
$$

On the other hand, turning to the set II of diagrams depicted in Fig. F.2, the corresponding computation comes almost straightforwardly at this point. The only difference with respect to the previous set relies on the ordering of the quark spinors and how color indices are contracted. More precisely, the amplitude for our set II of box diagrams in Fig. F.2 reads

$$\begin{aligned} i\mathcal{M}_{\rm II} = -\frac{iG_F^2 M_W^2}{2\pi^2} &\left[(\lambda^t_{bq})^2 S_0(x_t) + (\lambda^c_{bq})^2 S_0(x_c) + 2\lambda^c_{bq}\lambda^t_{bq} S_0(x_c,x_t)\right] \\ &\times \delta_{\alpha_1\alpha_2}\delta_{\alpha_3\alpha_4}\left[\bar{u}_q(0)\gamma^\mu P_L v_b(0)\right]\left[\bar{v}_q(0)\gamma_\mu P_L u_b(0)\right] . \end{aligned} \tag{F.28}$$

Then, we can write down the total amplitude $i\mathcal{M}$ as

$$i\mathcal{M} = i(\mathcal{M}_{\rm I} - \mathcal{M}_{\rm II}) = -\frac{iG_F^2 M_W^2}{2\pi^2}\mathcal{F}_0 \begin{pmatrix} \delta_{\alpha_1\alpha_4}\delta_{\alpha_2\alpha_3}\left[\bar{u}_q(0)\gamma^\mu P_L u_b(0)\right]\left[\bar{v}_q(0)\gamma_\mu P_L v_b(0)\right] \\ -\delta_{\alpha_1\alpha_2}\delta_{\alpha_3\alpha_4}\left[\bar{u}_q(0)\gamma^\mu P_L v_b(0)\right]\left[\bar{v}_q(0)\gamma_\mu P_L u_b(0)\right] \end{pmatrix}, \tag{F.29}$$

where we have introduced

$$\mathcal{F}_0 = (\lambda^t_{bq})^2 S_0(x_t) + (\lambda^c_{bq})^2 S_0(x_c) + 2\lambda^c_{bq}\lambda^t_{bq} S_0(x_c,x_t) . \tag{F.30}$$

It is important to notice that there is a relative minus sign between the two sets of diagrams. We can then use Fierz identities for spinors [10], namely,

$$\left(\bar{\psi}_1\gamma^\mu P_L\psi_2\right)\left(\bar{\psi}_3\gamma^\mu P_L\psi_4\right) = -\left(\bar{\psi}_1\gamma^\mu P_L\psi_4\right)\left(\bar{\psi}_3\gamma^\mu P_L\psi_2\right) , \tag{F.31}$$

in order to write

$$i\mathcal{M} = -\frac{iG_F^2 M_W^2}{2\pi^2}\mathcal{F}_0\left[\bar{u}_q(0)\gamma^\mu P_L u_b(0)\right]\left[\bar{v}_q(0)\gamma_\mu P_L v_b(0)\right]\left(\delta_{\alpha_1\alpha_4}\delta_{\alpha_2\alpha_3} + \delta_{\alpha_1\alpha_2}\delta_{\alpha_3\alpha_4}\right) . \tag{F.32}$$

In terms of an effective $\Delta B = 2$ Hamiltonian, $i\mathcal{M}$ arises from the matrix element of a single dim-6 local operator $[\bar{q}_\alpha(x)\gamma^\mu P_L b_\alpha(x)]\,[\bar{q}_\beta(x)\gamma_\mu P_L b_\beta(x)]$. With two pairs of identical operators, contraction of the fields with external particle states requires some care. As we will address later in this section, one can write

$$\begin{aligned} &\left[\bar{u}_q(0)\gamma^\mu P_L u_b(0)\right]\left[\bar{v}_q(0)\gamma_\mu P_L v_b(0)\right]\left(\delta_{\alpha_1\alpha_4}\delta_{\alpha_2\alpha_3} + \delta_{\alpha_1\alpha_2}\delta_{\alpha_3\alpha_4}\right) = \\ &= \frac{1}{2}\langle B_q|\left[\bar{q}_\alpha(x)\gamma^\mu P_L b_\alpha(x)\right]\left[\bar{q}_\beta(x)\gamma_\mu P_L b_\beta(x)\right]|\bar{B}_q\rangle , \end{aligned} \tag{F.33}$$

being α and β color indices. This yields

$$\begin{aligned} i\mathcal{M} &= -\frac{iG_F^2 M_W^2}{4\pi^2}\mathcal{F}_0\langle B_q|\left[\bar{q}_\alpha(x)\gamma^\mu P_L b_\alpha(x)\right]\left[\bar{q}_\beta(x)\gamma_\mu P_L b_\beta(x)\right]|\bar{B}_q\rangle \\ &= -\frac{iG_F^2 M_W^2}{16\pi^2}\mathcal{F}_0\langle B_q|\left[\bar{q}_\alpha(x)\gamma^\mu(1-\gamma_5) b_\alpha(x)\right]\left[\bar{q}_\beta(x)\gamma_\mu(1-\gamma_5) b_\beta(x)\right]|\bar{B}_q\rangle . \end{aligned} \tag{F.34}$$

The resulting $\mathcal{H}^{\Delta B=2}_{\rm dis,eff}$ effective Hamiltonian reads

$$\mathcal{H}^{\Delta B=2}_{\rm dis,eff} = \frac{G_F^2 M_W^2}{16\pi^2}\mathcal{F}_0 O^{\Delta B=2}_{V-A} + {\rm H.c.} , \tag{F.35}$$

with

$$O^{\Delta B=2}_{V-A} \equiv \left[\bar{q}_\alpha(x)\gamma^\mu(1-\gamma_5) b_\alpha(x)\right]\left[\bar{q}_\beta(x)\gamma_\mu(1-\gamma_5) b_\beta(x)\right] . \tag{F.36}$$

We can now obtain $M_{12}^{q,\mathrm{SM}}$, at lowest order in perturbation theory, as

$$M_{12}^{q,\mathrm{SM}} = \frac{1}{2M_{B_q}} \langle B_q | \mathcal{H}_{W,\mathrm{eff}}^{\Delta B=2} | \bar{B}_q \rangle \,. \tag{F.37}$$

Note that we have inserted at this point a $(2M_{B_q})^{-1}$ factor, so that the meson states that appear in Eq. (F.37) are covariantly normalized.

In principle, in order to compute the matrix element of the operator $O_{V-A}^{\Delta B=2}$ between these meson states one relies on the vacuum insertion approximation. This means separating the matrix element of our four-quark operator into the product of two matrix elements of quark bilinears by inserting solely the vacuum state, instead of a complete set of states. The correction to this approximation is expressed in terms of a bag parameter that accounts for all other states neglected in the sum. Therefore, in the relativistic normalization approach, one can write (see App. C from [58])

$$\langle B_q | O_{V-A}^{\Delta B=2} | \bar{B}_q \rangle = -\frac{8}{3} e^{i(\xi_b - \xi_q - \xi_{B_q})} M_{B_q}^2 f_{B_q}^2 B_{B_q} \,, \tag{F.38}$$

where ξ_{B_q}, ξ_b and ξ_q are the CP transformation phases of the B_q meson state and the quark fields, M_{B_q} is the common mass of the mesons (in the absence of weak interactions), f_{B_q} is the meson decay constant encoding all the information about strong interactions, and B_{B_q} is the bag factor. The meson decay constant and the bag parameter are determined non-perturbatively in the framework of QCD sum rules [214–216] or lattice QCD [212,213]. One usually assumes a CP transformation in which $\xi_b = \xi_q = 0$. Furthermore, in this work we are assuming $\xi_{B_q} = \pi$, *i.e.*, $\mathcal{CP}|B_q\rangle = -|\bar{B}_q\rangle$. With these choices, we can finally write the well-known result for $M_{12}^{q,\mathrm{SM}}$:

$$M_{12}^{q,\mathrm{SM}} = \frac{G_F^2 M_W^2}{12\pi^2} (\lambda_{bq}^t)^2 S_0(x_t) M_{B_q} f_{B_q}^2 B_{B_q} \hat{\eta}_B \,. \tag{F.39}$$

Numerically, the dominant contribution comes from virtual top quarks running in the loop because $m_t \gg m_c$, and thus Eq. (F.30) is simply written as $\mathcal{F}_0 \simeq (\lambda_{bq}^t)^2 S_0(x_t)$. For completeness, we have included in the final result the factor $\hat{\eta}_B$ [218] which takes into account short distance (perturbative) QCD corrections at two loops.

At this point, we find useful to point out that the majority of references addressing the study of neutral meson mixing make use of the covariant normalization of the states, such as [237,238,294] and more recent references. However, for the sake of clarity, we should highlight that other works like [58, 292, 295, 296] opt to write Eqs. (F.37) and (F.38) maintaining the non-covariant normalization of the states, so that

$$M_{12}^{q,\mathrm{SM}} = \langle B_q | \mathcal{H}_{W,\mathrm{eff}}^{\Delta B=2} | \bar{B}_q \rangle \,, \qquad \langle B_q | O_{V-A}^{\Delta B=2} | \bar{B}_q \rangle = -\frac{8}{6} e^{i(\xi_b - \xi_q - \xi_{B_q})} M_{B_q} f_{B_q}^2 B_{B_q} \,. \tag{F.40}$$

Likewise, there might be different choices for the CP transformation phase ξ_{B_q}, *e.g.*, Ref. [292] sets $\xi_{B_q} = 0$.

To close this section, let us come back to the obtention of Eq. (F.33).

Effective local operator $O_{V-A}^{\Delta B=2}$

Our aim is to compute the matrix element $\langle B_q | \bar{q}_\alpha(x) \gamma^\mu P_L b_\alpha(x) \bar{q}_\beta(x) \gamma_\mu P_L b_\beta(x) | \bar{B}_q \rangle$ in terms of spinor currents. Adopting the momentum and color indices assignments presented in Fig. F.3, our initial and final states are defined by

$$|\bar{B}_q\rangle = a^{(b)\dagger}_{\alpha_2}(p_2) b^{(q)\dagger}_{\alpha_1}(p_1)|0\rangle\,, \qquad |B_q\rangle = b^{(b)\dagger}_{\alpha_4}(p_4) a^{(q)\dagger}_{\alpha_3}(p_3)|0\rangle\,, \tag{F.41}$$

being $|0\rangle$ the vacuum state, and $a^{(\psi)\dagger}_{\alpha}(p)$ and $b^{(\psi)\dagger}_{\alpha}(p)$ the creation operators of particles and antiparticles of fermion ψ with color index α and momentum p. All possible contractions of the quark fields with the creation and annihilation operators of the external states read

$$\begin{aligned}
&\langle B_q|\bar{q}_\alpha(x)\gamma^\mu P_L b_\alpha(x)\bar{q}_\beta(x)\gamma_\mu P_L b_\beta(x)|\bar{B}_q\rangle \\
&= \langle 0|a^{(q)}_{\alpha_3}(p_3) b^{(b)}_{\alpha_4}(p_4)\bar{q}_\alpha(x)\gamma^\mu P_L b_\alpha(x)\bar{q}_\beta(x)\gamma_\mu P_L b_\beta(x) a^{(b)\dagger}_{\alpha_2}(p_2) b^{(q)\dagger}_{\alpha_1}(p_1)|0\rangle \\
&+ \langle 0|a^{(q)}_{\alpha_3}(p_3) b^{(b)}_{\alpha_4}(p_4)\bar{q}_\alpha(x)\gamma^\mu P_L b_\alpha(x)\bar{q}_\beta(x)\gamma_\mu P_L b_\beta(x) a^{(b)\dagger}_{\alpha_2}(p_2) b^{(q)\dagger}_{\alpha_1}(p_1)|0\rangle \\
&+ \langle 0|a^{(q)}_{\alpha_3}(p_3) b^{(b)}_{\alpha_4}(p_4)\bar{q}_\alpha(x)\gamma^\mu P_L b_\alpha(x)\bar{q}_\beta(x)\gamma_\mu P_L b_\beta(x) a^{(b)\dagger}_{\alpha_2}(p_2) b^{(q)\dagger}_{\alpha_1}(p_1)|0\rangle \\
&+ \langle 0|a^{(q)}_{\alpha_3}(p_3) b^{(b)}_{\alpha_4}(p_4)\bar{q}_\alpha(x)\gamma^\mu P_L b_\alpha(x)\bar{q}_\beta(x)\gamma_\mu P_L b_\beta(x) a^{(b)\dagger}_{\alpha_2}(p_2) b^{(q)\dagger}_{\alpha_1}(p_1)|0\rangle\,.
\end{aligned} \tag{F.42}$$

There is a minus sign for each crossing among the Wick contraction lines, which accounts for the anti-commutation of the fermionic operators in order to perform the corresponding contraction. Therefore, we obtain

$$\begin{aligned}
&\langle B_q|\bar{q}_\alpha(x)\gamma^\mu P_L b_\alpha(x)\bar{q}_\beta(x)\gamma_\mu P_L b_\beta(x)|\bar{B}_q\rangle \\
&= -\delta_{\alpha\alpha_3}\delta_{\alpha\alpha_4}\delta_{\beta\alpha_1}\delta_{\beta\alpha_2}\,[\bar{u}_q(p_3)\gamma^\mu P_L v_b(p_4)]\,[\bar{v}_q(p_1)\gamma_\mu P_L u_b(p_2)]\,e^{-i(p_1+p_2-p_3-p_4)x} \\
&\quad + \delta_{\alpha\alpha_1}\delta_{\alpha\alpha_4}\delta_{\beta\alpha_2}\delta_{\beta\alpha_3}\,[\bar{v}_q(p_1)\gamma^\mu P_L v_b(p_4)]\,[\bar{u}_q(p_3)\gamma_\mu P_L u_b(p_2)]\,e^{-i(p_1+p_2-p_3-p_4)x} \\
&\quad + \delta_{\alpha\alpha_2}\delta_{\alpha\alpha_3}\delta_{\beta\alpha_1}\delta_{\beta\alpha_4}\,[\bar{u}_q(p_3)\gamma^\mu P_L u_b(p_2)]\,[\bar{v}_q(p_1)\gamma_\mu P_L v_b(p_4)]\,e^{-i(p_1+p_2-p_3-p_4)x} \\
&\quad - \delta_{\alpha\alpha_1}\delta_{\alpha\alpha_2}\delta_{\beta\alpha_3}\delta_{\beta\alpha_4}\,[\bar{v}_q(p_1)\gamma^\mu P_L u_b(p_2)]\,[\bar{u}_q(p_3)\gamma_\mu P_L v_b(p_4)]\,e^{-i(p_1+p_2-p_3-p_4)x} \\
&= 2\begin{pmatrix} \delta_{\alpha_1\alpha_4}\delta_{\alpha_2\alpha_3}\,[\bar{u}_q(p_3)\gamma^\mu P_L u_b(p_2)]\,[\bar{v}_q(p_1)\gamma_\mu P_L v_b(p_4)] \\ -\delta_{\alpha_1\alpha_2}\delta_{\alpha_3\alpha_4}\,[\bar{u}_q(p_3)\gamma^\mu P_L v_b(p_4)]\,[\bar{v}_q(p_1)\gamma_\mu P_L u_b(p_2)] \end{pmatrix} e^{-i(p_1+p_2-p_3-p_4)x}\,.
\end{aligned} \tag{F.43}$$

Using the Fierz identity in Eq. (F.31), we can write down

$$\begin{aligned}
&\langle B_q|\bar{q}_\alpha(x)\gamma^\mu P_L b_\alpha(x)\bar{q}_\beta(x)\gamma_\mu P_L b_\beta(x)|\bar{B}_q\rangle \\
&\quad = 2(\delta_{\alpha_1\alpha_4}\delta_{\alpha_2\alpha_3} + \delta_{\alpha_1\alpha_2}\delta_{\alpha_3\alpha_4})\,[\bar{u}_q(p_3)\gamma^\mu P_L u_b(p_2)]\,[\bar{v}_q(p_1)\gamma_\mu P_L v_b(p_4)]\,e^{-i(p_1+p_2-p_3-p_4)x}\,.
\end{aligned} \tag{F.44}$$

Finally, if we take the limit of zero external momenta, we are left with

$$\begin{aligned}
&\langle B_q|\bar{q}_\alpha(x)\gamma^\mu P_L b_\alpha(x)\bar{q}_\beta(x)\gamma_\mu P_L b_\beta(x)|\bar{B}_q\rangle \\
&\quad = 2(\delta_{\alpha_1\alpha_4}\delta_{\alpha_2\alpha_3} + \delta_{\alpha_1\alpha_2}\delta_{\alpha_3\alpha_4})\,[\bar{u}_q(0)\gamma^\mu P_L u_b(0)]\,[\bar{v}_q(0)\gamma_\mu P_L v_b(0)]\,,
\end{aligned} \tag{F.45}$$

which is precisely the result anticipated in Eq. (F.33).

F.1.2 Decay width mixing $\Gamma_{12}^{q,\mathrm{SM}}$

Let us now move on to the analysis of $\Gamma_{12}^{q,\mathrm{SM}}$. It corresponds to two $\Delta B = 1$ transitions via real (on-shell) intermediate states, *i.e.*, through decay modes that are common to both B_q and $\bar{B}_q$, as one can readily check by inspection of Eq. (F.2). Consequently, $\Gamma_{12}^{q,\mathrm{SM}}$ is sensitive to light states with masses below $M_{B_q} \sim m_b$, thus only containing up and/or charm quarks.

The theoretical determination of $\Gamma_{12}^{q,\mathrm{SM}}$ is cumbersome because it is not given by the matrix element of a local operator. In light of this, one relies on the validity of the heavy quark expansion, where $\Gamma_{12}^{q,\mathrm{SM}}$ is expressed as a power series in Λ/m_b, being Λ a mass scale related to non-perturbative interactions, and the strong coupling α_s (see, *e.g.*, [234] for a detailed description). Although this is a well-known approach where higher order corrections have already been calculated, it might be instructive for the reader to briefly review the details on the computation of the lowest order contribution to $\Gamma_{12}^{q,\mathrm{SM}}$ in the previous expansion [296–301], that is, at $\mathcal{O}(\Lambda^3/m_b^3)$ and $\mathcal{O}(\alpha_s^0)$ in QCD.

To this aim, one has to extract the *absorptive* (imaginary) part of the box diagrams in Figs. F.1 and F.2. Aiming for simplicity, we perform the computations in the unitary gauge (corresponding to the limit $\xi_W \to \infty$ in the R_ξ-gauge), so that only the diagrams in Figs. F.1a and F.2a containing two physical W bosons have to be considered. A simplifying assumption can be carried out on that regard, namely, neglecting the momentum dependence in the bosonic propagators, as they are bounded to be $k_W^2 \lesssim m_b^2 \ll M_W^2$. One can further take the momentum of external light quarks $p_1, p_3 \to 0$ since $p_2^2 = p_4^2 = m_b^2 \gg p_1^2 = p_3^2 = m_q^2$, which implies $p_2 \simeq p_4 \equiv p$. With these approximations, we can start writing

$$
\begin{aligned}
i\mathcal{M} &= i\left(\mathcal{M}_{\mathrm{I}} - \mathcal{M}_{\mathrm{II}}\right) \\
&= \left(-i\eta\frac{g}{\sqrt{2}}\right)^4 \sum_{i,j=u,c,t} \lambda_{bq}^i \lambda_{bq}^j \int \frac{\mathrm{d}^d k}{(2\pi)^d} \\
&\times \Bigg\{ \sum_{\beta_1,\beta_2} \delta_{\alpha_1\beta_2}\delta_{\alpha_2\beta_1}\delta_{\alpha_3\beta_1}\delta_{\alpha_4\beta_2} \frac{[\bar{u}_q(0)\gamma^\rho P_L i(\not{k}+m_i)\gamma^\nu P_L u_b(p)]\,[\bar{v}_q(0)\gamma^\mu P_L i(\not{k}-\not{p}+m_j)\gamma^\sigma P_L v_b(p)]}{D_i(k)D_j(k-p)} \\
&\qquad \times i\frac{g_{\mu\nu}}{M_W^2} \times i\frac{g_{\rho\sigma}}{M_W^2} \\
&\quad - \sum_{\beta_1,\beta_2} \delta_{\alpha_1\beta_1}\delta_{\alpha_2\beta_1}\delta_{\alpha_3\beta_2}\delta_{\alpha_4\beta_2} \frac{[\bar{v}_q(0)\gamma^\mu P_L i(\not{p}-\not{k}+m_i)\gamma^\nu P_L u_b(p)]\,[\bar{u}_q(0)\gamma^\rho P_L i(-\not{k}+m_j)\gamma^\sigma P_L v_b(p)]}{D_i(p-k)D_j(-k)} \\
&\qquad \times i\frac{g_{\mu\sigma}}{M_W^2} \times i\frac{g_{\nu\rho}}{M_W^2} \Bigg\}.
\end{aligned}
\tag{F.46}
$$

Notice the relative minus sign between the two partial amplitudes. Since the denominator of the fermionic propagators is quadratic in the corresponding momentum, it is clear that $D_i(p-k) = D_i(k-p)$ and $D_j(-k) = D_j(k)$. Exchanging the labels $i \leftrightarrow j$ in the second term in the curly brackets, and taking into account the Dirac algebra identities quoted in Eq. (F.5), we are left with

$$
\begin{aligned}
i\mathcal{M} &= \frac{g^4}{4M_W^2} \sum_{i,j=u,c,t} \lambda_{bq}^i \lambda_{bq}^j \int \frac{\mathrm{d}^d k}{(2\pi)^d} \frac{k_\alpha (k-p)^\beta}{D_i(k)D_j(k-p)} \\
&\times \begin{pmatrix} \delta_{\alpha_1\alpha_4}\delta_{\alpha_2\alpha_3}\,[\bar{u}_q(0)\gamma^\mu\gamma^\alpha\gamma^\nu P_L u_b(p)]\,[\bar{v}_q(0)\gamma_\nu\gamma_\beta\gamma_\mu P_L v_b(p)] \\ -\delta_{\alpha_1\alpha_2}\delta_{\alpha_3\alpha_4}\,[\bar{u}_q(0)\gamma^\mu\gamma^\alpha\gamma^\nu P_L v_b(p)]\,[\bar{v}_q(0)\gamma_\nu\gamma_\beta\gamma_\mu P_L u_b(p)] \end{pmatrix}.
\end{aligned}
\tag{F.47}
$$

One may notice that the remaining one-loop integral is divergent in $d = 4$ dimensions: this is just a consequence of having neglected the momentum dependence in the bosonic propagators. Nevertheless, one should not worry about it, as we are interested in the absorptive (imaginary) part of the diagrams. The latter yields

$$i\mathcal{M} = \frac{ig^4}{64\pi^2 M_W^2} \sum_{i,j=u,c,t} \lambda_{bq}^i \lambda_{bq}^j \left\{ - \begin{pmatrix} \delta_{\alpha_1\alpha_4}\delta_{\alpha_2\alpha_3}\,[\bar{u}_q(0)\gamma^\mu P_L u_b(p)]\,[\bar{v}_q(0)\gamma_\mu P_L v_b(p)] \\ -\delta_{\alpha_1\alpha_2}\delta_{\alpha_3\alpha_4}\,[\bar{u}_q(0)\gamma^\mu P_L v_b(p)]\,[\bar{v}_q(0)\gamma^\mu P_L u_b(p)] \end{pmatrix} A(m_b^2, m_i^2, m_j^2) \right.$$
$$\left. + \begin{pmatrix} \delta_{\alpha_1\alpha_4}\delta_{\alpha_2\alpha_3}\,[\bar{u}_q(0)P_R u_b(p)]\,[\bar{v}_q(0)P_R v_b(p)] \\ -\delta_{\alpha_1\alpha_2}\delta_{\alpha_3\alpha_4}\,[\bar{u}_q(0)P_R v_b(p)]\,[\bar{v}_q(0)P_R u_b(p)] \end{pmatrix} B(m_b^2, m_i^2, m_j^2) \right\}, \tag{F.48}$$

with

$$A(m_b^2, m_i^2, m_j^2) = \frac{\pi\,\lambda(m_b^2, m_i^2, m_j^2)\sqrt{\lambda(m_b^2, m_i^2, m_j^2)}}{3m_b^4}, \tag{F.49}$$

$$B(m_b^2, m_i^2, m_j^2) = \frac{2\pi\left[m_b^4 + m_b^2(m_i^2 + m_j^2) + 4m_i^2 m_j^2 - 2(m_i^4 + m_j^4)\right]\sqrt{\lambda(m_b^2, m_i^2, m_j^2)}}{3m_b^4}, \tag{F.50}$$

being $\lambda(x, y, z) = x^2 + y^2 + z^2 - 2xy - 2xz - 2yz$ the Källen function. We should stress that the sum only includes the contributions from the light up and charm quarks. Similarly to what has been done in Eqs. (F.42) and (F.43), it is straightforward to obtain

$$i\mathcal{M} = -\frac{iG_F^2}{16\pi^2} \sum_{i,j=u,c} \lambda_{bq}^i \lambda_{bq}^j \left\{ A(m_b^2, m_i^2, m_j^2)\langle B_q|\,[\bar{q}_\alpha(x)\gamma^\mu(1-\gamma_5)b_\alpha(x)]\,[\bar{q}_\beta(x)\gamma_\mu(1-\gamma_5)b_\beta(x)]\,|\bar{B}_q\rangle \right.$$
$$\left. - B(m_b^2, m_i^2, m_j^2)\langle B_q|\,[\bar{q}_\alpha(x)(1+\gamma_5)b_\alpha(x)]\,[\bar{q}_\beta(x)(1+\gamma_5)b_\beta(x)]\,|\bar{B}_q\rangle \right\}, \tag{F.51}$$

where we have introduced the Fermi coupling constant in the prefactor by using $G_F/\sqrt{2} = g^2/(8M_W^2)$. The resulting effective Hamiltonian $\mathcal{H}_{\text{abs,eff}}^{\Delta B=2}$ that allows to compute the absorptive part of the mixing reads

$$\mathcal{H}_{\text{abs,eff}}^{\Delta B=2} = \frac{G_F^2}{16\pi^2} \sum_{i,j=u,c} \lambda_{bq}^i \lambda_{bq}^j \left\{ A(m_b^2, m_i^2, m_j^2)\, O_{V-A}^{\Delta B=2} - B(m_b^2, m_i^2, m_j^2)\, O_{S+P}^{\Delta B=2} \right\} + \text{H.c.}, \tag{F.52}$$

with dim-6 four-quark operators given by

$$O_{V-A}^{\Delta B=2} \equiv [\bar{q}_\alpha(x)\gamma^\mu(1-\gamma_5)b_\alpha(x)]\,[\bar{q}_\beta(x)\gamma_\mu(1-\gamma_5)b_\beta(x)], \tag{F.53}$$

$$O_{S+P}^{\Delta B=2} \equiv [\bar{q}_\alpha(x)(1+\gamma_5)b_\alpha(x)]\,[\bar{q}_\beta(x)(1+\gamma_5)b_\beta(x)]. \tag{F.54}$$

Besides the $(V-A)\times(V-A)$ contribution that was already present in the computation of $M_{12}^{q,\text{SM}}$, we have $(S+P)\times(S+P)$ quark currents. Then, we can obtain $\Gamma_{12}^{q,\text{SM}}$ from

$$\frac{\Gamma_{12}^{q,\text{SM}}}{2} = -\frac{1}{2M_{B_q}} \langle B_q|\mathcal{H}_{\text{abs,eff}}^{\Delta B=2}|\bar{B}_q\rangle. \tag{F.55}$$

The previous formula is an assumption to reduce a complicated hadron phase space problem into a manageable one-loop integral. Again, we are using the covariant normalization of the meson states.

The matrix element of the operator $O^{\Delta B=2}_{S+P}$ is given by

$$\langle B_q|O^{\Delta B=2}_{S+P}|\bar{B}_q\rangle = \frac{5}{3}e^{i(\xi_b-\xi_q-\xi_{B_q})}\frac{M^4_{B_q}f^2_{B_q}}{(m_b+m_q)^2}B'_{B_q} \simeq \frac{5}{3}e^{i(\xi_b-\xi_q-\xi_{B_q})}M^2_{B_q}f^2_{B_q}B'_{B_q}\,, \tag{F.56}$$

where the B'_{B_q} is the bag factor accounting for the deviation from the vacuum insertion approximation. In the second-to-last step we have used that $m_q \ll m_b \sim M_{B_q}$. Together with Eq. (F.38), and setting $\xi_{B_q} = \pi$ and $\xi_b = \xi_q = 0$, the result for $\Gamma^{q,\mathrm{SM}}_{12}$ turns out to be

$$\Gamma^{q,\mathrm{SM}}_{12} = -\frac{G^2_F M_{B_q} f^2_{B_q}}{72\pi m^4_b}\sum_{i,j=u,c}\lambda^i_{bq}\lambda^j_{bq}\sqrt{\lambda(m^2_b,m^2_i,m^2_j)} \times\left\{4\lambda(m^2_b,m^2_i,m^2_j)B_{B_q} + 5\left[m^4_b + m^2_b(m^2_i+m^2_j) + 4m^2_i m^2_j - 2(m^4_i+m^4_j)\right]B'_{B_q}\right\}. \tag{F.57}$$

At this order, the non-perturbative scale Λ is given by $\Lambda^3 \sim 16\pi^2 M_{B_q} f^2_{B_q} \times$ "numerical suppression factor" [234]. Currently, higher order QCD corrections are only known for the leading term in the Λ/m_b expansion, while the contribution from subleading powers of Λ/m_b is only known at leading order in QCD. For a recent update on the state of the art, see [160,302] and references therein. It is easy to check that our previous result coincides with the one computed in [298] when considering the vacuum insertion approximation $B_{B_q} = B'_{B_q} = 1$ and taking the limit $m_u \to 0$. In the latter case, and further using 3×3 CKM unitarity in the form of Eq. (F.8), one can readily obtain

$$\Gamma^{q,\mathrm{SM}}_{12} = -\frac{G^2_F M_{B_q} f^2_{B_q} m^2_b}{8\pi}\left[(\lambda^t_{bq})^2 + \frac{8}{3}\frac{m^2_c}{m^2_b}\lambda^t_{bq}\lambda^c_{bq} + \mathcal{O}\left(\frac{m^4_c}{m^4_b}\right)\right]. \tag{F.58}$$

For completeness, we finally include the alternative form for Eqs. (F.55) and (F.56) that makes use of the non-covariant normalization of the states, namely,

$$\frac{\Gamma^{q,\mathrm{SM}}_{12}}{2} = -\langle B_q|\mathcal{H}^{\Delta B=2}_{\mathrm{abs,eff}}|\bar{B}_q\rangle\,, \qquad \langle B_q|O^{\Delta B=2}_{S+P}|\bar{B}_q\rangle \simeq \frac{5}{6}e^{i(\xi_b-\xi_q-\xi_{B_q})}M_{B_q}f^2_{B_q}B'_{B_q}\,. \tag{F.59}$$

F.2 Calculation within vector-like quark models

In this section, we compute the contributions to neutral $B_q-\bar{B}_q$ meson mixing that arise in vector-like quark singlet extensions of the SM. In particular, App. F.2.1 is devoted to UVLQ models with a new up-type quark singlet, while App. F.2.2 focuses on DVLQ models with an extra down-type quark singlet.

F.2.1 UVLQ models

In UVLQ models, we only get new contributions to the mass mixing M^q_{12}. They correspond to additional SM-like box diagrams, as the ones presented in Figs. F.1 and F.2, with the new up-type quark T running in the loop. Therefore, the computation of $M^{q,\mathrm{UVLQ}}_{12}$ follows analogously to the SM case, with cancellation of gauge dependence through

$$\sum_{i=u,c,t,T}\lambda^i_{bq} = \lambda^u_{bq} + \lambda^c_{bq} + \lambda^t_{bq} + \lambda^T_{bq} = 0\,, \qquad (q=d,s)\,, \tag{F.60}$$

similarly to Eq. (F.8). Taking this into account, Eq. (F.22) is modified as

$$\begin{aligned}\sum_{i,j=u,c,t,T} \lambda_{bq}^i \lambda_{bq}^j F(x_i, x_j) = &- (\lambda_{bq}^T)^2 \left[2F(x_u, x_T) - F(x_u, x_u) - F(x_T, x_T)\right] \\ &- 2\lambda_{bq}^c \lambda_{bq}^T \left[F(x_u, x_c) + F(x_u, x_T) - F(x_u, x_u) - F(x_c, x_T)\right] \\ &- 2\lambda_{bq}^t \lambda_{bq}^T \left[F(x_u, x_t) + F(x_u, x_T) - F(x_u, x_u) - F(x_t, x_T)\right] + [\text{SM-like}] \,,\end{aligned} \tag{F.61}$$

where the [SM-like] part corresponds precisely to the result quoted in Eq. (F.22). Then, in the limit $x_u \to 0$, the function $\mathcal{F}_0$ in Eq. (F.30) is now given by

$$\mathcal{F}_0 = [\text{SM-like}] + (\lambda_{bq}^T)^2 S_0(x_T) + 2\lambda_{bq}^c \lambda_{bq}^T S_0(x_c, x_T) + 2\lambda_{bq}^t \lambda_{bq}^T S_0(x_t, x_T) \,, \tag{F.62}$$

with [SM-like] denoting the result in Eq. (F.30). For a heavy T quark mass $m_T > 1.6$ TeV, the only numerically relevant contributions are

$$\begin{aligned}\mathcal{F}_0 &\simeq (\lambda_{bq}^t)^2 S_0(x_t) + (\lambda_{bq}^T)^2 S_0(x_T) + 2\lambda_{bq}^t \lambda_{bq}^T S_0(x_t, x_T) \\ &= (\lambda_{bq}^t)^2 S_0(x_t) \left[1 + \frac{\lambda_{bq}^T}{\lambda_{bq}^t} \frac{2S_0(x_t, x_T)}{S_0(x_t)} + \left(\frac{\lambda_{bq}^T}{\lambda_{bq}^t}\right)^2 \frac{S_0(x_T)}{S_0(x_t)}\right] .\end{aligned} \tag{F.63}$$

Finally, assuming that two-loop perturbative QCD corrections encoded in the parameter $\hat{\eta}_B$ are similar to the SM case, the mass mixing M_{12}^q in UVLQ models reads

$$\frac{M_{12}^{q,\text{UVLQ}}}{M_{12}^{q,\text{SM-like}}} = 1 + \frac{\lambda_{bq}^T}{\lambda_{bq}^t} \frac{C_1^{\text{UVLQ}}(x_t, x_T)}{S_0(x_t)} + \left(\frac{\lambda_{bq}^T}{\lambda_{bq}^t}\right)^2 \frac{C_2^{\text{UVLQ}}(x_T)}{S_0(x_t)} \,, \tag{F.64}$$

where

$$C_1^{\text{UVLQ}}(x_t, x_T) = 2S_0(x_t, x_T) \,, \qquad C_2^{\text{UVLQ}}(x_T) = S_0(x_T) \,. \tag{F.65}$$

The $M_{12}^{q,\text{SM-like}}$ piece is of the form of Eq. (F.39), although in this case one could have different values for the CKM couplings since 3×3 unitarity does not hold. As we can check, the new contributions in this scenario appear linearly and quadratically in the deviation of unitarity λ_{bq}^T.

F.2.2 DVLQ models

In DVLQ, there are new contributions to mass mixing M_{12}^q and decay width mixing Γ_{12}^q. Nevertheless, the latter happen to be negligible, as discussed in chapter 7, so in what follows we will exclusively focus on the computation of $M_{12}^{q,\text{DVLQ}}$. We must point out that Ref. [256] already addressed in detail the relevant contributions to $\Delta B = 2$ processes within down-type vector-like singlet extensions. Our aim here is to be more explicit on how the different contributions emerge, which might be of interest for practitioners on this topic.

Before we going into details, two important features of DVLQ must be recalled. First, 3×3 CKM unitarity does not hold, but instead the orthogonality relation between columns is modified as

$$\sum_{i=u,c,t} \lambda_{bq}^i = \lambda_{bq}^u + \lambda_{bq}^c + \lambda_{bq}^t = (D_L)_{qb} \,, \qquad (q = d, s) \,, \tag{F.66}$$

with $(D_L)_{qb}$ parametrizing the deviation of unitarity. Second, there are new tree-level flavor-changing couplings of the Z boson to down-type quarks, which are precisely proportional to the deviation of unitarity. Therefore, we will get novel tree-level contributions to meson mixing as well as one-loop penguin contributions in addition to the usual boxes. As in previous calculations, we will work in a general R_ξ-gauge and take the limit of vanishing external masses and momenta. Finally, it is important to notice that in each category of diagrams (tree, boxes, and penguins) two distinct sets of topologies emerge depending on the ordering of quark spinors and how color indices are contracted, in a similar fashion to what occurs in our SM calculation with the set I of boxes in Fig. F.1 and the set II in Fig. F.2, which are Fierz-related. Since in general the two sets share the same effective Wilson coefficient generated by the weak interactions, we will only show explicitly the computation of one of these sets—say set I, *i.e.*, the one in which the b ($\bar{q}$) quark of the initial $\bar{B}_q$ state is connected with the q ($\bar{b}$) quark of the final B_q meson state. In any case, our final result will appropriately include all contributions, taking into account that there is again a relative minus sign between the two sets of topologies.

Tree-level diagrams

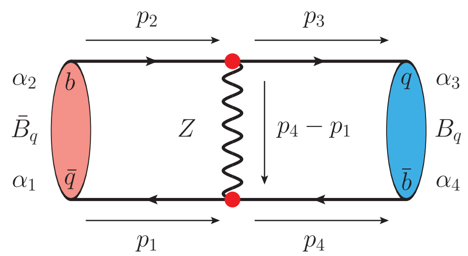

Figure F.4: Set I (t-channel) of tree-level contributions to neutral B_q ($q = d, s$) meson mixing in DVLQ models. The momentum flow and color indices assignments are indicated. The vertices in red correspond to the flavor-changing couplings of the Z boson to down-type quarks.

The amplitude for the set I of tree-level diagrams in Fig. F.4 reads

$$\begin{aligned} i\mathcal{M}_{\rm I}^{\rm tree} &= \left[i\eta\eta_Z \frac{g}{2c_W}(D_L)_{qb}\right]^2 \delta_{\alpha_1\alpha_4}\delta_{\alpha_2\alpha_3}\left[\bar{u}_q(0)\gamma^\nu P_L u_b(0)\right]\left[\bar{v}_q(0)\gamma^\mu P_L v_b(0)\right] \times i\frac{g_{\mu\nu}}{M_Z^2} \\ &= -\frac{ig^2}{4M_W^2}(D_L)_{qb}^2 \delta_{\alpha_1\alpha_4}\delta_{\alpha_2\alpha_3}\left[\bar{u}_q(0)\gamma^\mu P_L u_b(0)\right]\left[\bar{v}_q(0)\gamma_\mu P_L v_b(0)\right] , \end{aligned} \tag{F.67}$$

where $c_W \equiv \cos\theta_W$, and $M_W = c_W M_Z$. The parameters η and η_Z can be ± 1 depending on the sign convention used in the definition of the $SU(2)_L$ covariant derivative and the Glashow rotation, respectively—see [17] for details. Furthermore, the simple form used for the Z propagator arises because we are taking the limit of zero external momenta, which is justified by the fact that $k_Z^2 = (p_4 - p_1)^2 = (p_2 - p_3)^2 \ll M_Z^2$, with $p_1, p_3 \sim m_q$ and $p_2, p_4 \sim m_b$. One can readily check that tree-level diagrams generate a contribution $\propto G_F (D_L)_{qb}^2$.

Box diagrams

As in the SM, the set I of box diagrams depicted in Fig. F.1, with momentum flow and color indices assignments indicated in Fig. F.3a, also contribute to neutral meson mixing in DVLQ models at one-loop. The key difference with respect to the SM is the lack of 3×3 CKM unitarity, as shown in Eq. (F.66).

Taking this into account, we can resume the calculation from Eq. (F.7), namely,

$$
\begin{aligned}
i\mathcal{M}_{\mathrm{I}}^{\mathrm{box}} = \delta_{\alpha_1\alpha_4}\delta_{\alpha_2\alpha_3}\frac{g^4}{4M_W^2}\sum_{i,j=u,c,t}\lambda_{bq}^i\lambda_{bq}^j\int\frac{\mathrm{d}^dk}{(2\pi)^d}\frac{1}{D_i(k)D_j(k)} \\
\times\Bigg\{\frac{1}{D_W^2(k)}\left(\frac{k^4}{M_W^2}\left[\not{k}P_L\right]\left[\not{k}P_L\right]-2k^4\left[\gamma^\mu P_L\right]\left[\gamma_\mu P_L\right]+M_W^2\left[\gamma^\nu\not{k}\gamma^\mu P_L\right]\left[\gamma_\mu\not{k}\gamma_\nu P_L\right]\right) \\
+\frac{k^4-m_i^2m_j^2}{M_W^2}\left(\frac{1}{D_g^2(k)}-\frac{2}{D_W(k)D_g(k)}\right)\left[\not{k}P_L\right]\left[\not{k}P_L\right]+\frac{2(k^4-m_i^2m_j^2)}{D_W(k)D_g(k)}\left[\gamma^\mu P_L\right]\left[\gamma_\mu P_L\right]\Bigg\},
\end{aligned}
\tag{F.68}
$$

where we have used the shorthand $[\ldots][\ldots] = [\bar{u}_q(0)\ldots u_b(0)]\,[\bar{v}_q(0)\ldots v_b(0)]$. For convenience, let us introduce the following notation:

$$
i\mathcal{M}_{\mathrm{I}}^{\mathrm{box}} = \delta_{\alpha_1\alpha_4}\delta_{\alpha_2\alpha_3}\frac{g^4}{4M_W^2}\sum_{a=1}^{6}\sum_{i,j=u,c,t}\lambda_{bq}^i\lambda_{bq}^jI_{ij}^{(a)}\,,
\tag{F.69}
$$

with $I_{ij}^{(a)}$ denoting each of the one-loop integrals that appear in Eq. (F.68). By means of Eq. (F.9), these can be reexpressed as

$$
\begin{aligned}
I_{ij}^{(1)} &= \int\frac{\mathrm{d}^dk}{(2\pi)^d}\frac{k^4}{D_i(k)D_j(k)D_W^2(k)}\frac{[\not{k}P_L][\not{k}P_L]}{M_W^2} \\
&= \int\frac{\mathrm{d}^dk}{(2\pi)^d}\frac{1}{D_W^2(k)}\left[k^2\left(\frac{1}{D_i(k)}+\frac{1}{D_j(k)}\right)+\frac{m_i^2m_j^2}{D_i(k)D_j(k)}-1\right]\frac{[\not{k}P_L][\not{k}P_L]}{M_W^2}\,,
\end{aligned}
\tag{F.70}
$$

$$
\begin{aligned}
I_{ij}^{(2)} &= \int\frac{\mathrm{d}^dk}{(2\pi)^d}\frac{(-2k^4)}{D_i(k)D_j(k)D_W^2(k)}[\gamma^\mu P_L][\gamma_\mu P_L] \\
&= \int\frac{\mathrm{d}^dk}{(2\pi)^d}\frac{(-2)}{D_W^2(k)}\left[k^2\left(\frac{1}{D_i(k)}+\frac{1}{D_j(k)}\right)+\frac{m_i^2m_j^2}{D_i(k)D_j(k)}-1\right][\gamma^\mu P_L][\gamma_\mu P_L]\,,
\end{aligned}
\tag{F.71}
$$

$$
\begin{aligned}
I_{ij}^{(3)} &= \int\frac{\mathrm{d}^dk}{(2\pi)^d}\frac{1}{D_i(k)D_j(k)D_W^2(k)}M_W^2\left[\gamma^\nu\not{k}\gamma^\mu P_L\right]\left[\gamma_\mu\not{k}\gamma_\nu P_L\right] \\
&= \int\frac{\mathrm{d}^dk}{(2\pi)^d}\frac{k^2}{D_i(k)D_j(k)D_W^2(k)}M_W^2[\gamma^\mu P_L][\gamma_\mu P_L] \\
&= \int\frac{\mathrm{d}^dk}{(2\pi)^d}\frac{1}{D_i(k)D_j(k)D_W^2(k)}4M_W^2[\not{k}P_L][\not{k}P_L]\,,
\end{aligned}
\tag{F.72}
$$

$$
\begin{aligned}
I_{ij}^{(4)} &= \int\frac{\mathrm{d}^dk}{(2\pi)^d}\int\frac{\mathrm{d}^dk}{(2\pi)^d}\frac{k^4-m_i^2m_j^2}{D_i(k)D_j(k)D_g^2(k)}\frac{[\not{k}P_L][\not{k}P_L]}{M_W^2} \\
&= \int\frac{\mathrm{d}^dk}{(2\pi)^d}\frac{1}{D_g^2(k)}\left[k^2\left(\frac{1}{D_i(k)}+\frac{1}{D_j(k)}\right)-1\right]\frac{[\not{k}P_L][\not{k}P_L]}{M_W^2}\,,
\end{aligned}
\tag{F.73}
$$

$$
\begin{aligned}
I_{ij}^{(5)} &= \int\frac{\mathrm{d}^dk}{(2\pi)^d}\int\frac{\mathrm{d}^dk}{(2\pi)^d}\frac{(-2)(k^4-m_i^2m_j^2)}{D_i(k)D_j(k)D_W(k)D_g(k)}\frac{[\not{k}P_L][\not{k}P_L]}{M_W^2} \\
&= \int\frac{\mathrm{d}^dk}{(2\pi)^d}\frac{(-2)}{D_W(k)D_g(k)}\left[k^2\left(\frac{1}{D_i(k)}+\frac{1}{D_j(k)}\right)-1\right]\frac{[\not{k}P_L][\not{k}P_L]}{M_W^2}\,,
\end{aligned}
\tag{F.74}
$$

$$
\begin{aligned}
I_{ij}^{(6)} &= \int \frac{\mathrm{d}^d k}{(2\pi)^d} \int \frac{\mathrm{d}^d k}{(2\pi)^d} \frac{2(k^4 - m_i^2 m_j^2)}{D_i(k) D_j(k) D_W(k) D_g(k)} [\gamma^\mu P_L][\gamma_\mu P_L] \\
&= \int \frac{\mathrm{d}^d k}{(2\pi)^d} \frac{(-2)}{D_W(k) D_g(k)} \left[k^2 \left(\frac{1}{D_i(k)} + \frac{1}{D_j(k)} \right) - 1 \right] [\gamma^\mu P_L][\gamma_\mu P_L] \,.
\end{aligned}
\tag{F.75}
$$

In particular, for $I_{ij}^{(3)}$ we have applied Lorentz invariance in the form

$$
\int \frac{\mathrm{d}^4 k}{(2\pi)^4} f(k^2) k_\alpha k^\beta = \frac{g_\alpha^\beta}{4} \int \frac{\mathrm{d}^4 k}{(2\pi)^4} f(k^2) k^2 \,,
\tag{F.76}
$$

together with the Dirac identity in Eq. (F.17). Both forms of $I_{ij}^{(3)}$ will be used later. Notice that all $I_{ij}^{(a)}$ integrals are symmetric under the exchange $i \leftrightarrow j$. On the other hand, we can apply Eq. (F.66) in order to eliminate λ_{bq}^u from Eq. (F.69), leading to

$$
\begin{aligned}
i\mathcal{M}_{\mathrm{I}}^{\mathrm{box}} = \delta_{\alpha_1\alpha_4}\delta_{\alpha_2\alpha_3} \frac{g^4}{4M_W^2} \sum_{a=1}^{6} \Bigg[& \sum_{i,j=c,t} \lambda_{bq}^i \lambda_{bq}^j \left(I_{ij}^{(a)} - I_{iu}^{(a)} - I_{uj}^{(a)} + I_{uu}^{(a)} \right) \\
& + 2(D_L)_{qb} \sum_{i=c,t} \lambda_{bq}^i \left(I_{iu}^{(a)} - I_{uu}^{(a)} \right) + (D_L)_{qb}^2 I_{uu}^{(a)} \Bigg] \,.
\end{aligned}
\tag{F.77}
$$

Now we perform the sums over index a by using Eqs. (F.70) to (F.75). On this regard, it is convenient to use the first form of $I_{ij}^{(3)}$ for the linear terms in $(D_L)_{qb}$, and its second form for the terms that are independent of $(D_L)_{qb}$. This yields

$$
i\mathcal{M}_{\mathrm{I}}^{\mathrm{box}} = i\mathcal{M}_{\mathrm{I}}^{\mathrm{box},0} + i\mathcal{M}_{\mathrm{I}}^{\mathrm{box},1} + i\mathcal{M}_{\mathrm{I}}^{\mathrm{box},2} \,,
\tag{F.78}
$$

where

$$
\begin{aligned}
i\mathcal{M}_{\mathrm{I}}^{\mathrm{box},0} &= \delta_{\alpha_1\alpha_4}\delta_{\alpha_2\alpha_3} \frac{g^4}{4M_W^2} \sum_{i,j=c,t} \lambda_{bq}^i \lambda_{bq}^j \int \frac{\mathrm{d}^d k}{(2\pi)^d} \frac{1}{D_W^2} \\
&\times \Bigg\{ \frac{m_i^2 m_j^2}{M_W^2} \frac{[\not{k} P_L][\not{k} P_L]}{D_i D_j} + 4M_W^2 \left(\frac{1}{D_i} - \frac{1}{D_u} \right) \left(\frac{1}{D_j} - \frac{1}{D_u} \right) [\not{k} P_L][\not{k} P_L] - \frac{2 m_i^2 m_j^2}{D_i D_j} [\gamma^\mu P_L][\gamma_\mu P_L] \\
&- \frac{m_u^2}{D_u} \left[\left(\frac{x_i}{D_i} + \frac{x_j}{D_j} - \frac{x_u}{D_u} \right) [\not{k} P_L][\not{k} P_L] - 2 \left(\frac{m_i}{D_i} + \frac{m_j}{D_j} - \frac{m_u}{D_u} \right) [\gamma^\mu P_L][\gamma_\mu P_L] \right] \Bigg\} \,,
\end{aligned}
\tag{F.79}
$$

$$
\begin{aligned}
i\mathcal{M}_{\mathrm{I}}^{\mathrm{box},1} &= \delta_{\alpha_1\alpha_4}\delta_{\alpha_2\alpha_3} \frac{g^4}{2M_W^2} (D_L)_{qb} \sum_{i=c,t} \lambda_{bq}^i \int \frac{\mathrm{d}^d k}{(2\pi)^d} \\
&\times \Bigg\{ \frac{1}{D_W^2} \left[\left(\frac{x_i}{D_i} - \frac{x_u}{D_u} \right) [\not{k} P_L][\not{k} P_L] - 2 \left(\frac{m_i^2}{D_i} - \frac{m_u^2}{D_u} \right) [\gamma^\mu P_L][\gamma_\mu P_L] + M_W^2 \left(\frac{1}{D_i} - \frac{1}{D_u} \right) [\gamma^\mu P_L][\gamma_\mu P_L] \right] \\
&+ \frac{m_u^2}{D_u D_W^2} \left[\left(\frac{x_i}{D_i} - \frac{x_u}{D_u} \right) [\not{k} P_L][\not{k} P_L] - 2 \left(\frac{m_i^2}{D_i} - \frac{m_u^2}{D_u} \right) [\gamma^\mu P_L][\gamma_\mu P_L] + M_W^2 \left(\frac{1}{D_i} - \frac{1}{D_u} \right) [\gamma^\mu P_L][\gamma_\mu P_L] \right] \\
&+ \frac{1}{D_g} \left[\frac{2}{D_W} \left(\frac{m_i^2}{D_i} - \frac{m_u^2}{D_u} \right) [\gamma^\mu P_L][\gamma_\mu P_L] + \left(\frac{1}{D_g} - \frac{2}{D_W} \right) \left(\frac{x_i}{D_i} - \frac{x_u}{D_u} \right) [\not{k} P_L][\not{k} P_L] \right] \Bigg\} \,,
\end{aligned}
\tag{F.80}
$$

$$
i\mathcal{M}_{\mathrm{I}}^{\mathrm{box},2} = \delta_{\alpha_1\alpha_4}\delta_{\alpha_2\alpha_3} \frac{g^4}{4M_W^2} (D_L)_{qb}^2 \sum_{a=1}^{6} I_{uu}^{(a)} \,.
\tag{F.81}
$$

Notice that we have omitted the momentum k dependence in the denominators for conciseness. All in all, the contribution to neutral meson mixing arising from box diagrams can be split in three pieces: (i) the SM-like $i\mathcal{M}_{\mathrm{I}}^{\mathrm{box},0}$, (ii) $i\mathcal{M}_{\mathrm{I}}^{\mathrm{box},1} \propto G_F\alpha(D_L)_{qb}$, and (iii) $i\mathcal{M}_{\mathrm{I}}^{\mathrm{box},2} \propto G_F\alpha(D_L)_{qb}^2$, being α the fine structure constant in QED. The latter consists of a radiative correction to tree-level diagrams and thus it is neglected. On the other hand, the second piece is linear in $(D_L)_{qb}$, which means that, in the decoupling limit of the heavy down quark, it goes to zero more slowly than tree-level diagrams that are quadratic in $(D_L)_{qb}^2$. Hence, *a priori*, this second piece should not be neglected, at least in the limit of small $(D_L)_{qb}$. Furthermore, the terms proportional to m_u^2 in both $i\mathcal{M}_{\mathrm{I}}^{\mathrm{box},0}$ and $i\mathcal{M}_{\mathrm{I}}^{\mathrm{box},1}$ will safely vanish in the limit $m_u \to 0$ as the one-loop integrals involved are convergent in $d = 4$ dimensions—in fact, in this limit $i\mathcal{M}_{\mathrm{I}}^{\mathrm{box},0}$ generates the result quoted in Eq. (F.25). Finally, one should worry about canceling the gauge dependence[2] of the box contributions that are linear in $(D_L)_{qb}$. To this aim, different penguin topologies must be added, as we explain next.

Penguin diagrams

They consist of a Z tree-level flavor-changing vertex and another one where the change of flavor is obtained through the exchange of W bosons at one loop. Let us classify these penguin topologies into three different subsets: (i) subset I.A illustrated in Fig. F.5, (ii) subset I.B illustrated in Fig. F.7, and (iii) subset I.C illustrated in Fig. F.9. Within each subset, one can in turn distinguish two different groups depending on how the loop and the flavor-changing coupling of the Z boson to down-type quarks are placed. These two groups, 1 and 2, give rise to the very same amplitude, and thus we will simply compute one of them and include a factor of 2 in the calculation of the amplitude. In particular, Figs. F.5, F.7 and F.9 only show one of the aforementioned groups, say group 1. On the other hand, our choice for the momentum flow and quark color indices is represented in Fig. F.6 for subsets I.A and I.B, and Fig. F.10 for subset I.C. The latter will deserve special attention, since the limit of vanishing external momenta and masses cannot be taken straightforwardly. Some additional remarks are in order.

(i) In the loops, we can apply $\sum_{i=u,c,t} \lambda_{bq}^i = 0$, that is, ignoring the deviation of unitarity $(D_L)_{qb}$, since this would generate a contribution $\propto G_F\alpha(D_L)_{qb}^2$, which is a radiative correction to tree-level diagrams. Therefore, we can effectively apply 3×3 CKM unitarity in a SM fashion.

(ii) In topology C, the coupling of the Z boson in the fermion line that contains the loop must be flavor-conserving (SM-like). If not, we would get a contribution $\propto (D_L)_{qb}(D_L)_{qk}V_{ib}V_{ik}^*$ or $\propto (D_L)_{qb}(D_L)_{kb}V_{iq}^*V_{ik}$, which are subleading.

Then, our result will be the sum of three different pieces, namely

$$i\mathcal{M}_{\mathrm{I}}^{\mathrm{peng}} = i\mathcal{M}_{\mathrm{I}}^{\mathrm{peng,A}} + i\mathcal{M}_{\mathrm{I}}^{\mathrm{peng,B}} + i\mathcal{M}_{\mathrm{I}}^{\mathrm{peng,C}}\,, \tag{F.82}$$

that we proceed to address separately.

[2] One of the advantages of working in an R_ξ-gauge is that gauge dependence is explicitly manifest. This provides insight into which additional contributions must be included in order to obtain a gauge-invariant result, while also offering a self-consistency check for our calculations.

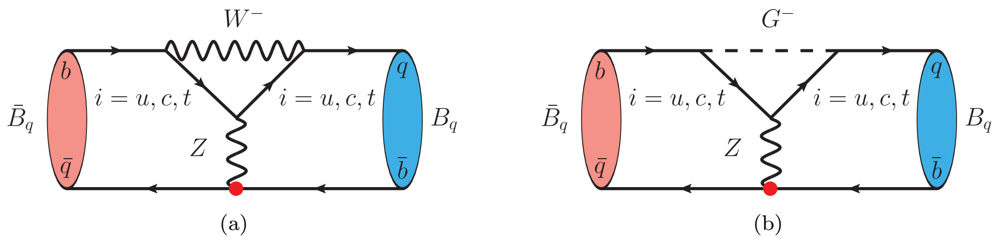

Figure F.5: Set I.A.1 of penguin diagrams triggering neutral B_q ($q = d, s$) meson mixing: (a) W^- contribution, and (b) G^- contribution. The vertices in red correspond to the flavor-changing couplings of the Z boson to down-type quarks. There exists an analogous set I.A.2 of diagrams where the red vertex is instead placed in the upper fermion line, while the loop is moved to the lower one. Both sets I.A.1 and I.A.2 generate the very same amplitude, and thus we will simply include a factor of 2 in our calculations.

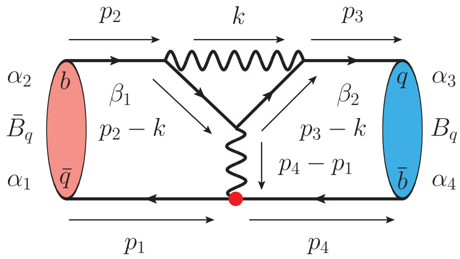

Figure F.6: Momentum flow and color indices assignments in penguin topology A triggering neutral B_q ($q = d, s$) meson mixing.

Topology A—. The amplitude corresponding to subset I.A of penguin diagrams (see Figs. F.5 and F.6) reads

$$\begin{aligned}
i\mathcal{M}_{\mathrm{I}}^{\mathrm{peng,A}} &= 2 \times \frac{(-1)}{2} \left(i\eta\eta_Z \frac{g}{c_W}\right)^2 \left(i\frac{g}{\sqrt{2}}\right)^2 (D_L)_{qb} \sum_{i=u,c,t} \lambda_{bq}^i \sum_{\beta_1,\beta_2} \delta_{\alpha_1\alpha_4}\delta_{\alpha_2\beta_1}\delta_{\alpha_3\beta_2}\delta_{\beta_1\beta_2} \int \frac{\mathrm{d}^d k}{(2\pi)^d} \\
&\times \Bigg\{ (-\eta)^2 \frac{[\bar{u}_q(0)\gamma^\sigma P_L i(-\not{k} + m_i)\gamma^\nu \left(\frac{1}{2}P_L - Q_u s_W^2\right) i(-\not{k} + m_i)\gamma^\rho P_L u_b(0)][\bar{v}_q(0)\gamma^\mu P_L v_b(0)]}{D_i^2(k)} \\
&\qquad \times i\frac{g_{\mu\nu}}{M_Z^2} \times i\left[-\frac{g_{\rho\sigma}}{D_W(k)} + \frac{k_\rho k_\sigma}{M_W^2}\left(\frac{1}{D_W(k)} - \frac{1}{D_g(k)}\right)\right] \\
&\quad + \frac{m_i^2}{M_W^2} \frac{[\bar{u}_q(0)P_R i(-\not{k} + m_i)\gamma^\nu \left(\frac{1}{2}P_L - Q_u s_W^2\right) i(-\not{k} + m_i)P_L u_b(0)][\bar{v}_q(0)\gamma^\mu P_L v_b(0)]}{D_i^2(k)} \\
&\qquad \times i\frac{g_{\mu\nu}}{M_Z^2} \times i\frac{1}{D_g(k)} \Bigg\}.
\end{aligned} \tag{F.83}$$

The first factor 2 accounts for the topologies, not shown in Fig. F.5, where the flavor-changing coupling of the Z boson is moved into the upper fermion line while the loop is moved to the lower one. The parameter Q_u denotes the electric charge of up-type quarks. The Dirac structure in the spinor currents can be reduced as

$$\begin{aligned}
&\gamma^\sigma P_L(-\not{k}+m_i)\gamma^\nu\left(\frac{1}{2}P_L - Q_u s_W^2\right)(-\not{k}+m_i)\gamma^\rho P_L = \\
&\qquad = \left(\frac{1}{2} - Q_u s_W^2\right)\gamma^\sigma \not{k}\gamma^\nu \not{k}\gamma^\rho P_L - Q_u s_W^2 m_i^2 \gamma^\sigma\gamma^\nu\gamma^\rho P_L\,, \qquad \text{(F.84)}\\
&P_R(-\not{k}+m_i)\gamma^\nu\left(\frac{1}{2}P_L - Q_u s_W^2\right)(-\not{k}+m_i) P_L = \\
&\qquad = \left(\frac{1}{2} - Q_u s_W^2\right) m_i^2 \gamma^\nu P_L - Q_u s_W^2 \not{k}\gamma^\nu\not{k} P_L\,, \qquad \text{(F.85)}
\end{aligned}$$

by means of Eq. (F.5). This yields

$$\begin{aligned}
i\mathcal{M}_{\mathrm{I}}^{\text{peng,A}} = &-\frac{g^4}{2M_W^2}(D_L)_{qb}\delta_{\alpha_1\alpha_4}\delta_{\alpha_2\alpha_3}[\bar{v}_q(0)\gamma_\mu P_L v_b(0)]\sum_{i=u,c,t}\lambda_{bq}^i \int\frac{\mathrm{d}^d k}{(2\pi)^d}\frac{1}{D_i^2(k)} \\
&\times\left\{\left[\left(\frac{1}{2} - Q_u s_W^2\right)[\bar{u}_q(0)\gamma^\sigma\not{k}\gamma^\mu\not{k}\gamma^\rho P_L u_b(0)] - Q_u s_W^2 m_i^2[\bar{u}_q(0)\gamma^\sigma\gamma^\mu\gamma^\rho P_L u_b(0)]\right]\right.\\
&\qquad\times\left[-\frac{g_{\rho\sigma}}{D_W(k)} + \frac{k_\rho k_\sigma}{M_W^2}\left(\frac{1}{D_W(k)} - \frac{1}{D_g(k)}\right)\right]\\
&\left.+\frac{x_i}{D_g(k)}\left[\left(\frac{1}{2} - Q_u s_W^2\right) m_i^2[\bar{u}_q(0)\gamma^\mu P_L u_b(0)] - Q_u s_W^2[\bar{u}_q(0)\not{k}\gamma^\mu\not{k}P_L u_b(0)]\right]\right\}, \qquad \text{(F.86)}
\end{aligned}$$

with $x_i = m_i^2/M_W^2$. We can then contract the fermion currents in the second line with the corresponding propagator structure, taking into account that

$$\gamma^\rho\not{k}\gamma^\mu\not{k}\gamma_\rho = -(2-\epsilon)\not{k}\gamma^\mu\not{k}\,, \qquad \gamma^\rho\gamma^\mu\gamma_\rho = -(2-\epsilon)\gamma^\mu\,, \qquad \text{(F.87)}$$

and $\not{k}^2 = k^2$, where we are setting $d = 4-\epsilon$ in dimensional regularization. On that regard, it is important to maintain full generality in the previous identities when they are used within integrals that are not convergent in $d = 4$ dimensions; otherwise, one can fix $d = 4$, *i.e.*, taking $\epsilon \to 0$. Hence, we obtain

$$\begin{aligned}
i\mathcal{M}_{\mathrm{I}}^{\text{peng,A}} = &-\frac{g^4}{2M_W^2}(D_L)_{qb}\delta_{\alpha_1\alpha_4}\delta_{\alpha_2\alpha_3}[\bar{v}_q(0)\gamma_\mu P_L v_b(0)]\sum_{i=u,c,t}\lambda_{bq}^i \int\frac{\mathrm{d}^d k}{(2\pi)^d}\frac{1}{D_i^2(k)} \\
&\times\left\{\frac{1}{D_W(k)}\left[\left(\frac{1}{2} - Q_u s_W^2\right)(2-\epsilon)[\bar{u}_q(0)\not{k}\gamma^\mu\not{k}P_L u_b(0)] - 2Q_u s_W^2 m_i^2[\bar{u}_q(0)\gamma^\mu P_L u_b(0)]\right.\right.\\
&\qquad\left.+\left(\frac{1}{2} - Q_u s_W^2\right)\frac{k^4}{M_W^2}[\bar{u}_q(0)\gamma^\mu P_L u_b(0)] - Q_u s_W^2 x_i[\bar{u}_q(0)\not{k}\gamma^\mu\not{k}P_L u_b(0)]\right]\\
&\left.+\frac{1}{D_g(k)}\left(\frac{1}{2} - Q_u s_W^2\right)\left(x_i m_i^2 - \frac{k^4}{M_W^2}\right)[\bar{u}_q(0)\gamma^\mu P_L u_b(0)]\right\}, \qquad \text{(F.88)}
\end{aligned}$$

where all gauge dependence is contained in the last line of the previous expression. At this point, it is convenient to reexpress

$$\frac{1}{D_i^2(k)}\left(x_i m_i^2 - \frac{k^4}{M_W^2}\right) = -\frac{1}{M_W^2} - \frac{2x_i}{D_i(k)}\,, \qquad \frac{1}{D_i^2(k)}\frac{k^4}{M_W^2} = \frac{1}{M_W^2} + \frac{x_i(2k^2 - m_i^2)}{D_i^2(k)}\,, \qquad \text{(F.89)}$$

in such a way that the $1/M_W^2$ terms can be dropped by means of the SM-like 3×3 unitarity, as pointed out before. Further using that $\sum_{i=u,c,t} \lambda^i_{bq} = 0$ to eliminate λ^u_{bq}, we are left with

$$
\begin{aligned}
i\mathcal{M}_{\mathrm{I}}^{\mathrm{peng,A}} = \frac{g^4}{2M_W^2} (D_L)_{qb} \delta_{\alpha_1\alpha_4}\delta_{\alpha_2\alpha_3} \sum_{i=c,t} \lambda^i_{bq} \int \frac{\mathrm{d}^d k}{(2\pi)^d} \\
\times \Bigg\{ -\frac{1}{D_W}\left(\frac{1}{2} - Q_u s_W^2\right) \Bigg[\left(\frac{x_i(2k^2 - m_i^2)}{D_i^2} - \frac{x_u(2k^2 - m_u^2)}{D_u^2} \right) [\gamma^\mu P_L][\gamma_\mu P_L] \\
+ \left(\frac{1}{D_i^2} - \frac{1}{D_u^2} \right) (2-\epsilon) [\not{k}\gamma^\mu P_L \not{k} P_L][\gamma_\mu P_L] \Bigg] \\
+ \frac{Q_u s_W^2}{D_W} \left[2\left(\frac{m_i^2}{D_i^2} - \frac{m_u^2}{D_u^2} \right) [\gamma^\mu P_L][\gamma_\mu P_L] + \left(\frac{x_i}{D_i^2} - \frac{x_u}{D_u^2} \right) [\not{k}\gamma^\mu P_L \not{k} P_L][\gamma_\mu P_L] \right] \\
+ \frac{2}{D_g}\left(\frac{1}{2} - Q_u s_W^2\right)\left(\frac{x_i}{D_i} - \frac{x_u}{D_u} \right) [\gamma^\mu P_L][\gamma_\mu P_L] \Bigg\} ,
\end{aligned}
\tag{F.90}
$$

where we have introduced the shorthand $[\ldots][\ldots] = [\bar{u}_q(0)\ldots u_b(0)]\,[\bar{v}_q(0)\ldots v_b(0)]$ and omitted the momentum k dependence in the denominators for conciseness. All gauge dependence is contained in the last line.

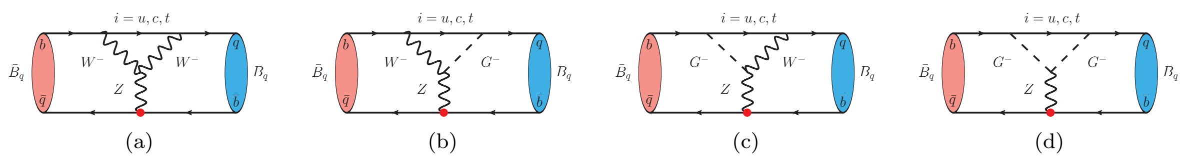

Figure F.7: Set I.B.1 of penguin diagrams triggering neutral B_q ($q = d, s$) meson mixing: (a) W^-W^- contribution, and (b) W^-G^- contribution, (c) G^-W^- contribution, and (d) G^-G^- contribution. The vertices in red correspond to the flavor-changing couplings of the Z boson to down-type quarks. There exists an analogous set I.B.2 of diagrams where the red vertex is instead placed in the upper fermion line, while the loop is moved to the lower one. Both sets I.B.1 and I.B.2 generate the very same amplitude, and thus we will simply include a factor of 2 in our calculations.

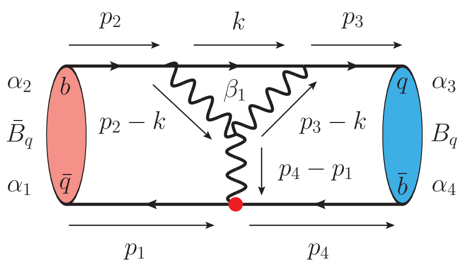

Figure F.8: Momentum flow and color indices assignments in penguin topology B triggering neutral B_q ($q = d, s$) meson mixing.

Topology B—. The amplitude corresponding to subset I.B of penguin diagrams (see Figs. F.7 and F.8) reads

$$
\begin{aligned}
i\mathcal{M}_{\mathrm{I}}^{\text{peng,B}} &= 2\times\left(i\eta\eta_Z\frac{g}{2c_W}\right)(i\eta\eta_Z g)\left(i\frac{g}{\sqrt{2}}\right)^2(D_L)_{qb}\sum_{\beta_1}\delta_{\alpha_1\alpha_4}\delta_{\alpha_2\beta}\delta_{\alpha_3\beta}\sum_{i=u,c,t}\lambda^i_{bq}\int\frac{\mathrm{d}^dk}{(2\pi)^d}\\
&\times\Bigg\{(-1)^2\eta^2 c_W\frac{[\bar{u}_q(0)\gamma^\sigma P_L i(\not{k}+m_i)\gamma^\rho P_L u_b(0)][\bar{v}_q(0)\gamma^\mu P_L v_b(0)]}{D_i(k)}\left(2g^{\alpha\beta}k^\nu-g^{\beta\nu}k^\alpha-g^{\nu\alpha}k^\beta\right)\\
&\quad\times i\left[-\frac{g_{\alpha\rho}}{D_W(k)}+\frac{k_\alpha k_\rho}{M_W^2}\left(\frac{1}{D_W(k)}-\frac{1}{D_g(k)}\right)\right]\times i\left[-\frac{g_{\beta\sigma}}{D_W(k)}+\frac{k_\beta k_\sigma}{M_W^2}\left(\frac{1}{D_W(k)}-\frac{1}{D_g(k)}\right)\right]\times i\frac{g_{\mu\nu}}{M_Z^2}\\
&\quad+(-1)^2\frac{s_W^2}{c_W}m_i\frac{[\bar{u}_q(0)P_R i(\not{k}+m_i)\gamma^\rho P_L u_b(0)][\bar{v}_q(0)\gamma^\mu P_L v_b(0)]}{D_i(k)}g^{\nu\alpha}\\
&\quad\times i\left[-\frac{g_{\alpha\rho}}{D_W(k)}+\frac{k_\alpha k_\rho}{M_W^2}\left(\frac{1}{D_W(k)}-\frac{1}{D_g(k)}\right)\right]\times\frac{i}{D_g(k)}\times i\frac{g_{\mu\nu}}{M_Z^2}\\
&\quad+(-1)^2\frac{s_W^2}{c_W}m_i\frac{[\bar{u}_q(0)\gamma^\sigma P_L i(\not{k}+m_i)P_L u_b(0)][\bar{v}_q(0)\gamma^\mu P_L v_b(0)]}{D_i(k)}g^{\nu\beta}\\
&\quad\times i\left[-\frac{g_{\beta\sigma}}{D_W(k)}+\frac{k_\beta k_\sigma}{M_W^2}\left(\frac{1}{D_W(k)}-\frac{1}{D_g(k)}\right)\right]\times\frac{i}{D_g(k)}\times i\frac{g_{\mu\nu}}{M_Z^2}\\
&\quad-\frac{1-2s_W^2}{c_W}\frac{m_i^2}{M_W^2}\frac{[\bar{u}_q(0)P_R i(\not{k}+m_i)P_L u_b(0)][\bar{v}_q(0)\gamma^\mu P_L v_b(0)]}{D_i(k)}k^\nu\times\frac{i}{D_g(k)}\times\frac{i}{D_g(k)}\times i\frac{g_{\mu\nu}}{M_Z^2}\Bigg\},
\end{aligned}
\tag{F.91}
$$

where the factor 2 in the first line accounts for the topologies, not shown in Fig. F.7, in which the flavor-changing coupling of the Z boson is moved into the upper fermion line. Taking into account the properties of the chiral projectors in Eq. (F.5), the previous expression can be simplified as

$$
\begin{aligned}
i\mathcal{M}_{\mathrm{I}}^{\text{peng,B}} &= \frac{g^4}{2M_W^2}(D_L)_{qb}\delta_{\alpha_1\alpha_4}\delta_{\alpha_2\alpha_3}[\bar{v}_q(0)\gamma_\mu P_L v_b(0)]\sum_{i=u,c,t}\lambda^i_{bq}\int\frac{\mathrm{d}^dk}{(2\pi)^d}\frac{1}{D_i(k)}\\
&\times\Bigg\{c_W^2[\bar{u}_q(0)\gamma^\sigma\not{k}\gamma^\rho P_L u_b(0)]\left(2g^{\alpha\beta}k^\nu-g^{\beta\nu}k^\alpha-g^{\nu\alpha}k^\beta\right)\\
&\qquad\times\left[-\frac{g_{\alpha\rho}}{D_W(k)}+\frac{k_\alpha k_\rho}{M_W^2}\left(\frac{1}{D_W(k)}-\frac{1}{D_g(k)}\right)\right]\left[-\frac{g_{\beta\sigma}}{D_W(k)}+\frac{k_\beta k_\sigma}{M_W^2}\left(\frac{1}{D_W(k)}-\frac{1}{D_g(k)}\right)\right]\\
&\qquad+\frac{2s_W^2m_i^2}{D_g(k)}[\bar{u}_q(0)\gamma^\rho P_L u_b(0)]\left[-\frac{g^\mu_\rho}{D_W(k)}+\frac{k_\rho k^\mu}{M_W^2}\left(\frac{1}{D_W(k)}-\frac{1}{D_g(k)}\right)\right]\\
&\qquad-\frac{(1-2s_W^2)x_i}{c_W}[\bar{u}_q(0)\not{k}P_L u_b(0)]k^\mu\Bigg\}.
\end{aligned}
\tag{F.92}
$$

Then, considering the second identity in Eq. (F.87) and $\not k^2 = k^2$, after some algebra we get

$$
\begin{aligned}
i\mathcal{M}_{\rm I}^{\rm peng,B} = {}& \frac{g^4}{2M_W^2}(D_L)_{qb}\delta_{\alpha_1\alpha_4}\delta_{\alpha_2\alpha_3}\sum_{i=u,c,t}\lambda^i_{bq}\int\frac{\mathrm{d}^dk}{(2\pi)^d}\frac{1}{D_i(k)} \\
&\times\Bigg\{-\frac{2c_W^2}{D_W^2(k)}\Bigg[\Big(2-\epsilon+\frac{k^2}{M_W^2}\Big)[\not k P_L][\not k P_L]+\Big(1-\frac{k^2}{M_W^2}\Big)k^2[\gamma^\mu P_L][\gamma_\mu P_L]\Bigg] \\
&\quad+\frac{1}{D_g(k)}\Bigg[\frac{1}{D_W(k)}\Big(\frac{2(1-s_W^2)k^2}{M_W^2}+2s_W^2x_i\Big)[\not k P_L][\not k P_L] \\
&\qquad-\frac{1}{D_W(k)}\Big(\frac{2(1-s_W^2)k^4}{M_W^2}+2s_W^2m_i^2\Big)[\gamma^\mu P_L][\gamma_\mu P_L]-\frac{x_i}{D_g(k)}[\not k P_L][\not k P_L]\Bigg]\Bigg\},
\end{aligned}
\tag{F.93}
$$

with $[\ldots][\ldots] = [\bar{u}_q(0)\ldots u_b(0)]\,[\bar{v}_q(0)\ldots v_b(0)]$. Since $k^2 = m_i^2 + D_i(k)$, the SM-like unitarity relation leads us to

$$
\begin{aligned}
i\mathcal{M}_{\rm I}^{\rm peng,B} = {}& \frac{g^4}{2M_W^2}(D_L)_{qb}\delta_{\alpha_1\alpha_4}\delta_{\alpha_2\alpha_3}\sum_{i=u,c,t}\lambda^i_{bq}\int\frac{\mathrm{d}^dk}{(2\pi)^d}\frac{1}{D_i(k)} \\
\times\Bigg\{&-\frac{2c_W^2}{D_W^2(k)}\Bigg[(2-\epsilon+x_i)[\not k P_L][\not k P_L]+m_i^2\Big(1-\frac{k^2}{M_W^2}\Big)[\gamma^\mu P_L][\gamma_\mu P_L]\Bigg] \\
&+\frac{1}{D_g(k)}\Bigg[-\Big(\frac{1}{D_g(k)}-\frac{2}{D_W(k)}\Big)x_i[\not k P_L][\not k P_L]-\frac{2x_ik^2}{D_W(k)}[\gamma^\mu P_L][\gamma_\mu P_L]+2s_W^2x_i[\gamma^\mu P_L][\gamma_\mu P_L]\Bigg]\Bigg\}.
\end{aligned}
\tag{F.94}
$$

Finally, we eliminate λ^u_{bq} using, again, the SM-like CKM orthogonality relation:

$$
\begin{aligned}
i\mathcal{M}_{\rm I}^{\rm peng,B} = {}& \frac{g^4}{2M_W^2}(D_L)_{qb}\delta_{\alpha_1\alpha_4}\delta_{\alpha_2\alpha_3}\sum_{i=u,c,t}\lambda^i_{bq}\int\frac{\mathrm{d}^dk}{(2\pi)^d} \\
\times\Bigg\{&-\frac{2c_W^2}{D_W^2}\Bigg[\Big(\frac{2-\epsilon+x_i}{D_i}-\frac{2-\epsilon+x_u}{D_u}\Big)[\not k P_L][\not k P_L]+\Big(\frac{m_i^2}{D_i}-\frac{m_u^2}{D_u}\Big)\Big(1-\frac{k^2}{M_W^2}\Big)[\gamma^\mu P_L][\gamma_\mu P_L]\Bigg] \\
&+\frac{1}{D_g(k)}\Bigg[-\Big(\frac{1}{D_g}-\frac{2}{D_W}\Big)\Big(\frac{x_i}{D_i}-\frac{x_u}{D_u}\Big)[\not k P_L][\not k P_L] \\
&\qquad-\frac{2}{D_W}\Big(\frac{m_i^2}{D_i}-\frac{m_u^2}{D_u}\Big)\frac{k^2}{M_W^2}[\gamma^\mu P_L][\gamma_\mu P_L]+2s_W^2\Big(\frac{x_i}{D_i}-\frac{x_u}{D_u}\Big)[\gamma^\mu P_L][\gamma_\mu P_L]\Bigg]\Bigg\},
\end{aligned}
\tag{F.95}
$$

omitting the k dependence in the denominators.

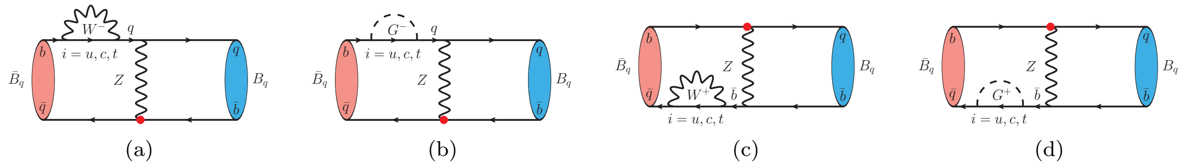

Figure F.9: Set I.C.1 of penguin diagrams triggering neutral B_q ($q = d, s$) meson mixing: (a) W^- contribution, and (b) G^- contribution, (c) W^+ contribution, and (d) G^+ contribution. The vertices in red correspond to the flavor-changing couplings of the Z boson to down-type quarks. There exists an analogous set I.C.2 of diagrams where the self-energy loop is in the final state. Both sets I.C.1 and I.C.2 generate the very same amplitude, and thus we will simply include a factor of 2 in our calculations.

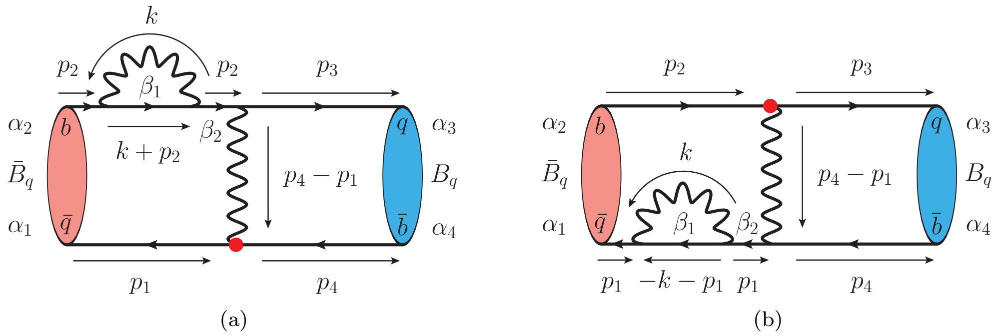

Figure F.10: Momentum flow and color indices assignments in penguin topology C triggering neutral B_q ($q = d, s$) meson mixing.

Topology C—. The last penguin topology corresponds to self-energy diagrams as the ones presented in Fig. F.9. In this case, one should be careful when taking the limit of vanishing external momenta and quark masses: there is a q propagator with momentum $p_2^2 = m_b^2$ in Figs. F.9a and F.9b, and a $\bar{b}$ propagator with momentum $p_1^2 = m_q^2$ in Figs. F.9c and F.9d. Therefore, we will keep all masses and momenta of external quarks, and take them to zero at the end of the calculation.

Before writing down the amplitude for diagrams in Fig. F.9, let us first compute separately the corresponding self-energy structures. On the one hand, from Figs. F.9a and F.9b, with momenta given in Fig. F.10a and omitting quark spinors, we have

$$
\begin{aligned}
i\mathcal{M}_1^{\text{self-energy}} = {} & \left(i\frac{g}{\sqrt{2}}\right)^2 \sum_{\beta_1} \delta_{\alpha_2\beta_1}\delta_{\beta_1\beta_2} \sum_{i=u,c,t} \lambda_{bq}^i \int \frac{\mathrm{d}^d k}{(2\pi)^d} \\
& \times \Bigg\{ (-\eta)^2 \frac{[\gamma^\sigma P_L i(\not{k} + \not{p}_2 + m_i \gamma^\rho P_L)]}{D_i(k+p_2)} \times i \left[-\frac{g_{\rho\sigma}}{D_W(k)} + \frac{k_\rho k_\sigma}{M_W^2}\left(\frac{1}{D_W(k)} - \frac{1}{D_g(k)}\right)\right] \\
& + \frac{1}{M_W^2} \frac{[(m_i P_R - m_q P_L) i(\not{k} + \not{p}_2 + m_i)(m_i P_L - m_q P_R)]}{D_i(k+p_2)} \times \frac{i}{D_g(k)} \Bigg\}.
\end{aligned}
\tag{F.96}
$$

Using Eq. (F.5) it reduces to

$$
\begin{aligned}
i\mathcal{M}_1^{\text{self-energy}} = {} & \frac{g^2}{2}\delta_{\alpha_2\beta_2} \sum_{i=u,c,t} \lambda_{bq}^i \int \frac{\mathrm{d}^d k}{(2\pi)^d} \frac{1}{D_i(k+p_2)} \\
& \times \Bigg\{ [\gamma^\sigma(\not{k} + \not{p}_2)\gamma^\rho P_L] \left[-\frac{g_{\rho\sigma}}{D_W(k)} + \frac{k_\rho k_\sigma}{M_W^2}\left(\frac{1}{D_W(k)} - \frac{1}{D_g(k)}\right)\right] \\
& + \frac{1}{M_W^2 D_g(k)} [(m_i P_R - m_q P_L)(\not{k} + \not{p}_2 + m_i)(m_i P_L - m_q P_R)] \Bigg\}.
\end{aligned}
\tag{F.97}
$$

We can then expand both lines in the curly brackets taking into account Eq. (F.5), the second identity in Eq. (F.87), and

$$
\not{k}(\not{k} + \not{p}_2)\not{k} = \left[(k+p_2)^2 - p_2^2\right]\not{k} - k^2 \not{p}_2 \,, \tag{F.98}
$$

where we have used $\not{k}^2 = k^2$ and $\{\not{k}, \not{p}_2\} = 2k \cdot p_2$, in order to obtain

$$\begin{aligned}
i\mathcal{M}_1^{\text{self-energy}} = \frac{g^2}{2}\delta_{\alpha_2\beta_2} \sum_{i=u,c,t} \lambda_{bq}^i \int \frac{\mathrm{d}^d k}{(2\pi)^d} \frac{1}{D_i(k+p_2)} \\
\times \Bigg\{ \frac{1}{D_W(k)} \left[\frac{(k+p_2)^2 - p_2^2}{M_W^2} [\not{k} P_L] - \frac{k^2}{M_W^2} [\not{p}_2 P_L] + (2-\epsilon)(\not{k} + \not{p}_2) P_L \right] \\
+ \frac{1}{M_W^2 D_g(k)} \Big[(k^2 + m_i^2)[\not{p}_2 P_L] - [(k+p_2)^2 - p_2^2 - m_i^2][\not{k} P_L] \\
+ m_b m_q (\not{k} + \not{p}_2) P_R - m_i^2 (m_q P_L + m_b P_R) \Big] \Bigg\} .
\end{aligned} \tag{F.99}$$

One can trade $(k+p_2)^2 - p_2^2 = m_i^2 - p_2^2 + D_i(k+p_2)$, so that SM-like 3×3 CKM unitarity allows us to write

$$\begin{aligned}
i\mathcal{M}_1^{\text{self-energy}} = \frac{g^2}{2}\delta_{\alpha_2\beta_2} \sum_{i=u,c,t} \lambda_{bq}^i \int \frac{\mathrm{d}^d k}{(2\pi)^d} \frac{1}{D_i(k+p_2)} \\
\times \Bigg\{ \frac{1}{D_W(k)} \left[\frac{m_i^2 - p_2^2}{M_W^2} [\not{k} P_L] - \frac{k^2}{M_W^2} [\not{p}_2 P_L] + (2-\epsilon)(\not{k} + \not{p}_2) P_L \right] \\
+ \frac{1}{M_W^2 D_g(k)} \left[(k^2 + m_i^2)[\not{p}_2 P_L] + p_2^2 [\not{k} P_L] + m_b m_q (\not{k} + \not{p}_2) P_R - m_i^2 (m_q P_L + m_b P_R) \right] \Bigg\} .
\end{aligned} \tag{F.100}$$

By means of Lorentz invariance, the previous result can be written as

$$\begin{aligned}
i\mathcal{M}_1^{\text{self-energy}} &= \frac{g^2}{2}\delta_{\alpha_2\beta_2} \sum_{i=u,c,t} \lambda_{bq}^i \left[A_i(p_2^2) \not{p}_2 P_L + B_i(p_2^2) m_b m_q \not{p}_2 P_R - C_i(p_2^2)(m_q P_L + m_b P_R) \right] \\
&= \frac{g^2}{2}\delta_{\alpha_2\beta_2} \sum_{i=u,c,t} \lambda_{bq}^i \Pi_i(p_2) ,
\end{aligned} \tag{F.101}$$

where we have defined

$$\Pi_i(p_2) \equiv A_i(p_2^2) \not{p}_2 P_L + B_i(p_2^2) m_b m_q \not{p}_2 P_R - C_i(p_2^2)(m_q P_L + m_b P_R) , \tag{F.102}$$

with

$$A_i(p^2)\not{p} = \int \frac{\mathrm{d}^d k}{(2\pi)^d} \frac{1}{D_i(k+p)} \left\{ \frac{1}{D_W(k)} \left[\frac{m_i^2 - p^2}{M_W^2} \not{k} - \frac{k^2}{M_W^2} \not{p} + (2-\epsilon)(\not{k} + \not{p}) \right] + \frac{(k^2 + m_i^2)\not{p} + p^2 \not{k}}{M_W^2 D_g(k)} \right\} , \tag{F.103}$$

$$B_i(p^2)\not{p} = \int \frac{\mathrm{d}^d k}{(2\pi)^d} \frac{1}{D_i(k+p)} \frac{\not{k} + \not{p}}{M_W^2 D_g(k)} , \tag{F.104}$$

$$C_i(p^2) = \int \frac{\mathrm{d}^d k}{(2\pi)^d} \frac{1}{D_i(k+p)} \frac{m_i^2}{M_W^2 D_g(k)} . \tag{F.105}$$

On the other hand, the self-energy amplitudes from Figs. F.9c and F.9d, with the choice of momentum flow given in Fig. F.10b, can be computed in a similar way, leading to

$$\begin{aligned} i\mathcal{M}_2^{\text{self-energy}} &= -\frac{g^2}{2}\delta_{\alpha_1\beta_2}\sum_{i=u,c,t}\lambda_{bq}^i\Big[A_i(p_1^2)\not{p}_1 P_L + B_i(p_1^2)m_b m_q \not{p}_1 P_R + C_i(p_1^2)(m_q P_L + m_b P_R)\Big] \\ &= -\frac{g^2}{2}\delta_{\alpha_1\beta_2}\sum_{i=u,c,t}\lambda_{bq}^i\widetilde{\Pi}_i(p_1)\,, \end{aligned} \tag{F.106}$$

where

$$\widetilde{\Pi}_i(p_1) \equiv A_i(p_1^2)\not{p}_1 P_L + B_i(p_1^2)m_b m_q \not{p}_1 P_R + C_i(p_1^2)(m_q P_L + m_b P_R)\,. \tag{F.107}$$

We are now in good position to compute the full amplitude for subset I.C of penguins diagrams (see Figs. F.7 and F.8). This reads

$$\begin{aligned} i\mathcal{M}_{\rm I}^{\text{peng,C}} &= 2\times\left(-\frac{g^2}{4}\right)\left(i\eta_Z\frac{g}{c_W}\right)^2(D_L)_{qb}\delta_{\alpha_1\alpha_4}\delta_{\alpha_2\alpha_3}\sum_{i=u,c,t}\lambda_{bq}^i \\ &\times\Bigg\{\frac{\Big[\bar{u}_q(p_3)\gamma^\nu\left(-\tfrac{1}{2}P_L-(Q_u-1)s_W^2\right)i(\not{p}_2+m_q)\Pi_i(p_2)u_b(p_2)\Big]\left[\bar{v}_q(p_1)\gamma^\mu P_L v_b(p_4)\right]}{D_q(p_2)}\times i\frac{g_{\mu\nu}}{M_Z^2} \\ &\quad-\frac{\Big[\bar{v}_q(p_1)\widetilde{\Pi}_i(p_1)i(-\not{p}_1+m_b)\gamma^\mu\left(-\tfrac{1}{2}P_L-(Q_u-1)s_W^2\right)v_b(p_4)\Big]\left[\bar{u}_q(p_3)\gamma^\nu P_L u_b(p_2)\right]}{D_b(-p_1)}\times i\frac{g_{\mu\nu}}{M_Z^2}\Bigg\}\,, \end{aligned} \tag{F.108}$$

where the factor of 2 in the first line accounts for the topologies, not shown in Fig. F.9, in which the self-energy is in the final state. We should point out that we have already considered the limit of vanishing external momenta when writing the propagator of the Z boson, as this will not modify our final result. After a fair amount of algebra, and implementing the on-shell conditions $p_1^2 = p_3^2 = m_q^2$ and $p_2^2 = p_4^2 = m_b^2$, we obtain

$$\begin{aligned} i\mathcal{M}_{\rm I}^{\text{peng,C}} &= -\frac{g^4}{2M_W^2}(D_L)_{qb}\delta_{\alpha_1\alpha_4}\delta_{\alpha_2\alpha_3}\sum_{i=u,c,t}\lambda_{bq}^i\times\frac{1}{m_b^2-m_q^2} \\ &\times\Bigg\{\left(-\frac{1}{2}-(Q_u-1)s_W^2\right)\begin{pmatrix}A(m_b^2)m_b^2 - A(m_q^2)m_q^2 + m_b^2 m_q^2\left[B(m_b^2)-B(m_q^2)\right] \\ -(m_b^2+m_q^2)\left[C(m_b^2)-C(m_q^2)\right]\end{pmatrix} \\ &\qquad\times[\bar{u}_q(p_3)\gamma^\mu P_L u_b(p_2)][\bar{v}_q(p_1)\gamma_\mu P_L v_b(p_4)] \\ &\quad-(Q_u-1)s_W^2 m_b m_q\begin{pmatrix}A(m_b^2)-A(m_q^2)+B(m_b^2)m_b^2-B(m_q^2)m_q^2 \\ -2\left[C(m_b^2)-C(m_q^2)\right]\end{pmatrix} \\ &\qquad\times[\bar{u}_q(p_3)\gamma^\mu P_R u_b(p_2)][\bar{v}_q(p_1)\gamma_\mu P_R v_b(p_4)]\Bigg\}\,. \end{aligned} \tag{F.109}$$

At this point, we can take the limit of zero external momenta and masses. To this aim, we can make use of the fact that

$$\lim_{x_1,x_2\to 0}\frac{f(x_1)x_1 - f(x_2)x_2}{x_1-x_2} = \frac{\mathrm{d}}{\mathrm{d}x}[f(x)x]\bigg|_{x=0} = f(0)\,, \tag{F.110}$$

$$\lim_{x_1,x_2\to 0}\frac{f(x_1)-f(x_2)}{x_1-x_2} = \frac{\mathrm{d}}{\mathrm{d}x}f(x)\bigg|_{x=0} = f'(0)\,, \tag{F.111}$$

yielding

$$i\mathcal{M}_{\mathrm{I}}^{\mathrm{peng,C}} = \frac{g^4}{2M_W^2}(D_L)_{qb}\delta_{\alpha_1\alpha_4}\delta_{\alpha_2\alpha_3}\sum_{i=u,c,t}\lambda_{bq}^i\left(\frac{1}{2}+(Q_u-1)s_W^2\right)A_i(0)[\gamma^\mu P_L][\gamma_\mu P_L]\,, \tag{F.112}$$

with the shorthand $[\ldots][\ldots] = [\bar{u}_q(0)\ldots u_b(0)]\,[\bar{v}_q(0)\ldots v_b(0)]$. Finally, the SM-like CKM orthogonality relation allows us to eliminate λ_{bq}^u:

$$i\mathcal{M}_{\mathrm{I}}^{\mathrm{peng,C}} = \frac{g^4}{2M_W^2}(D_L)_{qb}\delta_{\alpha_1\alpha_4}\delta_{\alpha_2\alpha_3}\sum_{i=c,t}\lambda_{bq}^i\left(\frac{1}{2}+(Q_u-1)s_W^2\right)[A_i(0)-A_u(0)][\gamma^\mu P_L][\gamma_\mu P_L]\,. \tag{F.113}$$

Canceling out gauge dependence

As previously commented, gauge dependence in $i\mathcal{M}_{\mathrm{I}}^{\mathrm{box,1}}$ should be canceled out by adding all penguin topologies in $i\mathcal{M}_{\mathrm{I}}^{\mathrm{peng}}$, both linear in the deviation of unitarity $(D_L)_{qb}$. More precisely, gauge-dependent terms sum up to

$$\begin{aligned}
i\mathcal{M}_{\mathrm{I}}^{\mathrm{box,1}} + i\mathcal{M}_{\mathrm{I}}^{\mathrm{peng}}\Big|_{\mathrm{GD}} &= \frac{g^4}{2M_W^2}(D_L)_{qb}\delta_{\alpha_1\alpha_4}\delta_{\alpha_2\alpha_3}[\gamma^\mu P_L][\gamma_\mu P_L]\sum_{i=c,t}\lambda_{bq}^i\left(\frac{1}{2}+(Q_u-1)s_W^2\right)\\
&\times\left[\left(A_i(0)-\int\frac{\mathrm{d}^dk}{(2\pi)^d}\frac{2x_i}{D_i(k)D_g(k)}\right)-\left(A_u(0)-\int\frac{\mathrm{d}^dk}{(2\pi)^d}\frac{2x_u}{D_u(k)D_g(k)}\right)\right]\\
&= \frac{ig^4}{32\pi^2M_W^2}(D_L)_{qb}\delta_{\alpha_1\alpha_4}\delta_{\alpha_2\alpha_3}[\gamma^\mu P_L][\gamma_\mu P_L]\sum_{i=c,t}\lambda_{bq}^i\left(\frac{1}{2}+(Q_u-1)s_W^2\right)\\
&\times\left\{\left[-\frac{3x_i}{2}\left(\frac{2}{\epsilon}-\gamma+\ln\frac{4\pi\mu^2}{M_W^2}\right)+\frac{x_i(11-5x_i)}{4(x_i-1)}+\frac{3x_i^2(x_i-2)\ln x_i}{2(x_i-1)^2}\right]-[i\leftrightarrow u]\right\},
\end{aligned} \tag{F.114}$$

where γ is the Euler-Mascheroni constant, and μ is the 't Hooft parameter. The result is indeed gauge-independent, but it is not zero because the $A_i(0)$ integral contained a gauge-independent piece—see Eq. (F.103). One can also check that there is a one-loop divergence in the form of a $2/\epsilon$ pole near 4 dimensions. The latter, nevertheless, cancels out when taking into account the remaining gauge-independent terms not included in Eq. (F.114). All in all, in the limit $m_u\to 0$, we are left with

$$i\mathcal{M}_{\mathrm{I}}^{\mathrm{box,1}} + i\mathcal{M}_{\mathrm{I}}^{\mathrm{peng}} = \frac{ig^4}{16\pi^2M_W^2}(D_L)_{qb}\delta_{\alpha_1\alpha_4}\delta_{\alpha_2\alpha_3}[\gamma^\mu P_L][\gamma_\mu P_L]\sum_{i=c,t}\lambda_{bq}^iY(x_i)\,, \tag{F.115}$$

where $Y(x_i)$ is the well-known Inami-Lim function

$$Y(x_i) = \frac{x_i}{4(x_i-1)}\left[x_i-4+\frac{3x_i\ln x_i}{x_i-1}\right]. \tag{F.116}$$

Notice that the result is independent of the electric charge Q_u and of the weak mixing angle θ_W.

Final result

The total amplitude corresponding to set I of diagrams contributing to neutral B_q meson mixing is

$$
\begin{aligned}
i\mathcal{M}_{\rm I} &= i\mathcal{M}_{\rm I}^{\rm box,0} + \left(i\mathcal{M}_{\rm I}^{\rm box,1} + i\mathcal{M}_{\rm I}^{\rm peng}\right) + i\mathcal{M}_{\rm I}^{\rm tree} \\
&= -i\frac{g^4}{64\pi^2 M_W^2}\delta_{\alpha_1\alpha_4}\delta_{\alpha_2\alpha_3}[\bar{u}_q(0)\gamma^\mu P_L u_b(0)][\bar{v}_q(0)\gamma_\mu P_L v_b(0)]\sum_{i,j=c,t}\lambda_{bq}^i\lambda_{bq}^j S_0(x_i,x_j) \\
&\quad + i\frac{g^4}{16\pi^2 M_W^2}(D_L)_{qb}\delta_{\alpha_1\alpha_4}\delta_{\alpha_2\alpha_3}[\bar{u}_q(0)\gamma^\mu P_L u_b(0)][\bar{v}_q(0)\gamma_\mu P_L v_b(0)]\sum_{i=c,t}\lambda_{bq}^i Y(x_i) \\
&\quad - i\frac{g^2}{4M_W^2}(D_L)_{qb}^2\delta_{\alpha_1\alpha_4}\delta_{\alpha_2\alpha_3}[\bar{u}_q(0)\gamma^\mu P_L u_b(0)][\bar{v}_q(0)\gamma_\mu P_L v_b(0)]\,. \qquad \text{(F.117)}
\end{aligned}
$$

Numerically, only the top quark contributions are relevant. Therefore, we can write down

$$
\begin{aligned}
i\mathcal{M}_{\rm I} &= -i\frac{G_F^2 M_W^2}{2\pi^2}\delta_{\alpha_1\alpha_4}\delta_{\alpha_2\alpha_3}[\bar{u}_q(0)\gamma^\mu P_L u_b(0)][\bar{v}_q(0)\gamma_\mu P_L v_b(0)](\lambda_{bq}^t)^2 S_0(x_t) \\
&\quad\times\left[1 - \frac{(D_L)_{qb}}{\lambda_{bq}^t}\frac{4Y(x_t)}{S_0(x_t)} + \left(\frac{(D_L)_{qb}}{\lambda_{bq}^t}\right)^2\frac{2\pi^2\sqrt{2}/(G_F M_W^2)}{S_0(x_t)}\right], \qquad \text{(F.118)}
\end{aligned}
$$

where we have used that $G_F/\sqrt{2} = g^2/(8M_W^2)$. It is straightforward to include the contribution from set II of diagrams as

$$
\begin{aligned}
i\mathcal{M} = i(\mathcal{M}_{\rm I} - \mathcal{M}_{\rm II}) &= -i\frac{G_F^2 M_W^2}{2\pi^2}\begin{pmatrix}\delta_{\alpha_1\alpha_4}\delta_{\alpha_2\alpha_3}[\bar{u}_q(0)\gamma^\mu P_L u_b(0)][\bar{v}_q(0)\gamma_\mu P_L v_b(0)] \\ -\delta_{\alpha_1\alpha_2}\delta_{\alpha_3\alpha_4}[\bar{u}_q(0)\gamma^\mu P_L v_b(0)][\bar{v}_q(0)\gamma_\mu P_L u_b(0)]\end{pmatrix}(\lambda_{bq}^t)^2 S_0(x_t) \\
&\quad\times\left[1 - \frac{(D_L)_{qb}}{\lambda_{bq}^t}\frac{4Y(x_t)}{S_0(x_t)} + \left(\frac{(D_L)_{qb}}{\lambda_{bq}^t}\right)^2\frac{2\pi^2\sqrt{2}/(G_F M_W^2)}{S_0(x_t)}\right], \qquad \text{(F.119)}
\end{aligned}
$$

Assuming that two-loop perturbative QCD corrections encoded in the parameter $\hat{\eta}_B$ are similar to the ones computed within the SM, we finally obtain

$$
\frac{M_{12}^{q,\rm DVLQ}}{M_{12}^{q,\rm SM-like}} = 1 + \frac{(D_L)_{qb}}{\lambda_{bq}^t}\frac{C_1^{\rm DVLQ}(x_t)}{S_0(x_t)} + \left(\frac{(D_L)_{qb}}{\lambda_{bq}^t}\right)^2\frac{C_2^{\rm DVLQ}}{S_0(x_t)}\,, \qquad \text{(F.120)}
$$

where

$$
C_1^{\rm DVLQ}(x_t) = -4Y(x_t), \quad C_2^{\rm DVLQ} = \frac{2\sqrt{2}\pi^2}{G_F M_W^2}\,. \qquad \text{(F.121)}
$$

As in the UVLQ case, two new terms linear and quadratic in the deviation of unitarity $(D_L)_{qb}$ arise within this scenario.

Bibliography

[1] B. Grinstein, X. Lu, C. Miró and P. Quílez, *Most general EFTs from spurion analysis Hilbert series and minimal lepton flavor violation*, *JHEP* **07** (2025) 259 [2412.16285]. i, 31

[2] C. Miró, M. Nebot and D. Queiroz, *Light states in real multi-Higgs models with spontaneous CP violation*, *Phys. Rev. D* **111** (2025) L111703 [2411.00084]. i, 78

[3] C. Miró, M. Escudero and M. Nebot, *How large could the CP violation in neutral B-meson mixing be? Implications for baryogenesis and upcoming searches*, *Phys. Rev. D* **110** (2024) 115033 [2410.13936]. i

[4] J.M. Alves, F.J. Botella, C. Miró and M. Nebot, *Spontaneous CP violation and $\mu - \tau$ symmetry in two-Higgs-doublet models with flavour conservation*, *Eur. Phys. J. C* **83** (2023) 940 [2306.14952]. i

[5] C. Miró, M. Escudero and M. Nebot, *How large could CP violation in B meson mixing be? Implications for baryogenesis and future searches*, *PoS* **DISCRETE2024** (2025) 023. i

[6] B. Grinstein, X. Lu, C. Miró and P. Quílez, *Accidental symmetries, Hilbert series, and friends*, *JHEP* **03** (2025) 172 [2412.05359]. ii, 31, 71

[7] F.J. Botella, F. Cornet-Gomez, C. Miró and M. Nebot, *New physics hints from τ scalar interactions and $(g-2)_{e,\mu}$*, *J. Phys. G* **51** (2024) 025001 [2302.05471]. ii, 41, 100, 101

[8] F.J. Botella, F. Cornet-Gomez, C. Miró and M. Nebot, *Muon and electron $g-2$ anomalies in a flavor conserving 2HDM with an oblique view on the CDF M_W value*, *Eur. Phys. J. C* **82** (2022) 915 [2205.01115]. ii, 41, 100, 101

[9] C. Miró, *Addressing leptonic $g-2$ anomalies in a flavor conserving two-Higgs-doublet model*, *Frascati Phys. Ser.* **72** (2022) 1. ii

[10] M.D. Schwartz, *Quantum Field Theory and the Standard Model*, Cambridge University Press (3, 2014). 3, 178, 179, 191, 193

[11] P. Langacker, *The Standard Model and Beyond*, Taylor & Francis (2017), 10.1201/b22175. 3, 187

[12] S. Weinberg, *The Quantum theory of fields. Vol. 1: Foundations*, Cambridge University Press (6, 2005), 10.1017/CBO9781139644167. 3

[13] S. Weinberg, *The quantum theory of fields. Vol. 2: Modern applications*, Cambridge University Press (8, 2013), 10.1017/CBO9781139644174. 3

[14] S.L. Glashow, *Partial Symmetries of Weak Interactions*, *Nucl. Phys.* **22** (1961) 579. 4

[15] S. Weinberg, *A Model of Leptons*, *Phys. Rev. Lett.* **19** (1967) 1264. 4

[16] A. Salam, *Weak and Electromagnetic Interactions*, *Conf. Proc. C* **680519** (1968) 367. 4

[17] J.C. Romao and J.P. Silva, *A resource for signs and Feynman diagrams of the Standard Model*, *Int. J. Mod. Phys. A* **27** (2012) 1230025 [1209.6213]. 4, 175, 189, 200

[18] P.W. Higgs, *Broken Symmetries and the Masses of Gauge Bosons*, *Phys. Rev. Lett.* **13** (1964) 508. 4, 6

[19] F. Englert and R. Brout, *Broken Symmetry and the Mass of Gauge Vector Mesons*, *Phys. Rev. Lett.* **13** (1964) 321. 4, 6

[20] Y. Nambu, *Quasiparticles and Gauge Invariance in the Theory of Superconductivity*, *Phys. Rev.* **117** (1960) 648. 6

[21] J. Goldstone, *Field Theories with Superconductor Solutions*, *Nuovo Cim.* **19** (1961) 154. 6

[22] G. 't Hooft and M.J.G. Veltman, *Regularization and Renormalization of Gauge Fields*, *Nucl. Phys. B* **44** (1972) 189. 6

[23] Particle Data Group collaboration, *Review of particle physics*, *Phys. Rev. D* **110** (2024) 030001. 8, 13, 41, 96, 105, 108, 114, 115, 116

[24] ATLAS collaboration, *Observation of a new particle in the search for the Standard Model Higgs boson with the ATLAS detector at the LHC*, *Phys. Lett. B* **716** (2012) 1 [1207.7214]. 8, 77

[25] CMS collaboration, *Observation of a New Boson at a Mass of 125 GeV with the CMS Experiment at the LHC*, *Phys. Lett. B* **716** (2012) 30 [1207.7235]. 8, 77

[26] A. Santamaria, *Masses, mixings, Yukawa couplings and their symmetries*, *Phys. Lett. B* **305** (1993) 90 [hep-ph/9302301]. 11

[27] N. Cabibbo, *Unitary Symmetry and Leptonic Decays*, *Phys. Rev. Lett.* **10** (1963) 531. 12

[28] M. Kobayashi and T. Maskawa, *CP Violation in the Renormalizable Theory of Weak Interaction*, *Prog. Theor. Phys.* **49** (1973) 652. 12, 23, 105

[29] S.L. Glashow, J. Iliopoulos and L. Maiani, *Weak Interactions with Lepton-Hadron Symmetry*, *Phys. Rev. D* **2** (1970) 1285. 13

[30] L.-L. Chau and W.-Y. Keung, *Comments on the Parametrization of the Kobayashi-Maskawa Matrix*, *Phys. Rev. Lett.* **53** (1984) 1802. 13, 96, 114

[31] L. Wolfenstein, *Parametrization of the Kobayashi-Maskawa Matrix*, *Phys. Rev. Lett.* **51** (1983) 1945. 13

[32] A.J. Buras, M.E. Lautenbacher and G. Ostermaier, *Waiting for the top quark mass, $K^+ \to \pi^+ \nu \bar{\nu}$, $B_s^0 - \bar{B}_s^0$ mixing and CP asymmetries in B decays*, *Phys. Rev. D* **50** (1994) 3433 [hep-ph/9403384]. 14

[33] C. Jarlskog, *Commutator of the Quark Mass Matrices in the Standard Electroweak Model and a Measure of Maximal CP Nonconservation*, *Phys. Rev. Lett.* **55** (1985) 1039. 15

[34] L. Vale Silva, *2023 update of the extraction of the CKM matrix elements*, in *12th International Workshop on the CKM Unitarity Triangle*, 5, 2024 [2405.08046]. 18

[35] F.J. Botella, G.C. Branco, M. Nebot and M.N. Rebelo, *Unitarity triangles and the search for new physics*, Nucl. Phys. B **651** (2003) 174 [hep-ph/0206133]. 18

[36] Super-Kamiokande collaboration, *Evidence for oscillation of atmospheric neutrinos*, Phys. Rev. Lett. **81** (1998) 1562 [hep-ex/9807003]. 19, 28

[37] SNO collaboration, *Direct evidence for neutrino flavor transformation from neutral current interactions in the Sudbury Neutrino Observatory*, Phys. Rev. Lett. **89** (2002) 011301 [nucl-ex/0204008]. 19, 28

[38] P. Minkowski, *$\mu \to e\gamma$ at a Rate of One Out of 10^9 Muon Decays?*, Phys. Lett. B **67** (1977) 421. 19

[39] M. Gell-Mann, P. Ramond and R. Slansky, *Complex Spinors and Unified Theories*, *Conf. Proc. C* **790927** (1979) 315 [1306.4669]. 19

[40] T. Yanagida, *Horizontal gauge symmetry and masses of neutrinos*, *Conf. Proc. C* **7902131** (1979) 95. 19

[41] R.N. Mohapatra and G. Senjanovic, *Neutrino Masses and Mixings in Gauge Models with Spontaneous Parity Violation*, Phys. Rev. D **23** (1981) 165. 19

[42] J. Schechter and J.W.F. Valle, *Neutrino Masses in SU(2) x U(1) Theories*, Phys. Rev. D **22** (1980) 2227. 19

[43] R. Foot, H. Lew, X.G. He and G.C. Joshi, *Seesaw Neutrino Masses Induced by a Triplet of Leptons*, Z. Phys. C **44** (1989) 441. 19

[44] Y. Cai, J. Herrero-García, M.A. Schmidt, A. Vicente and R.R. Volkas, *From the trees to the forest: a review of radiative neutrino mass models*, Front. in Phys. **5** (2017) 63 [1706.08524]. 19

[45] F. Feruglio and A. Romanino, *Lepton flavor symmetries*, Rev. Mod. Phys. **93** (2021) 015007 [1912.06028]. 19

[46] S. Weinberg, *Baryon and Lepton Nonconserving Processes*, Phys. Rev. Lett. **43** (1979) 1566. 19, 22, 61

[47] B. Pontecorvo, *Neutrino Experiments and the Problem of Conservation of Leptonic Charge*, *Zh. Eksp. Teor. Fiz.* **53** (1967) 1717. 19

[48] Z. Maki, M. Nakagawa and S. Sakata, *Remarks on the unified model of elementary particles*, Prog. Theor. Phys. **28** (1962) 870. 19

[49] I. Esteban, M.C. Gonzalez-Garcia, M. Maltoni, I. Martinez-Soler, J.P. Pinheiro and T. Schwetz, *NuFit-6.0: updated global analysis of three-flavor neutrino oscillations*, JHEP **12** (2024) 216 [2410.05380]. 20, 97

[50] F. Capozzi, E. Di Valentino, E. Lisi, A. Marrone, A. Melchiorri and A. Palazzo, *Unfinished fabric of the three neutrino paradigm*, Phys. Rev. D **104** (2021) 083031 [2107.00532]. 20, 97

[51] P.F. de Salas, D.V. Forero, S. Gariazzo, P. Martínez-Miravé, O. Mena, C.A. Ternes et al., *2020 global reassessment of the neutrino oscillation picture*, *JHEP* **02** (2021) 071 [2006.11237]. 20, 97

[52] DESI collaboration, *DESI 2024 VI: cosmological constraints from the measurements of baryon acoustic oscillations*, *JCAP* **02** (2025) 021 [2404.03002]. 20

[53] D. Naredo-Tuero, M. Escudero, E. Fernández-Martínez, X. Marcano and V. Poulin, *Critical look at the cosmological neutrino mass bound*, *Phys. Rev. D* **110** (2024) 123537 [2407.13831]. 20

[54] KATRIN collaboration, *Direct neutrino-mass measurement based on 259 days of KATRIN data*, 2406.13516. 20

[55] J.A. Casas and A. Ibarra, *Oscillating neutrinos and $\mu \to e, \gamma$*, *Nucl. Phys. B* **618** (2001) 171 [hep-ph/0103065]. 21, 22

[56] M.J. Dolinski, A.W.P. Poon and W. Rodejohann, *Neutrinoless Double-Beta Decay: Status and Prospects*, *Ann. Rev. Nucl. Part. Sci.* **69** (2019) 219 [1902.04097]. 21

[57] J.H. Christenson, J.W. Cronin, V.L. Fitch and R. Turlay, *Evidence for the 2π Decay of the K_2^0 Meson*, *Phys. Rev. Lett.* **13** (1964) 138. 22

[58] G.C. Branco, L. Lavoura and J.P. Silva, *CP Violation*, vol. 103 (1999), 10.1093/oso/9780198503996.001.0001. 23, 27, 41, 50, 51, 90, 109, 187, 194

[59] J. Bernabeu, G.C. Branco and M. Gronau, *CP Restrictions on Quark Mass Matrices*, *Phys. Lett. B* **169** (1986) 243. 23, 25

[60] F.J. Botella and J.P. Silva, *Jarlskog - like invariants for theories with scalars and fermions*, *Phys. Rev. D* **51** (1995) 3870 [hep-ph/9411288]. 25, 45, 49, 50, 90, 95

[61] F.J. Botella and L.-L. Chau, *Anticipating the Higher Generations of Quarks from Rephasing Invariance of the Mixing Matrix*, *Phys. Lett. B* **168** (1986) 97. 26

[62] C. Abel et al., *Measurement of the Permanent Electric Dipole Moment of the Neutron*, *Phys. Rev. Lett.* **124** (2020) 081803 [2001.11966]. 29

[63] PLANCK collaboration, *Planck 2018 results. VI. Cosmological parameters*, *Astron. Astrophys.* **641** (2020) A6 [1807.06209]. 29

[64] A.D. Sakharov, *Violation of CP Invariance, C asymmetry, and baryon asymmetry of the universe*, *Pisma Zh. Eksp. Teor. Fiz.* **5** (1967) 32. 29

[65] HEAVY FLAVOR AVERAGING GROUP (HFLAV) collaboration, *Averages of b-hadron, c-hadron, and τ-lepton properties as of 2023*, 2411.18639. 29, 106, 109, 110, 114, 115

[66] BELLE-II collaboration, *Evidence for $B^+ \to K^+\nu\bar{\nu}$ decays*, *Phys. Rev. D* **109** (2024) 112006 [2311.14647]. 29

[67] CMS collaboration, *Search for the lepton-flavor violating decay of the Higgs boson and additional Higgs bosons in the $e\mu$ final state in proton-proton collisions at $\sqrt{s}$ = 13 TeV*, *Phys. Rev. D* **108** (2023) 072004 [2305.18106]. 29

[68] A. Crivellin and B. Mellado, *Anomalies in particle physics and their implications for physics beyond the standard model*, *Nature Rev. Phys.* **6** (2024) 294 [2309.03870]. 29

[69] A. Crivellin and B. Mellado, *Anomalies in Particle Physcis*, *PoS* **DIS2024** (2025) 007. 29

[70] P. Colangelo, F. De Fazio, F. Loparco and N. Losacco, *Flavour anomalies, correlations, hadronic uncertainties, and all that*, *Nuovo Cim. C* **47** (2024) 145 [2401.02796]. 29, 55

[71] E.E. Jenkins and A.V. Manohar, *Algebraic Structure of Lepton and Quark Flavor Invariants and CP Violation*, *JHEP* **10** (2009) 094 [0907.4763]. 31, 38, 56

[72] A. Hanany, E.E. Jenkins, A.V. Manohar and G. Torri, *Hilbert Series for Flavor Invariants of the Standard Model*, *JHEP* **03** (2011) 096 [1010.3161]. 31, 38, 56

[73] B. Yu and S. Zhou, *Hilbert series for leptonic flavor invariants in the minimal seesaw model*, *JHEP* **10** (2021) 017 [2107.11928]. 31, 56

[74] Y. Wang, B. Yu and S. Zhou, *Flavor invariants and renormalization-group equations in the leptonic sector with massive Majorana neutrinos*, *JHEP* **09** (2021) 053 [2107.06274]. 31, 56

[75] L. Lehman and A. Martin, *Hilbert Series for Constructing Lagrangians: expanding the phenomenologist's toolbox*, *Phys. Rev. D* **91** (2015) 105014 [1503.07537]. 31, 56

[76] L. Lehman and A. Martin, *Low-derivative operators of the Standard Model effective field theory via Hilbert series methods*, *JHEP* **02** (2016) 081 [1510.00372]. 31, 56

[77] B. Henning, X. Lu, T. Melia and H. Murayama, *Hilbert series and operator bases with derivatives in effective field theories*, *Commun. Math. Phys.* **347** (2016) 363 [1507.07240]. 31, 56

[78] B. Henning, X. Lu, T. Melia and H. Murayama, *2, 84, 30, 993, 560, 15456, 11962, 261485, ...: Higher dimension operators in the SM EFT*, *JHEP* **08** (2017) 016 [1512.03433]. 31, 56

[79] B. Henning, X. Lu, T. Melia and H. Murayama, *Operator bases, S-matrices, and their partition functions*, *JHEP* **10** (2017) 199 [1706.08520]. 31, 33, 56

[80] D. Kondo, H. Murayama and R. Okabe, *23, 381, 6242, 103268, 1743183, ... : Hilbert series for CP-violating operators in SMEFT*, *JHEP* **03** (2023) 107 [2212.02413]. 31, 56

[81] Q. Bonnefoy, E. Gendy, C. Grojean and J.T. Ruderman, *Opportunistic CP violation*, *JHEP* **06** (2023) 141 [2302.07288]. 31, 56

[82] L. Gráf, B. Henning, X. Lu, T. Melia and H. Murayama, *Hilbert series, the Higgs mechanism, and HEFT*, *JHEP* **02** (2023) 064 [2211.06275]. 31, 56

[83] L. Graf, B. Henning, X. Lu, T. Melia and H. Murayama, *2, 12, 117, 1959, 45171, 1170086, . . . : a Hilbert series for the QCD chiral Lagrangian*, *JHEP* **01** (2021) 142 [2009.01239]. 31, 56

[84] B. Feng, A. Hanany and Y.-H. He, *Counting gauge invariants: The Plethystic program*, *JHEP* **03** (2007) 090 [hep-th/0701063]. 31, 56

[85] S. Benvenuti, B. Feng, A. Hanany and Y.-H. He, *Counting BPS Operators in Gauge Theories: Quivers, Syzygies and Plethystics*, *JHEP* **11** (2007) 050 [hep-th/0608050]. 31, 56

[86] J. Gray, A. Hanany, Y.-H. He, V. Jejjala and N. Mekareeya, *SQCD: A Geometric Apercu*, *JHEP* **05** (2008) 099 [0803.4257]. 31, 56

[87] B. Grinstein, X. Lu, L. Merlo and P. Quílez, *Hilbert series for covariants and their applications to minimal flavor violation*, *JHEP* **2024** (2024) 154 [2312.13349]. 31, 33, 34, 36, 37, 56, 58, 59, 61, 62, 159

[88] M. Brion, *Sur les modules de covariants*, *Annales scientifiques de l'École Normale Supérieure* **26** (1993) 1. 31, 37, 58, 59

[89] B. Broer, *Hilbert series for modules of covariants*, *Algebraic Groups and Their Generalizations: Classical Methods (University Park, PA, 1991)* **56** (1994) 321. 36, 37, 58, 59

[90] F.J. Botella, F. Cornet-Gomez and M. Nebot, *Electron and muon $g-2$ anomalies in general flavour conserving two Higgs doublets models*, *Phys. Rev. D* **102** (2020) 035023 [2006.01934]. 41

[91] I.P. Ivanov, *Building and testing models with extended Higgs sectors*, *Prog. Part. Nucl. Phys.* **95** (2017) 160 [1702.03776]. 41

[92] G.C. Branco, P.M. Ferreira, L. Lavoura, M.N. Rebelo, M. Sher and J.P. Silva, *Theory and phenomenology of two-Higgs-doublet models*, *Phys. Rept.* **516** (2012) 1 [1106.0034]. 41, 44

[93] B.W. Lee, C. Quigg and H.B. Thacker, *The Strength of Weak Interactions at Very High-Energies and the Higgs Boson Mass*, *Phys. Rev. Lett.* **38** (1977) 883. 42, 77

[94] B.W. Lee, C. Quigg and H.B. Thacker, *Weak Interactions at Very High-Energies: The Role of the Higgs Boson Mass*, *Phys. Rev. D* **16** (1977) 1519. 42, 77

[95] T.D. Lee, *A Theory of Spontaneous T Violation*, *Phys. Rev. D* **8** (1973) 1226. 44, 77, 89

[96] T.D. Lee, *CP Nonconservation and Spontaneous Symmetry Breaking*, *Phys. Rept.* **9** (1974) 143. 44, 77, 89

[97] I.F. Ginzburg and M. Krawczyk, *Symmetries of two Higgs doublet model and CP violation*, *Phys. Rev. D* **72** (2005) 115013 [hep-ph/0408011]. 44

[98] S. Davidson and H.E. Haber, *Basis-independent methods for the two-Higgs-doublet model*, *Phys. Rev. D* **72** (2005) 035004 [hep-ph/0504050]. 44

[99] M.P. Bento, H.E. Haber, J.C. Romão and J.a.P. Silva, *Multi-Higgs doublet models: physical parametrization, sum rules and unitarity bounds*, *JHEP* **11** (2017) 095 [1708.09408]. 45

[100] C.C. Nishi, *The Structure of potentials with N Higgs doublets*, *Phys. Rev. D* **76** (2007) 055013 [0706.2685]. 45

[101] H. Georgi and D.V. Nanopoulos, *Suppression of Flavor Changing Effects From Neutral Spinless Meson Exchange in Gauge Theories*, *Phys. Lett. B* **82** (1979) 95. 45, 90, 95

[102] J.F. Donoghue and L.F. Li, *Properties of Charged Higgs Bosons*, *Phys. Rev. D* **19** (1979) 945. 45, 90, 95

[103] S.L. Glashow and S. Weinberg, *Natural Conservation Laws for Neutral Currents*, *Phys. Rev. D* **15** (1977) 1958. 47, 89

[104] E.A. Paschos, *Diagonal Neutral Currents*, *Phys. Rev. D* **15** (1977) 1966. 47

[105] A. Pich and P. Tuzon, *Yukawa Alignment in the Two-Higgs-Doublet Model*, *Phys. Rev. D* **80** (2009) 091702 [0908.1554]. 47

[106] T.P. Cheng and M. Sher, *Mass Matrix Ansatz and Flavor Nonconservation in Models with Multiple Higgs Doublets*, *Phys. Rev. D* **35** (1987) 3484. 48

[107] G.C. Branco, W. Grimus and L. Lavoura, *Relating the scalar flavor changing neutral couplings to the CKM matrix*, *Phys. Lett. B* **380** (1996) 119 [hep-ph/9601383]. 48

[108] G. D'Ambrosio, G.F. Giudice, G. Isidori and A. Strumia, *Minimal flavor violation: An Effective field theory approach*, *Nucl. Phys. B* **645** (2002) 155 [hep-ph/0207036]. 48, 55

[109] V. Cirigliano, B. Grinstein, G. Isidori and M.B. Wise, *Minimal flavor violation in the lepton sector*, *Nucl. Phys. B* **728** (2005) 121 [hep-ph/0507001]. 48, 55, 56, 72

[110] J.M. Alves, F.J. Botella, G.C. Branco, F. Cornet-Gomez and M. Nebot, *Controlled Flavour Changing Neutral Couplings in Two Higgs Doublet Models*, *Eur. Phys. J. C* **77** (2017) 585 [1703.03796]. 48

[111] M. Nebot, F.J. Botella and G.C. Branco, *Vacuum Induced CP Violation Generating a Complex CKM Matrix with Controlled Scalar FCNC*, *Eur. Phys. J. C* **79** (2019) 711 [1808.00493]. 49, 78, 95

[112] L. Lavoura and J.P. Silva, *Fundamental CP violating quantities in a $SU(2) \times U(1)$ model with many Higgs doublets*, *Phys. Rev. D* **50** (1994) 4619 [hep-ph/9404276]. 50

[113] A. Mendez and A. Pomarol, *Signals of CP violation in the Higgs sector*, *Phys. Lett. B* **272** (1991) 313. 50

[114] M. Nebot and J.a.P. Silva, *Self-cancellation of a scalar in neutral meson mixing and implications for the LHC*, *Phys. Rev. D* **92** (2015) 085010 [1507.07941]. 51

[115] B. Capdevila, A. Crivellin and J. Matias, *Review of semileptonic B anomalies*, *Eur. Phys. J. ST* **1** (2023) 20 [2309.01311]. 55

[116] A. Cerri et al., *Report from Working Group 4: Opportunities in Flavour Physics at the HL-LHC and HE-LHC*, *CERN Yellow Rep. Monogr.* **7** (2019) 867 [1812.07638]. 55, 89, 105

[117] V. Cirigliano and B. Grinstein, *Phenomenology of minimal lepton flavor violation*, *Nucl. Phys. B* **752** (2006) 18 [hep-ph/0601111]. 56

[118] B. Grinstein, V. Cirigliano, G. Isidori and M.B. Wise, *Grand Unification and the Principle of Minimal Flavor Violation*, *Nucl. Phys. B* **763** (2007) 35 [hep-ph/0608123]. 56

[119] M. Raidal et al., *Flavour physics of leptons and dipole moments*, *Eur. Phys. J. C* **57** (2008) 13 [0801.1826]. 56

[120] B. Grzadkowski, M. Iskrzynski, M. Misiak and J. Rosiek, *Dimension-Six Terms in the Standard Model Lagrangian*, *JHEP* **10** (2010) 085 [1008.4884]. 60, 61, 73, 74

[121] R. Alonso, H.-M. Chang, E.E. Jenkins, A.V. Manohar and B. Shotwell, *Renormalization group evolution of dimension-six baryon number violating operators*, *Phys. Lett. B* **734** (2014) 302 [1405.0486]. 61, 74

[122] A. Kobach, *Baryon Number, Lepton Number, and Operator Dimension in the Standard Model*, *Phys. Lett. B* **758** (2016) 455 [1604.05726]. 65

[123] A. Helset and A. Kobach, *Baryon Number, Lepton Number, and Operator Dimension in the SMEFT with Flavor Symmetries*, *Phys. Lett. B* **800** (2020) 135132 [1909.05853]. 65

[124] R. Alonso, E.E. Jenkins, A.V. Manohar and M. Trott, *Renormalization Group Evolution of the Standard Model Dimension Six Operators III: Gauge Coupling Dependence and Phenomenology*, *JHEP* **04** (2014) 159 [1312.2014]. 73

[125] Y. Liao and X.-D. Ma, *Operators up to Dimension Seven in Standard Model Effective Field Theory Extended with Sterile Neutrinos*, *Phys. Rev. D* **96** (2017) 015012 [1612.04527]. 76

[126] R. Alonso, E. Fernandez Martinez, M.B. Gavela, B. Grinstein, L. Merlo and P. Quilez, *Gauged Lepton Flavour*, *JHEP* **12** (2016) 119 [1609.05902]. 72

[127] Gfitter collaboration, *Updated Status of the Global Electroweak Fit and Constraints on New Physics*, *Eur. Phys. J. C* **72** (2012) 2003 [1107.0975]. 77

[128] A.D. Linde, *Dynamical Symmetry Restoration and Constraints on Masses and Coupling Constants in Gauge Theories*, *JETP Lett.* **23** (1976) 64. 77

[129] S. Weinberg, *Mass of the Higgs Boson*, *Phys. Rev. Lett.* **36** (1976) 294. 77

[130] D.A. Dicus and V.S. Mathur, *Upper bounds on the values of masses in unified gauge theories*, *Phys. Rev. D* **7** (1973) 3111. 77

[131] G.J. Gounaris, R. Kogerler and H. Neufeld, *Relationship Between Longitudinally Polarized Vector Bosons and their Unphysical Scalar Partners*, *Phys. Rev. D* **34** (1986) 3257. 77

[132] M.J.G. Veltman, *Second Threshold in Weak Interactions*, *Acta Phys. Polon. B* **8** (1977) 475. 77

[133] H.D. Politzer and S. Wolfram, *Bounds on Particle Masses in the Weinberg-Salam Model*, *Phys. Lett. B* **82** (1979) 242. 77

[134] N. Cabibbo, L. Maiani, G. Parisi and R. Petronzio, *Bounds on the Fermions and Higgs Boson Masses in Grand Unified Theories*, *Nucl. Phys. B* **158** (1979) 295. 77

[135] D.J.E. Callaway, *Nontriviality of Gauge Theories With Elementary Scalars and Upper Bounds on Higgs Masses*, *Nucl. Phys. B* **233** (1984) 189. 77

[136] P. Langacker and H.A. Weldon, *A Mass Sum Rule for Higgs Bosons in Arbitrary Models*, *Phys. Rev. Lett.* **52** (1984) 1377. 77

[137] H.A. Weldon, *Constraints on scalar masses implied by spontaneous symmetry breaking*, *Phys. Lett. B* **146** (1984) 59. 77

[138] H. Huffel and G. Pocsik, *Unitarity Bounds on Higgs Boson Masses in the Weinberg-Salam Model With Two Higgs Doublets*, *Z. Phys. C* **8** (1981) 13. 78

[139] R. Casalbuoni, D. Dominici, F. Feruglio and R. Gatto, *Tree Level Unitarity Violation for Large Scalar Mass in Multi - Higgs Extensions of the Standard Model*, *Nucl. Phys. B* **299** (1988) 117. 78

[140] J. Maalampi, J. Sirkka and I. Vilja, *Tree level unitarity and triviality bounds for two Higgs models*, *Phys. Lett. B* **265** (1991) 371. 78

[141] S. Kanemura, T. Kubota and E. Takasugi, *Lee-Quigg-Thacker bounds for Higgs boson masses in a two doublet model*, *Phys. Lett. B* **313** (1993) 155 [hep-ph/9303263]. 78

[142] J. Horejsi and M. Kladiva, *Tree-unitarity bounds for THDM Higgs masses revisited*, *Eur. Phys. J. C* **46** (2006) 81 [hep-ph/0510154]. 78

[143] I.F. Ginzburg and I.P. Ivanov, *Tree-level unitarity constraints in the most general 2HDM*, *Phys. Rev. D* **72** (2005) 115010 [hep-ph/0508020]. 78

[144] S. Kanemura and K. Yagyu, *Unitarity bound in the most general two Higgs doublet model*, *Phys. Lett. B* **751** (2015) 289 [1509.06060]. 78

[145] H.E. Haber and Y. Nir, *Multiscalar Models With a High-energy Scale*, *Nucl. Phys. B* **335** (1990) 363. 78

[146] F. Faro, J.C. Romao and J.P. Silva, *Nondecoupling in Multi-Higgs doublet models*, *Eur. Phys. J. C* **80** (2020) 635 [2002.10518]. 78

[147] S. Carrolo, J.C. Romão, J.a.P. Silva and F. Vazão, *Symmetry and decoupling in multi-Higgs boson models*, *Phys. Rev. D* **103** (2021) 075026 [2102.11303]. 78

[148] G. Barenboim, M. Gorbahn, U. Nierste and M. Raidal, *Higgs Sector of the Minimal Left-Right Symmetric Model*, *Phys. Rev. D* **65** (2002) 095003 [hep-ph/0107121]. 78

[149] M. Nebot, *Bounded masses in two Higgs doublets models, spontaneous CP violation and $\mathbb{Z}_2$ symmetry*, *Phys. Rev. D* **102** (2020) 115002 [1911.02266]. 78

[150] U. Nierste, M. Tabet and R. Ziegler, *Cornering Spontaneous CP Violation with Charged-Higgs-Boson Searches*, *Phys. Rev. Lett.* **125** (2020) 031801 [1912.11501]. 78

[151] J.F. Gunion and H.E. Haber, *The CP conserving two Higgs doublet model: The Approach to the decoupling limit*, *Phys. Rev. D* **67** (2003) 075019 [hep-ph/0207010]. 86

[152] M. Carena, I. Low, N.R. Shah and C.E.M. Wagner, *Impersonating the Standard Model Higgs Boson: Alignment without Decoupling*, *JHEP* **04** (2014) 015 [1310.2248]. 86

[153] A. Pilaftsis, *Symmetries for standard model alignment in multi-Higgs doublet models*, *Phys. Rev. D* **93** (2016) 075012 [1602.02017]. 86

[154] G.C. Branco, *Spontaneous CP Violation in Theories with More Than Four Quarks*, *Phys. Rev. Lett.* **44** (1980) 504. 89, 90, 92, 103, 140

[155] G. Ecker, W. Grimus and H. Neufeld, *A CP Violating Mixing Matrix Compatible With Neutral Flavor Conservation and Spontaneous CP Violation*, *Phys. Lett. B* **194** (1987) 251. 89, 91, 93, 94, 103, 140

[156] M. Gronau, A. Kfir, G. Ecker, W. Grimus and H. Neufeld, *Do Flavor Conservation and Spontaneous CP Violation Lead to a Real Kobayashi-Maskawa Matrix?*, *Phys. Rev. D* **37** (1988) 250. 89, 91, 92, 94, 95, 103, 140

[157] P.F. Harrison and W.G. Scott, *$\mu - \tau$ reflection symmetry in lepton mixing and neutrino oscillations*, *Phys. Lett. B* **547** (2002) 219 [hep-ph/0210197]. 89, 96

[158] T.S. Roussy et al., *An improved bound on the electron's electric dipole moment*, *Science* **381** (2023) adg4084 [2212.11841]. 101

[159] V. Ilisie, *New Barr-Zee contributions to $(g-2)_\mu$ in two-Higgs-doublet models*, *JHEP* **04** (2015) 077 [1502.04199]. 102, 185

[160] J. Albrecht, F. Bernlochner, A. Lenz and A. Rusov, *Lifetimes of b-hadrons and mixing of neutral B-mesons: theoretical and experimental status*, *Eur. Phys. J. ST* **233** (2024) 359 [2402.04224]. 105, 110, 111, 112, 198

[161] G. Elor, M. Escudero and A. Nelson, *Baryogenesis and Dark Matter from B Mesons*, *Phys. Rev. D* **99** (2019) 035031 [1810.00880]. 105, 113, 126, 127, 131, 132

[162] A.E. Nelson and H. Xiao, *Baryogenesis from B Meson Oscillations*, *Phys. Rev. D* **100** (2019) 075002 [1901.08141]. 105, 131, 132

[163] G. Alonso-Álvarez, G. Elor and M. Escudero, *Collider signals of baryogenesis and dark matter from B mesons: A roadmap to discovery*, *Phys. Rev. D* **104** (2021) 035028 [2101.02706]. 105, 106, 109, 126, 127, 128, 129, 131, 132

[164] A. Ghalsasi, D. McKeen and A.E. Nelson, *Baryogenesis via Mesino Oscillations*, *Phys. Rev. D* **92** (2015) 076014 [1508.05392]. 105

[165] D. McKeen and A.E. Nelson, *CP Violating Baryon Oscillations*, *Phys. Rev. D* **94** (2016) 076002 [1512.05359]. 105

[166] K. Aitken, D. McKeen, T. Neder and A.E. Nelson, *Baryogenesis from Oscillations of Charmed or Beautiful Baryons*, *Phys. Rev. D* **96** (2017) 075009 [1708.01259]. 105

[167] G. Alonso-Álvarez, G. Elor, A.E. Nelson and H. Xiao, *A Supersymmetric Theory of Baryogenesis and Sterile Sneutrino Dark Matter from B Mesons*, *JHEP* **03** (2020) 046 [1907.10612]. 105, 113

[168] G. Elor and R. McGehee, *Making the Universe at 20 MeV*, *Phys. Rev. D* **103** (2021) 035005 [2011.06115]. 105

[169] F. Elahi, G. Elor and R. McGehee, *Charged B mesogenesis*, *Phys. Rev. D* **105** (2022) 055024 [2109.09751]. 105

[170] G. Elor, R. Houtz, S. Ipek and M. Ulloa, *The Standard Model CP Violation is Enough*, 2408.12647. 105

[171] G. Alonso-Álvarez, M. Escudero, B. Grinstein, J. Martin-Camalich and C. Murgui, *B-Mesogenesis, revisited*, *In preparation* (2024) . 106

[172] C.W. Bauer and N.D. Dunn, *Comment on new physics contributions to Γ_{12}^s*, *Phys. Lett. B* **696** (2011) 362 [1006.1629]. 106, 124, 125

[173] Z. Ligeti, M. Papucci, G. Perez and J. Zupan, *Implications of the dimuon CP asymmetry in $B_{d,s}$ decays*, *Phys. Rev. Lett.* **105** (2010) 131601 [1006.0432]. 106, 113

[174] A.J. Lenz, *A simple relation for B_s mixing*, *Phys. Rev. D* **84** (2011) 031501 [1106.3200]. 106, 113

[175] C. Bobeth and U. Haisch, *New Physics in Γ^s_{12}: $(\bar{s}b)(\bar{\tau}\tau)$ Operators*, Acta Phys. Polon. B **44** (2013) 127 [1109.1826]. 106, 113, 126

[176] A. Lenz, U. Nierste, J. Charles, S. Descotes-Genon, H. Lacker, S. Monteil et al., *Constraints on new physics in $B-\bar{B}$ mixing in the light of recent LHCb data*, Phys. Rev. D **86** (2012) 033008 [1203.0238]. 106, 113

[177] A. Bevan et al., *Standard Model updates and new physics analysis with the Unitarity Triangle fit*, Nucl. Phys. B Proc. Suppl. **241-242** (2013) 89. 106, 113

[178] J. Charles, S. Descotes-Genon, Z. Ligeti, S. Monteil, M. Papucci and K. Trabelsi, *Future sensitivity to new physics in B_d, B_s, and K mixings*, Phys. Rev. D **89** (2014) 033016 [1309.2293]. 106, 113

[179] M. Artuso, G. Borissov and A. Lenz, *CP violation in the B^0_s system*, Rev. Mod. Phys. **88** (2016) 045002 [1511.09466]. 106, 112, 113, 115

[180] J. Charles, S. Descotes-Genon, Z. Ligeti, S. Monteil, M. Papucci, K. Trabelsi et al., *New physics in B meson mixing: future sensitivity and limitations*, Phys. Rev. D **102** (2020) 056023 [2006.04824]. 106, 113

[181] K. De Bruyn, R. Fleischer, E. Malami and P. van Vliet, *New physics in B^0_q-mixing: present challenges, prospects, and implications for*, J. Phys. G **50** (2023) 045003 [2208.14910]. 106, 113

[182] B.A. Dobrescu, P.J. Fox and A. Martin, *CP Violation in B_s Mixing from Heavy Higgs Exchange*, Phys. Rev. Lett. **105** (2010) 041801 [1005.4238]. 106, 124

[183] M. Trott and M.B. Wise, *On Theories of Enhanced CP Violation in $B_{s,d}$ Meson Mixing*, JHEP **11** (2010) 157 [1009.2813]. 106, 113, 124

[184] Y. Bai and A.E. Nelson, *CP Violating Contribution to $\Delta\Gamma$ in the B_s System from Mixing with a Hidden Pseudoscalar*, Phys. Rev. D **82** (2010) 114027 [1007.0596]. 106, 124, 130

[185] F.J. Botella, G.C. Branco, M. Nebot and A. Sánchez, *Mixing asymmetries in B meson systems, the D0 like-sign dimuon asymmetry and generic New Physics*, Phys. Rev. D **91** (2015) 035013 [1402.1181]. 106, 113, 124

[186] I. Doršner, S. Fajfer, A. Greljo, J.F. Kamenik and N. Košnik, *Physics of leptoquarks in precision experiments and at particle colliders*, Phys. Rept. **641** (2016) 1 [1603.04993]. 106, 113

[187] D. Buttazzo, A. Greljo, G. Isidori and D. Marzocca, *B-physics anomalies: a guide to combined explanations*, JHEP **11** (2017) 044 [1706.07808]. 106, 113

[188] S. Iguro and Y. Omura, *Status of the semileptonic B decays and muon g-2 in general 2HDMs with right-handed neutrinos*, JHEP **05** (2018) 173 [1802.01732]. 106, 113

[189] L. Di Luzio, M. Kirk, A. Lenz and T. Rauh, *ΔM_s theory precision confronts flavour anomalies*, JHEP **12** (2019) 009 [1909.11087]. 106, 113

[190] A. Crivellin, D. Müller and C. Wiegand, *$b \to s\ell^+\ell^-$ transitions in two-Higgs-doublet models*, JHEP **06** (2019) 119 [1903.10440]. 106, 113

[191] P. Athron, C. Balazs, T.E. Gonzalo, D. Jacob, F. Mahmoudi and C. Sierra, *Likelihood analysis of the flavour anomalies and g – 2 in the general two Higgs doublet model*, *JHEP* **01** (2022) 037 [2111.10464]. 106, 113

[192] J. Bonilla, A. de Giorgi, B. Gavela, L. Merlo and M. Ramos, *The cost of an ALP solution to the neutral B-anomalies*, *JHEP* **02** (2023) 138 [2209.11247]. 106, 113

[193] M.-D. Zheng, F.-Z. Chen and H.-H. Zhang, *Explaining anomalies of B-physics, muon $g-2$ and W mass in R-parity violating MSSM with seesaw mechanism*, *Eur. Phys. J. C* **82** (2022) 895 [2207.07636]. 106, 113

[194] A. Datta, A. Hammad, D. Marfatia, L. Mukherjee and A. Rashed, *Dark photon and dark Z mediated B meson decays*, *JHEP* **03** (2023) 108 [2210.15662]. 106, 113

[195] J. Davighi, A. Gosnay, D.J. Miller and S. Renner, *Phenomenology of a Deconstructed Electroweak Force*, *JHEP* **05** (2024) 085 [2312.13346]. 106, 113

[196] P. Athron, R. Martinez and C. Sierra, *B meson anomalies and large $B^+ \to K^+ \nu\bar{\nu}$ in non-universal $U(1)'$ models*, *JHEP* **02** (2024) 121 [2308.13426]. 106, 113

[197] B. Allanach and A. Mullin, *Plan B: new Z' models for $b \to s\ell^+\ell^-$ anomalies*, *JHEP* **09** (2023) 173 [2306.08669]. 106, 113

[198] T. Li, Z. Qian, M.A. Schmidt and M. Yuan, *The quark flavor-violating ALPs in light of B mesons and hadron colliders*, *JHEP* **05** (2024) 232 [2402.14232]. 106, 113

[199] D0 collaboration, *Evidence for an Anomalous Like-Sign Dimuon Charge Asymmetry*, *Phys. Rev. D* **82** (2010) 032001 [1005.2757]. 106, 113, 124

[200] D0 collaboration, *Measurement of the anomalous like-sign dimuon charge asymmetry with 9 fb^{-1} of $p\bar{p}$ collisions*, *Phys. Rev. D* **84** (2011) 052007 [1106.6308]. 106, 113, 124

[201] D0 collaboration, *Study of CP-violating charge asymmetries of single muons and like-sign dimuons in $p\bar{p}$ collisions*, *Phys. Rev. D* **89** (2014) 012002 [1310.0447]. 106, 113, 124

[202] V. Weisskopf and E. Wigner, *Over the natural line width in the radiation of the harmonius oscillator*, *Z. Phys.* **65** (1930) 18. 107

[203] V. Weisskopf and E.P. Wigner, *Calculation of the natural brightness of spectral lines on the basis of Dirac's theory*, *Z. Phys.* **63** (1930) 54. 107

[204] LHCb collaboration, *Physics case for an LHCb Upgrade II - Opportunities in flavour physics, and beyond, in the HL-LHC era*, 1808.08865. 109, 110

[205] Belle-II collaboration, *The Belle II Physics Book*, *PTEP* **2019** (2019) 123C01 [1808.10567]. 109, 110

[206] H. Aihara et al., *The Belle II Detector Upgrades Framework Conceptual Design Report*, 2406.19421. 109

[207] FCC collaboration, *FCC-ee: The Lepton Collider: Future Circular Collider Conceptual Design Report Volume 2*, *Eur. Phys. J. ST* **228** (2019) 261. 109, 134

[208] S. Monteil and G. Wilkinson, *Heavy-quark opportunities and challenges at FCC-ee*, *Eur. Phys. J. Plus* **136** (2021) 837 [2106.01259]. 109, 134

[209] A. Buras, *Gauge Theory of Weak Decays*, Cambridge University Press (6, 2020), 10.1017/9781139524100. 109

[210] T. Inami and C.S. Lim, *Effects of Superheavy Quarks and Leptons in Low-Energy Weak Processes* $K_L \to \mu\bar{\mu}$, $K^+ \to \pi^+\nu\bar{\nu}$, *and* $K^0 \leftrightarrow \bar{K}^0$, *Prog. Theor. Phys.* **65** (1981) 297. 110

[211] W.A. Bardeen, A.J. Buras, D.W. Duke and T. Muta, *Deep Inelastic Scattering Beyond the Leading Order in Asymptotically Free Gauge Theories*, *Phys. Rev. D* **18** (1978) 3998. 110

[212] Fermilab Lattice, MILC collaboration, $B^0_{(s)}$*-mixing matrix elements from lattice QCD for the Standard Model and beyond*, *Phys. Rev. D* **93** (2016) 113016 [1602.03560]. 110, 111, 115, 194

[213] R.J. Dowdall, C.T.H. Davies, R.R. Horgan, G.P. Lepage, C.J. Monahan, J. Shigemitsu et al., *Neutral B-meson mixing from full lattice QCD at the physical point*, *Phys. Rev. D* **100** (2019) 094508 [1907.01025]. 110, 111, 194

[214] A.G. Grozin, R. Klein, T. Mannel and A.A. Pivovarov, $B^0 - \bar{B}^0$ *mixing at next-to-leading order*, *Phys. Rev. D* **94** (2016) 034024 [1606.06054]. 110, 111, 194

[215] M. Kirk, A. Lenz and T. Rauh, *Dimension-six matrix elements for meson mixing and lifetimes from sum rules*, *JHEP* **12** (2017) 068 [1711.02100]. 110, 111, 194

[216] D. King, A. Lenz and T. Rauh, B_s *mixing observables and* $|V_{td}/V_{ts}|$ *from sum rules*, *JHEP* **05** (2019) 034 [1904.00940]. 110, 111, 194

[217] J.T. Tsang and M. Della Morte, *B-physics from lattice gauge theory*, *Eur. Phys. J. ST* **233** (2024) 253 [2310.02705]. 110

[218] A.J. Buras, M. Jamin and P.H. Weisz, *Leading and Next-to-leading QCD Corrections to* ϵ *Parameter and* $B^0 - \bar{B}^0$ *Mixing in the Presence of a Heavy Top Quark*, *Nucl. Phys. B* **347** (1990) 491. 110, 116, 194

[219] Flavour Lattice Averaging Group (FLAG) collaboration, *FLAG Review 2024*, 2411.04268. 110

[220] A.B. Carter and A.I. Sanda, *CP Violation in B Meson Decays*, *Phys. Rev. D* **23** (1981) 1567. 110

[221] I.I.Y. Bigi and A.I. Sanda, *Notes on the Observability of CP Violations in B Decays*, *Nucl. Phys. B* **193** (1981) 85. 110

[222] R. Fleischer, *CP violation in B decays: recent developments and future perspectives*, *Eur. Phys. J. ST* **233** (2024) 391 [2402.00710]. 110

[223] M.Z. Barel, K. De Bruyn, R. Fleischer and E. Malami, *In pursuit of new physics with* $B^0_d \to J/\psi K^0$ *and* $B^0_s \to J/\psi\phi$ *decays at the high-precision Frontier*, *J. Phys. G* **48** (2021) 065002 [2010.14423]. 110, 115

[224] LHCb collaboration, *Measurement of CP violation parameters and polarisation fractions in* $B^0_s \to J/\psi\bar{K}^{*0}$ *decays*, *JHEP* **11** (2015) 082 [1509.00400]. 110

[225] P. Frings, U. Nierste and M. Wiebusch, *Penguin contributions to CP phases in $B_{d,s}$ decays to charmonium*, Phys. Rev. Lett. **115** (2015) 061802 [1503.00859]. 110, 115

[226] K. De Bruyn and R. Fleischer, *A Roadmap to Control Penguin Effects in $B_d^0 \to J/\psi K_S^0$ and $B_s^0 \to J/\psi\phi$*, JHEP **03** (2015) 145 [1412.6834]. 110

[227] LHCb collaboration, *Measurement of the CP-violating phase β in $B^0 \to J/\psi\pi^+\pi^-$ decays and limits on penguin effects*, Phys. Lett. B **742** (2015) 38 [1411.1634]. 110

[228] M. Jung, *Determining weak phases from $B \to J/\psi P$ decays*, Phys. Rev. D **86** (2012) 053008 [1206.2050]. 110

[229] M. Ciuchini, M. Pierini and L. Silvestrini, *Theoretical uncertainty in sin 2β: An Update*, in *6th International Workshop on the CKM Unitarity Triangle*, 2, 2011 [1102.0392]. 110

[230] S. Faller, M. Jung, R. Fleischer and T. Mannel, *The Golden Modes $B^0 \to J/\psi K_{S,L}$ in the Era of Precision Flavour Physics*, Phys. Rev. D **79** (2009) 014030 [0809.0842]. 110

[231] M. Ciuchini, M. Pierini and L. Silvestrini, *The Effect of penguins in the $B_d \to J/\psi K^0$ CP asymmetry*, Phys. Rev. Lett. **95** (2005) 221804 [hep-ph/0507290]. 110

[232] LHCb collaboration, *Measurement of CP Violation in $B^0 \to \psi(\to \ell^+\ell^-)K_S^0(\to \pi^+\pi^-)$ Decays*, Phys. Rev. Lett. **132** (2024) 021801 [2309.09728]. 110, 113, 114

[233] LHCb collaboration, *Improved Measurement of CP Violation Parameters in $B_s^0 \to J/\psi K^+K^-$ Decays in the Vicinity of the ϕ(1020) Resonance*, Phys. Rev. Lett. **132** (2024) 051802 [2308.01468]. 110, 113, 114

[234] A. Lenz, *Lifetimes and heavy quark expansion*, Int. J. Mod. Phys. A **30** (2015) 1543005 [1405.3601]. 111, 196, 198

[235] M. Beneke, G. Buchalla, C. Greub, A. Lenz and U. Nierste, *Next-to-leading order QCD corrections to the lifetime difference of B(s) mesons*, Phys. Lett. B **459** (1999) 631 [hep-ph/9808385]. 111

[236] M. Beneke, G. Buchalla, A. Lenz and U. Nierste, *CP Asymmetry in Flavor Specific B Decays beyond Leading Logarithms*, Phys. Lett. B **576** (2003) 173 [hep-ph/0307344]. 111

[237] M. Ciuchini, E. Franco, V. Lubicz, F. Mescia and C. Tarantino, *Lifetime differences and CP violation parameters of neutral B mesons at the next-to-leading order in QCD*, JHEP **08** (2003) 031 [hep-ph/0308029]. 111, 194

[238] A. Lenz and U. Nierste, *Theoretical update of $B_s - \bar{B}_s$ mixing*, JHEP **06** (2007) 072 [hep-ph/0612167]. 111, 194

[239] H.M. Asatrian, A. Hovhannisyan, U. Nierste and A. Yeghiazaryan, *Towards next-to-next-to-leading-log accuracy for the width difference in the $B_s - \bar{B}_s$ system: fermionic contributions to order $(m_c/m_b)^0$ and $(m_c/m_b)^1$*, JHEP **10** (2017) 191 [1709.02160]. 111

[240] H.M. Asatrian, H.H. Asatryan, A. Hovhannisyan, U. Nierste, S. Tumasyan and A. Yeghiazaryan, *Penguin contribution to the width difference and CP asymmetry in $B_q - \bar{B}_q$ mixing at order $\alpha_s^2 N_f$*, Phys. Rev. D **102** (2020) 033007 [2006.13227]. 111

[241] M. Gerlach, U. Nierste, V. Shtabovenko and M. Steinhauser, *Two-loop QCD penguin contribution to the width difference in B_s–$\overline{B}_s$ mixing*, JHEP **07** (2021) 043 [2106.05979]. 111

[242] M. Gerlach, U. Nierste, V. Shtabovenko and M. Steinhauser, *The width difference in $B-\bar{B}$ mixing at order α_s and beyond*, JHEP **04** (2022) 006 [2202.12305]. 111

[243] M. Gerlach, U. Nierste, V. Shtabovenko and M. Steinhauser, *Width Difference in the $B-\bar{B}$ System at Next-to-Next-to-Leading Order of QCD*, Phys. Rev. Lett. **129** (2022) 102001 [2205.07907]. 111

[244] M. Beneke, G. Buchalla and I. Dunietz, *Width Difference in the $B_s-\bar{B}_s$ System*, Phys. Rev. D **54** (1996) 4419 [hep-ph/9605259]. 111

[245] A. Badin, F. Gabbiani and A.A. Petrov, *Lifetime difference in B_s mixing: Standard model and beyond*, Phys. Lett. B **653** (2007) 230 [0707.0294]. 111

[246] HPQCD collaboration, *Lattice QCD matrix elements for the $B_s^0-\bar{B}_s^0$ width difference beyond leading order*, Phys. Rev. Lett. **124** (2020) 082001 [1910.00970]. 111

[247] C. Bobeth, U. Haisch, A. Lenz, B. Pecjak and G. Tetlalmatzi-Xolocotzi, *On new physics in $\Delta\Gamma_d$*, JHEP **06** (2014) 040 [1404.2531]. 112, 125

[248] G.-y. Huang and S. Zhou, *Precise Values of Running Quark and Lepton Masses in the Standard Model*, Phys. Rev. D **103** (2021) 016010 [2009.04851]. 116

[249] F. del Aguila and M.J. Bowick, *The Possibility of New Fermions With $\Delta I = 0$ Mass*, Nucl. Phys. B **224** (1983) 107. 118

[250] V.D. Barger, M.S. Berger and R.J.N. Phillips, *Quark singlets: Implications and constraints*, Phys. Rev. D **52** (1995) 1663 [hep-ph/9503204]. 118

[251] M. Carena, A.D. Medina, B. Panes, N.R. Shah and C.E.M. Wagner, *Collider phenomenology of gauge-Higgs unification scenarios in warped extra dimensions*, Phys. Rev. D **77** (2008) 076003 [0712.0095]. 118

[252] O. Matsedonskyi, G. Panico and A. Wulzer, *Light Top Partners for a Light Composite Higgs*, JHEP **01** (2013) 164 [1204.6333]. 118

[253] G.C. Branco and L. Lavoura, *On the Addition of Vector Like Quarks to the Standard Model*, Nucl. Phys. B **278** (1986) 738. 118

[254] P. Langacker and D. London, *Mixing Between Ordinary and Exotic Fermions*, Phys. Rev. D **38** (1988) 886. 118

[255] Y. Nir and D.J. Silverman, *Z Mediated Flavor Changing Neutral Currents and Their Implications for CP Asymmetries in B^0 Decays*, Phys. Rev. D **42** (1990) 1477. 118

[256] G. Barenboim and F.J. Botella, *$\Delta F = 2$ effective Lagrangian in theories with vector - like fermions*, Phys. Lett. B **433** (1998) 385 [hep-ph/9708209]. 118, 199

[257] G. Barenboim, F.J. Botella, G.C. Branco and O. Vives, *How sensitive to FCNC can B^0 CP asymmetries be?*, Phys. Lett. B **422** (1998) 277 [hep-ph/9709369]. 118

[258] F. del Aguila, M. Perez-Victoria and J. Santiago, *Observable contributions of new exotic quarks to quark mixing*, *JHEP* **09** (2000) 011 [hep-ph/0007316]. 118

[259] J.A. Aguilar-Saavedra, R. Benbrik, S. Heinemeyer and M. Pérez-Victoria, *Handbook of vectorlike quarks: Mixing and single production*, *Phys. Rev. D* **88** (2013) 094010 [1306.0572]. 118

[260] K. Ishiwata, Z. Ligeti and M.B. Wise, *New Vector-Like Fermions and Flavor Physics*, *JHEP* **10** (2015) 027 [1506.03484]. 118

[261] J.M. Alves, G.C. Branco, A.L. Cherchiglia, C.C. Nishi, J.T. Penedo, P.M.F. Pereira et al., *Vector-like singlet quarks: A roadmap*, *Phys. Rept.* **1057** (2024) 1 [2304.10561]. 118, 120

[262] CMS collaboration, *Search for pair production of vector-like quarks in leptonic final states in proton-proton collisions at $\sqrt{s}$ = 13 TeV*, *JHEP* **07** (2023) 020 [2209.07327]. 120

[263] A. Banerjee, E. Bergeaas Kuutmann, V. Ellajosyula, R. Enberg, G. Ferretti and L. Panizzi, *Vector-like quarks: Status and new directions at the LHC*, *SciPost Phys. Core* **7** (2024) 079 [2406.09193]. 120

[264] S. Jäger, M. Kirk, A. Lenz and K. Leslie, *Charming new physics in rare B-decays and mixing?*, *Phys. Rev. D* **97** (2018) 015021 [1701.09183]. 125

[265] A. Lenz and G. Tetlalmatzi-Xolocotzi, *Model-independent bounds on new physics effects in non-leptonic tree-level decays of B-mesons*, *JHEP* **07** (2020) 177 [1912.07621]. 125

[266] S. Jäger, M. Kirk, A. Lenz and K. Leslie, *Charming New B-Physics*, *JHEP* **03** (2020) 122 [1910.12924]. 125

[267] A. Lenz, J. Müller, M.L. Piscopo and A.V. Rusov, *Taming new physics in $b \to c\bar{u}d(s)$ with $\tau(B^+)/\tau(B_d)$ and a^d_{sl}*, *JHEP* **09** (2023) 028 [2211.02724]. 125

[268] W. Altmannshofer and P. Stangl, *New physics in rare B decays after Moriond 2021*, *Eur. Phys. J. C* **81** (2021) 952 [2103.13370]. 125

[269] A. Greljo, J. Salko, A. Smolkovič and P. Stangl, *Rare b decays meet high-mass Drell-Yan*, *JHEP* **05** (2023) 087 [2212.10497]. 125

[270] R. Bause, H. Gisbert, M. Golz and G. Hiller, *Model-independent analysis of $b \to d$ processes*, *Eur. Phys. J. C* **83** (2023) 419 [2209.04457]. 125

[271] M. Bordone and M. Fernández Navarro, *τ_{B_s}/τ_{B_d} and $\Delta\Gamma_s$ confront new physics in $b \to s\tau\tau$*, *Eur. Phys. J. C* **83** (2023) 842 [2307.07013]. 126

[272] LHCb collaboration, *Search for the decays $B^0_s \to \tau^+\tau^-$ and $B^0 \to \tau^+\tau^-$*, *Phys. Rev. Lett.* **118** (2017) 251802 [1703.02508]. 126

[273] A. Crivellin and M. Kirk, *Diquark explanation of $b \to s\ell^+\ell^-$*, *Phys. Rev. D* **108** (2023) L111701 [2309.07205]. 126

[274] C. Cornella, D.A. Faroughy, J. Fuentes-Martin, G. Isidori and M. Neubert, *Reading the footprints of the B-meson flavor anomalies*, *JHEP* **08** (2021) 050 [2103.16558]. 126

[275] ATLAS collaboration, *A search for pair-produced resonances in four-jet final states at $\sqrt{s}$ = 13 TeV with the ATLAS detector*, *Eur. Phys. J. C* **78** (2018) 250 [1710.07171]. 128

[276] CMS collaboration, *Search for pair-produced resonances decaying to quark pairs in proton-proton collisions at $\sqrt{s} = 13$ TeV*, Phys. Rev. D **98** (2018) 112014 [1808.03124]. 128

[277] CMS collaboration, *Search for supersymmetry in proton-proton collisions at 13 TeV in final states with jets and missing transverse momentum*, JHEP **10** (2019) 244 [1908.04722]. 128

[278] ATLAS collaboration, *Search for squarks and gluinos in final states with jets and missing transverse momentum using 139 fb^{-1} of $\sqrt{s}$ =13 TeV pp collision data with the ATLAS detector*, JHEP **02** (2021) 143 [2010.14293]. 128

[279] P. Agrawal, M. Blanke and K. Gemmler, *Flavored dark matter beyond Minimal Flavor Violation*, JHEP **10** (2014) 072 [1405.6709]. 129

[280] S. Oh and J. Tandean, *Anomalous CP-Violation in $B_s - \bar{B}_s$ Mixing Due to a Light Spin-One Particle*, Phys. Lett. B **697** (2011) 41 [1008.2153]. 130

[281] A. Crivellin, C.A. Manzari, W. Altmannshofer, G. Inguglia, P. Feichtinger and J. Martin Camalich, *Toward excluding a light Z' explanation of $b \to s\ell^+\ell^-$*, Phys. Rev. D **106** (2022) L031703 [2202.12900]. 130

[282] Belle collaboration, *Search for B^0 meson decays into Λ and missing energy with a hadronic tagging method at Belle*, Phys. Rev. D **105** (2022) L051101 [2110.14086]. 131

[283] BaBar collaboration, *Search for B mesogenesis at BaBar*, Phys. Rev. D **107** (2023) 092001 [2302.00208]. 131

[284] BaBar collaboration, *Search for Evidence of Baryogenesis and Dark Matter in $B^+ \to \psi_D + p$ Decays at BABAR*, Phys. Rev. Lett. **131** (2023) 201801 [2306.08490]. 131

[285] A. Khodjamirian and M. Wald, *B-meson decay into a proton and dark antibaryon from QCD light-cone sum rules*, Phys. Lett. B **834** (2022) 137434 [2206.11601]. 131

[286] G. Elor and A.W.M. Guerrera, *Branching fractions of B meson decays in Mesogenesis*, JHEP **02** (2023) 100 [2211.10553]. 131

[287] A. Boushmelev and M. Wald, *Higher twist corrections to B-meson decays into a proton and dark antibaryon from QCD light-cone sum rules*, Phys. Rev. D **109** (2024) 055049 [2311.13482]. 131

[288] Y.-J. Shi, Y. Xing and Z.-P. Xing, *Semi-inclusive decays of B meson into a dark anti-baryon and baryons*, Eur. Phys. J. C **83** (2023) 744 [2305.17622]. 131

[289] J. Aebischer, W. Dekens, E.E. Jenkins, A.V. Manohar, D. Sengupta and P. Stoffer, *Effective field theory interpretation of lepton magnetic and electric dipole moments*, JHEP **07** (2021) 107 [2102.08954]. 175

[290] M. Jung and A. Pich, *Electric Dipole Moments in Two-Higgs-Doublet Models*, JHEP **04** (2014) 076 [1308.6283]. 185

[291] A. Cherchiglia, P. Kneschke, D. Stöckinger and H. Stöckinger-Kim, *The muon magnetic moment in the 2HDM: complete two-loop result*, JHEP **01** (2017) 007 [1607.06292]. 185

[292] I.I. Bigi and A.I. Sanda, *CP violation*, vol. 9, Cambridge University Press (9, 2009), 10.1017/CBO9780511581014. 187, 194

[293] H.H. Patel, *Package-X 2.0: A Mathematica package for the analytic calculation of one-loop integrals*, *Comput. Phys. Commun.* **218** (2017) 66 [1612.00009]. 191

[294] G. Buchalla, A.J. Buras and M.E. Lautenbacher, *Weak decays beyond leading logarithms*, *Rev. Mod. Phys.* **68** (1996) 1125 [hep-ph/9512380]. 194

[295] H.-Y. Cheng, *CP Violating Effects in Heavy Meson Systems*, *Phys. Rev. D* **26** (1982) 143. 194

[296] A.J. Buras, W. Slominski and H. Steger, *$B^0 - \bar{B}^0$ Mixing, CP Violation and the B Meson Decay*, *Nucl. Phys. B* **245** (1984) 369. 194, 196

[297] J.R. Ellis, M.K. Gaillard, D.V. Nanopoulos and S. Rudaz, *The Phenomenology of the Next Left-Handed Quarks*, *Nucl. Phys. B* **131** (1977) 285. 196

[298] J.S. Hagelin, *Mass Mixing and CP Violation in the $B^0 - \bar{B}^0$ system*, *Nucl. Phys. B* **193** (1981) 123. 196, 198

[299] E. Franco, M. Lusignoli and A. Pugliese, *Strong Interaction Corrections to CP Violation in $B_0 - \bar{B}_0$ Mixing*, *Nucl. Phys. B* **194** (1982) 403. 196

[300] L.-L. Chau, *Quark Mixing in Weak Interactions*, *Phys. Rept.* **95** (1983) 1. 196

[301] V.A. Khoze, M.A. Shifman, N.G. Uraltsev and M.B. Voloshin, *On Inclusive Hadronic Widths of Beautiful Particles*, *Sov. J. Nucl. Phys.* **46** (1987) 112. 196

[302] A. Dziurda et al., *Summary of Working Group 4: Mixing and mixing-related CP violation in the B system: Δm, $\Delta\Gamma$, ϕ_s, ϕ_1/α, ϕ_2/β, ϕ_3/γ*, in *12th International Workshop on the CKM Unitarity Triangle*, 4, 2024 [2404.03945]. 198